Time Based Load-flow Analysis and Loss Costing in Electrical Distribution Systems

Christopher Neil Macqueen

Abstract

This thesis describes research into the problem of load-flow analysis of electrical distribution systems. A discrete time simulation approach is presented which models the steady state behaviour of the system as individual load and generation profiles change with time. The approach is shown to provide improved modelling accuracy when compared with approaches based upon typical daily load curves, particularly when applied to systems serving diverse loads. The feasibility of studying systems of realistic size over simulation periods of a year on current workstation technology is demonstrated.

An enhanced version of the Newton-Raphson load-flow algorithm of Irving and Sterling is presented which performs selective updating of the Jacobian over multiple time steps. The resulting method is shown to be substantially quicker than the original algorithm.

An original load allocation algorithm is presented which utilises available distribution company data to assign active and reactive power profiles to individual loads and generators in the absence of full metered data.

Applications of discrete time simulation are outlined. A new constrained simulation algorithm, based upon Ridders' algorithm, is presented which determines the maximum load or generation which can be accommodated at a specified location as a function of time, without violating selected operational constraints.

Three new time based algorithms for the calculation of distribution system losses are presented. The first algorithm performs a full discrete time analysis and is shown to be suitable for applications in which high accuracy is required. The second and third algorithms offer reduced execution times through the use of interpolation.

A detailed loss allocation algorithm is presented which uses a directed graph technique to assign losses in individual lines and transformers to the consumers supplied by them. The algorithm is shown to be suitable for allocating both demand and energy losses.

The design of an open software environment is described which employs a common relational database and interactive network graphics system, and integrates the time based analysis algorithms and third party applications in a flexible way. The use of advanced graphical techniques to permit efficient management of large volumes of analysis data is described. Such techniques are shown to be of importance in time based analysis.

Time Based Load-flow Analysis and Loss Costing in Electrical Distribution Systems

Christopher Neil Macqueen

A thesis presented for the degree of
Doctor of Philosophy

University of Durham
School of Engineering and Computer Science

January, 1994

Acknowledgements

I am indebted to a large number of people who have provided support, guidance and technical information during the course of the research. In particular I should like to thank my supervisor Dr. J. R. Bumby for his guidance and kind encouragement throughout the project. Thanks are due to Dr. M. R. Irving, Mr. J. O. Gann and the members of the OCEPS research group for technical support and friendship. I am also grateful to Prof. G. Musgrave for providing opportunities to complete the work at Brunel University.

I am grateful to staff of the three 'Northern RECs' for technical help and advice, in particular Mr. N. Robson, Mr. M. Wild and Mr. J. E. Morrell of Northern Electric, Mr. N. Grandidge of Norweb Electricity, and Miss R. Isaac of Yorkshire Electricity.

I should like to thank Mr. C. J. Mortley, Mr. M. Weller and Mr. E. South of SEEBOARD plc for the provision of valuable technical assistance.

Thanks to my immediate and extended family, and to friends at Coldharbour Lane, for their encouragement.

Finally, I want to express my deep-felt appreciation to my wife Cathy for her loving support and constant encouragement.

To

Cathy

Contents

Figures

Tables

Declaration

The work described in this thesis has not previously been submitted for a degree in this or any other university, and unless otherwise referenced it is the author's own work.

Statement of Copyright

Author's Note

The work described in this thesis was conducted as part of a five year research project undertaken by the OCEPS Research Group in collaboration with three Regional Electricity Companies in the North of England.

The OCEPS Group has become well established in the field of power systems research and has developed a wide range of analysis software. The work described here draws upon certain software modules developed by other members of the Group, namely the core Newton-Raphson load-flow algorithm, the Power~PACS graphics system and associated electrical plant database, and the PACS API communication interface. All the other software described in the thesis, including the Insight Simulation, Load Allocation, Load Library and Tariff Library application software, and the Discrete Time Simulator with modified load-flow, constrained simulation, loss costing and loss allocation algorithms, is the original work of the author.

List of Symbols

Symbols

B	Susceptance, Ω^{-1}
$\mathbf{B}$, $\mathbf{B}_0$, B_{00}	Loss formula B-coefficients
C	Capacity, VA
C_L	Cost of losses, £/MWh
e	Real component of voltage
E	Complex voltage
f	Imaginary component of voltage
F_C	Cost function
F_D	Load Factor
$F_{Distrib}$	Distribution factor
F_{Div}	Diversity factor
F_L	Loss factor (general)
F_{Lr}	Active loss factor
F_{Lx}	Reactive loss factor
F_{PLR}	Peak load ratio
G	Conductance, Ω^{-1}
I	Current, A
H	Element of Jacobian matrix. Rate of change of P with respect to θ.
J	Jacobian matrix
k_1, k_2	Load loss factor coefficients
K	Line code coefficient
L	Element of Jacobian matrix. Rate of change of Q with respect to V.
L	Line length, m
LA	Loss assignment to a vertex
LC	Loss coefficient
LD	Load diversity
m	Iteration number
M	Element of Jacobian matrix. Rate of change of Q with respect to θ.
n	Number of nodes in the system

n_B	Number of branches (lines) in the system
n_D	Number of loads in the system
n_{gsp}	Number of Grid Supply Points in the system
n_G	Number of generators in the system
n_T	Number of transformers in the system
N	Element of Jacobian matrix. Rate of change of P with respect to V.
N_{Case}	Number of load-flow cases
N_{Day}	Number of typical days
N_{Level}	Number of discrete loading levels
N_{Step}	Number of time steps in a day
N_{TStep}	Total number of time steps in a simulation
P	Active power, W
P_D	Active power demand, W
P_G	Active power generation, W
P_L	Active demand loss, W
PF	Penalty factor
Q	Reactive power, VAr
Q_D	Reactive power demand, VAr
Q_L	Reactive demand loss, VAr
R	Resistance, Ω.
S	Apparent power, VA
t	Time step
T	Time, hours
V	Voltage magnitude, V
W_L	Active energy loss, Wh
X	Reactance, Ω.
Y_{ik}	Admittance between nodes i and k
$\alpha_1, \alpha_2, \alpha_3$	Active power polynomial load modelling coefficients
$\beta_1, \beta_2, \beta_3$	Reactive power polynomial load modelling coefficients
μ_1, μ_2, μ_3	Active power polynomial load modelling exponents
ν_1, ν_2, ν_3	Reactive power polynomial load modelling exponents
γ	Impedance angle, radians
θ	Voltage angle, radians.

Subscripts and Superscripts

act	Actual value
arch	Archetypal value
av	Average value
A	Autotransformer value

D	Load (demand) value
day	Daily value
$fixed$	Fixed loss value
G	Generator value
lib	Library value
(m)	Iteration number
max	Maximum value
min	Minimum value
$noload$	No-load value
nom	Nominal value
r	Active value
R	Reference generator value
rem	Remaining value
sp	Specified value
sys	Total value for the system
var	Variable loss value
V	Voltage dependent component
x	Reactive value
$year$	Annual value
θ	Angle dependent component

Notation Conventions

$\bar{I}$	Complex quantity
$\bar{I}^*$	Complex conjugate
$\Re$	Real part of a complex quantity
$\Im$	Imaginary part of a complex quantity
$\mathbf{I}$	Vector (column matrix)
$[\mathbf{Y}]$	Matrix
$[\mathbf{Y}]^T$	Matrix transpose

Acronyms

REC	Regional Electricity Company
CEGB	Central Electricity Generating Board

Chapter 1. Introduction

1.1 Aims of the Thesis

1.1.1 Introduction and Background to the Research

The work described in this thesis concerns the development of a new approach to the analysis of electrical distribution systems which models the variations in the state of the system as a function of time, thereby providing greater insight into the performance of the system and achieving higher levels of modelling accuracy than existing techniques.

The need to achieve greater accuracy in the modelling of the system for operations and planning purposes has been driven by the privatisation of the electricity supply industry in the United Kingdom, which was initiated in 1988 with the government's White Paper "Privatising Electricity" [69] and completed on vesting day in April 1990.

The effects of privatisation on the distribution sector are wide ranging. The more important of these are listed below:

- The regulatory environment has been redesigned to encourage competition in the supply side of the business, while maintaining tight control in the distribution side of the business, which is a natural monopoly.
- The obligation to supply electricity at acceptable levels of quality and reliability has been placed at the distribution level, and consumers have been given new rights regarding standards of supply. The result is that distribution companies are more accountable than was the case prior to privatisation.
- Competition in the supply business currently permits consumers with maximum demands above 1MW to place contracts for electricity with alternative energy suppliers, and to utilise the transmission and distribution networks of third parties where necessary to transfer the electricity from the point of supply to the point of consumption. Distribution companies are obliged to offer 'Use of System' tariffs which do not discriminate between franchise and non-franchise customers.

- Competition in the generation sector of the industry has led to a proliferation of mostly small independent generating companies. Distribution companies are having to respond to increasing numbers of connection requests from prospective generators.
- The transfer of the distribution companies to public ownership has led to a much greater emphasis on the economics of electricity supply. The primary objective of these Regional Electricity Companies (RECs) is to meet their regulatory obligations while simultaneously maintaining the interests of shareholders and maximising profits.
- RECs are required to calculate loss factors for Use of System tariffs and for major industrial consumers. Initial regulation concerning charging for electrical losses passed costs through to the consumer, with the result that there has been little motivation on the part of the RECs to reduce system losses. This aspect of regulatory policy is currently under review, and it is anticipated that incentives towards loss reduction at the distribution level will be increased.

The results of these changes on the operation and planning of the distribution system can be summarised as follows:

- The incentives to make the fullest use of existing assets, to put off capital investment by increasing levels of utilisation, are significantly greater now than pre-privatisation.
- The requirement for greater accountability has brought the need for additional information concerning the performance of the system, and improved methods of analysis to assist in the operation and planning of the system, and in the design of cost-reflective tariff structures.
- The new regulatory environment has required the RECs to adapt increasingly quickly to change, and to respond to inquiries from the regulator and from customers.
- The growth in the numbers of independent generating companies poses problems for RECs in the areas of protection co-ordination and system security.
- Charging for system losses has recently come under review, and the calculation and reduction of system losses is likely to become an increasingly important aspect of REC operations.

1.1.2 Aims of the Research

The primary aim of the research presented in the thesis is to develop an improved approach to load-flow analysis in electric distribution systems which is able to address the issues raised in the previous section. Particular attention is paid to the evaluation and costing of losses.

The state of any power system varies continuously as a function of time in response to changing consumer demands, generator outputs, switch states and so on. Existing approaches to steady-state analysis of the system provide a solution for a single operating condition. Several solutions under different conditions are used to cover a range of system states. The work described here investigates methods which model more faithfully the variations in system operating conditions with time.

The research also addresses the problems associated with inadequate levels of metered loading data required to perform time-based load-flow analysis. Many of the RECs are investing in new telemetry systems and corporate database management systems to improve access to system data. However, allocation techniques are still required to provide accurate estimates of load profiles in cases where metered data is not available.

The volumes of input data and results associated with time-based analysis are much greater than for conventional 'snapshot' approaches. Techniques for the minimisation and efficient storage of this data are crucial to the success of the time-based approach. Similarly the provision of facilities for efficient management of large volumes of data is of great importance. The latest interactive graphic user interface standards offer considerable potential in this respect.

Another aspect of time-based analysis is the large computational requirement when compared with conventional approaches. For studies of large systems over extended periods of time it may be necessary to reduce the execution time using techniques such as interpolation. This area is explored with regard to the calculation of losses.

1.2 The Electricity Supply Industry

The origins of the electricity supply industry date back to the early 1870s to the development of the first practical self-excited generators by the Belgian, Gramme, and the German firm of Siemens & Halske. Subsequent improvements to the designs of the electric arc lamp and the electric motor provided commercial applications for electricity in the form of urban street lighting and motive power for the transport and mining industries [21].

The first public electricity supply scheme was established in the Surrey town of Godalming in 1881 [110], and by May 1882 it supplied the town's streets and 'eight or ten' private customers. During the succeeding years there was a rapid growth in both the industrial and domestic usage of electricity. The earliest supply schemes operated over small distances and at low voltage, and suffered from poor voltage regulation and high losses. As the demand for electricity grew technical and economic considerations dictated that power stations be located near sources of fuel and cooling water, and that power be transmitted over longer distances at higher voltages.

Modem power systems generally comprise generation, transmission, sub-transmission or secondary transmission) and distribution systems, as shown in Figure 1.1. The work described here focuses on the sub-transmission and distribution levels of the system, which will be referred to as 'the distribution system'. In the United Kingdom this corresponds to voltage levels of 132kV and below.

1.3 Distribution System Configuration

The function of the distribution system is to transfer power from the transmission grid to the ultimate consumer. Figure 1.2 illustrates the configuration typically used in distribution system design. Power from the grid is supplied to the distribution system via a small number of Grid Supply Points (GSPs). These GSPs feed the sub-transmission network which supplies HV or primary substations located in major areas of demand. Large industrial or commercial consumers may be supplied directly from these substations. In the case of smaller consumers, primary feeders distribute power to consumer substations serving individual streets and housing estates. Power is transferred to consumers' premises at domestic voltage via the secondary distribution system.

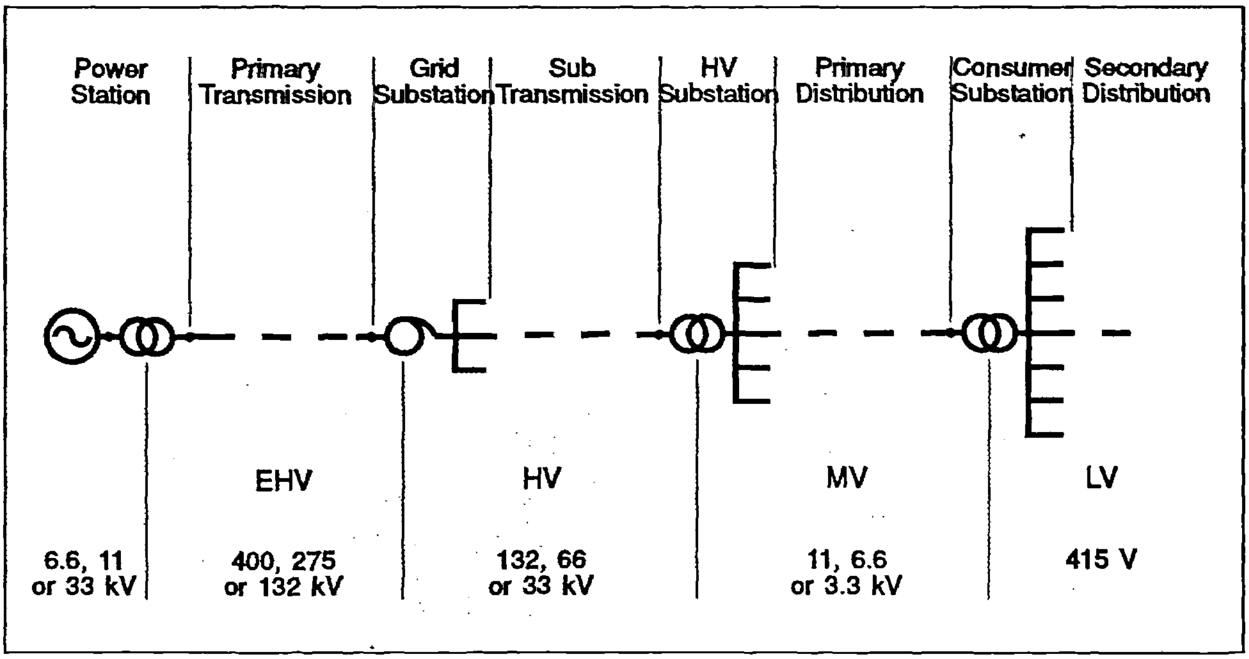

Figure 1.1 Components of a Power System

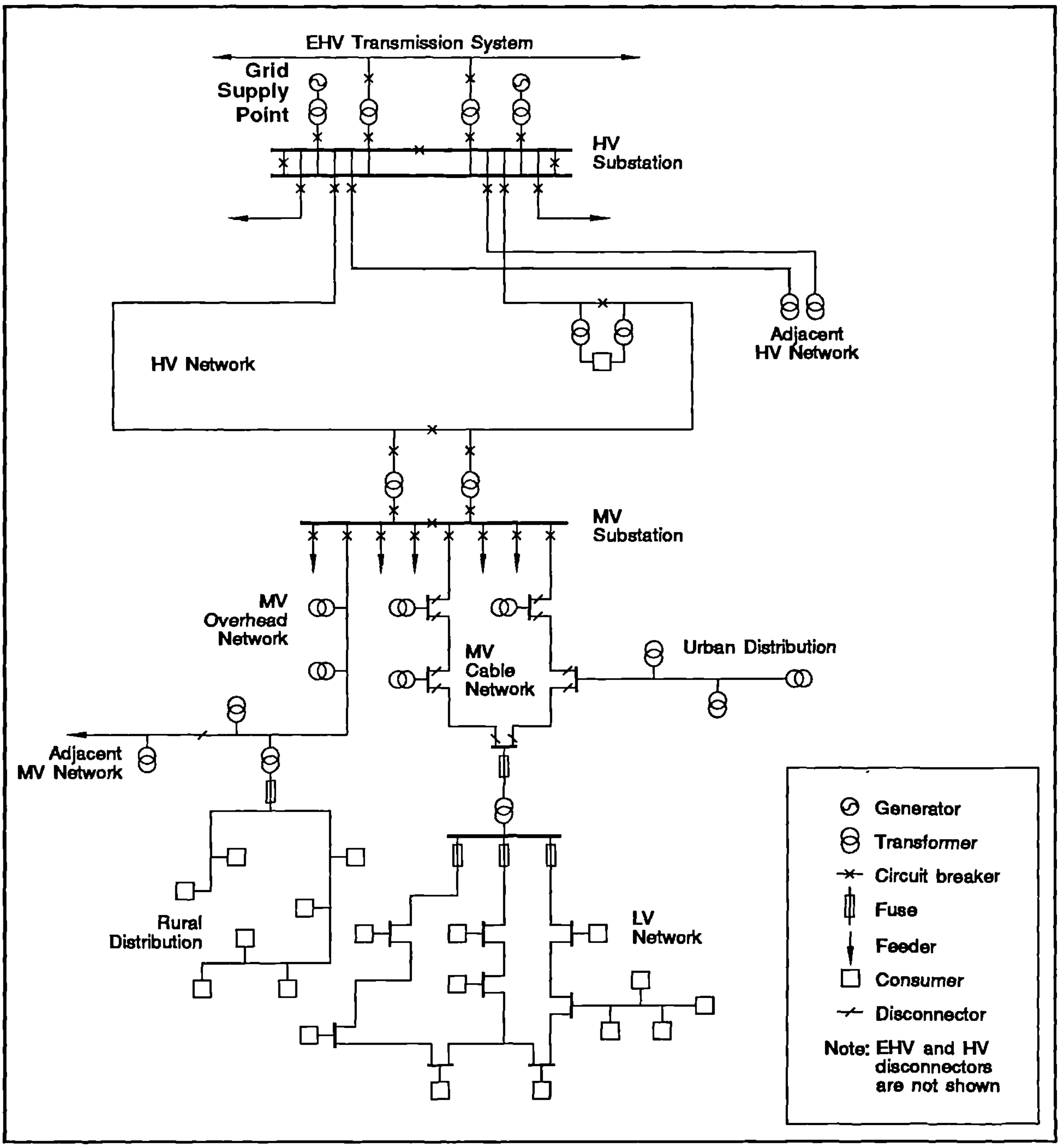

Figure 1.2 Typical Distribution System Structure

Source: Lakervi and Holmes, [81].

A number of network configurations are used by different distribution companies throughout the world. The more common configurations are illustrated in Figure 1.3.

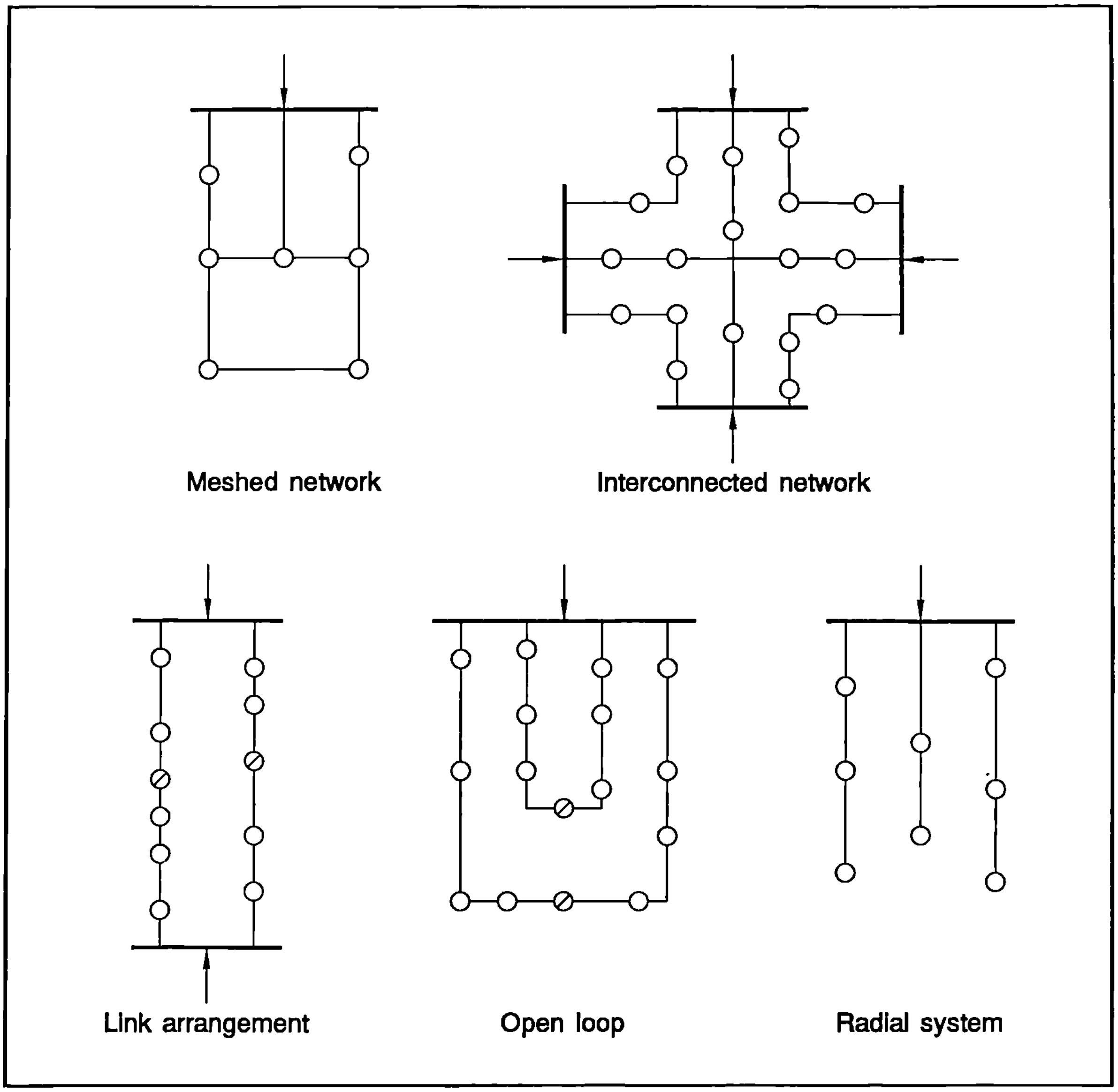

Figure 1.3 Distribution Network Configurations

Source: Lakervi and Holmes, [81].

The sub-transmission system is normally operated in a meshed or interconnected configuration to provide a secure supply to primary substations. In the event of outages in the system, continuity of supply can more easily be maintained in an interconnected system than in a radially connected system.

The primary distribution system is also interconnected, but is normally operated in a radial configuration through the use of open points. Examples include the link arrangement and open loop configurations shown in Figure 1.3. Radial systems at this level are necessary for the co-ordination of the protective devices required to isolate areas of the system in the event of a fault. In addition, the location of faults on the system in the absence of telemetered data is simplified in a radial network, as compared with a meshed configuration.

The use of open points provides flexibility in maintaining supplies of power to consumers during outage conditions.

1.4 Distribution System Operation and Planning Functions

The operation and planning of the distribution system comprises a complex set of tasks that represent a balance between minimising capital and running costs while maintaining acceptable standards of quality and security of supply to the customer. These tasks can be broken down into three categories according to their associated lead times [35], as illustrated in Figure 1.4.

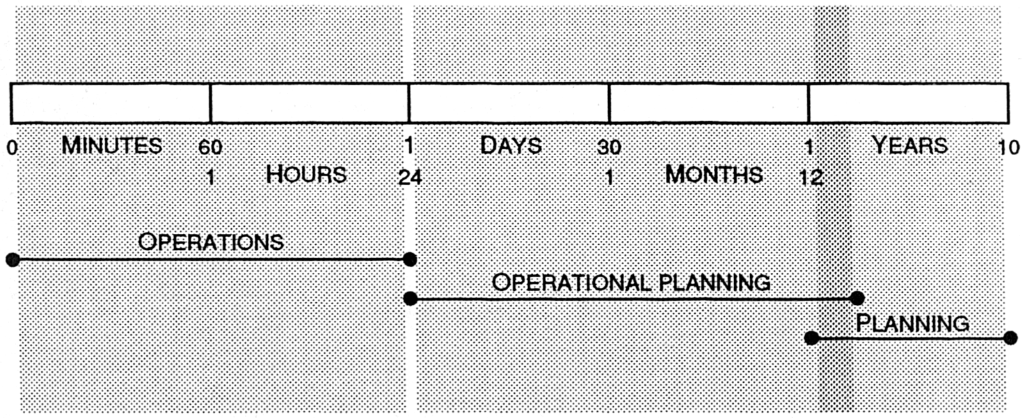

Figure 1.4 Distribution System Operation and Planning Functions

Source: British Electricity International, [24].

1.4.1 Operations Functions

The operations function covers the period from the present time to 24 hours in advance, and concerns:

- dealing with contingencies in order to minimise supply interruptions
- maintenance of the distribution system within constraints defined by thermal and stability limits and regulations concerning voltage variation

1.4.2 Operational Planning Functions

The operational planning function covers the period from 24 hours to three years, and concerns:

- demand forecasting
- demand control, including voltage reduction, load management and load shedding schemes
- short term maintenance of the system and outage planning
- response to third party connection requests

- security assessment
- co-ordination of protective devices
- configuration of the network for loss reduction
- testing and monitoring of the system

1.4.3 Planning Functions

The system planning function is concerned with the longer term, and covers the period one to more than ten years in advance. System planning involves:

- long term outage planning
- system reinforcement to meet projected growth in demand.
- replacement of ageing plant

1.4.4 Commercial Functions

In addition to the operations and planning functions outlined above, a wide range of analysis related to the commercial side of the business is performed, including:

- energy contracting
- energy accounting
- tariff design

1.4.5 Analysis Tools for Distribution System Operations and Planning

A wide range of computerised analysis tools have been developed to assist operations and planning engineers to perform these functions. Figure 1.5 lists the more widely used of these tools.

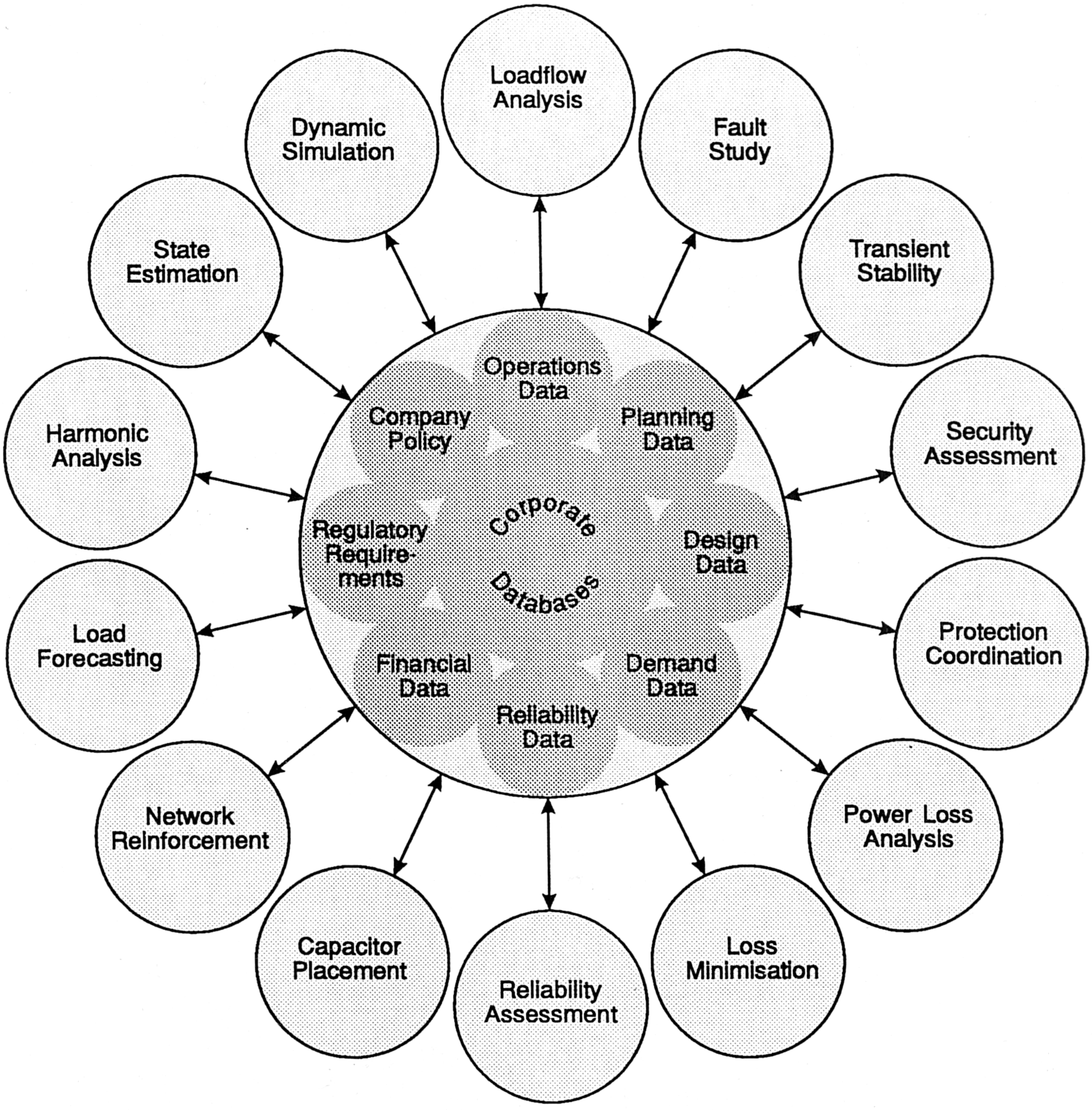

Figure 1.5 Analysis Tools Commonly Used in Distribution System Operations and Planning

Of prime importance in power system analysis is the load-flow program which forms the basis of many of these tools.

The load-flow is used primarily to assess the steady state of the system under different loading conditions and system configurations. It is also used to calculate the initial conditions for other analysis programs such as fault study and transient stability, and is used for solving the algebraic equations in dynamic simulation programs. Optimal load-flows are used in the dispatch of generation, interchange evaluation and real time pricing programs.

1.5 Nature of Distribution Systems

In the past new analysis algorithms have often been applied to transmission systems first, where potential benefits are greatest, before being applied to the distribution level. However, distribution systems possess certain characteristics which are of particular significance when conducting analysis at this level. These can render some assumptions made at the transmission level invalid, requiring different approaches to a given problem.

1.5.1 Load Diversity

When the demands of two or more consumers are combined, the peak of the combined load is likely to be less than the sum of the individual peaks. This occurs when the individual peak demands do not coincide, and is referred to as load diversity.

Two definitions are in general use: Load Diversity and Diversity Factor. These are given in Appendix A.

1.5.1.1 Causes of Load Diversity

Load diversity arises from the power consumption patterns of the electrical equipment which make up a given consumer load. The demand profiles of most electrical appliances are not smooth and continuous, but comprise a series of sudden shifts in demand. This is particularly true of domestic appliances, such as immersion heaters, cookers, refrigerators and so on, which switch on and off under the control of timers and thermostats. Some industrial loads exhibit similar behaviour. The demand pattern for a given consumer is therefore a combination of the demand profiles of various appliances, leading to an erratic profile, such as that shown in Figure 1.6(a). The figure shows a daily profile for a particular domestic consumer, sampled at 30 second intervals.

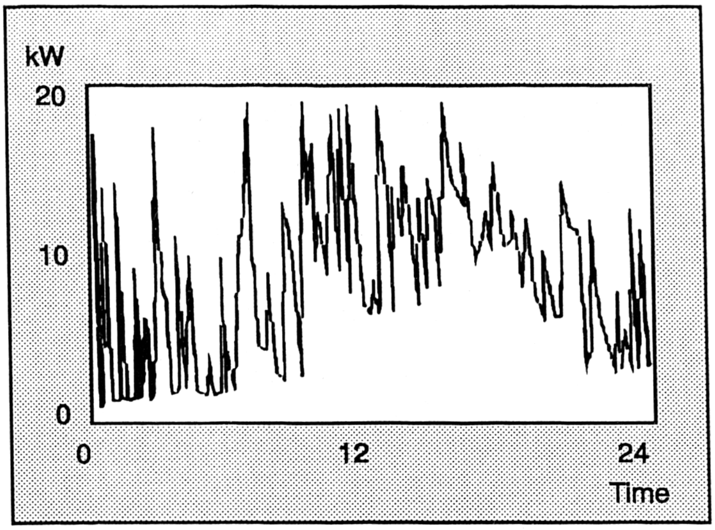

(a) Single Consumer

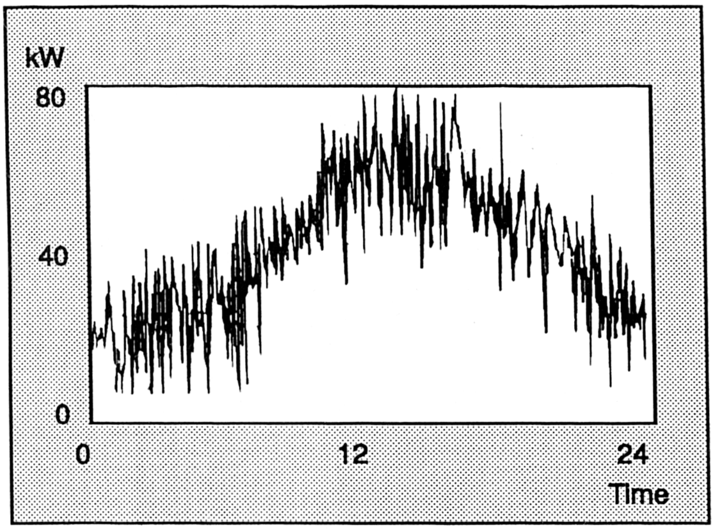

(b) Group of 5 Consumers

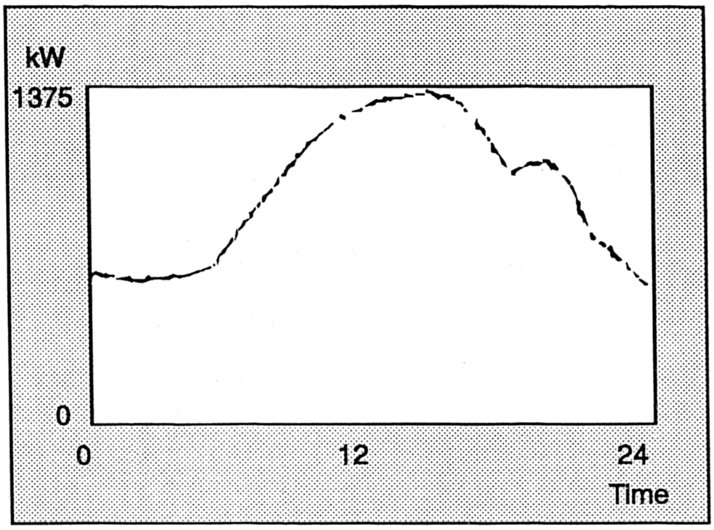

(c) Group of 125 Consumers

Figure 1.6 Load Diversity of Groups of Domestic Consumers

Source: Willis et al, [151].

1.5.1.2 The Effect of Sample Size on Load Diversity

Although the profile of an individual consumer is erratic and unpredictable, when the profiles of large numbers of consumers of the same type are aggregated, the resulting demand profile is smooth and continuous. The spikes and troughs in individual profiles do not always coincide, and are effectively removed by an averaging process. Figure 1.6(b) shows the demand profile for 5 domestic consumers, while Figure 1.6(c) shows the profile for a group of 125 consumers.

Figure 1.6(a) indicates that the peak demand of the single domestic consumer is approximately 20kW. For five consumers the average peak demand is approximately 16kW, while for 125 consumers it has fallen to approximately 11kW. Figure 1.7 shows a graph of diversity factor against number of consumers for these three cases. Extrapolating for larger groups of consumers the diversity factor for this type of consumer tends towards a value of approximately 2.

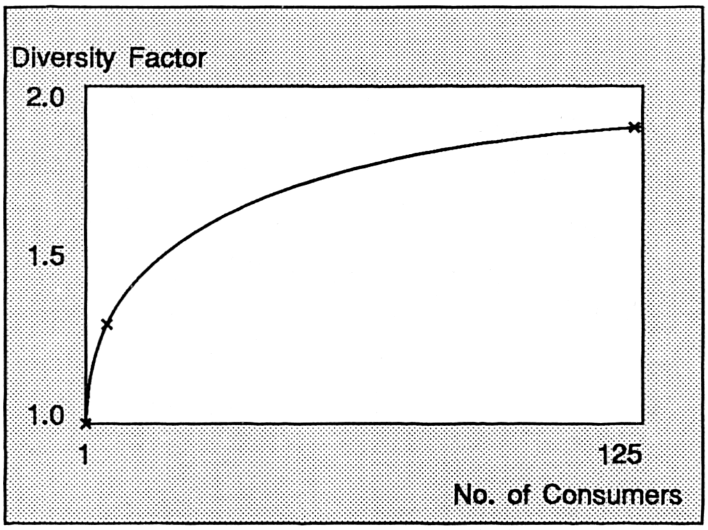

Figure 1.7 Diversity Factor against Sample Size for Domestic Consumer Groups

Source: Willis et al, [151].

From this example it can be seen that when modelling the demand of a given consumer type, the sample size has a significant effect on both the demand profile shape and the diversity factor.

1.5.1.3 The Effect of Demand Profile Shape on Load Diversity

In the example given above it was assumed that all the consumers in the sample belonged to the same basic consumer category. Demand profiles from different groups of consumers in this category would be expected to conform, provided the sample sizes were sufficiently large.

The combination of profiles for consumers groups in different categories, such as industrial and residential, can lead to high levels of diversity due to the non-coincidence of peaks in the different profile shapes. This is complicated by the fact that consumer demand profiles can differ significantly on different days of the week and seasons of the year, giving rise to diversity factors which change from day to day. Figure 1.8 compares the demand profiles for three different categories of consumer for a winter Sunday and Monday: a domestic feeder, a manufacturing plant and a major chemical works. The data was taken from neighbouring 11kV feeders in the North of England. The domestic profile shows the expected lunchtime peak on the Sunday, and the early evening peak on the weekday. The manufacturing plant can be seen to be operating a shift pattern, with peak demand overnight, perhaps due to a beneficial off-peak tariff. The chemical works can be seen to operate a continuous process which is run up on the Sunday afternoon. The figure serves to illustrate the large differences in demand profile which can arise on a given system.

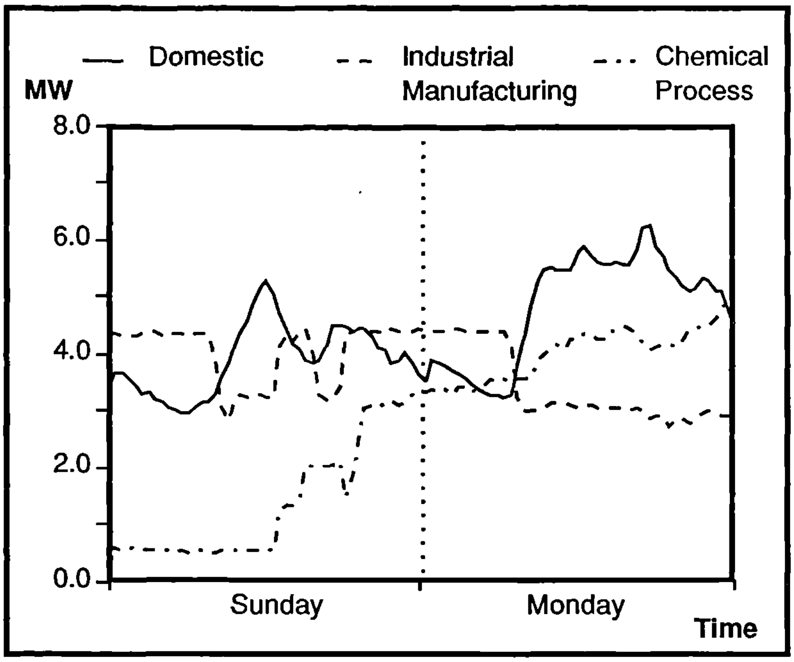

Figure 1.8 Consumer Demand Profiles on Neighbouring 11kV Feeders

1.5.1.4 The Implications of Load Diversity for Load-Flow Analysis

The effects of load diversity are dependent upon the voltage level of the system under study. In analysis of a transmission system the flow of power in a grid transformer or sub-transmission line may be modelled as a single load. In this case the load comprises many thousands of individual consumers of different size and category. The demand profiles of loads modelled in this way tend to conform, with the result that load diversity at this level is relatively insignificant.

Analysis at the higher voltage levels of distribution systems can often be treated in the same way. However, the further the analysis is taken down the system towards the ultimate consumers, the greater are the effects of load diversity. In the United Kingdom major consumers are frequently connected directly to 11kV substations, with the result that loads modelled at this voltage level can exhibit large differences in demand profile shape, load factor and load diversity. The modelling of loads may therefore require different treatment at the distribution level as compared with the transmission level. Chapter 2 reviews the general approaches to modelling loads in distribution system load-flow analysis.

1.5.2 Availability of Demand Data

In general both the quantity and quality of demand data available for power system analysis decreases with voltage level. At higher voltages, typically 400kV down to 33kV in the UK, SCADA (Supervisory Control and Data Acquisition) systems measure voltage, current, and possibly power and power factor at intervals of approximately one minute, and store values of half-hour averages. At voltages of 11kV and below demand data is more scarce, and measuring devices are less accurate. Figure 1.9 shows the sources of demand data typically found at different levels of distribution systems in the United Kingdom.

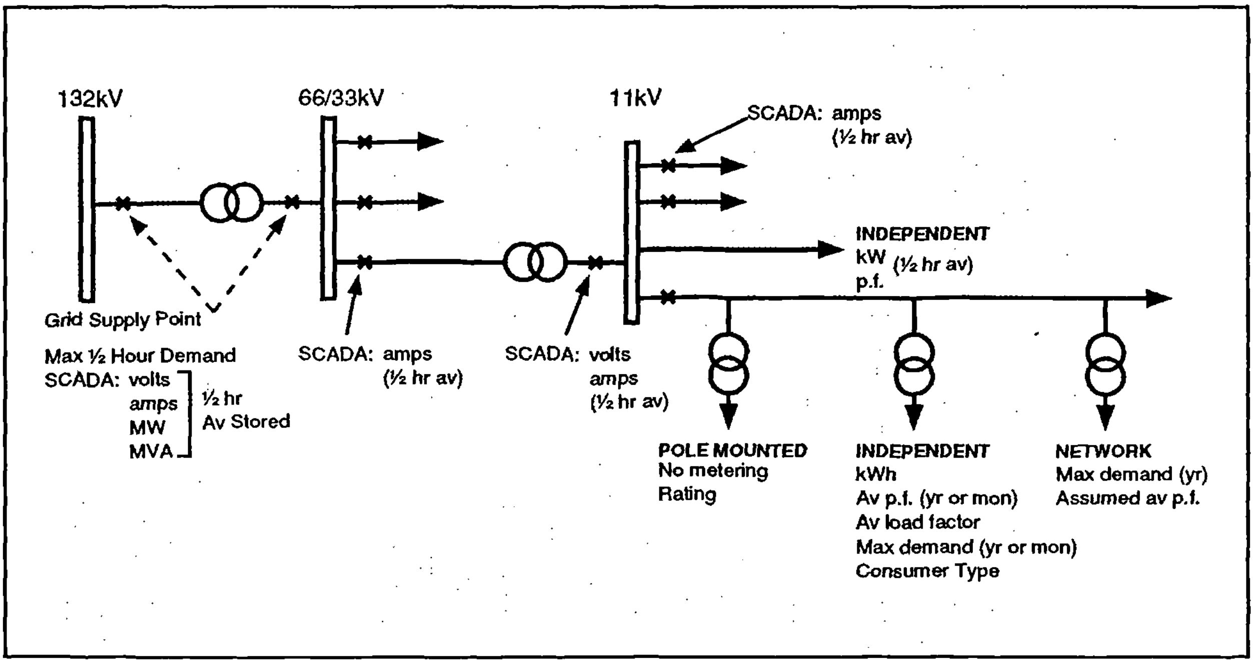

Figure 1.9 Distribution System Data Sources

Although levels of metering will vary from one distribution company to the next, the figure illustrates that the availability of time-based demand data at voltages of 11kV and below cannot be assumed, and techniques for estimating demand profiles in the absence of data may be required. The data typically available can be summarised as follows:

- For substations at 33kV and above, measurements of active and reactive power are generally available on a half hour basis via SCADA systems.

- For primary 11kV substations measurements of voltage and current are generally available on a half hour basis via SCADA systems. Power factor is available either on a half hour basis, or as a yearly average.

- At the 11kV level, the nature of the consumers supplied by a given feeder determines which measurements are available. Major independent consumers may have metering equipment which records active power and power factor on a half hour basis. Other independent consumers may not have a large enough demand for electricity to warrant full metering, but are nevertheless significant enough to have an individual record in the distribution company's consumer billing file, listing information such as total energy taken, average power factor, average load factor, monthly maximum demand and the kind of activity the consumer is engaged in. Network transformers may be equipped with maximum demand equipment which is read and reset on an annual basis. Pole mounted transformers usually have no metering, the only related information being the transformer rating itself.

1.5.3 Transmission Line Resistance to Reactance Ratios

The impedances of transmission lines used in the EHV transmission grid are largely reactive, with reactance to resistance (X/R) ratios typically in the range 3 to 10. In transmission lines used at lower voltages the impedance is more resistive. At 11kV and below the X/R ratios of lines are typically less than unity. Table 1.1 illustrates the variation typically found, and lists representative values for the impedances of transmission lines at the different voltage levels.

Table 1.1 Typical Distribution System Line Parameters

Line Type	Voltage Level kV	Conductor Size mm^2 (Matl)	Rating MVA (° C)	Resistance R Ω/km	Reactance X Ω/km	X/R Ratio
O/H	275	400 (Al/St)	207.0 (75)	0.07	0.21	3.0
	132	500 (Al/St)	139.0 (75)	0.06	0.20	3.3
	33	175 (Al)	30.0 (65)	0.16	0.38	2.4
	11	100 (Al)	6.8 (65)	0.28	0.33	1.2
	0.415	70 (Al)		0.26	0.29	1.1
	0.415	35 (Al)		0.54	0.33	0.6
U/G	33	400 (Al)	27.1 (65)	0.10	0.08	0.8
	33	240 (Cu)	27.4 (65)	0.10	0.08	0.8
	11	240 (Al)	6.2 (65)	0.15	0.08	0.5
	0.415	185 (Al)	0.2 (80)	0.21	0.07	0.3

The table serves to demonstrate the decrease in X/R ratio with decreasing voltage level. In addition to the general variation in impedance with voltage level, significant differences in impedance at a given voltage level can occur through the use of lines of different rating, and of widely differing length.

The practical implications of this for load-flow analysis are that at the transmission level, the 'coupling' of active and reactive components in some of the load-flow equations is weak, allowing for treatment of these components separately with subsequent savings in storage and computational requirements. In addition line resistance can frequently be neglected in the calculations, simplifying the analysis. At the distribution level the low X/R ratios of lines can render the decoupling assumptions invalid, with the result that decoupled algorithms may require many iterations to converge, and may fail to converge altogether.

1.6 Developments in Computer Hardware and Software

The rate of increase in the capabilities of computer hardware and software seen in recent years shows no sign of diminishing. Two developments in particular have provided new impetus for the design of software for power systems analysis.

1.6.1 The Advent of Low Cost High Performance Workstations

Performance which until recently was available only on the most powerful mainframe computers can now be found on entry level workstations. Figure 1.10 illustrates the typical increases in performance/price for workstation hardware from one manufacturer since 1987. Inflation has not been included in the analysis, hence the real increases are greater than the figure suggests.

Similarly, reductions in the cost of RAM and disk-based storage have been dramatic during recent years.

The implications for power system analysis software are profound; algorithms which had hitherto been rejected as impractical on the grounds of excessive computational and memory requirements can now be used with profit on the latest machines. For other methods, which have found widespread use, restrictions on the size and complexity of the problems to which they can be applied have been greatly reduced.

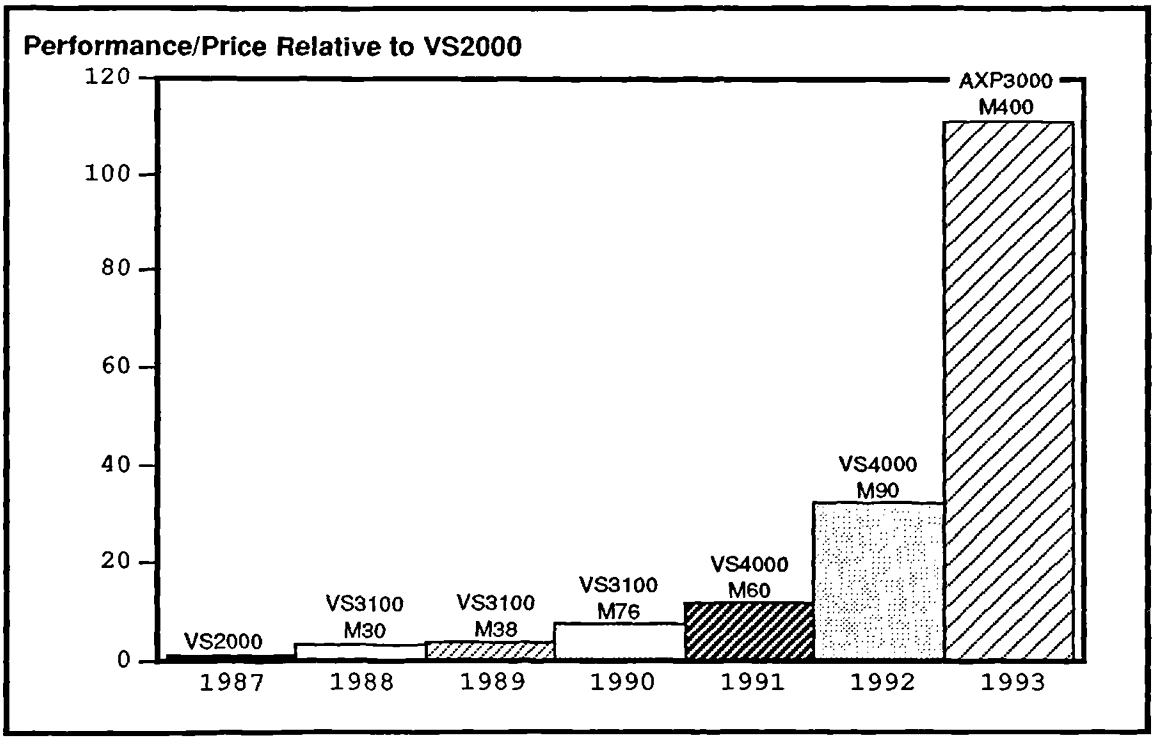

Figure 1.10 Increases in Performance/Price for Workstation Hardware Since 1987

Source: Digital Equipment Corporation

1.6.2 The Development of Window-based Graphic User Interface (GUI) Software

The rich development environments provided by software such as X/Motif and Windows NT provide great potential for designing power systems analysis software which is both more powerful and easier to use than previous user interface software permitted. The graphics capabilities of these systems can be exploited to allow efficient management of large volumes of input data and results, and the event handling and communications facilities allow for the development of open, multi-tasking environments for the integration of analysis programs.

As the complexity of power systems analysis software increases the rôle of the man-machine interface grows in importance, to the extent that the success of the software becomes dependent upon the quality of both the numerical algorithms and the Graphic User Interface used to access them. The work described in this thesis focuses on both of these areas.

1.7 Contents of the Thesis

The thesis reviews existing methods for load-flow analysis in distribution systems, including the problems of load modelling, load-flow algorithms and the software environments in which these algorithms are used, and presents a new time-based approach to load-flow analysis which addresses these three problems. The thesis describes the most important applications of the proposed method and presents new algorithms for the calculation and allocation of electrical losses. The contents of the thesis are described by chapter in more detail in the following sections.

In Chapter 2 the general approaches used for load-flow analysis in distribution system planning are reviewed. Three deterministic approaches are studied; the first of these covers conventional static methods in which the analysis is conducted at a few selected loading conditions, from which results pertaining to peak or average conditions are determined. The second approach covers load duration methods in which the analysis is conducted at different levels across a typical day load duration curves. The last approach covers chronological methods in which the analysis is conducted step by step across typical daily load curves. Two probabilistic approaches are reviewed: probabilistic load-flow, and Monte Carlo simulation. These approaches model the uncertainty in the state of the system; the probabilistic load-flow uses an analytical method, the Monte Carlo simulation method performs repeated load-flow studies using random input variables. Towards the end of the chapter the proposed chronological approach, Discrete Time Simulation, is described. All of the approaches are compared in terms of accuracy, and data and computational requirements, with particular emphasis placed on the modelling of consumer demand patterns.

In Chapter 3 the load-flow problem is addressed, and the most important and widely used load-flow algorithms are described. A brief history of the development of the load-flow is given, and the early methods, Y-Matrix Iterative Methods and Z-Matrix Methods, are outlined. The more recent methods are considered in detail: the Newton Raphson Method, the Fast Decoupled Method and Second Order methods. These algorithms are considered in terms of their suitability for the analysis specifically of distribution systems, and in terms of the proposed time-based analysis approach. The Efficient Newton Raphson Method of Irving and Sterling is described, and proposed as the most suitable algorithm in the light of these criteria. The remainder of the chapter describes the development of this load-flow for use in the context of time-based analysis, including improvements in speed of execution.

Chapter 4 covers the design and implementation of a distribution planning system: a software environment which integrates the analysis routines, databases and network graphics, and provides a graphic user interface via which analysis can be set up and performed, and the results studied. The first part of the chapter is devoted to a review of existing approaches to this problem. The requirements of such systems are listed and the application of recent advances in hardware and software technology to the problem are outlined. The remaining sections describe the proposed Insight planning environment, outlining the structure of the software and describing each of the primary components.

In Chapter 5 the problem of load allocation and modelling is addressed. The sources of load data typically found in distribution systems are reviewed briefly, and the need for an algorithm to estimate load profiles in the absence of available data is described. A load allocation algorithm designed around the available sources of data is proposed, and results from studies on a real system are presented.

Chapter 6 describes applications of the proposed time-based analysis approach which are not covered in Chapters 7 to 9. These include the analysis of voltage problems and the placement and sizing of reactive compensation, the study of the impact of embedded generation, and assessment of the available network capacity to support additional load and generation.

In Chapter 7 the problem of calculating electrical losses in distribution systems is introduced. The energy and demand components of loss are described, and sources of losses in distribution systems are listed. Existing methods for calculating demand loss are reviewed: loss formula methods, percentage loading methods, load-flow methods and optimal load-flow methods. Methods for calculating energy losses are studied, including loss-load factor methods, methods which use historical metered data and statistical modelling, and methods which derive energy losses from demand losses. The proposed method of loss calculation by Discrete Time Simulation is described and compared with existing techniques.

Chapter 8 describes techniques to reduce the computational requirements of the proposed loss calculation method through the use of interpolation. Two techniques are described: loss calculation using archetypal days, loss calculation using loss coefficients. Results from tests on these algorithms are presented and compared with the original method.

In Chapter 9 the problem of allocating losses to consumers supplied by the system is described. A loss allocation algorithm is proposed which assigns demand and energy losses to consumers according to the burden they impose on the system. A number of formulae for sharing losses between multiple consumers supplied at a given location are proposed and assessed in the light of economic theory concerning electricity pricing objectives and cost allocation.

In Chapter 10 the main conclusions of the thesis are presented, and proposals for future work are made.

Chapter 2. Load-flow Analysis Approaches in Distribution System Planning

2.1 Introduction

The chief use of load-flow analysis in distribution system planning is to assess the impact on system performance of a variety of changes, including load growth, and changes in the configuration of the system. Typical performance indices include maintaining the system within operational constraints, meeting service continuity and reliability obligations, and minimising power losses.

A load-flow solution provides a steady state solution for the system corresponding to a particular loading condition. By repeating the load-flow analysis for different loading conditions information concerning the range of possible system states can be derived. The following sections outline different approaches to this problem of deriving information for planning purposes from a limited number of load-flow solutions. The features and attributes of each of the approaches are summarised in Tables 2.7 to 2.12.

One of the criteria used in the assessment is the data required by each approach. It should be noted that the data requirements common to all load-flow based methods are excluded from consideration. In each case it is assumed that an accurate model of the system under study, which includes the parameters of the electrical plant in the system and its configuration, is available. This data will be referred to as 'Plant Data' and will be considered separately from time related load and generation data which will be referred to as 'Profiles Data'. The Plant Data attributes required to run a load-flow study are listed in Appendix D.

The approaches used by utilities when conducting this kind of load-flow analysis can be described in terms of two broad categories: deterministic approaches and probabilistic approaches.

2.2 Deterministic Approaches

Deterministic approaches to load-flow analysis do not attempt to model the uncertainty in input data such as consumer demand patterns and the availability of plant. Such data are assumed to be known in advance. Uncertainty in the data is dealt with, when necessary, by applying safety factors to design ratings derived from the load-flow analysis [5].

The advantage of deterministic approaches is their simplicity compared with probabilistic approaches, in regard to both the analysis algorithms and the power system data required. This simplicity is achieved at the expense of information concerning the variability of certain operating conditions, information which can be of great benefit in the planning and design process.

2.2.1 Single Case Load-flow Approach

2.2.1.1 Description of the Approach

In this approach load-flow studies for a particular system are performed at a small number of loading conditions, which are carefully selected by the planning engineer to cover the full extent of the range of system operating conditions. The most important loading condition corresponds to the time of system annual maximum demand. Other conditions studied may include the time of system annual minimum demand and other maximums and minimums related to different seasons of the year.

When conducting a particular planning study the engineer will decide how much of the system it is necessary to model. The radial configuration commonly used in distribution systems at lower voltages frequently gives rise to primary feeders which can conveniently be considered in isolation. Other areas at higher voltages may also be loosely connected permitting treatment of these areas separately in the analysis.

In addition to selecting the geographical area of the system to model, the engineer will decide which voltage levels to include. There is little benefit in taking the analysis to lower voltage levels than is required by the planning study. Lower voltage feeders can simply be represented by equivalent loads for the purposes of the analysis. When aggregating the demands on individual feeders in this way, it is necessary to use diversity factors to ensure the correct total.

From the results of this small number of load-flow studies the planning engineer can assess the limits of system performance for the configurations studied, including maximum and minimum values of voltage regulation, power flows, power losses, and transformer tap positions.

To determine values such as the total number of units of power or loss in a given circuit over a period of time, the engineer must make use of load factors and loss factors which relate the average and peak values of load and loss respectively. Section 7.5.1 describes the method often used.

2.2.1.2 Data Requirements

In addition to the plant data required to run any load-flow study, the Single Case method requires loading data and running configuration for each of the load-flow cases studied.

Assuming that active and reactive power are specified for each load, and that active power and voltage are specified for each generator, the loading data requirements for N_{Case} cases are given by

$$\text{Loading data} = 2N_{Case}(n_D + n_G) \times 4 \text{ Bytes}$$

where n_D and n_G are the numbers of loads and generators respectively, and 32 bit word length is assumed. The data requirements are very low in comparison with alternative methods described in this section.

2.2.1.3 Computational Requirements

The computational requirements for the method are very low, since only one load-flow for each case studied is required.

2.2.1.4 Modelling Accuracy

The simplicity of the analysis can give rise to a number of difficulties:

1. Conducting the analysis at the time of system annual maximum demand does not guarantee that the maximum loading conditions on every circuit will be covered. In particular, the peak demands on feeders serving industrial loads may occur at quite different times of the day, or during different weeks of the year than the times of system peak demand.

2. The approach does not provide any information concerning how often, or for how long a particular loading condition occurs.

3. The loss factors used to determine losses over a period must be derived empirically. Although published values for the coefficients in the loss factor equation (7-25) are available [42, 46], work by Gustafson [61] has shown that these coefficients can differ significantly from one system to the next. As an example of this, the typical values cited by Gustafson for k_1 and k_2 of 0.08 and 0.92 are not in agreement with the values of 0.3 and 0.7 published by Buller and Woodrow [29] and EPRI [46]. Clearly these discrepancies can give rise to significant errors in the loss values calculated using these coefficients.

4. The use of fixed diversity factors when aggregating loads can potentially lead to errors when studying loading conditions other than the system annual maximum demand.

5. Fixed tariffs and simple time-of-day tariffs can be applied by performing the analysis for each time band in the tariff. More complex time-varying tariffs cannot accurately be applied.

2.2.1.5 Discussion

The benefits of the single case approach are its speed, simplicity and low data requirements. It requires engineering judgement in the selection of loading conditions at which to run the analysis, but is capable of providing adequate information concerning the limits of system operation. However, the simplicity of the approach is achieved at the expense of modelling accuracy.

2.2.2 Multiple Case Duration Curve Approach

2.2.2.1 Description of the Approach

This approach models the time-varying nature of loads on the system using load duration curves. Load duration curves present the demand measurements, recorded normally at half-hourly or hourly intervals, in decreasing order of magnitude rather than in chronological order. The resulting curves provide information concerning how long a given load exceeds any particular level. Figure 2.2 illustrates the load duration curve derived from the demand data for a typical winter weekday shown in Figure 2.1 for three types of consumer.

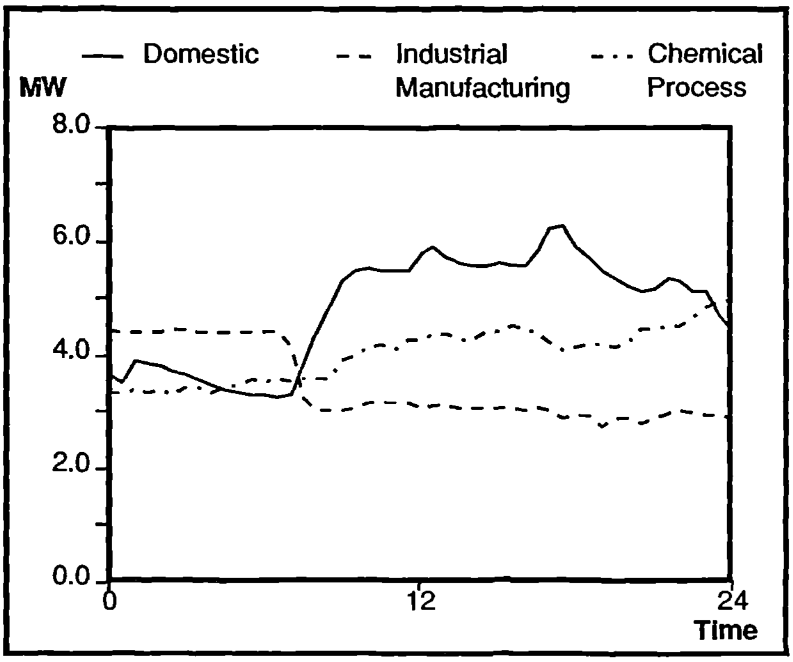

Figure 2.1 Chronological Load Curves for Three Consumer Types

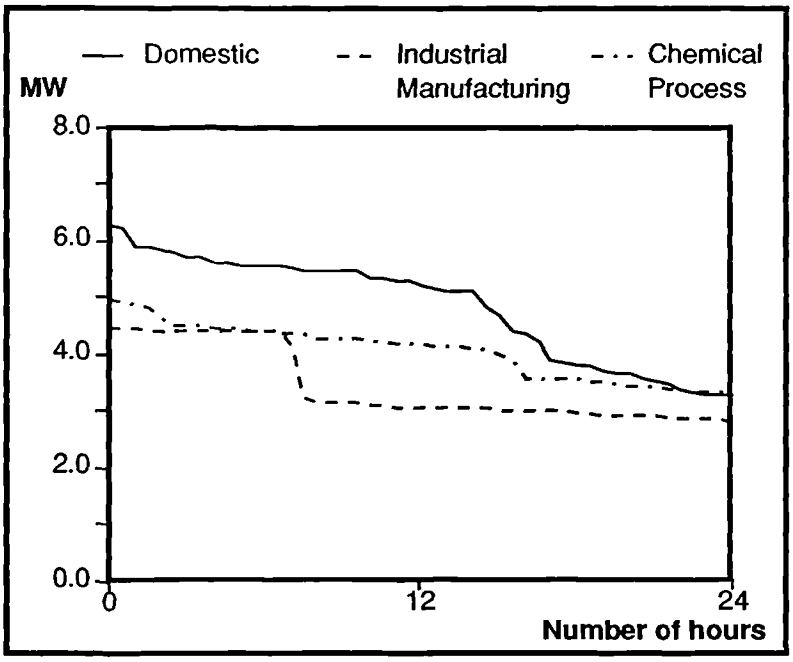

Figure 2.2 Load Duration Curves for Three Consumer Types

The method of Sun et al. [138] is perhaps the best known example of this approach. The general approach has also been adopted by EPRI for the calculation of transmission system losses [44]. The procedure is as follows:

1. A set of typical daily load curves for different days of the week and seasons of the year is compiled for each load in the system from measurements and load research data.

2. A set of load duration curves is derived from the typical daily curves for each load.

3. Each load duration curve is approximated by a number of discrete load levels, as illustrated in Figure 2.3. Load-flow (and other power system analysis) studies are conducted at each of these levels to provide results for the full range of system operating conditions, for each of the typical days included in the study. In the example shown in Figure 2.3 seven discrete levels have been used to approximate the duration curve, requiring seven load-flow solutions.

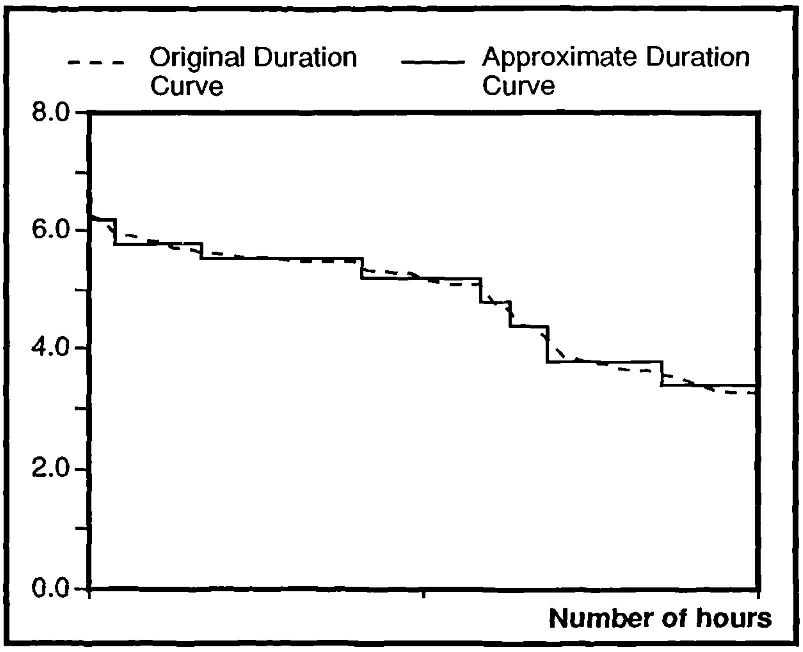

Figure 2.3 Approximation of a Load Duration Curve

By integrating the results for power flow and losses, the total number of units of power and loss for each of the typical days can be determined. Values for energy flows and losses over the simulation period can be obtained by summing daily totals corresponding to the appropriate day types.

2.2.2.2 Data Requirements

In addition to the plant data required to run any load-flow study, the Multiple Case Duration Curve approach requires running configurations for each of the typical days studied. Loading data must be specified for each discrete level in each of the duration curves used. Assuming N_{Day} typical days, and N_{Level} discrete levels for each duration curve the loading data requirements are

$$\text{Loading data} = 2N_{Day}N_{Level}(n_D + n_G) \times 4 \text{ Bytes}$$

2.2.2.3 Computational Requirements

The computational requirements for the approach are moderate, and depend upon the number of typical days used, and the number of discrete levels used to approximate each duration curve. The number of load-flow solutions required is given by

$$\text{Number of load flows} = N_{Day}N_{Level}$$

In the method of Sun et al. [138] six daily curves were used, and approximately six levels were used to approximate each curve, resulting in 36 load-flow solutions for each of the systems modelled.

2.2.2.4 Modelling Accuracy

Compared with the Single Case approach the Duration Curve approach provides improved modelling of time-varying loads in two respects:

1. The use of a collection of curves covering different day types and seasons of the year captures more accurately the diversity of different types of load. For example the significant differences in the demand patterns of many industrial loads on weekdays and weekends can be accounted for more accurately.

2. The use of duration curves incorporates to some extent the load factors of the individual loads, permitting greater accuracy in the calculation of energy flows and losses over a period of time.

However, the use of duration curves, instead of chronological load curves, carries with it the implicit assumption that all loads in the study conform; that is, the demand patterns for all the loads have the same shape. The demand of every load on the system is assumed to be a fixed proportion of the total load on the system. This assumption fails to hold in many cases, particularly when modelling industrial loads with widely differing demand patterns. The result is a subsequent reduction in modelling accuracy.

In addition, the use of a small number of representative curves to model the behaviour of a system throughout the year assumes that the demand patterns of the loads in the system are predictable and follow a repetitive cycle. Loads whose demand patterns are erratic and unpredictable, and therefore cannot be represented by a small number of typical curves, are not handled well by this approach.

It should also be noted that because the chronological sequence of load changes is not retained, time-varying tariffs can only be applied correctly to duration curve results if the results profile and the tariff conform. Only under these conditions can a tariff be converted to duration form and applied correctly. When applying a volatile tariff such as the UK Pool Selling Price, or in networks supplying diverse loads such an assumption is likely to be rendered invalid, and this must be recognised as a disadvantage of the method when used to calculate the costs of energy.

2.2.2.5 Discussion

The Multiple Case Duration Curve approach provides improved accuracy over the Single Case approach, and is an efficient way to study the range of system operating conditions, and for calculating energy flows and losses.

The implicit assumption that individual load profiles conform, and that the profiles follow a predictable, repetitive cycle can fail to hold, particularly in the case of industrial loads, with subsequent loss of accuracy.

2.2.3 Multiple Case Chronological Approach

2.2.3.1 Description of the Approach

The Multiple Case Chronological approach represents the variation of system conditions with time using a set of typical daily demand curves for each load on the system. The minimum number of curves required for a year's study is typically six: weekday and weekend curves for winter, summer and shoulder seasons. Unlike the Duration Curve approach the load-flow analysis is performed chronologically across each of these typical days, at hourly or half-hourly intervals.

The results of the analysis cover typical system operating conditions for different types of day, from which planning and design studies can be performed. By integrating power flow and loss results over each of the daily curves, energy flow and loss figures can be derived for each typical day studied. The daily totals can be summed to give totals for the complete study period.

An example of this approach is the method of Broadwater et al. [25], in which the analysis is performed at hourly intervals across nine typical daily curves: weekday, weekend and one other day type (not specified) for summer, winter and shoulder seasons.

2.2.3.2 Data Requirements

In addition to the plant data required to run any load-flow study, the Multiple Case Chronological approach requires running configurations for each of the typical days studied. Loading data must be specified for each time step of each typical daily curve used. Assuming N_{Day} typical days, and N_{Step} steps per day the loading data requirements are

$$\text{Loading data} = 2N_{Day}N_{Step}(n_D + n_G) \times 4\text{ Bytes}$$

2.2.3.3 Computational Requirements

The computational requirements for the approach are significantly greater than the Duration Curve approach, due to the chronological modelling of each of the typical daily curves. The number of load-flow solutions required is given by

$$\text{Number of load flows} = N_{Day}N_{Step}$$

In the method of Broadwater et al. [25] nine daily curves were used, and the analysis conducted at hourly step intervals, resulting in 216 solutions for each of the systems modelled.

2.2.3.4 Modelling Accuracy

By retaining the chronological information concerning the variation of individual loads on the system, a much more accurate picture of the behaviour of the system can be obtained than is possible using Single Case or Duration Curve approaches. Loads whose peak and off-peak demands do not coincide can be modelled comparatively accurately.

In spite of the improvement in accuracy over the previous methods, the chronological approach described here relies on the assumption that the demand patterns for individual loads modelled on the system are predictable and follow a repetitive pattern. If the annual demand pattern for a given load cannot be represented by a small number of daily curves, this method will be prone to significant inaccuracy.

The method accommodates the use of fixed time-of-day tariffs to calculate the costs of energy for different typical days. The method does not support the use of continuously varying tariffs such as the UK Pool Price.

2.2.3.5 Discussion

The Multiple Case Chronological approach achieves higher levels of modelling accuracy than the preceding approaches, particularly in the case of non-conforming industrial loads. This is at the expense of computation and data requirements, typically several times greater than those of the Duration Curve Approach.

The approach is subject to inaccuracy in the case of loads whose demand profiles do not follow a repetitive pattern for each type of day modelled. The success of the method is therefore dependent upon the presence of 'well-behaved' loads on the system under study.

2.3 Probabilistic Approaches

Probabilistic approaches model the uncertainty in the data used in the load-flow analysis in order to provide information concerning the likelihood of the occurrence of a given set of operating conditions. Probabilistic approaches to this problem generally belong to two categories: Probabilistic Load-flow (PLF) analysis and Monte Carlo Simulation.

2.3.1 Probabilistic Load-flow Analysis

In probabilistic load-flow analysis the load and generation values which comprise the input data to the load-flow are considered as random variables, as are the resulting voltages and angles. In addition, since plant in the system can fail, plant availabilities can also be considered as random variables. The objective of probabilistic load-flow analysis is to obtain the probability density functions (PDFs) of the voltages and angles within the system, given a probabilistic description of load and generation values (Borkowska [157]). The problem consists of two parts:

2.3.1.1 Determining Probability Density Functions for the Input Variables

Load and generation levels, and system configuration are random variables which in general are not independent (Allan [1], Anders [5], Leite da Silva et al [83, 84]), and need therefore to be described by a joint probability density function. Such a task may not be feasible, due to a lack of statistical data relating these variables. In practice network configuration is considered independent of load and generation levels, and the analysis is carried out either for a number of network configurations with the network topology considered fixed for each configuration [84], or with network configurations considered as independent discrete random variables and included in the analysis.

The remaining problem of defining the interdependence of load and generation levels may still be infeasible due to lack of data, and these variables are often considered as independent as well. However, load levels at different nodes in the system have been found to be highly correlated [83] and cannot in general be considered as independent.

Perhaps the most awkward problem to overcome in calculating probability density functions for the load and generation values is deriving a realistic model of the 'dispatching law'. The dispatching law determines how imbalances in load and generation are eliminated. For example, a shortage of generation may be made up solely by the slack bus. Alternatively the outputs of specific generators within the system may be increased in a. predetermined manner. Although a number of attempts have been made to solve this problem [5], further work is required to provide satisfactory, practical techniques.

2.3.1.2 Calculating Values and Probability Density Functions for the State Vector

Having obtained the PDFs of the input variables (the load and generation values), the PDFs of the voltages and angles (the state vector) need to be derived from these values and from the network equations. Deterministic load-flow algorithms rely upon iterative numerical techniques to solve the resulting non-linear equations. To obtain the PDFs of the state vector requires expressing these values as linear combinations of the input variables. To achieve this the load-flow equations must be linearised about the expected values of P and Q. The state vector can then be represented as a linear combination of the input variables, and the PDFs of the desired variables can be obtained via convolution (Allan et al. [2])

Three linearised formulations of the load-flow have been used: the dc load-flow, the ac decoupled formulation and the ac coupled formulation. Work by Allan et al. [2], and Anders [5] has shown that these three methods give comparable results when used to calculate active power flows and voltage angles and their associated PDFs (the P-θ problem), but that they vary greatly in accuracy when used to calculate reactive power flows and voltage magnitudes and their associated PDFs (the Q-V problem). This is due to the greater nonlinearity of the Q-V problem.

To account for the time-varying nature of system load and generation levels PLF analysis can be combined with the multiple case duration curve or chronological approaches outlined in Sections 2.2.2 and 2.2.3, in which the analysis is performed for a number of operating conditions.

2.3.1.3 Discussion

The advantages offered by Probabilistic Load-flow methods are attractive. Probability Density Functions of the load-flow results can be used to assess the likelihood of specified conditions occurring on the system, information which can be highly beneficial in certain, but not all, types of planning study.

A number of practical problems have restricted the use of these methods, particularly at the distribution level:

- The linearisation of the load-flow equations can lead to errors, particularly with reactive power and voltage magnitude results, and in the case of large variances in the input variables.
- The modelling of rules concerning the dispatch of power to maintain the balance between load and generation has not been completely resolved.
- Another difficulty concerns the acquisition of probabilistic data of sufficient quality to justify the use of probabilistic techniques. The modelling of the interdependence between individual loads, and between load, generation and network configuration presents a formidable problem. The assumptions made to circumvent this problem can compromise the reliability of the results.

In conclusion, further development of these techniques, and improvements in the quantity and quality of data from the system are needed before a probabilistic load-flow approach can be fully justified for the proposed load-flow analysis approach for distribution systems.

2.3.2 Monte Carlo Simulation

The PLF approach is an analytical method; the load-flow equations were solved explicitly to obtain the solution. The Monte Carlo Simulation approach involves a number of repeated simulation studies, each one using values for the random input variables generated using their respective probability distributions. As such it is not an analytical method. The results of all of these samples can be used to derive probability density functions for the state vector. Because the simulations themselves are deterministic, the simplifying assumptions that are required for the solution of load-flow equations in the PLF approach are not necessary, with the result that the system can be modelled more accurately [2].

Monte Carlo Simulation methods consist of three steps: generation of the random input variables, simulation of the system, and accumulation and statistical analysis of the results. The first two steps are performed repeatedly, enough times to reduce the variance of the state vector sufficiently to achieve a specified confidence level in the expected values.

2.3.2.1 Generation of Values for Random Input Variables

The load and generation levels and network configuration are considered as random variables, whose probability density functions are known. Joint density functions can be accommodated if the data is available, without greatly increasing the complexity of the method. This contrasts with the PLF methods in which random variables normally have to be considered as independent to reduce the complexity of the method.

To account for the time-varying nature of system load and generation levels Monte Carlo simulation can be used in conjunction with the multiple case duration curve or chronological approaches outlined in Sections 2.2.2 and 2.2.3. Perhaps the most suitable method is to derive PDFs on an hourly or half hourly basis, from daily profiles of loads and generators taken from SCADA and load research data, and to perform 24 hour simulations for different types of day.

The method requires generation of a number of appropriate values for the random variables which correspond to their PDFs. This is achieved through the use of a pseudo-random number generator to generate numbers uniformly distributed between 0 and 1, and then by evaluating the inverses of the appropriate PDF (or joint density function) at those levels.

2.3.2.2 Simulation of the System

Monte Carlo methods use the same simulation models as are used in deterministic analysis. In the case of load-flow based distribution system analysis is concerned, standard ac load-flow algorithms can be used. However, to improve computational efficiency linearised ac load-flows can be used (Allan et al. [2]).

2.3.2.3 Analysis of the results

The results from the Monte Carlo simulations can be treated as samples of experimental observations, and the normal methods of statistical analysis apply. The accuracy of the results depends upon the number of simulation studies performed: the error in the estimation of the mean of the sample values is inversely proportional to the square root of the sample size (Siddall [129]). In practice large numbers of simulations are required to reach convergence to acceptable levels of error.

Variance reduction techniques have been applied in certain cases to reduce the number of required samples with some success. An example is the use of a control variable together with stratified sampling by Breipohl et al [23] to reduce the number of samples in chronological production simulation from approximately 10000 to 10. Examples of such methods applied to load-flow analysis in distribution systems have not been reported.

2.3.2.4 Discussion

Monte Carlo Simulation approaches for load-flow based distribution system planning are relatively simple to implement, in comparison with PLF methods. They do not contain the simplifying approximations in the modelling of the network which are required in the PLF approaches. In addition, they are able to handle dependent random variables.

The greatest problem associated with Monte Carlo simulation is the large numbers of simulations required to achieve convergence to practical levels of accuracy. The corresponding computational overhead can become prohibitively large, particularly in the case of load-flow solutions on large distribution networks. Variance reduction techniques have been applied to certain power system problems to reduce the required number of simulations.

In common with PLF methods, Monte Carlo simulation is subject to the problem of evaluating joint probability density functions for the random input variables.

2.4 The Proposed Load-flow Analysis Approach - Discrete Time Simulation

2.4.1 Description of the Approach

The load-flow analysis approach adopted for this work is a chronological, multiple case method in which load-flows are conducted at regular intervals across the entire period of interest. In this respect it differs from the methods described in the preceding sections which build up a picture of the behaviour of the system from a number of typical operating conditions. Simulation periods vary according to the planning function, from a day to perhaps a year at half-hourly steps. Long term studies might extend far beyond this, but use longer step intervals.

All the results derived from the load-flow simulation are time related, and provide the planning engineer with a clear picture of the behaviour of the system as a function of time [89]. Simple analysis of the data yields the maximum and minimum values of load, voltage, loss and other parameters in any part of the system over the specified time period. Figures for energy flow and loss in the system can be obtained directly by integrating the respective spot values over the period.

2.4.2 Data Requirements

In addition to the plant data required to run any load-flow study, the proposed discrete time simulation method requires load and generation profiles, recorded at regular intervals over the time period of interest, for every load and generator in the system under study. If the total number of discrete time steps is N_{TStep} the loading data requirements are given by

$$\text{Loading Data} = 2N_{TStep}(n_D + n_G) \times 4 \text{ Bytes}$$

Clearly this represents a large volume of data, not all of which may be available. Techniques for handling this data and for providing estimates in the absence of a full set of data are described in Chapter 5. Section 2.5.4 gives memory requirements for simulations of different length on a selection of networks.

2.4.3 Computational Requirements

The computational requirements of the approach depend upon the length of the simulation period, and can become large for lengthy simulations. The number of load-flow solutions is given by

$$\text{Number of load flows} = N_{TStep}$$

A full year's simulation at hourly steps therefore implies 8760 load-flow solutions. Section 2.5.4 gives execution times for simulations on different systems on a variety of hardware.

2.4.4 Modelling Accuracy

The proposed Discrete Time Simulation approach achieves the highest level of modelling accuracy by performing chronological analysis over the entire study period. The diversity of individual demand profiles on the system can be accounted for without the simplifying assumptions concerning demand patterns made in the alternative approaches. As a result, industrial loads whose demand profiles are erratic and unpredictable, being heavily dependent upon different industrial processes, can be modelled accurately [91].

All standard types of tariff, including the continuously varying UK Pool Price tariff, can be applied at both the system level and for individual network components to give the costs of energy and losses over the study period.

2.4.5 Discussion

The proposed Discrete Time Simulation approach provides the most detailed, and potentially most accurate, picture of the state of the system of all the approaches outlined. One of the most important aspects of this is the ability of the approach to study the changing behaviour of the system with time, as individual load and generation patterns change. This feature is common to the alternative multiple case approaches, but only partially due to their use of a small number of typical days.

Better knowledge of the system as a function of time allows planning engineers to make decisions with greater confidence, and to achieve greater utilisation of the system without compromising security.

The costs of achieving the high levels of modelling accuracy are the greatly increased storage and computational requirements of the proposed approach. In previous years, these requirements have precluded the use of the approach at the distribution level. However, the rapid increase in power of the latest workstations, and the falling cost of disk and RAM based storage, mean that the proposed approach is now feasible when combined with techniques for minimising storage and maximising computational efficiency.

2.5 Test Results

2.5.1 Test Objectives

The approaches described in the preceding sections employ different techniques to model the changing state of the distribution system as a function of time. Inevitably there is a conflict between achieving high levels of modelling accuracy and minimising data requirements and execution times. In this section the results of tests are given which attempt to quantify these factors for a range of typical distribution system configurations.

The first series of tests compare the use of full chronological loading data, load curves derived from typical daily profiles, and load duration curves derived from typical daily profiles, and assess the accuracy of calculated results for energy losses and system utilisation levels.

It is important to note that in these tests a unique set of typical daily curves is derived for each load and generator from actual metered data. In practice it is unlikely that unique curves would be derived for each load or generator. Instead, a collection of typical curves corresponding to the more important types or classes of consumer would be derived from load research data. Typical curves would be assigned to individual loads and generators using the closest consumer type category. The tests conducted here therefore represent the best performance obtainable from approaches based upon typical curves.

In the second series of tests, the execution times of the approaches are compared on each of the distribution test networks.

The final series of tests compare the storage requirements for the simulation of a year at half hour steps on each test network.

2.5.2 Test Networks

The distribution networks used in the tests are summarised in Table 2.1. These networks are described in more detail in Appendix E. The systems have been chosen to provide a combination of configurations and load types which reflects the range typically found in distribution companies in the United Kingdom. The 15 node system can be considered typical of systems serving residential areas, where individual load diversity is very small. The 10 node system represents the opposite end of the spectrum, serving a mixture of highly diverse industrial loads. The 348 node system is a complete distribution system down to 33kV with selected 11kV feeders. Discussions with REC operations and planning engineers have indicated that load-flow studies are normally carried out on small portions of the system, rarely exceeding a few hundred nodes.

Table 2.1 Load-flow Analysis Approach Test Systems

No. of Nodes	Real System	Voltage levels	Loading Data	Remarks
7	✓	66-20kV	12 months	Radial primary feeder serving a mixture of rural and industrial loads
10	✓	66-11kV	6 months Jan - June	Radial primary feeder with a mixture of domestic and non-conforming industrial loads
15	✓	132-11kV	12 months	Interconnected system serving mainly conforming domestic loads
348	✓	400-11kV	1 month January	Complete distribution network down to 33kV with selected 11kV feeders, serving a largely domestic load

2.5.3 Test 1. Comparison of Simulation Results for Three Analysis Approaches

In this test the proposed Discrete Time Simulation approach is used as a reference, against which two other deterministic approaches are compared.

2.5.3.1 Test Procedure

The test procedure used three approaches to simulate the performance of each test system at half hour steps over an extended period.

1. Discrete Time Simulation

   Full time-based load and generation data from metering and SCADA systems was used. From the simulation results the following values were calculated:

   a) Line loading. For each line in the system the MVA power flow at the sending end was determined at each time step, and the maximum, average and minimum loadings for each line were calculated.

   b) Demand losses, P_L. The detailed loss calculation algorithm described in Chapter 7 was used to determine the demand loss in every line and transformer in the system at each time step.

2. Multiple Case Chronological Simulation.

   A simulation was performed over the same period, in which the load and generation data was derived from a number of 'typical' daily curves. These curves were derived as follows:

a) Nine typical day types were used to model each load and generation pattern over the year: Weekday, Saturday and Sunday curves for Summer, Winter and Shoulder seasons. This follows the method of Broadwater et al [25].

b) For each load and generator the time based profile data used in Approach 1 was used to derive typical daily curves for each of the nine day types using the following method:

   i. For each day type, an average daily curve was derived by identifying all occurrences of the day type in the year's data, summing the individual half hour values for each occurrence, and dividing the total sum by the number of occurrences.

   ii. For each day type, a typical daily curve was obtained by calculating the Euclidean Distance between each day in the year's data and the relevant average daily curve derived in i. The day with the minimum Euclidean Distance was chosen as the typical curve for that day type.

c) For each day of the simulation period the data for each load and generator was derived by selecting the appropriate typical daily curve. A list of bank holiday dates for the year in question was included, and the standard practice of treating these as Sundays in the analysis was adopted.

Once the discrete time simulation was completed the line loadings and demand losses were calculated as before.

3. Multiple Case Duration Curve Simulation
   A simulation was performed over the same period. The load and generation data was derived as in the previous case, with the exception that duration curves were derived from each of the nine typical daily curves for each load and generator. Six load-flow solutions were performed across each duration curve instead of the 48 solutions performed in the previous case. This follows the method of Sun et al. [138] and EPRI [44].

   The system line loadings and demand losses were calculated as before. When assessing these results in the light of values from the discrete time simulation approach, the discrete time simulation results were first rearranged into duration curves for each day of the simulation period, to provide a basis for the comparison.

2.5.3.2 Test Results - Graphical Analysis of Simulation Input Data and Derived Results

Before conducting a quantitative analysis of the three approaches it is instructive to study samples of input data and results for different categories of load.

Figures 2.4 to 2.6 compare data from actual chronological measurements with data derived from typical daily curves over a period of four days in February for three loads: a 66kV domestic feeder, a mineral ore extraction and processing plant supplied at 11kV, and a chemical processing plant also supplied at 11kV. Three typical day-types were used to cover the four day period: winter Saturday, winter Sunday and winter weekday.

In each figure the first graph compares the MW demand data for the relevant load. This represents the input data to the simulation. The second graph compares the allocated MW losses for the load. Given the demand profiles from actual data and typical days the figure shows the proportion of system losses assigned to each load using the loss allocation algorithm described in Chapter 9. The allocation was performed on the basis of demand. The third graph applies a time-varying tariff to the allocated losses to give the respective costs of losses over the sample period. The tariff used was the half-hourly UK Pool Selling Price for the year 1992/93.

Figures 2.7 to 2.9 repeat the comparison using approximate duration curves in place of the typical chronological curves, as detailed above. It is important to note that in order to apply the time-varying tariff to loss duration curves it was necessary to assume that the loss profiles and the tariff conform. Only in such circumstances can such a tariff be converted to duration form and applied correctly to determine the costs of losses.

From the figures the following observations can be made:

1. It is clear from the Figure 2.4 that the domestic profile is approximated reasonably well using typical days. In the case of demand profiles typical day values for individual half hours lie within 20% of the actual values throughout the sample period, and the area under the two profiles differs by less than 1.5%.

   It can be seen that in the case of allocated losses the half-hourly discrepancies are exaggerated slightly. This is also reflected in the areas under the curves, which now differ by 5.8%. The application of a time-based tariff increases the discrepancies a little further: integration of the curves leads to a difference of 5.9% over the period.

2. Figure 2.5 shows that the approximation of the actual data using typical days is less successful in the case of mineral extraction plant than for the domestic load. In the graph of demand profiles typical day values differ from actual values by as much as 300% for certain half hours, and the area under the two profiles differs by approximately 15%. The figure indicates that the use of a single day-type to model weekdays during winter gives rise to substantial errors in this case because the Monday demand pattern differs appreciably from that of the Tuesday. Further analysis of the demand data for the rest of the winter season indicates that the demand patterns for the remaining weekdays are relatively close to the Tuesday pattern. Another source of error in the approximation of

this demand profile is the change in working pattern which occurs late on the Saturday evening in the sample period.

As in the case of the domestic load the discrepancies between the actual and typical curves are greater when determining allocated losses, both in terms of the half-hourly variations and the areas under the curves. The energy losses derived from typical days are in error by 18.9% over the sample period. The error increases to 19.6% when the time-based tariff is applied.

3. Figure 2.6 illustrates the poor approximation afforded by the typical daily curves when the actual data is volatile and unpredictable. The demand profile of the chemical processing plant exhibits a slight repetitive pattern, particularly during the early hours of the morning, but is generally erratic. Differences between typical day values and actual values differ substantially over much of the sample period, and the area under the two demand profiles differs by approximately 14%. The errors for the corresponding allocated losses and cost of losses curves are 15.7% and 16.5% respectively.

4. The use of duration curves derived from typical daily curves to model the domestic demand profile in Figure 2.7 is marginally less accurate than the chronological case of Figure 2.4. The use of just six data points for each 24 hour period does not appear to compromise accuracy to a significant extent. The graphs of allocated losses and costs of losses follow the same trend as for the chronological case, with decreasing modelling accuracy.

5. It might be expected that for industrial loads with erratic demand profiles the use of duration curves, which neglect the time sequence of load changes, would lead to improved modelling of these profiles. This can be seen in the case of the mineral extraction plant in Figure 2.8 on the Sunday and Tuesday, where half hourly discrepancies are reduced compared with the chronological case. The major errors which occur on the Saturday evening and Monday are still evident, however.

6. Similarly, the poor modelling of the erratic profile of the chemical processing plant is not improved through the use of duration curves, as shown in Figure 2.9.

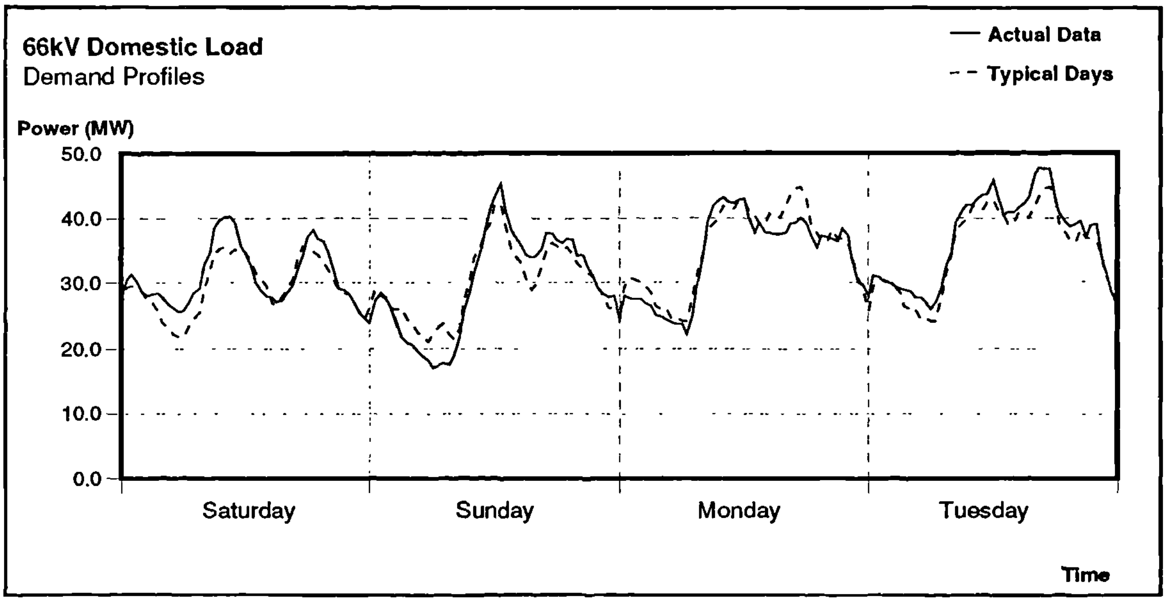

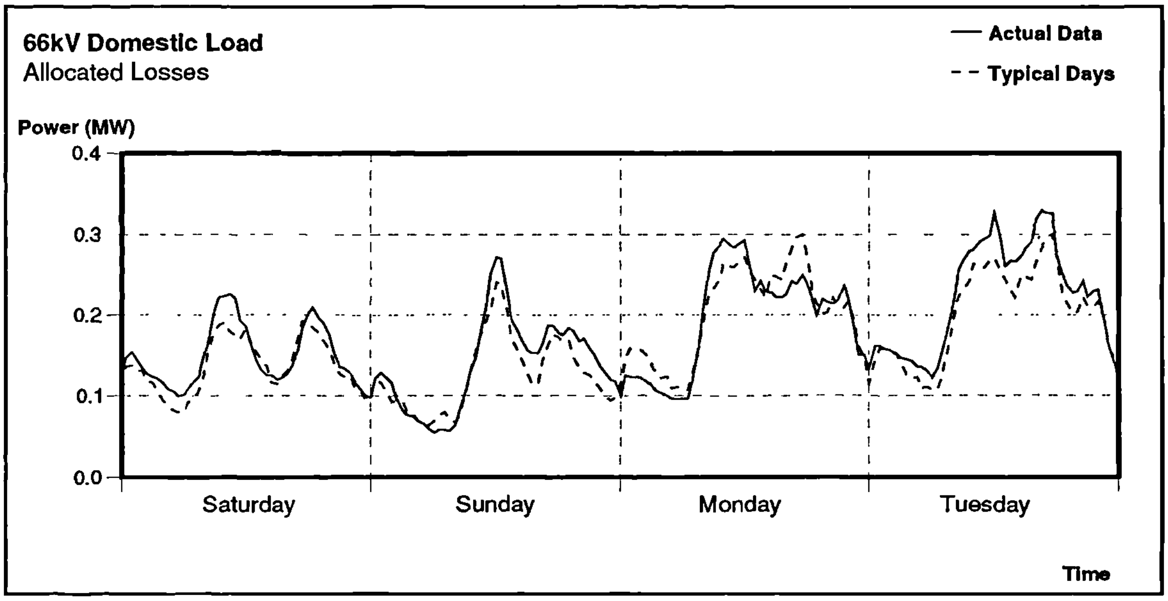

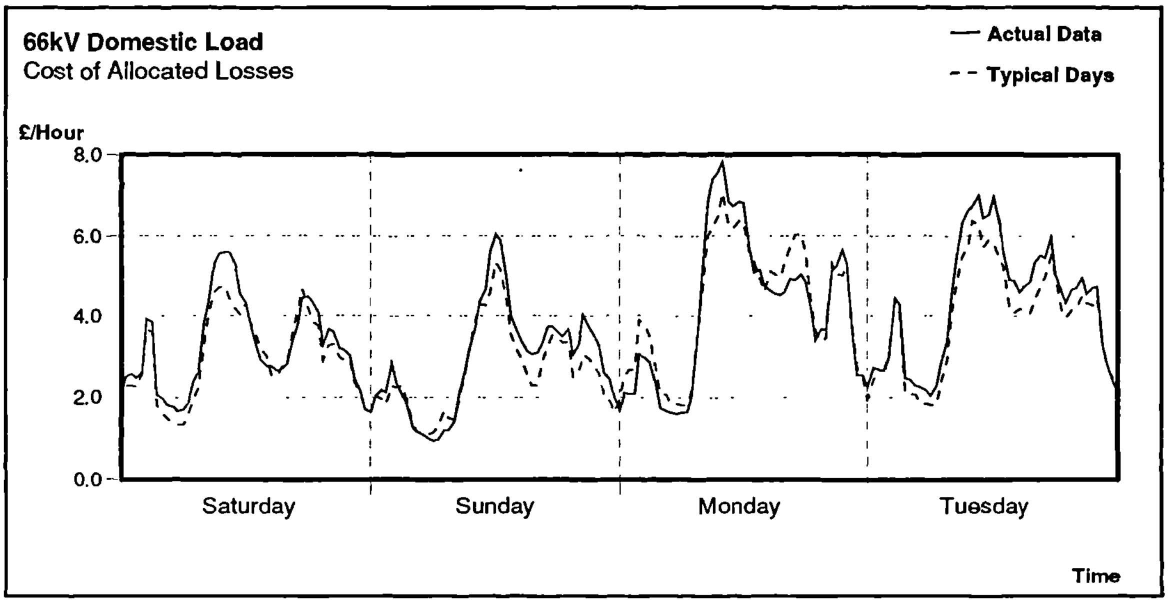

Figure 2.4 Actual Data and Typical Days for 66kV Domestic Load

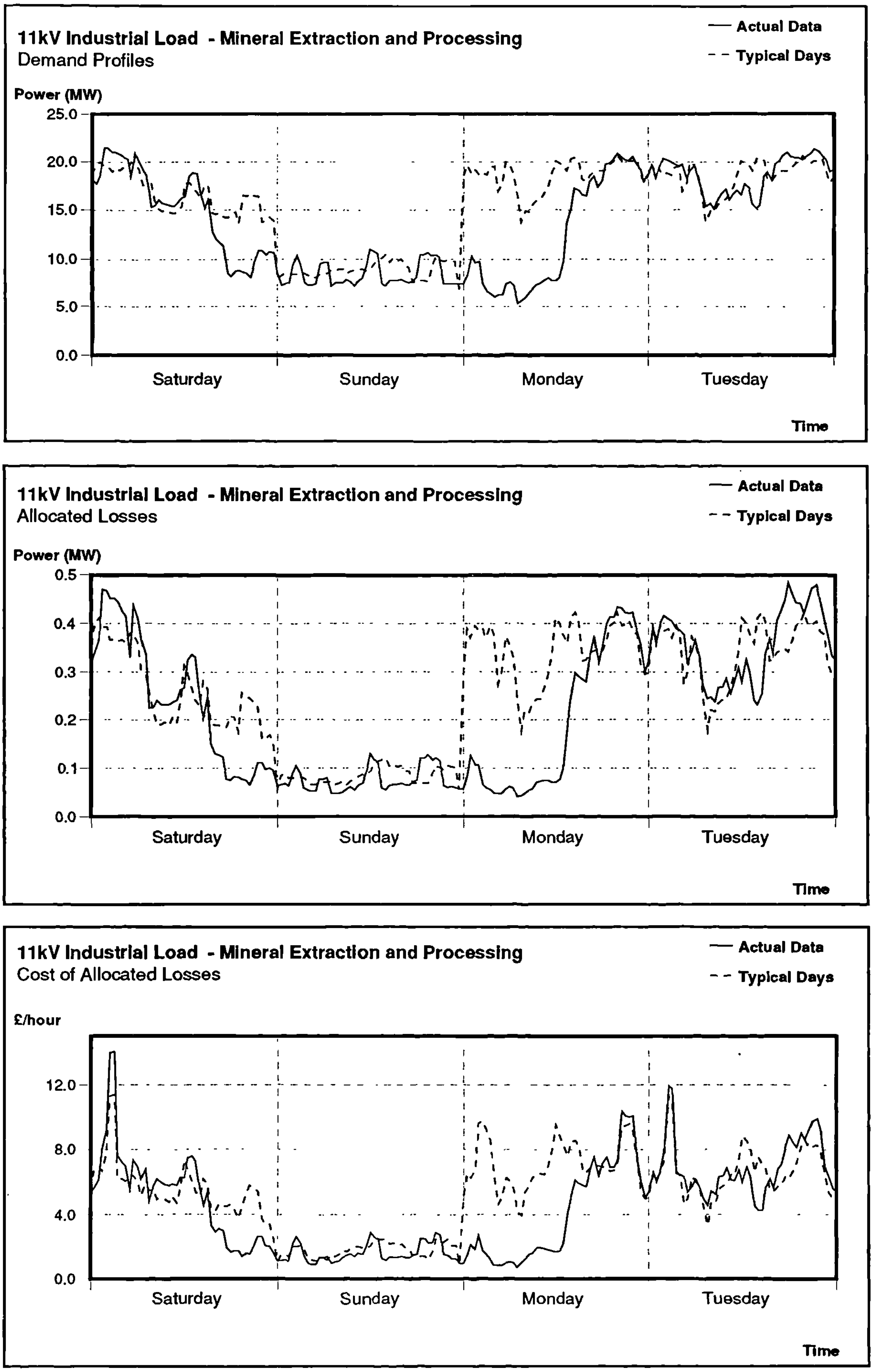

Figure 2.5 Actual Data and Typical Days for 11kV Mineral Extraction Plant

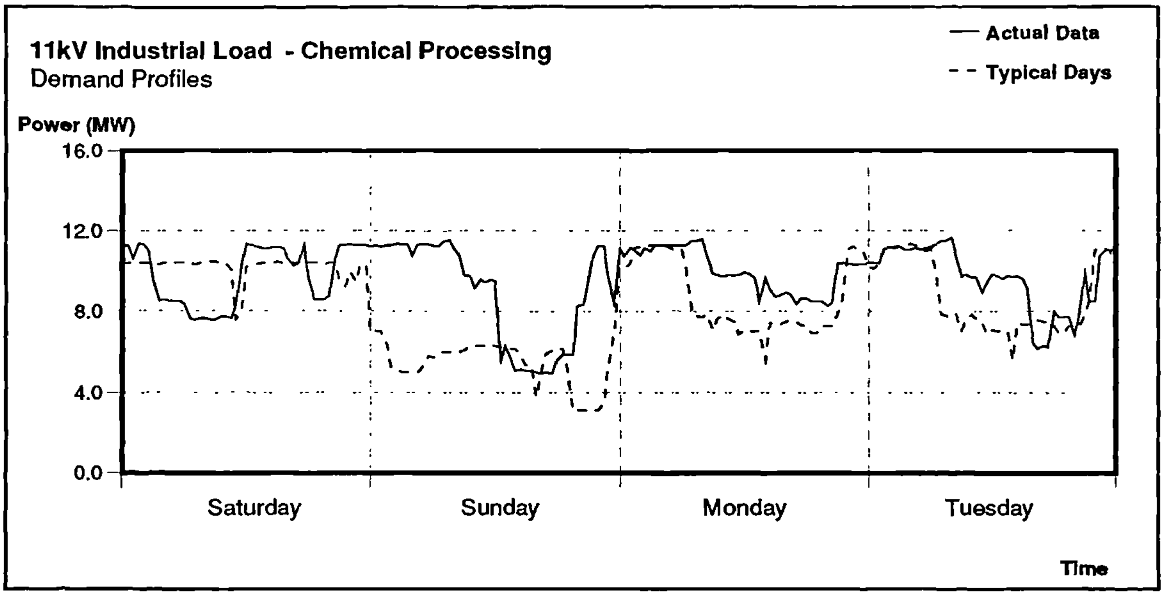

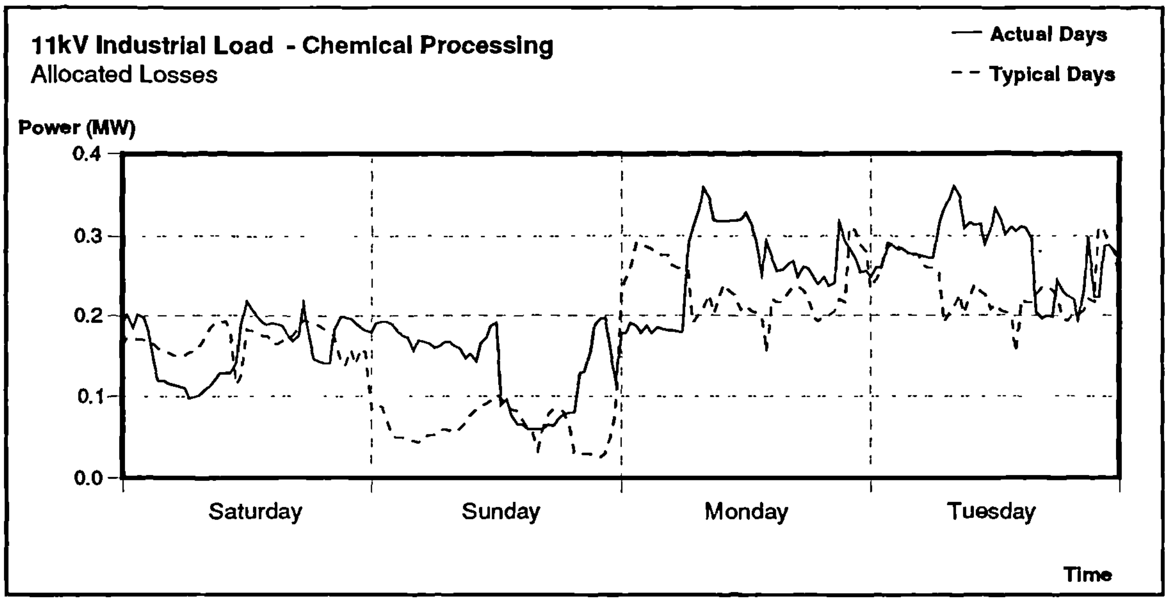

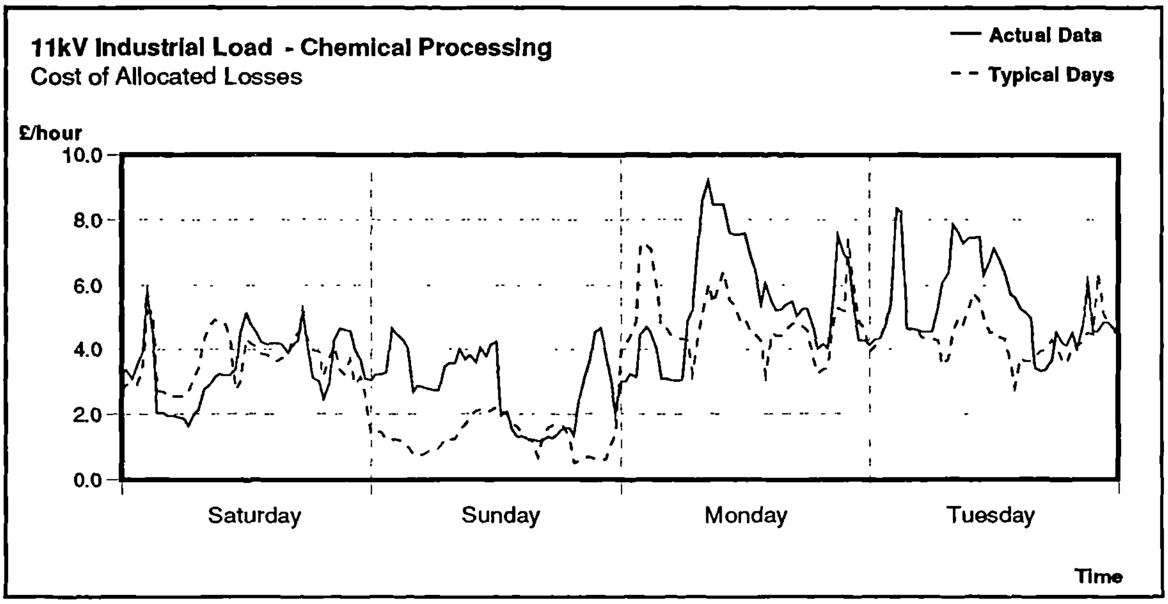

Figure 2.6 Actual Data and Typical Days for 11kV Chemical Processing Plant

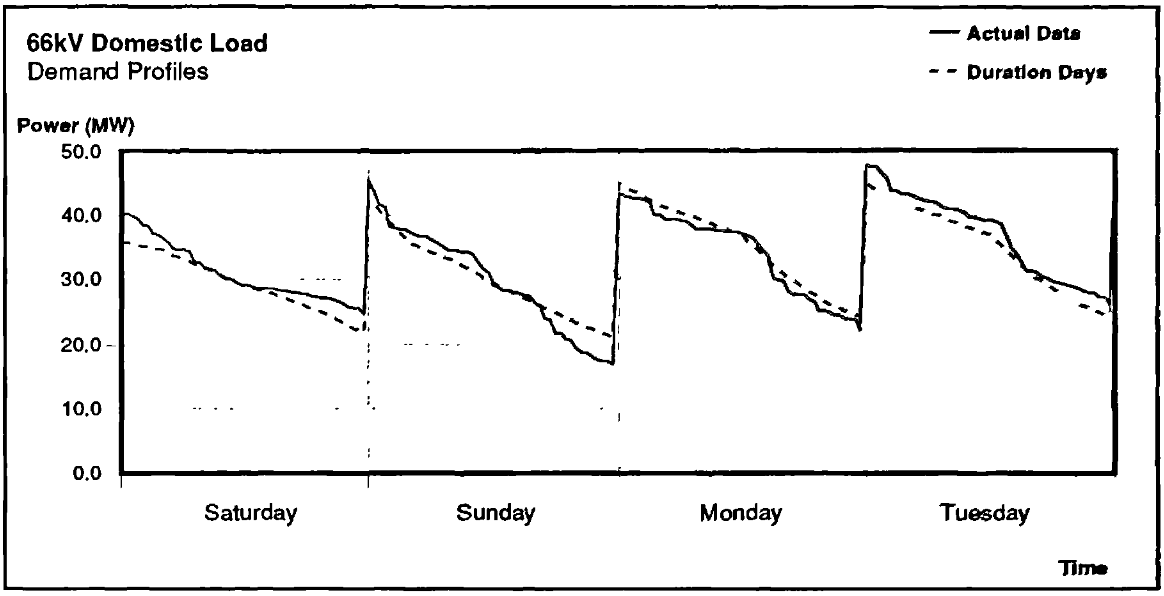

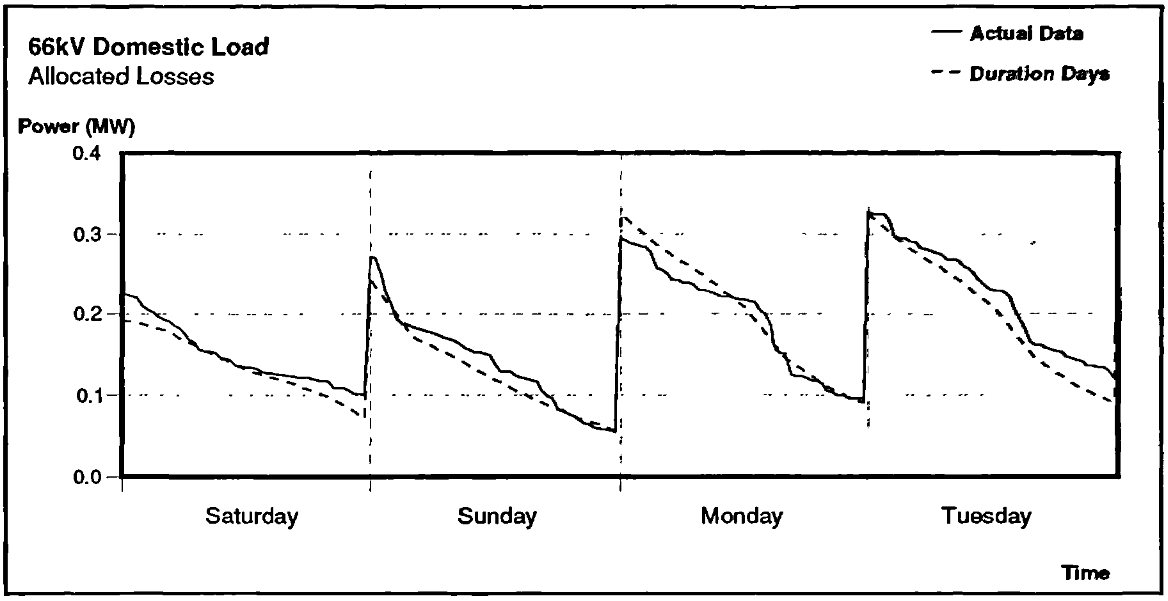

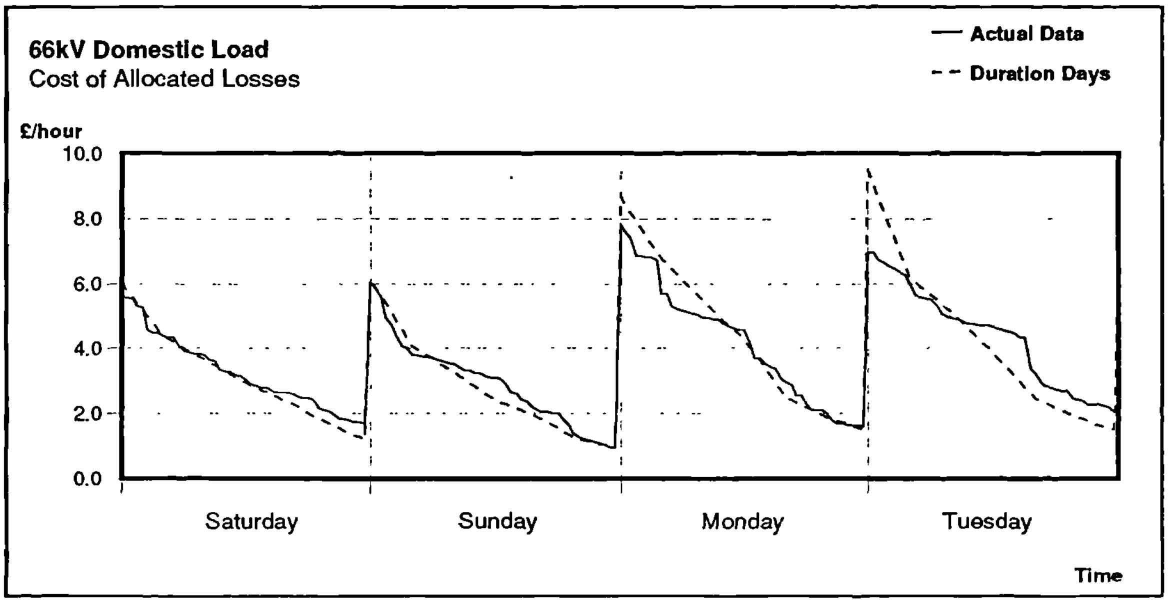

Figure 2.7 Actual Data and Duration Days for 66kV Domestic Load

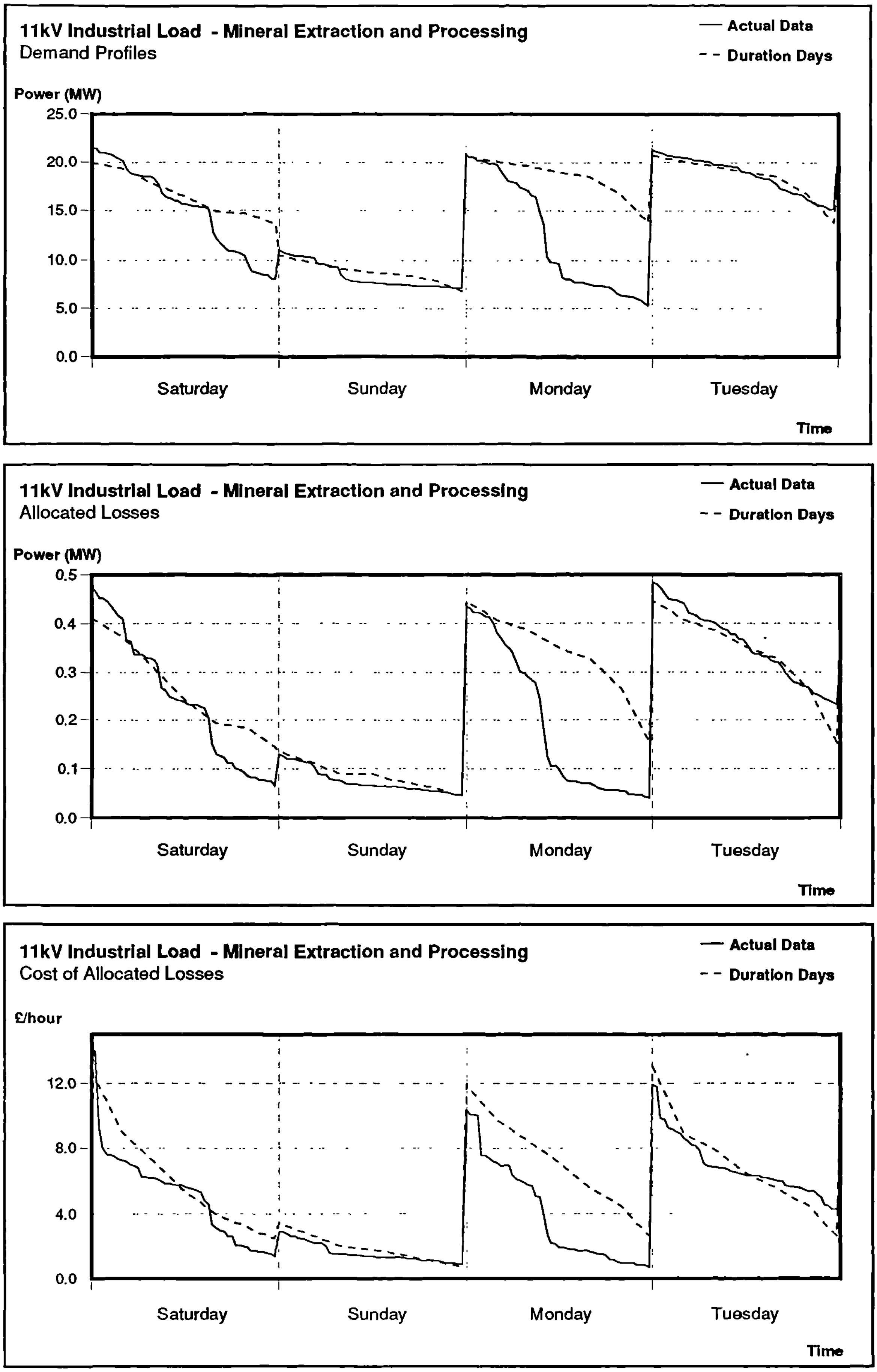

Figure 2.8 Actual Data and Duration Days for 11kV Mineral Extraction Plant

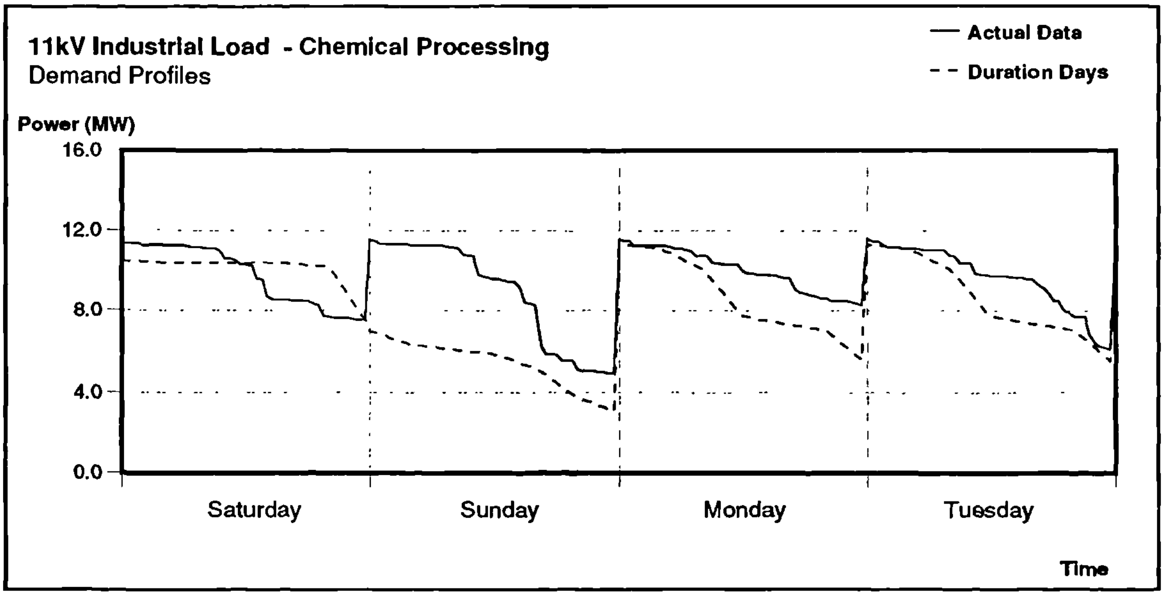

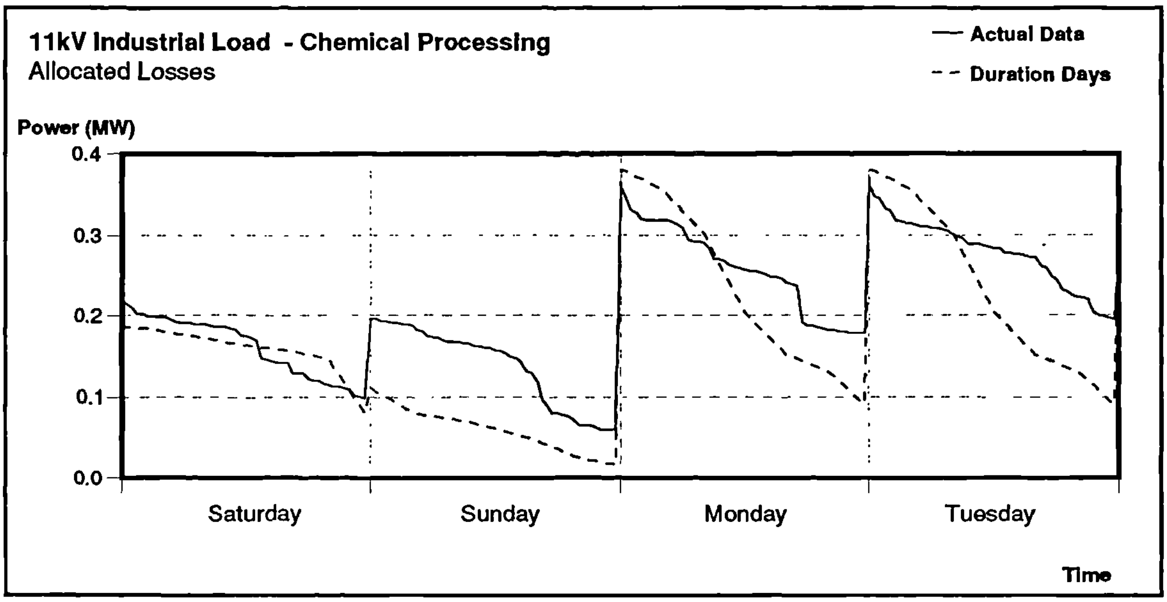

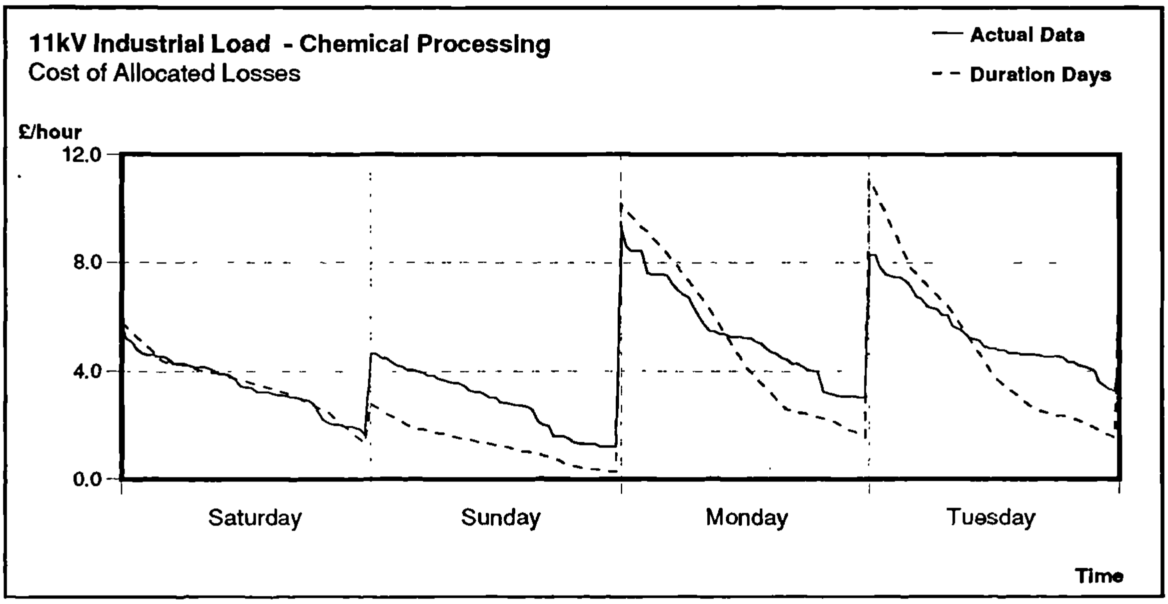

Figure 2.9 Actual Data and Duration Days for 11kV Chemical Processing Plant

2.5.3.3 Test Results - Statistical Analysis of Simulation Input Data and Results

Tables 2.2 to 2.4 provide summaries of comparisons of demand data, line loading results and line loss results for the three analysis approaches outlined above. Comprehensive results for each node and line are listed in Appendix B.

The tables list results summed over all plant in the system; for example demands summed over all the loads in the system. The first two results columns give system maximum and minimum values in MW. The third column gives energy values in GWh, which are derived by integrating the half-hour results over the study period.

The discrete time simulation approach is used as a reference against which the approaches based upon typical days are compared. The discrepancies are expressed as percentages of the reference values.

The final column in the tables lists the mean half hour deviations between the results for the typical days approaches and the reference results. For each item of plant in the system the mean deviations over the study period are calculated. These are summed over all items of plant and expressed as a percentage of the system mean reference value. For example, in the case of loss results, the mean deviation is calculated as shown in Equation (2-1).

$$\bar{d} = \frac{\sum_{i=1}^{n_B}\left[\sum_{t=1}^{N_{TStep}} \left|(P_{L,i}(t) - P_{Lref,i}(t))\right|\right]}{\sum_{i=1}^{n_B}\left[\sum_{t=1}^{N_{TStep}} P_{Lref,i}(t)\right]} \times 100 \qquad (2\text{-}1)$$

Table 2.2 Comparison of System Demand Results for Three Analysis Approaches

Test System	Simulation Type	Comparison with Discrete Time Simulation						
		System Demand			Errors			Deviation
		Demand Max (MW)	Demand Min (MW)	Energy (GWh)	Demand Max (%)	Demand Min (%)	Energy (%)	Mean Half hour (%)
7 Node	DTS	68.40	17.70	361.4				
	MC Chron	59.13	23.88	362.1	-13.5	34.9	0.2	13.3
	MC Dur	63.08	20.86	361.9	-7.8	17.8	0.1	11.7
10 Node	DTS	42.18	3.56	120.6				
	MC Chron	38.04	12.17	122.3	-9.8	241.8	1.4	20.3
	MC Dur	40.81	7.65	122.5	-3.2	114.9	1.5	17.7
15 Node	DTS	243.90	73.50	1316.8				
	MC Chron	215.20	79.10	1312.3	-11.8	7.6	-0.3	8.6
	MC Dur	221.70	78.30	1311.6	-9.1	6.5	-0.4	7.7
348 Node	DTS	6846.16	3812.20	3925.8				
	MC Chron	6326.02	3988.43	3821.7	-7.6	4.6	-2.7	3.5
	MC Dur	6366.62	3974.29	3821.7	-7.0	4.3	-2.7	3.1

Table 2.3 Comparison of System Line Load Results for Three Analysis Approaches

Test System	Simulation Type	Comparison with Discrete Time Simulation						
		System Line Loading			Errors			Deviation
		Loading Max (MW)	Loading Min (MW)	Energy (GWh)	Loading Max (%)	Loading Min (%)	Energy (%)	Mean Half hour (%)
7 Node	DTS	94.30	26.99	527.9				
	MC Chron	81.35	38.42	532.1	-13.7	42.3	0.8	10.1
	MC Dur	91.07	31.57	532.1	-3.4	17.0	0.8	9.8
10 Node	DTS	94.30	7.77	264.4				
	MC Chron	83.48	26.12	265.4	-11.5	236.2	0.4	18.3
	MC Dur	88.51	15.98	265.5	-6.1	105.7	0.4	16.2
15 Node	DTS	648.44	200.17	3499.6				
	MC Chron	569.06	215.59	3487.4	-12.2	7.7	-0.3	7.6
	MC Dur	586.67	213.51	3485.1	-9.5	6.7	-0.4	6.9
348 Node	DTS	31962.	23546.	19718.4				
	MC Chron	29568.	23683.	19444.8	-7.5	1.0	-1.4	3.3
	MC Dur	29706.	23087.	19445.5	-7.1	-1.9	-1.4	8.4

Table 2.4 Comparison of System Loss Results for Three Analysis Approaches

Test System	Simulation Type	Comparison with Discrete Time Simulation						
		System Loss			Errors			Deviation
		Demand Max (MW)	Demand Min (MW)	Energy (GWh)	Demand Max (%)	Demand Min (%)	Energy (%)	Mean Half hour (%)
7 Node	DTS	0.799	0.062	3.25				
	MC Chron	0.590	0.128	3.29	-26.2	105.1	1.3	21.3
	MC Dur	0.786	0.087	3.36	-1.7	39.8	3.2	20.7
10 Node	DTS	1.054	0.008	1.91				
	MC Chron	0.770	0.070	1.84	-26.9	775.0	-3.6	29.8
	MC Dur	0.851	0.029	1.85	-23.9	262.5	-3.2	25.8
15 Node	DTS	4.737	0.439	16.16				
	MC Chron	3.724	0.509	15.90	-21.4	15.9	-1.6	14.3
	MC Dur	3.913	0.499	15.91	-17.4	13.7	-1.6	13.0
348 Node	DTS	183.227	79.765	84.94				
	MC Chron	153.829	82.136	81.82	-16.0	3.0	-3.7	5.6
	MC Dur	155.603	79.269	82.02	-15.1	-0.6	-3.4	7.0

2.5.3.4 Discussion of the Results

Before discussing the test results it is important to note that, as explained in Section 2.5.1, the typical curves used in the tests were derived from the metered data used in the discrete time simulation reference, and that a set of unique curves were derived for each load and generator in the system. Hence the results for system energy in Table 2.2 should match the reference results closely. The results which are of particular importance in this assessment are the errors in the energy results for line flows and losses, and the mean half hour deviations from the reference results.

From a study of the results in Tables 2.2 to 2.4 the following observations can be made.

2.5.3.4.1 Demand Results. Table 2.2.

The errors on the system energy results are small for both typical and duration day methods, as expected.

The results indicate that the methods based upon typical days underestimate the system maximum demand and overestimate the system minimum demand. This is also to be expected, because the typical days represent average loading conditions.

The errors on system maximum and minimum demand indicate that the duration curve approach models the extreme operating conditions more accurately than the method based upon chronological typical days, particularly for the networks serving diverse industrial loads (7 and 10 Nodes). This is because the process of converting typical daily curves in chronological format to duration format eliminates the diversity between individual load profiles. The maximum and minimum demands of load profiles in duration format will by definition coincide, resulting in a diversity factor of unity for the system. The errors which remain between the duration curve approach and discrete time simulation simply comprise the differences between the average data and the actual data on the days of system maximum and minimum demand.

The mean deviations can be seen to coincide with the degree of diversity in a given network. These results also indicate that the duration curve approach consistently achieves slightly lower mean deviations than the chronological approach. By neglecting the chronological sequence of load changes the duration curve approach is less sensitive to small erratic variations in demand, with subsequent reductions in deviations.

2.5.3.4.2 Line Loading Results. Table 2.3.

The results for line loading taken system-wide show little difference when compared with the results for system demand. This indicates that given loading patterns whose average values coincide with the reference results, the average values for power flows in lines will also coincide with reference results.

2.5.3.4.3 Loss Results. Table 2.4.

The results show that errors in the calculation of system losses are significantly higher than for the line loading case. This finding is repeated in the results for mean deviations. The 'square law' effect of losses can be seen to exaggerate the discrepancies between the results for typical days and the discrete time simulation.

The results for system energy losses can be regarded as respectable, with errors of less than 4% in all cases. As noted above these figures should be regarded as the upper limit of accuracy for these networks. The mean deviations lie in the range 6 - 30% which indicates that errors in loss results for particular lines and transformers may be large for part or all of the study period.

2.5.4 Test 2. Comparison of Execution Times for Three Analysis Approaches

In this test the execution times of the three approaches are compared. In each case the elapsed time required to conduct a simulation of a year at half hour steps was recorded. The following processes were included in the recorded execution time:

1. Reading of plant data from relational database
2. Reading of profiles data from profiles database
3. Load-flow solutions

4. Writing of load-flow state vector to local storage.

In each case the analysis software had dedicated access to the resources of the hardware platform used in the tests.

2.5.4.1 Test Results

Table 2.5 Execution Times for Three Analysis Approaches

Test	Approach	Execution Time for Simulation of a Year at Half Hour Steps			
		VAXstation 4000-60		Alpha AXP 3000-60	
		Elapsed Time Min:Secs	Speed Relative to DTS	Elapsed Time Min:Secs	Speed Relative to DTS
7 Node	DTS	2:44	1.0	0:24	1.0
	MC Chron	0:08	20.5	0:02	12.0
	MC Dur	0:05	32.8	0:02	12.0
10 Node	DTS	3:50	1.0	0:34	1.0
	MC Chron	0:10	23.0	0:03	11.3
	MC Dur	0:06	38.0	0:02	17.0
15 Node	DTS	7:11	1.0	0:54	1.0
	MC Chron	0:14	30.8	0:04	13.5
	MC Dur	0:08	53.9	0:03	18.0
348 Node	DTS	461:21	1.0	59:02	1.0
	MC Chron	9:09	50.4	1:30	39.4
	MC Dur	2:35	178.6	0:40	88.6

2.5.4.2 Discussion

The results from Table 2.5 indicate that the execution times for discrete time simulation are substantially longer than for the other two approaches: between 11 and 50 times longer than the approach based upon typical days, and between 12 and 180 times longer than the approach based upon duration days.

It can be seen that for the smallest systems the execution overhead associated with accessing the relational plant database reduces the differences in performance between the three approaches. For the large system the differences in execution time are largely related to the different numbers of load-flow solutions performed in each approach.

It is clear that the comparatively short execution times of the two approaches based upon typical days are attractive in a distribution operations and planning environment; results for a year's simulation can be obtained in seconds on current workstations. It is important to note, however, that the Alpha AXP workstation has made it possible to run full discrete time simulations of a year's duration on realistic systems such as the 348 Node system in less than an hour. When allowing for the fact that load-flow studies are frequently conducted on systems significantly smaller than the 348 node system used here, it can be seen that the widespread use of discrete time simulation for operations and planning purposes is feasible, given the performance of current workstations.

2.5.5 Test 3. Comparison of Storage Requirements for Three Analysis Approaches

2.5.5.1 Test Results

Table 2.6 compares the storage requirements for the three approaches outlined in Section 2.5.3. Two categories of data are compared: input demand profiles and results profiles. Input demand profiles data comprises active and reactive demands at each time step for each load and generator in the system. Results profiles data comprises voltage and angle at every load-flow node in the system, and tap position for every transformer, at each time step.

Table 2.6 Storage Requirements for Three Analysis Approaches

Test System	Approach	Storage Requirements for Simulation of a Year at Half Hour Steps (MByte)	
		Input Demand Profiles	Results Profiles
7 Node	DTS	0.668	1.069
	MC Chron	0.017	0.026
	MC Dur	0.002	0.003
10 Node	DTS	0.535	·1.538
	MC Chron	0.013	0.038
	MC Dur	0.002	0.005
15 Node	DTS	0.936	2.406
	MC Chron	0.023	0.059
	MC Dur	0.003	0.007
348 Node	DTS	20.585	56.040
	MC Chron	0.508	1,382
	MC Dur	0.063	0.173

2.5.5.2 Discussion

Table 2.6 illustrates the very large differences in storage requirements for the three approaches. Discrete time simulation requires approximately 40 times the storage of the multiple case chronological approach and over 300 times the storage of the multiple case duration curve approach. These results are to be expected from the fact that discrete time simulation models the performance of the system at every half hour of the year.

The figures show that the storage requirements for all four test systems can be accommodated comfortably on current workstation technology. As an example, the Alpha AXP 3000-60 workstation used in the tests is configured with a 1000MByte hard disk as standard, and can be expanded relatively cheaply.

2.6 Conclusions

In this chapter the most widely used approaches to load-flow analysis in distribution systems have been described with particular reference to the modelling of the variations in load and generation profiles with time. These are summarised in Tables 2.7 to 2.12.

Three deterministic approaches have been described. The single case load-flow approach employs a small number of load-flow solutions at extreme loading conditions to determine the limits of system performance. It has been noted that the speed and low storage requirements of this approach are attractive, but that the simplicity of the analysis provides little information concerning the variation in system state with time and can lead to significant errors in calculated results. The multiple case duration curve approach has been described and shown to be an efficient method for providing improved modelling of time related variations in the performance of the system. The inability of the approach to account accurately for load diversity has been highlighted. The multiple case chronological approach has been described and shown to provide improved modelling of non-conforming loads, at the expense of additional computational and storage requirements. The limitations of the method with respect to the modelling of loads with erratic, unpredictable profiles have been discussed.

Two probabilistic approaches have been outlined: probabilistic load-flow and Monte Carlo simulation. The advantages of probabilistic techniques in modelling the uncertainty in the input data and providing information concerning the likelihood of certain operating conditions have been described. The difficulties associated with modelling the interdependencies of random variables such as load and generation profiles and network topology, and the approximations made in the load-flow equations, have also been discussed, and it has been proposed that because of these problems deterministic analysis provides a better solution for the time based modelling of distribution systems.

A new approach entitled discrete time simulation has been presented, which accounts for the variations in individual load and generation profiles with time by modelling the system at regular intervals throughout the study period. The advantages of the approach in terms of improved modelling of non-conforming and unpredictable loads have been outlined. It has also been noted that the approach provides a sound basis on which to perform detailed studies for the costing of energy and allocation of costs to consumers. The disadvantages of the approach, specifically the substantial data and computational requirements have also been discussed.

Test results have been presented which compare the accuracy, execution times and storage requirements of the proposed discrete time simulation approach with the two multiple case approaches based upon typical days.

The accuracy test results confirm that the methods based upon typical days perform best on systems containing predictable, conforming loads. In such cases mean discrepancies on individual items of plant were found to lie between 3% and 15%. On systems with high proportions of non-conforming industrial loads these approaches are subject to substantial errors, with mean discrepancies of up to 30%. The results also show that the errors in the loss results are greater than the errors in power flow results, due to the 'square law' effect of losses.

The performance results indicate that the execution times for discrete time simulation are many times greater than for the alternative approaches, although it has been demonstrated that the advances in the latest workstations have reduced the times required for the full simulation of a year at half hour steps to less than an hour in typical cases.

The results for storage requirements have shown that the requirements of discrete time simulation are typically between 40 and 300 times greater than those of the alternative approaches. However, it has been noted that the input and results data required for a simulation of a year on test systems of realistic size can easily be accommodated on current workstations.

Table 2.7 Summary of the Single Case Load-flow Approach.

Criterion	Description
Model system annual maximum and minimum demand conditions	Yes, by running cases at these conditions.
Model system as a function of time	Only by running a large number of individual cases. The manual effort required is large, since each case must be set up individually. Results are approximate at best.
Model load diversity	Approximate at best. Requires engineering judgement in the selection of cases to capture the effects of diversity on specific circuits.
Model energy flows and energy losses over a period of time	Requires the use of load and loss factors in conjunction with the solution from the system peak loading condition. Results rely on the accuracy of these factors.
Model energy and loss costs through the application of time-varying tariffs	Approximate. Simple time-of-day tariffs can be accommodated by performing the analysis for different tariff periods. More complex tariffs cannot be accurately applied.
Data requirements	Very low. Loading data required for a small number of cases. Measurements of annual maximum and minimum demands are usually available or can be inferred.
Computational requirements	Very low. A small number of load-flow solutions.

Table 2.8 Summary of the Multiple Case Duration Curve Approach

Criterion	Description
Model system annual maximum and minimum demand conditions	No. Typical days basedupon average loading conditions do not provide a good basis for modelling extreme loading conditions.
Model system as a function of time	Duration curves provide information concerning how long the system was in a certain state. They provide no information concerning the time or sequence of events or system states.
Model load diversity	Not modelled accurately. Demand profiles for all loads in the system are assumed to conform to the system demand profile, an assumption which often fails to apply, particularly in industrial areas.
Model energy flows and energy losses over a period of time	Results from typical daily curves can be integrated and summed over each day to give figures for total energy flow and loss over a period of time.
Model energy and loss costs through the application of time-varying tariffs	Approximate. Time-varying tariffs cannot in general be accurately applied to duration curves, due to the lack of chronological information.
Data requirements	Low. Loading data required for a small number of load levels on each of a small number of duration curves, and can be derived from measurements or load research data.
Computational requirements	Low. A relatively small number of load-flow solutions.

Table 2.9 Summary of the Multiple Case Chronological Approach

Criterion	Description
Model system annual maximum and minimum demand conditions	No. Typical days basedupon average loading conditions do not provide a good basis for modelling extreme loading conditions.
Model system as a function of time	Yes, for each of the typical days studied.
Model load diversity	Modelled reasonably accurately. Demand profiles for all loads in the system are assumed to follow a predictable cyclic pattern, such that a year's profile can be modelled by a small number of daily curves. This assumption fails to apply to a relatively small number of industrial loads.
Model energy flows and energy losses over a period of time	Results from typical daily curves can be integrated and summed over each day to give figures for total energy flow and loss over a period of time.
Model energy and loss costs through the application of time-varying tariffs	Certain fixed time-of-day tariffs are well handled. Continuously varying tariffs can only be applied in an approximate manner.
Data requirements	Moderate. Loading data required for 24 or 48 load levels on each of a small number of daily curves. Data can be derived from measurements or load research data.
Computational requirements	Moderate.

Table 2.10 Summary of the Probabilistic Load-flow Approach

Criterion	Description
Model system annual maximum and minimum demand conditions	Yes, provided these loading conditions are studied. The results also provide probabilities of certain loading conditions being exceeded.
Model system as a function of time	Yes, provided the analysis is combined with a multiple case duration curve or chronological approach.
Model load diversity	Potentially accurate, if the relationships between load and generation levels can be derived, and their PDFs calculated. In practice simplifying approximations are used in the absence of data, and these reduce modelling accuracy.
Model energy flows and energy losses over a period of time	Results from analysis performed across typical daily curves can be integrated and summed over each day to give figures for total energy flow and loss over a period of time.
Model energy and loss costs through the application of time-varying tariffs	Depends upon the method used to model the system as a function of time. Refer to comments for those methods.
Data requirements	Moderate requirements in terms of quantity, but may be difficult to obtain. Expected loading data and PDFs required for each operating condition studied.
Computational requirements	Depends upon the specific method. Linearised load-flow equations can be solved much more quickly than the non-linear equations in the conventional deterministic case, but additional computations can be substantial.

Table 2.11 Summary of the Monte Carlo Simulation Approach

Criterion	Description
Model system annual maximum and minimum demand conditions	Yes. The results also provide probabilities of certain loading conditions being exceeded.
Model system as a function of time	Yes, for each of the typical days studied.
Model load diversity	Potentially accurate, if the relationships between load and generation levels can be derived, and their PDFs calculated. In practice simplifying approximations are used in the absence of data, and these reduce modelling accuracy.
Model energy flows and energy losses over a period of time	Results from analysis performed across typical daily curves can be integrated and summed over each day to give figures for total energy flow and loss over a period of time.
Model energy and loss costs through the application of time-varying tariffs	Certain fixed time-of-day tariffs are well handled. Continuously varying tariffs can only be applied in an approximate manner.
Data requirements	Moderate requirements in terms of quantity, but may be difficult to obtain. Mean loading data and PDFs required for 24 or 48 load levels on each of a small number of daily curves.
Computational requirements	Very large. Many thousands of load-flow solutions are required to derive accurately the resulting expected values and PDFs.

Table 2.12 Summary of Proposed Discrete Time Simulation Approach

Criterion	Description
Model system annual maximum and minimum demand conditions	Yes, by simulating the periods during which these conditions occur.
Model system as a function of time	Yes, throughout the simulation period.
Model load diversity	Modelled accurately. No simplifying assumptions are made.
Model energy flows and energy losses over a period of time	Yes. Accurate values can be obtained directly by integrating over the period.
Model energy and loss costs through the application of time-varying tariffs	Yes. All standard time-varying tariffs can be applied at a system-wide or individual component level
Data requirements	Very large. Loading data required for each time step throughout the simulation. Usually readily available at higher voltages. Special techniques may be required to derive it from load research data at lowest voltages.
Computational requirements	Very large. Several thousand load-flow solutions are required to simulate a year.

Chapter 3. Load-flow Algorithms

3.1 Formulation of the Load-flow Problem

3.1.1 Basic Equations

The load-flow provides a solution for the steady state operating condition of a power system. Derivations of the load-flow equations can be found in standard texts by Arrillaga and Arnold [7], Del Toro [34], El-Abiad [40], Gross [59], Stagg and El-Abiad [131], Wood and Wollenburg [152], and others.

The basic formulation assumes a balanced three-phase system, represented by a positive sequence network of nodes, connected by series and shunt branches. Linear mathematical equations are used to model transmission lines, transformers and shunt and series reactances, such that the relationship between the nodal currents I and the nodal voltages E (with respect to a base voltage) in a network of n nodes is given in matrix form by

$$\mathbf{I} = [\mathbf{Y}]\mathbf{E} \tag{3-1}$$

and for node i

$$\bar{I}_i = \sum_{k=1}^{n} \bar{Y}_{ik} \bar{E}_k \tag{3-2}$$

3.1.2 Node Constraints

The steady state operating condition of the system is determined by the constraints on power and possibly voltage at each node. Three categories of node are defined, and equations developed which define the relationship between power and voltage and current at that node, as follows:

1. PQ Type

   For nodes in this category the active and reactive components of injected power are specified.

$$\begin{aligned} \bar{S}_i^{sp} &= P_i^{sp} + jQ_i^{sp} \\ &= P_{Gi}^{sp} - P_{Di}^{sp} + j(Q_{Gi}^{sp} - Q_{Di}^{sp}) \\ &= \bar{E}_i \bar{I}_i^{\,*} \end{aligned} \tag{3-3}$$

Substituting from (3-2) gives

$$\overline{S}_i^{sp} = \overline{E}_i \sum_{k=1}^{n} \overline{Y}_{ik}^{*} \, \overline{E}_k^{*} \tag{3-4}$$

2. PV Type

   For nodes in this category the active component of injected power is specified, and the reactive component varies to maintain the voltage at a constant value.

$$P_i^{sp} = P_{Gi}^{sp} - P_{Di}^{sp} = \Re(\overline{E}_i \overline{I}_i^{*}) \tag{3-5}$$

$$V_i^{sp} = (e_i^2 + f_i^2)^{1/2} = V_i = |E_i| \tag{3-6}$$

3. Slack

   Because the transmission losses on the system are not known in advance of the load-flow calculation it is not possible to specify the injected power at every node. Instead, one of the nodes is chosen as the slack node. The voltage magnitude and angle are specified at this node, while the active and reactive power vary to make up any differences between generation, load and losses on the system.

3.1.3 Nodal Mismatch Equations

Because the equations for power at each node are non-linear an iterative.scheme must be employed to solve them. Progress towards the solution is then indicated by the differences or mismatches in specified and calculated values of power at each node. These mismatches are derived from (3-3) and (3-4)

$$\begin{aligned} \Delta S_i &= \overline{S}_i^{sp} - \overline{E}_i \overline{I}_i^{*} \\ &= P_i^{sp} + jQ_i^{sp} - \overline{E}_i \sum_{k=1}^{n} \overline{Y}_{ik}^{*} \, \overline{E}_k^{*} \end{aligned} \tag{3-7}$$

Separating real and imaginary components

$$\Delta P_i = P_i^{sp} - \Re\Big((e_i + jf_i)\sum_{k=1}^{n} (G_{ik} - jB_{ik})(e_k - jf_k)\Big) \tag{3-8}$$

$$\Delta Q_i = Q_i^{sp} - \Im\Big((e_i + jf_i)\sum_{k=1}^{n} (G_{ik} - jB_{ik})(e_k - jf_k)\Big) \tag{3-9}$$

In polar co-ordinates these are expressed as

$$\Delta P_i = P_i^{sp} - V_i \sum_{k=1}^{n} (G_{ik}\cos\theta_{ik} + B_{ik}\sin\theta_{ik})V_k \tag{3-10}$$

$$\Delta Q_i = Q_i^{sp} - V_i \sum_{k=1}^{n} (G_{ik}\sin\theta_{ik} - B_{ik}\cos\theta_{ik})V_k \tag{3-11}$$

Alternatively, current mismatch equations are sometimes used

$$\Delta \bar{I}_i = \frac{\Delta \bar{S}_i^*}{\bar{E}_i^*} = \left(\frac{(P_i^{sp} - jQ_i^{sp})}{\bar{E}_i^*}\right) - \sum_{k=1}^{n} \bar{Y}_{ik} \bar{E}_k \tag{3-12}$$

In most load-flow algorithms convergence is considered to have been reached when the largest mismatch is less than a specified tolerance.

3.2 Review of Existing Load-Flow Algorithms

3.2.1 Early Load-Flow Methods

3.2.1.1 Y Matrix Iterative Method

The first successful computer-based load-flow technique was the Y Matrix Iterative Method, applications of which were developed in the late 1950s by Ward and Hale [149], Glimn and Stagg [53], and Brown and Tinney [28].

From an expression of the current mismatch at each bus:

$$\Delta \bar{I}_i = \bar{I}_i - \sum_{k=1}^{n} \bar{Y}_{ik} \bar{E}_k \tag{3-13}$$

a relaxation algorithm is applied which eliminates ΔI_i by recalculating E_i

$$\bar{E}_i = \frac{\left(\bar{I}_i - \sum_{k=1}^{n} \bar{Y}_{ik} \bar{E}_k\right)}{\bar{Y}_{ii}} \tag{3-14}$$

The Gauss-Seidel method of successive displacements is normally used to apply this algorithm. Most variations of this method differ in their treatment of the non-linear node constraints. The basic method is to rewrite equation (3-3) in terms of current

$$\bar{I}_i = \frac{(P_i^{sp} - jQ_i^{sp})}{\bar{E}_i} \tag{3-15}$$

and substitute this into (3-14).

The principal advantage of the Y Matrix Iterative Method is a low storage requirement, arising from the fact that the sparse, often symmetrical, admittance matrix can be stored efficiently. For small networks the computational requirements of the method are also small, but because the computation time of the Gauss-Seidel successive displacements method is proportional to the number of buses n, and because the number of iterations required is also of order n, the total computation time of the method varies approximately with n^2. Hence for larger networks the method rapidly becomes uncompetitive when compared with newer methods. In addition the Gauss-Seidel method can fail to converge if the admittance matrix does not possess diagonal dominance. Diagonal dominance is weakened in networks containing combinations of very high and low impedances and significant values of capacitance.

3.2.1.2 Z Matrix Iterative Method

The development of the Z Matrix Iterative Method sought to improve on the slow and often unreliable convergence of the Y Matrix approach. The most important Z Matrix algorithms were published by Gupta and Humphrey Davies [60], Brameller and Denmead [22] and Brown et al [26,27] between 1961 and 1968. As the name implies the impedance matrix is used directly to calculate the node voltages

$$\mathbf{E} = [\mathbf{Z}]\mathbf{I} \tag{3-16}$$

The node power constraints are incorporated in the same way as for the Y Matrix Methods. The Gauss-Seidel method of successive displacements is normally used to solve this equation. However because the voltage of each node is coupled to the currents at all the buses, rather than just those to which it is connected as in the Y Matrix method, convergence is comparatively rapid. The principal disadvantage, however, is that the use of the non-sparse impedance matrix results in large storage requirements. Computation times also become excessive for large problems [134].

The following sections review the most important and widely used load-flow algorithms.

3.2.2 The Newton-Raphson Method

3.2.2.1 Formulation of the Basic Method

The Newton-Raphson method is the multivariable form of the Newton method. The Newton method is an iterative algorithm for solving an equation of the form

$$f(x) = 0 \tag{3-17}$$

A Taylor's series expansion of this equation about a known value $x^{(m)}$ gives

$$f(x) = f(x^{(m)}) + \frac{1}{1!}f'(x)(x - x^{(m)}) + \frac{1}{2!}f''(x)(x - x^{(m)})^2 + \ldots \tag{3-18}$$

In the Newton method the second and higher order terms are discarded, and from (3-17) and (3-18) we have

$$x - x^{(m)} = 0 - \frac{f(x^{(m)})}{f'(x^{(m)})} + \varepsilon \tag{3-19}$$

The value x is not a root of $f(x) = 0$, because of the error term ε introduced by neglecting the higher order terms. However x generally represents a better estimate of the root than $x^{(m)}$. Hence the problem is formulated as

$$f(x^{(m)}) = -f'(x^{(m)})\Delta x \tag{3-20}$$

where Δx is a correction term which is solved for at each iteration, and used to provide a better estimate of the root

$$x^{(m+1)} = x^{(m)} + \Delta x \tag{3-21}$$

The iterative procedure is repeated until one of the following conditions occurs:

$$\begin{array}{rcll} \Delta x & \leq & \Delta x_{tol} & \text{(Convergence)} \\ \Delta x & > & x_{max} & \text{(Divergence)} \\ m & > & m_{max} & \text{(Failure to converge after } m_{max} \text{ iterations)} \end{array}$$

In the application of the Newton-Raphson method to the load-flow problem, equation (3-20) is expressed in terms of the power mismatches at each node

$$\begin{bmatrix} \Delta \mathbf{P} \\ \Delta \mathbf{Q} \end{bmatrix} = [\mathbf{J}] \begin{bmatrix} \Delta \theta \\ \Delta \mathbf{V}/\mathbf{V} \end{bmatrix} \tag{3-22}$$

where J is the Jacobian matrix of partial derivatives

$$[\mathbf{J}] = \begin{bmatrix} [\mathbf{H}] & [\mathbf{N}] \\ [\mathbf{M}] & [\mathbf{L}] \end{bmatrix} = \begin{bmatrix} \left[\dfrac{\partial \mathbf{P}}{\partial \theta}\right] & \left[\dfrac{\partial \mathbf{P}}{\partial \mathbf{V}}\right] \\ \left[\dfrac{\partial \mathbf{Q}}{\partial \theta}\right] & \left[\dfrac{\partial \mathbf{Q}}{\partial \mathbf{V}}\right] \end{bmatrix} \tag{3-23}$$

The elements H, N, M and L are (in polar form)

$$\begin{aligned} H_{kk} &= -B_{kk}V_k^2 - Q_k \\ H_{ki} &= L_{ki} = V_k V_i (G_{ki}\sin\theta_{ki} - B_{ki}\cos\theta_{ki}) \\ N_{kk} &= G_{kk}V_k^2 + P_k \\ N_{ki} &= -M_{ki} = V_k V_i (G_{ki}\cos\theta_{ki} + B_{ki}\sin\theta_{ki}) \\ M_{kk} &= -G_{kk}V_k^2 + P_k \\ L_{kk} &= -B_{kk}V_k^2 + Q_k \end{aligned} \tag{3-24}$$

The Newton-Raphson method was first applied to the load-flow problem by Van Ness [145] and Van Ness and Griffin [146]. These early implementations suffered from large memory and computational requirements when applied to networks of realistic size. The method of

Tinney and Hart [141] overcame these limitations through the use of optimally ordered Gaussian elimination and an efficient storage scheme for the sparse Jacobian matrix.

The procedure followed for an iteration *m* of the method is to evaluate the Jacobian using equations (3-24) and to invert it using triangular factorisation [126, 142, 141, 156]. The power mismatches are evaluated using equations (3-10) and (3-11). The voltage and angle corrections are then computed from (3-22):

$$\begin{bmatrix} \Delta\theta \\ \Delta V/V \end{bmatrix} = [J]^{-1} \begin{bmatrix} \Delta P \\ \Delta Q \end{bmatrix} \tag{3-25}$$

and used in the next iteration.

The principal advantages of the Newton-Raphson method are its reliability, even when applied to networks which are difficult to solve by other methods, and its very high rate of convergence. The rate of convergence becomes quadratic when close to the solution.

Disadvantages include relatively high memory requirements, and because the Jacobian needs to be built and inverted at every iteration the computational requirements for each iteration can also be high.

A number of improvements to the basic method have been developed.

3.2.2.2 The Newton-Raphson Starting Process of Stott

Stott [132] reported an effective starting process for Newton Raphson load flows which employs a d.c. load-flow to calculate approximate voltage angles for each node. These in turn are used in an approximate a.c. method used to calculate corresponding voltage magnitudes. The use of these voltages as the starting point for the full Newton Raphson load flow is reported to reduce the numbers of iterations required for solution by between 1 and 3 compared with a flat voltage start, and to improve significantly convergence characteristics on difficult networks.

3.2.2.3 The Minimisation Technique of Sasson et al.

Another method developed to improve convergence for difficult cases was published by Sasson et al [125], who used a Fletcher-Powell minimisation technique to provide a solution for cases in which the standard method diverged, due either to ill-conditioned or insoluble problems.

This method is very useful tool for solving difficult cases, and for identifying the causes of difficulty in cases where standard load-flow algorithms fail to converge. The method generally takes longer than the Newton-Raphson method for practical cases [140].

3.2.2.4 The Efficient Formulation of Irving and Sterling

The Jacobian matrix in equation (3-22) is of order $(n_{PQ} + n_{PV} + n_{PQ})$, where n_{PV} and n_{PQ} are the numbers of PV and PQ nodes in the network respectively. The inversion of a matrix of this order by bifactorisation requires significant computational effort in the optimal ordering and sparse indexing procedures. Tinney and Hart [141] reduce this by arranging the variables in equation (3-22) as shown.

$$\begin{bmatrix} \Delta P_1 \\ \Delta Q_1 \\ \Delta P_2 \\ \Delta Q_2 \\ \vdots \\ \Delta P_n \\ \Delta Q_n \end{bmatrix} = [J'] \begin{bmatrix} \Delta\theta_1 \\ \Delta V_1/V_1 \\ \Delta\theta_2 \\ \Delta V_2/V_2 \\ \vdots \\ \Delta\theta_n \\ \Delta V_n/V_n \end{bmatrix} \qquad (3\text{-}26)$$

The Jacobian [J′] is now naturally partitioned into 2 x 2, 2 x 1, 1 x 2, and 1 x 1 submatrices. Considering each of these submatrices as a single element the order of the Jacobian is reduced to $(n_{PV} + n_{PQ})$. This is achieved at the expense of some additional calculations and logic in dealing with the different submatrices.

Irving and Sterling [73] take this a stage further and eliminate the logic required to deal with submatrices of different forms through the use of 2 x 2 submatrices throughout. This is achieved by adopting a proposal by Dodson [36] in which the order of matrices N, M and L of equation (3-23) are extended to that of H through the introduction of elementary rows and columns:

$$[J''] = \begin{bmatrix} [H] & [N'] \\ [M'] & [L'] \end{bmatrix} = \begin{bmatrix} [H] & [N] & [0] \\ [M] & [L] & [0] \\ [0] & [0] & [I] \end{bmatrix} \qquad (3\text{-}27)$$

where [0] and [I] are appropriate zero and unit matrices. The equations are then rearranged as for equation (3-26), with the result that the Jacobian is partitioned into 2 x 2 submatrices. The extra processing saved by using uniform submatrices greatly outweighs the additional floating point calculations, since the calculations on the elements of each submatrix can be handled very efficiently by modern optimising compilers and virtual memory architecture. The overall result is greatly improved efficiency over the basic algorithm.

Test results by Zhang and Irving [155] have shown that the performance of the method is generally approximately three and a half times quicker than the basic algorithm.

3.2.3 The Fixed Jacobian Method

The Fixed Jacobian method seeks to reduce the computation time of the Newton-Raphson method by repeated use of the Jacobian, thereby avoiding the need to build and factorise the Jacobian at each iteration.

The Fixed Jacobian method has been reported by Tinney and Hart [141], and Miesel and Barnard [93], who also developed criteria for the convergence of the method. The Jacobian is evaluated at the initial conditions and inverted by triangular factorisation to obtain voltage corrections as in the standard Newton method. The lower and upper triangular matrices are stored. On subsequent iterations the voltage corrections are applied to calculate new power mismatches, and the forward elimination and back substitution steps of the inversion process are repeated to obtain new voltage corrections and so on.

Avoiding the need to factorise the Jacobian can reduce the computation time per iteration by up to four times. However, because the quadratic convergence of the Newton method is normally significantly degraded, the number of iterations is increased, and any speed advantages may be lost. However, when the Fixed Jacobian method is used in conjunction with the Newton-Raphson method, such that the Jacobian is used more than once before being updated, the overall execution times can be significantly shorter than either of the methods used in isolation [37, 93, 141].

3.2.4 The Decoupled Newton Method

Decoupled methods in power system analysis exploit the strong interdependence between active power P and voltage angle θ, and between reactive power Q and voltage magnitude V. The coupling between the P-θ and Q-V components is therefore relatively weak. Decoupled algorithms neglect these weak relationships, solving the P-θ and Q-V problems separately.

The best known decoupled load-flow method is that of Stott [133]. The decoupling assumptions are

$$[\mathbf{N}] = \left[\frac{\partial \mathbf{P}}{\partial \mathbf{V}}\right] = 0 \tag{3-28}$$

$$[\mathbf{M}] = \left[\frac{\partial \mathbf{Q}}{\partial \theta}\right] = 0 \tag{3-29}$$

Equation (3-22) then becomes

$$[\Delta\mathbf{P}] = [\mathbf{H}][\Delta\theta] \tag{3-30}$$

$$[\Delta\mathbf{Q}] = [\mathbf{L}][\Delta\mathbf{V}/\mathbf{V}] \tag{3-31}$$

Each iteration of the method involves constructing and solving (3-30) for $\Delta\theta$, then updating θ and using it to construct and solve (3-31) for ΔV.

The decoupling results in a saving in storage of between 30 and 40 percent, and a saving in computation time per iteration of 10 to 20 percent [134]. However, because the quadratic convergence of the coupled method is lost, more iterations may be required.

3.2.5 The Fast Decoupled Method

In the Fast Decoupled method further assumptions and approximations are used to reduce execution time. The method was developed from a number of emerging techniques, by Stott and Alsac [136]. The decoupling assumptions of the Decoupled Newton method are made, and in addition the following simplifications are made

$$\begin{aligned} \cos\theta_{ki} &\simeq 1 \\ G_{ki}\sin\theta_{ki} &\ll B_{ki} \\ Q_{ki} &\ll B_{kk}V_k^2 \end{aligned} \tag{3-32}$$

Equations (3-30) and (3-31) then become

$$[\Delta\mathbf{P}] = [\mathbf{V}\mathbf{B}'\mathbf{V}][\Delta\theta] \tag{3-33}$$

$$[\Delta\mathbf{Q}] = [\mathbf{V}\mathbf{B}''\mathbf{V}][\Delta\mathbf{V}/\mathbf{V}] \tag{3-34}$$

where [B′] and [B″] are elements of [-B]. The decoupling process is taken further by omitting from [B′] any network elements which affect reactive power flows, such as shunt reactances and off-nominal transformer taps, and omitting elements from [B″] which affect phase angles, such as phase shifters. Lastly the left hand V terms are taken across to the left hand sides of the equations, which reduces the non-linearity of the Q-V problem, and the right hand V terms in equation (3-33) are set to 1.0 per unit. The resulting equations are

$$[\Delta\mathbf{P}/\mathbf{V}] = [\mathbf{B}'][\Delta\theta] \tag{3-35}$$

$$[\Delta\mathbf{Q}/\mathbf{V}] = [\mathbf{B}''][\Delta\mathbf{V}] \tag{3-36}$$

Equations (3-35) and (3-36) are solved in turn at each iteration as for the Decoupled Newton method. The matrices [B′] and [B″] are only one quarter of the size of the Jacobian matrix, and are factorised at the first iteration only. Hence, the speed per iteration is approximately 5 times that of the Newton-Raphson method [134]. Although the rate of convergence of the method is not as high, the overall speed of the Fast Decoupled method can be significantly better than that of the basic Newton method (Stott [134], Sasson et al [124], Masiello and Wollenberg [92] and Sasaki [123]).

Since the Fast Decoupled method was developed in 1974, it has been widely adopted by the power industry, and has been subject to a number of modifications aimed at improving its speed and/or convergence characteristics: Bacher and Tinney [10], Keyhani [77], Babic [9], Benham-Guilani [13], Amerongen [4], Haley and Ayres [64], Wang et al [148].

3.2.6 Second Order Newton Raphson Method

In the Second Order Newton Raphson method the second order terms of the Taylor series are retained. Second order methods have been published in polar form by Sachdev and Medicherla [120], and in rectangular form by Roy [118], Iwamoto and Tamura [74], El-Hawary and Wellon [43], Rao et al [115], and Hubbi [70].

Although these methods vary in their treatment of the problem, they are based around the Taylor series expansion of Equation (3-17) about an initial estimate vector x_e up to and including the second order terms

$$\begin{bmatrix} \mathbf{f(x)} \end{bmatrix} = \begin{bmatrix} \mathbf{f(x_e)} \end{bmatrix} + \begin{bmatrix} \mathbf{J} \end{bmatrix} \begin{bmatrix} \Delta \mathbf{x} \end{bmatrix} + \frac{1}{2} \begin{bmatrix} \quad \mathbf{H} \quad \end{bmatrix} \begin{bmatrix} \Delta x_1 \Delta x_1 \\ \Delta x_1 \Delta x_2 \\ \vdots \\ \Delta x_i \Delta x_j \\ \vdots \\ \Delta x_n \Delta x_n \end{bmatrix} \tag{3-37}$$

In the rectangular form the third and higher order terms are zero; in the polar form they are neglected. Equation (3-37) in rectangular form is therefore 'exact' and can be rearranged [74] to give

$$[\Delta \mathbf{x}] = [\mathbf{J}(\mathbf{x_e})]^{-1}[\mathbf{f(x)} - \mathbf{f(x_e)} - \mathbf{f}(\Delta \mathbf{x})] \tag{3-38}$$

in which the Jacobian is evaluated at the initial value only, and $f(\Delta x)$ is a vector function of corrections in the unknown variables. The iterative form of this equation is

$$[\Delta \mathbf{x}]^{(m+1)} = [\mathbf{J}(\mathbf{x_e})]^{-1}[\mathbf{f(x)} - \mathbf{f(x_e)} - \mathbf{f}(\Delta \mathbf{x}^{(m)})] \tag{3-39}$$

Expressed in terms of the load flow equations (3-39) becomes, in rectangular form,

$$\begin{bmatrix} \Delta \mathbf{f}^{(m+1)} \\ \Delta \mathbf{e}^{(m+1)} \end{bmatrix} = \begin{bmatrix} \mathbf{J}_0 \end{bmatrix}^{-1} \begin{bmatrix} \mathbf{P} - \mathbf{P}_0 - \mathbf{P}(\Delta \mathbf{e}^{(m)}, \Delta \mathbf{f}^{(m)}) \\ \mathbf{Q} - \mathbf{Q}_0 - \mathbf{Q}(\Delta \mathbf{e}^{(m)}, \Delta \mathbf{f}^{(m)}) \\ |\mathbf{E}|^2 - |\mathbf{E}_0|^2 - |\Delta \mathbf{E}^{(m)}|^2 \end{bmatrix} \tag{3-40}$$

which is solved iteratively for $\Delta f^{(m+1)}$ and $\Delta e^{(m+1)}$. Decoupled versions of the Second Order method based upon the decoupling assumptions first proposed by Stott and Alsac [136] have also been reported by Babic [9], Roy and Rao [119], and Nanda et al [99].

The advantages claimed for the method are that using the second-order terms results in improved convergence over the Newton Raphson method, and the use of a fixed Jacobian matrix results in significant reductions in computation time per iteration.

Although the Second Order methods have been presented in the literature as essentially new approaches to the load-flow problem, it has been pointed out by Duran [37] and by Hubbi [70] that these methods are in fact variants of the Fixed Jacobian method. Hubbi developed a Mismatch Theorem and used it to demonstrate that at each iteration the second order terms of equation (3-37) are exactly equal to the power and voltage mismatches of the Fixed Jacobian method with Jacobian evaluated at the first iteration, which can be calculated using equations (3-8), (3-9) and (3-6). Nevertheless, Second Order methods have attracted widespread interest for application to a variety of problem areas [39, 32, 76].

3.2.7 Other Load Flow Algorithms

A number of load-flow methods have been developed specifically for radial distribution systems. Radial systems, and systems which are only weakly meshed, can be solved directly, resulting in significant improvements in speed and reductions in storage requirements when compared with the iterative methods described in the preceding sections. Examples of such algorithms include the method of Goswami and Baku [56] and the method of Baran and Wu [11].

Although the computational efficiency of these methods is attractive, they are not suitable for application to the kinds of meshed or interconnected system which occur at HV or MV voltage levels, or to systems with significant numbers of voltage controlled buses. For this reason direct methods are not considered further here.

3.3 Criteria for the Selection of a Load-flow Algorithm

In view of the range of techniques available for the solution of the load-flow problem, and the different assumptions used, it is not surprising that specific load-flow algorithms are well suited to particular types of problems. It is therefore important to select the algorithm best suited to a given problem. Stott [134] lists the properties generally used to assess load-flow methods in general. This section outlines the most important criteria to be considered when selecting a load-flow specifically for discrete time simulation, and describes the advantages and disadvantages of the methods given in the preceding sections.

3.3.1 Convergence Characteristics

The proposed load-flow algorithm must converge reliably on the systems to which the discrete time simulator is applied, that is, on practical distribution systems. Such systems cover a wide range of voltages and contain a mixture of plant with widely differing electrical characteristics. Table 1.1 in Chapter 1 illustrates the variation typically found, and lists representative values for the impedances of transmission lines at the different voltage levels.

In addition to the general variation in impedance with voltage level, significant differences in impedance at a given voltage level can occur through the use of lines of different rating, and of widely differing length. These features affect load-flow algorithms in different ways.

3.3.1.1 The Effects of Low X/R Ratios on Convergence

The decoupling assumptions central to the Decoupled Newton and Fast Decoupled methods neglect matrices N and M from the Jacobian by assuming that the real parts of the network admittances G are small in comparison with the imaginary parts B (Equations 3-28 and 3-29). The additional simplifications of the Fast Decoupled method (Equation 3-32) also assume that G is small in comparison with B.

In cases where transmission line X/R ratios approach unity these assumptions fail to hold, which results in poorer convergence, or failure to converge at all. It is well known that decoupled algorithms can perform badly in these circumstances [112, 113, 114, 115, 135, 153]. Wu [153] derives a mathematical relationship between convergence of the Fast Decoupled method and X/R ratio. Rao et al [114] develop an empirical criterion for the convergence of the method.

Because the Newton-Raphson, Fixed Jacobian and Second Order methods retain the coupling of the P-θ and Q-V problems these methods are not affected by low X/R ratios.

3.3.1.2 The Effects of High System Loading on Convergence

At high levels of system loading the coupling between the P-θ and Q-V components increases, which affects the convergence of the decoupled methods in the same way as low X/R ratios [135]. Indeed the convergence of all the load-flow algorithms described above is affected to some degree by high system loading.

Another consequence of high system loading is that the initial conditions normally used at the start of the load-flow calculations may differ significantly from the final solution, with the result that the method may diverge. Methods of higher order require better initial estimates than those of lower order [120, 121]. In this respect the Second Order methods are more susceptible to convergence difficulties on heavily loaded systems than the Newton-Raphson methods, as shown by the results of Hubbi [70].

3.3.1.3 The Effects of Ill-Conditioning on Convergence

A system is said to be ill-conditioned when a small change in one or more of the parameters results in a large change in the solution [144]. Two common causes of ill-conditioning in load flow analysis include:

1. Transmission line series capacitors
   The negative reactance of series capacitors cancels with the positive inductive reactance of the lines in which they are installed, resulting in comparatively small diagonal elements in the Jacobian matrix. This can lead to numerical instability in the solution of the Jacobian.

All the popular load flow techniques are affected by this form of ill-conditioning. However, the Newton-Raphson algorithm of Irving and Sterling [73], which uses a partitioned Jacobian matrix, is less susceptible since each diagonal 'element' is a 2 x 2 submatrix. The inverse of such an element only approaches singularity if capacitive/inductive reactance cancellation occurs *and* the resistance modelled at the node is negligible.

The Newton-like method of Tripathy and Purge Prasad [144] displays improved convergence over the Newton-Raphson method for ill-conditioned systems, but at the expense of longer execution times.

2. Lines of greatly differing impedance terminating at the same bus.
   This form of ill-conditioning affects all of the popular load flow algorithms, and gives rise to numerical instability through round-off error. It can be overcome by applying higher precision arithmetic in the solution process. The use of 64-bit floating point numbers is generally sufficient to counter the problem [73].

3.3.2 Execution Time

The discrete time simulator must be able operate on systems of realistic size over lengthy periods of time, and provide solutions without excessive delays on workstation hardware. These requirements are discussed in Section 2.5.4. It is clear, however, that execution speed is a high priority in the selection of a load flow algorithm for discrete time simulation.

3.3.2.1 General Properties

Comparing the execution times of different load flow techniques is not as straightforward as it might appear at first sight. A number of factors combine to make direct comparisons difficult:

1. In most cases the speed of a load flow algorithm is highly dependent upon the skill with which the method is implemented or coded. This applies particularly to the Newton-based methods [134]; efficient programming of the Jacobian matrix factorisation routines is crucial to the success of the methods, both in terms of speed and memory requirements.

   As a result it is often difficult to compare published results for different methods, since the programming and underlying assumptions differ widely from one implementation of a given method to another.

2. Published results relating to the performance of load flow algorithms are frequently expressed solely in terms of ratios of execution times. The execution time of a proposed method is given as a ratio of the execution time of an existing method. Alternatively the performance is expressed in terms of the number of iterations, and assumptions are made

concerning the comparative execution times of each iteration. If no actual times are given for a particular machine it is not possible to assess the true performance of the method. The problem is compounded by the differences due to specific implementations described in 1.

This approach can lead to discrepancies in published performance figures, when hypothetical figures do not match results obtained in practice. An example of this is the claim by Rao et al. [115] that their Second Order load flow is 70 - 80% quicker than the standard Newton-Raphson method. This claim is not consistent with the results of Hubbi [70] which suggest a much smaller margin in the performance of the two methods.

3. The assumptions concerning the use of a given load flow can bias the performance figures. As an example, Iwamoto and Tamura claim that for multiple case solutions their Second Order method requires 1/12th of the time than the Newton-Raphson method, assuming just one iteration is required for solution [74]. This claim assumes that the formation and solution of the Jacobian which is necessary in the first iteration of Second Order methods is an *off-line* process, not included in the timing comparison, while the same calculation in the Newton-Raphson is considered as an *on-line* process which is included in the comparison [75]. If the two methods were compared on the same basis their performance figures would almost be identical.

4. The test systems used to demonstrate the performance of load flow methods are frequently small, relatively easy to solve, and often do not contain the electrical plant which causes convergence difficulties, but which is found in most practical systems, such as generators which reach reactive limits, automatic tap-changing transformers, and reactive compensation equipment. This can be justified, since the inclusion of these types of plant can lead to confusion when studying the convergence characteristics of a given method. The convergence and subsequent speed of a method may be quite different on practical systems, however.

The factors outlined above illustrate the difficulties inherent in comparisons of the speed of different load flow techniques. It is possible, however to make the following general observations, based upon results published in the literature:

- The Fast Decoupled load flow is in most cases the fastest available technique, particularly on well behaved systems with high X/R ratios [10, 39, 136, 137].
- The Second Order and Fixed Jacobian methods are capable of execution times similar to those of the Fast Decoupled method on well behaved systems when good initial estimates are available [39].
- The basic Newton-Raphson method is perhaps the slowest of the methods in widespread use, due to the overhead involved in refactorising the Jacobian at each iteration. The

performance shortfall compared with other methods is greatly reduced, however, when applied to systems that are difficult to solve or heavily loaded. In addition, the efficient Newton-Raphson algorithm of Irving and Sterling [73] has been shown to be substantially quicker than the basic algorithm [155].

3.3.2.2 Execution Times for Multiple Case Solutions

Multiple case load-flow solutions, which arise in discrete time simulation and other applications such as outage studies, offer potential time savings compared with the general single case solution. By using the solution from the first load-flow as the starting point for subsequent load-flows, instead of the flat voltage start traditionally employed, the numbers of iterations subsequently required to reach the solution can often be greatly reduced. All of the popular load-flow methods can benefit from such improvements in the initial conditions. In addition, the following advantages apply to multiple case solutions for certain load-flow methods:

- In Second Order methods such as that of Iwamoto and Tamura [74], the Jacobian is formed and factorised at the initial iteration only, using a flat voltage start. The Jacobian is therefore independent of loading conditions, and subsequent load-flow solutions can be obtained using the same factorised Jacobian and repeatedly applying back substitution to obtain new voltage corrections. Topology changes, and transformer tap and generator reactive limit adjustments require further processing which erode the general improvements in execution times. However, the overall saving in execution times can be substantial [39].
- The Newton-Raphson method gains the maximum benefit from good initial conditions on account of its convergence characteristic. The work of Keyhani [77] and Stott [134] has shown that although the convergence rate of the method is quadratic near to the solution, it can be significantly less than quadratic when far from the solution, particularly when transformer tap and generator reactive limit adjustments are made. Therefore the use of previous solutions as initial conditions serves to shift the convergence pattern into the quadratic region of the characteristic.

3.3.3 Storage Requirements

In the early years of the development of the load-flow, the small core memory sizes of computers dictated that storage requirements be kept to a minimum. Methods with low storage requirements still offer positive benefits, allowing larger networks to be solved on relatively small machines. However lack of memory is no longer the pressing problem that it once was. In the proposed time-based analysis approach the storage requirements of the load-flow are only a small proportion of the total requirements of the software.

The storage requirements for the most widely used load-flow techniques are listed in Table 3.1. The storage requirements are expressed in terms of the number of nodes, n, in the system and constitute the memory required to store and solve the Jacobian matrix equation.

Table 3.1 Load-flow Storage Requirements

Loadflow Method	Storage Requirements	Source of Data
Newton-Raphson	17 - 18n	[134, 70]
Fixed Jacobian	23n	[70, 141]
Decoupled Newton	11 - 12n	[134]
Fast Decoupled	12n	[134, 136]
Second Order	13 - 27n	[70]

The decoupled methods require the least storage because the two decoupled matrices derived from the Jacobian require only one quarter of the memory of the original Jacobian. The overall saving in storage is of the order 35 to 40 percent over the basic Newton-Raphson method.

The Newton-Raphson method needs only to store the upper triangle of the Jacobian unless repeat solutions are performed, as in the Fixed Jacobian method, in which case the lower triangle is stored to allow repetition of the forward elimination phase of the factorisation process. This increases the storage requirement by approximately 40 percent.

The Second Order methods vary in their storage requirements, depending upon whether they use a symmetric Jacobian, permitting storage of the upper triangle only, and whether they update the Jacobian after the first iteration [70].

3.4 The Proposed Load-flow Algorithm

3.4.1 Selection of the Proposed Algorithm

The selection of a load-flow algorithm for discrete time simulation takes into account the criteria outlined in the preceding sections and the nature of the application.

The algorithm considered to be most suitable for this application combines the Efficient Newton-Raphson algorithm of Irving and Sterling [73] with techniques used in the Fixed Jacobian method [93, 141]. The resulting algorithm retains the excellent convergence characteristics of the Efficient Newton-Raphson method while benefiting from the speed improvements of the Fixed Jacobian method. The justification for such a choice is as follows:

- The Newton-Raphson method provides excellent convergence characteristics at all voltage levels, particularly when close to the solution. Its reliability is generally second to none. The penalty for the high rate of convergence is the long execution time per iteration. The algorithm of Irving and Sterling provides improved convergence and numerical stability, with reduced execution times, over the basic algorithm.

- The Decoupled Newton and Fast Decoupled methods are discounted in this case because of convergence difficulties associated with the decoupling assumptions used in these algorithms. The combinations of high and low X/R ratios of lines regularly encountered in distribution system studies, and high levels of system loading associated with certain planning studies render the decoupling assumptions invalid. In cases which do not give rise to convergence problems the speed and simplicity of the Fast Decoupled method are valuable assets. However, reliability of convergence is considered to be of greater importance in this application.
- The Fixed Jacobian method can provide improved performance on well behaved systems, particularly when close to the solution. In the absence of these conditions the method can exhibit poor convergence. The method can offer improvements in speed when used in conjunction with the Newton Raphson method.
- The basic Second Order methods have been shown to be variants of the Fixed Jacobian method. They offer execution times approaching those of the Fast Decoupled method on well behaved systems, but on heavily loaded systems and when converging to high accuracy the numbers of iterations increase markedly, with corresponding increases in execution times.

3.4.2 Details of the Proposed Algorithm

The proposed load-flow algorithm takes full advantage of the nature of discrete time simulation to maximise computational efficiency. The flow chart for the proposed algorithm is compared with that of the existing algorithm in Figures 3.1 to 3.3.

The details of the algorithm are as follows:

1. A flag is passed to the load-flow each time it is called, indicating whether a topology change has occurred since the last load-flow solution. The flag is also set at the first time step of the discrete time simulation.
2. In the event of the topology change flag being set, data integrity checks are carried out, and the Jacobian matrix is evaluated and factorised at each iteration until solution. This is equivalent to performing a full Efficient Newton Raphson load-flow (Irving and Sterling [73]), and ensures maximum reliability of convergence for the first time step of a simulation, and in the event of a significant change in the system state due to changes in topology.

3. If the topology change flag is not set, data integrity checks are not performed. The voltage solution from the previous load-flow solution is used as the initial conditions for the current load-flow, to calculate the initial mismatch vector. The factorised Jacobian from the previous load-flow solution is re-used by applying the solution phase of the Zollenkopf bifactorisation algorithm [156] to the mismatch vector to derive new voltage corrections. This takes the Fixed Jacobian method a stage further by holding the Jacobian fixed over successive time steps.

4. Changes in the Jacobian due to transformer tap adjustments and generator node switching are accommodated by forcing an update and refactorisation of the Jacobian matrix. In practice this occurs comparatively rarely, since changes in the system loading condition from one time step to the next are usually small.

5. The maximum power mismatch is monitored from one iteration to the next, and should the rate of convergence fall below a predefined threshold an update of the Jacobian matrix is performed in order to maintain progress towards the solution. This follows the recommendations of Meisel and Barnard [93] who propose that the Jacobian should be held constant once convergence is guaranteed. The convergence of the Constant Jacobian load-flow is approximately linear, and therefore this is used as the criteria for forcing an update of the Jacobian.

   In practical cases the solution vector changes only gradually from one time step of a simulation to the next, with the result that a single factorised Jacobian can be used to provide reliable convergence for many load-flow solutions before an update is required.

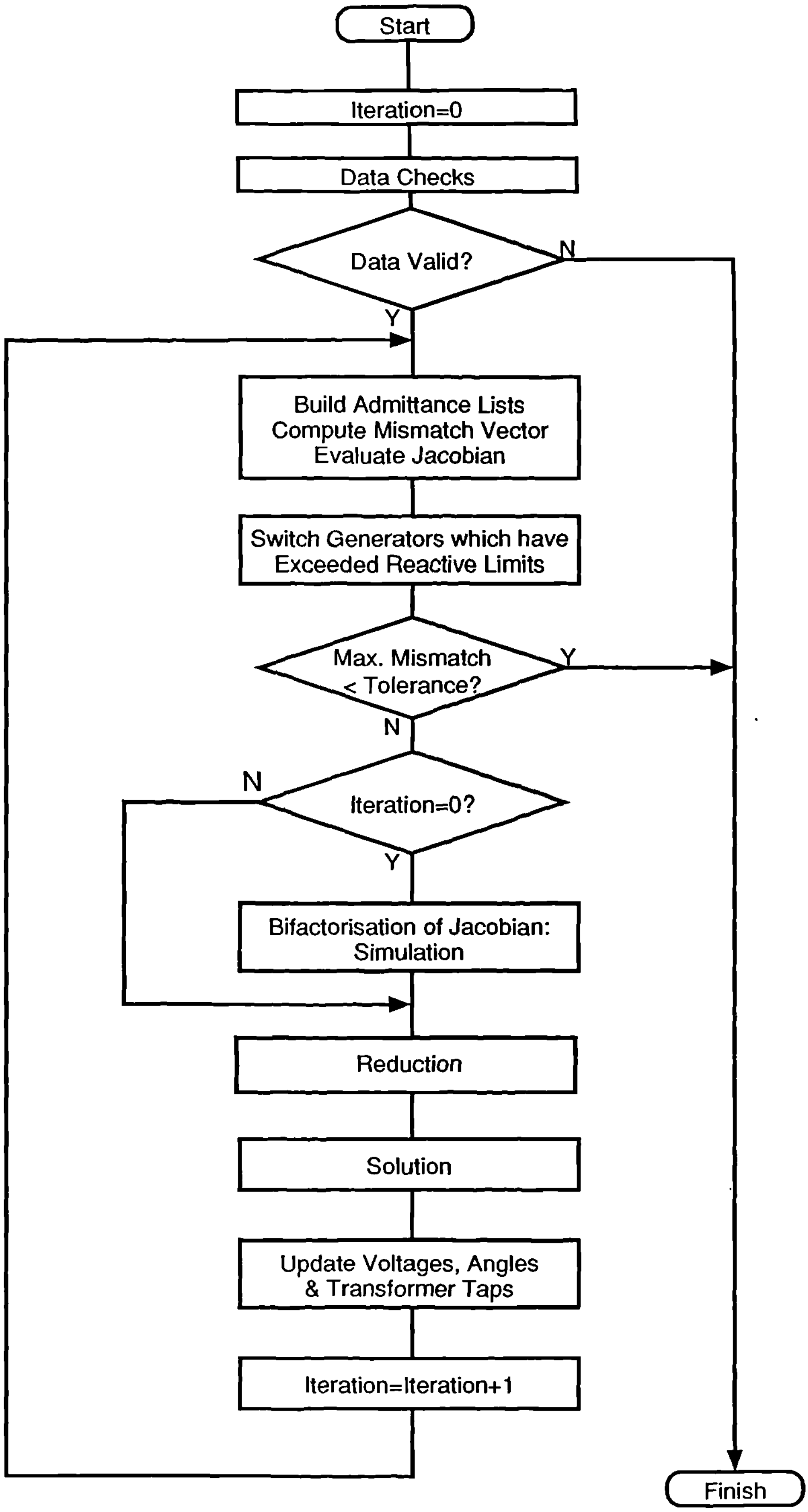

Figure 3.1 Flow Chart for Existing Efficient Newton-Raphson Load-flow

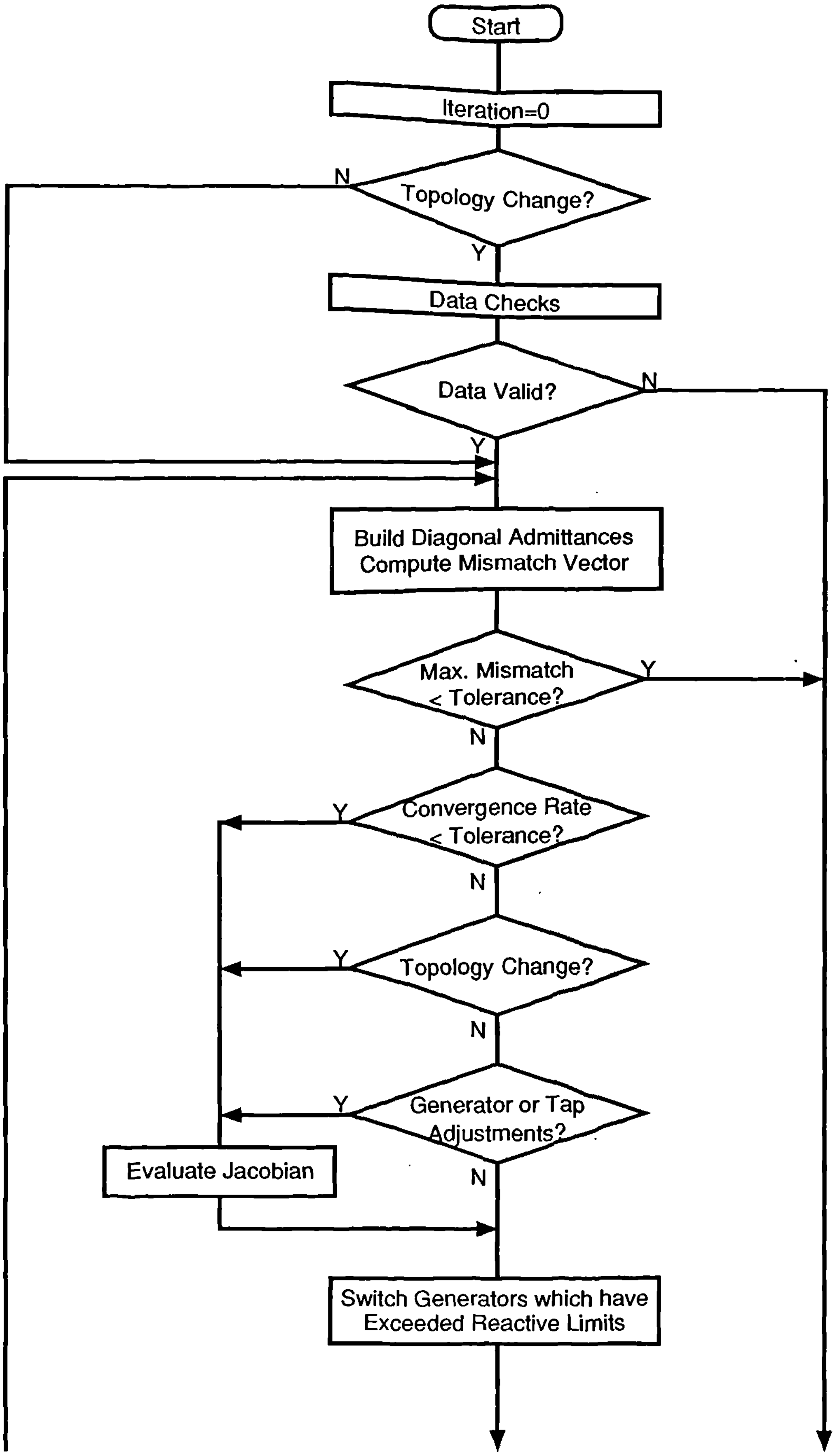

Figure 3.2 Flow Chart for Proposed Load-flow

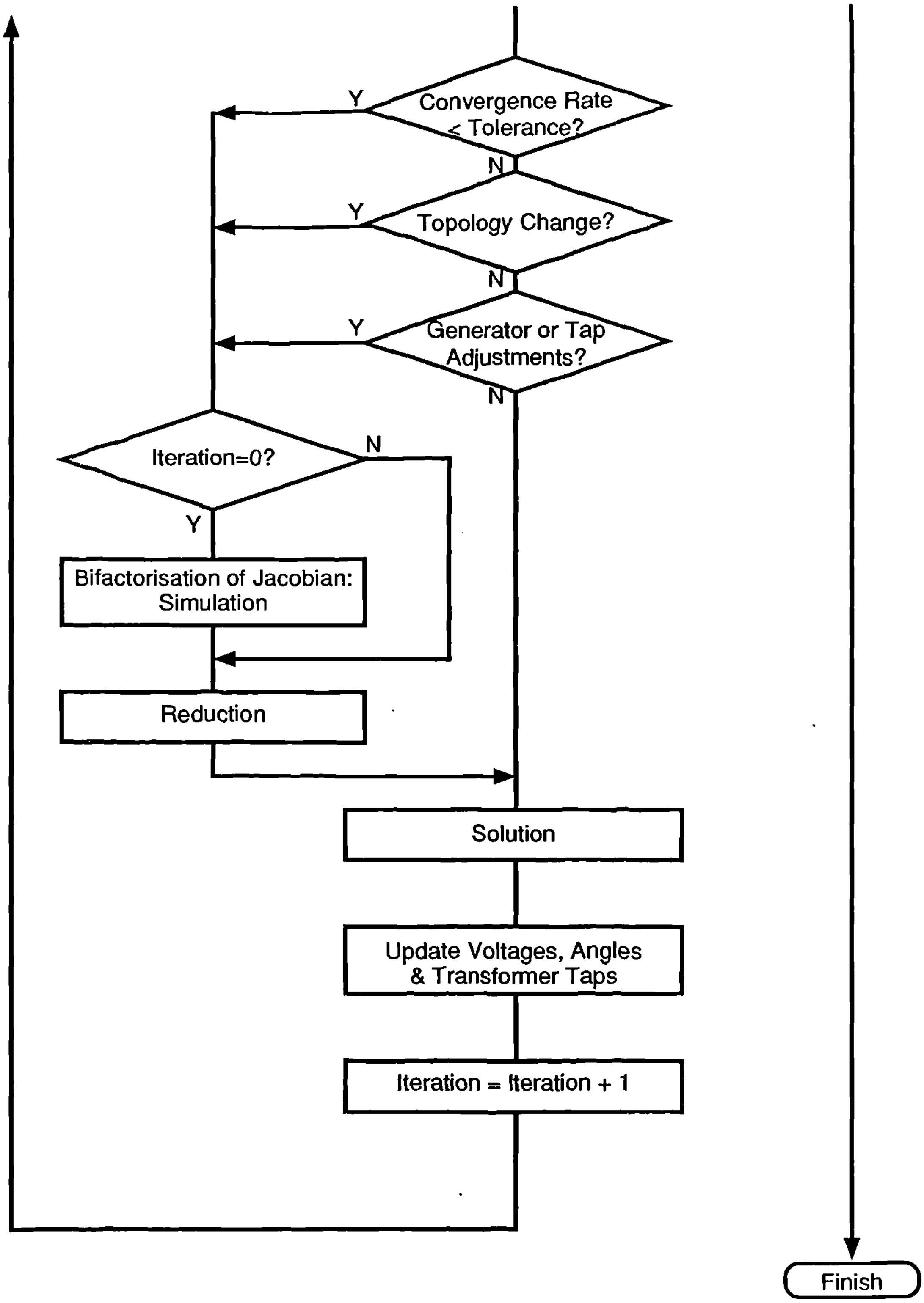

Figure 3.3 Flow Chart for Proposed Load-flow - Continued

3.4.3 Test Results

By monitoring the rate of convergence and updating the Jacobian when necessary, the proposed algorithm achieves the same reliability of convergence as the Newton-Raphson method from which it was derived.

The improvements in performance realised in the proposed algorithm depend upon the nature of the problems to which the algorithm is applied. The test results presented in this section cover a range of systems of differing size and difficulty.

3.4.3.1 Load-flow Test Systems

The systems used to test the proposed load-flow are described briefly in Table 3.2. These networks are described in more detail in Appendix E.

Table 3.2 Load-flow Test Systems

Test System	Voltage levels	On-load Tap changing	Generator node switching	Reactive compensation
7 Node	132 - 20kV	✓	✗	✗
10 Node	66 - 11kV	✓	✗	✗
15 Node	132 - 11kV	✓	✗	✗
30 Node	33kV	✗	✓	✓
348 Node	400-11kV	✓	✓	✓

3.4.3.2 Test 1. Performance Coverage

The execution time of the proposed load-flow is dependent upon how often the Jacobian is updated during the course of a discrete time simulation. This in turn depends upon factors such as the number of changes in network topology during a simulation, how often transformer taps are adjusted, and whether generators in the system reach their reactive limits.

Table 3.3 lists the major functions of the proposed load-flow algorithm, and outlines the time typically required to perform each of these functions, as a percentage of the sum total for each of the test systems. The timings were recorded using the 30 Node test system.

The table shows that the most time-consuming functions within the load-flow algorithm are the calculation of the mismatch vector and the evaluation and bifactorisation of the Jacobian matrix.

Not all of the functions listed in Table 3.3 are performed in a given iteration. From the flow charts in Figures 3.2 and 3.3, three different types of iteration can be defined as shown in Table 3.4. From the tables it can be seen that the Updated Jacobian iteration requires approximately 70% of the time of the Full Newton-Raphson Iteration. The Constant Jacobian iteration requires approximately 34% of the time of the Full Newton-Raphson Iteration.

The Constant Jacobian iteration is therefore approximately twice as fast as the Updated Jacobian used in conventional load-flow programs.

Table 3.3 Major Functions within the Proposed Load-flow Algorithm

Function No.	Description		Approx. Time (% of Total)
1	Data checks		7
2	Build diagonal admittances		3
3	Calculate mismatch vector		18
4	Evaluate Jacobian matrix		19
5	Switch generators which have exceeded reactive limits		3
6	Bifactorisation of Jacobian	Simulation	23
7		Reduction	17
8		Solution	7
9	Update voltages, angles and transformer taps		3
TOTAL			100

Table 3.4 Iteration Types for the Proposed Load-flow Algorithm

Iteration Type	Iteration No.	Func-tions	Conditions of Execution
Full Newton-Raphson	First	1, 2, 3, 4, 5, 6, 7, 8, 9	First load-flow in a discrete time simulation Topology change
Updated Jacobian	Subsequent	2, 3, 4, 5, 7, 8, 9	First load-flow in a discrete time simulation Topology change Generator or transformer tap adjustments Convergence rate less than tolerance
Constant Jacobian	Any	2, 3, 5, 8, 9	Subsequent load-flows in a discrete time simulation No topology change No generator or transformer tap adjustments Convergence rate greater than tolerance

3.4.3.3 Test 2. Execution Times for the Proposed Load-flow

In this test the execution times of the proposed load-flow are compared with the Newton-Raphson load-flow of Irving and Sterling. Table 3.5 lists the total and average elapsed times for a simulation of a winter week at half hour steps, comprising a total of 336 load-flow solutions. Also recorded are the average numbers of iterations.

The times were recorded on a VAXstation 4000-60 workstation. A flat start was used for the first load-flow, subsequent load-flows used the previous solution as the initial conditions. In all cases the convergence tolerance was 10^{-6} per unit on the nodal power mismatches.

Table 3.5 Execution Times for Proposed Load-flow Algorithm

Test System	Load-flow Algorithm	Elapsed Time (Seconds)			Iterations
		Total 336 Load-flows	Average per Load-flow	Relative Time	Average per Load-flow
7 Node	Newton-Raphson	10.0	0.0298	3.4	1.9
	Proposed Algorithm	2.9	0.0086	1.0	3.0
10 Node	Newton-Raphson	12.0	0.0357	2.9	2.0
	Proposed Algorithm	4.2	0.0123	1.0	3.1
15 Node	Newton-Raphson	14.9	0.0446	1.9	2.2
	Proposed Algorithm	7.9	0.0234	1.0	3.5
348 Node	Newton-Raphson	585.9	1.7440	1.1	8.1
	Proposed Algorithm	528.3	1.5630	1.0	9.2

The test results indicate that the proposed algorithm is two to three times faster than the standard method on systems that are relatively easy to solve. However, on the 348 Node system only a 10% improvement in speed was achieved. This system is relatively difficult to solve, as shown by the average number of iterations recorded for both algorithms. A total of 9 generators typically reach their reactive limits at different stages during the course of the solution, and as a result the Jacobian is frequently updated and the rate of convergence is poor. There is little scope for improving the speed through the use of the constant Jacobian.

3.4.3.4 Test 3. Initial Conditions - Flat Start versus Previous Load-flow Solution

In this test the use of a previous load-flow solution to provide initial voltage estimates is compared with the normal flat voltage start, in terms of the number of iterations and execution time required to reach a solution.

The time period studied is a twenty four hour period at half hour steps on a winter weekday loading profile. The results for the networks studied are shown in Table 3.6.

Table 3.6 Effect of Initial Conditions on Load-flow Execution Times

Test System	Initial Conditions	Elapsed Time (Seconds)			Iterations
		Total 336 Load-flows	Average per Load-flow	Relative Time	Average per Load-flow
7 Node	Flat Start	20.0	0.0595	6.9	6.1
	Previous Solution	2.9	0.0086	1.0	3.0
10 Node	Flat Start	33.0	0.0982	7.9	7.0
	Previous Solution	4.2	0.0123	1.0	3.1
15 Node	Flat Start	23.1	0.0685	2.9	5.8
	Previous Solution	7.9	0.0234	1.0	3.5
348 Node	Flat Start	991.9	2.9520	1.9	14.2
	Previous Solution	528.3	1.5630	1.0	9.2

The results indicate that very large improvements in speed can be achieved through the use of previous solutions for the initial voltage estimates of successive load-flows. In all cases the number of iterations required to reach the solution was approximately halved.

3.5 Conclusions

In this chapter the most widely used load-flow algorithms have been described and their suitability for application to the discrete time simulation of distribution networks has been assessed.

The Newton-Raphson algorithm has been described, and its procedure outlined. The principal advantages of the method: its reliability and high rate of convergence, have been noted, with particular reference to discrete time simulation in which previous load-flow solutions can provide good initial conditions for subsequent load-flows. The performance penalty associated with the requirement to update and invert the Jacobian at each iteration has also been described. Three variations on the method by Stott, Sasson et al, and Irving and Sterling have been outlined.

The Fixed Jacobian method has been described and shown to offer reduced iteration times, but at the expense of reduced convergence rates. The advantages associated with combining conventional Newton-Raphson and Constant Jacobian iterations during the course of a solution have been noted.

The Decoupled and improved Fast Decoupled methods have been presented, and the decoupling assumptions described. The speed and simplicity of the methods have been noted. It has also been noted that the reliability of convergence of these methods can be badly affected when the decoupling assumptions fail to apply, as is often the case in systems at lower voltages, or under heavy loading conditions. For this reason a decoupled method was not adopted for the proposed load-flow algorithm.

The Second Order Newton-Raphson method has been described and shown to be a variant of the Fixed Jacobian method, with similar advantages and disadvantages.

A new load-flow algorithm based upon the Newton-Raphson and Fixed Jacobian methods has been proposed for discrete time simulation of distribution systems. The algorithm has been shown to benefit from the basic speed and reliability of the efficient Newton-Raphson algorithm of Irving and Sterling, with further improvements in speed brought by the application of the constant Jacobian method proposed by Miesel and Barnard. This technique is extended with selected updating of the Jacobian across multiple time steps during a simulation. Test results have been presented which indicate improvements in speed of between 10% and 300% when compared with the basic Newton-Raphson algorithm.

Chapter 4. Software Environments for Distribution System Planning

4.1 Review of Existing Planning Environment Architectures

4.1.1 Introduction

As illustrated in Figure 1.5 in Chapter 1, a wide variety of computer-based analysis tools are employed in the operation and planning of the distribution system. Historically many of these analysis programs have been designed as stand-alone tools with their own unique data structures and power system models, often running on specific proprietary hardware platforms. The need to improve the efficiency and effectiveness of these tools has led to the design of software environments which provide access to a number of analysis applications, and contain common facilities for the input and display of data.

This chapter outlines briefly the existing approaches to the design of software environments for distribution system planning, and discusses advantages and disadvantages of each approach. In the light of this assessment objectives for the design of such systems are developed and discussed. The subsequent sections describe the proposed software environment, and describe how the design of the environment meets these objectives. The components of the environment are described with particular emphasis on the time based Insight applications which contain the analysis algorithms reported elsewhere in the thesis.

4.1.2 Outline of Existing Approaches

A large number of software systems exist for the analysis and planning of distribution systems. This review does not attempt to provide a comprehensive survey, but aims instead to highlight some of the features of these systems.

4.1.2.1 Alphanumeric Systems

The use of interactive graphical interfaces for power systems software is comparatively recent, the first systems appearing in the early 1980s. Earlier systems, and many systems currently in use are based upon alphanumeric interfaces; references [12] and [41] provide lists of examples. Features of these systems are listed below.

- Plant data is entered from the keyboard into forms or tables on the screen, or imported from another system via an interchange format.
- In certain cases data from one application can be passed to another within the environment, normally via an intermediate data file.
- The majority of systems do not support the use of more than one application simultaneously.
- Facilities may exist for the display of results on a one-line diagram. In many cases this diagram is built using a design system such as AutoCad, and acts as a template on which data is displayed. Some systems permit the user to define library symbols to represent items of plant, other systems provide little flexibility in this respect.
- Data can be imported and exported via a limited number of interchange formats, but these systems are not open in the wider sense: new third party applications cannot easily be integrated with the environment. Not surprisingly, these systems also provide limited support for recent open systems standards.

4.1.2.2 Early Interactive Graphical Systems

Early software environments for power systems analysis which employed interactive graphics permitted the user to build network diagrams and enter data graphically, using a mouse or digitising tablet. An example is the Dinis system which contains applications for load-flow and fault analysis, and simple reliability studies (Thomas et al [139], ICL [71]). Features of such systems are listed below.

- The workload involved in building and editing the network model is greatly reduced compared with equivalent alphanumeric systems.
- Designed prior to the emergence of standards for graphical user interface and application design, these systems use their own graphics and application management routines. The implications of this include:
    - Limited access to the environment and its data. New third party applications cannot easily be integrated with the environment.
    - Limited support for multiple windows with applications running simultaneously.
    - Increased difficulty in porting of the environment to other hardware platforms and software systems.
    - Lack of support for distributed processing
- Some flexibility is provided in defining the symbols used on the diagram. However, many aspects of the display of data can not be altered by the user.

4.1.2.3 Current Interactive Graphical Systems

There has been much debate recently on the design of interactive graphical software for power systems analysis, and significant numbers of new systems are under development. Changes taking place in the computer industry include moves towards:

- Open system architectures and standards which facilitate porting and evolutionary development of existing systems, and integration of new applications
- Sharing of information and resources between applications
- Distributed processing
- Object oriented design concepts
- Improved interactive capabilities, where system supporting activity is transparent to the user. Greater flexibility in the display of information.

Studies by EPRI [31] and by Imhof and Arias [72] have been directed towards man-machine interface design and an assessment of techniques for the display of power systems data. Geisler et al [52] have proposed a generalised information management system for electrical distribution. This work is of particular interest because it embraces the changes taking place in the computer industry outlined above. Foley et al [48] have explored the use of an object oriented approach for the design of a power system software environment.

4.2 Objectives for the Design of Software Planning Environments

4.2.1 Introduction

From the discussion of existing approaches to the design of software environments for power system planning a set of objectives can be drawn up which seek to build on the improvements achieved in recent years, while addressing deficiencies in earlier generations of these systems. These objectives are described in the following sections.

4.2.2 Design Objectives

4.2.2.1 Open System Design

The term 'open' is used to describe a system which complies with a set of accepted standards in areas such as the graphic user interface, communications and networking protocols, operating system calls, database access and so on. The adoption of such standards in the design of a software system greatly improves the portability of the system and the ease with which it can be integrated with other open systems. The use of standard data access and communications protocols facilitates the transfer of data to and from other systems.

In addition to complying with open systems standards, it is important that the software environment is open in the wider sense, in that the integration of new analysis programs and modification of existing applications can be performed easily without the need to alter or recompile the environment itself.

4.2.2.2 Flexibility

The environment should provide the flexibility to permit the user to perform a wide range of tasks and to customise the display of data. To achieve this it is important that the design of the environment itself should not be specific to particular applications, in order that it should be able to cater for different user requirements. Specific features should be implemented instead at the application level.

4.2.2.3 Modular Architecture

It is also important that the architecture of the environment be modular, with clear interfaces between modules. This facilitates maintenance and development of the software to meet future changes in requirements; specific modules can be upgraded as required with minimal disturbance to remaining modules.

4.2.2.4 Efficient Management of Data

The environment should provide database facilities accessible by all the integrated applications. The system should permit straightforward import and export of data, and sharing of data between applications. Graphical techniques should where possible obviate the need for laborious selection and input of data via the keyboard.

4.2.2.5 Graphic User Interface

A standard Graphic Use Interface (GUI) should be employed to provide a uniform, easy to use front end for the system and its applications. Multiple windows and multi-tasking are desirable to improve operator efficiency by allowing more than one application to run simultaneously.

4.2.2.6 Distributed Applications

A desirable feature is the ability to support distributed processes on different hardware platforms, to allow for the spreading of computational and storage requirements across a number of networked machines.

4.3 The Proposed Software Environment

The proposed environment comprises a number of programs developed at Brunel University, together with the time based analysis applications developed by the author for this thesis. The architecture of the environment has been designed to meet the objectives outlined in the preceding sections.

4.3.1 Environment Architecture

4.3.1.1 Primary Components

The primary components of the proposed software environment are shown in Figure 4.1.

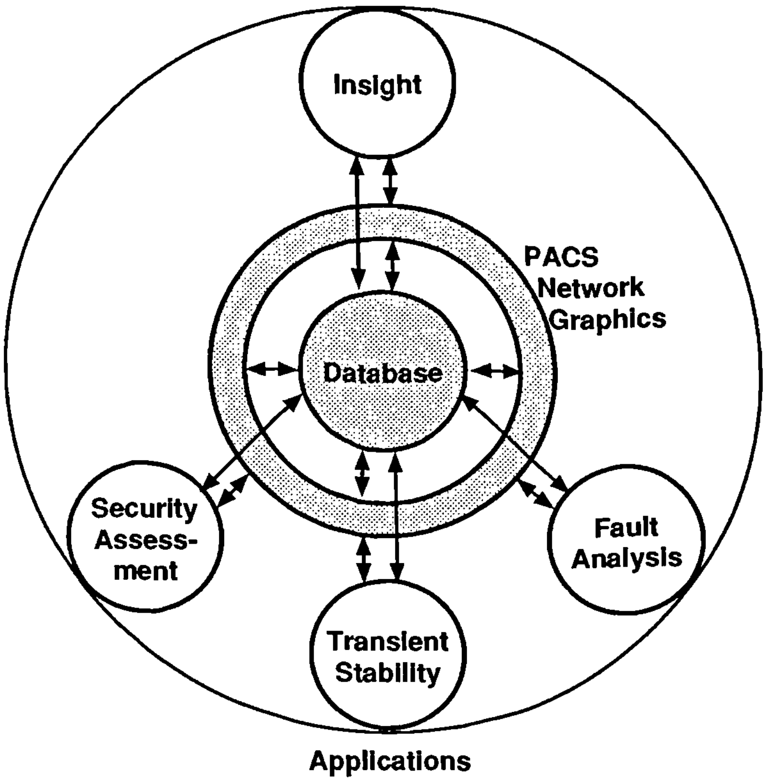

Figure 4.1 Primary Components of the Proposed Environment

The environment comprises:

- Database.
  At the heart of the proposed environment is a relational plant database, accessed via SQL. This database is used by all the applications in the environment for the storage of input data and results. The design of the database is described in Section 4.3.3.

- Network graphics.
  The Power~PACS (Planning Analysis and Control System) network graphics module, is used by all the application programs for the editing and display of network data, and for the display of results. The PACS graphics system is described in Section 4.3.2.

- Application Programmers Interface (API).
  Application programs can communicate with the PACS system and with each other via an Application Programmers Interface. The API is described in Section 4.3.4.

- Insight Application.
  The Insight application contains the proposed time-based analysis algorithms. The Insight Application is described in Section 4.3.5.

- Other Applications.
  In addition to the load-flow analysis performed by the Insight application, a range of power system analysis can be performed by integrated applications, developed at Brunel University. These are described in Section 4.3.6.

4.3.1.2 Client-Server Architecture

The environment employs a client-server architecture, as shown in Figure 4.2.

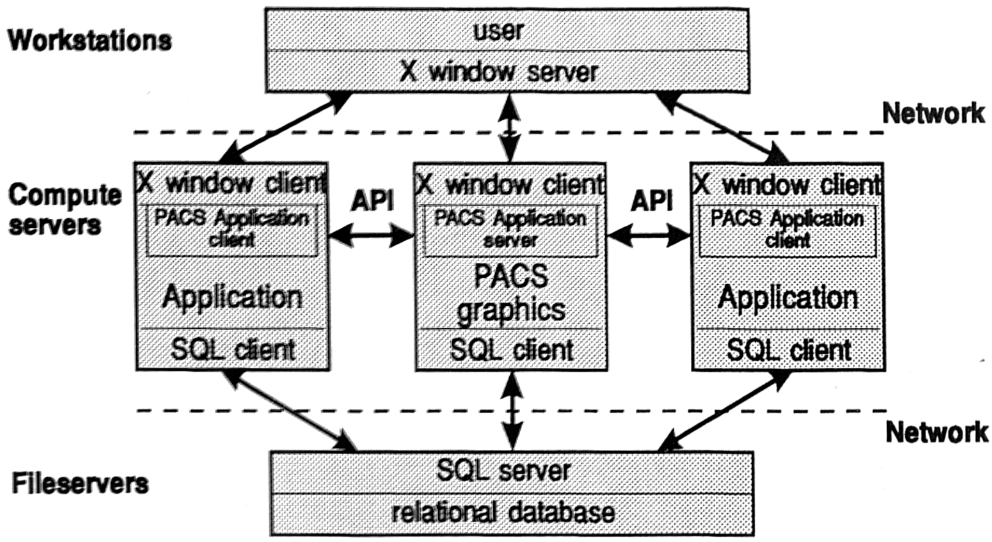

Figure 4.2 Client-Server Architecture of the Proposed Environment

Within this architecture the PACS graphics system acts as an application server to other applications in the environment. Applications can be spawned as subprocesses from the PACS system and can communicate with the graphics via the Application Programmers Interface. The PACS system, via the API, provides facilities for the graphical selection of plant within the diagram and the updating of results. Each of the applications has access to the central relational database via an SQL server.

The proposed architecture supports distributed processes; each of the X window clients can be located on a different platform if required.

4.3.1.3 Integration of Applications

The structure of the environment allows for the flexible integration of applications, at one of three levels:

1. Proprietary database access routines. No API.

   In the simplest case the name of the application is installed in the applications menu of the PACS system, together with the operating system command required to run the application. The PACS user interface allows this procedure to be performed interactively, without changes to program code. The application can now be initiated from the PACS applications menu, and it updates the relational database via its own SQL-based routines. Once the application has completed, the user forces an update of the PACS display in order to view any changes to data in the database.

2. Brunel database access routines. No API.

   A step up in the integration hierarchy occurs when the application uses the public database access routines developed at Brunel University [101]. The use of these routines serves to isolate the application from all but the most substantial changes to the structure of the database which might occur to accommodate new applications and facilities.

3. Brunel database access routines. Brunel API.

   Applications which are fully integrated with the environment employ the API to communicate with the PACS system. The simplest example is the use of the API to instruct the PACS system to update its display once an application has placed new values into the database.

4.3.1.4 Graphic User Interface Design

The graphic user interface (GUI) of the applications in the environment is based upon the X Window System standard, and employs the DECwindows widget set (although it is soon to be transferred to OSF Motif). An overview of the implementation is shown in Figure 4.3.

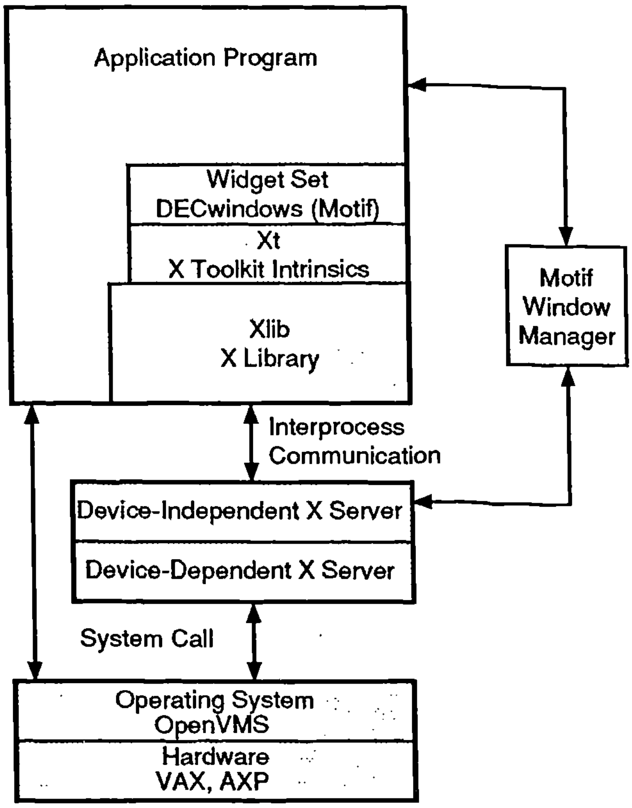

Figure 4.3 Graphic User Interface Architecture

Source: Peddle [108].

The environment is currently implemented under the OpenVMS operating system running on Digital VAX and AXP hardware platforms.

4.3.2 PACS Network Graphics System

The PACS network graphics system, developed by OCEPS [100], is an interactive system for building and displaying network diagrams. The PACS system allows the user to build library symbols for power system plant graphically using a mouse. Data from the relational database can be displayed next to the graphical symbols as the user requires it, and the colours or representation of symbols can be made dependent on values in the database. The network graphics itself is independent of the database model, with the result that changes to entities or relations in the database can be made without the need to alter or re-compile the graphics.

Once a library of standard symbols has been completed the user can build a network diagram by selecting plant from the library and connecting it together. Complex items of plant can be constructed from simpler library symbols to provide an accurate representation of the actual network. The model of the network is built and maintained automatically in the relational database during this process, with the result that any changes to electrical connectivity produced by adding or deleting plant from the diagram or changing the status of switches will result in automatic changes to the electrical models used by the analysis programs.

One of the top priorities in the design of the graphics system was to maximise drawing speed in order to accommodate complete distribution network diagrams.

4.3.3 Database Structure and Implementation

The entity-relation model used to store power system plant data is shown in Figure 4.4. The mechanism for connecting plant together uses the junction entity as the general point of connection. The primary items of plant, shown in the middle row in Figure 4.4, are connected to junctions via their own terminals. The database structure and implementation are described more fully in reference [101]

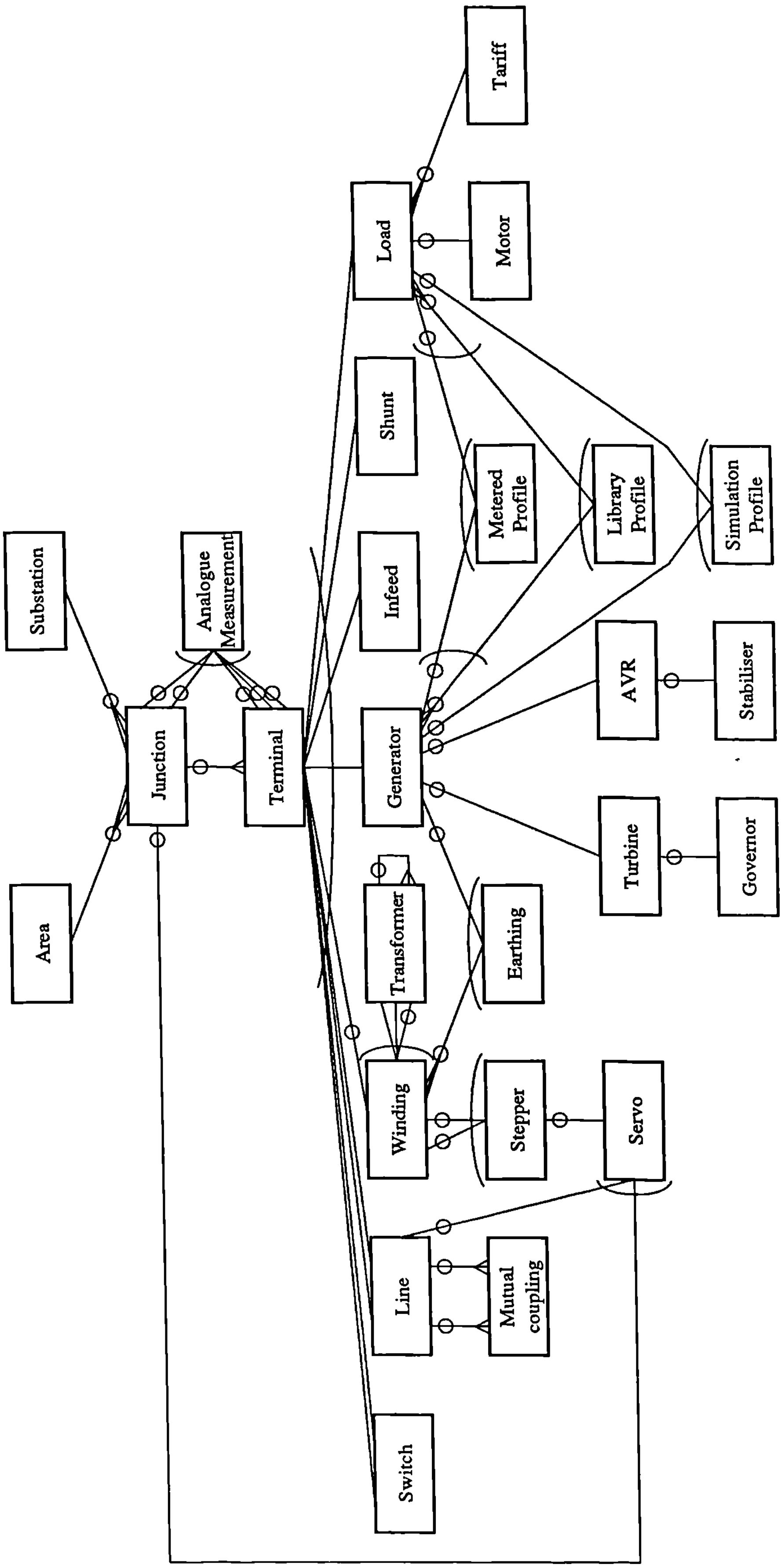

Figure 4.4 Software Environment Database Entity Relation Model

4.3.4 Application Programmers Interface Design

The Application Programmers Interface was developed at Brunel University by Morrison [91, 95] to provide communication channels between applications within the environment. The API employs a client-server architecture. In the case of communications with the PACS graphics system the API server is located in the PACS application. Each of the compliant applications is an API client.

The API uses facilities within the X Window System to exchange data between X Window clients connected to the same X server. The mechanism for the transfer of information is illustrated in Figure 4.5.

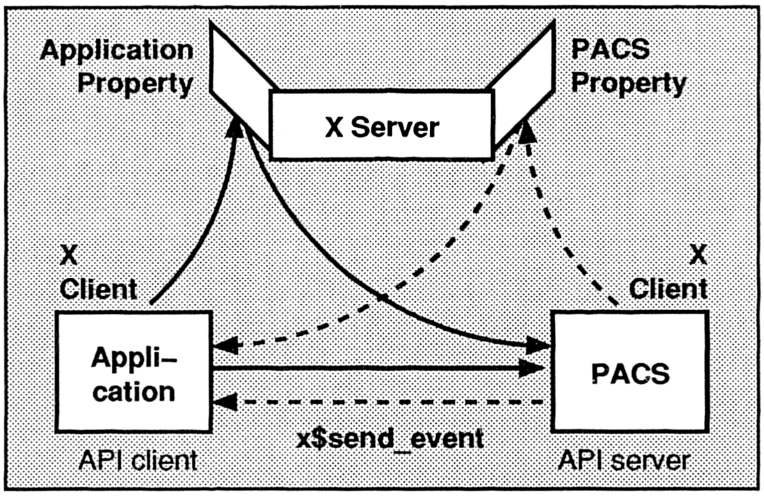

Figure 4.5 Inter-Application Communication Via the API

The X server allows X clients to reserve areas of memory, called 'properties' on the server machine. When an API client first wishes to establish a communication link with the API server it reserves a property using standard Xlib procedures, and registers the identifier of this property with the API server.

To send a message via the API, an application loads a request message into its own property and notifies the API server via a specific X event. The server retrieves the message from the property and returns a response, if required, using the same mechanism with its own property. Individual API clients can use multiple properties to permit communication on more than one 'channel' simultaneously. Similarly the API server supports multiple properties which allow several applications running simultaneously within the environment to communicate with the network graphics.

Applications use the API via a set of public routines for initialising an API client, opening a connection with the API server, and sending a message to the server. Responses from the server are provided via the 'callback' mechanism: when a client sends a message it provides the address of a callback subroutine. This routine is called when the server sends the response, and one of the arguments to the routine is the response message itself.

The most common message types used in API communications with the PACS system are listed in Table 4.1.

Table 4.1 Common API Message Types

Message	Description	Response
REQgetfilename	Requests the database filename of the network currently displayed in PACS	Filename
REQsearchcomplianttotal	Requests the number of selected plant items which match specified search criteria	Number of search compliant items, and database reference of first item in list
REQfetchnext	Requests the details of the next plant item in the list established by REQsearchcomplianttotal	Database reference of next search compliant item in list
REQupdategraphics	Instructs PACS to update its display of values in the database	Completion status

The efficiency of the X Window System in manipulating properties and sending and processing events ensures that the API is able to transfer data between applications quickly, as illustrated in Table 4.2, which lists the number of messages processed per second on two hardware platforms. In this test each message required the client to send a message to the server, the server to retrieve the response from its display list and to send the response message to the client.

Table 4.2 API Performance

Computer Hardware	Messages Per Second
Digital VAXstation 4000-60	83
Digital AXP 3000-60	515

4.3.5 Insight Application

The Insight application contains the time-based analysis algorithms, including discrete time simulation, load allocation, constrained simulation, loss calculation and loss allocation, which are reported in Chapter 2 and Chapters 5 to 9.

The Insight application software and its primary components are described in detail in Sections 4.4 to 4.8.

4.3.6 Other Analysis Applications

A number of power system analysis applications have been developed at Brunel University, and have been integrated with the environment. These applications are described briefly below.

4.3.6.1 Short Circuit Fault Analysis

The fault analysis program performs a steady state analysis of a faulted power system network. The algorithm applies symmetrical components theory, and applies sparse factorisations of positive, negative and zero sequence nodal admittance matrices, (Cheung [30]).

4.3.6.2 Transient Stability

The transient stability program performs a time domain simulation, via numerical integration of machine dynamic equations combined with non-linear algebraic network equation solution (OCEPS [102]).

4.3.6.3 Security Assessment

The security assessment program performs a steady state analysis of the system under a set of hypothetical outage conditions, using a variation of the efficient Newton-Raphson load-flow algorithm (Irving and Sterling [73]).

4.4 The Proposed Insight Analysis Application

4.4.1 Introduction

The following sections describe the structure and implementation details of the Insight application via which the time based analysis algorithms are accessed and controlled. The implementation details are given in some depth, which is justified for two reasons:

1. Historically, chronological algorithms of the type described in this work have been ruled out due to the considerable volumes of input data required and results data generated, together with substantial computational requirements (EPRI [44]). The specific implementations of these methods clearly have a substantial impact on the success of the underlying algorithms. The design of software which enables the user to handle with ease large volumes of data both at the input stage and during the study of results, and the development of techniques which store and retrieve the data efficiently play a very important role in determining whether a particular analysis approach is feasible. The solution of these problems therefore constitutes an important part of the work presented in the thesis.

2. Certain techniques employed in the design of the user interface software have not been reported in the power systems literature.

4.4.2 Overview of the Insight Analysis Application

The proposed Insight application comprises several components which fall naturally into three categories, as shown in Figure 4.6. The figure also shows the sources of data for the Insight application.

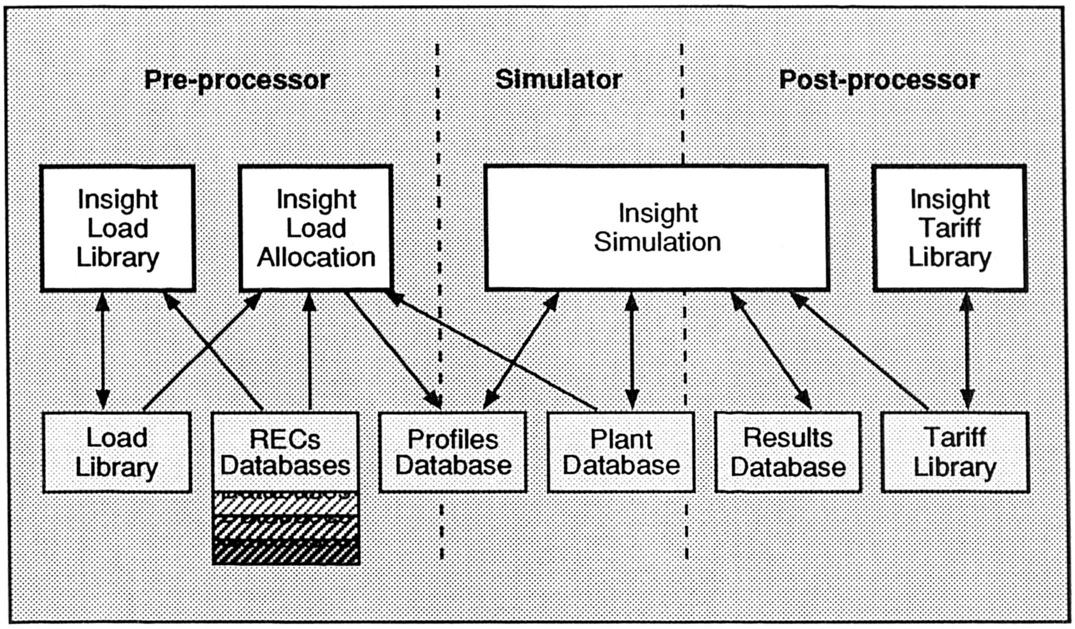

Figure 4.6 Insight Application Components

The Load Library and Load Allocation components comprise the Pre-processor stage which concerns the preparation of input data for the simulator.

The Insight Simulation component represents the Simulator stage, which contains the discrete time simulator and other time-based analysis algorithms.

The Post-processor stage contains facilities for the selection and display of results, and further analysis including loss calculation, allocation and costing.

4.4.3 Data Storage Considerations

4.4.3.1 Categories of Analysis Data

The data required for time-based load-flow analysis can be classified into three categories:

1. Static plant data, which includes network impedances, generator limits, transformer tap step limits and so on. This will be referred to as plant data.

2. Time-based power data for loads and generators, which will be referred to as profiles data.

3. Time-based results which define the state of the network, including power injections for loads and generators, voltages and angles at junctions and transformer tap positions, which will be referred to as results data.

The specific attributes stored in each of these categories for each item of plant are listed in Appendix D.

Two factors which affect the selection of methods for the storage of data in each category are the frequency with which the data needs to be accessed and the volume of data in the category. Table 4.3 describes the access characteristics of each category for time based load-flow analysis. The table also lists the volume of data required for a year's simulation at hourly intervals (8760 time steps) on the 348 node distribution test system. The figures are based upon the database attributes listed in Appendix D.

Table 4.3 Analysis Data Characteristics for Time Based Load-flow Analysis

Category	Access Characteristics		Volume/MByte 1 yr, 348 node
	Read	Write	
Plant Data	Prior to editing of input data Prior to discrete time simulation	At end of discrete time simulation At each step during results playback	0.7
Profiles Data	Prior to discrete time simulation	During load allocation	10.3
Results Data	During display of simulation results Prior to further analysis such as loss costing	At each step of discrete time simulation	828.7

The following section discusses the potential methods for the storage of data in each category.

4.4.3.2 Database Technology

Four of the most widely used database options for the storage of power system analysis data are summarised in Table 4.4 in terms of four criteria: speed of data access, facilities for data access and manipulation, flexibility in the modelling of power system plant, including the ease with which models can be extended, and security features to prevent loss or corruption of data. These options are:

1. Flat File Database

   In a flat file system, data is stored sequentially as a series of records along with indexing information. The structure of the file normally mimics the data structures used in the application program. Flat file database systems are normally custom-built for specific applications, and are therefore application specific.

2. Network Database

   A network database consists of a set of records, and a set of links which relate a parent record type to multiple occurrences of a child record type (Date, [33]). Hierarchical databases are a restricted form of network database in which a child record can have only one parent. In network database systems a child record can have any number of parents. Network data manipulation languages exist for locating specific records and traversing the record-link structure.

In this approach complex data structures can be represented within the database using the parent child hierarchies. The penalty for the direct modelling of complex data is increased complexity in the querying and modification of such databases.

3. Relational Database

   In a relational database system the data is represented as a series of tables. Operators for data retrieval essentially generate new tables out of existing ones (Date [33]). Relational databases store complex data structures as sets of simple tables. The implications of this approach include reduced complexity and improved flexibility in the querying and modification of the database, but at the expense of poor performance when modelling complex data structures. Since the early 1980s relational systems have become the predominant database system approach.

4. Object Oriented Database

   In the object oriented approach data is represented as a series of discrete objects which incorporate both data structure and behaviour (Rumbaugh et al. [117]). Objects generally possess certain characteristics, including a unique *identity*, *class* membership, a set of *polymorphic operations* which define how a particular object behaves, and *inheritance* of attributes and operations from other classes via a hierarchical relationship.

   Complex data structures can be modelled directly using objects, and through the mechanism of *encapsulation* irrelevant data can be hidden from the user, thereby reducing complexity when it comes to queries and modifications to the database. It should be noted however, that these characteristics also serve to reduce flexibility when querying the database or performing substantial modifications.

   Object oriented database systems are still comparatively recent, and are still evolving towards a mature technology. Widely adopted standards for object models and query languages do not yet exist [48].

Table 4.4 Database Options for the Storage of Power Systems Analysis Data

Criterion	Database Assessment			
	Flat File	**Network**	**Relational**	**Object-oriented**
Speed	Potentially fast, but depends upon access characteristics	Potentially fast	Comparatively slow	Potentially fast, depending upon access characteristics
Data Access	Custom built routines are normally required. Flexibility is poor	Data access can be complex.	Good. Flexible import/export via the SQL standard	Difficult until standards for object models and query languages become established
Data Modelling Flexibility	Poor. Extensions to data models normally require changes to entire database	Extensions to data models may require substantial and complicated changes to database	Relatively good. Extensions to data models can often be made without disturbing existing data	Good. Changes to data model for one object class are independent of other classes
Security	Poor, unless facilities to improve security are built into the access routines.	Generally good.	Good. Most relational databases provide a range of security features.	Generally good. Many object-oriented databases provide security features

From the table it can be seen that relational database systems currently provide the best combination of data access facilities, modelling flexibility and security, but suffer from long access times. Object oriented databases are showing promise, but as yet no widely adopted object models for power system data and object oriented query languages have become established. Network databases and flat data files can achieve high speed at the expense of flexibility in the modelling of data. Network databases become complicated to use in the case of complex data structures. Flat files are too primitive for use with complex data structures, but may be suitable for the storage of simple data structures which need to be accessed sequentially.

Based upon the above criteria, the most desirable method for storing all three categories of data, from the standpoint of security and flexibility and openness, would use a single relational database.

4.4.3.3 Evaluation of Relational Database Management Systems for Time Based Load-flow Analysis

The suitability of two relational database management systems (RDBMS) for time based load-flow analysis has been assessed in terms of performance by Gann [50, 51]. Database access rates were reported for a number of network sizes, using a variety of database configurations. The general database model developed at Brunel University [101] was used, Figure 4.4.

The best results obtained from tests conducted on a generalised 500 substation network are summarised in Table 4.5, for database configurations with and without a Ram disk.

Table 4.5 RDBMS Performance for Time Based Load-flow Analysis

RDBMS Configuration	Accessing Performance for 500 Substation Network			
	Elapsed time	Elapsed time per time step		Total Elapsed Time for 24 Steps (min)
	Read Plant Data (secs)	Read Profiles Data (secs)	Write Results Data (secs)	
Ingres	145	41	118	66
Ingres Ram Disk	100	24	78	42
Rdb	109	10	31	18
Rdb Ram Disk	95	9	22	14

Performance figures were recorded on a VAX8600 minicomputer

The test network comprised generalised generator and load substations as shown in Figure 4.7. The database records required for each substation type are listed in Table 4.6.

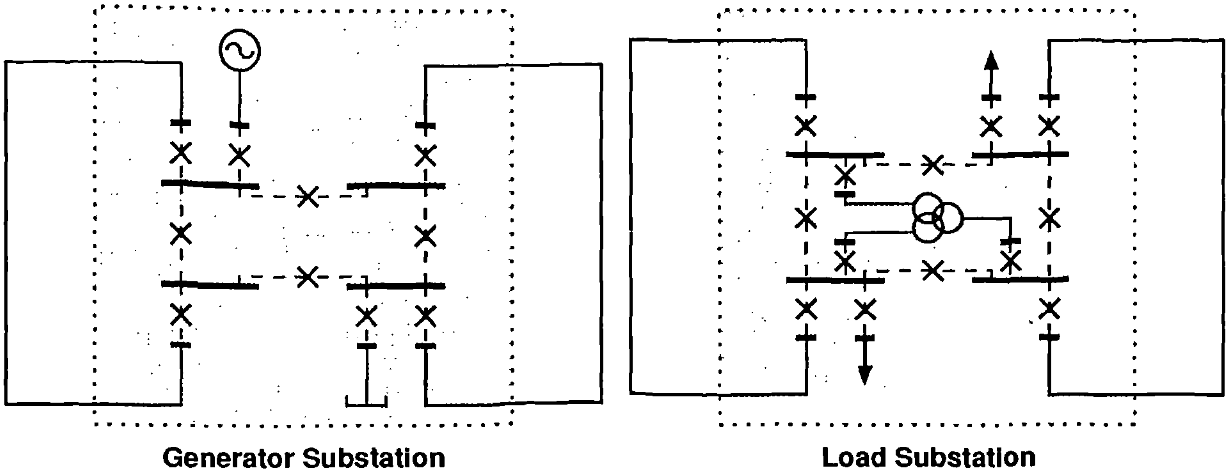

Figure 4.7 Generalised Substation Configurations for the RDBMS Evaluation Test Network

Source: Gann [51]

Table 4.6 Substation Details for RDBMS Evaluation Test Network

Substation Details	Substation Type	
	Generator	Load
Number of substations in test network	50	450
Number of records of plant data	51	71
Number of records of profiles data per time step	2	2
Number of records of results data per time step	13	18

The 500 substation test network represents the largest system likely to be studied in practice, and the performance figures therefore apply to the 'worst case'. Nevertheless it is clear, as concluded by Gann [51], that the performance obtained is not adequate for the indiscriminate use of a relational database system for time based load-flow analysis, particularly in view of the fact that the figures for total elapsed time apply to a simulation of just 24 time steps. In spite of the fact that the latest workstations are very much quicker than the VAX8600 machine used for the tests, this conclusion still applies for longer studies on larger systems. The performance of RDBMSs in connection with power systems applications has been reported elsewhere, Rumbaugh et al. [117].

The following section describes the methods employed to overcome this limitation in the proposed Insight application.

4.4.3.4 Method for Storage of Plant Data for Time Based Load-flow Analysis

A relational database system was selected for the storage of plant data, for a number of reasons:

1. The plant data comprises a small proportion of the total, particularly in the case of lengthy simulation studies. The database access times are therefore relatively small, even when using a relational database.
2. The plant data is required by other applications within the proposed software environment. A relational database provides the best support for open access to such data.
3. Through the inclusion of attributes such as voltage, power injections, currents and so on in the plant database model, the relational database can be used to hold a 'snapshot' of the state of the system at a particular instant in time. Time based results for a particular time step can be copied to the relational database for subsequent display on the PACS diagram, and for use as initial conditions by other applications such as fault study and transient stability.

4.4.3.5 Method for Storage of Profiles Data for Time Based Load-flow Analysis

An optimised file-based database is used for the storage of profiles data. The following factors were influential in the choice of this approach:

1. The performance of relational database systems was considered insufficient at the present time for use with the substantial volumes of profiles data required in practice.
2. Efficient access is an important requirement in achieving acceptable simulation times. File based databases offer very high rates of data transfer if the data can be read sequentially in large blocks.

   The data structure for the storage of a power profile is simple, comprising the times to which the data relates, and pairs of active and reactive power values for each time step. Such a structure is well suited to storage in a flat file, since the indexing is essentially very simple and the data is accessed sequentially in blocks.

3. Profiles data is imported from a variety of distribution company sources using the proposed Load Allocation application. The transfer of data from these sources is frequently a slow and inefficient process. It is important that this process is performed as infrequently as possible, and that profiles data is held in a form in which it can be accessed efficiently as and when required for simulation studies.

The proposed profiles database structure comprises a header and a body, stored in different files, as shown in Figure 4.8.

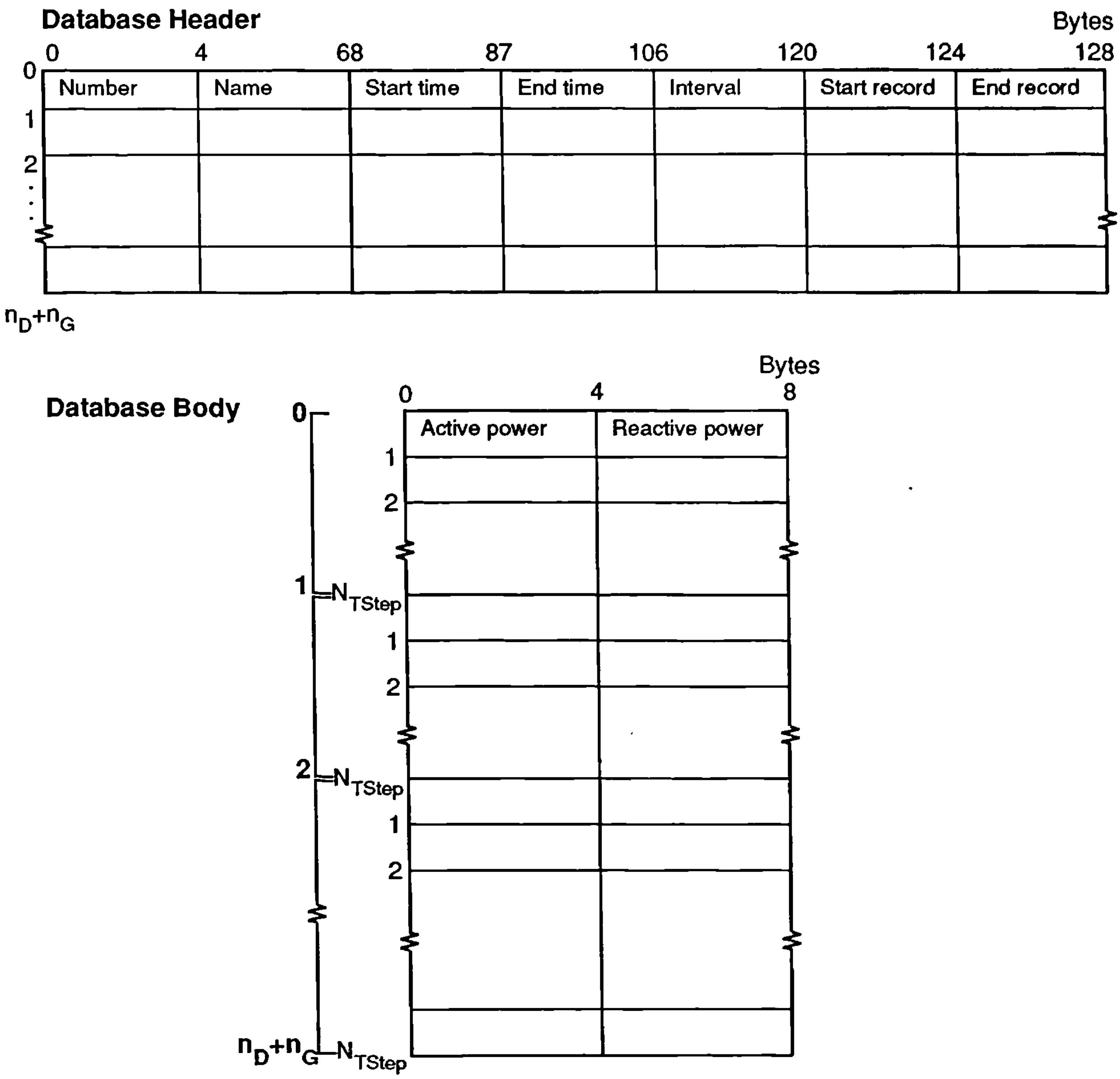

Figure 4.8 Profiles Database Structure

For maximum efficiency both the header and body are organised as fixed length unformatted records, with direct mode of access. Indexing information in the database header specifies the location of the profile data for a particular load or generator, providing direct access to specific profiles. The database body contains active and reactive power values arranged sequentially for each load or generator.

To improve levels of security a library of self contained publicly defined routines provide the sole means of access to the database. This library includes routines to reorganise the database should it become fragmented due to repeated deletion and insertion of profiles of different lengths.

The name and number of each profile stored in the profiles database match the name and database reference of the corresponding load or generator entity in the relational plant database. The Load Allocation application maintains the consistency between the two databases.

The performance of the profiles database is compared with that of most efficient relational database configuration used by Gann [51] in Table 4.7. The table clearly shows that there is a computational overhead associated with the proposed profiles database, which results in poor overall access times for profiles of very short duration, compared with the relational database system. The subsequent rate of data transfer is many times quicker than that of the relational database however, with the result that the profiles database achieves much higher levels of performance for profiles comprising more than a handful of time steps.

Table 4.7 Performance of the Proposed Profiles Database for Time Based Load-flow Analysis

Database	**Accessing Performance Elapsed time to read profiles data for 500 substations for profiles of different duration (secs)**			
	1 step	**12 steps**	**24 steps**	**1488 steps**
Proposed Profiles Database	45	50	52	442
Rdb Ram Disk	9	108	216	13392

Performance figures were recorded on a Digital VAX8600 minicomputer

4.4.3.6 Method for Storage of Results Data for Time Based Load-flow Analysis

Of the three data categories, the storage of the results data poses the most difficult problem, due to the volume of data generated. The problem is compounded by the relational database model used for the storage of plant data. This model provides great flexibility in the modelling of complex arrangements of electrical plant, but at the expense of large numbers of junction and terminal entities (Gann [50]). Time based results must be available for each of these entities.

The proposed approach adopts the following techniques:

1. Time based results are stored in the node-branch form used by the load-flow program to reduce storage requirements. Indices set up by a topology program are used to map the full relational database model of the network to the node-branch form and vice versa. The use of the node-branch model greatly reduces the volume of results data which

needs to be stored, as shown in Figure 4.9, which compares the node-branch model with the full database model for three of the load-flow test systems. Please refer to Appendix E for further information concerning the configuration of the test systems.

2. Only the state vector from the load-flow solution is stored. All other results are calculated as and when they are required. The state vector comprises the voltage magnitude and angle at every node, plus transformer tap positions. Figure 4.9 shows the reductions in storage achieved for each of the test systems using just the state vector, compared with storing all the node and branch results. It should be noted that some additional temporary storage is required to hold calculated results for display or further analysis.

3. Results data is stored in virtual memory. The state vector at each time-step is not written explicitly to disk but is held in in-memory data structures. The results are therefore paged on and off the disk efficiently by the operating system. The effect of this approach is that while the user is studying the results the data will automatically be paged off the disk into memory, and can be accessed extremely quickly. If the user performs other tasks the operating system will divert resources in that direction.

4. In cases where results are needed by other applications, three approaches are available. For applications requiring a 'snapshot' of the results at a specific point in time, such as the fault study application, the state vector is used to calculate a full set of results in node-branch form, which are subsequently mapped into the full database form and copied to the relational plant database. For applications requiring results in time based form, the API is used to transfer results profiles directly to the application. An example of this approach is the Graph application which plots a series of values transferred via the API. Finally, if an application is not integrated with the environment, results can be saved to disk in ascii tabular form, suitable for subsequent importing into the application.

The use of these techniques serves to reduce the volume of results data to a level that is manageable on today's workstations, and to maximise the efficiency with which results can be accessed for display or further analysis. The calculation of results from the state vector, rather than saving them explicitly results in a transfer of the workload away from the hard disk and towards the cpu. This will permit greater exploitation of future developments in computer hardware in which increases in cpu speed tend greatly to outstrip increases in disk access rates.

Table 4.8 Comparison of Results Storage Requirements Using Different Data Models for Simulation of a Year

Test System	Storage Requirements 1 Year Simulation (MByte)		
	Full Database Model	Node Branch Model	State Vector Model
348 Node	828.7	165.9	32.8

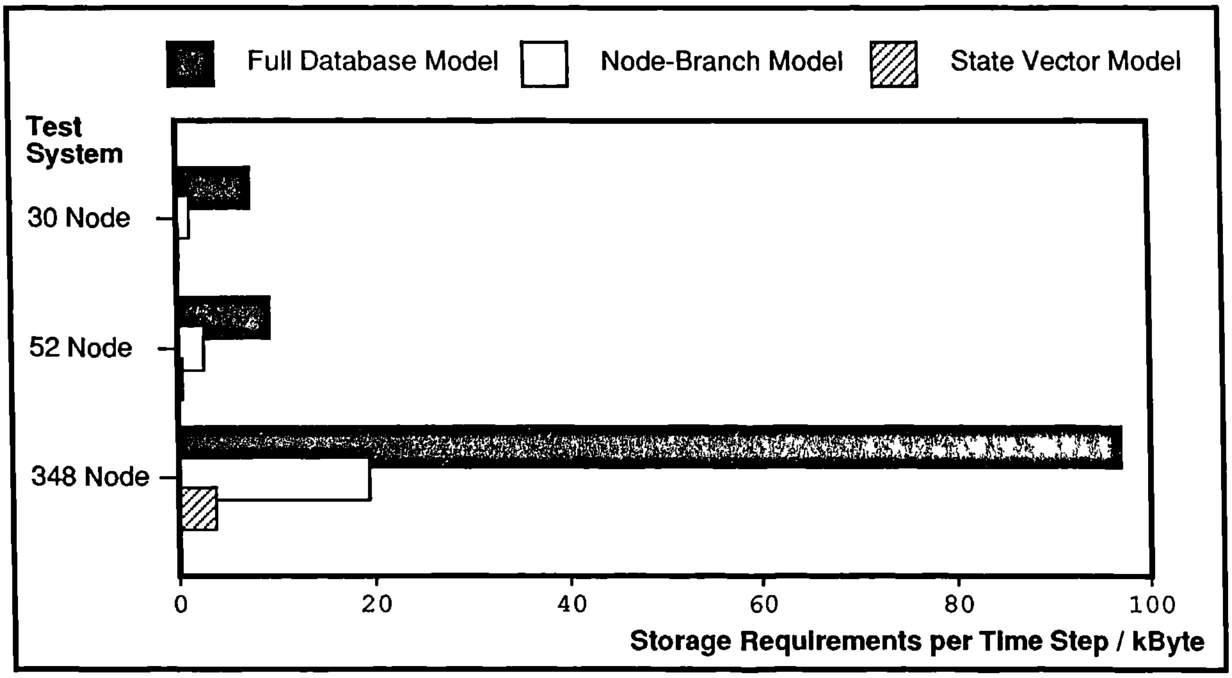

Figure 4.9 Reduction in Storage Requirements for Results Data

4.4.3.7 Summary

It has been shown that the storage and handling of data associated with time based load-flow analysis is a difficult problem, due to the large volumes of information and the speed with which data must be accessed to maintain acceptable levels of program performance. In addition any solution must allow for the sharing of data with other applications within the environment.

The solution to this problem has taken into account the different volumes and access characteristics of data in the three categories: plant data, profiles data and results data. A method of storage has been designed for each category to achieve the requirements stated above.

A relational database system is used for the storage of plant data, which provides flexible modelling of power system plant, sharing of the plant data between applications and a mechanism for passing simulation results for a particular point in time to other analysis applications as initial conditions.

A file-based database system has been implemented for the storage of profiles data which provides compact storage coupled with efficient access.

Results data is stored in virtual memory for the quickest possible access. The use of the node-branch data model and the storage of just the state vector have substantially reduced the storage requirements to well within the capabilities of current workstation hardware for simulations of a year on systems of realistic size.

4.4.4 Application and Interface Management

4.4.4.1 Separation of Form and Function

A common approach to the design of power system analysis software in the past has been to embed the user interface in the application itself, without clear interfaces between the interface and the application routines.

However, important benefits can be gained by separating the form of an application (the user interface) from its function (the analysis routines). This is particularly true of the latest interactive graphic user interfaces. Potential advantages apply to the following areas:

- Software development and maintenance
  Modifications to the software can be made more easily if there is a clearly defined interface between interface and application. Changes to the interface can often be made without disturbing the application routines and vice versa.

- Software portability
  Normally in power system analysis software the analysis routines are relatively portable, because they do not rely heavily on external, operating system dependent functions. Separation of the interface and application routines improves portability by defining more clearly the parts of the code which are hardware or operating system dependent.

  An example of this is the provision of different user interfaces for different hardware platforms, but retaining the same application routines. A simple text-based interface could be provided for a system accessed via alphanumeric terminals, while an interactive GUI could be provided for the same application accessed via workstation X-terminals.

- Macros
  Separation of form and function within an application permits calls to the application routines to be recorded and stored as a macro. Macros can be played back at a later stage by repeating the application calls in the correct sequence. Such a facility offers substantial benefits in power system planning studies in which a particular type of study needs to be repeated for a number of network configurations, but this facility has not been reported in the literature.

- Auditing

  As in the case of macros the separation of interface and application routines facilitates the recording of sequences of actions by the user. These actions can be stored in a log file to provide a record of the session. In addition, should the system fail for whatever reason, the log file could be used to reconstruct the session by repeating the actions in sequence.

The following sections describe how these potential advantages are realised in the design.

4.4.4.2 Structure of the Proposed Insight Applications

The top level interface between the GUI and the application routines for the proposed Insight Applications is shown in Figure 4.10.

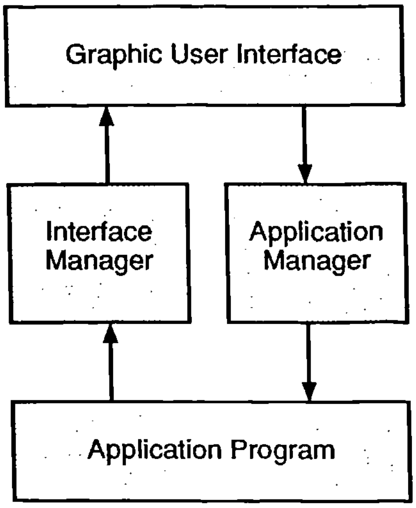

Figure 4.10 Overview of the Interface Between GUI and Application for Insight Application Programs

Actions performed using the GUI generate commands which are sent to a routine called the Application Manager. The Application Manager interprets the commands and calls the appropriate application routines. In a similar way information is returned to the interface via commands to the Interface Manager which in turn calls routines within the GUI for updating graphical displays and so on. The components involved in the transfer of information from interface to application are shown in Figure 4.11. The procedure by which the application returns information to the interface is similar.

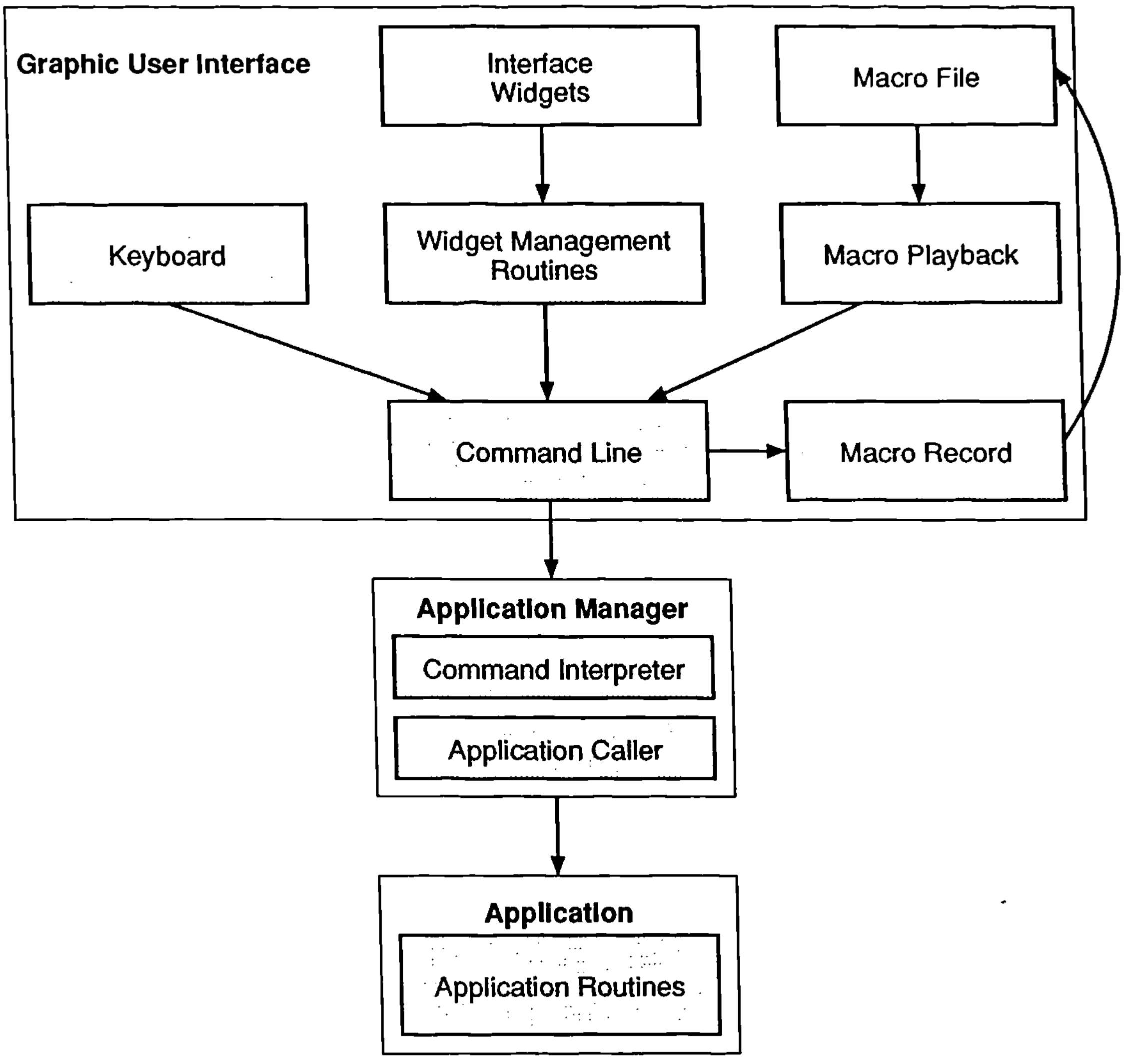

Figure 4.11 Components of the Interface Between GUI and Application for Insight Application Programs

These components are described in the following sections.

4.4.4.3 Command Line Interface

At the centre of the GUI is a command line, which receives commands from three sources:

1. Interface Widgets

   During normal operation of the program using the GUI, actions performed by the user on widgets in the interface generate 'callbacks' to widget management subroutines. These routines build appropriate commands which are sent to the command line.

2. Keyboard

   As an alternative to interacting with the program via menus and dialogs using the mouse, commands can be typed into the command line directly from the keyboard. The syntax of the command language is straightforward, and commands comprise standard English keywords as described in the following section.

3. Macros

During interaction with the program, commands sent to the command line can be recorded and stored in a macro file. A macro playback feature reads commands from a macro file and sends them to the command line one after the other. A flag set by the user dictates whether the program continues in the event of an error occurring during the playback of a macro, or whether execution is halted. An example of a macro file is given in Figure 4.13.

An additional feature of the Insight applications is an 'autostart macro'. The user can specify a macro to be executed automatically when the program starts up. This feature allows the user to perform standard tasks which are required whenever the program is used, such as the specification of particular plant and profiles databases for example. It also permits the applications to be run in batch mode without user interaction. If the user creates a macro file containing a complete simulation study, including 'Quit' as the last command, the program can be set up to run during off-peak hours to generate a set of results completely automatically, thus minimising the workload on computer systems during busy periods. This is of particular benefit when conducting lengthy simulations on large networks.

4.4.4.4 Command Syntax

Command syntax is illustrated in Figure 4.12. A command comprises command verb, command option, parameter and a set of optional keyword-value pairs. Figure 4.13 gives examples.

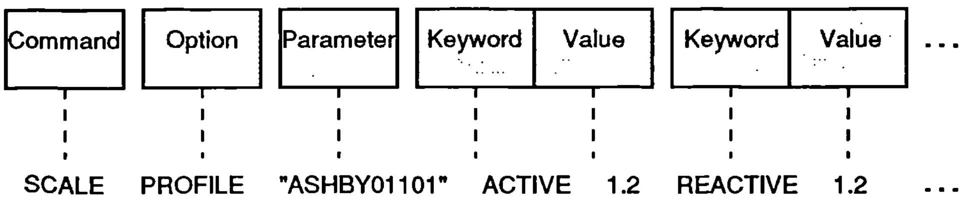

Figure 4.12 Command Syntax for Proposed Command Line Interface

```
!
! MACRO FILE EXAMPLE
!
! Set up simulation
!
open database demo_v291
set times start_time "01/01/1990.00:30:00" -
   end_time "01/02/1990.00:00:00" -
   interval "00000.00:30:00"
!
! Run simulation
!
start simulation
!
! Plot results for Ashby and Cuffley substations
!
plot results "ASHBY01101,CUFFL01101" attribute "VOLT_MAG" -
   device "NEW" display_format "CHRONOLOGICAL"
!
! End of Macro
!
```

Figure 4.13 Macro File Example

4.4.5 Graphical Techniques for Data Selection

4.4.5.1 Introduction

As indicated in Section 4.4.1 an important requirement in the design of software for time based load-flow analysis is the efficient management of large volumes of data. This section describes two techniques employed in the Insight application programs to achieve this aim.

4.4.5.2 Graphical Selection of Plant

During a planning study it is frequently necessary to specify particular items of plant for editing or for the display of results. The Insight application uses graphical techniques in conjunction with the PACS network graphics system to allow the user to select plant from a large volume of data. To select one or more items of plant, the procedure is as follows:

1. In the PACS window the user selects the Select Variables function and with the mouse drags a box around the area of interest on the network diagram.
2. In the Insight application window the user selects the appropriate editing facility. At this point the Insight application sends a message to the PACS graphics system via the API requesting the database references for the items of plant (variables) selected by the user. When it has received the response the Insight application filters out any irrelevant items of plant and presents the names of the remaining items to the user in a list box.
3. The user selects the required items from the list by clicking on them with the mouse.

4. New selections can be made by performing another Select Variables operation in the PACS window, and pressing an Update button in the Insight editing window, which forces Insight to query the PACS system for another selection.

Figure 4.14 illustrates this procedure for the selection of loads and generators for editing of profiles data. In this example the user has selected a total of 92 miscellaneous items of plant by dragging a box around four of the 11kV substations using the mouse. When the user subsequently selects the Edit profiles option in the Insight application the program queries the PACS system as to which plant is selected, and presents just the loads and generators to the user. In this case there are four loads in the user's selection.

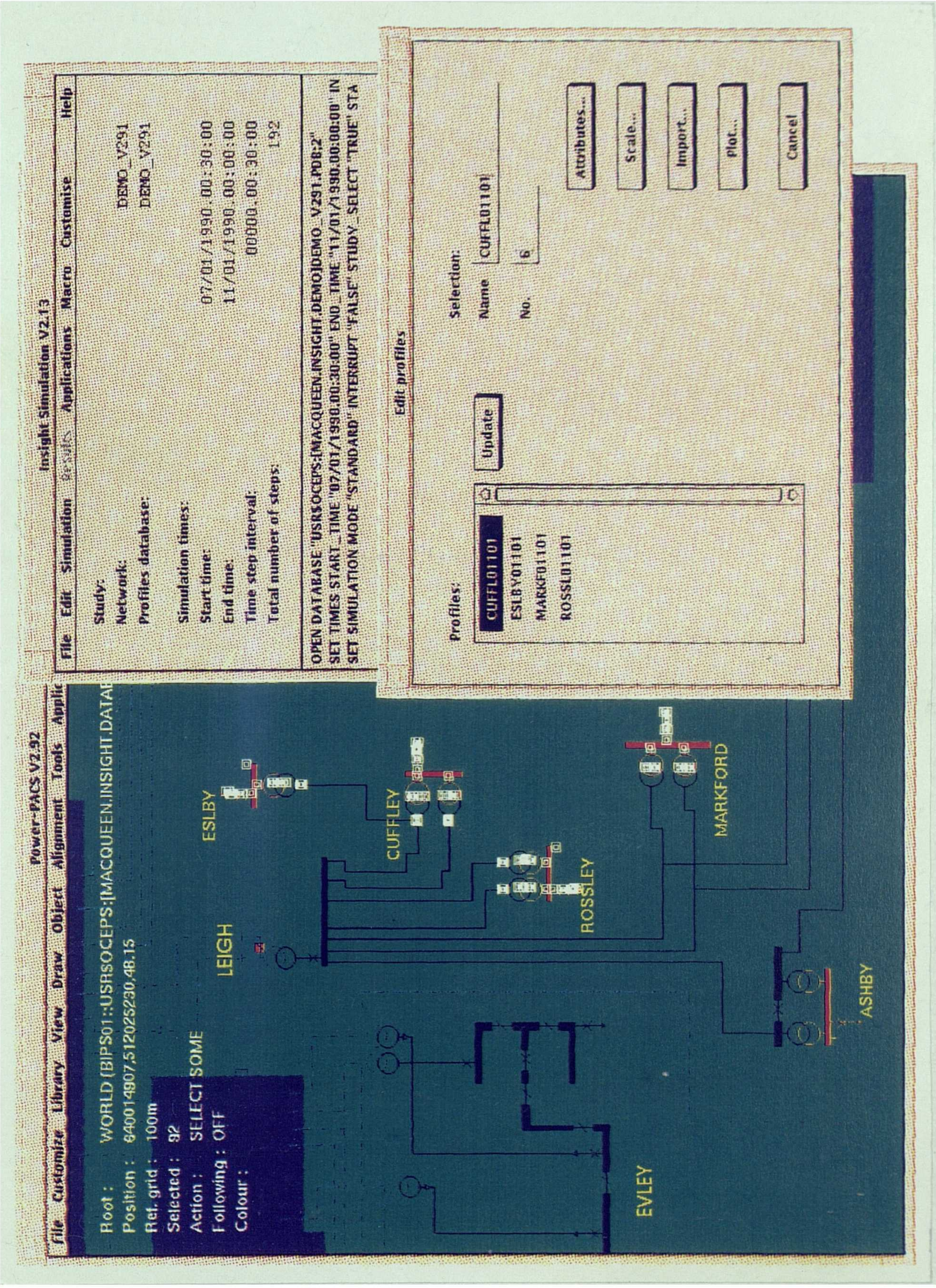

Figure 4.14 Graphical Selection of Plant Within the Insight Application

4.4.5.3 Selection of Electrical Circuits

All items of plant in the plant database have a logical attribute named 'In Study'. The concept of a study permits certain database entities to be included or excluded from particular operations. The In Study attribute can be set manually to True or False, or it can be set automatically using a Study Select application developed at Brunel University. The Study Select program operates in two ways, depending upon whether any items of plant are selected in the PACS diagram at the time it is initiated:

1. If items of plant are selected in the diagram the Study Select application identifies all the items of plant which are electrically connected to the selected plant and sets the In Study attribute to True for these items, and to False for the remaining items.
2. If no items of plant are selected in the diagram the Study Select application identifies all the items of plant in the system that are 'live' and sets the In Study attribute to True for these items, and to False for the remaining items.

Using the Study Select application it is therefore possible to identify and select a specific electrical circuit.

In addition the Insight application provides an option which allows the user to specify whether the program should use the In Study attribute when performing its analysis. In this way the user can perform simulations on a subset of the system, thereby reducing computation time and storage requirements.

4.4.5.4 Conclusions

The graphical methods described above provide an effective means of identifying and selecting desired items of plant from a large volume of data. This is particularly true in the case of results data, where the number of individual items to choose from can run into tens of thousands on a system of realistic size.

4.5 The Insight Load Allocation Component

4.5.1 Overview of Insight Load Allocation

The Load Allocation component is a program for the creation and maintenance of profiles databases containing power profiles for loads and generators which reside in a corresponding plant database.

The primary function of this component is the automatic load allocation procedure which is described in Chapter 5. Other facilities are provided for the editing and display of individual profiles in the database.

The program is designed to interface to distribution company databases for the collection of load and generation data for use in the allocation process. The macro facility described in Section 4.4.4.3 allows the program to be operated in batch mode, performing a load allocation at periodic intervals, such as weekly or monthly, and updating the profiles database automatically.

4.5.2 Program Functionality

The functions of the Load Allocation component are summarised in Figure 4.15 as they appear in the program menus and dialog boxes. The implementation details of the program are given in Appendix F.

- **MAIN WINDOW**
  - **FILE FUNCTIONS**
    - NEW PROFILES DATABASE
    - OPEN PROFILES DATABASE
    - SAVE PROFILES DATABASE
    - SPECIFY PLANT DATABASE
    - EXIT
  - **EDIT FUNCTIONS**
    - EDIT PROFILES
      - Set Profile Attributes
      - Scale Profile
      - Import Profile
      - Plot Profile
    - EDIT DATABASE
      - Delete Profile
      - Database Maintenance
    - EDIT LOAD LIBRARY
  - **LOAD ALLOCATION PROCEDURE**
  - **MACRO FUNCTIONS**
    - RECORD MACRO
    - EDIT MACRO
    - RUN MACRO
  - **CUSTOMISE OPTIONS**
    - ALLOCATION OPTIONS
      - Set Scope of Allocation
      - Specify Time Period of Allocation
      - Specify Metered Data Formats
      - Specify Load Library
      - Specify System Demand Profile
      - Select Error Handling Option
    - MACRO OPTIONS
      - Specify Macro to Run at Program Start-up
      - Select Error Handling Option
    - SAVE OPTIONS TO DISK
    - LOAD OPTIONS FROM DISK

Figure 4.15 Functions of the Load Allocation Component

4.6 The Insight Simulation Component

4.6.1 Overview of Insight Simulation

The Insight Simulation houses the time based load flow routines and provides facilities for the selective display of results in graphical and tabular form. Also included are algorithms for further analysis, including the costing of losses and the allocation of losses to individual consumers.

The Insight Simulation program reads plant data from the relational database and profiles data from a profiles database prepared using the Load Allocation component.

4.6.2 Program Functionality

The functions of the Insight Simulation component are summarised in Figure 4.16 as they appear in program menus and dialog boxes. Further implementation details can be found in Appendix F.

- MAIN WINDOW
  - FILE FUNCTIONS
    - SPECIFY PLANT DATABASE
    - SPECIFY PROFILES DATABASE
    - EXIT
  - EDIT FUNCTIONS
    - SET SIMULATION TIMES
    - EDIT PROFILES
      - Set Profile Attributes
      - Scale Profile
      - Import Profile
      - Plot Profile
  - DISCRETE TIME SIMULATION
  - RESULTS FUNCTIONS
    - DISPLAY SIMULATION STATISTICS
    - DISPLAY RESULTS
      - Plot Selected Results on a Graph
      - List Selected Results in a Table
      - Print Selected Results
      - Export Selected Results to Disk
    - RESULTS PLAYBACK
      - Start Playback
      - Pause Playback
      - Rewind to a Specified Time
      - Fast Forward to a Specified Time
  - APPLICATIONS
    - INSIGHT LOAD ALLOCATION
    - INSIGHT LOAD LIBRARY
    - INSIGHT TARIFF LIBRARY
  - MACRO FUNCTIONS
    - RECORD MACRO
    - EDIT MACRO
    - RUN MACRO
  - CUSTOMISE OPTIONS
    - SIMULATION OPTIONS
      - Set Simulation Mode
        - Standard Mode
        - Constrained Mode
          - Specify Constraint Options
            - Select Constrained Plant
            - Specify Constraint Type
            - Select Plant to Monitor for Constraint Violations
            - Specify Constrained Algorithm Options
      - Select Simulation Options
    - LOAD-FLOW OPTIONS
    - COST OPTIONS
      - Pool Price Tariff Options
      - Time of Day Tariff Options
    - MACRO OPTIONS
      - Specify Macro to Run at Program Start-up
      - Select Error Handling Option
    - SAVE OPTIONS TO DISK
    - LOAD OPTIONS FROM DISK

Figure 4.16 Functions of the Insight Simulation Component

4.7 The Insight Load and Tariff Library Components

4.7.1 Overview of the Load and Tariff Libraries

The Load and Tariff Library components are programs with which the user can create and maintain libraries of daily load and time of day tariff curves respectively. The Load Library curves are used by the Load Allocation procedure to estimate the demand profiles for particular types of consumer, and are used by the loss costing algorithm based upon archetypal daily load curves. The Tariff Library curves are used to apply time of day tariffs to power and loss profiles to determine costs.

In the following sections the Load Library is described. The functionality of the Tariff Library program is essentially identical.

4.7.2 Library Structure

4.7.2.1 Entity Relation Model

The entity relation model of the load and tariff libraries is shown in Figure 4.17. A library comprises a number of Consumer Types which represent categories of consumer. Each of these Consumer Types can have a number of Profiles, each of which comprises two daily curves of 48 values at half hour intervals, one active and one reactive. Each Profile is associated with one or more Day Types and one or more Seasons, which determine which Profiles apply to which days of the week and seasons of the year.

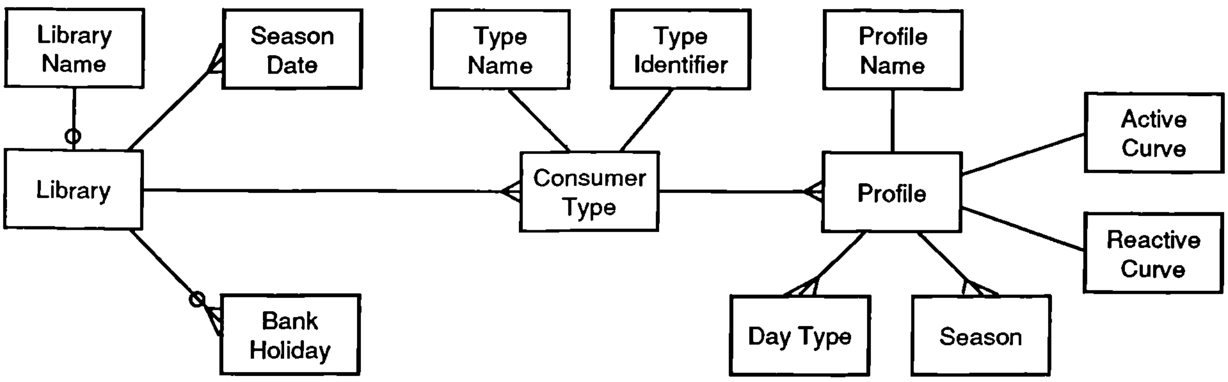

Figure 4.17 Entity Relation Model of the Load and Tariff Library Data Structures

4.7.2.2 Consumer Type Examples

Two examples are given here to illustrate the modelling of different categories of consumer.

4.7.2.2.1 Example 1. Domestic with Economy 7

The first consumer type models a domestic consumer with an Economy 7 tariff. Nine profiles are used to model the annual variation in demand. The details of these profiles are listed in Table 4.9.

Table 4.9 Load Library Profiles for a Domestic Consumer Type

Profile		Applicable Seasons	Applicable Day Types
No.	Name		
1	Winter Weekday	Winter	Mon, Tues, Wed, Thurs, Fri
2	Winter Saturday	Winter	Sat
3	Winter Sunday	Winter	Sun, Bank Holiday
4	Shoulder Weekday	Spring, Autumn	Mon, Tues, Wed, Thurs, Fri
5	Shoulder Saturday	Spring, Autumn	Sat
6	Shoulder Sunday	Spring, Autumn	Sun, Bank Holiday
7	Summer Weekday	Summer	Mon, Tues, Wed, Thurs, Fri
8	Summer Saturday	Summer	Sat
9	Summer Sunday	Summer	Sun, Bank Holiday

The active profile curves are plotted in Figure 4.18.

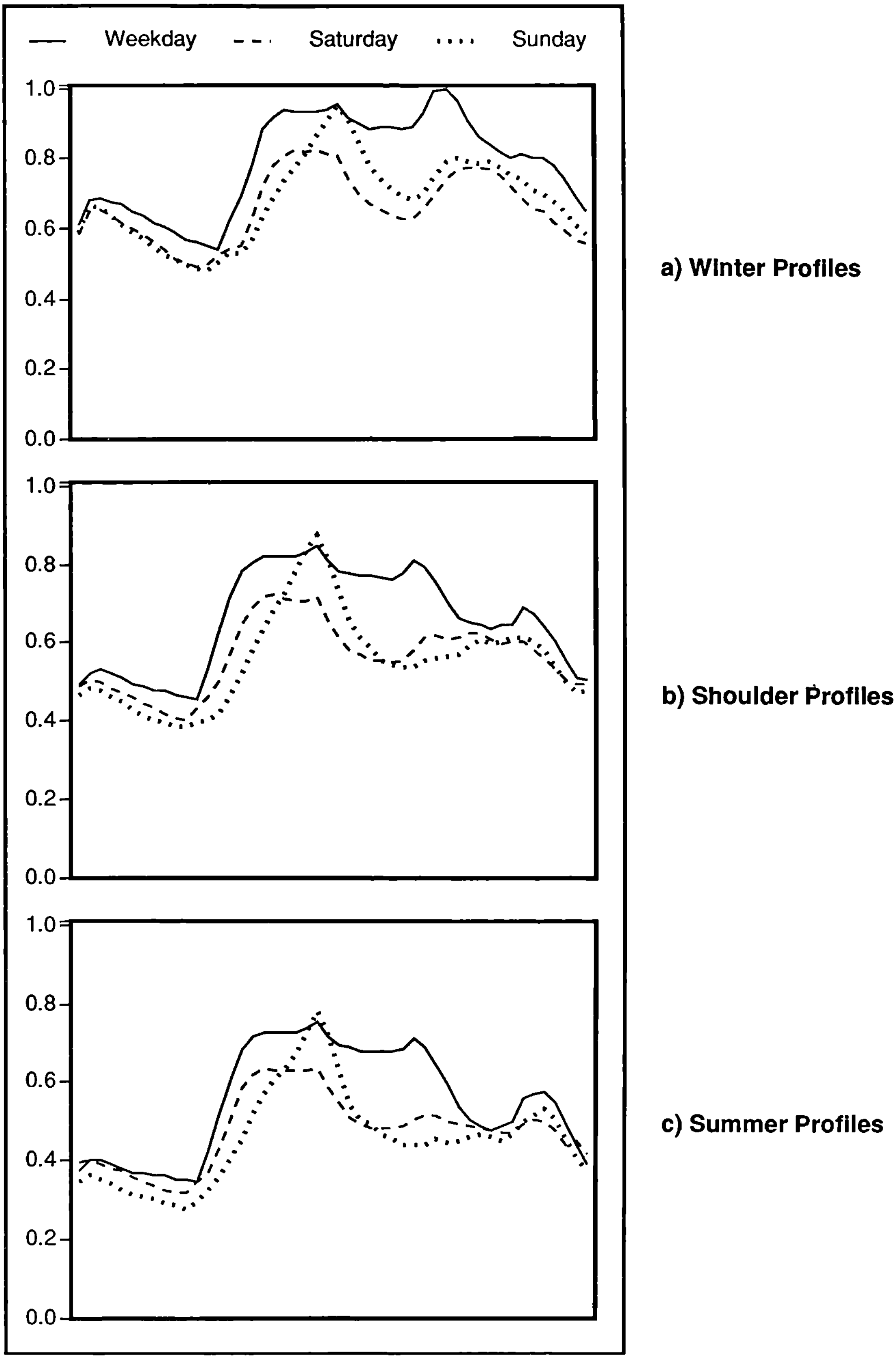

Figure 4.18 Profiles for Domestic Consumer Type

4.7.2.2.2 Example 2. Industrial Consumer

In this example a major industrial consumer (a rolling mill) exhibits a repetitive demand pattern that does not show a seasonal variation. In addition there is little difference between the Saturday and Sunday demand patterns. The consumer type used to model this consumer therefore requires just two profiles: Weekday and Weekend, as summarised in Table 4.10.

Table 4.10 Load Library Profiles for an Industrial Consumer Type

Profile		Applicable Seasons	Applicable Day Types
No.	Name		
1	Weekday	Winter, Spring, Summer, Autumn	Mon, Tues, Wed, Thurs, Fri
2	Weekday	Winter, Spring, Summer, Autumn	Sat, Sun, Bank Holiday

The active demand curves for these profiles are plotted in Figure 4.19.

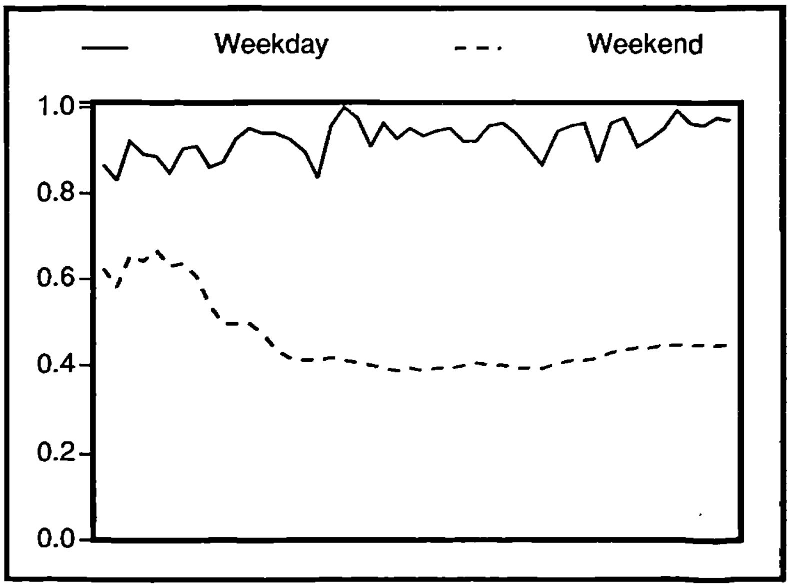

Figure 4.19 Profiles for an Industrial Consumer Type

4.7.3 Program Functionality

The functions of the Load and Tariff Library programs are summarised in Figure 4.20. Further implementation details are given in Appendix F.

- MAIN WINDOW
  - MAIN MENU
    - FILE FUNCTIONS
      - NEW LIBRARY
      - OPEN LIBRARY
      - SAVE LIBRARY
      - EXIT
    - EDIT FUNCTIONS
      - EDIT SEASONS
        - Set Season Start dates
        - Specify Bank Holidays
    - CUSTOMISE OPTIONS
      - PROGRAM OPTIONS
        - Set Curve Display Options
        - Set Graphical Curve Shaping Options
      - SAVE OPTIONS TO DISK
      - LOAD OPTIONS FROM DISK
  - MAIN DIALOG
    - EDIT CONSUMER TYPE
      - ADD PROFILE
      - DELETE PROFILE
      - EDIT PROFILE DATA
        - Import Curve Data
        - Scale Curve
        - Screen Edit Curve Data
        - Shape Curve Graphically
      - EDIT PROFILE DAYS AND SEASONS
        - Specify Applicable Day Types
        - Specify Applicable Seasons
    - ADD CONSUMER TYPE
    - DELETE CONSUMER TYPE
    - COPY CONSUMER TYPE

Figure 4.20 Functions of the Insight Load and Tariff Library Components

4.8 Graphical Display Facilities

4.8.1 Overview of the Graphical Display Facilities

The PACS graphics system provides an effective means of displaying plant and results data on a one-line diagram. Within the PACS system the colours and graphical representation of symbols on the diagram can be made dependent upon values in the database, with the result that constraint violations and other operating conditions can be highlighted to the user.

For the graphical display of time based data a Graph utility has been developed and integrated with the other components in the Insight application.

4.8.2 The Insight Graph Utility

4.8.2.1 Overview

The Graph program is a general utility for displaying graphical data in two dimensions. The drawing routines use the xlib graphics functions of the X Window System to achieve high levels of performance as required to plot lengthy profiles efficiently.

The standard facilities for customising the appearance of the graph, saving graphs to disk and obtaining hardcopy output have been built into the program. Additional facilities perform scaling of individual curves and numerical integration to calculate the area under the curves.

4.8.2.2 Client Server Architecture

The Graph utility provides a service for application clients which use the API to transfer data for plotting, as shown in Figure 4.21.

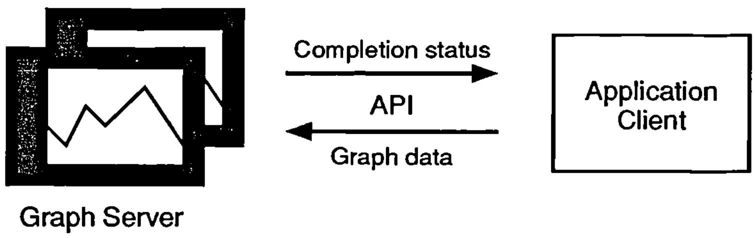

Figure 4.21 Graph Utility Client Server Architecture

Within the client server architecture the client spawns the Graph application as a subprocess and opens an API communication channel. The client subsequently sends data and formatting information as and when required via a set of standard messages.

4.9 Conclusions

4.9.1 The Proposed Software Environment

This chapter has described a software environment for distribution system planning. The designs of earlier generations of software planning systems have been outlined, and a list of design objectives has been developed. The proposed software environment has been described, with reference made to these objectives.

The relational database, flexible PACS network graphics system and API communications interface have been described and shown to provide open access for the integration of new analysis applications through a client-server architecture. The central relational database has been shown to permit the sharing of data between integrated applications within the environment.

The use of a graphic user interface based upon the X Window System to provide a consistent front end to the different components of the environment has been reported. This approach supports multi-tasking of applications and distributed processing across multiple hardware platforms.

4.9.2 The Proposed Insight Application

The design features of the time-based Insight application have been described, with reference to the execution of time-based analysis.

The problem associated with the storage and manipulation of large volumes of data has been outlined. The most widely used data storage methods have been listed, and three techniques for the storage of time based analysis data have been proposed which account for the storage requirements and data access characteristics of each of the categories of analysis data. Additional techniques for reducing storage requirements have been described, and test results have been presented which illustrate the significant reductions which can be achieved in practical cases.

The design of the interface and application management architecture has been described and shown to provide benefits in the areas of software development, portability, and the provision of macros and auditing facilities.

Graphical techniques have been described which provide an effective means by which the user can select specific plant items and electrical circuits from large volumes of data.

The components of the Insight application have been described, and their primary functions listed.

Chapter 5. Load Allocation

5.1 Overview of the Problem

When conducting a load-flow study on a particular system, it is necessary to specify the active and reactive components of power at every load node, and the voltage and active power at every generation node throughout the system. In the proposed load-flow analysis approach this requirements dictates that profiles of active and reactive power and, in theory, voltage, recorded at regular intervals across the simulation period, be specified in place of spot values.

In practice in the proposed discrete time simulator, reactive power profiles are specified for generators instead of voltage profiles, and a constant voltage target is assumed. This is done to accommodate the possibility of generators operating in different modes; both as PV-type nodes and PQ-type nodes. It also ensures that during the allocation procedure the system reactive power demand can be more accurately established and allocated to loads, as described in Section 5.2.3.

As outlined in Section 1.5.2 in Chapter 1, profiles of active and reactive power are normally available at voltages of 33kV and above via SCADA systems. At lower voltages, however, time-based data may not be available [88]. Where this is the case, techniques must be used to estimate the demand, and it is important that the best possible use is made of the existing information, in order to maximise accuracy. This is particularly true in regard to accounting for load diversity. As explained in Chapter 2, the strength of the proposed discrete time simulation approach is its ability to model this diversity. It is important to avoid compromising this advantage through the use of unnecessary approximations in the preparation of the input data.

5.2 The Proposed Load Allocation Algorithm

The general allocation procedure is shown in block diagram form in Figure 5.1, the objective being to derive profiles of active and reactive power for each generator and load defined in the system under study.

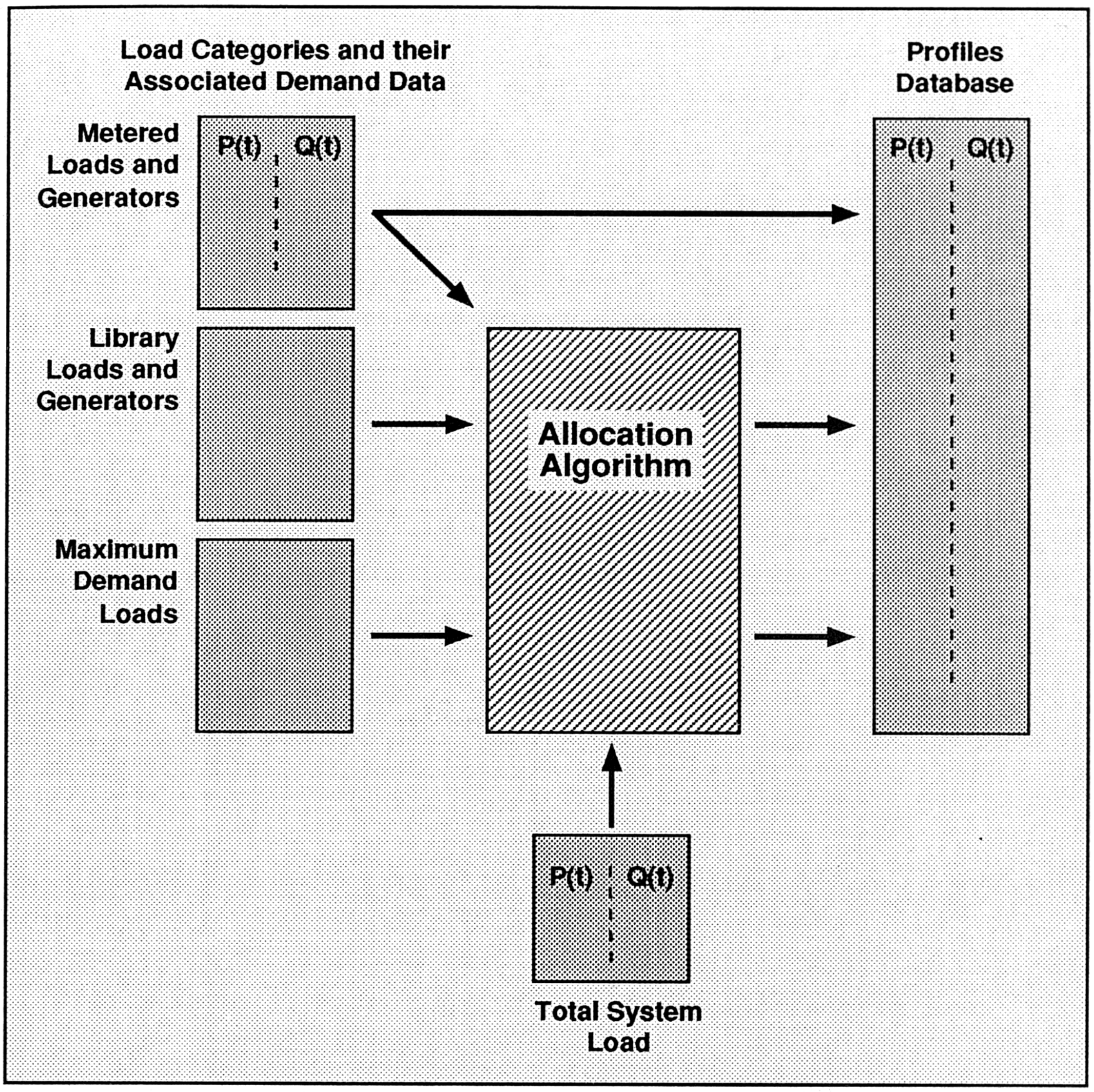

Figure 5.1 General Procedure for Load Allocation

The major stages of the allocation procedure are shown in Figure 5.2. These stages are described in the following sections.

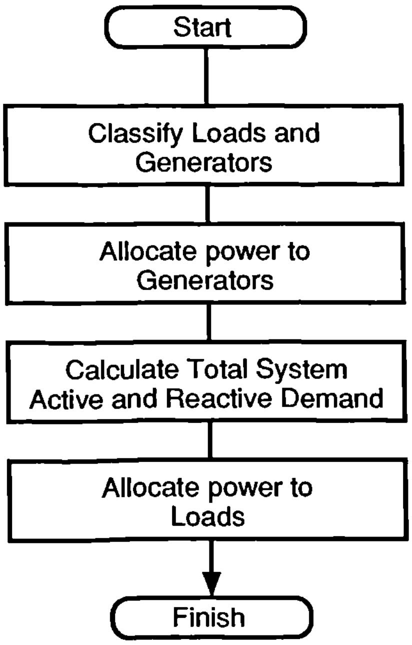

Figure 5.2 Flow Chart of Load Allocation Procedure

5.2.1 Classification of Load Types

Loads and generators in the system fall naturally into three broad categories according to the information available at each. The categories are described in terms of generators in Table 5.1, and in terms of loads in Table 5.2.

Table 5.1 Generator Type Categories

Category	Data Available	Typical generator types
Metered	Metered data sufficient to derive active power at regular intervals (normally half hour) for the period of interest. This data may also be supplied by a generator scheduling program.	Centrally dispatched generators. Major independent generators.
Library	Data sufficient to determine the nature of the generation profile. Such information might include the generator type/fuel and values such as maximum MW output, average load factor and total energy supplied, all recorded on a monthly basis.	Small independent generators.

Table 5.2 Load Type Categories

Category	Data Available	Typical load types
Metered	Metered data sufficient to derive active and reactive power at regular intervals (normally half hour) for the period of interest.	Feeders possessing metering for SCADA systems Major industrial consumers
Library	Data sufficient to determine the nature of the demand profile. Such information is normally available for large consumers in the distribution company's consumer billing database. This database stores the consumer type/industrial activity and values such as average power factor, average load factor, maximum demand and total energy taken, all recorded on a monthly basis.	Large industrial and commercial consumers. Certain feeders at 11kV and below
Maximum Demand	Annual active and reactive maximum demand values. In the worst case transformer rating and assumed average power factor can be used in the absence of maximum demands.	Low voltage feeders supplied by network and pole-mounted transformers

The classification of the generators and loads defined in the system is performed at the same time as the network model is built. In the proposed software environment, the type classification for each load and generator is defined using the Meter File Type, Profile Library Type and Annual Active and Reactive Power Maximum attributes in the relational database model. These attributes are described in Appendix D.

When modelling the higher voltage levels of the distribution system, at 33kV and above, most loads and generators fall into the Metered category. The modelling of 11kV systems may require the use of the Library category to describe industrial and commercial loads and small independent generators. The Maximum Demand category may also be required for low voltage feeders supplying domestic loads, and in other cases where data is particularly scarce.

5.2.2 Allocation to Generators

Power is allocated to generators first, because it is only after the generation in the system is known that the total system demand can be calculated, information which is required in the allocation procedure to loads in the system.

5.2.2.1 Allocation to Metered Generators

Wherever metered data is available, it is used directly to give the active and reactive components of power at those locations. If the active and reactive components are not measured explicitly, power factor measurements are used to derive them.

5.2.2.2 Allocation to Library Generators

In cases where the only available data for a generator is a set of monthly or yearly average and peak values as outlined in Table 5.1, the output profile for the generator must be reconstructed. The procedure is exactly the same as that performed for loads, which is the more general case, and is described in Section 5.2.4.2.

5.2.3 Calculation of the Total System Load

It is necessary to specify the total load supplied by the system under study, in order to allocate load to areas where detailed loading information is incomplete. The total system load at time t can be determined from SCADA measurements at the appropriate grid supply points and from the output of any generators within the distribution system:

$$P_{D,sys}(t) = \sum_{i=1}^{n_{gsp}} P_{G,i}(t) + \sum_{j=1}^{n_G} P_{G,j}(t) \tag{5-1}$$

$$Q_{D,sys}(t) = \sum_{i=1}^{n_{gsp}} Q_{G,i}(t) + \sum_{j=1}^{n_G} Q_{G,j}(t) \tag{5-2}$$

where the subscripts *sys*, *gsp*, and *G* denote system, grid supply point and generator values respectively.

5.2.4 Allocation to Loads

Loads are allocated by category. Categories with greater levels of data are allocated first. The load allocation procedure is summarised in Figure 5.3.

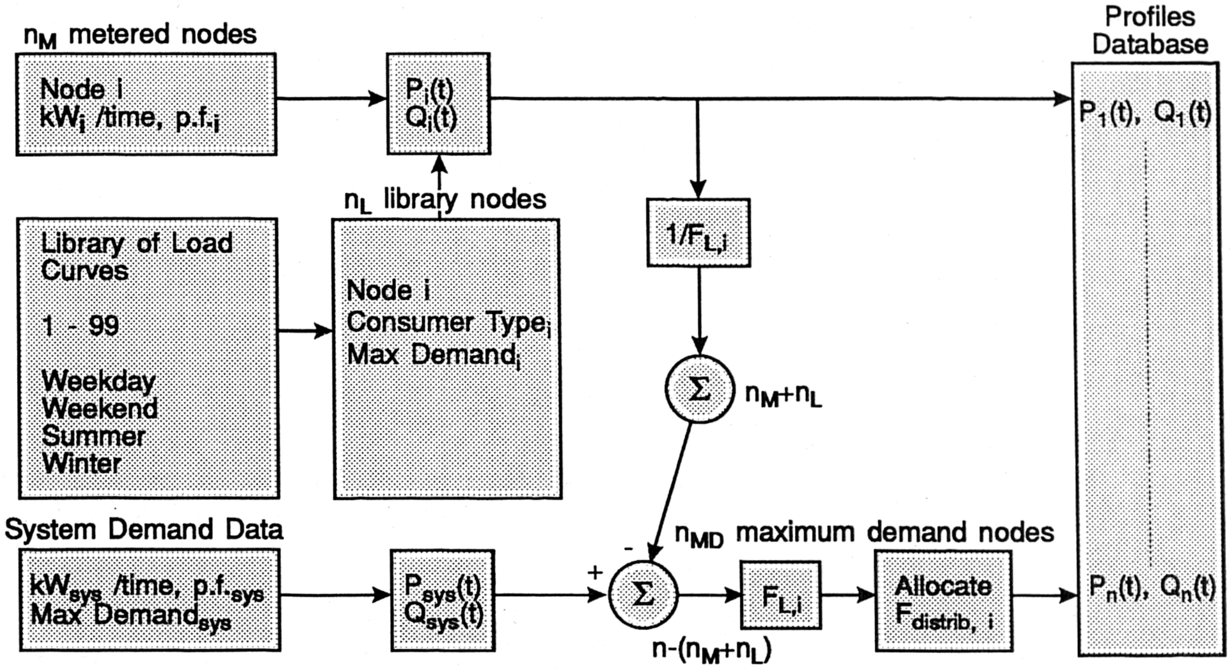

Figure 5.3 Load Allocation Summary

5.2.4.1 Allocation to Metered Loads

Wherever metered data is available, it is used directly to give the active and reactive components of load at those nodes. If the active and reactive components are not measured explicitly, power factor measurements are used to derive them.

5.2.4.2 Allocation to Library Loads

In cases where the only available data for a load is a set of monthly or yearly average and peak values as outlined in Table 5.2, the demand profile for the load must be reconstructed. Research undertaken by organisations such as the Electricity Association [3] has shown that representative demand profiles for particular types of consumer can be defined, and that the variation in demand throughout the year for each consumer type can be described using a small number of typical daily demand curves.

The consumer type category defines loads with similar demand patterns, such as Domestic Economy 7, Retail Superstore, particular types of industrial company and so on.

The number of daily curves used to describe a particular demand profile depends upon the nature of the profile and the available load research data. The minimum number of curves normally required is four: weekday and weekend curves for summer and winter seasons. Additional curves can be defined if required to cover spring and autumn seasons, to differentiate between Saturdays and Sundays, and to model Bank Holidays.

In the proposed load allocation procedure the typical daily demand curves for each consumer type are stored in a load library. The application software developed to build and maintain the load library is described in Section 4.7.

The procedure for allocating a demand profile to a Library load , i, is as follows:

1. The consumer type of the load is identified, and a group of library profile curves corresponding to the consumer type is selected. Each library profile curve, c, comprises a vector of active and reactive power defined at half hour steps for a day.

$$\mathbf{P}_{Dlib,c} = \begin{bmatrix} \mathrm{p}_1 \\ \mathrm{p}_2 \\ \vdots \\ \mathrm{p}_{48} \end{bmatrix} , \quad \mathbf{Q}_{Dlib,c} = \begin{bmatrix} \mathrm{q}_1 \\ \mathrm{q}_2 \\ \vdots \\ \mathrm{q}_{48} \end{bmatrix} \tag{5-3}$$

   Each group of curves is stored in normalised form such that the maximum active power value in the group is equal to 1 per unit.

2. For each day, d, of the load allocation period the season and day of the week are identified. The library curve corresponding to this season and day is selected and scaled by multiplying by the annual maximum demand for the load in question, i.e.

$$\begin{aligned} \mathbf{P}_{Dday,i} &= \mathbf{P}_{Dlib,c} \times P_{Dmax,i} \\ \mathbf{Q}_{Dday,i} &= \mathbf{Q}_{Dlib,c} \times Q_{Dmax,i} \end{aligned} \tag{5-4}$$

5.2.4.3 Allocation to Maximum Demand Loads

There is insufficient data concerning loads in this category to reconstruct a demand profile as in the previous case. The annual maximum demands and transformer ratings can be used, however, to derive a set of linear distribution factors, $F_{Distrib}$, which define the relative magnitudes of the loads, such that

$$\sum_{i=1}^{n_{MD}} F_{Distrib,i} = 1 \tag{5-5}$$

where n_{MD} is the number of loads in this category.

By subtracting the demand profiles of the loads in the first two categories from the total system demand, the real and reactive power remaining to be allocated, P_{Drem} and Q_{Drem} can be determined as shown in Equations (5-6) and (5-7).

$$P_{Drem}(t) = P_{Dsys}(t) - \sum_{i=1}^{n_M} \left(\frac{P_{D,i}(t)}{1 - F_{Lr,i}} \right) - \sum_{j=1}^{n_L} \left(\frac{P_{D,j}(t)}{1 - F_{Lr,j}} \right) \tag{5-6}$$

$$Q_{Drem}(t) = Q_{Dsys}(t) - \sum_{i=1}^{n_M} \left(\frac{Q_{D,i}(t)}{1 - F_{Lx,i}} \right) - \sum_{j=1}^{n_L} \left(\frac{Q_{D,j}(t)}{1 - F_{Lx,j}} \right) \tag{5-7}$$

F_{Lr} and F_{Lx} are active and reactive allocation loss factors, defined in Appendix A, which are included to account for the losses which occur in the system between each load and the point at which the total system load was measured. Initially approximate loss factors are assumed, based upon the average losses occurring at each voltage level. Once results from a discrete time simulation are available, accurate loss factors can be calculated using the loss allocation algorithm described in Chapter 9.

The remaining system load is allocated around the maximum demand loads using the distribution factors as follows

$$P_{D,i}(t) = P_{Drem}(t) \times F_{Distrib,i} \times (1 - F_{Lr,i}) \tag{5-8}$$

$$Q_{D,i}(t) = Q_{Drem}(t) \times F_{Distrib,i} \times (1 - F_{Lx,i}) \tag{5-9}$$

One of the effects of using 'linear' distribution factors in this stage of the allocation is that the resulting load profiles will conform, i.e. they will have the same profile shape as the remaining system load. However, this effect is actually desirable, since it fits in well with the nature of distribution system loads and their associated measurement data.

It is the major industrial consumers whose demand profiles show the greatest diversity. At the same time the greater levels of information available for these consumers mean that this diversity can be accounted for accurately. Demand profiles for residential feeders, on the other hand, tend to conform closely to a standard residential profile.

By subtracting the profiles for the major industrial consumers from the total system demand, the resulting system demand profile will be made up largely of small residential loads all with similar demand profile shapes. So despite the lack of detailed information, an accurate allocation can be performed for these loads on the basis of linear distribution factors.

5.3 Test Results

The theory behind the load allocation algorithm suggests that provided the major loads on the system, which show the greatest levels of diversity, are sufficiently well defined that their demand patterns are available either directly from stored measurements or indirectly via other information, the remaining loads on the system can be allocated accurately in the absence of detailed data, because their demand patterns conform.

Where this situation fails to exist, as a result of diverse loads on the system not being accounted for, the accuracy of the allocation algorithm will clearly be diminished. It is necessary therefore to study the accuracy of the algorithm when applied to a typical area of a distribution network.

5.3.1 Test Results on a Distribution Network Primary Feeder

5.3.1.1 Test Network

The section of distribution network used in the test is a simplified primary feeder as shown in Figure 5.4. The feeder runs from a Grid Supply Point at 132kV down to 11kV and serves a mixture of industrial and residential loads. In particular, Load L1 is primarily residential, Load L2 is a major industrial consumer, and Load L3 is largely residential, but with one major industrial consumer.

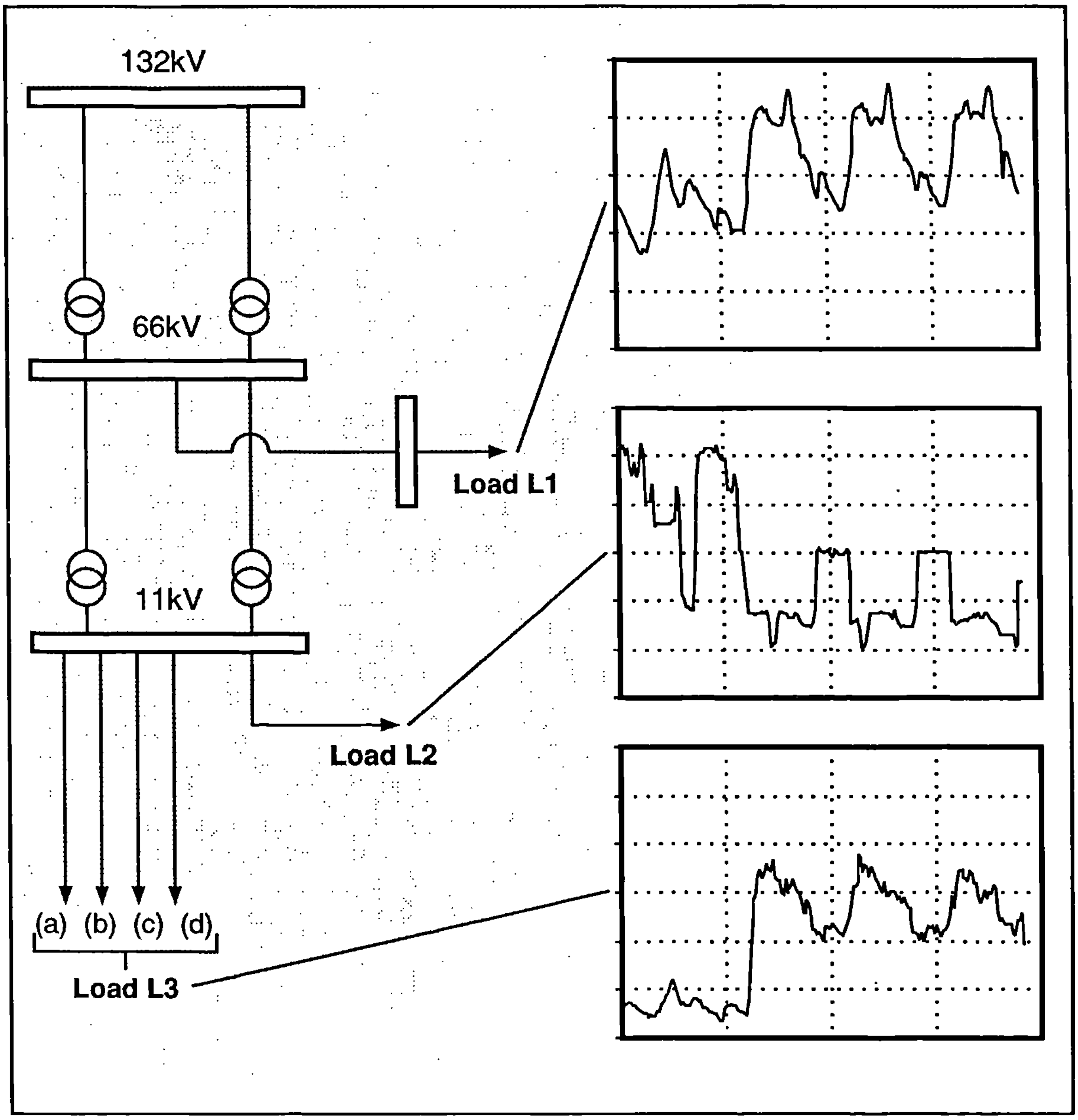

Figure 5.4 Distribution Primary Feeder with Associated Demand Data

Demand measurements for these loads were taken for a four day winter period, Sunday to Wednesday, to provide a reference against which the performance of the algorithm could be assessed.

5.3.1.2 Test Results with Minimal Demand Data

Insofar as the demand data available to the algorithm was concerned, initially a 'worst case' was chosen. The minimum amount of demand data that might be expected for a feeder of this type was assumed to be available: half hourly metered data for the major consumer, but no data except the annual maximum demands for loads L1 and L3. In practice it is likely that considerably more information would be available.

The allocation algorithm had therefore to use the metered data for load L2, and then to allocate to loads L1 and L3 on the basis of distribution factors calculated from their respective annual maximum demands. Figure 5.5 compares the demand profiles produced by the allocation algorithm with the reference profiles for loads L1 and L3.

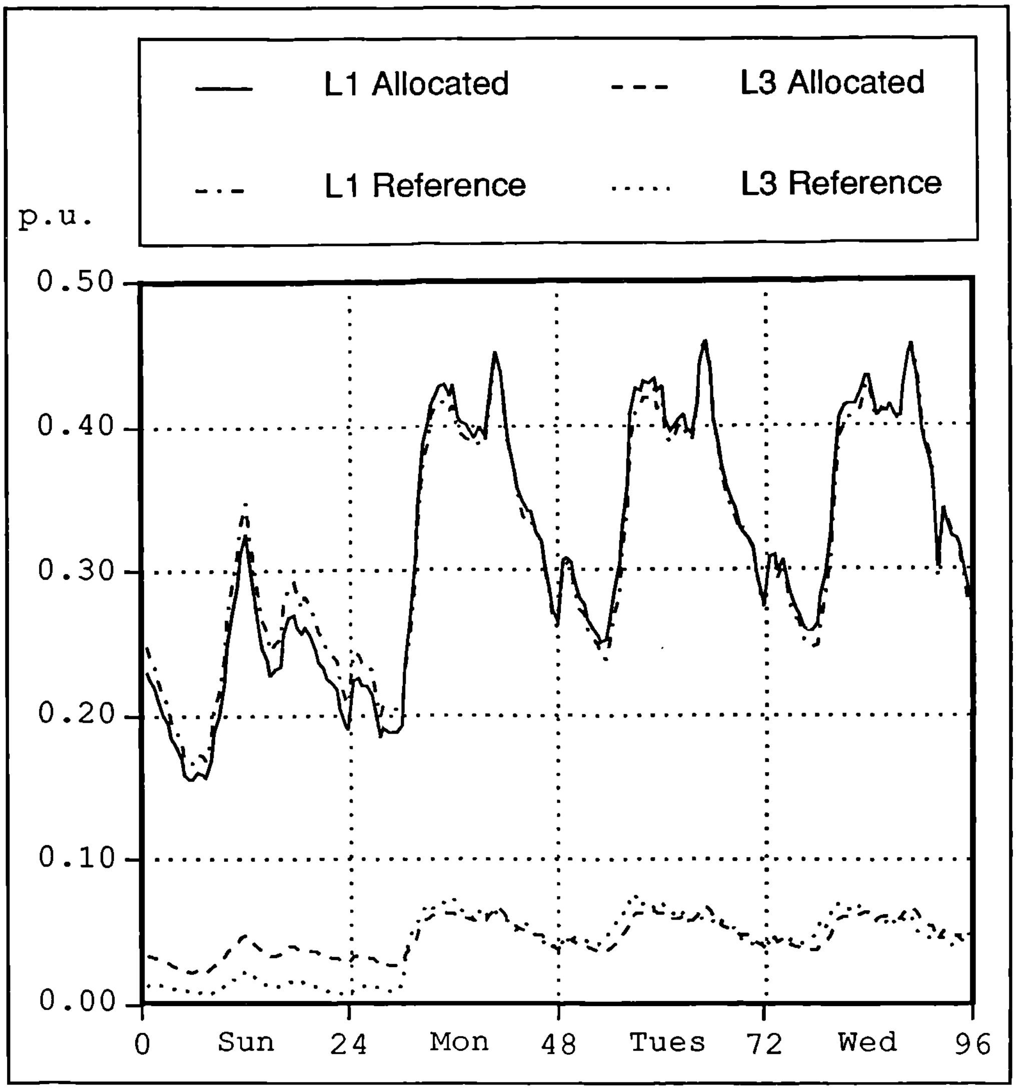

Figure 5.5 Load Allocation Results with Minimal Demand Data

The results show that the demand profiles allocated to loads L1 and L3 agree closely with the reference profiles during the weekdays, but that there are significant errors during the

Sunday. The reason for this becomes clear when the individual loads making up L3 are studied. Load L3 comprises four individual loads as shown in Figure 5.6.

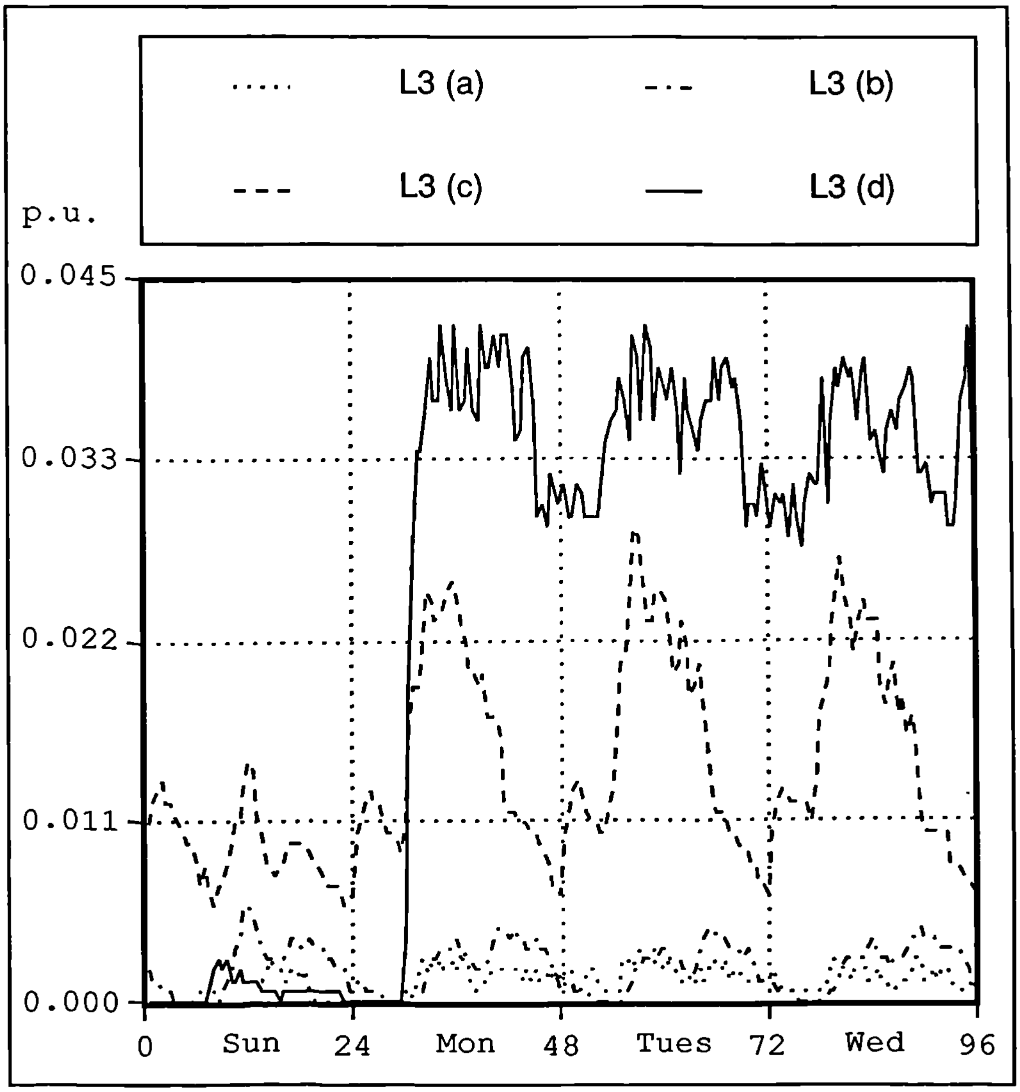

Figure 5.6 Individual Loads Making Up Load L3

Individual loads (a), (b) and (c) are all residential in nature, but (d) is clearly industrial, with no demand on a Sunday and a two-shifting work pattern during the week. In the allocation algorithm, it is assumed that all loads that are allocated by distribution factors, i.e. loads with limited data, conform to a residential load pattern. This is clearly not the case for load L3(d), which gives rise to the errors shown in Figure 5.5. The errors in the allocation are directly related to how poorly a given load in this category conforms to the residential load pattern. In this case load L3(d) differs most from a residential load on the Sunday, and this explains the large errors in the allocation for that day.

5.3.1.3 Test Results with Additional Demand Data

In practice a significant industrial consumer such as load L3(d) would have an individual record in the distribution company's consumer billing file, which would contain additional demand information to that which was assumed for the test in the previous section. This would enable library profiles for the consumer to be selected for each day, as shown in Figure 5.7.

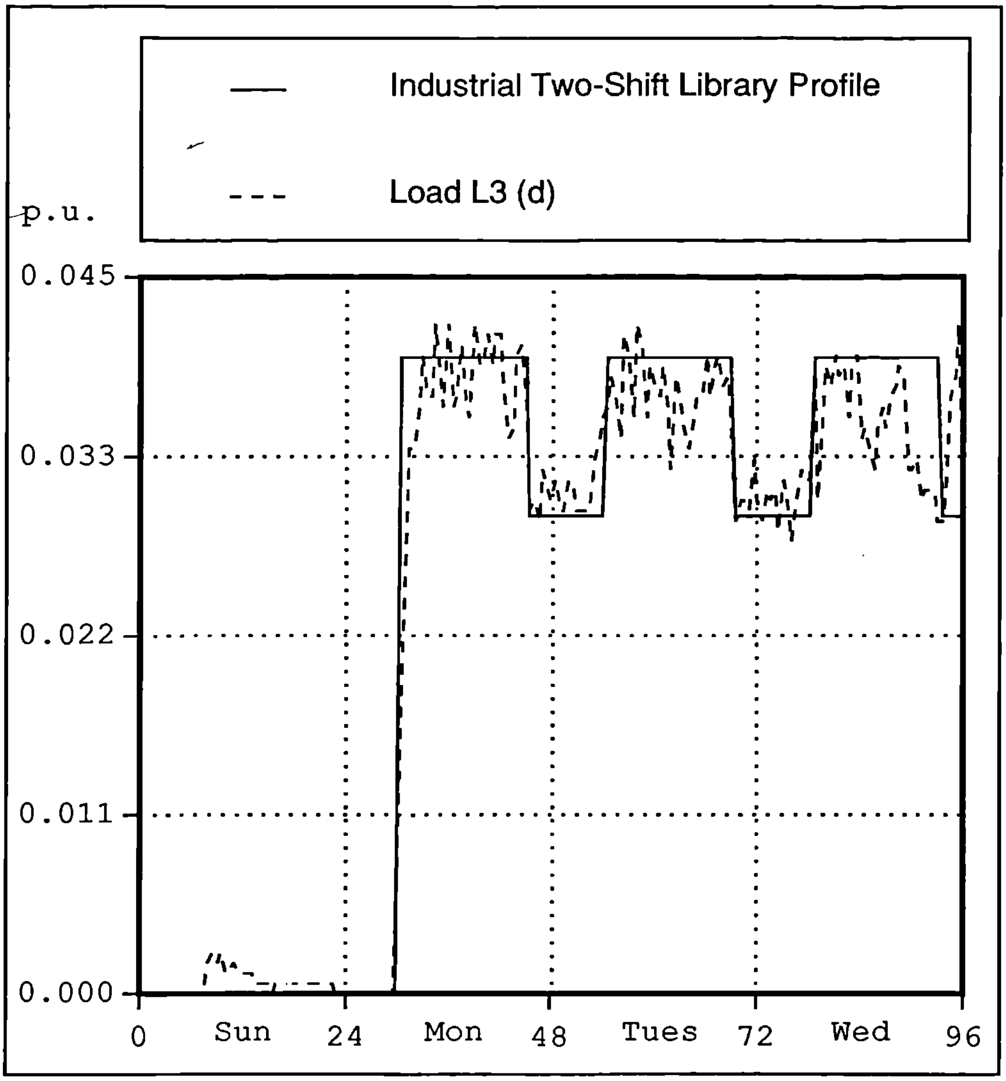

Figure 5.7 Library Profiles for Load L3(d)

Although the demand profile for Load L3(d) does vary in an unpredictable manner during the day, the library profile does serve as a useful approximation in the absence of more detailed information. This is illustrated in the marked improvement in the allocation results for the other loads, as shown in Figure 5.8.

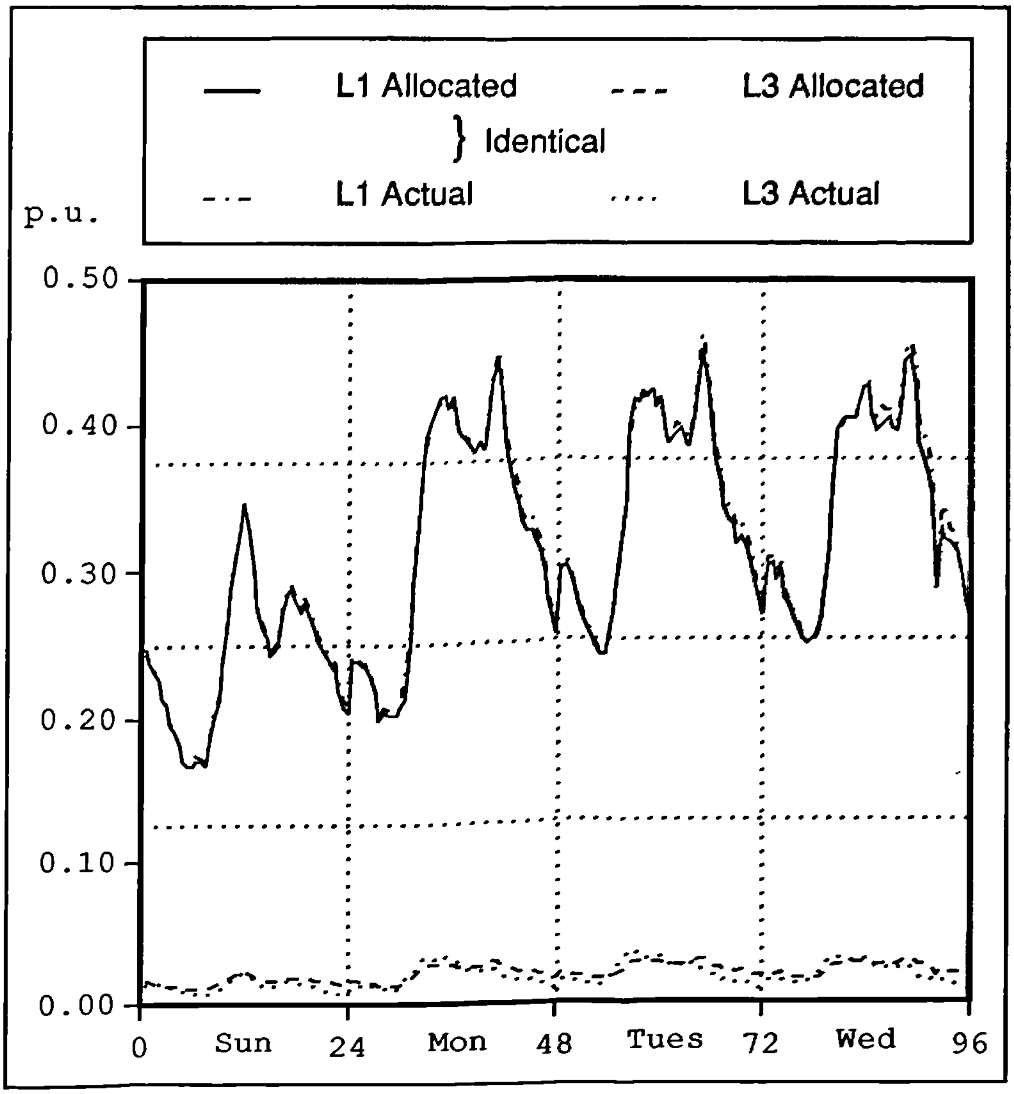

Figure 5.8 Load allocation Results with Additional Demand Data

The allocated and actual measurements for Load L1 are now very close, while the results for Load L3 are greatly improved.

5.4 Conclusions

A load allocation algorithm has been described which aims to make use of available data to assign time-based power profiles to all the loads and generators in the system. Advantage has been taken of the nature of demand patterns of consumers in a distribution system and their associated measurement data, to allocate load accurately even in the absence of detailed demand information.

Test results on a real system have demonstrated the effectiveness of the algorithm.

Chapter 6. Analysis Applications

6.1 Introduction

This chapter describes practical applications of the discrete time simulation approach. Particular emphasis is placed on applications concerned with problems which have arisen from the restructuring of the electricity supply industry in the UK, or which have grown in importance as a result, although clearly some of these problems are common to utilities world-wide.

The applications related to the costing of losses form a major part of the thesis, and are therefore described in later chapters.

6.2 Analysis of Voltage Related Problems

The proposed discrete time simulator is capable of producing accurate voltage profiles for substations throughout the system during the period of interest, information which is of value for a number of studies.

6.2.1 Accurate Assessment of Voltage Violations

In the event of voltage violations the Insight Simulation application allows the planning engineer to assess the severity of the problem: how frequently and for how long is the voltage outside limits, and by how much. Figure 6.1 shows a voltage profile for Load Ld10 (Node 36) on the 52 Node test network, produced by a discrete time simulation for January and February at half hour steps. In this example the 33/11kV transformers have reached their tap limit at peak periods during winter weekdays. The horizontal guide line at 10.34kV on the figure denotes the nominal 6% voltage lower limit. Figure 6.2 shows the same information presented as a duration curve. Given an accurate picture of the state of the system the engineer can assess whether reactive compensation or some other measure is required, or whether, because the violations occur only for short periods during peak winter days, the situation can be tolerated.

Should the planning engineer decide to take action the proposed software can be used to determine the most cost effective strategy. An example is the placement and sizing of capacitors in the system for voltage support.

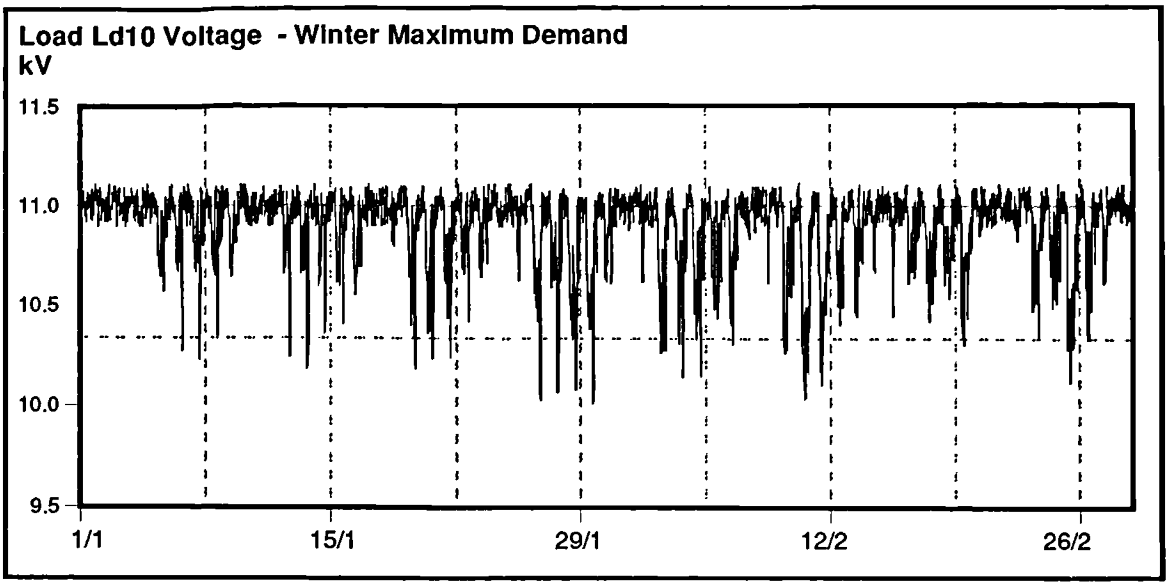

Figure 6.1 Voltage Profile Example - Chronological Display

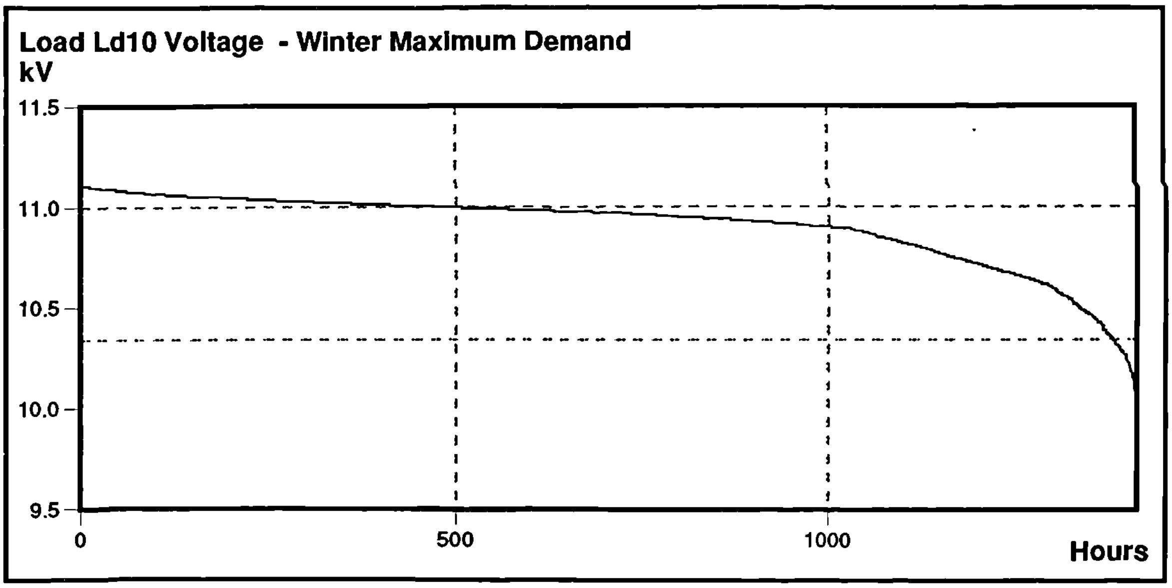

Figure 6.2 Voltage Profile Example - Duration Display

6.2.2 Capacitor Placement and Sizing

6.2.2.1 Procedure Using the Proposed Software Environment

Should the planning engineer elect to install reactive compensation to provide voltage support, it is necessary to determine the reactive power requirements at the specified location. In the case of simpler compensation schemes such as fixed capacitors, it is also necessary to study the effect of a proposed scheme, since solution of low voltage problems during peak periods may give rise to overvoltages during off-peak periods. The issues to be considered when planning reactive compensation are discussed by Grainger [57] and by Osborn [104].

Using the proposed Insight application, the procedure for determining the reactive power needed at a given location to maintain the voltage at a specified level is as follows:

1. Perform a discrete time simulation of the network for the period of the year during which the peak demand occurs on the area of system under study. From the resulting voltage profiles, identify a suitable location for reactive compensation.
2. Determine the reactive power requirement at the chosen location:
   a) Select a voltage level which represents the lowest permissible voltage for the chosen location.
   b) Install a generator at the chosen location using the PACS graphics system. This requires selection of a generator from the plant library, placing it into the diagram and connecting it to a busbar at the chosen substation. Set the following attributes for the generator:
      i. Set the reactive limits of the generator to a very large value (±10000 MVAr, for example).
      ii. Set the voltage magnitude of the generator to the voltage limit defined in a).
   c) Import a power profile for the generator which covers the time period of interest, using the Import facility in the Insight Simulation application. Set the active and reactive power values at each time step to zero using the Scale facility. This action specifies that the generator will supply no active power, but will supply (or absorb) reactive power to maintain the voltage at the specified level.
   d) Perform a discrete time simulation across the period of interest. Plot the reactive power profile for the new generator. This represents the reactive power required at the specified location to maintain the voltage at the target level.
3. Select the size of a capacitor based upon the maximum reactive power requirement determined in stage 2.
4. Install a capacitor of the selected size using the PACS graphics system. This requires selection of a shunt capacitor from the plant library, placing it into the diagram and connecting it to the appropriate busbar. The previously installed generator is deleted or switched out at this stage.
5. Perform a discrete time simulation across the year to assess the affect of the capacitor under all operating conditions, including off-peak periods such as the August holiday period.
6. Repeat if required for other suitable capacitor locations.

It is important to note that the design of the PACS and Insight Simulation applications obviates the need to perform each of these steps when repeating the procedure for other capacitor locations. The generator, once it has been placed into the diagram and its attributes specified, can be simply disconnected and moved to new locations as required. The actions required initially to specify the generator's power profile do not need to be repeated. In addition Insight macros can be recorded which perform a discrete time simulation and plot the specified results, thereby reducing the effort required to obtain simulation results.

6.2.2.2 Worked Example

Figures 6.3 to 6.5 illustrate the procedure for the example given in Section 6.2.1 above. In this example the voltage at Node 36 drops to approximately 10kV during peak winter periods, which represents a voltage drop of 9% on the nominal value (Figure 6.1). In the UK RECs are obliged to maintain the voltage to their consumers between ±6%.

In this case the reactive power required to bring the voltage up to -4% (10.56kV) of the nominal voltage during peak periods is found by placing a generator whose voltage target is set to this value into the system at Node 36, and performing a discrete time simulation. The resulting reactive power profile for the generator is shown in Figure 6.3 and denotes the reactive power required at each half hour to maintain the voltage at 10.56kV. The peak point on the figure is approximately 6MVAr, and indicates the maximum reactive power required. A static compensator of this size can now be connected at Node 36 to supply the required reactive power. Repeating the discrete time simulation and plotting the voltage profile at this point shows that the voltage problem has been solved, Figure 6.4. If it is likely that the static compensator will give rise to overvoltages during summer minimum loading conditions, a further discrete time simulation should be performed during this period. Figure 6.5 shows the corresponding voltage profile for July and August, which indicates that the transformers supplying Load Ld10 are operating within their tap range under these conditions, and maintaining the voltage within limits.

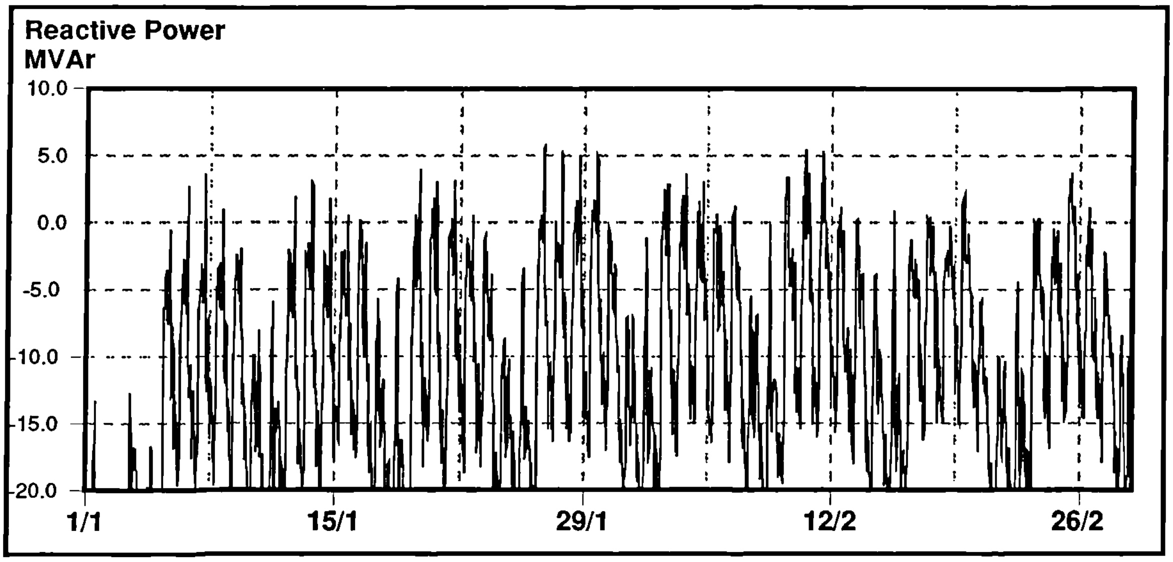

Figure 6.3 Capacitor Placement - Reactive Power Required to Hold Voltage at -4%

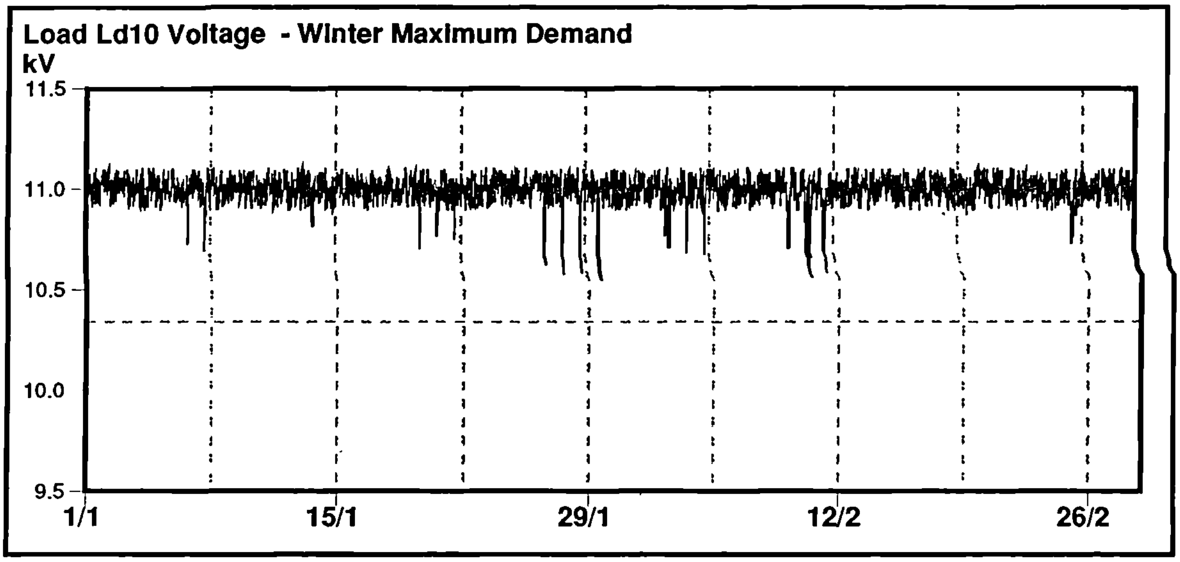

Figure 6.4 Voltage Profile After Installation of Static Compensator

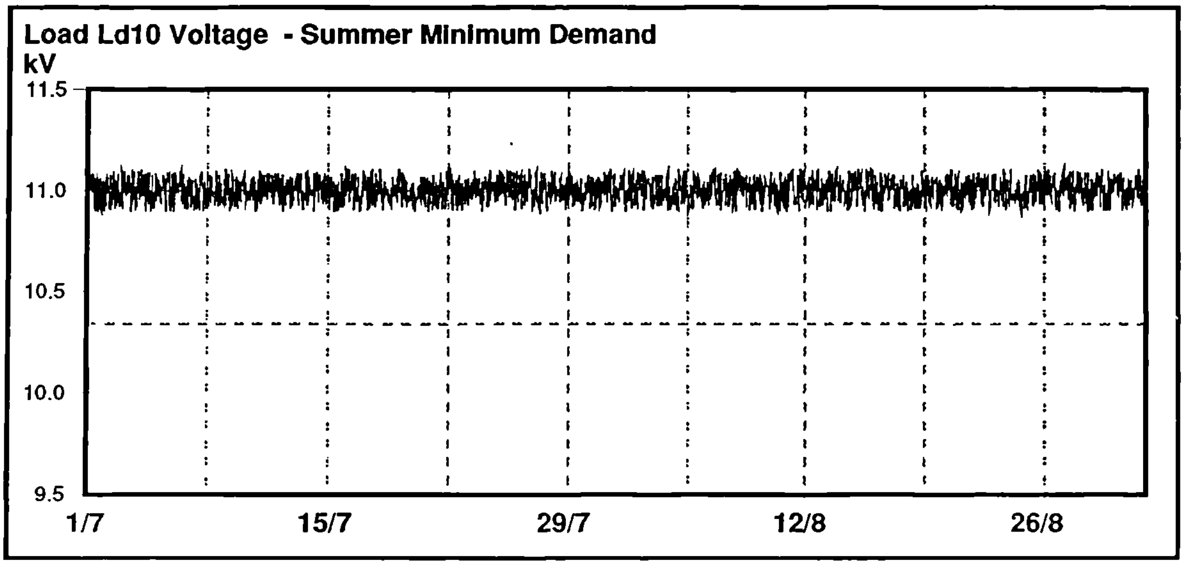

Figure 6.5 Voltage Profile During Period of Annual Minimum Demand

6.2.3 Voltage Regulation

6.2.3.1 Introduction

The chronological analysis performed by the Insight application coupled with the modelling of both the voltage dependency of loads and the resistance heating of lines provides an accurate basis for the study of the effects of various control settings on the voltage profiles of individual consumers. Studies by Gnadt et al [54] have shown that in particular the accurate modelling of the voltage dependency of loads is crucial to achieve meaningful results in these kinds of studies.

6.2.3.2 Analysis of the Effects of Primary Transformer Voltage and Line Drop Compensation Settings

At voltages of 11kV and below, increases in system loading are normally accompanied by increased voltage drops along primary and secondary feeders. Transformers serving primary feeders often incorporate line drop compensation (LDC) or voltage compounding to counteract this effect and to reduce voltage regulation at consumer terminals. In most cases values of equivalent resistance and reactance for LDC can be determined easily using standard formulae, without the need for more detailed analysis. Some cases however can give rise to difficulties. Figure 6.6 illustrates a situation in which a primary substation serves both a local urban load and a remote rural network. In this case standard LDC settings to reduce voltage regulation on the rural system may lead to unsatisfactory variations in voltage locally, in particular overvoltages during periods of peak demand.

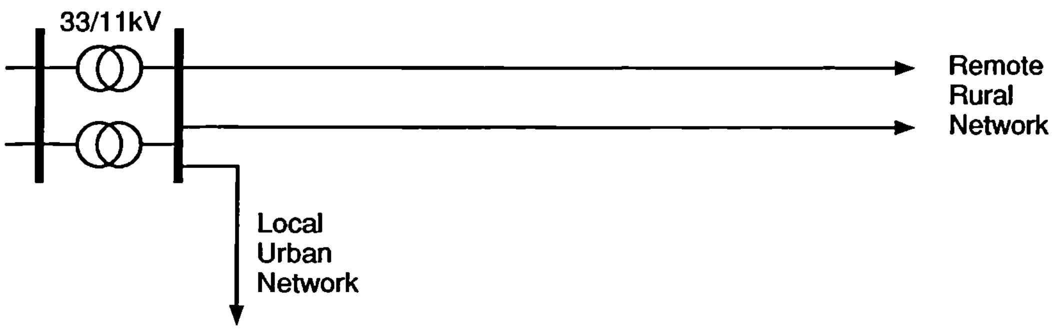

Figure 6.6 Voltage Regulation Problems on Rural 11kV Feeders

Time-based analysis can be used to good effect to help solve these kinds of problems. The effects of different LDC settings and off load tap positions on LV transformers can be modelled accurately as a function of time.

In addition, the constrained simulation algorithm described in Section 6.4.2 can be used to optimise the tap positions of the primary transformers to observe both local and remote voltage constraints. The Insight application could form the basis of an automatic voltage control scheme in which the load allocation and simulation components run as batch processes at regular intervals, calculating a set of optimised tap positions for selected transformers which account for the loading conditions pertaining at the time..

6.2.3.3 Voltage Reduction Studies

As in the previous case, the modelling accuracy of the proposed time based analysis permits the study of voltage reduction strategies on the steady state operation of the system.

In the event of certain abnormal circumstances which result in a deficiency in generation, transmission or distribution system capability, voltage reduction may be required to reduce temporarily the demand on the system. In cases where a large proportion of the demand is made up of resistance heating or lighting loads, a reduction in supply voltage results in a corresponding reduction in the power requirements. Motor loads, on the other hand, are essentially unaffected by small changes in supply voltage.

The effects of a voltage reduction scheme on the system demand can be established by discrete time simulation provided the nature of the voltage dependency of consumer loads is known. The efficient Newton-Raphson load-flow algorithm employed in the discrete time simulator uses a polynomial to model the voltage dependency of individual loads. The active and reactive power demands for a load i are determined from their nominal values by:

$$P_{Di} = P_{Dnom,i}(\alpha_1 V_i^{\mu_1} + \alpha_2 V_i^{\mu_2} + \alpha_3 V_i^{\mu_3}) \qquad (6\text{-}1)$$

$$Q_{Di} = Q_{Dnom,i}(\beta_1 V_i^{\nu_1} + \beta_2 V_i^{\nu_2} + \beta_3 V_i^{\nu_3}) \qquad (6\text{-}2)$$

where α and β are active and reactive coefficients, and μ and ν are active and reactive exponents respectively.

Care is required in lowering the voltage on feeders supplying low voltage networks, so that load shed by one feeder is not picked up by other feeders whose voltage has not been lowered. This may result in the operation of protection equipment on the original feeder, leading to overloads on alternative feeders and causing them to trip out in cascade (Pansini [106]). The effects of a voltage reduction scheme on neighbouring areas can be predicted using discrete time simulation.

6.3 Analysis of Problems Related to Embedded Generation

6.3.1 Growth in Embedded Generation in the UK Since Privatisation

One of the most important effects of the restructuring of the electricity supply industry in the UK has been the opening up of the system to private generating companies. The result of this change in legislation has been a proliferation of independent generating stations, many of which are small in size and embedded in the distribution system. Figure 6.7 illustrates the growth in independent generators which has occurred since privatisation in 1990. The figure shows the numbers of generation licences, required for power stations larger than 50MW, issued since vesting day (Offer [103]). Many small generators of less than 50MW capacity have also been constructed during this period.

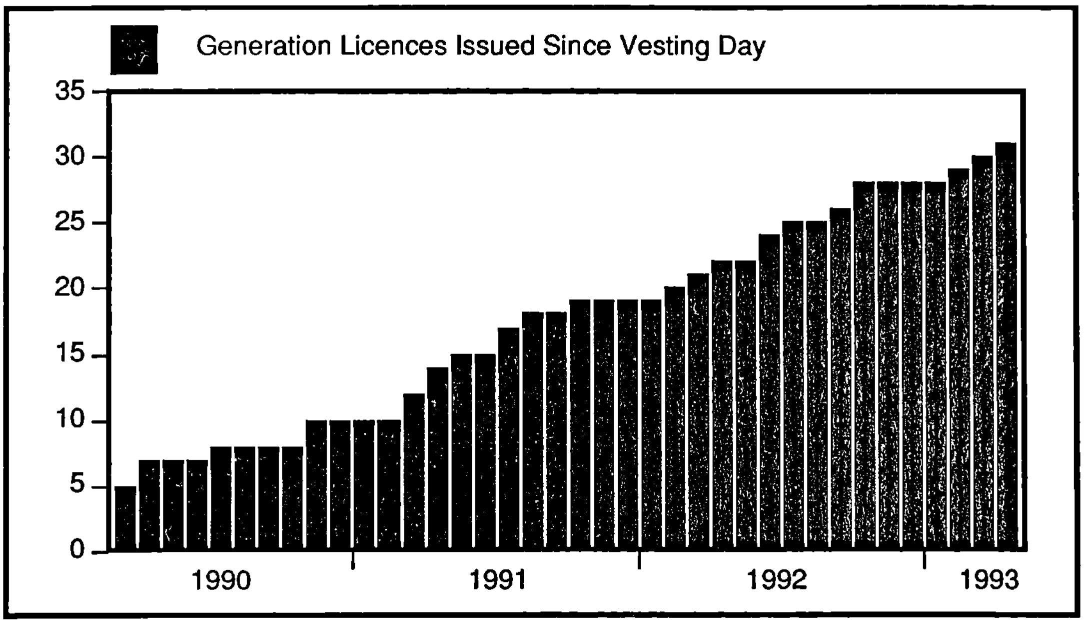

Figure 6.7 Growth in Independent Generation in the UK Since Privatisation

The substantial rate of growth in embedded generation seen in recent years has created new problems for distribution system planning engineers. Distribution companies faced with connection requests from prospective generators need to assess the impact of embedded generation on system security, operational constraints such as voltage and power flow limits, and system economics. These areas are described in greater detail in the following sections. The application of discrete time simulation to the solution of these problems is discussed.

6.3.2 Analysis of the Impact on the System of Embedded Generation

6.3.2.1 The Effect of Embedded Generation on Local Voltage Conditions

The proposed discrete time simulation approach provides an accurate means by which the effect of an embedded generator on local voltages can be gauged. The procedure normally performed is as follows:

1. Using the PACS graphics system a suitable generator is placed into the diagram and connected via a switch to the desired substation.

2. A discrete time simulation is performed under base case conditions, with the embedded generator switched out, for the period of interest. Voltages of neighbouring substations are plotted and stored.

3. The discrete time simulation is repeated with generator switched in and generating according to its normal or expected schedule. Voltage profiles for the same collection of substations are plotted. The base case voltages can be retrieved and plotted simultaneously to display the changes in voltage resulting from the connection of the generator. Duration curves of voltage can be used in the case of lengthy simulations to improve the clarity of the results.

6.3.2.2 The Effect of Embedded Generation on Protection Co-ordination

The co-ordination of protective devices on much of the UK distribution system relies on the assumption that the direction of power flow in individual circuits is constant. The time/current characteristics of time-delay overcurrent relays in widespread use are set to ensure the correct sequence of operation of primary and backup relays in the event of a fault. The protection scheme is designed to provide for the rapid isolation of the faulted section, without isolating healthy sections of the system.

The addition of embedded generators to the system can compromise the efficacy of the existing protection scheme by altering the directions of local power flows. The reliability of operation of protective devices may be degraded. The severity of the problem is dependent upon several factors, including the size and location of the generator, local loading conditions and network configuration, and varies as a function of time.

Time-based load-flow analysis can be used effectively to identify potential problems arising from the presence of embedded generators in the system, by determining the effects they have on power flows under different system loading conditions.

6.3.2.3 The Effect of Embedded Generation on System Losses

An increasingly important issue in the privatised UK electricity supply industry is the calculation of 'scaling factors' for embedded generators. These scaling factors determine the charge (or compensation) generators incur for the change in system losses arising from their connection to the system. The scaling factor is therefore the mechanism for the allocation of the costs of incremental system losses due to the generator in question.

Discrete time simulation provides an accurate means for calculating generator scaling factors. The procedure is similar to those of the previous sections:

1. A discrete time simulation is performed under base case conditions for the period of interest, with the embedded generator switched out. The total demand losses for the system are calculated at each step and integrated to give the energy losses over the period.

2. The embedded generator is switched in, and the simulation is repeated. A new system energy loss is calculated.

3. The marginal system energy loss is determined by subtracting the base case energy loss figure.

4. The generator scaling factor is determined by dividing the marginal energy loss by the energy output by the generator during the period.

6.3.3 Determination of Embedded Generation Output Limits

6.3.3.1 Description of the Problem

In many cases the installation of a generator in the distribution system will result in reduced local power flows, improved voltage regulation and lower losses. However, at certain sites the capacity of the system to absorb additional power output imposes limits on the size of generator which can be accommodated. Two common causes of this are:

1. Cases in which the generator output reinforces local power flows. In such cases local thermal and stability limits will restrict the output of the generator during peak periods.

2. In remote regions with little local load. In such cases the local load may be unable to absorb sufficient of the generator's output, with the result that local voltages may increase beyond regulatory limits. Thermal limits in rural feeders may also restrict the output of the generator. This problem is particularly common with wind farm generation, which is normally located in remote regions, and is most acute during off-peak periods.

6.3.3.2 Outline of the Proposed Constrained Simulation Algorithm

In order to assess the capacity of the system to accept generation at a particular location, a constrained simulation algorithm is presented which uses a simple optimisation to maximise the output of the generator as a function of time while observing operating constraints such as voltage and current.

The algorithm is described fully in Section 6.4.2. For each time step of the simulation the algorithm performs load-flows under base case and 'maximum generation' conditions, while monitoring selected constraints. A root finding algorithm is used to predict the maximum generation output level which can be accommodated without violating these constraints. The algorithm performs a number of iterations until the difference between load-flow results and the corresponding constraints is less than a specified tolerance.

6.4 Analysis of System Capacity

6.4.1 System Utilisation

The restructuring of the electricity supply industry in the UK has resulted in a much greater emphasis on the economics of electricity supply. At the same time the obligation to supply electricity, previously held with the CEGB, has been placed with the distribution companies. The primary objective of the distribution companies is meet this obligation while simultaneously maintaining the interests of their shareholders by maximising profits. Clearly the incentives to make the fullest use of existing assets within the system have never been greater.

One of the keys to achieving this objective is improved information concerning the performance of the system. The proposed time based load-flow analysis achieves this by modelling the individual variations in load and generation patterns with time.

Another important requirement in the maximisation of system utilisation, while maintaining adequate levels of security, is an assessment of the capacity of the system at different locations to support additional load or generation. The constrained simulation algorithm presented in the following sections calculates the maximum load or generation which can be supported at a given location within the system without violating operational constraints such as voltage regulation and thermal limits.

6.4.2 The Proposed Constrained Simulation Algorithm

6.4.2.1 Formulation of the Problem

The proposed algorithm performs a simple optimisation, in which the power of a specified load or generator is maximised at each time step of a discrete time simulation, subject to voltage or current constraints.

The resulting power profile for the load or generator represents the spare capacity of the system at that location in terms of the additional load or generation which can be accommodated.

The optimisation process is formulated as a one-dimensional root finding problem of the form given in Equation (6-3), where in this case the independent variable x is the active power of the specified load or generator. Note that although the reactive power of the load or generator also varies, the power factor angle is kept constant, with the result that the reactive power is linearly dependent upon the active power.

$$f(x) = 0 \tag{6-3}$$

Assuming that a particular constraint is applied to n_M monitored items of plant, the function whose root must be found is given by the maximum amount by which the constraint is violated for any of the monitored plant, as shown in Equation (6-4). The actual values for each item of plant are determined from a load-flow solution.

$$f(x) = \max_{1 \leq i \leq n_M} (value_i - limit_i) \tag{6-4}$$

For example, in the case of voltage limits forming the constraint, the value of the function is given by the maximum difference between any monitored plant voltage and its corresponding limit. The root of the function corresponds with the condition at which none of the voltages of monitored items of plant exceed their corresponding voltage limits, and in the 'worst' case, the voltage lies on the constraint within a tolerance specified by the user.

6.4.2.2 Root Finding Methods

A number of methods are available for finding the roots of one-dimensional functions. Press et al. [111] provide a good selection. Two methods are applied here: the Secant Search Method and Ridders' Method [116].

In the Secant Search Method the function is assumed to be approximately linear in the region of interest. Two function evaluations are performed for different values of x, and a straight line is drawn through the two points. This line is interpolated or extrapolated to the point at which it crosses the axis, which is used as the next approximation of the root, as shown in Figure 6.8.

The updating formula for the Secant method is given by Equation (6-5).

$$x_3 = x_2 + (x_1 - x_2)\frac{f(x_2)}{(f(x_2) - f(x_1))} \tag{6-5}$$

In general the Secant method achieves a rate of convergence equal to 1.618 [111], and is simple to implement. However the use of extrapolation to derive successive approximations of the root ensures that convergence cannot be guaranteed. Local variations in the function can upset the algorithm, and hence it performs best with smooth, well-behaved functions.

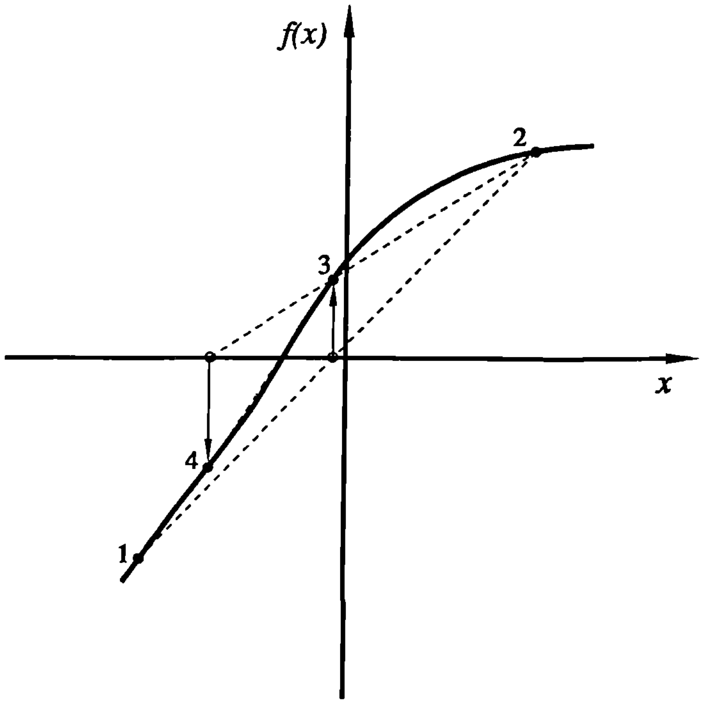

Figure 6.8 Secant Method for Root Finding in One Dimension

Ridders' Method is a variant of the False Position Method [111]. Given two values x_1 and x_2 which bracket the root, the method evaluates the function at the midpoint $x_3 = (x_1 + x_2)/2$ and subsequently linearizes the function about these three points by creating a new function

$$h(x) = f(x)e^Q \tag{6-6}$$

with the requirement that

$$f(x_1) - 2f(x_3)e^Q + f(x_2)e^{2Q} = 0 \tag{6-7}$$

i.e.

$$h(x_1) - 2h(x_3) + h(x_2) = 0 \tag{6-8}$$

Equation (6-7) is a quadratic in e^Q which can be solved analytically using the standard formula

$$e^Q = \frac{f(x_3) + \mathrm{sign}[f(x_2)]\sqrt{f(x_3)^2 - f(x_1)f(x_2)}}{f(x_2)} \tag{6-9}$$

Now an approximation to the root x_4 is determined using the false position method on the values $f(x_1)$, $f(x_3)e^Q$, $f(x_2)e^{2Q}$. Combining this with Equation (6-9) gives the updating formula

$$x_4 = x_3 + (x_3 - x_1)\frac{\mathrm{sign}[f(x_1) - f(x_2)]f(x_3)}{\sqrt{f(x_3)^2 - f(x_1)f(x_2)}} \tag{6-10}$$

The principal advantage of the method is that it is robust. The order of convergence is $\sqrt{2}$, but reliability is greatly improved as compared with the Secant method.

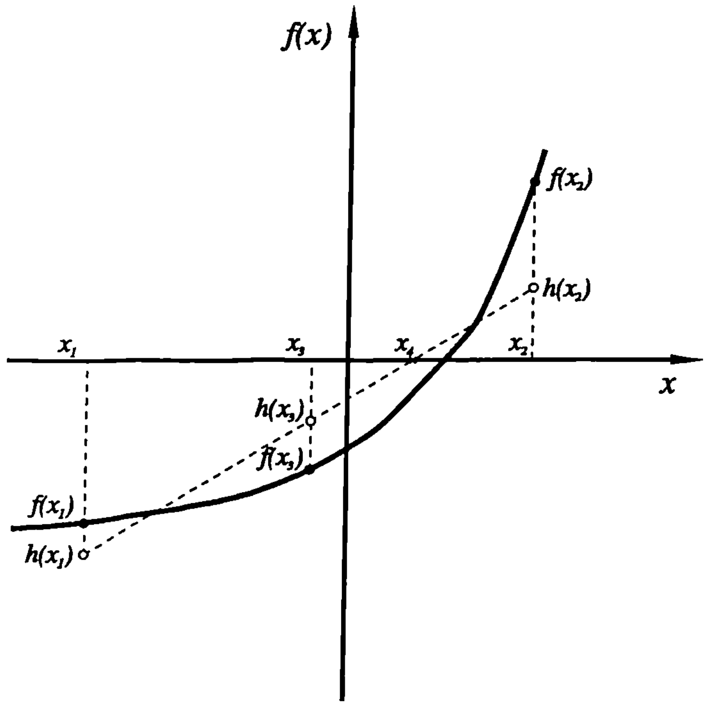

Figure 6.9 Ridders' Method for Root Finding in One Dimension

It should be noted that one of the most effective general methods for root finding, the Newton Method described in Section 3.2.2.1, is not applicable in this case because the derivative of the function in Equation (6-4) with respect to the power of the load or generator is not easily computed.

6.4.2.3 Input Data Requirements

The input data requirements are identical for the two root finding methods, and are listed in Table 6.1.

Table 6.1 Constrained Simulation Data Requirements

Category	Data Required	Storage Location
Constrained Plant	Identity of load or generator to be maximised	Program settings
	Maximum active and reactive power of load or generator	Plant database
Constraint Type	Type of constraint to be observed, e.g. voltage	Program settings
	Identity of plant to be monitored for constraint violations	Program settings
	Appropriate limits for each item of plant to be monitored	Plant database
Algorithm Parameters	Maximum number of iterations before failure	Program settings
	Accuracy to which constraints must be observed	Program settings
Simulation Data	Standard data for a discrete time simulation (refer to Section 4.4.3)	Plant and profiles databases

The constrained simulation algorithm employs the same data set as the standard discrete time simulation, with additional parameters, the majority of which are stored in the program settings file.

The Constrained Plant settings define which load or generator is to be maximised, provide maximum active and reactive power values which are used to restrict the magnitude of power applied during the iterative process.

The Constraint Type settings define which operational limits are to be observed and which items of plant are to be monitored for limit violations. These items are used to evaluate the function in Equation (6-4). The appropriate limits are stored in the relational plant database.

The Algorithm Parameters contain the convergence criteria. The algorithm attempts to find the root of the function to within the accuracy dictated by the user. If the algorithm fails to find a solution within the maximum number of iterations specified by the user it returns with an error message.

6.4.2.4 Procedure for the Proposed Algorithm using the Secant Search Method

The procedure for the method, using the Secant Search method, is summarised in Figures 6.10 and 6.11. The following steps are performed:

1. At the first time step, suitable values for x_1 and x_2 must be selected for the specified load or generator. The Secant method does not require that these values bracket the root, but convergence is more reliable if this is the case. The first estimate corresponds to $P_D = 0$, $Q_D = 0$. The second estimate uses the maximum values for the load or generator, which in many cases will lead to constraint violations, i.e. the root will be bracketed.

   At subsequent time steps the algorithm exploits the fact that system loading conditions tend to change little from one time step to the next, and hence the solution from the previous time step is likely to be close to the solution for the current step. The algorithm uses the previous solution as the initial estimate, and evaluates the error function for this condition. Then, depending upon whether the error is positive or negative a small increment (10%) is added to or subtracted from the initial estimate to give the second estimate. In most cases the resulting pair of estimates will bracket the root.

Loads and generators are treated slightly differently when calculating successive estimates for the solution. In the case of loads, and generators operating in PQ mode with specified active *and* reactive power, the power factor is determined from nominal active and reactive values at the start of the algorithm. Whenever the active power is varied the reactive power is also varied to maintain this power factor. In the case of generators operating in PV mode, where active power is specified and reactive power varies to maintain a specified voltage, just the active power is varied and the reactive power is determined from the load-flow solution.

2. The pair of estimates are passed to a bracketing algorithm which adjusts them if necessary to ensure that they bracket the root. This algorithm is described in Section 6.4.2.6.

3. The algorithm enters the main loop. If the value of the function is smaller than the minimum accuracy specified by the user the algorithm proceeds to the next time step, Step 1.

4. Provided the maximum number of iterations has not been exceeded the algorithm derives a new estimate of the solution from the two most recent estimates using the Secant updating formula of Equation (6-5). If the maximum number of iterations are exceeded the algorithm terminates with an error status.

5. The error function of Equation (6-4) is evaluated using the latest estimate. Should the load-flow fail to converge because the estimate is excessively large, the algorithm reduces the estimate, by halving and then subtracting the increment added in Step 4., and runs another load-flow.

6. If the load-flow converges the algorithm returns to Step 3.

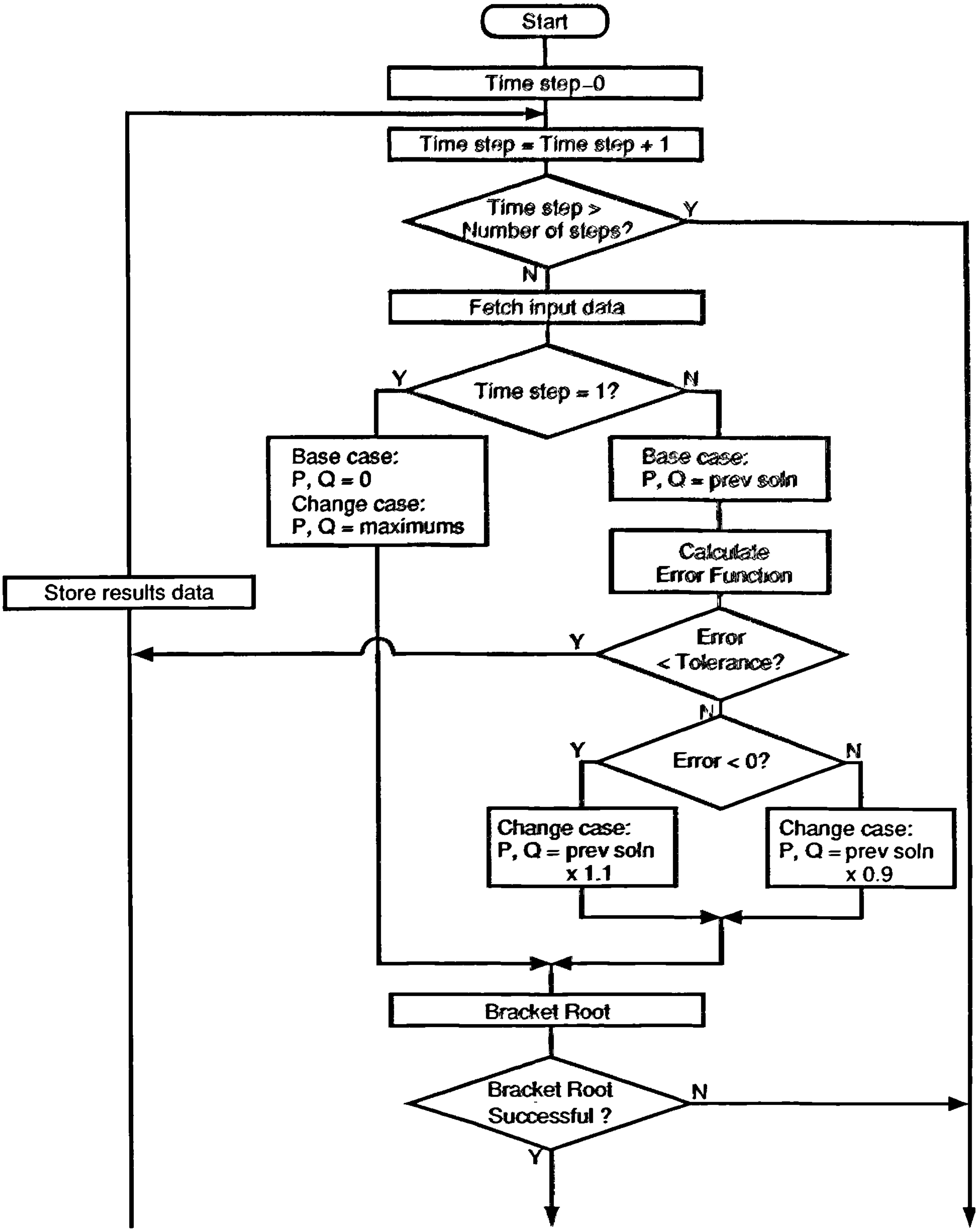

Figure 6.10 Flow Chart of the Constrained Simulation Algorithm Using the Secant Search Method

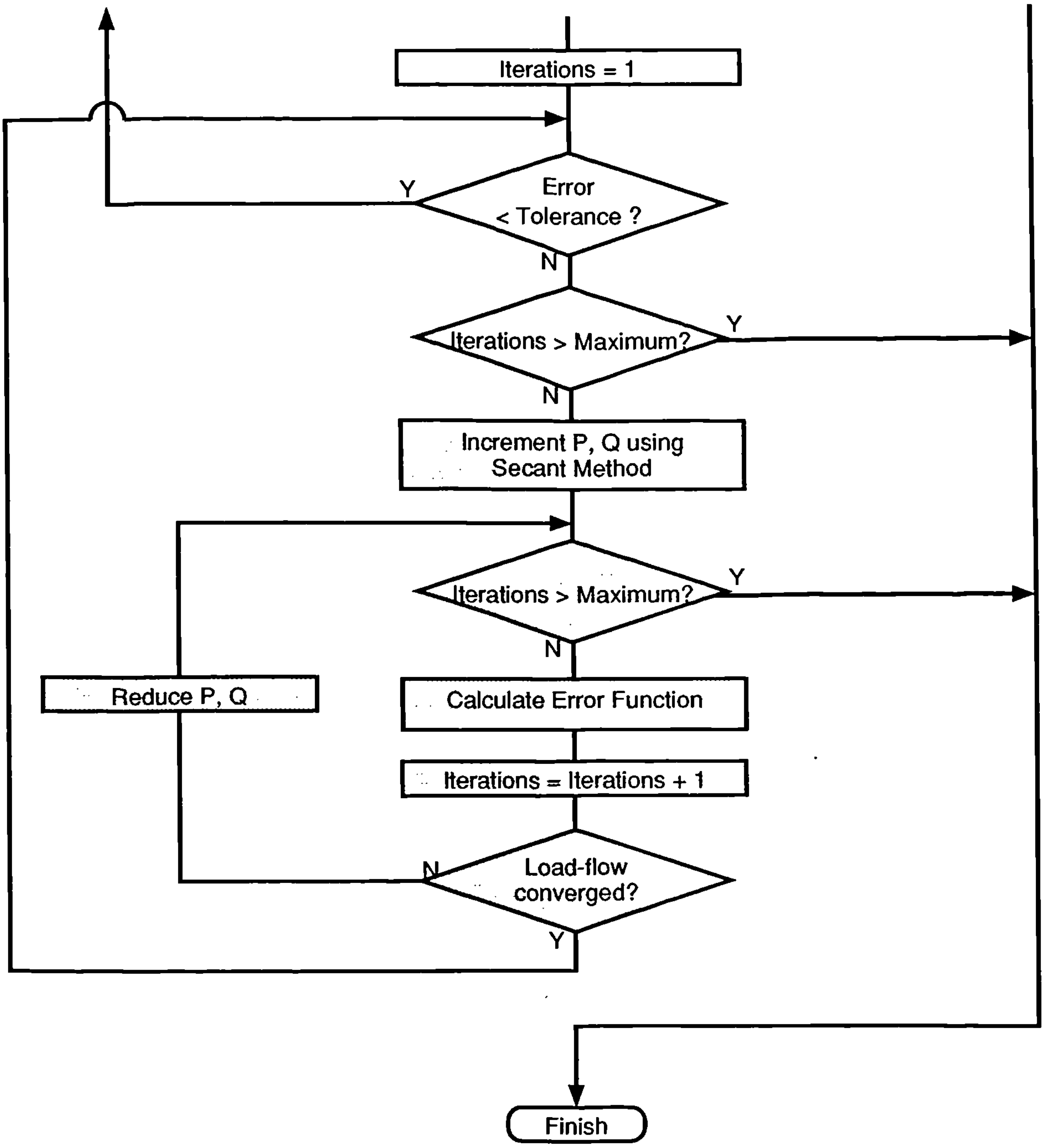

Figure 6.11 Flow Chart for Constrained Simulation Algorithm Using the Secant Search Method (Cont.)

6.4.2.5 Procedure for the Proposed Algorithm Using Ridders' Method

The procedure in the case of Ridders' method is very similar to that of the Secant method. The shaded steps in Figure 6.11 are replaced by Ridders' root-finding algorithm. Two error function evaluations are performed in each iteration of the method, and Equation (6-10) is used to compute a new estimate.

6.4.2.6 Root Bracketing Algorithm

The root bracketing algorithm is based upon standard techniques, such as the method cited by Press et al. [111], with additional logic to reduce the likelihood of load-flow failures due to excessively large estimates and to overcome such failures when they occur. A flow chart of the algorithm is shown in Figure 6.12.

```
ROOT BRACKETING ALGORITHM
  CALCULATE ERROR FUNCTION FOR FIRST ESTIMATE P1
    REPEAT
    CALCULATE ERROR FUNCTION ERROR1 FOR P1
    INCREMENT ITERATION COUNT
      IF LOAD-FLOW FAILS
      REDUCE ESTIMATE P1:   P1 = P1/ 1.3
    UNTIL LOAD-FLOW CONVERGES OR ITERATION COUNT EXCEEDED
  CALCULATE ERROR FUNCTION FOR SECOND ESTIMATE P2
    REPEAT
    CALCULATE ERROR FUNCTION ERROR2 FOR P2
    INCREMENT ITERATION COUNT
      IF LOAD-FLOW FAILS
      REDUCE ESTIMATE P2:   P2 = P2 - (P2-P1) x 0.618
    UNTIL LOAD-FLOW CONVERGES OR ITERATION COUNT EXCEEDED
  BRACKET ROOT
    WHILE ROOT IS NOT BRACKETED AND ITERATION COUNT NOT EXCEEDED
      IF ERROR2 < ERROR1
      INCREMENT P2 USING MODIFIED SECANT METHOD
        REPEAT
        CALCULATE ERROR FUNCTION ERROR2 FOR P2
        INCREMENT ITERATION COUNT
          IF LOAD-FLOW FAILS
          HALVE INCREMENT AND SUBTRACT FROM P2
        UNTIL LOAD-FLOW CONVERGES OR ITERATION COUNT EXCEEDED
      ELSE IF ERROR2 > ERROR1
      INCREMENT P1 USING MODIFIED SECANT METHOD
        REPEAT
        CALCULATE ERROR FUNCTION ERROR1 FOR P1
        INCREMENT ITERATION COUNT
          IF LOAD-FLOW FAILS
          HALVE INCREMENT AND SUBTRACT FROM P1
        UNTIL LOAD-FLOW CONVERGES OR ITERATION COUNT EXCEEDED
      ELSE ERROR2 = ERROR1
      EXPAND BOUNDS ON P1 AND P2:   P1 = P1 + (P1 - P2) x 0.618, P2 = P2 + (P2 - P1) x 0.618
        REPEAT
        CALCULATE ERROR FUNCTION ERROR1 FOR P1
        INCREMENT ITERATION COUNT
          IF LOAD-FLOW FAILS
          HALVE INCREMENT AND SUBTRACT FROM P1
        UNTIL LOAD-FLOW CONVERGES OR ITERATION COUNT EXCEEDED
        REPEAT
        CALCULATE ERROR FUNCTION ERROR2 FOR P2
        INCREMENT ITERATION COUNT
          IF LOAD-FLOW FAILS
          HALVE INCREMENT AND SUBTRACT FROM P2
        UNTIL LOAD-FLOW CONVERGES OR ITERATION COUNT EXCEEDED
```

Figure 6.12 Constrained Simulation Bracketing Algorithm

6.4.2.7 Load Constrained Simulation Example

When interpreting performance results for the constrained simulation algorithms it is important to study the characteristic of the function being solved. This function is dependent upon factors such as network topology, the siting and operation of transformers, generators and reactive compensation equipment, and the demand profiles of neighbouring loads. However, from a typical example it is still possible to draw some general conclusions concerning the performance of the algorithms.

Figure 6.13 shows a section of the 52 Node test system. In this example the demand at Load Ld14 is varied and the error function is based upon voltage constraints. Figure 6.14 shows the error function against active power demand for Load Ld14 for three transformer tap settings. These settings are:

1. On-load tap changing on all transformers in the system
2. On-load tap changing on all transformers except T27 whose tap is fixed at its nominal position
3. Taps on all transformers fixed at nominal positions.

For case 1. Figure 6.15 shows the operation of three transformers feeding the Ld14 feeder. For transformers T18 and T27 the tap changer is located on the primary (high voltage) side. On transformer T1 the tap changer is on the secondary (low voltage) side and hence operates in the opposite sense.

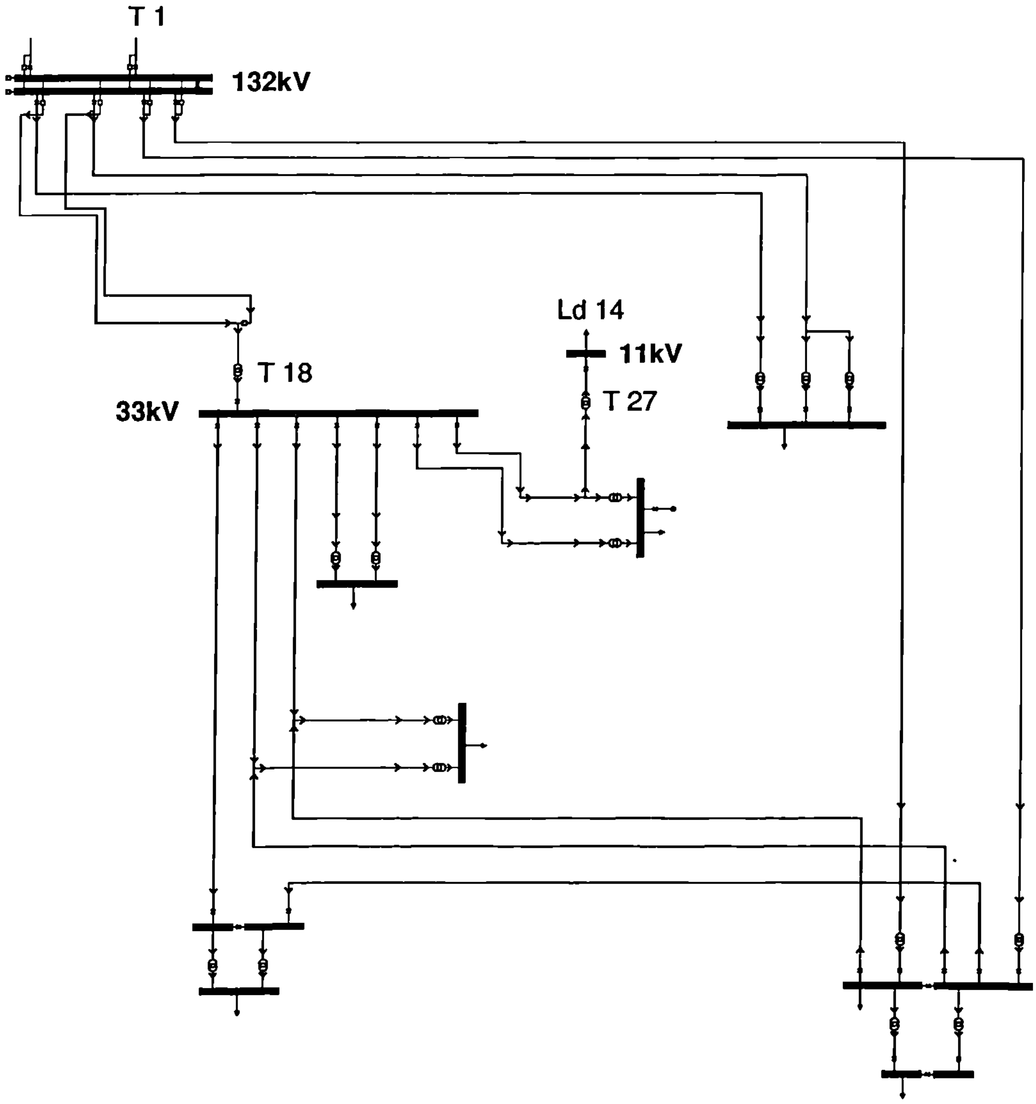

Figure 6.13 Constrained Simulation Test System

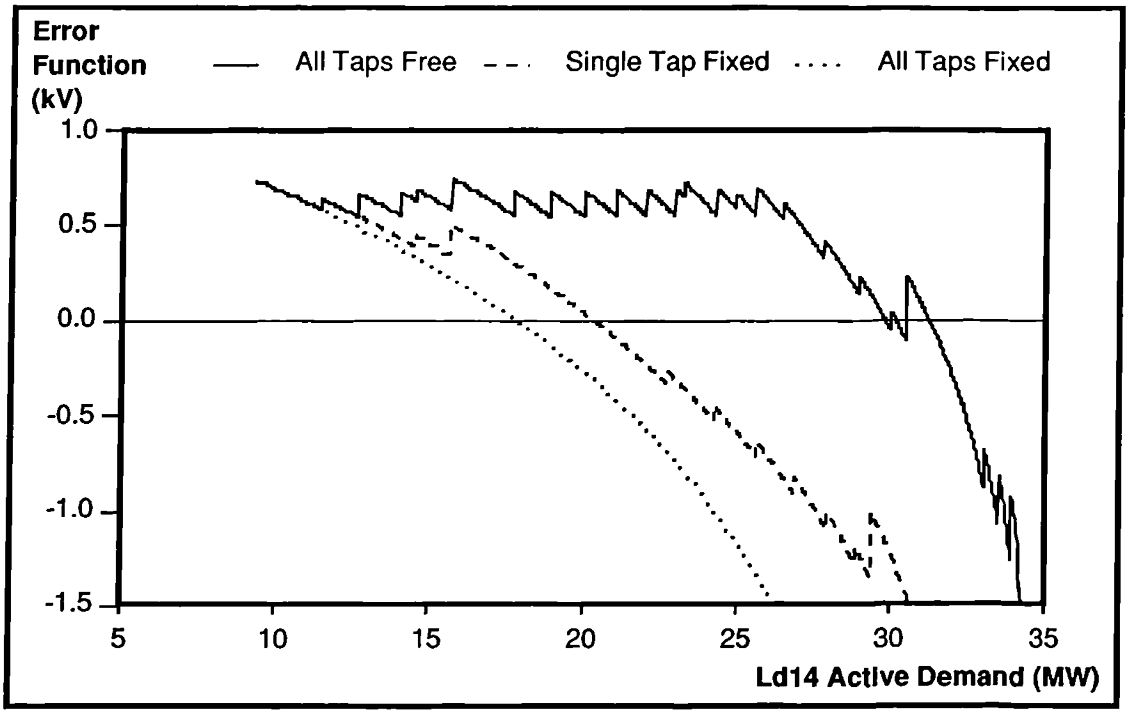

Figure 6.14 Load Ld14 Error Function for 3 Different Transformer Tap Settings

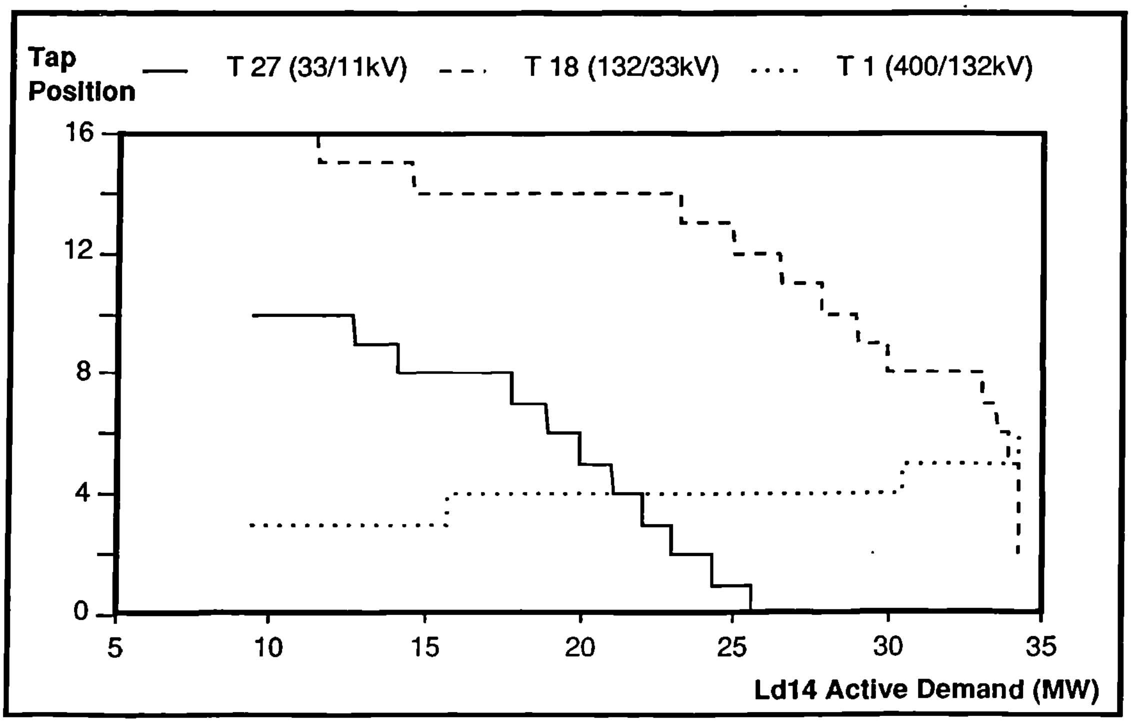

Figure 6.15 Transformer Tap Operation for Different Values of Load Ld14

Figure 6.14 illustrates the effects of transformers with on-load tap changing on the nature of the error function. (On-load tap changing is commonplace in the UK at these voltage levels.) The following effects are noted:

1. The error function is not smooth and continuous, but has a saw-tooth profile as taps change at different locations in the system.
2. There is no guarantee of a single root. In this example there are five roots.
3. There is no guarantee that the root can be obtained to the specified accuracy. Because transformer taps operate in discrete steps, should a tap change transition coincide with the root it may be impossible to reach it.
4. While local transformers operate within their tap limits the error function curve exhibits very little variation with demand.
5. As transformers reach their tap limits the error function curve drops sharply. In this case the voltage collapses when the demand is between 35 and 36 MW.

Figure 6.16 compares the convergence characteristics of the Secant Method and Ridders' Method for the three transformer tap settings.

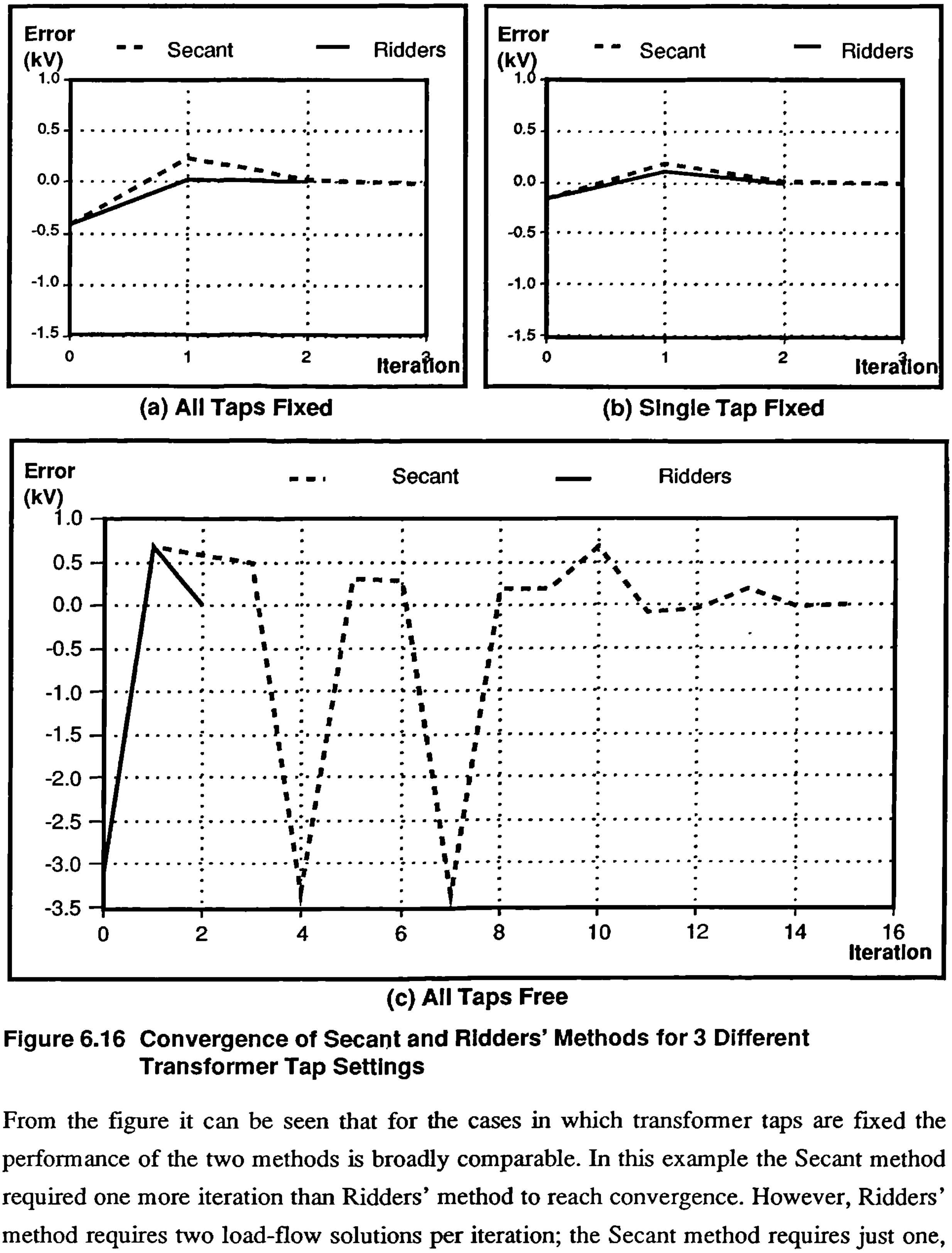

Figure 6.16 Convergence of Secant and Ridders' Methods for 3 Different Transformer Tap Settings

From the figure it can be seen that for the cases in which transformer taps are fixed the performance of the two methods is broadly comparable. In this example the Secant method required one more iteration than Ridders' method to reach convergence. However, Ridders' method requires two load-flow solutions per iteration; the Secant method requires just one, and hence works out marginally quicker overall.

For the case in which transformers were set to on-load tap-changing the Secant method converges slowly and erratically. Ridders' method converges in two iterations as before.

The reasons behind the poor performance of the Secant method are better understood by superimposing the convergence characteristic on the error function, as shown in Figure 6.17.

During convergence whenever the root is bracketed by the two latest estimates, convergence is slow due to the asymptotic nature of the error function curve. This is a well known weakness of the method (Press et al [111]). In addition when the two latest estimates do not bracket the root, but lie on the upper portion of the error function curve the shallow gradient results in extrapolation to large values of demand. When this occurs the load-flow fails to converge, and the algorithm must reduce the demand in stages until a load-flow solution can be obtained. Such a process can disrupt progress towards the solution.

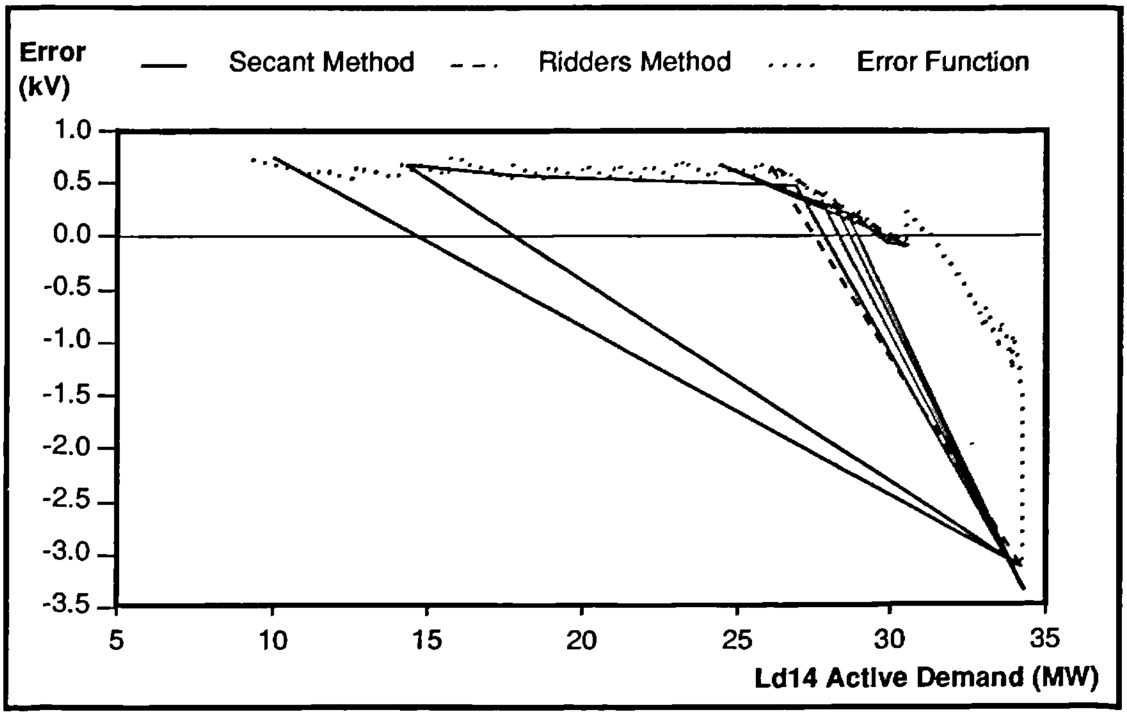

Figure 6.17 Convergence Characteristic of the Secant Method with On-Load Tap Changing

6.4.2.8 Generator Constrained Simulation Example

In many respects the constrained simulation algorithm operates in the same manner when maximising generation output as it does for maximising load demand. In the generator constrained case maximum voltage limits form the constraint in place of the minimum voltage limits in the load constrained case.

An additional problem arises when generators are operating in PV mode; that is, with active power specified while reactive power varies to maintain a constant specified voltage. While the generator is operating within its reactive limits the voltage will not vary with active power. However, once a reactive limit has been reached the generator switches to PQ mode of operation and the voltage varies with active power. Figure 6.18 shows the error function and reactive power output for a generator connected in place of load Ld14 in the 52 node test system. The generator has reactive limits of ±10MVAr, and transformers are set to on-load tap changing.

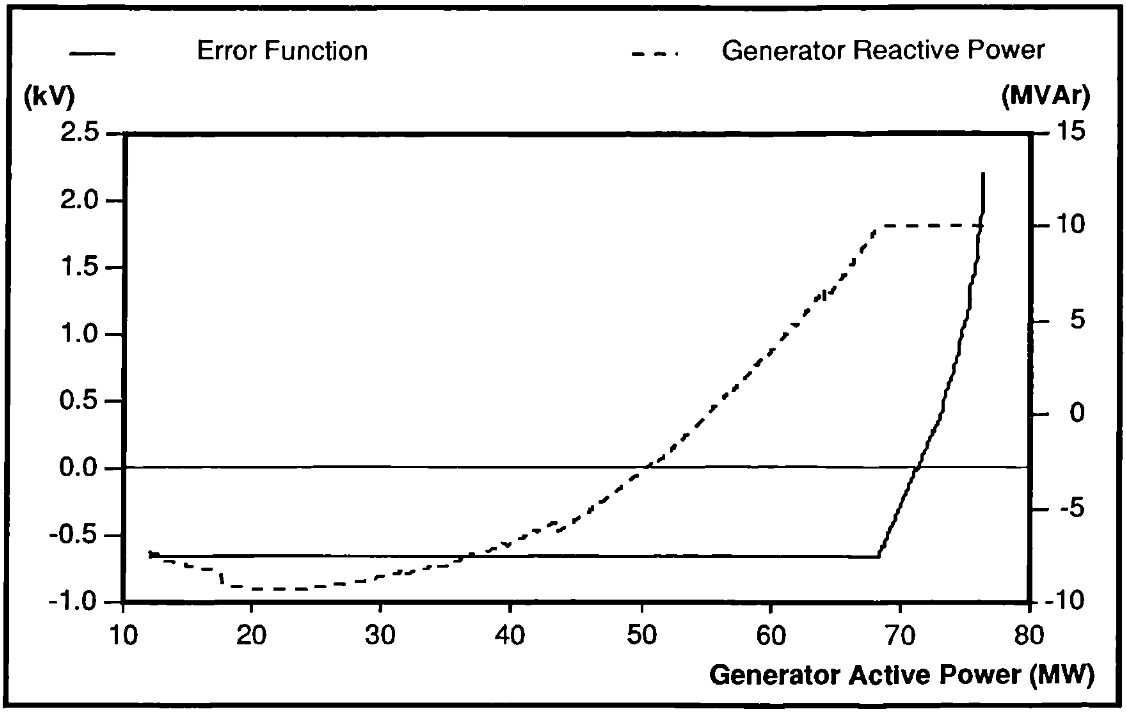

Figure 6.18 Error Function for PV Generator Connected at Node 43

The sharp increase in voltage once the generator's 10MVAr limit has been reached would be expected to cause problems for the Secant method. Figure 6.19 shows the corresponding convergence characteristic, and confirms that this is indeed the case.

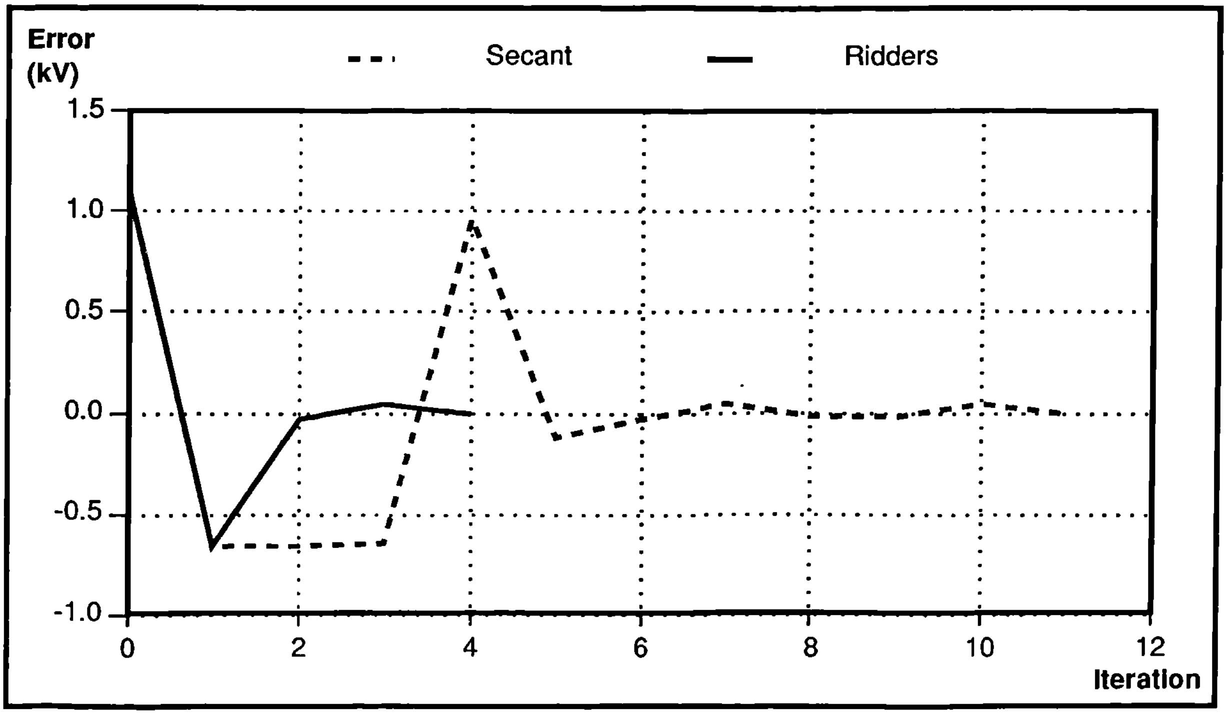

Figure 6.19 Convergence of Secant and Ridders' Methods for PV Generator

6.4.2.9 Test Results

The execution speed and reliability of the two methods were compared through a series of 24 hour constrained simulation studies. A total of 8 substations were selected from the available test systems. The third Wednesday in January was chosen as a typical winter weekday, and simulation runs were performed for this day at half hour steps. The maximum number of load-flow solutions allowed for each method was 50 for each time step, and the convergence tolerance on the error function was 0.1%.

For the first time step two initial estimates of active power for the selected load or generator were derived as follows: the first estimate was zero in each case, the second estimate was obtained by increasing the annual maximum active power for the load or generator by 20%.

For subsequent time steps the solution for the previous time step was adjusted by ±5% to obtain the two initial estimates. In each case the estimates were passed to the bracketing algorithm for possible modification to ensure that the solution was bracketed. Table 6.2 lists the number of load-flow solutions and load-flow iterations required to bracket the solution at the first and subsequent time steps. This provides a measure of how non-linear the error function was for each case, and hence the difficulty of the problem.

The first time step represents a more difficult problem for the constrained simulation algorithms than the subsequent time steps, because although the solution is bracketed the initial estimates are likely to be some distance from the solution. Initial estimates at succeeding steps are likely to be much closer to the solution. The test results have therefore been presented in two tables: Table 6.3 applies to the first step, and Table 6.4 applies to the complete simulation including the first step.

Table 6.2 Test Results for the Constrained Simulation Bracketing Algorithm

Test System	Load/ Gen	First Time Step		Subsequent Time Steps	
		Load-flow Solutions	Total Load-flow Iterations	Av. Load-flow Solutions	Av. Load-flow Iterations
9 Node	Gen2	10	47	1.94	12.13
30 Node	Gen4	40	733	1.87	38.15
52 Node	Ld14	2	18	1.87	12.71
	Gen3	3	29	2.79	18.04
348 Node	Ld14	2	30	2.06	22.73
	Ld28	6	130	2.04	24.96
	Ld83	5	151	1.42	22.06
	Ld114	11	260	2.10	26.81

Table 6.3 Constrained Simulation Results for First Time Step

Test System	Load/ Generator	Method	First Time Step		
			Method Iterations	Load-flow Solutions	Load-flow Iterations
9 Node	Gen2	Secant	0	0	0
		Ridders	0	0	0
30 Node	Gen4	Secant	Convergence not obtained after 50 LF solutions		
		Ridders	4	8	59
52 Node	Ld14	Secant	10	13	152
		Ridders	5	10	87
	Gen3	Secant	1	1	10
		Ridders	2	4	40
348 Node	Ld14	Secant	9	13	291
		Ridders	2	4	68
	Ld28	Secant	8	18	268
		Ridders	2	4	68
	Ld83	Secant	7	13	329
		Ridders	4	8	136
	Ld114	Secant	11	28	654
		Ridders	2	4	68
Average over all cases (Excl. 30 Node Gen4)		Secant	6.57	12.29	243.43
		Ridders	2.43	4.86	66.71

Table 6.4 **Constrained Simulation Results for the Complete Simulation**

Test System	Load/ Generator	Method	Average Method Iterations	Average Load-flow Solutions	Average Load-flow Iterations	Average CPU Time per Time Step (s)
9 Node	Gen2	Secant	0.44	0.44	2.77	0.42
		Ridders	0.44	0.87	5.52	0.48
30 Node	Gen4	Secant	Convergence not obtained after 50 LF solutions			
		Ridders	0.54	1.08	8.50	4.46
52 Node	Ld14	Secant	2.06	2.13	8.77	0.60
		Ridders	1.17	2.33	8.21	0.56
	Gen3	Secant	1.33	1.33	9.52	0.96
		Ridders	0.19	0.37	2.71	0.69
348 Node	Ld14	Secant	1.51	1.67	23.80	8.54
		Ridders	0.98	1.96	21.49	9.05
	Ld28	Secant	1.52	1.73	20.88	7.90
		Ridders	0.97	1.96	22.63	8.35
	Ld83	Secant	0.54	0.67	11.00	4.26
		Ridders	0.42	0.83	9.83	5.15
	Ld114	Secant	1.38	1.73	26.06	10.04
		Ridders	0.94	1.87	21.06	8.54
Average over all cases (Excl. 30 Node Gen4)		Secant	1.25	1.38	14.69	4.67
		Ridders	0.73	1.46	13.06	4.69

CPU times were recorded on a Digital VAXstation 4000-60 workstation

6.4.2.10 Discussion

The results for the bracketing algorithm, Table 6.2, show that in the majority of cases the algorithm requires less than 10 load-flow solutions to locate a pair of estimates which bracket the solution.

In one case, Generator 4 in the 30 Node system, the algorithm struggled to bracket the solution. In this case the solution lay very close to the limit beyond which the load-flow failed to converge. In addition the generator's reactive limits were reached at a point very close to the solution, and hence the voltage for the generator remained constant over a very large part of the feasible operating region. Under these conditions any bracketing algorithm will struggle to converge, because there is no information to direct the search.

The results comparing the two constrained simulation algorithms for the first time step, Table 6.3, indicate that Ridders' Method is superior to the Secant Method when the initial estimates are some way from the solution. In all but one case Ridders' Method required fewer load-flow solutions to reach the solution, and was on average approximately three times quicker than the Secant Method on the test cases used. In the difficult case in the 30 Node system, the Secant method failed to find a solution in 50 load-flow solutions, while

Ridders' Method required 8 solutions. This finding is in line with expectations outlined in preceding sections.

The results comparing the two algorithms for the complete simulation, Table 6.4, indicate that there is little difference in performance when the initial estimates are close to the solution. Ridders' Method converges in fewer method iterations than the Secant Method, but requires twice as many load-flow solutions per method iteration, hence the overall levels of performance are similar. It is to be expected that performance of Ridders' Method will prove to be more robust in 'difficult' cases, for example when system conditions change significantly from one time step to the next. This factor, together with the greater reliability of the method under the difficult conditions at the first time step make it the method of choice for constrained simulation applications.

6.5 Conclusions

This chapter has outlined practical applications for the discrete time simulation approach described in earlier chapters of the thesis. Applications relevant to the analysis of voltage problems, the impact of embedded generation and the study of system capacity have been described.

6.5.1 Analysis of Voltage Related Problems

It has been noted that discrete time simulation is capable of providing an accurate assessment of the voltage conditions on the system as a function of time, which includes the times of occurrence, duration and severity of any voltage violations on the system under study.

It has been shown that this approach also serves as a valuable planning tool in the sizing and placement of capacitors to alleviate voltage problems on the system. The procedure followed in the Insight application to model the effects of capacitive compensation has been outlined and demonstrated by way of a worked example.

Additional applications of the software relating to voltage regulation have been described. It has been noted that the Insight application is well suited to model the voltage regulation problems on rural feeders, and provides a means by which the Line Drop Compensation settings of primary transformers can be adjusted to meet the voltage regulation requirements of both local and remote loads. The use of the Insight application in an automatic voltage control scheme to optimise tap positions in areas with severe voltage regulation problems has also been described. Another important area of application is the assessment of voltage reduction schemes. It has been noted that time based analysis coupled with the polynomial modelling of the voltage dependency of loads provides an accurate means of calculating the effect on system demands of selective voltage reduction measures.

6.5.2 Analysis of Problems Related to Embedded Generation

The sharp increase in numbers of embedded generators commissioned and under construction since deregulation of this sector of the industry has been described and shown to pose difficulties for REC planning engineers in connection with voltage regulation, protection co-ordination and system economics. The procedure for assessing the impact of prospective embedded generators on the local voltages and power flows has been outlined. The calculation of embedded generator scaling factors to account for incremental system losses has also been described.

It has also been noted that the output of embedded generators may be restricted in certain locations and at certain times of the day by constraints related to voltage and current limits. A constrained simulation algorithm has been proposed to determine the maximum permissible output of a generator as a function of time, while observing such constraints.

6.5.3 Analysis of System Capacity

It has been noted that the ability of discrete time simulation to account for load diversity makes it possible to assess the utilisation of the system with greater levels of accuracy than more approximate methods.

The constrained simulation algorithm has been proposed to determine the maximum additional load that can be supported at a given location without violating operational constraints.

Two root finding algorithms for determining the maximum load or generation have been compared: the Secant Search Method and Ridders' Method. A bracketing algorithm based upon established techniques but tailored to the needs of this application has been presented for determining two initial estimates which bracket the solution.

The nature of the problem to be solved has been assessed using a worked example, through which it has been demonstrated that the presence of on-load tap changing transformers and generators operating in PV mode can make the error function difficult, and in certain cases impossible, to solve. It has been shown that the Secant Method is particularly susceptible to these problems when the initial estimates are not close to the solution.

The execution speed and reliability of the two methods have been compared for loads and generators at eight locations in a variety of test systems. The results for the bracketing algorithm demonstrate that it operates reliably even in difficult cases, normally requiring between 2 and 11 load-flow solutions to bracket the solution. Constrained simulation results for the first time step confirm the findings of the worked example: that the convergence of the Secant Method is erratic and relatively slow when the initial estimates are not very close to the solution. In comparison the convergence of Ridders' Method is reliable and approximately three times as fast. The results for a full twenty four hour simulation indicate that the two methods are broadly comparable in terms of execution speed when initial conditions are close to the solution. In the final analysis Ridders' Method is proposed as the method of choice on the grounds of greater reliability.

The following chapters describe the application of the discrete time simulation approach to the evaluation, costing and allocation of electrical losses.

Chapter 7. Calculation of Losses

7.1 Introduction

Losses are a highly important issue in the operation and planning of the distribution system. Energy dissipated as losses at the distribution level comprises a significant proportion, usually in the region 5 to 10 percent, of the total energy supplied to the system. The proportion of the capacity of the system which is tied up to supply these losses during periods of peak demand can often exceed 10 percent. It is clear that losses at the distribution level give rise to substantial costs both in terms of wasted energy, and in bringing forward necessary capital investment in all three sectors of the industry: generation, transmission and distribution [57].

The first step in developing a loss management strategy is to identify the different components of loss, and to locate and quantify each component within the system. In this chapter the existing methods for calculating losses are reviewed and a new algorithm based upon discrete time simulation is proposed.

7.2 Demand Loss and Energy Loss

Electrical losses are generally expressed in terms of two components: demand or power loss, and energy loss. These terms are defined in Appendix A.

Demand loss is typically calculated at the time of system peak demand to determine the capacity required to serve the maximum load and loss.

Energy losses are evaluated for a particular period of time, typically a year, and can be derived from demand losses using Equation (7-1).

$$W_L = \int_{t_0}^{t_0+T} P_L(t)\,dt \qquad (7\text{-}1)$$

The concepts of demand and energy components are normally retained when applying a cost to electrical losses. A demand or capacity component of cost is defined which reflects the investment costs of new plant required to supply the losses during peak load. An energy component of cost is defined which covers the cost of supplying the energy loss.

7.3 Sources of Loss in a Distribution System

Electrical losses can be considered in terms of two broad categories: technical losses and non-technical or commercial losses. The primary sources of these losses are listed in Table 7.1. Other minor sources of loss include circuit breakers and switchgear, reactors, and capacitors. A comprehensive list of components, with representative percentage loss figures is provided by Hickok [67].

Table 7.1 Primary Sources of Distribution System Loss

Loss Type	Sources
Technical Losses	Joule effect losses in lines, cables and transformer windings
	Iron losses in transformer cores
	Dielectric losses in cables
	Corona effect losses in high voltage lines
Non-technical Losses	Theft
	Metering and accounting errors

The calculation of non-technical losses is beyond the scope of this work, which instead addresses the different components of technical loss. The technical losses can further be classified under the headings fixed and variable losses. The terms no-load and load losses are also used.

Fixed losses are considered independent of system loading, and normally include transformer iron losses, dielectric losses and corona losses. Of these, iron losses are by far the most significant.

Variable losses are dependent upon loading level and include Joule effect (I^2R) losses.

7.4 Review of Existing Methods for Evaluating Demand Losses

A variety of methods for evaluating demand losses have been developed over a period of many years. The more important methods are outlined in the following sections. The methods are then assessed in the light of criteria developed later in the chapter.

7.4.1 Calculation of Demand Losses Using Loss Formulae

7.4.1.1 Introduction

The earliest methods for evaluating demand losses arose from research into the economic dispatch problem. Loss formulae were developed to relate the losses in the system to the active power outputs of the generators. The traditional form of the loss formula is given in Equation (7-2).

$$P_L = \mathbf{P}_G^T[\mathbf{B}]\mathbf{P}_G + \mathbf{P}_G^T\mathbf{B}_0 + B_{00} \qquad (7\text{-}2)$$

where $[\mathbf{B}]$, $\mathbf{B}_0$ and B_{00} are called the B-coefficients. A number of methods have been developed for calculating the the B-coefficients, the most widely used of which are outlined in the following sections. In most cases the coefficients are calculated from the results of two load-flow solutions at system 'base' and 'off-base' conditions. Strictly the loss formula applies only to these conditions. However, the formula remains valid over a certain range of conditions provided the following conditions are met:

- Individual load currents are a linear function of the system load current, i.e. they conform.
- The reactive power output of each generator is a linear function of its real power output.
- Generator voltages and angles do not deviate significantly from their base case values.

7.4.1.2 Calculation of B-Coefficients Using Invariant Transformations

This method was first developed by Kron [79, 80] in the early 1950s and uses concepts from tensor analysis. From a linear open-circuit network, as shown in Figure 7.1, the equation for 'Reference Frame 1_0' is defined as

$$\mathbf{E}_0 = [\mathbf{Z}_0]\mathbf{I}_0$$

$$\begin{bmatrix} E_1 - E_R \\ \vdots \\ E_N - E_R \\ E_A - E_R \end{bmatrix} = \begin{bmatrix} Z_{11} & \cdots & Z_{1N} & Z_{1A} \\ \vdots & & \vdots & \vdots \\ Z_{N1} & \cdots & Z_{NN} & Z_{NA} \\ Z_{A1} & \cdots & Z_{AN} & Z_{AA} \end{bmatrix} \begin{bmatrix} I_1 \\ \vdots \\ I_N \\ I_A \end{bmatrix} \qquad (7\text{-}3)$$

where subscript R refers to the reference generator, and subscript A refers to autotransformers in the system.

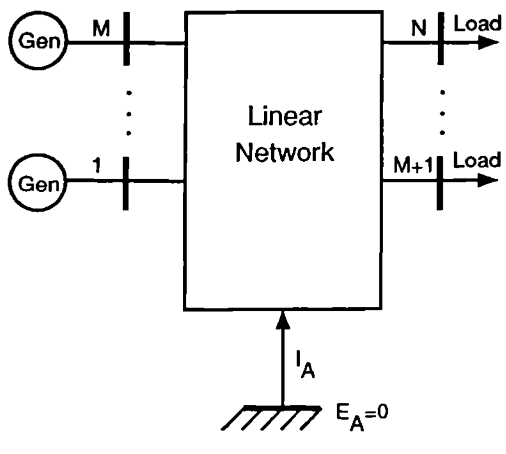

Figure 7.1 Kron Network Diagram Conventions

The loss formula of Equation (7-2) is derived from Equation (7-3) by performing a series of invariant transformations which convert existing system variables to new variables, while keeping power injections and losses constant. The purpose of the transformations is to eliminate from the equation the load currents, and to express the generator currents in terms of generator powers, in order that the losses might be expressed in terms of generator powers.

7.4.1.3 Calculation of B-Coefficients Using the Bus Impedance Matrix

In 1979 Shoults et al [127] published a simplified method for calculating B-coefficients using the standard bus impedance matrix, Z.

$$\mathbf{E} = [\mathbf{Z}]\mathbf{I} \tag{7-4}$$

Two transformations are performed: the first to express the load currents in terms of the generator currents, and the second to express the generator currents in terms of the generator real power outputs.

As in the Kron-based methods of invariant transformations the load currents are assumed to conform to the total load current, and the reactive output of each generator is assumed to be a linear function of its active output. Unlike the Kron based methods the constants of proportionality that define these relationships are calculated from the results of two load-flows using the method of least squares.

Rather than forming the bus impedance matrix explicitly the method uses optimally ordered bifactorisation of the bus admittance matrix. Once the bifactorisation of the admittance matrix has been completed once, the direct solution stage is all that is subsequently required to solve all the equations involving Z.

Shoults et al state that the method is simpler and quicker both in implementation and execution time than the Kron-based methods.

7.4.1.4 Loss Formula Based Upon the AC Load-flow Jacobian

Penalty factors have traditionally been used in economic dispatch calculations to define the incremental losses at each bus, as shown in Equation (7-5).

$$PF_i = \left(\frac{1}{1 - \frac{\partial P_L}{\partial P_{G,i}}} \right) \tag{7-5}$$

Early methods calculated penalty factors from the B-coefficients of the Loss Formula of Equation (7-2). Penalty factors can also be calculated using the AC load-flow Jacobian, or from a DC load-flow solution.

Practical methods to calculate system losses directly from penalty factors have not been found. However, by linearising the loss equation around a particular operating condition, as in Equation (7-6), penalty factors can be used to derive an approximation for the losses.

$$P_L = P_L^0 + \Delta P_L \qquad (7\text{-}6)$$

Dy Liacco [38] presents a suitable formulation, which starts with a statement of the economic dispatch problem

$$\begin{aligned} \min f(x,P) &= \sum_{i \in g} F_{C,i}(P_{G,i}) \\ g(x,P) &= 0 \end{aligned} \qquad (7\text{-}7)$$

where $F_{C,i}(P_{G,i})$ is the cost function for real generated power, x represents the dependent variables, P represents the active variables, g represents the load-flow equations and G is the set of generators. Solving the Lagrangian equation for this optimisation problem, the reduced gradient can be derived as

$$\nabla f = \frac{\partial \mathbf{F}_C}{\partial \mathbf{P}} - \alpha_P \frac{\partial F_{C,R}}{\partial P_R} = 0 \qquad (7\text{-}8)$$

where subscript R denotes reference bus, and α_P is given by

$$\alpha_P = \left(- \left[\frac{\partial \mathbf{g}}{\partial \mathbf{x}} \right]^T \right)^{-1} \frac{\partial \mathbf{P}_R}{\partial \mathbf{x}} \qquad (7\text{-}9)$$

but consists only of the terms corresponding to the real power equations in the load-flow equations. Note that $\left[\frac{\partial \mathbf{g}}{\partial \mathbf{x}}\right]$ is the Jacobian equation.

The reference bus penalty factor for generator i can be derived as

$$PF_i = \frac{1}{\alpha_{p,i}} \qquad (7\text{-}10)$$

However, when considering losses we note that since for a particular generator bus i, $\alpha_{p,i} = \frac{\partial P_R}{\partial P_{G,i}}$ we can substitute into Equation (7-6) to obtain an expression for the total losses given in Equation (7-11).

$$P_L = P_L^0 + \sum_{i=1, i \neq R}^{M} \alpha_{p,i} \Delta P_{G,i} \qquad (7\text{-}11)$$

7.4.1.5 Loss Formula Based Upon DC Load-flow Equations

Podmore [109] developed a straightforward technique for deriving a loss formula from the equations of a DC load-flow. From a description of the active power loss in a branch:

$$P_{L_{ij}} = |E_i - E_j|^2 g_{ij} \qquad (7\text{-}12)$$

an expression is derived which expresses the total losses in terms of two components: a voltage dependent component and an angle dependent component, as shown in Equation (7-13).

$$P_L = P_L^{\theta} + P_L^V \tag{7-13}$$

$$\text{where} \quad P_L^{\theta} = \sum_{ij}^{\text{n branch}} E_i E_j \theta^2 g_{ij}$$

$$\text{and} \quad P_L^V = \sum_{ij}^{\text{n branch}} (E_i - E_j)^2 g_{ij}$$

The DC load-flow equations are then used to express the bus angles as linear functions of the bus powers, making the assumption that the angles are small. The resulting expressions are substituted into Equation (7-13) to give the loss formula.

$$P_L = \mathbf{P}_G^T[\mathbf{E}_{GG}]\mathbf{P}_G + \mathbf{P}_G^T\mathbf{E}_{G0} + E_{00} + P_L^V \tag{7-14}$$

The coefficients E_{GG}, E_{G0} and E_{00} consist of combinations of bus injections, voltages and branch impedances.

The benefits of the method are its relative simplicity and speed compared with the traditional B-coefficients methods. In addition the assumption that generator reactive powers are linearly related to their active powers is avoided in this formulation. Instead the underlying assumption is that voltage magnitudes remain constant.

7.4.1.6 Loss Formula Based Upon a Loop-Based Method

In 1986 Zhang et al [154] proposed a method for calculating losses by a loop-based method. The method initially expresses the active power loss in each branch in terms of voltage and angle dependent components, in the same way as the method of Podmore [109] in Equations (7-12) and (7-13).

As in Podmore's method, the assumption that voltage magnitudes are constant under variations of active power is made to enable $P^V{}_{Lij}$ to be considered constant. The angle dependent component $P^{\theta}{}_{Lij}$ is then expressed in terms of 'generalised flows' $f^{\theta}{}_{ij}$ through a 'generalised impedance' r_{ij}, Equation (7-15).

$$P_{L_{ij}}^{\theta} = r_{ij}(f_{ij}^{\theta})^2 \tag{7-15}$$

The losses in the system are then expressed as

$$P_L = (\mathbf{f}^{\theta})^T[\mathbf{R}]\mathbf{f}^{\theta} + P_L^V \tag{7-16}$$

where **R** is a diagonal matrix of generalised impedances.

The method proceeds by calculating a θ network with the same topology as the original network, but with new calculated impedances and nodal injections. The θ flows in this network are calculated using a loop-based algorithm. From these results, and from Equation (7-16) the coefficients of a traditional loss formula can be derived.

$$P_L = \mathbf{P}_G^T[\mathbf{B}]\mathbf{P}_G + \mathbf{B}_0^T\mathbf{P}_G + B_{00} + P_L^V \tag{7-17}$$

Zhang et al present results which show that their algorithm is several times faster than the fastest of the other loss formula methods, due mainly to the efficiency of the loop-based algorithm compared with traditional node-branch algorithms.

7.4.1.7 Discussion

Loss formulae have traditionally been applied to transmission systems in connection with the economic dispatch problem. They have been used widely over a period of many years, and are still in use today. Test results on a variety of transmission systems have shown that these loss formulae are capable of yielding acceptably accurate loss figures (Hill and Stevenson [68], Kirchmayer and Stagg [78], Shoults et al [127], Walker and Hutchins [147]).

In order to establish a simple relationship between system losses and the active power outputs of the generators, a number of assumptions are necessary. These assumptions are listed in Table 7.2.

Table 7.2 Loss Formulae Assumptions

Assumption	Loss Formula Method				
	1	2	3	4	5
Individual load currents are a linear function of the system load current, i.e. they conform	✓	✓			
The reactive power output of each generator is a linear function of its real power output.	✓	✓			
Bus voltages are constant under variations of active power				✓	✓
Generator voltages and angles do not deviate significantly from their base case values.	✓	✓	✓	✓	✓

Loss Formula Method	
1	Invariant transformations
2	Bus impedance matrix
3	AC load-flow Jacobian
4	DC load-flow equations
5	Loop-based method

The accuracy of the loss formula methods is dependent upon how well these assumptions hold in practice.

It is important to note that the assumptions will in general apply more accurately to transmission systems than to distribution systems, for the following reasons:

- Loads modelled at the transmission level represent the sum of many more individual loads than at the distribution level, and the resulting profiles conform to a greater extent.
- Bus voltages are in general more constant at the transmission level, than at the distribution level, due to the interconnected nature of the system (as opposed to a radial configuration), and the greater proportion of voltage regulated buses at the transmission level.

The coefficients in a loss formula strictly apply to the system operating condition at which they were calculated. They remain valid over a limited range, provided the assumptions in Table 7.2 continue to hold. For substantial changes in operating condition, including topology changes, new sets of coefficients need to be calculated; the coefficients themselves do not have any physical meaning, and cannot be used to derive information concerning the results of a change in conditions.

Of the loss formula methods described in the preceding sections the methods of Podmore [109] and Zhang [154] appear to provide the best combination of execution speed, accuracy and ease of implementation.

7.4.2 Calculation of Demand Losses as a Percentage of Peak Demand

In this approach the demand losses in individual components, or in the system as a whole are expressed as a percentage of the peak demand. The percentages used are system dependent and are derived from measurements taken over a period of several years. Examples of this method are given by Flaten [47] and Slominski [130]. In the method of Flaten losses calculated for a sample of representative items of plant under typical operating conditions are used to derive losses for the system as a whole.

The advantages of these methods are their simplicity and speed. Since they are based upon actual measurements they are capable of reasonable accuracy. However, when used as predictive tools load-flow and other studies may need to be run to assess the effects on losses of changes to the system (Slominski [130]).

7.4.3 Calculation of Demand Losses Using Load-flows

A load-flow solution for a system operating condition provides the power injections, voltages and angles at all the nodes of the system. From this solution the power losses can easily be evaluated, either by taking the difference between generation and load for the system,

$$P_L = \sum_{i=1}^{n}(P_{G,i} - P_{D,i}) \qquad (7\text{-}18)$$

or by adding up the losses in individual components of the system

$$P_L = \sum_{i=1}^{n_B}\sum_{j=1}^{n_B} P_{L_{ij}}^{\text{Joule}} + \sum_{i=1}^{n_T}(P_{L_i}^{\text{Joule}} + P_{L_i}^{\text{Iron}}) \qquad (7\text{-}19)$$

where n_B and n_T are the numbers of lines and transformers respectively.

Commercial load-flow programs are in widespread use, and many have facilities for calculating demand losses. The dramatic increases in speed and memory of both PC and workstation hardware mean that load-flow solutions can be performed in a matter of seconds on the largest of systems.

A problem with this approach, however, is that a complete description of the network must be provided, including network parameters, switching configuration, and values of load and generation. These requirements can represent a very large volume of data, although in many cases such data is held in utility databases, and is accessible using increasingly sophisticated software tools.

7.4.4 Calculation of Demand Losses Using Optimal Load-flows

7.4.4.1 Introduction

Optimal load-flows explicitly include the load-flow equations, and in addition minimise an objective function (generator fuel costs or transmission losses, for example) while observing operational constraints. This can be particularly important in the study of transmission systems where the output of reactive power equipment has a large impact on losses, and may not be known.

The disadvantage of optimal load-flows for this application is that the time required to prepare and execute a given study is considerably longer than that of the standard load-flow.

7.4.4.2 Optimal Load-flow Method of EPRI

In 1990 EPRI [44] proposed a method for evaluating losses in transmission systems using a fully coupled optimal load-flow based upon the augmented Lagrangian technique, originally developed by Arrow and Solow [8]. The method forms the basis of their ‘high level’ program for accurate loss calculation, and is implemented in a nonlinear optimisation package called MINOS, developed by Murtagh and Saunders [98].

The objective function used in this approach is generation cost, which was chosen because minimisation of generation cost 'represents the typical objective of many electric utilities' [44].

The vector of controlled variables comprises:

- generator active power
- generator reactive power or voltage magnitude
- transformer and phase shifter tap position
- HVDC link setting

Results for the IEEE 118 bus system and a 530 bus system are presented, for a number of different operating conditions. EPRI state that the optimal load-flow converged reliably in all cases to a unique solution in which all the constraints were observed. Reliability of convergence was affected by neither the loading level nor the quality of the initial conditions. Speed of convergence increased approximately in proportion to loading level. EPRI state that 'convergence may take more time as the starting point gets worse'.

Comparisons with 'the PECO load-flow program' were made which illustrated that the quality of the initial conditions has a large effect on the accuracy of the loss solution given by the standard load-flow. In the results presented, all of the load-flow solutions were in some way infeasible due to violation of certain constraints. The inability of the load-flow to observe such constraints is clearly a problem in the types of system presented.

The results demonstrate clearly the speed advantage of the standard load-flow over the optimal load-flow. The cpu time of the standard load-flow was approximately 1/20th that of the optimal load-flow for the 530 bus system, and varied approximately in proportion to the number of nodes in the system. By comparison, the cpu time of the optimal load-flow increased by 12 times between the two test systems for a fourfold increase in number of nodes.

7.4.4.3 Security Constrained Dispatch Method of EPRI

In addition to the fully coupled optimal load-flow method for the accurate calculation of demand losses, EPRI proposed a quicker, approximate optimal load-flow approach [44], which involves the execution of one or more simplified iterations of a decoupled optimal load-flow procedure.

The method starts from a statement of the classical dispatch problem.

$$\min \left(F_C(P_G) = \sum_{i=1}^{n_G} F_{C,i}(P_{G,i})\right) \tag{7-20}$$

subject to $g_r(x_r) = 0$ (Active load-flow equation)

$P_{Gmin} \leq P_G < P_{Gmax}$ (Active generation limits)

$$\text{where } x_r^T = \left[\theta^T, P_G^T\right] \tag{7-21}$$

The active load-flow equation in Equation (7-20) is now linearised as shown in Equation (7-22).

$$\sum_{i=1}^{n_G} \beta_i \, \Delta P_{G,i} = \beta^T \Delta \mathbf{P}_G = 0 \tag{7-22}$$

where β_i is the incremental transmission loss factor, equivalent to $\alpha_{p,\,i}$ in Equation (7-11). The dispatch problem is now solved as a linearly constrained optimisation using the MINOS system. The solution often represents a good approximation to the full optimal load-flow solution.

However, should the solution result in the violation of active constraints the user can execute a security constrained dispatch, equivalent to an active optimal load-flow, which minimises generation costs subject to active constraints while assuming that the reactive variables are fixed. The security constrained dispatch problem is formulated as in Equation (7-23).

$$\min \left(F_C(P_G) = \sum_{i=1}^{n_G} F_{C,i}(P_{G,i})\right) \tag{7-23}$$

subject to $g_r(x_r) = 0$ (Active load-flow equation)

$h_r(x_r) \geq 0$ (Active inequality constraints)

This problem is linearised and solved using the MINOS system. A load-flow is run using the results of this optimisation, to compute updated loss factors and to study line flow violations. The procedure is repeated until the system losses stabilise.

If at the end of the first stage (economic dispatch) there are significant numbers of reactive constraint violations, the user can opt to execute a reactive constraint enforcement phase, effectively a reactive optimal load-flow, which is formulated as shown in Equation (7-24).

$$\min \left(\sum_{i=1}^{n_x} w_i (u_{x,i} - u_{x,i}^0)^2\right) \tag{7-24}$$

subject to $g_x(x_x) = 0$ (Reactive load-flow equation)

$x_x^{\min} \leq x_x \leq x_x^{\max}$ (Bounds on reactive variables)

u_x is a vector of reactive control variables (a subset of x_x), u^0_x is a vector of set points of u_x, and w is a vector of weights to control the deviations of certain control variables. This problem is a nonlinear one, due to the nonlinearity of the flow equations, and is solved as a nonlinearly constrained optimisation using MINOS.

Once a satisfactory solution has been obtained by a combination of the three stages described above the demand losses are calculated from a load-flow run, since the approximations made in the optimal load-flow stages prevent accurate calculation of losses directly from those stages.

Results published by EPRI [44] show that the method performed well on the well behaved IEEE 118 bus system, achieving loss results within 5% of those of the accurate optimal load-flow described in Section 7.4.4.2., in about a third of the time. However, the accuracy was poor when applied to a 530 bus system, with errors of up to 15%. EPRI state that this is due to the stronger coupling between active and reactive problems for this particular system, and it illustrates the weakness of decoupled algorithms in this respect.

In comparison with the load-flow used in the tests, the security constrained dispatch method was approximately four times slower than the load-flow for the 118 bus system, and five to six times slower for the 530 bus system. The loss results for the method were generally closer to the accurate method (full optimal load-flow) than those of the load-flow.

7.4.4.4 Discussion

The methods for loss calculation based upon optimal load-flows are capable of high levels of accuracy by incorporating the load-flow equations, and by modelling the operation of the system by utilities to minimise generator costs and avoid constraint violations. These methods have traditionally been applied at the transmission level, rather than the distribution level. There are a number of reasons for this:

- The dispatch of generation, and the control of power interchanges with neighbouring areas is normally carried out at the transmission level.
- At lower voltages the lack of controllable devices limits the scope and usefulness of the kind of optimisation performed by optimal load-flows.
- The computational and input data requirements of optimal load-flows are significantly greater than those of standard load-flow programs, and have precluded their use for large scale studies at the distribution level.

7.5 Review of Existing Methods for Evaluating Energy Losses

Energy losses pose a much more challenging problem than demand losses, because the calculation of energy losses requires accounting for the continuous variation in load and generation patterns with time, while demand losses are calculated at just the time of system peak demand. The following sections outline the existing methods for energy loss calculation.

7.5.1 Calculation of Energy Losses Using Loss Load Factors

7.5.1.1 Introduction

The loss load factor (LLF) method is in widespread use in utilities throughout the world. It is based upon an empirical relationship between load factor and loss factor within a power system. These terms are defined in Appendix A.

In the loss load factor method loss factors are derived from load factors using a formula originally developed by Buller and Woodrow [29] of the form

$$F_L = k_1 F_D + k_2 F_D^2 \tag{7-25}$$

where coefficients k_1 and k_2 are normally related by $k_2 = (1 - k_1)$. The values of k_1 and k_2 are system dependent.

7.5.1.2 Description of the Loss Load Factor Method

The energy losses for a period of time T are calculated from a knowledge of the system peak loss and load factor, as follows.

1. For a given system load factor, F_D, calculate the loss factor, F_L, using Equation (7-25).
2. The energy losses W_L for the period T are calculated using Equation (7-26).

$$W_L = P_{Lmax} \times F_L \times T \tag{7-26}$$

where T is expressed in hours.

7.5.1.3 Calculation of Loss Load Factor Coefficients

Standard values for the loss load factor coefficients have been published. Buller and Woodrow suggest that suitable values are $k_1 = 0.3$, $k_2 = 0.7$, although it should be noted that these values applied to losses in individual transmission lines, not complete systems. These values have also been adopted by EPRI [46]. Although these values are widely accepted, tests by Boice and Gursky [20] have resulted in values of 0.1 and 0.9 for their system. Clearly, significant differences can occur from one system to the next, giving rise to potential errors if values for a particular system are not validated.

Gustafson [61] states that provided the voltage, power factor and line resistance are assumed constant, the loss factor for a distribution system can be calculated from the load curve using

Equation (7-27).

$$F_L = \frac{1}{T}\int_0^T P_D^2(t)\,dt \tag{7-27}$$

where in this case the load curve $P_D(t)$ is normalised to its peak value.

Shultz et al. [128] have proposed a method for calculating loss factors for areas of the system where time-based load data is not available. They use a simple iterative technique, together with the network topology and branch impedance data, to derive a loss duration curve from which loss factors are derived.

Gustafson and Baylor [62, 63] have combined the use of the loss load factor method with other statistical techniques to account more accurately for the effects of generation schedules and energy interchanges with neighbouring utilities.

7.5.1.4 Discussion

The principal advantage of the method is its simplicity. It is particularly suitable for long term planning in which losses can be predicted for a period of years given the predicted growth in peak demand. However, there are a number of important limitations associated with the method:

- The results are approximate at best. Unless the loss factor coefficients are validated the method can be prone to significant errors.
- The method cannot account accurately for changes in system configuration, and as such is not ideally suited to many kinds of planning study.
- The underlying assumption in the loss load factor formula is that losses are dependent simply on loads. Gustafson and Baylor [62] have pointed out that this assumption fails when calculating losses in transmission systems, where loss is related to generation schedules, and in cases where power is transferred between utilities, where loss is related to the interchange of energy.
- The assumptions made in the calculation of loss factor coefficients using Equation (7-27) are unlikely to hold at lower voltages.
- The method does not account for fixed losses, which need to be calculated using an alternative method.

7.5.2 Calculation of Energy Losses Using Historical Metered Data

7.5.2.1 Introduction

In this approach the energy losses are computed by subtracting the energy output from the system during a period from the energy input to the system during that period. Energy output includes sales to customers and export of power to other utilities. Energy input includes generation and import from other utilities.

7.5.2.2 Calculation of Energy Input and Output

Normally the import of power via generators and tie lines is metered on a regular (half hour) basis (Tobin and Glynn [143]). In such cases, integrating the time-based power profiles over the required period will yield the energy.

As in the case of energy imported to the system, energy leaving the system via tie lines is normally accurately metered.

Calculating the sales of energy to consumers represents a much more difficult problem. This is because sales of energy to individual consumers are not measured at the same point in time. While measurements of the energy sales to major industrial consumers can be made to coincide, the reading of domestic consumers' meters is spread over the period of a month or a quarter. Meter readers will visit different consumers on different days of the billing period, resulting in a mismatch of reported sales as shown in Figure 7.2.

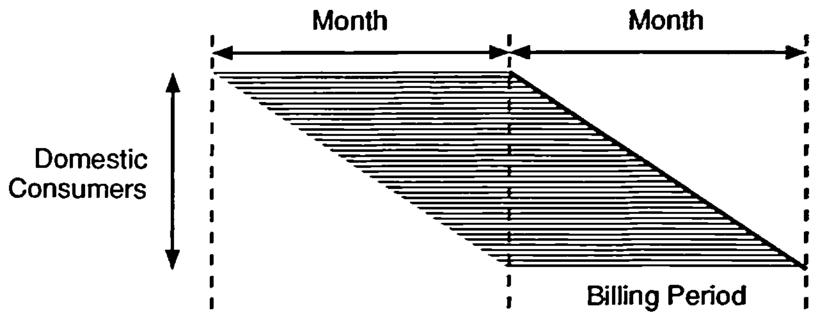

Figure 7.2 Mismatch in Reported Energy Sales

The result is that consumers' meters read early in the cycle will register energy sales which correspond largely to the previous period's purchased energy. This problem is compounded by the seasonal variations in demand which occur from one period to the next. In addition a significant number of measurements are based upon estimates, because meter readers are often unable to gain access in order to take a reading.

Sales data must be extensively pre-processed before it can be used in conjunction with purchases data for calculating losses. Two methods described by Slominski [130] are alignment of sales with purchases, and exponential smoothing of the resulting losses.

7.5.2.3 Discussion

This method to calculate energy losses has been used with success by many utilities. However, its value as a tool for planning purposes is limited, because it is unable to predict the effects on losses of changes in system configuration. It may also be difficult to identify the different components of losses at different voltage levels, and to distinguish between fixed and variable losses. Finally the pre-processing of sales data required calls into question the accuracy of the results.

7.5.3 Calculation of Energy Losses Using Statistical Modelling

7.5.3.1 Description of the Method

In this approach losses in representative items of plant within the system are calculated using typical or average operating conditions for different seasons of the year. These items of plant include different types of feeder, transformer, capacitor and so on. From this data the losses in the entire system are derived using statistical techniques.

Some of the more important methods are described in the following sections.

7.5.3.2 The Simplified Calculation Method of EPRI

The simplified method developed in 1983 by EPRI [45] calculates losses for two categories of plant:

1. Lines

   The energy losses for a line over period T are calculated using Equation (7-28)

$$(W_L)_T = \frac{K \times R \times L \times C^2 \times F_{Distrib} \times T \times F_L \times (F_{PLR})_T}{V^2 \times 1000} \tag{7-28}$$

2. Transformers

   The load losses for a transformer over period T are calculated using Equation (7-29)

$$(W_L)_T = P_L \times F_L \times F_{PLR} \times T \tag{7-29}$$

   The no-load losses are calculated using Equation (7-30).

$$(W_L)_T = P_{Lnoload} \times T \tag{7-30}$$

The input data for these equations is given below.

K	- Line code coefficient (0.33 for 3ϕ)		R	- Resistance per conductor	Ω/km
L	- Length	km	C	- Capacity	kVA
$F_{Distrib}$	- Distribution Factor	p.u.	T	- Time period	hours
F_L	- Loss Factor	p.u.	F_{PLR}	- Peak Load Ratio for Period	p.u.
V	- Operating Voltage (Line to line)	kV	P_L	- Load loss at rated load	kW
$P_{Lnoload}$	- No-load loss at rated load	kW			

The numbers of lines of different types are identified for the system and plant and circuit records are used to estimate the lengths of each type in the system. The energy losses for each type are calculated for the period of interest. Similarly, the numbers of transformers of each type are identified and the losses calculated.

7.5.3.3 The Detailed Calculation Method of EPRI

The detailed method for calculating distribution system losses proposed by EPRI in 1983 [45] combines the use of measurements from the system and statistical techniques to derive the energy losses for the system.

The method uses the concept of 'significant substations' and 'significant days' to reduce the quantities of data to be manipulated. In the case of significant substations, statistical analysis is used to identify groups of similar substations in terms of their loading patterns. A typical substation is chosen to represent each group. The same technique is used with the annual system demand profile, recorded at hourly intervals, to identify a small number of normalised daily load profiles which can be used to model the variation in demand throughout the year.

Once the significant groups have been defined the energy losses are calculated as follows:

1. Substation transformer losses.
   For each significant substation, *s*, the losses are calculated for each day of the year and summed. For each day, *d*, of the year, the daily peak substation load (measured data) is used to scale the relevant normalised significant day curve. Losses for the substation transformers are calculated for the day using conventional transformer equations, given the derived loading profiles.

2. Primary Feeder losses.
   A selection of feeders from the significant substation groups is chosen, and recorded measurements are used to estimate the demand patterns on each feeder. Losses are calculated using loss factors from the related significant substations.

3. Distribution transformer losses.
   Measured data is used to identify for each distribution transformer the number and type of customers served (residential, small commercial, large commercial) and the maximum demand in kVA. From this data losses are calculated using Equations (7-29) and (7-30).

4. Secondary feeder losses.
   Average losses for secondary feeders are calculated for a small number of groups of approximately 20 feeders, each group corresponding to a particular transformer kVA rating. Coincidence factors are used in conjunction with the load on the transformer serving the secondary to calculate the feeder load. An equation similar to (7-28) is used to determine the average energy losses.

5. The various components of loss are summed together to yield the system energy losses. To verify the calculation EPRI subtract metered sales to consumers from the measured energy leaving substation transformers, as in the method of Section 7.5.2

7.5.3.4 Results

Results for the two methods presented by EPRI [45] and by Grainger and Kendrew [58] compare the loss figures produced by each method on the Salt River Project system in Arizona. Overall, the simplified method gave energy losses which were 14% higher than those of the detailed method.

EPRI compared the results from the detailed method with results from the Historical Metered Data method of Section 7.5.2, and found a discrepancy of 13.2%.

7.5.3.5 Discussion

The methods for calculating energy losses which use statistical modelling and system measurements where they are available are widely used by the power industry. They can be tailored to suit the data available to a given utility, and once the data has been collected and prepared, can provide results quickly.

The disadvantages of the method are as follows:

- For detailed studies, the cost and time required to gather and prepare the input data is high.
- Significant errors can arise, even for detailed studies, as shown by the figures published by EPRI.

7.5.4 Calculation of Energy Losses from Demand Losses

7.5.4.1 Introduction

In this approach, energy losses are calculated from demand losses, using the relationship:

$$W_L = \int_{t_0}^{t_0+T} P_L(t)\,dt \qquad (7\text{-}31)$$

These methods differ primarily in the techniques used to account for the time-varying nature of the demand losses. The most important methods are outlined in the following sections.

7.5.4.2 The Load-flow Based Method of Sun et al.

In 1980 Sun et al [138] proposed a method for calculating energy losses in distribution systems which combines the use of an unbalanced load-flow program for calculating demand losses, with a load duration curve approach to modelling the time-based variations in demand, as described in Section 2.2.2 in Chapter 2. An important feature in the method was the use of an advanced load-modelling algorithm to model the variation of demand due to changes in voltage.

7.5.4.3 The Optimal Load-flow Based Method of EPRI

In 1990 EPRI [44] proposed the use of their Optimal Load-flow based methods for calculating demand losses in conjunction with a duration curve approach to determine energy losses.

The main features of this approach are described below.

1. A small number of 'operating modes' , each representing a 24 hour period, are defined for the system under study. The conditions which characterise a given operating mode are system topology, load profiles and generation schedules.
2. For each day of the study period the appropriate operating mode is identified, and its load duration curve obtained. The security constrained dispatch method, described in Section 7.4.4.3, is used to calculate demand losses at various points on this curve. A curve fitting technique is used to derive a loss-load relationship from the demand loss results.
3. The loss-load relationship is used to calculate demand losses at regular steps across the load duration curve. Energy losses are calculated by integrating the results.
4. The loss-load relationships are retained for future days corresponding to the same operational mode.
5. A 'fast' mode of operation permits the user to specify which operating modes should be used to develop loss-load relationships, which are calculated in advance. During the loss calculations, if the program encounters any operating modes for which loss-load relationships have not been calculated, it substitutes that of a 'similar' operating mode.

From the the results published by EPRI [44], it is clear that quadratic polynomials can be used with reasonable accuracy to describe the loss-load relationships. The errors compared with calculating demand losses explicitly at each point on the duration curve are less than 10% for the test systems used.

7.5.4.4 Discussion

This method inherits the advantages and disadvantages of the security constrained dispatch method for calculating demand losses, on which it is based.

- The modelling of the load-flow equations permits the effects on losses of changes in system configuration to be accurately assessed. The method is also able to observe operational constraints.

- The method used to calculate the demand losses is subject to error on systems for which the decoupling assumptions fail to hold.
- The execution time of the method is relatively slow, since several security constrained dispatch solutions are required for each of several operating modes.
- The use of duration curves to model the variation in demand is subject to errors in the case of diverse loads, as outlined in Section 2.2.2.4.

7.6 Assessment of Existing Loss Calculation Methods

7.6.1 Criteria for Evaluating Loss Calculation Methods

The following criteria for assessing loss calculation methods have been derived from distribution operations and planning functions.

7.6.1.1 General Criteria

The methods for calculating demand and energy losses should be capable of:

1. Calculating and distinguishing between fixed losses and variable losses.
2. Calculating losses in the system as a whole, and in individual components of the network.
3. Assessing the effects on losses of changes in system configuration, including changes in topology, and the addition and retirement of plant.
4. Assessing the effects on losses of changes in independent generation.

In addition the methods are assessed in terms of the times required to prepare and execute a loss study, and in terms of their general accuracy when applied to distribution systems.

7.6.1.2 Criteria Specific to Energy Loss Methods

In addition to the general criteria, methods for calculating energy losses should be capable of:

1. Modelling the time-varying nature of loads and generation patterns, and the resulting losses.
2. It is desirable that the losses should be obtained in a form which permits the application of time-related tariffs to deduce the true costs of losses.

7.6.2 Assessment of Methods for Calculating Demand Losses

An assessment of the methods for calculating demand losses outlined in the previous sections is given in Tables 7.3 to 7.6. The following conclusions are drawn.

- The use of loss formulae to calculate demand losses represents an important technique in economic dispatch problems on transmission systems. It is of limited use at the distribution level however, because the assumptions on which it is based are not valid in most distribution systems, particularly at lower voltages. Loss formulae do not provide sufficient information concerning the location of losses and their nature (fixed or variable), to be suitable for many kinds of planning study.

- Specifying losses as a percentage of peak demand is a useful technique for rapid, but approximate demand loss calculations. Because the method relies upon historical measurements and calculations performed for average operating conditions, the method lacks the accuracy and detailed modelling required in many planning calculations, in which the true operating conditions need to be accounted for.

- The load-flow and optimal load-flow methods are capable of high levels of accuracy because they employ a detailed model of the network and simulate actual system operating conditions. The penalty paid for this accuracy is the large quantity of input data required. However, in recent years there has been a significant improvement in the collection and storage of such data by distribution companies, with the result that in many cases acquiring data for load-flow studies is not the daunting problem it once was.

- Methods for calculating demand losses using standard load-flows are capable of providing a detailed analysis of the location and nature of losses throughout the system, suitable for planning studies. The accuracy of the results is closely related to the quality of the input data. Infeasible solutions, in which constraints are violated, are possible if there are inconsistencies in the input data.

- Optimal load-flows provide the network modelling accuracy of standard load-flows with the added advantage of optimisation of control variables to minimise costs and ensure that constraints are not violated. The execution time for optimal load-flows is many times greater than for standard load-flows, however, and increases at a greater rate with system size. In addition, the level of control of variables such as generator voltage and output offered by optimal load-flows is seldom available in distribution systems. Hence the solutions from optimal load-flows may be feasible, but not realistic. In view of this, it appears that while optimal load-flows are better suited for use at the transmission level, standard load-flows represent a better choice at the distribution level.

Table 7.3 Summary of Demand Losses using Loss Formulae

Criterion	Assessment
Calculate fixed and variable losses	Does not differentiate between fixed and variable losses
Calculate total and individual losses	Calculates just total losses
Account for changes in system configuration	Changes in system configuration generally require the calculation of a new set of loss formula coefficients
Account for independent generation	Changes in generation can generally be accounted for provided system voltages are not significantly affected.
Data preparation time	The methods vary in the time required to calculate the loss formula coefficients. Later methods greatly improved in this respect and moderately quick. In addition system operating conditions need to be specified.
Execution time	Very quick.
General accuracy on distribution systems	Poor. The assumptions made to develop the loss formulae seldom hold for distribution systems.

Table 7.4 Summary of Demand Losses as a Percentage of Peak Demand

Criterion	Assessment
Calculate fixed and variable losses	Calculates variable losses only. Fixed losses need to be calculated using another method.
Calculate total and individual losses	Designed to calculate total losses. Losses in individual components are based upon average operating conditions, and are therefore approximate at best.
Account for changes in system configuration	Most changes cannot be accounted for.
Account for independent generation	Cannot be accounted for.
Data preparation time	Depends upon the specific method. The simplest methods require just the system peak demand. More detailed methods require selection of a sample of plant and specification of parameters. Most data, however, is easily obtainable.
Execution time	Very quick.
General accuracy on distribution systems	Depends upon the level of detail used. Can achieve reasonable accuracy.

Table 7.5 Summary of Demand Losses using Load-flows

Criterion	Assessment
Calculate fixed and variable losses	Yes. Calculation of fixed losses requires line and transformer models which account for fixed losses.
Calculate total and individual losses	Yes.
Account for changes in system configuration	Yes.
Account for independent generation	Yes.
Data preparation time	A full model of the system must be specified. Data preparation time is therefore significant.
Execution time	Moderate. Load-flows can be completed in seconds on the largest of systems.
General accuracy on distribution systems	Very accurate, provided adequate network and loading data is available.

Table 7.6 Summary of Demand Losses using Optimal Load-flows

Criterion	Assessment
Calculate fixed and variable losses	Yes. Calculation of fixed losses requires line and transformer models which account for fixed losses.
Calculate total and individual losses	Yes.
Account for changes in system configuration	Yes.
Account for independent generation	Yes.
Data preparation time	A full model of the system must be specified. In addition a full set of constraints must be specified. Data preparation time is therefore long.
Execution time	Relatively slow. Optimal load-flows can take many minutes on larger systems.
General accuracy on distribution systems	Very accurate, provided adequate network and loading data is available.

7.6.3 Assessment of Methods for Calculating Energy Losses

An assessment of the methods for calculating energy losses outlined in the previous sections is given in Tables 7.7 to 7.10. The following conclusions are drawn.

- Loss load factors provide a quick and easy way to calculate energy losses with a minimum of data. As such, they are suitable for capital investment studies, but the poor accuracy and lack of detailed modelling of the system limit their suitability for many kinds of short to medium term planning studies.

- The use of historical metered data can provide a quick method to calculate energy losses, particularly in the absence of network data. However, the level of modelling detail is poor, and the method is unsuitable for predictive studies.

- Statistical modelling can be used effectively to reduce the quantity of data which must be collected to calculate system energy losses. To achieve reasonable levels of accuracy still demands substantial effort in the collection and preparation of data, however. The method is also limited for planning purposes, where predictive capabilities are required.
- The accuracy of energy losses calculated from demand losses depends upon the accuracy of the demand loss figures and the method used to model the variation in losses with time. Potentially this approach offers the most accurate loss solutions, and the greatest levels of detail in the modelling of the system, required for planning studies. The chief disadvantages of the approach are the long execution times and large volumes of input data required.

Table 7.7 Summary of Energy Losses using Loss Load Factors

Criterion	Assessment
Calculate fixed and variable losses	Calculates variable losses only.
Calculate total and individual losses	Yes. Losses in individual components require specifying loss load factors for each.
Account for time-varying nature of loads and losses	The load factor is used to account approximately for the time-varying nature of load profiles.
Account for changes in system configuration	Loss load factors apply to a base case configuration, and are not generally sensitive to changes in system configuration.
Account for changes in independent generation	Loss load factors cannot account accurately for changes in individual generation patterns.
Suitable for application of time-varying tariffs	No. Time based losses are not accessible for the application of time-varying tariffs.
Data preparation time	Very quick, although calculations on individual circuits may require more involved manual data preparation.
Execution time	Very quick.
General accuracy on distribution systems	Moderate. Can be poor if loss load factors have not been accurately validated.

Table 7.8 Summary of Energy Losses using Historical Metered Data

Criterion	Assessment
Calculate fixed and variable losses	Does not differentiate between fixed and variable losses.
Calculate total and individual losses	Calculates total losses only.
Account for time-varying nature of loads and losses	Accounts for the time varying nature of loads and resulting losses implicitly.
Account for changes in system configuration	No. Losses apply only to the configuration(s) used during the study period.
Account for changes in independent generation	No.
Suitable for application of time-varying tariffs	Yes.Time based losses are available for the application of time-varying tariffs.
Data preparation time	Purchases data is relatively quick to assemble and prepare. Sales data requires extensive preparation.
Execution time	Very quick.
General accuracy on distribution systems	Moderate. Accuracy depends upon the level of detail of the study and the pre-processing of the sales data.

Table 7.9 Summary of Energy Losses using Statistical Modelling

Criterion	Assessment
Calculate fixed and variable losses	Yes
Calculate total and individual losses	Yes, but losses in individual components are based on average operating conditions, and may not reflect the true conditions.
Account for time-varying nature of loads and losses	The variation in loads and losses with time is not modelled, since only average conditions are used in the calculations.
Account for changes in system configuration	No. Results are generally based on samples which are used to build a representative base case configuration.
Account for changes in independent generation	No. The method is insensitive to individual generation patterns.
Suitable for application of time-varying tariffs	No, since only average loss values are available.
Data preparation time	Depends upon the level of detail of the study. Representative plant has to be chosen using statistical techniques, and the data collected. Preparation time for a detailed study can be very long.
Execution time	Very quick.
General accuracy on distribution systems	Potentially good. Accurate results require detailed studies with large samples of plant data, which can be costly.

Table 7.10 Summary of Energy Losses using Demand Losses

Criterion	Assessment
Calculate fixed and variable losses	Depends upon the method for calculating demand losses. Normally fixed and variable losses are calculated.
Calculate total and individual losses	Depends upon the method for calculating demand losses. Normally total and individual losses are calculated.
Account for time-varying nature of loads and losses	Yes. Depends upon the specific method. Duration curve methods account for time-variation, but assume that loads conform. Chronological methods provide improved modelling of variation in loads and losses with time.
Account for changes in system configuration	Depends upon the method for calculating demand losses. Load-flow and optimal load-flow methods do account for changes in system configuration.
Account for changes in independent generation	Depends upon the method for calculating demand losses. Load-flow and optimal load-flow methods do account for changes in independent generation.
Suitable for application of time-varying tariffs	Depends upon the method for calculating demand losses. Chronological methods are generally suitable for application of time-varying tariffs.
Data preparation time	Depends upon the method for calculating demand losses. In general network data and load and generation profiles need to be specified, resulting in relatively long preparation times.
Execution time	Depends both on the method for calculating demand losses and the number of solutions required to calculate the energy losses. In general execution times are quite long.
General accuracy on distribution systems	Potentially very accurate. Accuracy depends on the method for calculating the demand losses and the assumptions made in integrating these results.

7.7 Calculation of Losses by Discrete Time Simulation

7.7.1 Overview of the Proposed Method

From the assessment of existing loss calculation methods carried out in the previous section, it appears that load-flow analysis best meets the criteria for calculating both demand and energy losses in distribution systems. Load-flow analysis offers the detailed modelling of the system which is required when conducting 'what if' studies to assess the merits of alternative planning options. It is capable of high levels of accuracy.

When using load-flow analysis to calculate energy losses, it is important to choose a technique that will model the variation in system loads with time with acceptable accuracy. The approaches to this problem are discussed in Chapter 2.

The method proposed here for calculating both demand and energy losses uses discrete time simulation to conduct the load-flow studies and to account for time-based variation of loads. Three algorithms based upon the same principle are proposed. The first is a detailed algorithm which performs a full analysis across the period of interest. The other two algorithms use interpolation of input data to reduce the computational requirements of the method.

The remainder of this chapter is devoted to a description of the detailed algorithm. The remaining algorithms are described in Chapter 8.

7.7.2 Description of the Detailed Loss Calculation Algorithm

7.7.2.1 Discrete Time Simulation

In the detailed algorithm, load-flow solutions are conducted at discrete intervals across the entire period of interest. In most cases this corresponds to half-hourly or hourly intervals across a year. The load-flow solution at each time step comprises the active and reactive power injections, and the voltage magnitudes and angles at every node, plus the transformer tap positions. From this information the demand and capacity losses can be calculated for the system as a whole, for smaller subsystems, or for individual network components.

7.7.2.2 Calculation of Demand Losses

The variable loss component for an area of the system is given by Equation (7-32).

$$P_{Lvar} = \sum_{i=1}^{n_B} P_{Lvar,i} + \sum_{i=1}^{n_T} P_{Lvar,i} \tag{7-32}$$

The individual line and transformer variable losses are given by

$$P_{L,ij} = G_{ij}(V_i^2 - 2V_iV_j\cos(\theta_i - \theta_j) + V_j^2) \tag{7-33}$$

where i and j denote the sending and receiving end nodes for the line and G is the series conductance.

The fixed loss component for an area of the system is given by Equation (7-34).

$$P_{Lfixed} = \sum_{i=1}^{n_B} P_{Lfixed,i} + \sum_{i=1}^{n_T} P_{Lfixed,i} + \sum_{i=1}^{n} P_{Lfixed,i} \tag{7-34}$$

Fixed losses for an individual line, k, with shunt conductance G are given by

$$P_{Lfixed,k} = \frac{G_k}{2}(V_i^2 + V_j^2) \tag{7-35}$$

Fixed losses for an individual transformer, k, modelled using a central magnetising branch with conductance G as described in Appendix D, are given by

$$P_{Lfixed,k} = V_k^2 G_k = P_{ij} + P_{ji} - P_{Lvar,k} \tag{7-36}$$

In practice it is easier to add the forward and reverse active power flows and subtract the variable loss component to derive the fixed loss than to evaluate the voltage at the magnetising branch.

Fixed losses for an individual node, i, with shunt conductance G are given by

$$P_{Lfixed,i} = V_i^2 G_i \tag{7-37}$$

7.7.2.3 Calculation of Energy Losses

If the power injections used to derive the demand losses represent spot values, energy losses are obtained by simply integrating the demand losses across the period of interest, i.e. for a year at hourly steps

$$W_L = \int_0^{8760} P_L(t)\,dt \tag{7-38}$$

The integration rule used is the trapezoidal method. Although higher order methods such as Simpson's rule provide smoother interpolation of the data points they can be susceptible to greater errors than the trapezoidal method when dealing with 'choppy' and erratic curves, as are found occasionally at the distribution level. Equation (7-39) gives the details of the integration, where N is the number of time steps and h is the time step interval in hours.

$$\int_{t_1}^{t_N} f(t)dt \simeq h\left[\frac{1}{2}(f_1 + f_N) + \sum_{i=2}^{N-1} f_i\right] \tag{7-39}$$

Alternatively, if the power injections represent average values, e.g. hourly averages, then the demand losses are summed to give the energy losses, i.e.

$$W_L = \sum_{i=1}^{8760} P_{L,i} \tag{7-40}$$

7.7.2.4 Discussion of the Proposed Method

The calculation of losses by discrete time simulation offers the following advantages.

- By simulating the operation of the system throughout the study period, without simplifying approximations concerning the conformance and cyclic behaviour of individual load profiles, the proposed method is potentially capable of higher accuracy than the existing methods described in the preceding sections.
- The calculation of demand losses on a time basis allows for the fact that the peak demands on certain feeders may not coincide with that of the system as a whole, due to the diversity of industrial loads.
- The calculation of energy losses on a time basis, while accounting for the diversity of individual loads, permits accurate costing of losses through the application of time related tariffs. In addition these time-based costs can be allocated to individual consumers in a manner which accounts for their specific demand patterns. Such an allocation results in charges to consumers which reflect the burden they place on the system, which is desirable from an economic point of view (Berrie [14, 15], Munasinghe [97]. A proposed loss allocation algorithm is described in Chapter 9.

The disadvantages of the proposed method are as follows.

- The input data required for lengthy studies on large systems, and the volume of results data generated, both require large quantities of disk based storage. The use of advanced graphical techniques for manipulating the data becomes essential. The results in Section 2.5 in Chapter 2 indicate that current workstation technology can accommodate complete UK distribution systems at voltages down to 33kV, plus 11kV primary feeders. To study the system losses at the lowest voltages still requires multiple separate studies, or the use of statistical modelling to infer from loss studies on representative low voltage feeders the losses on the low voltage system as a whole.
- The execution times for studies on large systems are lengthy, as illustrated in the results in Section 8.4.

7.7.3 Test Results

7.7.3.1 Introduction

The tests in this section attempt to quantify the improvements in accuracy achieved by the discrete time simulation approach to the calculation of losses. The substantial variations in the loss costing methods used by different distribution companies and the differences in availability of data from one company to the next make it difficult to conduct a set of definitive tests. The approach adopted here is to compare a subset of widely used techniques with the proposed method using a small number of real systems with a range of characteristics, in order to assess the likely range of performance to be expected in practice. Because the true losses for these systems are not known, it is possible only to assess the relative accuracy of the methods. The following assumptions are therefore made:

1. The plant data and associated profiles data is assumed to provide an accurate model of the system and its behaviour.
2. The load-flow solutions obtained using this data for a particular point in time provide an accurate representation of the state of the system at that point in time.

The solutions from the discrete time simulation approach are therefore used as a reference, against which the alternative methods are compared.

7.7.3.2 Comparison of Demand Loss Results

In Section 2.5.3 of Chapter 2 a comparison is made of the demand loss results of discrete time simulation and two multiple case load-flow methods: the multiple case chronological approach (typical days) and the multiple case duration curve approach.

The results show that for the calculation of system maximum demand losses discrepancies between these two approaches and discrete time simulation are typically in the range 15 - 27%. These differences arise from the use by the two multiple case approaches of typical daily demand curves. Differences between these typical curves and the actual demands on the day of system maximum demand loss can be substantial, and these approaches are normally reserved for the calculation of energy losses.

In practice, single case load-flows are normally used to determine maximum demand losses on the system. If the demand data used in such studies accounts for load diversity at the time of system maximum demand loss, the results will be of comparable accuracy to discrete time simulation. If diversity is not accounted for, the errors introduced will be dependent upon the degree of load diversity on the system, as shown in Table 7.11. The table lists the errors arising from the neglect of load diversity on four test systems, and indicates that these errors can be substantial.

Table 7.11 The Effects on Demand Loss Accuracy of Neglecting Load Diversity

Test System	System Max. Demand Loss (MW)		Error (%)
	Diversity Included	Diversity Neglected	
7 Node	0.805	0.991	23.1
10 Node	0.996	1.110	11.4
15 Node	4.737	5.107	7.8
348 Node	234.330	239.960	2.4

7.7.3.3 Comparison of Energy Loss Results

As with demand losses, a comparison of the energy loss results of discrete time simulation and two multiple case load-flow methods: the multiple case chronological approach (typical days) and the multiple case duration curve approach, is made in Section 2.5.3 in Chapter 2.

The results show that for the calculation of system energy losses discrepancies between these two approaches and discrete time simulation are in the range 1.3 - 3.7%. A study of the results for individual lines shows that discrepancies of approximately 10% are more common.

In addition to the multiple case load-flow methods, the loss load factor method is widely used for calculating system energy losses. The following test results compare the results from this approach with discrete time simulation for the four test systems used previously. Two variations of the basic loss load factor method are considered:

1. Derivation of the Loss Load Factor, F_L.
   The two widely used approaches for calculating the Loss Load Factor are compared:

   a) Derivation of Loss Load Factor from the Load Factor:

   $$F_L = k_1 F_D + k_2 F_D^2 \qquad (7\text{-}41)$$

   In this case the values $k_1 = 0.3$, $k_2 = 0.7$ are used, as recommended in the Electricity Council T8/6 document [42].

   b) Derivation of the Loss Load Factor from the system demands:

   $$F_L = \frac{1}{T}\int_0^T P_D^2(t)\,dt \qquad (7\text{-}42)$$

   where the demand values, P_D are normalised to their peak value.

2. Accounting for Load Diversity
   Results with load diversity included and excluded are compared.

Table 7.12 compares the system energy loss results for each variation of the loss load factor method with those of discrete time simulation for each of the test systems.

Table 7.12 Comparison of Loss Load Factor Method with Discrete Time Simulation

Test System	F_D	F_L Method	F_L	Diver-sity	Demand Loss MW	Energy Loss GWh		Error %
						DTS	F_L	
7 Node	0.603	F_D	0.435	Yes	0.805	3.258	3.067	-5.9
				No	0.991		3.775	15.9
		$\int P_D^2$	0.379	Yes	0.805		2.670	-18.0
				No	0.991		3.286	0.9
10 Node	0.655	F_D	0.497	Yes	0.996	1.854	2.138	15.3
				No	1.110		2.383	28.5
		$\int P_D^2$	0.462	Yes	0.996		1.988	7.2
				No	1.110		2.216	19.5
15 Node	0.612	F_D	0.446	Yes	4.737	16.163	18.497	14.4
				No	5.107		19.943	23.4
		$\int P_D^2$	0.391	Yes	4.737		16.240	0.5
				No	5.107		17.509	8.3
348 Node	0.771	F_D	0.648	Yes	234.330	110.03	112.86	2.6
				No	239.960		115.57	5.0
		$\int P_D^2$	0.601	Yes	234.330		104.76	-4.8
				No	239.960		107.28	-2.5

The energy loss errors for each variation of the method are displayed graphically in Figure 7.3.

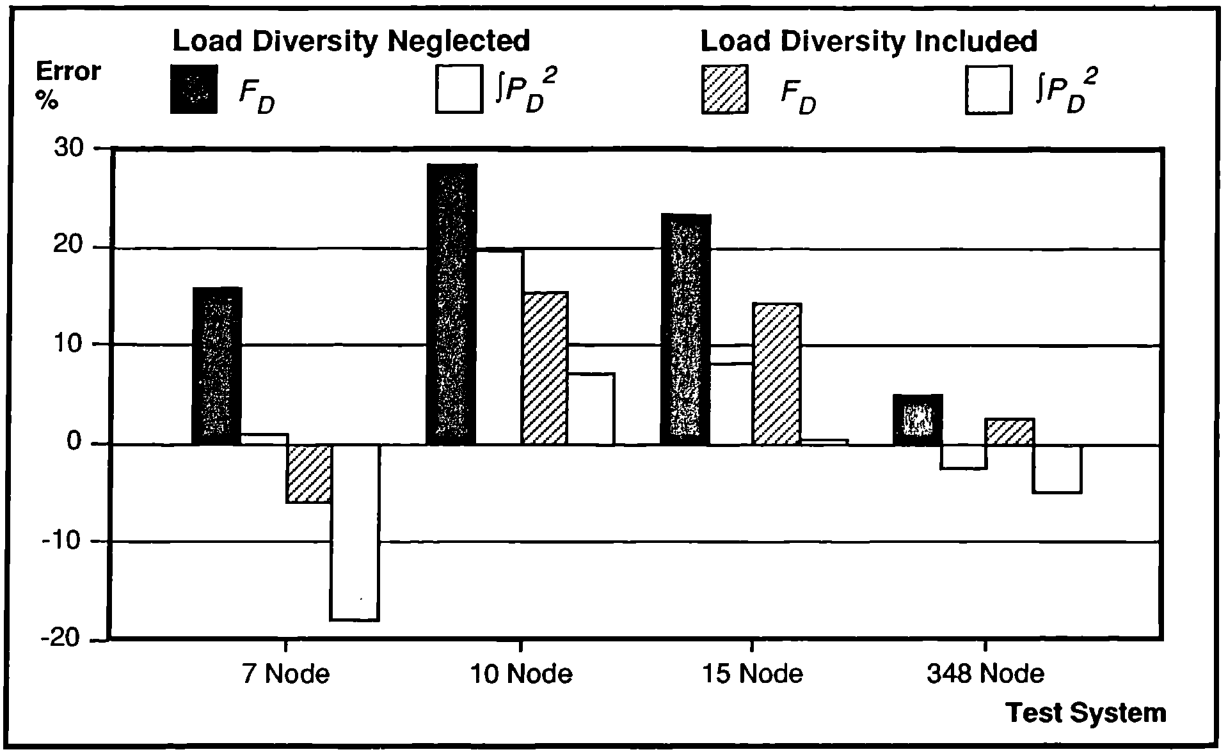

Figure 7.3 Energy Loss Errors for Variations of the Loss Load Factor Method

From the results the following observations can be made:

- In general, loss load factors derived by integrating the normalised system demand profile yield greater accuracy than those derived from the loss formula.
- In general, accounting for load diversity yields results of greater accuracy than neglecting diversity.
- Selected results show good accuracy when compared with discrete time simulation. For example the results for the 15 Node system, with loss load factors calculated from system demands and load diversity accounted for, agree to within 0.5%. However, the same method applied to the 7 Node system gives rise to an error of 18%.
- The performance of the method on the four test systems is erratic, and can lead to substantial errors.

7.7.3.4 Summary

In the calculation of demand losses, single case load-flows can be used in place of discrete time simulation with no loss of accuracy provided that load diversity is accounted for. If load diversity is neglected the results indicate that errors of between 2.5% and 23% arise in the cases studied.

The comparison of methods for calculating energy losses suggests that the discrete time simulation approach yields accuracies for system energy losses typically between one and four percent higher than the multiple case methods based upon typical daily load curves. This assumes that the typical daily curves are an accurate representation of the average load patterns throughout the system over the study period.

A comparison with the loss load factor method suggests that the discrete time simulation approach offers substantially greater reliability in the calculation of energy losses. Results from the loss load factor method showed a wide range of error from 0.5% to 28.5%.

7.8 Conclusions

In this chapter the most widely used methods for evaluating demand and energy losses have been reviewed, and a new method based upon discrete time simulation has been presented.

7.8.1 Review of Existing Methods for Evaluating Demand Losses

The most widely used variations of the method based upon loss formulae have been described, and the assumptions relating to their use identified. It has been noted that these formulae are better suited to application at the transmission level than at the distribution level.

The method of calculating demand losses as a percentage of peak demand has been outlined, and its potential accuracy and speed of analysis has been noted. The value of the method as a predictive tool for planning studies is shown to be limited.

The load-flow program has been presented as an accurate and relatively quick method for calculating demand losses. The problems associated with large volumes of input data have been noted, although moves by distribution companies towards increasingly comprehensive database management systems are easing these problems.

The use of optimal load-flows for loss calculation has been described with particular reference to the approaches used by EPRI. The advantages of this approach in terms of the accurate representation of the system and its constraints have been discussed. It has been argued that at the distribution level the costs associated with optimal load-flows, including substantially increased input data and execution times, can be seen to outweigh the benefits.

7.8.2 Review of Existing Methods for Evaluating Energy Losses

The Loss Load Factor method has been presented, and its inherent simplicity and speed have been described. The limitations and potential sources of error have been explained. Test results towards the end of the chapter have confirmed that although the method is capable of high accuracy, substantial errors can occur in practical cases.

The use of historical metered data in the evaluation of energy losses has been explained, and its successful use by many utilities has been noted. The problems associated with mismatches in reported energy sales have been shown to be a potential source of error.

Another widely used method employs statistical modelling of the system using a subset of representative items of plant. The approach adopted by EPRI has been described and their test results summarised.

The calculation of energy loss results from demand loss results has been described with reference to the methods of Sun et al and EPRI. It has been stated that this method provides potentially the most accurate and flexible means of calculating energy losses, although large data requirements and long execution times have been cited as disadvantages of the approach.

7.8.3 Assessment of the Methods

A set of criteria has been developed from the requirements of operations and planning engineers, and used to assess the loss calculation methods. The load-flow program has been identified as the most suitable method for calculating both demand and energy losses on account if its accuracy, flexibility and reasonable execution speed. This approach forms the basis of the proposed loss calculation algorithm.

7.8.4 The Detailed Loss Calculation Algorithm

A new loss calculation algorithm has been presented which calculates demand losses by discrete time simulation, from which energy losses are derived by integration over the study period. The method has been shown to offer high levels of accuracy by accounting for the variations in the power flows in individual feeders with time in the integration process. The detailed modelling of the system with time permits the application of time related tariffs for the costing of losses. The method has also been shown to provide a sound basis for the allocation of losses to the consumers supplied by the system.

The disadvantages of the method have been identified as the large data and computational requirements, which impose limits on the size of the system which can be studied or the duration of the study period. It has been noted however, that these limits on current workstation technology are not severely restrictive.

Test results have been presented which compare the results of the method with two load-flow based methods based upon typical days, and the loss load factor method. The results suggest that the alternative methods are capable of comparable accuracy in selected cases, but that the proposed method offers higher reliability over the full range of system configurations and loading conditions, and significantly greater accuracy in the results for individual items of plant.

Chapter 8. Calculation of Losses - Reduction in Computational Requirements by Interpolation

8.1 Introduction

The detailed method for the calculation of losses by discrete time simulation provides high levels of accuracy, and a sound basis on which to calculate and allocate costs of losses. This accuracy is achieved by performing a very detailed analysis, at the expense of long execution times.

Frequently in planning studies, a number of alternative strategies must be assessed in terms of their effect on the operation, security and efficiency of the system. In such cases, it is often acceptable to compromise a certain degree of accuracy during the early stages in order to achieve a faster turnaround in the planning studies. Detailed algorithms can be used towards the end of the process to provide accurate results, one a strategy has stabilised.

In this chapter, two algorithms based upon discrete time simulation are proposed, in which the execution times are reduced through the use of assumptions about the nature of loading data on the system. The performance of the algorithms is compared with that of the original detailed algorithm.

It should be noted that the algorithms described here are designed to calculate variable losses. Fixed losses are calculated separately and added in at the end of the calculation.

8.2 Loss Calculation Using Archetypal Days

8.2.1 Introduction

It has been established that the yearly variation in demand for many feeders exhibits a repetitive cyclic pattern permitting these demand profiles to be represented with reasonable accuracy by a small number of representative daily curves (Allera et al [3], Andersson et al [6], EPRI [45], Grainger and Kendrew [58], Lakervi and Holmes [81], Sarikas and Thacker [122]).

The proposed method uses representative or archetypal daily curves to represent the variation of individual loads throughout the year, as described in Section 2.2.3. Load-flows are conducted for each half hour of each of the archetypal days. In addition load-flows are conducted at a reference time for each day of the year. For each day of the year, the results for the appropriate archetypal curve are scaled using the results from the reference load-flow at that day.

8.2.2 Preparation of Input Data

1. A small number of archetypal day types is selected to represent the variations in demand throughout the year. Engineering judgement can be used to select the curves, or a numerical method such as the clustering algorithm used by EPRI [45].
2. From historical demand data, a specific date is chosen to represent each of the archetypal days.
3. System loading data, recorded at half hour intervals, is assembled for each of the dates chosen and a load allocation is performed, as described in Chapter 5. For each date the load allocation procedure assigns a 48 half-hour demand profile for each load modelled in the system under study.
4. In addition, system loading data, recorded at a reference time for each day of the study period (normally a year) is assembled, and a load allocation is performed. The load allocation procedure assigns a 365 day profile for each load in the system.

8.2.3 Description of the Method

A graphical overview of the method is shown in Figure 8.1. The procedure for the method is outlined in Figure 8.2 and described below. The description applies to the calculation of the system losses as a whole. The algorithm may also be applied to calculate the losses in individual lines and transformers.

1. Load-flows are conducted by discrete time simulation at half hour intervals across each of the archetypal days.
2. The demand losses $P_{Larch,\ t}$ for each half hour t of each archetypal day are calculated from the load-flow results, using Equation (7-32).
3. Load-flows are conducted by discrete time simulation at 24 hour intervals across the study period, to provide the system operating condition at the reference time for each day.
4. The demand losses $P_{Lact,\ ref}$ at the reference time for each day of the study period are calculated from the load-flow results, as described in Step 2.
5. For each day of the study period, the corresponding archetypal day type is identified. The 'actual' demand losses $P_{Lact,\ t}$ for each half hour time step t of each day of the study period are calculated by scaling the archetypal demand losses at each step for the

corresponding day type, using the ratio of actual to archetypal demand loss at the reference time.

$$P_{Lact,t} = P_{Larch,t}\left(\frac{P_{Lact,ref}}{P_{Larch,ref}}\right) \tag{8-1}$$

6. The 'actual' energy losses $W_{Lday,\,d}$ for each day d of the study period are calculated by summing the demand losses at each half hour.

$$W_{Lday,d} = \frac{1}{2}\sum_{t=1}^{48} P_{Lact,t} \tag{8-2}$$

7. The annual energy losses, W_{Lyear} are obtained by summing the daily losses.

$$W_{Lyear} = \sum_{d=1}^{365} W_{Lday,d} \tag{8-3}$$

The costs of losses can be determined by the application of time related costs, C_t , to the daily demand losses at Stage 6., as shown in Equation (8-4).

$$C_{Lday,d} = \frac{1}{2}\sum_{t=1}^{48} P_{Lact,t}.C_t \tag{8-4}$$

Stage 7 is performed as before to yield the annual costs of energy losses. This approach can accommodate both time of day tariffs and tariffs which vary throughout the year, such as the UK Pool Purchase Price.

8.2.4 Computational Requirements

The proposed algorithm using archetypal days requires 48 load-flow solutions for each of the day types, plus a load-flow solution for each day of the study period.

Assuming six archetypal days, and a study period of a year, the total number of load-flow solutions required is 653, compared with 17520 for the detailed algorithm.

8.2.5 Discussion of the Method

The reduction in the number of load-flow solutions required over the detailed algorithm relies upon the following assumptions.

1. Demand profiles for loads on the system do not necessarily conform, but do follow a repetitive daily cycle, and can therefore be approximated with reasonable accuracy using a small number of archetypal daily curves.

2. The current flowing in a given line is directly proportional to the sum of the MVA demands of loads supplied by the line. This permits archetypal loss profiles to be scaled linearly to match the loss at a given reference point. This shall be referred to as the

'Linearity Assumption'. It can be relaxed provided that for each of the days in the study period which correspond to a particular archetypal day type, the system operating conditions at each half hour are similar to those of the specific date chosen to represent that day type. In other words the degree of scaling performed in Equation (8-1) is small.

3. For any given day the effects which give rise to discrepancies in the magnitudes of archetypal load profiles and actual data apply equally to all the individual demands making up the profile and occur across the 24 hour period. For example, if weather and other effects on a particular day result in a 20% increase in demand on a given feeder as compared with the typical daily profile, this 20% increase occurs across all the individual loads supplied by the feeder and applies to the full day. This implies that linear *scaling* is the correct mechanism for reconciling the differences between archetypal and actual daily profiles, rather than 'shifting' the archetypal curve by adding or subtracting an increment.

The degree to which these assumptions hold in practical cases, and the resulting effects on accuracy are explored in Section 8.4.

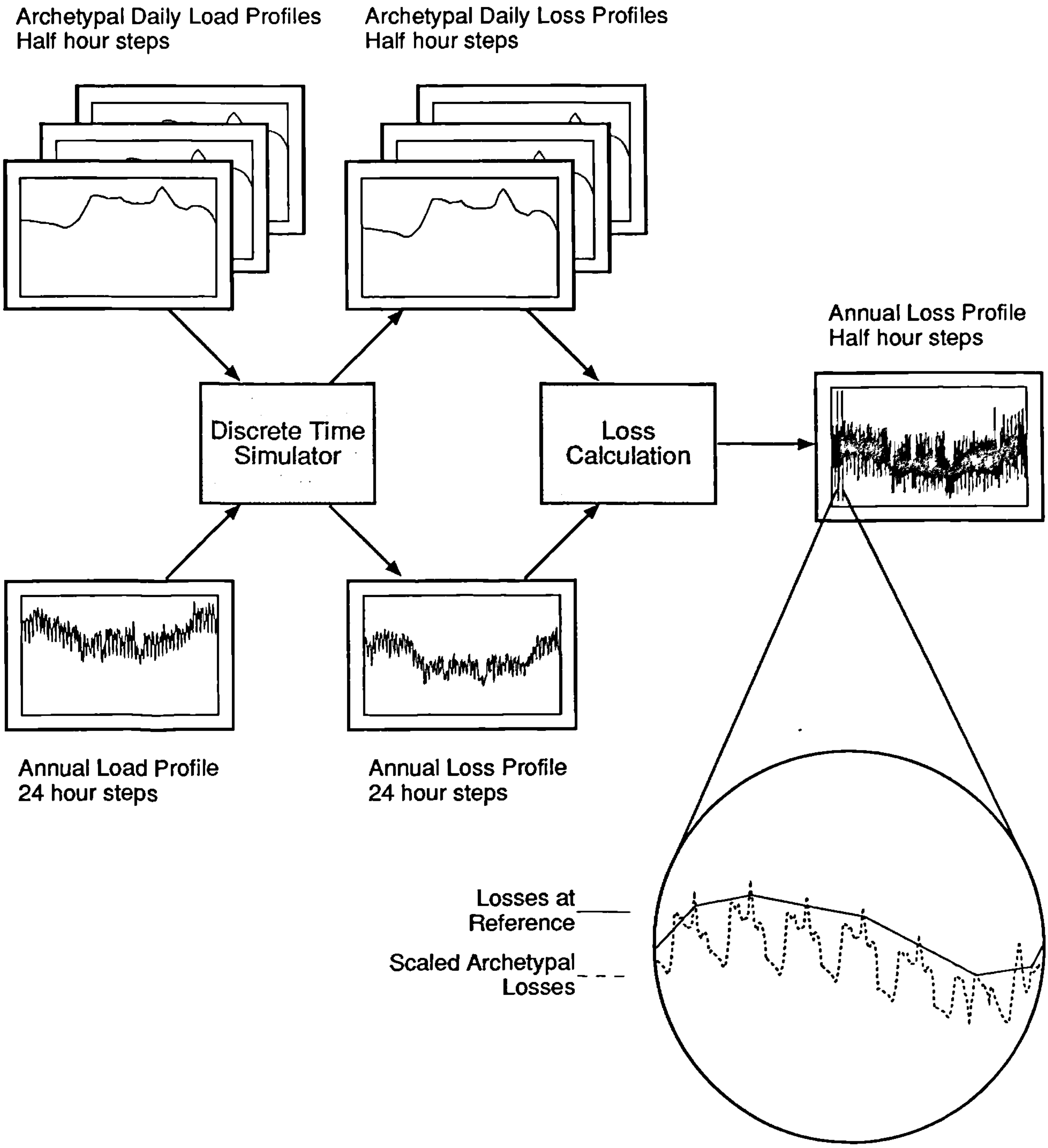

Figure 8.1 Graphical Overview of Loss Calculation Using Archetypal Days

- CALCULATE LOSSES FOR THE STUDY PERIOD
  - FOR ALL ARCHETYPAL DAYS
    - FOR ALL HALF HOURS
      - PERFORM LOAD-FLOW
      - CALCULATE ARCHETYPAL DEMAND LOSSES
  - FOR THE STUDY PERIOD
    - FOR ALL DAYS
      - PERFORM LOAD-FLOW AT REFERENCE TIME
      - CALCULATE ACTUAL DEMAND LOSSES AT REFERENCE TIME
      - IDENTIFY ARCHETYPAL DAY TYPE FOR THIS DAY
      - FOR ALL HALF HOURS
        - CALCULATE ACTUAL DEMAND LOSSES FROM ARCHETYPAL DEMAND LOSSES AND ACTUAL DEMAND LOSSES AT REFERENCE TIME
      - CALCULATE ACTUAL ENERGY LOSSES BY INTEGRATING ACTUAL DEMAND LOSSES OVER THE DAY
    - CALCULATE ACTUAL ENERGY LOSSES FOR STUDY PERIOD BY SUMMING ACTUAL DAILY ENERGY LOSSES

Figure 8.2 Procedure for Loss Calculation using Archetypal Days

8.3 Loss Calculation Using Loss Coefficients

8.3.1 Introduction

The method of loss calculation using loss coefficients attempts to establish a simple relationship between the losses in each line and transformer, and the system demand. The relationship is derived from a small number of load-flow solutions.

In the simplest case a single loss coefficient for each line and transformer is used to define a relationship between loss and system demand. Other, higher order methods are also explored.

8.3.2 Preparation of Input Data

1. A number of representative or average system operating conditions is selected, according to the specific variant of the algorithm.

2. For each condition a load allocation is performed as described in Chapter 5, to assign power injections to the loads and generators in the system.

8.3.3 Procedure for the Method Based Upon Single Loss Coefficients

This section describes the simplest variant of the algorithm: for each line and transformer in the system a single coefficient is derived which approximates the relationship between the loss in that component and the system demand squared. A variation of this method is described below.

1. A single average or peak system operating condition is chosen. A load-flow is conducted at this reference condition. Variable losses are calculated for all lines and transformers in the system.
2. For each line and transformer i a loss coefficient, LC_i is defined as shown in Equation (8-5).

$$LC_i = \frac{P_{L,i}}{S_{D,sys}^2} \tag{8-5}$$

3. The loss in any line or transformer are subsequently derived by applying the appropriate loss coefficient to the square of the system demand at the specified time.

$$P_{L,i} = S_{D,sys}^2 \times LC_i \tag{8-6}$$

4. For each time step of the study period, the system MVA demand $S_{D,\ sys}$ is determined and the demand losses in any line or transformer derived by simply applying the appropriate loss coefficient.

8.3.4 Discussion of the Method

The use of a loss factor for each line relating the loss in the line to the square of the system demand reduces greatly the data requirements and execution time of the method, but relies upon the following assumptions:

1. All loads in the system conform. For any given load the MVA demand is a fixed proportion of the total system MVA demand throughout the specified time period.
2. Given assumption 1., for any given line the current is directly proportional to the sum of the MVA demands supplied by the line. This is the Linearity Assumption which is also made by the method based upon archetypal days (assumption 2). It implies that voltage drops throughout the system are small.

8.3.5 Variation on the Method. Quadratic Loss Coefficients

8.3.5.1 Description

In this variation, three reference loading conditions are used in the calculation of loss coefficients. For each line and transformer the losses are calculated from a load-flow solution at each of the three loading conditions, and these are used to derive a unique quadratic polynomial that coincides with each condition:

$$P(x) = \frac{(x-x_2)(x-x_3)}{(x_1-x_2)(x_1-x_3)}y_1 + \frac{(x-x_1)(x-x_3)}{(x_2-x_1)(x_2-x_3)}y_2 + \frac{(x-x_1)(x-x_2)}{(x_3-x_1)(x_3-x_2)}y_3 \tag{8-7}$$

where in this case x represents the system demand squared and y represents the individual line or transformer loss. The losses in the line or transformer are subsequently derived for any loading condition by interpolating (or extrapolating) on this polynomial. The method used here to construct the interpolating polynomial is Neville's Algorithm [66, 111]. In this method the value of the interpolating polynomial at some point x is found recursively by updating a table of lower order polynomials:

$$\begin{array}{cccc} y_1 = P_1 & & & \\ & P_{12} & & \\ y_2 = P_2 & & P_{123} & \\ & P_{23} & & \\ y_3 = P_3 & & & \end{array} \tag{8-8}$$

where $P_{1\ldots n}$ is the polynomial of degree n - 1 passing through points (x_1,y_1) ... (x_n,y_n) given by Neville's form:

$$P_{i(i+1)\ldots(i+m)} = \frac{(x-x_{i+n})P_{i(i+1)\ldots(i+m-1)} + (x_i-x)P_{(i+1)(i+2)\ldots(i+m)}}{x_i-x_{i+m}} \tag{8-9}$$

In practice just the differences between each polynomial and its two lower order 'ancestors' are calculated and used together with y_1, y_2 and y_3 to obtain the final solution $y = P_{123}$ for a given value of x.

The principal benefit afforded by this variation is that it provides improved modelling of the relationship between the loss in a given line and the square of the system demand, particularly at the extreme loading conditions. However, as with the basic method the diversity of individual line loading patterns is not accounted for.

8.3.5.2 Implementation Details

- The three reference points were selected to span the range of system operating conditions: system maximum, minimum and average demand.
- For each of the three reference points the ten time steps at which the system demand was closest to the required values were identified. The active and reactive power values for each load and generator were derived by taking the mean of their respective values across the ten time steps. This process reduces the algorithm's sensitivity to extreme and unrepresentative loading conditions, while ensuring that the derived sets of power values are close to the values which occur in practice. The number ten was derived empirically from test results.

8.4 Evaluation of the Loss Calculation Algorithms

8.4.1 Objectives

The objectives of the tests are to determine the accuracy of the loss calculation algorithms under typical operating conditions, and to assess their sensitivity to algorithm parameters and changes in system operating conditions. The assumptions on which the algorithms rely are assessed in the light of test examples.

Throughout the tests the accurate loss calculation algorithm described in Chapter 7 is used as a reference against which the approximate algorithms are compared.

8.4.2 Accuracy of the Algorithms Under Typical Operating Conditions

In this test the accuracy of the approximate loss calculation algorithms is compared with that of discrete time simulation using actual network and loading data. The test systems cover a range of configurations, consumer load type mixes and voltage levels, and hence the results offer a guide to the levels of performance of the algorithms to be expected in practice.

8.4.2.1 System Demand and Energy Losses

Table 8.1 compares the system demand and energy loss results from the approximate loss calculation algorithms with the values obtained by discrete time simulation for four test systems. The errors in the loss results are presented as a percentage of the reference loss values.

Also listed are the mean deviations in the errors over the study period. These are derived by summing the deviations in the loss errors from the mean loss for every component in the system at each time step and taking the mean over the study period. The deviations are expressed as a percentage of the mean system demand loss over the period. Further information concerning the plant and loading data for these systems is given in Appendix E.

From the table the following observations can be made:

- In general the algorithms perform best on the networks in which load diversity is lowest. The loss results for the 15 and 348 node systems, which serve a higher proportion of domestic (conforming) loads, are closer to the reference than the results for the 7 and 10 node systems which serve a largely industrial load mix.
- The method based upon archetypal days in general provides greater accuracy than the methods based upon loss coefficients. An exception is found in the results for the 10 node system, where the method based upon archetypal days performs relatively poorly. In the other cases the system energy losses are obtained by this method to within 2% of reference values, and the system demand losses to within 10%.

- Of the two variations based upon loss coefficients the use of quadratic loss coefficients results in greater accuracy overall than in the linear case, although not in all cases: quadratic coefficients offer greater accuracy than linear coefficients in the systems serving largely diverse industrial loads, but the converse is true for the systems serving conforming domestic loads. Both methods based upon loss coefficients are susceptible to significant errors in the calculation of maximum and minimum demand losses, approaching 70% in two instances. However, the energy loss results are obtained to within 5% of reference values in all but one case.

These results are discussed in Sections 8.4.3 and 8.4.4 below.

The results in Table 8.1 can also be compared with equivalent results for the multiple case load-flow analysis approaches based upon typical and duration days which are described in Chapter 2. The methods of Sun et al [138] and EPRI [44] are examples of the multiple case load-flow approach based upon duration days. Comparison with the results of those algorithms in Table 2.4 leads to the following observations:

- The loss calculation method based upon archetypal days is significantly more accurate than the multiple case load-flow approaches in the calculation of system demand losses. In the calculation of energy losses there is little difference in the results. However the mean deviations for the archetypal days method are consistently lower than those of the multiple case load-flow approaches, which indicates greater reliability in the calculation of losses for individual lines and transformers

- The results for the loss calculation methods based upon loss coefficients are in general less accurate than those of the multiple case load-flow approaches.

Table 8.1 Comparison of System Losses for Different Loss Calculation Methods

Test System	Simulation Type	Comparison with Discrete Time Simulation						
		System Losses			Errors			Deviation
		Demand Max (MW)	Demand Min (MW)	Energy (GWh)	Demand Max (%)	Demand Min (%)	Energy (%)	Mean Half hour (%)
7 Node	DTS	0.621	0.047	1.32				
	Arch Days	0.669	0.043	1.34	7.7	-8.5	2.0	20.5
	Linear LC	1.052	0.067	1.69	69.4	42.6	28.4	27.2
	Quad LC	0.456	0.078	1.38	-26.6	65.9	4.6	38.3
10 Node	DTS	0.823	0.005	3.21				
	Arch Days	0.927	0.006	3.02	12.6	20.0	-5.7	24.7
	Linear LC	0.826	0.005	3.22	0.4	0.0	0.5	2.0
	Quad LC	0.731	0.006	3.21	-11.2	20.0	0.3	22.5
15 Node	DTS	4.737	0.439	16.16				
	Arch Days	4.811	0.416	15.92	1.6	-5.2	-1.5	10.6
	Linear LC	4.493	0.517	16.04	-5.2	17.8	-0.8	27.3
	Quad LC	4.620	0.442	15.37	-2.5	0.7	-4.8	32.0
348 Node	DTS	183.227	79.765	84.95				
	Arch Days	201.254	81.217	86.01	9.8	1.8	1.2	5.3
	Linear LC	192.820	59.427	86.21	5.2	-25.5	1.5	10.2
	Quad LC	184.829	81.033	88.85	0.9	1.6	4.6	10.7

8.4.2.2 Individual Component Demand and Energy Losses

The full results listing calculated losses for each line in each of the test systems are presented in Tables C.1 to C.13 in Appendix C.

The implementation details of the loss calculation algorithms are as for the system losses case.

The following observations can be made from the results:

- The loss results for individual lines lead to the same conclusions concerning the comparative performance of the methods as the results for the system as a whole.
- The methods based upon loss coefficients perform well on lines supplying loads whose demand profiles conform to the system demand, but are susceptible to large errors on lines supplying diverse loads. An example can be seen in the case of the 7 node system. Lines 1 and 2 supply the entire system load, and hence by definition the load supplied by these lines will conform to the system demand profile. Lines 3 and 4 supply a mixture of major industrial and domestic loads. The loss results for lines 1 and 2 can be seen to agree much more closely with the reference values than the results for lines 3 and 4. By contrast the method based upon archetypal days is much less sensitive to the nature of

the loads in this example because, although they do not all conform, the loads do exhibit a predictable repetitive pattern. Results for this system are given in Table C.1, page 289.

8.4.3 Assessment of the Method Based Upon Archetypal Days

Having identified the accuracy achieved by the loss calculation methods on real test cases, this section tests the assumptions that underlie the method based upon archetypal days, and attempts to quantify errors arising from their use.

8.4.3.1 Assessment of the Linearity Assumption

As stated in Section 8.2.5 the method assumes that the current in a given line is directly proportional to the MVA demand supplied by the line. The method relies on this assumption to scale the archetypal loss profiles using linear scaling factors to reconcile the differences between archetypal and actual losses at the reference time on a particular day.

In practice, although the current at a given bus i can be linearly related to the voltages throughout the system,

$$\bar{I}_i = \sum_{j=1}^{n} \bar{Y}_{ij}\bar{E}_j \tag{8-10}$$

the relationship between these voltages and system MVA demands is non-linear, as given by the well known load-flow equations (Arrillaga and Arnold [7], Del Toro [34], Gross [59], Stagg and El-Abiad [131], Wood and Wollenburg [152]):

$$\begin{aligned} \bar{S}_i &= V_i\sum_{j=1}^{n} Y_{ij}V_j \angle(\theta_i - \theta_j - \gamma_{ij}) \\ &= V_i\sum_{j=1}^{n} [Y_{ij}V_j(\cos(\theta_i - \theta_j - \gamma_{ij}) + j\sin(\theta_i - \theta_j - \gamma_{ij})] \end{aligned} \tag{8-11}$$

These effects are easily demonstrated. Figure 8.3 shows an LV feeder in the 122 node test system supplying a single load.

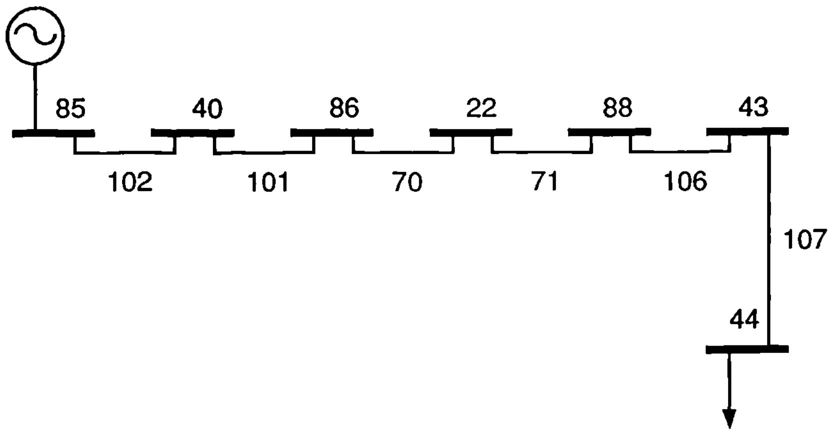

Figure 8.3 Radial Feeder on the 122 Node Test Network

If the load is increased in stages by adding a fixed kVA increment, the current flowing in the line will increase, but in a non-linear fashion, as shown in Figure 8.4. Voltage magnitudes along the feeder change non-linearly, as shown in Figure 8.5. Voltage angles increase along the feeder in a similar manner.

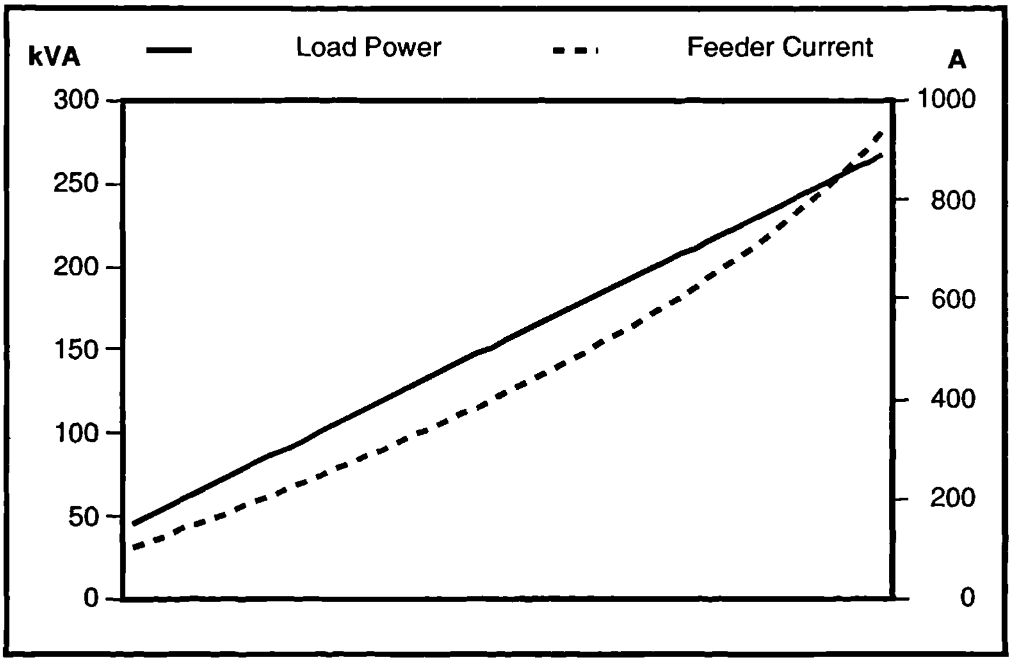

Figure 8.4 122 Node Test Network Feeder Current for Linearly Increasing Load

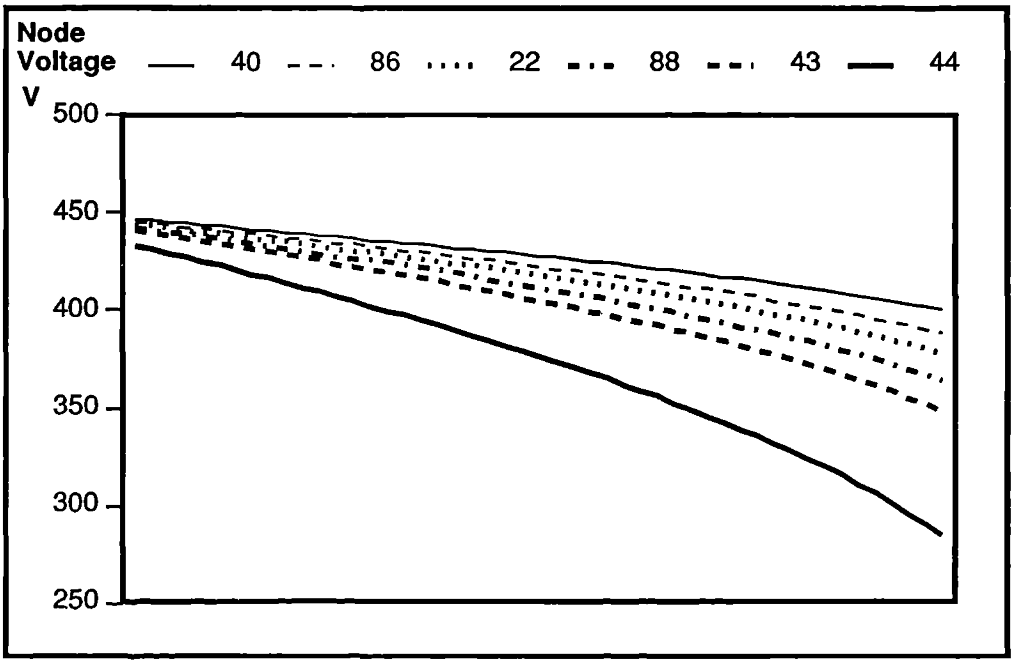

Figure 8.5 122 Node Test Network Feeder Voltage Profile for Linearly Increasing Feeder Load

Two factors which have an impact on the degree of non-linearity in the system are transmission line parameters and the voltage dependency of loads.

Transmission Line Parameters

The series and shunt admittances of transmission lines are normally modelled using a Π section model, as shown in Figure 8.6.

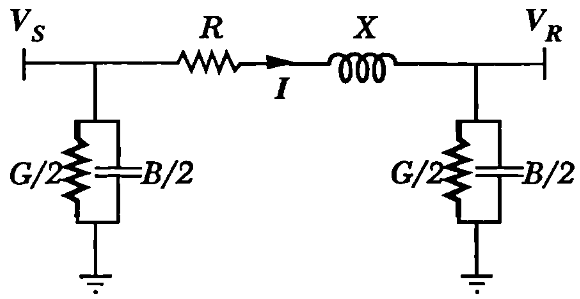

Figure 8.6 Π Section Model of a Transmission Line

The effect of the series inductive reactance is to increase the power factor angle (lagging) down the line, thereby absorbing reactive power, while the effect of the shunt capacitive reactance is to reduce the power factor angle (lagging), thereby supplying reactive power to the system. The reactive loss in a line is given approximately by

$$Q_L \simeq I^2X - V^2B \tag{8-12}$$

where

$$V \simeq V_S \simeq V_R \tag{8-13}$$

Q_L may be positive or negative depending on whether the inductive or capacitive component dominates. This depends partly on the line parameters, but is also affected by the loading of the line; as the load increases the increase in current and decrease in voltage cause the inductive component to become dominant, while the reverse is true for decreasing loads. The greater the net supply or absorption of reactive power by the transmission lines in the system, the greater the non-linearity between MVA demand and voltage. These effects are explored further in (Macqueen [85]).

Voltage Dependency of Loads

The nonlinear effects described above can be compounded by the way in which loads are modelled. Loads are commonly modelled such that the active and reactive power taken are fixed, regardless of the voltage at the terminals, whereas in practice most loads are voltage dependent. The effect of modelling loads as voltage *independent* exaggerates the variation in voltage with load in the system as follows. When system loading increases there is normally a corresponding reduction in voltage at the load terminals. In practice this would result in a reduction in the power taken by the loads. Indeed voltage reduction strategies which utilise this effect are often used to avert the need to disconnect loads under emergency conditions (Pansini [106]). However, when modelling loads as constant power a reduction in load voltage leads instead to an increase in load current in order that the load power be maintained. This in turn exacerbates the voltage problem.

8.4.3.2 The Effect of the Linearity Assumption on Accuracy Under Typical Conditions

Having identified the sources of error concerning the linearity assumption it is important to try to quantify the degree of error introduced in the use of archetypal loss profiles. It should be noted that the load-flow accounts for the non-linearity in the calculation of losses at the reference times, and for each of the archetypal days. It is only in the scaling of archetypal loss profiles that the linearity assumption is made. It follows that the error introduced depends upon the degree of scaling performed.

The four networks used in the earlier tests were employed. The test procedure was as follows:

1. For each load in the test system a collection of nine archetypal demand curves was derived from actual metered data using Stage 2 of the procedure described in Section 2.5.3 in Chapter 2.
2. For each load in the test system a demand profile for the simulation period (nominally one year) was built up by selecting, for each day, the archetypal curve matching the current day type and season.
3. A full discrete time simulation was performed at half hour steps using these demand profiles to yield reference losses.
4. Several runs of the loss calculation method based upon archetypal days were performed using the archetypal curves derived in Step 2, but scaled using a range of factors: -50%, -20%, 0%, +20%, +50%. The loss results were compared with the discrete time simulation reference.

Loads were modelled as voltage independent in the tests. The results of the tests are presented in Table 8.2. The table lists the errors in the system maximum and minimum demand losses, and the system energy losses compared with the reference case. Also listed are the mean half hour deviations in loss errors in individual components expressed as a percentage of the mean loss in each component over the study period.

A comparison of the results in the table with the results in Table 8.1 indicates that the errors introduced in the scaling of archetypal loss profiles generally comprise a small proportion of the errors as a whole. Given that the system peak demand typically varies by the ratio 2:1 winter to summer, and that archetypal profiles are calculated at some average loading condition for each season, the scaling of archetypal profiles is highly unlikely to exceed ±50%, and hence the errors in Table 8.2 for these scaling factors can be regarded as the maximum that will be introduced in practical cases.

Table 8.2 Comparison of Loss Errors for Different Archetypal Scaling Factors

Test System	Archetypal Load Scaling Factor (%)	Comparison with Base Case (0% Scaling)			
		Errors			Deviation
		Demand Max (%)	Demand Min (%)	Energy (%)	Mean Half Hour (%)
7 Node	-50	-0.73	1.10	0.16	0.26
	-20	-0.32	0.39	0.06	0.13
	0	0.00	0.00	0.00	0.00
	20	0.24	-0.47	-0.10	0.16
	50	0.90	-1.18	-0.19	0.39
10 Node	-50	0.36	9.49	1.00	1.11
	-20	0.08	2.06	0.29	0.29
	0	0.00	0.00	0.00	0.00
	20	-0.05	-1.58	-0.23	0.23
	50	-0.06	-3.64	-0.56	0.64
15 Node	-50	-1.11	13.34	1.38	1.44
	-20	-0.31	3.03	0.33	0.34
	0	0.00	0.00	0.00	0.00
	20	0.27	-1.90	-0.22	0.23
	50	0.65	-3.77	-0.47	0.49
348 Node	-50	-6.79	7.27	1.22	4.10
	-20	-3.93	0.26	-0.40	1.82
	0	0.00	0.00	0.00	0.00
	20	5.45	-1.93	-0.15	2.21
	50	Load-flow did not converge for this extreme loading condition			

8.4.3.3 Sensitivity of Results to Archetypal Reference Time

The loss calculation method based upon archetypal days performs scaling of archetypal loss values about a single reference point for each day. The results for the algorithm presented in Section 8.4.2 are based upon a reference time of 12 noon for each day of the study period. This section explores the effects of using alternative reference times on the accuracy of the results.

Tests were conducted on each of the four test networks used previously, as follows:

1. For each test network results from a full discrete time simulation were used as a reference.

2. Eight reference times were selected to cover the 24 hour period. For each of the eight cases the loss calculation method was run over the study period, using load-flow results at the appropriate reference time at each day for scaling of archetypal losses.

Figure 8.7 compares the errors in the system energy losses for each of the eight reference times. Figure 8.8 compares the mean errors in energy losses for individual lines.

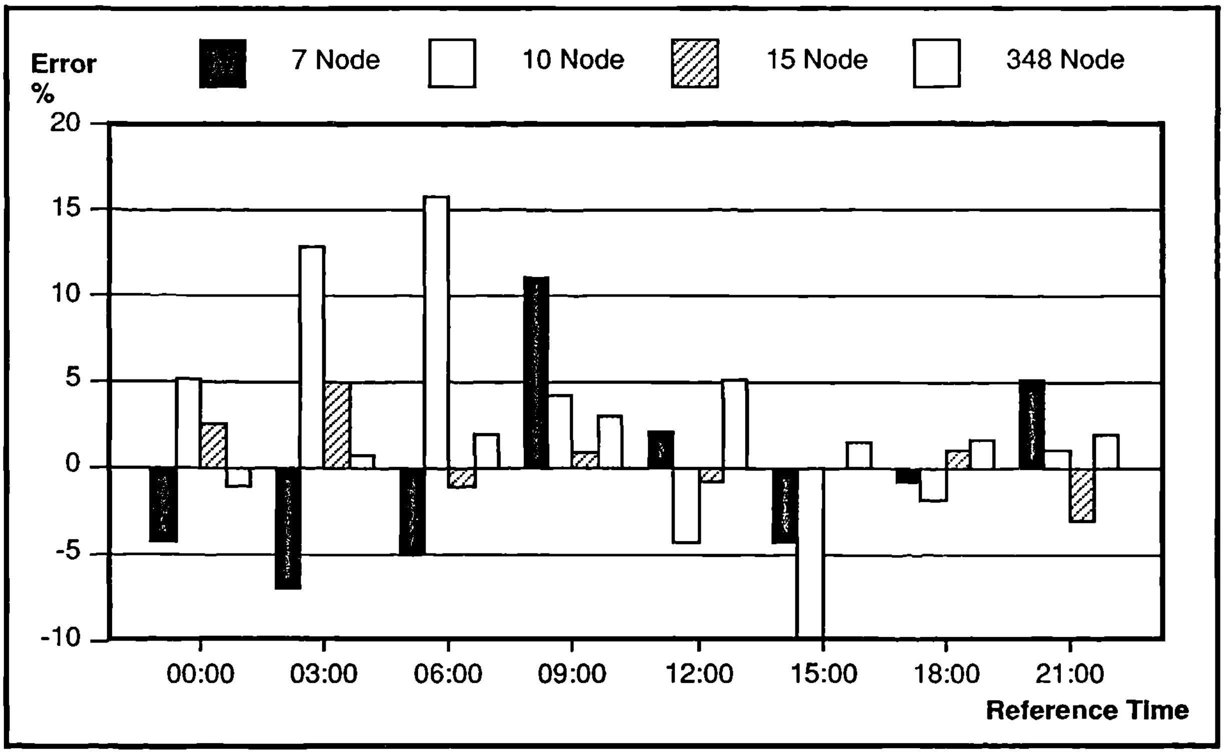

Figure 8.7 Errors in the Calculation of System Energy Loss for Different Reference Load-flow Times

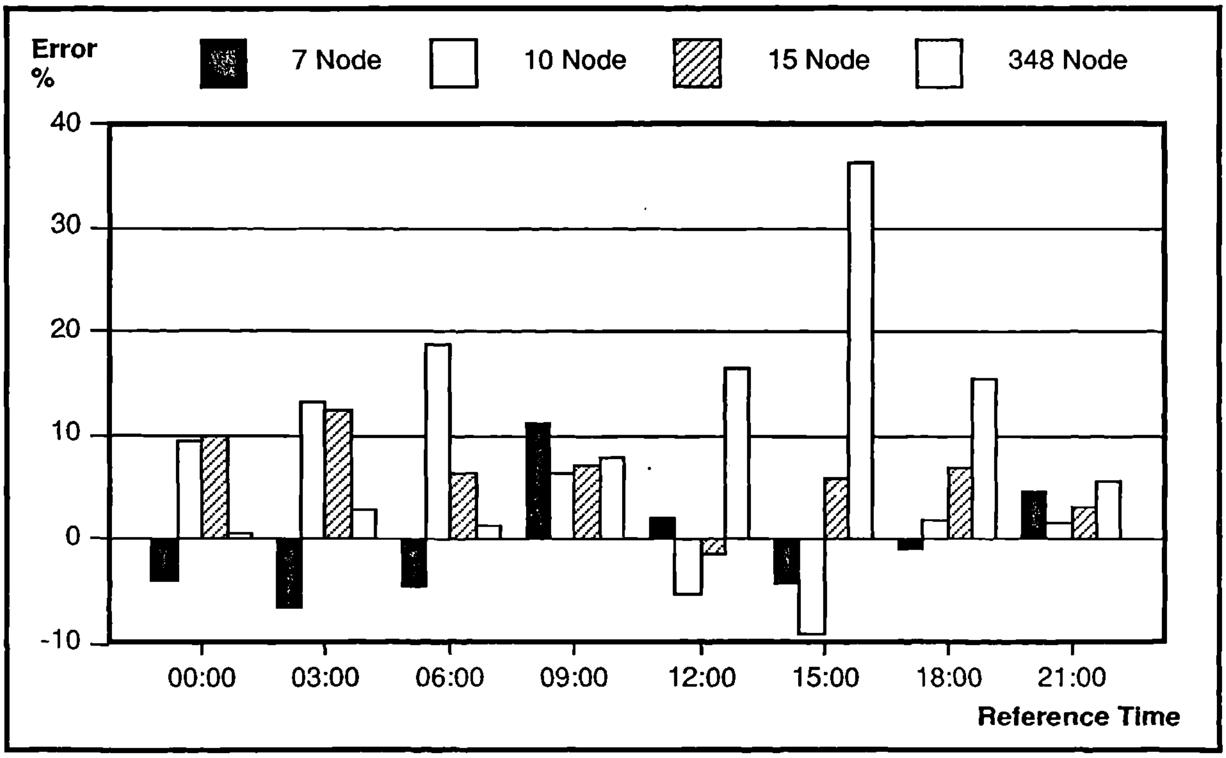

Figure 8.8 Mean Errors in the Calculation of Individual Energy Losses for Different Reference Load-flow Times

The figures show that there is considerable variation in the loss errors with reference time. From the figures it can be seen that three reference time periods yield system and individual losses with relatively small errors: 12:00, 18:00 and 21:00 hours. It is interesting to note that these times correspond to the peaks which occur in the typical domestic demand profiles throughout the year, as shown in Figure 4.18 in Chapter 4. These peaks correspond to domestic lunchtime cooking load, evening cooking/lighting load and evening lighting/heating loads respectively, and clearly offer greater stability in the scaling process.

8.4.4 Assessment of the Method Based Upon Loss Coefficients

8.4.4.1 Assessment of the Conforming Loads Assumption

In this method the loss coefficient for a given line relates the loss in the line to the system MVA demand. The implicit assumption is that the load supplied by the line conforms to the demand for the system as a whole. In networks with significant levels of load diversity this assumption leads to errors, as shown in the tables of results: Table 8.1 and Tables C.1 to C.13.

These effects can be seen by plotting the loss coefficients calculated at different points in time. Figure 8.9 shows the loss coefficients for Lines 1 and 3 of the 7 Node system, and Line 10 of the 15 Node system for four days in February. Line 1 supplies the whole system, and hence by definition the load supplied by the line conforms to the system demand. The resulting loss coefficients therefore form a straight line. Line 3 supplies a diverse group of loads which when summed together do not conform to the system demand, as shown in Figure 8.10. The variations in the loss coefficients for this line can be seen clearly to follow the discrepancies between the two profile shapes in Figure 8.10. Line 10 connects Nodes 1 and 3 of the 15 Node test system, which serves a rural/domestic area of largely conforming loads. The loss coefficient for this line is much more constant as expected.

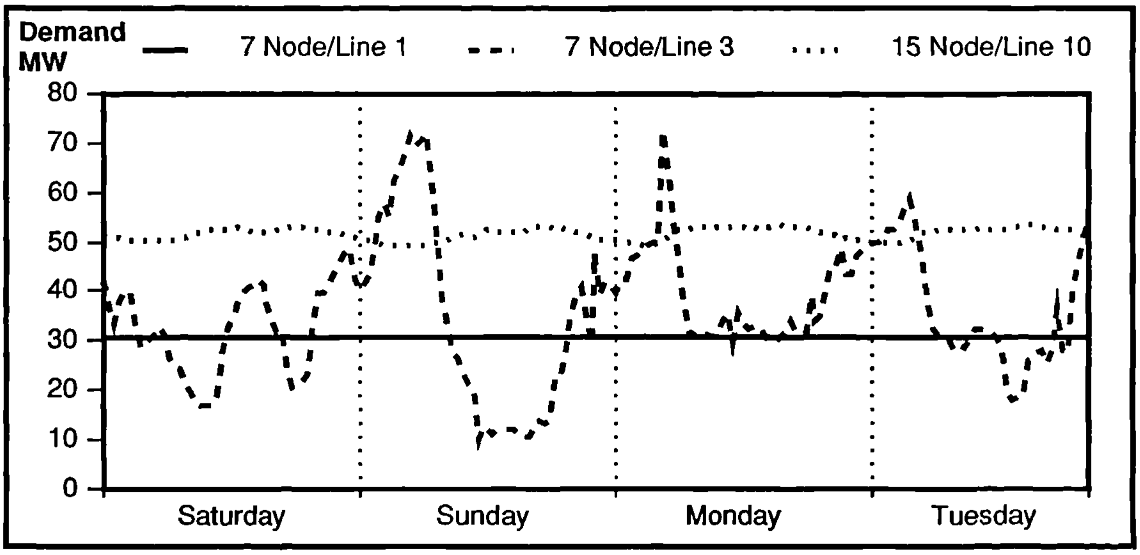

Figure 8.9 Variation in Loss Coefficients With Time With Load Diversity

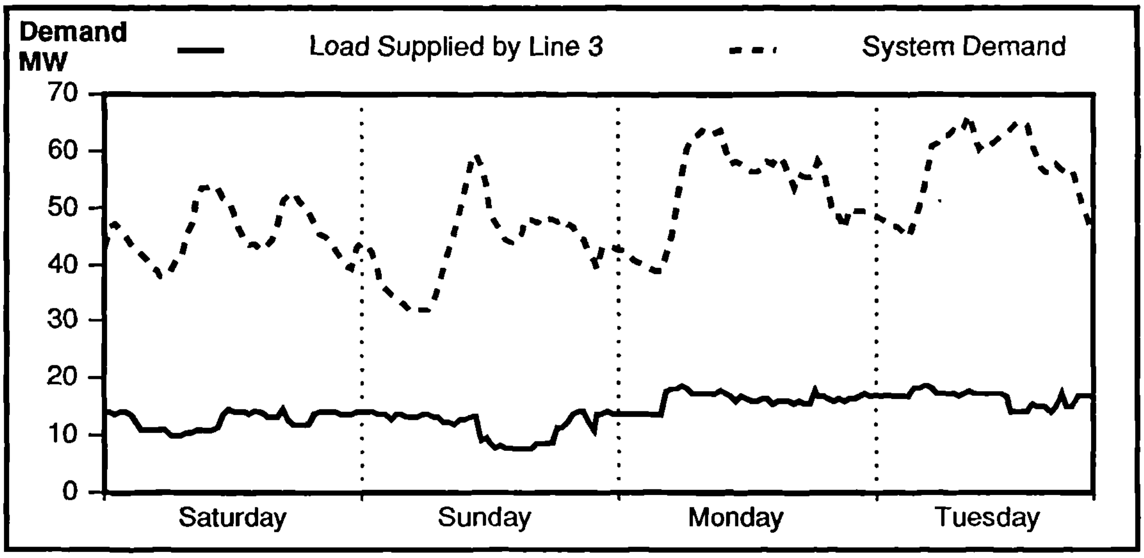

Figure 8.10 Comparison of Load Supplied By Line 3 with System Demand

True effects of load diversity on the loss coefficients, and hence on the accuracy of the loss calculation algorithm can be gauged by removing load diversity from these test systems and plotting the resulting loss coefficients. Figure 8.11 shows the corresponding loss coefficients for the previous examples with conforming loads. From these examples it is clear that load diversity has a very important impact on the accuracy of the loss calculation method based upon loss coefficients.

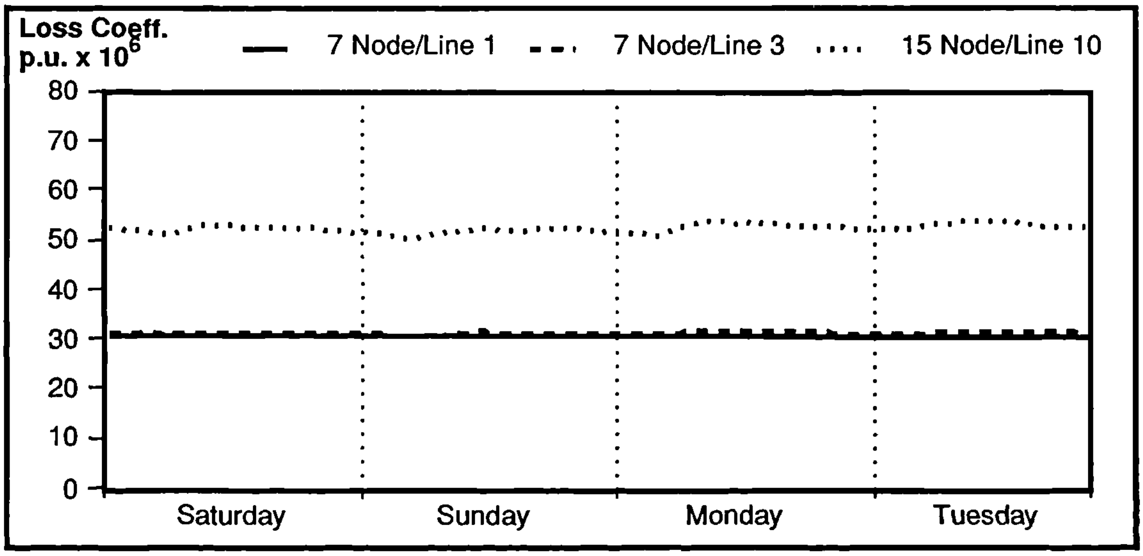

Figure 8.11 Variation in Loss Factors with Time Without Load Diversity

8.4.4.2 Assessment of the Linearity Assumption

Given a linear relationship between system MVA demand and the voltages and currents throughout the network the loss coefficients defined in Equation (8-5) should be constant for each line. However, as explained in Section 8.4.3.1, this relationship is nonlinear, and therefore the loss factors will vary with time, as indicated in Figure 8.11 above. These variations will depend upon the electrical characteristics of the lines and cables in the system, and on the loading conditions. The test examples used in the previous section provide a useful means of assessing these effects.

Figure 8.12 illustrates the effects of line reactance and susceptance on the loss factors for Line 3 of the 7 Node test system. The line is a 66kV overhead line with resistance 0.15p.u., reactance 0.27p.u., and negligible susceptance. The first curve shows the loss coefficients with the line parameters at their nominal values, which corresponds to the case shown in Figure 8.11 above. Three additional cases are shown: 1) with line reactance increased by 50% to 0.40p.u., 2) with susceptance set to 0.03p.u., and 3) with susceptance increased to 0.04p.u. The figure indicates that increasing the susceptance up to a point serves to reduce the lagging power factor angle and improve the stability of the loss coefficients as a result. However, beyond a value of approximately 0.03p.u. the susceptance begins to dominate the inductive reactance, with subsequent increases in loss factor variation. This supports the theory outlined in Section 8.4.3.1.

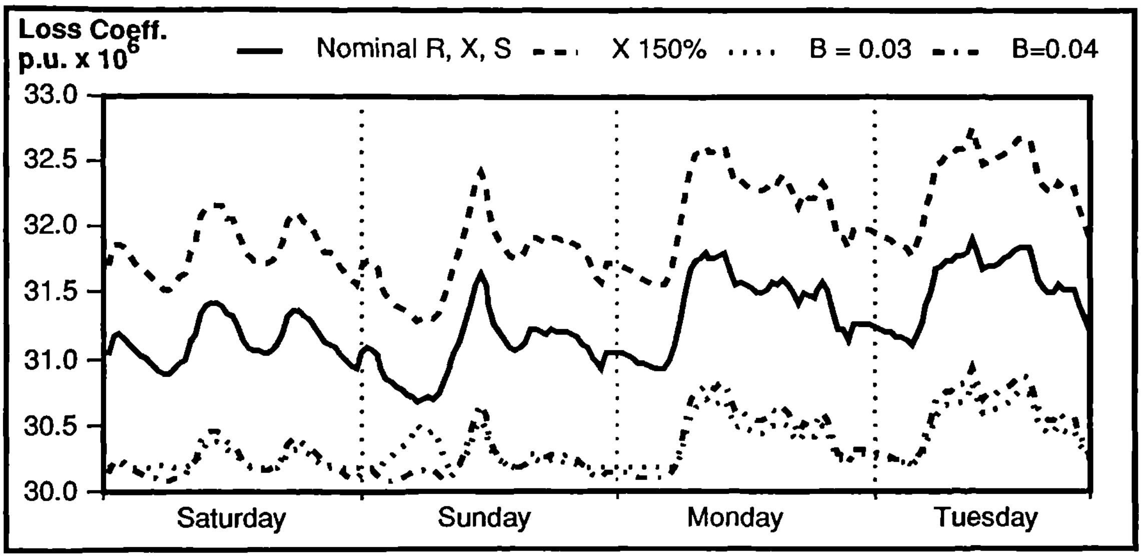

Figure 8.12 Variation in Loss Coefficients with Different Line Parameters

8.5 Conclusions

In this chapter two loss calculation algorithms based upon discrete time simulation have been presented which achieve significant reductions in execution time compared with the basic algorithm through the use of interpolation.

The first of the proposed methods, which uses archetypal daily load curves to represent the variation of individual loads throughout the year, has been described and shown to require only a small fraction of the load-flow solutions of the detailed loss calculation method. Test results have been presented which indicate that errors in the results lie typically in the range one to two percent for the calculation of energy losses, and within 20% when used to calculate demand losses. These results are shown to compare favourably with those of the two multiple case load-flow based approaches described in Chapter 2, which include the methods of Sun et al [138] and EPRI [44].

The assumptions used when performing the interpolation have been explored. Test results have been presented which indicate that errors introduced via the linear scaling of archetypal loss profiles are generally small in comparison with errors in the results generally. Additional tests have indicated that the use of reference times of 12:00, 18:00 or 21:00 hours in the scaling of archetypal loss profiles results in the lowest levels of error in the results.

The second of the proposed methods, which uses loss coefficients to relate the losses in individual lines to the system demand, has been described and shown to offer very low data and computational requirements. Test results have been presented for two variations of the algorithm, based upon linear and quadratic loss coefficients, which indicate that quadratic loss coefficients offer greater accuracy in systems with diverse industrial loads, while linear coefficients offer greater accuracy in systems with low levels of diversity. Errors on energy loss results are typically a few percent higher than those of the method based upon archetypal days, but the very low execution times of the method make it attractive for studies in which many different cases need to be run and compared.

The assumptions underlying the method have been outlined, and the implications of these assumptions explored through the use of representative test cases. It has been shown that the most significant source of error in this algorithm is high levels of load diversity.

In conclusion, the detailed loss calculation algorithm described in the previous chapter and the two algorithms based upon interpolation presented here are complementary, and offer a range of accuracy at a range of costs in terms of data and computational requirements.

Chapter 9. Allocation of Losses

9.1 Introduction

An aspect of loss accounting that is growing in importance, particularly in the United Kingdom, is the allocation of losses and their associated costs to the consumers on the system. Common practice among distribution companies world-wide is to determine the demand losses and the average energy losses incurred at each of the voltage levels in the system. Consumers are charged for losses on the basis of these average figures.

Such an approach is simple, but undesirable in economic terms, since it does not account for the fact that load losses are highly variable, and that the cost of supplying energy losses also varies continually during the day.

The loss results from the algorithms proposed in Chapters 7 and 8 are highly suitable for use in a more accurate method for apportioning losses and costs. The losses in each component of the system under study are available as a function of time, and can be related to time-based costing information.

In the design of new approaches to this problem, it is necessary first to consider the principle objectives in the pricing of electricity, and to study how these objectives can best be met in the case of allocating losses.

9.2 Objectives in the Allocation and Pricing of Losses

9.2.1 General Electricity Pricing Objectives

In the electricity industry, several objectives of pricing policy are widely recognised. The objectives are not necessarily mutually consistent, and compromises inevitably have to be made. The principle objectives are as follows [14, 15, 96, 97, 150].

9.2.1.1 Resource Allocation

Limited national resources must be allocated efficiently, both among different sectors of the economy, and within the electricity industry itself. This implies that prices must as far as possible reflect the true cost of supply, so that the consumer is aware of the economic cost of his consumption of electricity.

In the case of losses, it is important that the losses charged to a consumer reflect the costs of supplying the losses at the time they were produced.

9.2.1.2 Fairness and Equity in the Allocation of Costs

Prices must not discriminate between consumers. Costs must be allocated between consumers according to the burdens they impose on the system.

The burden placed by a consumer on the distribution system depends upon a number of factors, including the geographical location of the consumer and their proximity to sources of power and distribution system facilities, the maximum demand of the consumer, and the pattern of the demand.

In the specific case of losses, consumers at low voltage incur higher levels of loss than those at high or medium voltage, due to the lower efficiency of the low voltage system, and the additional transformation required to step the voltage down to these levels. This effect is compounded by the fact that losses produced in the low voltage system increase the loading of the system at higher voltages which in turn results in increased losses at those levels.

Another feature of losses is the square law relationship between loss and current. The result is that at high levels of system loading the marginal losses are very much greater than at low levels of loading. Hence a consumer whose demand for electricity coincides with system peak loading periods imposes a much greater burden on the system than a consumer whose demand occurs primarily during off-peak periods.

Energy generated to supply fixed losses, and variable losses during off-peak periods, is supplied from relatively cheap base-load plant. Variable losses at peak periods are supplied from expensive marginal plant.

To avoid discriminating between consumers when allocating losses and costs, it is necessary to model these effects; namely the square law effect between losses and demand, and the time-varying nature of losses and the associated costs of supplying them.

9.2.1.3 Revenue Requirements

Charges must raise sufficient revenues to meet the financial requirements of the utility concerned.

In the case of distribution system energy losses, the revenue received must cover the cost of additional energy purchased over and above that supplied to consumers.

Revenue received from demand loss charges, must provide for extension of the capacity of the network to meet projected growth in demand losses.

In addition, it is desirable that charging structures provide incentives towards loss reduction. Charging structures which pass all costs (and any savings due to loss reduction) through to the consumer do not achieve this aim. Instead the benefits brought about by loss reduction should be shared between the distribution company and the consumer, and conversely penalties associated with poor efficiency should be borne in part by the distribution company. These issues are currently under review in the UK by the electricity regulator.

9.2.1.4 Other Economic and Political Requirements

In addition, other economic or political requirements may need to be considered. These might include the assurance of a reasonable degree of price stability, tariff structures that are easily understood or subsidised supply to certain sectors to encourage economic growth, and so on.

Practical considerations limit the level of detail which can be accommodated in the allocation of costs. It is clear that the sheer number of domestic consumers in a distribution system requires that allocation methods and tariffs be kept simple. The relatively small numbers of larger industrial and commercial consumers permit the use of more sophisticated methods for these classes of consumer.

9.2.2 Pricing on an Average Cost or Marginal Cost Basis

Methods for pricing electricity normally fall into one of two broad categories: average or accounting cost pricing and marginal cost pricing. These categories are generally referred to in the context of pricing electricity in general.

In the average cost pricing approach, a utility's historic accounting costs are allocated to consumers via tariffs for different classes of consumer. Since it is based upon historic costs, the approach is essentially 'backward looking'.

Marginal cost pricing uses the marginal costs of supplying an extra unit of electricity at any given time as the basis for deriving tariffs. Short run marginal costs consider electricity supply costs with the system capacity taken as fixed. Long run marginal costs take the system capacity as variable and include the costs of changes in capacity in the analysis. Marginal cost pricing is 'forward looking', since it studies the cost implications of supplying additional demand, given that the existing levels of demand are already being served.

In the context of allocating and charging for losses described here the concepts of average cost and marginal cost pricing are used in a slightly different sense from the general case. In particular they are used to distinguish what happens when a new consumer is connected to the system.

9.2.2.1 Average Cost Pricing

The concept of average cost pricing used here describes methods in which the costs of losses are allocated between existing consumers according to the burden they place on the system. When a new consumer is connected to the system the same allocation procedure is used to allocate costs. The result is that the allocation to existing consumers may change, and is likely to increase significantly if system loading is increased, due to the quadratic growth of losses with respect to increases in load.

9.2.2.2 Marginal Cost Pricing

The concept of marginal cost pricing used here describes methods in which the costs of losses are allocated on a marginal basis. The sequence in which consumers are connected to the system is retained and whenever a new consumer is connected to the system, the marginal system losses generated as a result are allocated solely to the new consumer. The allocation to existing consumers is not affected.

9.2.2.3 Practical Pricing Schemes

In practice a distribution company may wish to adopt a strategy which combines the two approaches, for the following reasons:

1. A scheme based solely on average cost pricing for losses would be impractical since every major new consumer added to the system would affect the allocation to existing consumers. In addition, as levels of system loading increased, existing consumers would be forced to shoulder part of the costs attributable to new consumers, which departs from the fairness objective of Section 9.2.1.2.

2. A scheme based solely on marginal cost pricing is faced with the major difficulty of calculating and allocating costs to existing consumers. Consumers connected first enjoy the low levels of system loading with very low levels of loss. Consumers connected last generate a much higher marginal loss, due to the square law effect of losses.

3. A scheme employing both average and marginal cost pricing provides a practical and economically desirable solution. At the introduction of the scheme, or at some other suitable date, all existing consumers connected to the system are charged for losses on an average cost basis. Any consumers subsequently connected to the system are charged on a marginal cost basis.

The following sections describe proposed methods for average cost and marginal cost based allocation of losses.

9.2.3 Allocation of Demand and Energy Losses

Demand and energy losses are normally treated differently by distribution companies. As mentioned in Section 7.2, demand losses are related to the capacity of the system occupied to supply losses at the time of system peak demand, while energy losses relate to the units of electricity lost as heat over a period of time.

Demand losses have traditionally been calculated for a single point in time and allocated simply on the basis of consumer maximum demands, while energy losses are calculated as a function of time. The loss allocation algorithms proposed here therefore treat demand and energy losses differently.

9.3 Average Cost Based Loss Allocation - Allocation of Energy Losses

9.3.1 Introduction

The average cost based loss allocation method uses the model of the network employed by the discrete time simulator for conducting load-flow studies. The procedure is performed for each time step of the study period, and uses the load-flow results at each step to build a directed graph of the system based upon the directions of the active power flows. In order to deal with interconnected networks, a longest path algorithm is used to assign a 'potential' to each node, and the directed graph is traversed via a breadth first search of nodes, in which the loss in each line or transformer is assigned to the node supplied by it. Losses are accumulated in this way and allocated to the loads on the system.

This approach is well suited to allocating the variable losses in the system, which are dependent upon consumer demand patterns. A different treatment of fixed losses may be required, and this is discussed in Section 9.3.3.

Where more than one load is supplied from a given node, a formula is used to share the losses. Alternative formulae are described in Section 9.7, and the advantages and disadvantages of each are discussed.

9.3.2 Procedure for the Proposed Method

An overview of the loss allocation procedure is shown in Figures 9.1 and 9.2.

9.3.2.1 Calculation of Losses by Discrete Time Simulation

A prerequisite for a loss allocation study is a discrete time simulation run for the period of interest. In this case fixed losses are normally excluded from the load-flow studies, to ensure that just the variable losses are included in the allocation. The results from the discrete time simulation which are used in the loss allocation are the network connectivity, the directions and magnitudes of active power flowing in lines and transformers, the active power demand losses in lines and transformers and the active power injections for the loads.

9.3.2.2 Construction of a Directed Graph of the Network

Using standard nomenclature a directed graph consists of a number of vertices (nodes), linked by a set of arcs (branches). The directed graph is completely described by two arrays, *VFROM* and *VTO*, which store the numbers of the vertices at the sending and receiving ends of each arc respectively. In the implementation of the algorithm however, additional information is stored for each vertex, giving the numbers of the arcs in and out of the vertex. Although this information is redundant, it improves the computational efficiency of the algorithm.

The directed graph is built as follows.

1. Arc connections are renumbered where necessary by swapping vertices *VFROM* and *VTO*, to indicate the direction of active power flow. As a result, for each arc a, power flows from vertex *VFROM(a)* to vertex *VTO(a)*.
2. For each vertex v, a list of incoming and outgoing arc numbers is compiled.

9.3.2.3 Assignment of Potentials to the Directed Graph

Potentials are assigned to each vertex, which indicate the longest path to the vertex from the 'source' vertices. Vertices with no incoming arcs are labelled source vertices, and correspond to infeed and certain generation nodes in the network. Vertices with no outgoing arcs are labelled termination vertices, and correspond to certain load nodes in the network.

The assignment of potentials uses a longest path algorithm, which is essential to allow correctly for interconnected networks. The assignment proceeds as follows.

1. Identify the source vertices, for which the number of incoming arcs is zero, and assign a potential of 1. Add these vertices to a list of source vertices.
2. Begin the main loop.
3. For each vertex:
    a) If any of the incoming arcs comes from a vertex in the current source list:
        i. If the potential of the current vertex is less than the highest potential in the source list, assign to the current vertex a potential one greater than the highest.
        ii. Add the current vertex to a list of 'processed' vertices.
4. If any vertex potentials have been changed during Step 3:
    a) Add the list of processed vertices to the source list.
    b) Return to Step 2.
5. Finish.

9.3.2.4 Allocation of Losses using the Directed Graph

The loss allocation proceeds via a breadth-first traversal of the graph. That is, vertices are processed according to their potential, in ascending order. For each vertex the losses on incoming arcs are assigned to the vertex. Furthermore, the assigned losses at each vertex are shared between outgoing arcs using a formula specified by the user. Loads are treated as outgoing arcs during this process.

The details of the loss allocation process are as follows.

1. For each potential *p* (excluding potential 1):

   a) For each vertex *v* with potential *p*:

      i. For each incoming arc *a*:

         (i) Accumulate the loss at vertex *v* by adding the loss in *a* to the share of loss assigned to *a* from the vertex *VFROM(a)*. The share of the loss is determined using the specified formula, on the basis of the active power flowing in *a*, compared with the power flowing in the other outgoing arcs from vertex *VFROM(a)*.

2. For each vertex *v*:

   a) Determine the loss allocated to the load at *v* by applying the specified formula to share the accumulated loss between the load and the outgoing feeders at *v*.

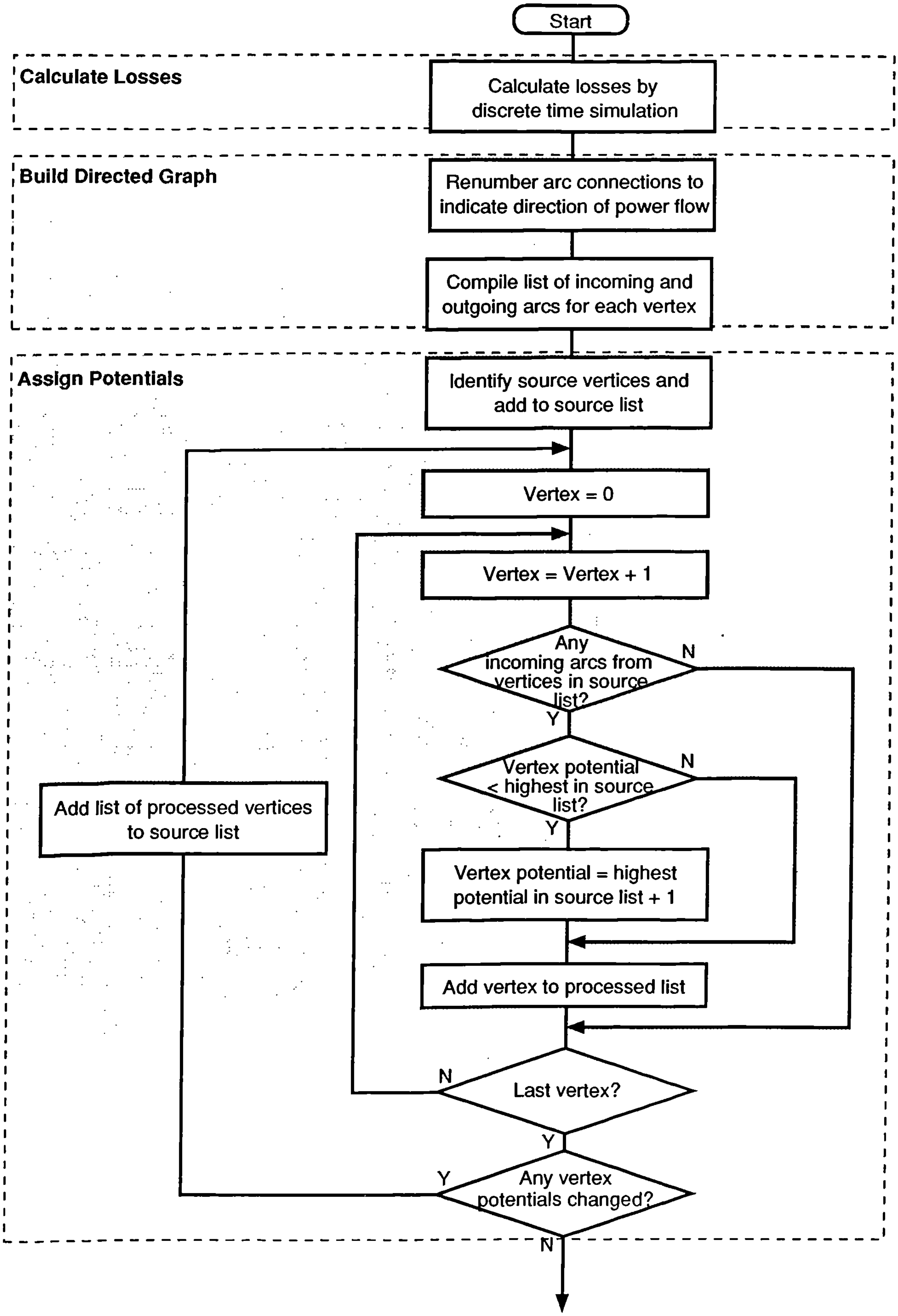

Figure 9.1 Flow Chart of the Average Cost Based Loss Allocation Procedure

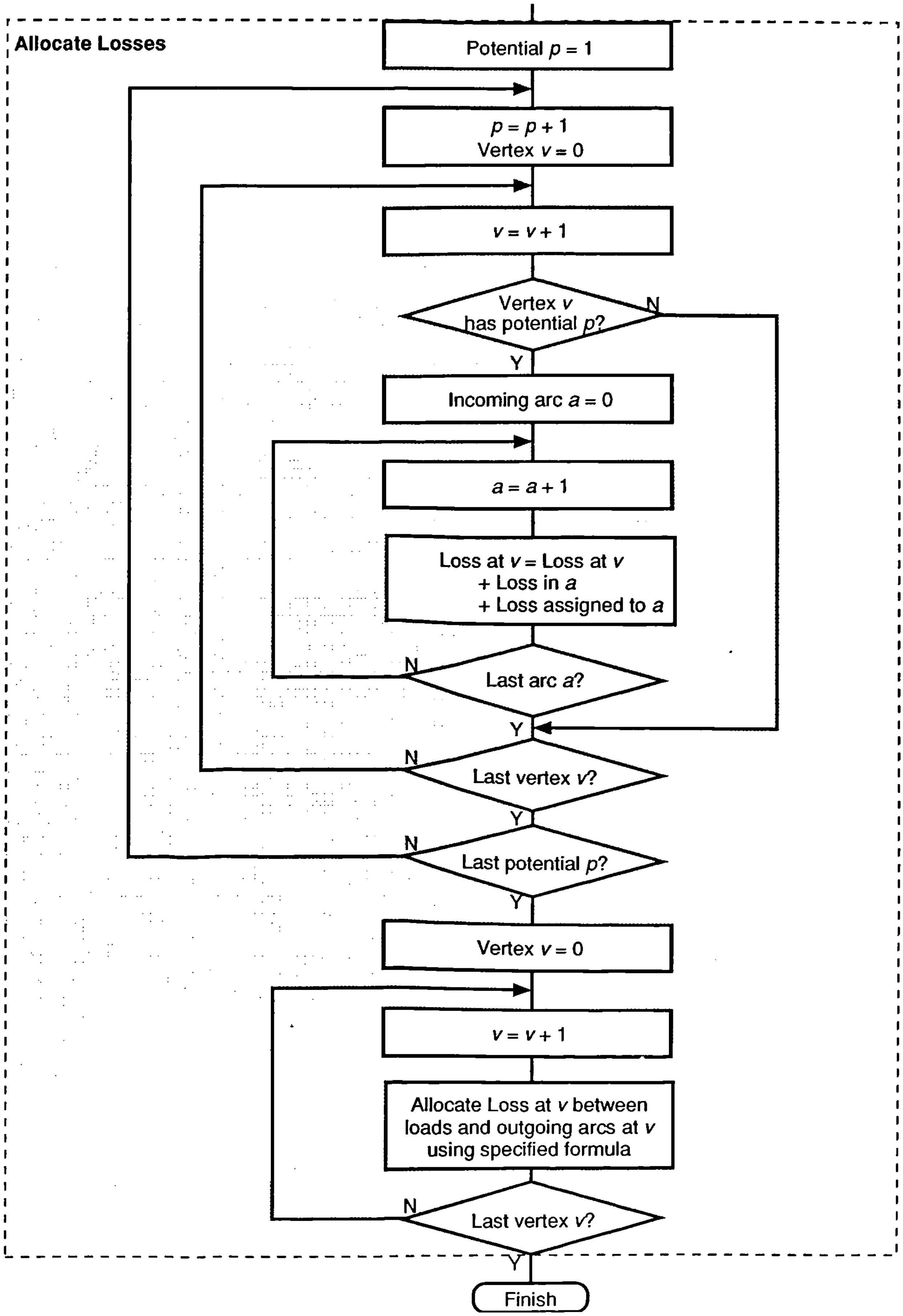

Figure 9.2 Flow Chart for the Average Cost Based Loss Allocation Procedure (Continued)

9.3.2.5 Loss Allocation Example

To illustrate the loss allocation algorithm, a simple example is given. Figure 9.3 shows the example network. The number in the square box adjacent to each vertex is the potential of the vertex, assigned using the longest path algorithm.

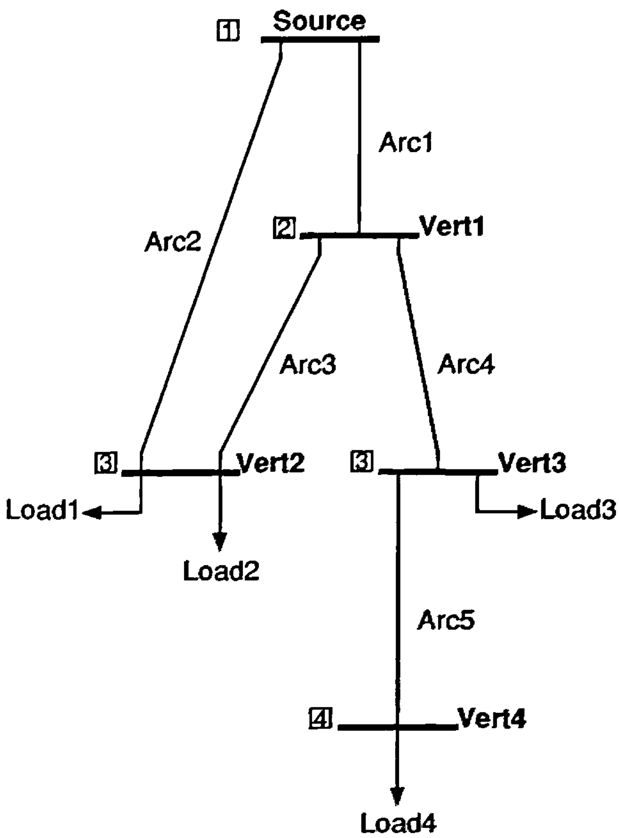

Figure 9.3 Loss Allocation Example Network

The allocation of losses for this network proceeds as shown in Tables 9.1 and 9.2. Table 9.1 shows the assignment of losses to each vertex in the sequence followed by the algorithm. Table 9.2 shows the final allocation of losses to each load in the system. In the tables the following simplified notation is used: F denotes active power flow in an arc, L denotes active loss in an arc, and D denotes active power injection at a load. The loss assigned to a particular vertex is denoted by LA.

The formula used in this example to share the losses between two or more parties assigns losses in proportion to the square of the active power demands. Loss allocation formulae are discussed in Section 9.7.

Table 9.1 Loss Allocation Example - Assignment of Losses to Vertices

Potential	Vertex	Arcs In	Arcs Out	Loss Assignment
2	Vert1	Arc1	Arc3, Arc4	$LA_1 = L_1$
3	Vert2	Arc2, Arc3	Load1, Load2	$LA_2 = L_2 + L_3 + LA_1\left(\frac{F_3^2}{F_3^2+F_4^2}\right)$
3	Vert3	Arc4	Arc5, Load3	$LA_3 = L_4 + LA_1\left(\frac{F_4^2}{F_3^2+F_4^2}\right)$
4	Vert4	Arc5	Load4	$LA_4 = L_5 + LA_3\left(\frac{F_5^2}{F_5^2+D_3^2}\right)$

Table 9.2 Loss Allocation Example - Final Allocation

Load	Vertex	Allocation
Load1	Vert2	$\text{Loss}_1 = LA_2\left(\frac{D_1^2}{D_1^2+D_2^2}\right)$
Load2	Vert2	$\text{Loss}_2 = LA_2\left(\frac{D_2^2}{D_1^2+D_2^2}\right)$
Load3	Vert3	$\text{Loss}_3 = LA_3\left(\frac{D_3^2}{D_3^2+F_5^2}\right)$
Load4	Vert4	$\text{Loss}_4 = LA_4$

9.3.3 Treatment of Fixed and Variable Losses

Because variable losses are related to consumer demand patterns, it is appropriate that they should be calculated and allocated on a time-basis. Fixed losses are related to voltage, and are often assumed to be constant. As such, they are sometimes considered to be part of the cost of providing the supply, and allocated according to consumers' maximum demands, as in the case of demand losses.

The policy adopted by a distribution company in regard to the allocation of fixed losses has a significant effect on the algorithm as described in the following sections.

9.3.3.1 Time Related Allocation of Fixed Losses on the Same Basis as Variable Losses

If fixed energy losses are allocated at each time step on the same basis as variable losses, for example on the basis of consumer demands at each step, they can be lumped together in the analysis. The allocation algorithm is as described above.

9.3.3.2 Time Related Allocation of Fixed Losses on a Different Basis to Variable Losses

If fixed energy losses are allocated at each step on a different basis to variable losses, for example fixed on the basis of consumer demands and variable on the basis of demands squared, the algorithm must distinguish between fixed and variable losses.

The separation of fixed and variable components of loss within the system is not straightforward, because the current drawn to supply fixed losses gives rise to additional variable losses at higher levels in the system, which are difficult to quantify. Two approaches to this problem are explored here:

1. Performing discrete time simulations with and without the modelling of fixed losses.
   The difference in losses in each component of the system corresponds to the fixed loss calculated on a marginal basis. Variable losses are allocated first using simulation results with the modelling of fixed losses excluded, and fixed losses are allocated using the difference in losses between the two simulation runs. The standard allocation algorithm is used in both cases, with appropriate allocation formulae in each case.

   The disadvantages of this approach include the extra computation time and storage associated with two simulation runs and, more importantly, the fact that treating fixed losses on a marginal basis will tend to overestimate the level of fixed losses and underestimate the level of variable losses, due to the square law effect. .

2. Using superposition with two passes of the allocation algorithm on different bases.
   This approach uses a modified form of the allocation algorithm. Losses are assigned first using the allocation formula for fixed losses. Sources of fixed loss P_{Lfixed} are treated differently from the standard case; each source of fixed loss is treated as a load, to which losses are allocated in the normal way. Hence for a given arc a feeding vertex v which supplies n_p other parties (feeders and loads) with demand P_D, the loss LA_a assigned to the source of fixed loss is given by

$$LA_a = (LA_0 + P_{Lvar,a})\frac{P^m_{Lfixed,a}}{\left(P^m_{Lfixed,a} + \sum_{j=1}^{n_p} P^m_{D,j}\right)} \tag{9-1}$$

   where LA_0 is the loss assigned to a from higher in the network and m is the exponent used in the specific allocation formula.

   Once this procedure has been completed each of these loads has been assigned a proportion of the variable losses P_{Lvar} which are generated to supply the fixed loss at that location. The variable loss in each arc is now set equal to this assignment plus the fixed loss component, for example the new loss in arc a is given by:

$$P_{L,a} = LA_a + P_{Lfixed,a} = P_{Lvar,a}\frac{P^m_{Lfixed,a}}{\left(P^m_{Lfixed,a}+\sum_{j=1}^{np}P^m_{D,j}\right)} + P_{Lfixed,a}$$

$$= P_{Lfixed,a}\left(1 + P^{m-1}_{Lfixed,a}\frac{P_{Lvar,a}}{\left(P^m_{Lfixed,a}+\sum_{j=1}^{np}P^m_{D,j}\right)}\right) \qquad (9\text{-}2)$$

This procedure effectively removes from the allocation all variable losses except those allocated to supplying the fixed losses. A standard loss allocation is now performed, using the loss allocation formula for fixed losses, to assign these fixed losses to all the loads in the system.

Finally the variable losses must be allocated. A standard allocation is performed using the loss allocation formula for variable losses, with the exception that the losses assigned to sources of fixed loss are subtracted from the accumulated loss at each vertex. Hence for arc a feeding vertex x, the accumulated loss at x is modified as shown in Equation (9-3).

$$LA_x = LA_x - LA_a = (LA_0 + P_{Lvar,a})\left(1 - \frac{P^m_{Lfixed,a}}{\left(P^m_{Lfixed,a}+\sum_{j=1}^{np}P^m_{D,j}\right)}\right) \qquad (9\text{-}3)$$

This procedure removes the effects of the fixed losses assigned earlier from the allocation of variable losses.

The disadvantages of this method include its complexity compared with the first method, and the computational requirements associated with three allocation passes, which may be significant for large networks. The most significant difference between the two approaches is that in the latter method the fixed losses are considered first, and are allowed for before allocating variable losses. Conceptually this is to be preferred since the fixed losses occur whenever the system is energised, irrespective of the load applied to the system.

9.3.3.3 Single Case Allocation of Fixed Losses

In cases where fixed losses are considered constant, and allocated for a single point in time, the allocation of fixed and variable losses is performed independently. Variable losses are allocated in the standard manner, but with fixed losses excluded from the analysis, either by neglecting fixed losses in the discrete time simulation, or by explicitly calculating fixed losses and subtracting them from the accumulated loss at each vertex, as in Method 2 of Section 9.3.3.2.

Fixed losses are allocated for a single peak or average loading condition, using the first stages of Method 2 in Section 9.3.3.2. Maximum demands can be used in the loss allocation formula if required.

9.3.4 Discussion of the Proposed Method

The proposed method is assessed in terms of the objectives outlined in Section 9.2.

9.3.4.1 Resource Allocation

The objective of efficient resource allocation requires that losses be calculated accurately, and that charges for losses reflect the true costs of supply. The proposed loss allocation provides accurate figures for losses at any point in the system, as a function of time. By applying appropriate time-related costs to the loss results, cost reflective charges for losses can be obtained.

The effectiveness of the proposed method in encouraging efficient use of energy is partly dependent upon the loss formula employed to share losses between consumers. This issue is explored in later sections.

9.3.4.2 Fairness and Equity in the Allocation of Costs

This objective requires that costs be allocated to consumers according to the burden they impose upon the system.

The proposed loss allocation method meets this objective by modelling the losses in detail as a function of time, and by relating the time-based loss results to consumers on the basis of their individual demand patterns and location within the system The method therefore takes into consideration all the factors which affect the burden which an individual consumer places on the system, as listed in Section 9.2.1.2.

9.3.4.3 Revenue Requirements

Revenue recovered from charges for losses must be sufficient to cover the financial obligations of the distribution company.

The proposed method is an aid for determining charges to consumers. It is the responsibility of the utility to derive charges on the basis of the loss results. The proposed method cannot therefore guarantee that revenue requirements will be satisfied, but instead it provides the information with which this objective can be met.

9.3.4.4 Other Economic and Political Requirements

Political or economic requirements may force the distribution company to diverge from the ideal methods for charging for losses.

The proposed loss allocation method provides the detailed analysis against which alternative methods can be assessed. For example, alternative simpler tariffs for domestic consumers can be compared using results from the proposed method as a benchmark.

9.4 Average Cost Based Loss Allocation - Allocation of Demand Losses

9.4.1 Introduction

Demand losses are normally calculated on a once-only basis at the time of system maximum demand, and the allocation procedure therefore follows the same approach.

Because the discrete time simulator is able to calculate demand losses as a function of time, a time-based allocation of demand losses could in theory be performed. By adopting the concept of a time-based capital cost for given lines and transformers, the consumer can be charged for the amount of capacity occupied by losses to serve their demand as a function of time. However, it is difficult to see how the extra data and computational requirements of such an approach could be justified in terms of the improvement in modelling accuracy.

9.4.2 Procedure for the Proposed Method

The loss allocation algorithm used for energy losses is run once, at the system maximum loading condition. A loss allocation formula appropriate to demand losses is used to share losses between consumers.

A question which needs to be addressed, is whether the loss allocation formula should assign losses on the basis of consumers' annual maximum demands, or on the basis of consumers' demands at the time of system maximum demand. Due to load diversity individual annual maximum demands are unlikely to coincide with the system annual maximum demand.

9.4.3 Discussion of the Proposed Method

9.4.3.1 Resource Allocation

The proposed method is able to determine accurate values for demand losses, and therefore forms a good basis for the calculation of cost reflective tariffs.

9.4.3.2 Fairness and Equity in the Allocation of Costs

The proposed method is able to determine accurately the proportion of the capacity of each line and transformer in the system occupied by the losses incurred in serving the demand of a given consumer at the system peak loading condition. The method is therefore able to allocate costs on the basis of the burden placed on the system by each consumer.

9.4.3.3 Revenue Requirements and Other Political and Economic Requirements

The proposed method is identical to the method for allocating energy losses in these respects, which are discussed in Sections 9.3.4.3 and 9.3.4.4.

9.5 Marginal Cost Based Loss Allocation - Allocation of Energy Losses

9.5.1 Introduction

The marginal cost based loss allocation method is a great deal simpler than the method based upon average costs.

The method employs one of the loss calculation algorithms described in Chapters 7 and 8 to calculate the system losses. The marginal losses are calculated for a single consumer at a time.

9.5.2 Procedure for the Proposed Method

A base case study is performed without the new consumer. A loss calculation algorithm is used to determine the system energy losses over the period of interest.

The loss calculation is repeated with the new consumer connected to give the new system losses. The incremental losses due to the consumer are obtained by simply subtracting the new losses from those of the base case, and these are allocated in total to the consumer. In this approach the fixed losses are excluded from the calculation, since they drop out naturally during the subtraction process. This is in line with standard policy to treat fixed and variable losses differently.

9.5.3 Discussion of the Proposed Method

The proposed method is assessed in terms of the objectives outlined in Section 9.2.

9.5.3.1 Resource Allocation

The proposed loss allocation provides accurate figures for marginal losses at any point in the system, as a function of time. By applying appropriate time-related costs to the loss results, cost reflective charges for losses can be obtained.

9.5.3.2 Fairness and Equity in the Allocation of Costs

Because the load-flow studies within the loss calculation algorithms model the state of the system the proposed method accounts implicitly for factors such as the demand profile of the new consumer, and the location of the consumer within the system. The method therefore takes into consideration all the factors which affect the burden which an individual consumer places on the system, as listed in Section 9.2.1.2.

9.5.3.3 Revenue Requirements

As with the method based upon average costs, the proposed method is an aid for determining charges to consumers. It cannot guarantee that revenue requirements will be satisfied, but instead it provides the information with which this objective can be met.

9.5.3.4 Other Economic and Political Requirements

In cases where other requirements force a utility to use alternative methods, the proposed loss allocation method provides the detailed analysis against which the alternatives can be assessed.

9.6 Marginal Cost Based Loss Allocation - Allocation of Demand Losses

9.6.1 Introduction

As in the average cost based approach, demand losses are calculated on a once-only basis at the time of system maximum demand. The marginal losses are calculated for a single consumer at a time.

9.6.2 Procedure for the Proposed Method

Two simulations are performed with and without the new consumer, for a single time step at the time of system maximum demand.

The incremental demand losses due to the consumer are obtained by simply subtracting the new losses from those of the base case, and these are allocated in total to the consumer.

9.6.3 Discussion of the Proposed Method

9.6.3.1 Resource Allocation

The proposed method is able to determine accurate values for incremental demand losses, and therefore forms a good basis for the calculation of cost reflective tariffs.

9.6.3.2 Fairness and Equity in the Allocation of Costs

The proposed method is able to determine accurately the proportion of the capacity of each line and transformer in the system occupied by the marginal losses incurred in serving the demand of a new consumer at the system peak loading condition. The method is therefore able to allocate costs on the basis of the additional burden placed on the system by the new consumer.

9.6.3.3 Revenue Requirements and Other Political and Economic Requirements

The proposed method is identical to the method for allocating energy losses in these respects, which are discussed in Sections 9.5.3.3 and 9.5.3.4.

9.7 Loss Allocation Formulae

In this section the effects of different formulae for sharing losses between two or more parties are discussed. The formulae are assessed in terms of engineering and economic criteria.

9.7.1 Loss Allocation on the Basis of Electrical Distance from Bulk Supply Point

In this formula the losses to be allocated, LA, at a given location are shared equally between parties. In the case of n_p parties, the proportion of the loss which is assigned to party i is given by Equation (9-4).

$$P_{L,i} = \frac{LA}{n_p} \tag{9-4}$$

The result of this formula when combined with the proposed loss allocation algorithm, is that consumers located at lower voltage levels attract higher losses than those at higher voltages, near to bulk supply points. Consumers supplied at the same location are assigned an equal share of the losses, regardless of their consumption of energy. This formula implies that consumers supplied from the same location benefit equally from the electrical supply. In economic terms it is inefficient since charges do not reflect the costs of supply.

The allocation formulae which follow, when used in conjunction with the loss allocation algorithm, are able to recognise the location of consumers within the system, and offer the additional benefits of accounting for consumers' demand patterns.

9.7.2 Loss Allocation on the Basis of Demand

In this formula the loss is allocated linearly in proportion to the individual demands, i.e. the loss allocated to party i with demand $P_{D,i}$ is given by Equation (9-5).

$$P_{L,i} = LA \frac{P_{D,i}}{\left(\sum_{j=1}^{n_p} P_{D,j}\right)} \tag{9-5}$$

This formula can be used to allocate variable losses, and by substituting maximum demand figures in place of time-based demands the formula is suitable for the allocation of demand losses. Because the allocation to a consumer is based upon the relative size of their demand at a given time it reflects to a certain extent the costs of supply, and can be regarded as efficient in economic terms. For this reason this formula is proposed as the most suitable for the allocation of both fixed and variable losses.

9.7.3 Loss Allocation on the Basis of Demand Squared

In this case the loss is allocated on the basis of the square of the individual demands, as given in Equation (9-6).

$$P_{L,i} = LA \frac{P_{D,i}^2}{\left(\sum_{j=1}^{np} P_{D,j}^2\right)} \tag{9-6}$$

This allocation reflects the fact that variable losses are proportional to the square of the demand. It should be noted however that the square law has already been accounted for implicitly in the discrete time simulation when calculating the losses. Sharing these losses using another square law relationship can give rise to large fluctuations in the loss assigned to a particular consumer due to changes in the relative size of their demand. This can serve to reduce the efficiency of the method.

9.7.4 Loss Allocation on the Basis of Demand^k

$$P_{L,i} = LA \frac{P_{D,i}^k}{\left(\sum_{j=1}^{np} P_{D,j}^k\right)} \tag{9-7}$$

This allocation is able to represent an intermediate position between allocating on the basis of demand and demand squared. An allocation corresponding to k=1.5 implies a greater emphasis on consumer demand than the linear allocation, but is less extreme than the demand squared case. However, the use of non-integer powers in the formula can be seen as a disadvantage with regard to general acceptance of the method.

9.8 Worked Examples

In this section worked examples are given to illustrate the characteristics of the allocation algorithms.

9.8.1 Average Cost Based Allocation

In this example the losses and costs of losses allocated using the proposed average cost based method to three loads in the 52 Node test system are compared. The loads are summarised in Table 9.3. The network diagram for this system is given in Appendix E. The example considers variable losses only.

Table 9.3 Average Cost Allocation Example Loads Summary

Load	Category	Voltage	Load Factor
Ld6	Industrial, heavy overnight demand	33kV	0.88
Ld8	Domestic/Economy 7 primary feeder	33kV	0.80
Ld10	Domestic primary feeder	11kV	0.74

Figure 9.4 shows the demand profiles for these loads for a winter weekday. For the purposes of this example the load profiles have been normalised such that the energy supplied during the 24 hour period is identical for each load.

Figure 9.5 shows the resulting losses allocated to these loads for the 24 hour period. The sharing of losses was performed on the basis of demand using Equation (9-5). The figure indicates that the 11kV load, Ld10, has been allocated a much higher proportion of the system losses than the 33kV loads. The reasons for this are threefold:

1. Electrical distance from the Grid Supply Point

   The 33kV loads are supplied by four parallel 132kV circuits with comparatively low percentage losses. The 11kV load is supplied by two parallel 33kV circuits with much higher percentage losses.

2. Voltage level

   An extra transformation is performed when supplying the 11kV load, as compared with the 33kV loads. In addition 33/11kV transformers are normally less efficient than 132/33kV transformers, which results in higher losses at lower voltage levels.

3. Local loading conditions

   The circuits supplying the 11kV load are more heavily loaded in this case than those supplying the 33kV loads. This results in substantially higher losses due to the quadratic relationship between loss and line current.

The allocated loss profiles for the 33kV loads are shown again in Figure 9.6, scaled up to permit analysis of the profile shapes. It can be seen that the allocated loss profile for each load follows the same pattern as the respective demand profile. This is to be expected, given the allocation formula used to share the losses.

Figure 9.7 illustrates the effect of applying a time related tariff to the loss profiles of Figure 9.6. The tariff is derived from the UK pool selling price for the day in question, and is shown in Figure 9.8.

Table 9.4 gives details of the total energy losses and costs allocated to each load over the 24 hour period. The following observations can be made from the results:

1. The 11kV load incurs over 4 times the energy loss over the period as the 33kV loads, due to its location within the system.

2. The two 33kV loads are allocated the same energy loss over the period. Because their respective demand profiles do not conform, the allocated loss profiles do not conform. As a result the application of a time varying tariff gives rise to different costs of losses for the two consumers.

3. The peak losses for the domestic loads coincide with the peak periods of the tariff, and therefore the total cost of losses is higher for these loads than for the diverse industrial load, whose peak loss occurs during the off-peak periods of the tariff. For the two 33kV loads this results in a 4% difference in the costs over the period.

In summary, it has been shown that when considering the losses incurred in supplying a given load, the electrical location of the load and the voltage at which it is supplied have a very substantial impact on the total loss. In addition the diversity of the demand profile of the load has an important effect on the costs of supplying the losses.

Table 9.4 Average Cost Allocation Example - Total Energy Losses and Costs Over the Study Period

Load	Totals Over the 24 Hour Study Period		
	Energy Taken (MWh)	Allocated Loss (MWh)	Allocated Cost (£)
Ld6	869.6	7.12	141.18
Ld8	869.6	7.17	147.02
Ld10	869.6	29.93	626.09

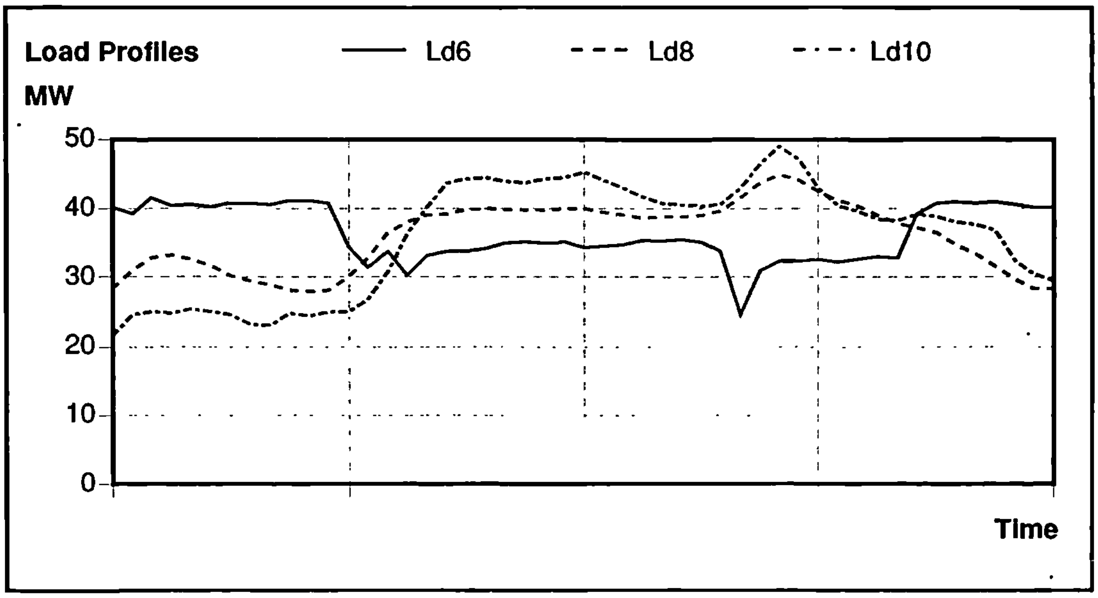

Figure 9.4 Average Cost Allocation Example - Load Profiles

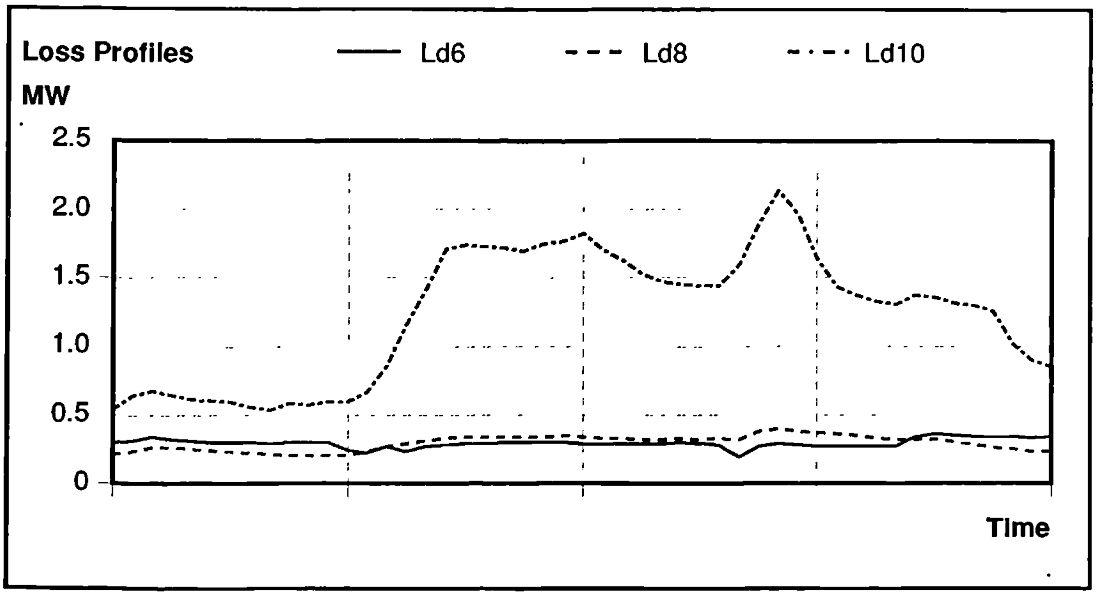

Figure 9.5 Average Cost Allocation Example - Allocated Losses

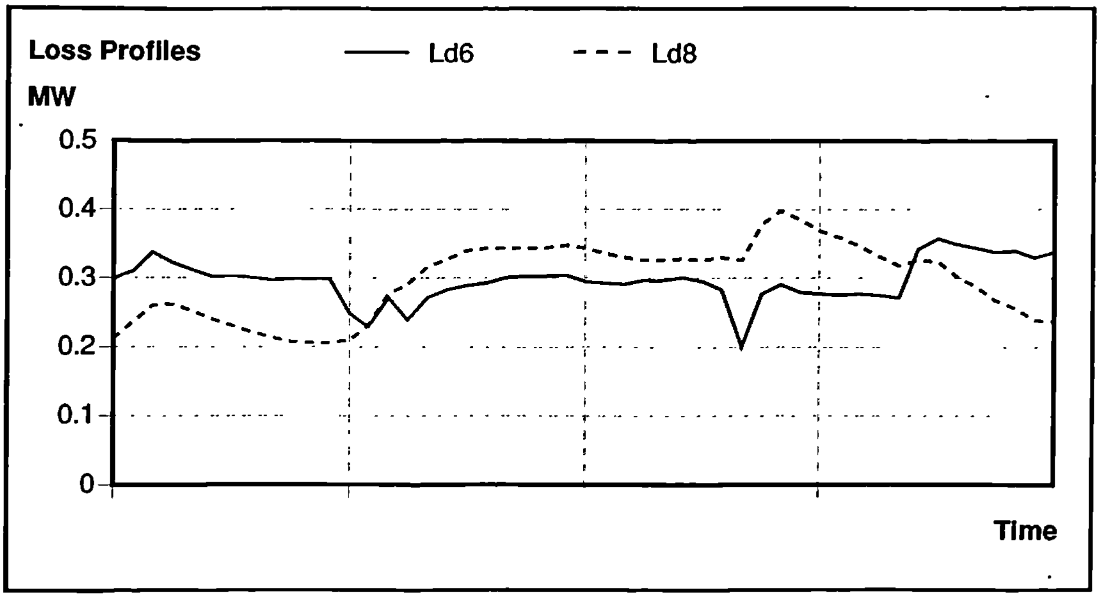

Figure 9.6 Average Cost Allocation Example - Allocated Losses for 33kV Loads

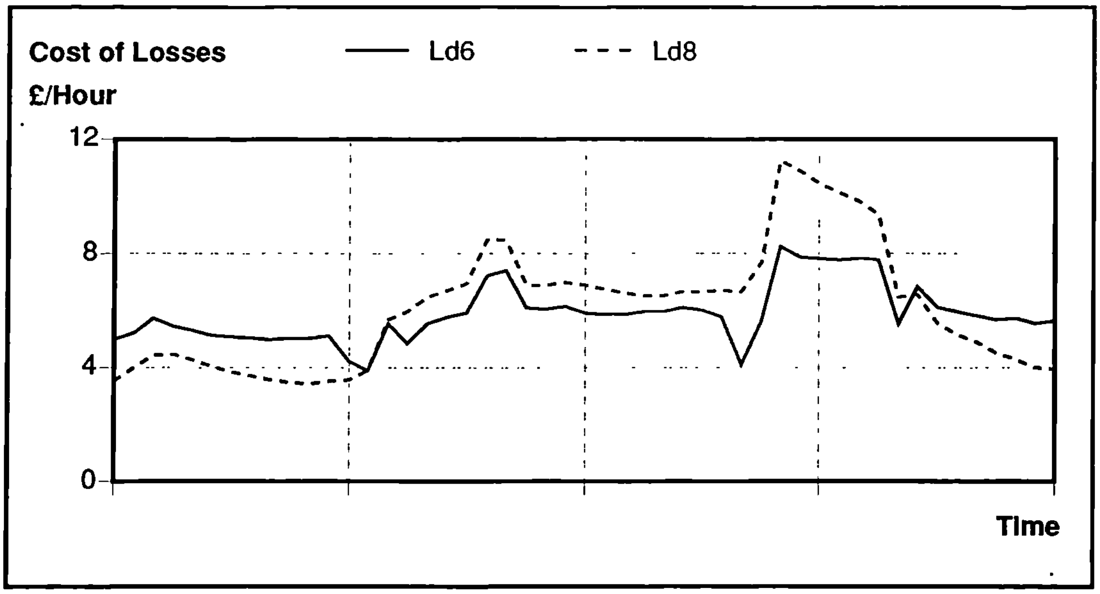

Figure 9.7 Average Cost Allocation Example - Costs of Losses for 33kV loads

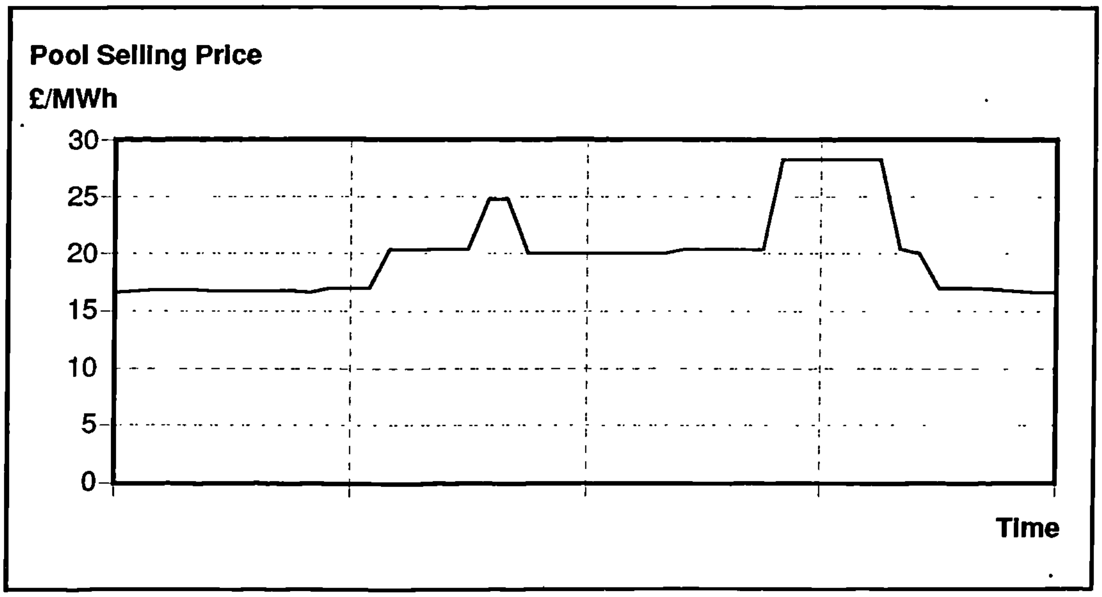

Figure 9.8 Average Cost Allocation Example - Pool Selling Price for Study Period

9.8.2 Marginal Cost Based Allocation

In this example the marginal losses due to the connection of a new load are considered. The results of using a marginal cost based allocation are compared with the equivalent results using an average cost based allocation. The new load is connected at Node 50, adjacent to the existing load, Ld11. In the example the demand profile of the new load is identical to that of the the existing load, hence the connection of the new load effectively doubles the demand at this location in the system. The existing load profile is shown in Figure 9.9.

Figure 9.10 shows the system losses before and after the connection of the load. The difference is the marginal loss allocated to the new load. Integrating the curves yields an energy loss of 2.73MWh.

Figure 9.11 compares the loss allocated to the new load using both the average and marginal cost based algorithms. In the average cost based method the total energy loss is 2.44MWh, a difference of approximately 10% compared with the marginal cost based method. The figure illustrates the differences in loss profiles for the two methods, and shows that the marginal cost based method is the more extreme, the large majority of losses occurring during periods of system peak demand. The average cost based method shares these losses across a number of local loads.

It should be noted that one of the effects of using the average cost based method is that the allocation to the existing load Ld11 will change as a result of the connection of the new load. Figure 9.12 illustrates this change, and shows that the allocation to the existing load increases by approximately 15%.

In summary, this example has illustrated the points made in the discussion in Section 9.2.2. Allocation on the basis of average costs leads to changes in existing allocations whenever new loads are connected to the system. Allocation on a marginal basis avoids this difficulty, but consumers connected earlier to the system enjoy lower marginal losses than those connected later. Consumers may be penalised particularly severely in heavily loaded areas where marginal losses are very high. This difficulty is compounded by the fact that marginal losses occur predominantly during peak periods when costs of energy are high, and hence the costs of losses for marginal consumers may be substantially higher than for consumers on average cost based rates.

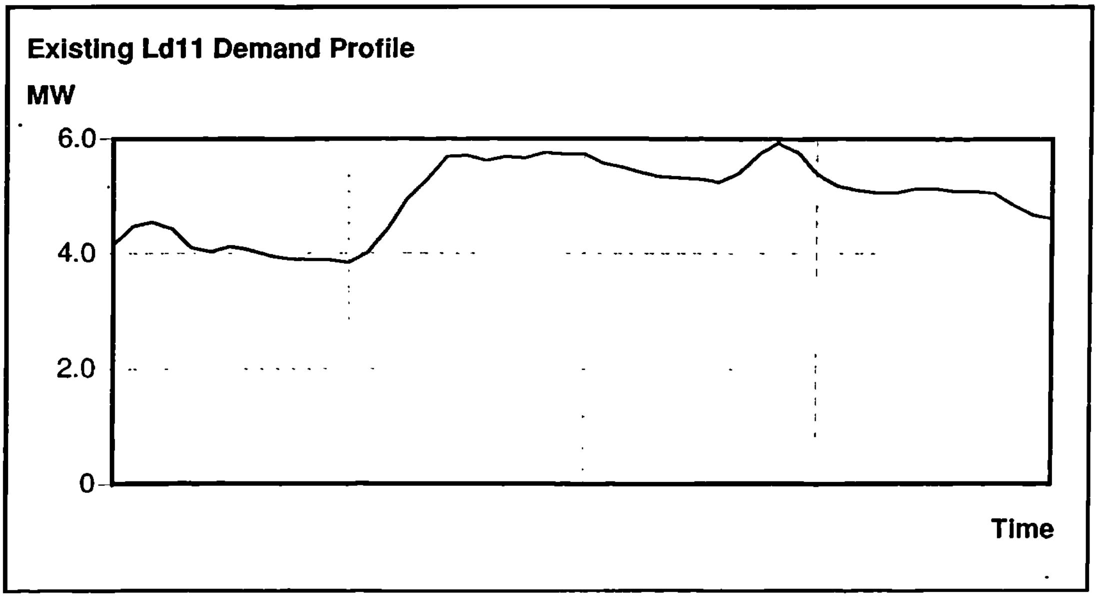

Figure 9.9 Marginal Cost Allocation Example - Existing Ld11 Demand Profile

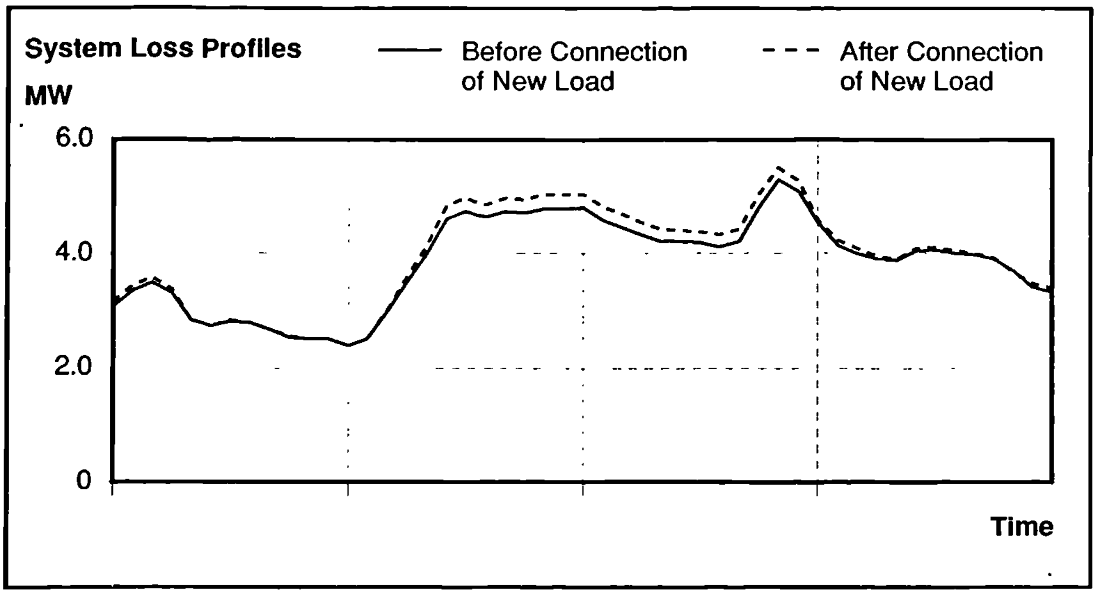

Figure 9.10 Marginal Cost Allocation Example - System Loss Profiles

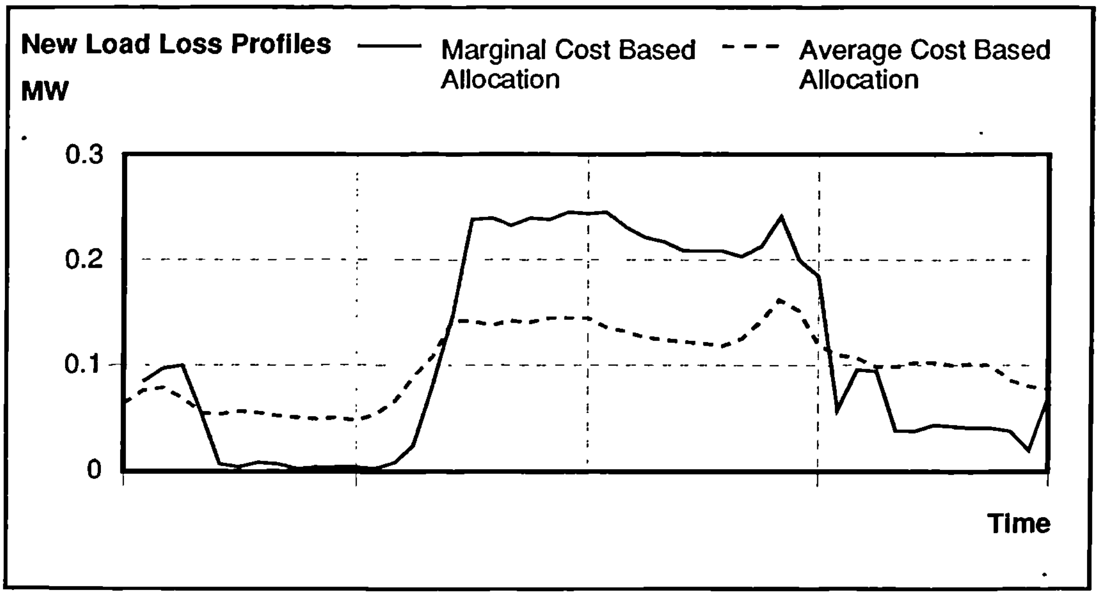

Figure 9.11 Marginal Cost Allocation Example - Comparison with Average Cost Based Method

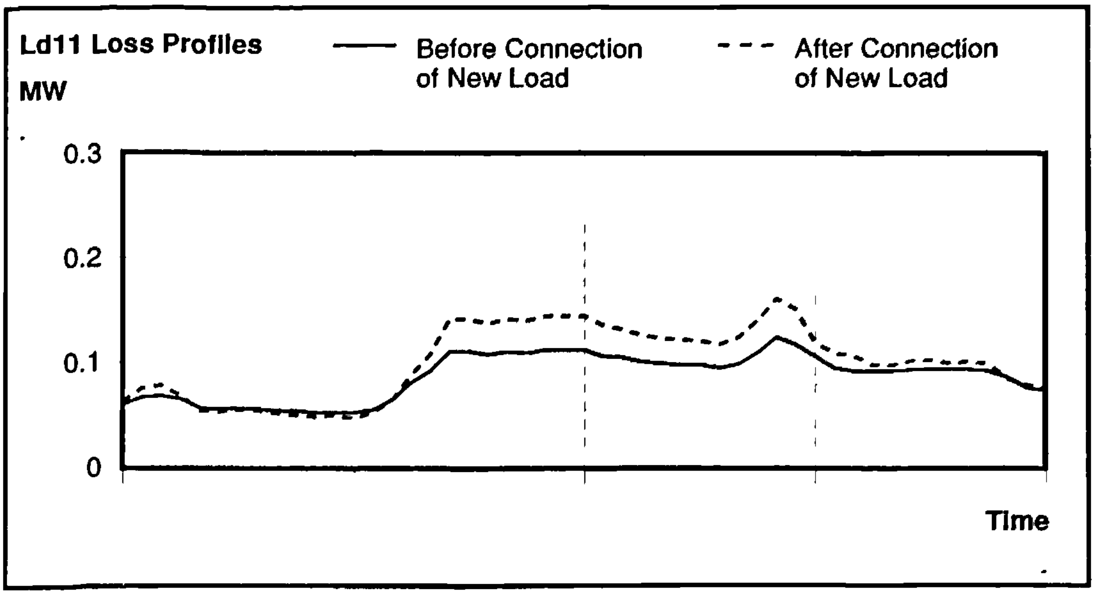

Figure 9.12 Marginal Cost Allocation Example - Ld11 Loss Allocation Before and After Connection of New Load

9.9 Conclusions

In this chapter the issues associated with the allocation of the costs of losses to consumers have been reviewed, and a set of commonly used pricing objectives have been outlined. The use of average and marginal cost methods for charging for losses have been discussed. The disadvantages associated with the exclusive use of average or marginal based cost allocation have been noted, and it has been suggested that a combination of both approaches provides the most effective means of catering for existing and new consumers.

A new method for the allocation of losses and costs of losses on an average basis has been presented, which uses graph theoretic techniques to assign losses in every line and transformer to the consumers supplied by it. The algorithm employs loss results from a discrete time simulation and can be applied to radial and interconnected systems. An example has been given which demonstrates the procedure. The treatment of variable and fixed losses has been discussed, and extensions to the basic algorithm have been described which permit allocation of fixed and variable losses on a different basis. It has been noted that the cost associated with such flexibility is increased complexity and computational requirements. The proposed method has been shown to meet the pricing objectives outlined at the beginning of the chapter, notably efficiency of resource allocation, and fairness in the allocation of costs.

A procedure which uses discrete time simulation results to allocate losses on a marginal basis has also been outlined.

A number of loss allocation formulae have been presented with which to ratio losses between two or more parties at a given location in the system. The features of each formula have been discussed, and it has been proposed that allocating losses on the basis of consumer demand is the most efficient method from an economic standpoint.

Worked examples have been presented which illustrate the features of allocation on both an average and a marginal basis.

In conclusion the proposed loss allocation algorithms provide an accurate means of charging for losses, and are therefore particularly well suited to application to major consumers. They also provide an important reference against which the effectiveness of simpler charging schemes can be assessed.

Chapter 10. Conclusions and Proposals for Further Work

10.1 Recapitulation of the Aims

The restructuring of the electricity supply industry in England and Wales has resulted in widespread changes to the operation of the system at the distribution level. Distribution companies have had to respond to requirements for greater accountability, maintenance of system security in the face of substantial changes, particularly in respect of embedded generation, and the increased emphasis on the economics of electricity supply. It has been recognised that access to improved information concerning the performance of the system and more effective management of this information are of key importance in meeting these requirements. Consequently distribution companies are investing in new systems to obtain and manage this data.

The primary aim of the research presented in this thesis has been to develop an improved approach to distribution system load-flow analysis which exploits recent improvements in the availability of system data and the speed of current workstations, to model more accurately the steady state performance of the system as load and generation patterns change over a period of time. The applications of this approach are wide-ranging, but the work described here has focused in particular on the accurate calculation, costing and allocation of electrical losses. Another aim of the research has been to design an open software environment which houses the analysis algorithms and associated database and graphics applications, and which provides sufficient flexibility to allow distribution system engineers to perform a wide range of analysis associated with the requirements outlined above.

10.2 Conclusions

10.2.1 Load-flow Analysis Approaches in Distribution System Planning

The most widely used approaches to the use of load-flow analysis in distribution system planning have been described in Chapter 2, with particular reference to the modelling of variations in load and generation patterns with time.

Deterministic approaches utilising single case load-flows, multiple case load-flows across typical load duration curves and multiple case load-flows across typical chronological load curves have been discussed. The multiple case approaches have been seen to provide an efficient means of modelling approximately the time based variations in generation and demand. These approaches have been shown to provide acceptable levels of accuracy on systems with conforming loads. The limitations of the duration curve approach in the case of demand profiles which do not conform, and in both approaches in the case of demand profiles which do not exhibit a repetitive daily cycle, have been highlighted and confirmed in tests using real data.

Probabilistic approaches based upon the probabilistic load-flow and Monte Carlo simulation have been described. The ability to model the likelihood of given system operating conditions with these approaches offers significant benefits in certain types of planning study, but the simplifying assumptions made in the modelling of the interdependencies between random input variables, and the approximations made in the probabilistic load-flow reduce the attractiveness of the approaches. It has been proposed that deterministic analysis offers a better solution to the distribution system problems to which this work is directed.

A new approach entitled discrete time simulation has been presented, which models the individual variations in load and generation profiles throughout the period of interest. The principal advantages of this approach are the ability to account accurately for load diversity and the provision of detailed time based results throughout the system, which provides an excellent resource for conducting additional analysis such as the costing of energy and allocation of costs to consumers. The costs associated with these improvements in accuracy include the substantial additional data requirements and execution times of this approach. However, test results on a system of realistic size have demonstrated that the data required to perform simulations of a year's duration at half hour steps can easily be accommodated on current workstations, and that execution times for such simulations are not excessive.

10.2.2 Load-flow Algorithms

In Chapter 3 the most widely used load-flow algorithms have been described, and their suitability for application to discrete time simulation of distribution systems has been assessed.

A new load-flow algorithm for discrete time simulation has been presented, based upon the efficient Newton-Raphson algorithm of Irving and Sterling [73], and employing an extended form of the Fixed Jacobian technique of Meisel and Barnard [93], with selective updating of the Jacobian across multiple time steps. This algorithm combines the reliable convergence of the fully coupled Newton-Raphson method with the speed improvements of both the Irving and Sterling 2 x 2 submatrix formulation and the Fixed Jacobian method.

Test results have been presented which compare the new algorithm with the existing efficient Newton-Raphson method, and indicate that the new algorithm is in most cases substantially quicker. In systems in which generators reach reactive limits in cascade at different stages of the iterative process the improvement in speed was found to be much smaller. In such cases the Jacobian needs to be updated frequently which reduces the scope for speed improvements through the use of a constant Jacobian. A proposal for improving the treatment of generator reactive limits to overcome this difficulty is made in Section 10.3.1.

10.2.3 Software Environments for Distribution System Planning

In Chapter 4 the design of software environments which provide access to analysis applications and contain common database and graphical display facilities has been discussed. Existing approaches have been described and a set of design objectives has been drawn up which seek to build on the strengths and address the deficiencies of earlier generations of such systems.

A new design has been presented which combines existing applications with new time based analysis applications an integrated, open environment. The proposed environment has been shown to meet the specified objectives with regard to flexibility, modularity, graphical management of data and distributed processing.

In the remainder of the chapter the proposed Insight analysis application, which provides access to the time based analysis algorithms described elsewhere in the thesis, is presented. The functionality of each component of the Insight application is described, with particular reference to features which contribute to the flexibility and ease of use of the underlying time based methods.

The problems associated with storage of the large volumes of data required for time based analysis have been discussed. The widely used database technologies have been outlined, and their suitability for the proposed application has been assessed. A solution has been proposed which combines the use of relational database management system, file-based database and virtual memory for storage of different categories of data. Techniques which store the data in reduced form are presented which reduce substantially the storage requirements for a given network. The proposed solution is shown to provide a good balance between speed of data access and flexible integration with the other components of the software environment.

Graphical techniques for the efficient selection and management of analysis data have been described and shown to play an important role in planning studies in which volumes of data are large.

10.2.4 Load Allocation

The proposed discrete time simulation approach requires that time based power profiles be specified for all loads and generators in the system under study. The problems associated with allocation of profiles to loads and generators in the absence of full metered data have been described in Chapter 5.

A new load allocation algorithm has been presented which makes use of data available in most distribution company billing records to assign time based load and generation profiles throughout the system. The algorithm takes advantage of the nature of demand patterns of different categories of consumers in a distribution system and their associated measurement data, to allocate load accurately even in the absence of detailed demand information.

Test results on a real system have demonstrated that the algorithm is capable of accurate results.

10.2.5 Analysis Applications

In Chapter 6 important applications of discrete time simulation analysis, not described in Chapters 7 to 9, have been described, and the procedures to be followed using the Insight application outlined.

Discrete time simulation has been shown to provide a convenient method for analysing voltage related problems, including the identification and correction of voltage violations, the setting of transformer line drop compensation settings on rural feeders, and prediction of the effects of voltage reduction.

Application of discrete time simulation to the study of the impact of embedded generation has also been discussed, with reference to local voltage problems, the co-ordination of protective devices and system losses. The ability of the discrete time simulation approach to model system performance over an extended period has been shown to offer advantages over single case methods in the study of these kinds of problems by providing the engineer with a clearer view of the nature and severity of the problem.

A new constrained simulation algorithm has been proposed with which to determine the maximum additional load or generation which can be supported at a given location within the system as a function of time without violating selected constraints. Two variants of the algorithm which employ the Secant Search method and Ridders' method respectively have been described A worked example has been presented which has identified potential convergence problems with the Secant based method due to the effects on the error function of on-load tap changing and generator reactive limits. These findings have been confirmed in tests on a number of networks, which indicate that although the Secant based method is marginally quicker on well behaved functions, the superior reliability of the Ridders' based method is to be preferred.

10.2.6 Calculation of Losses

In Chapter 7 the existing methods for the calculation of losses have been reviewed. Demand and energy losses are treated separately. A number of criteria have been developed from the requirements of operations and planning engineers in the Regional Electricity Companies, and used to assess each method.

The load-flow has been proposed as the most suitable method for calculating demand losses on the grounds of flexibility and execution time.

Of the existing methods for calculating energy losses the Loss Load Factor method has been shown to offer approximate results with very low data and computational requirements. However, the calculation of energy losses from demand losses as a function of time has been proposed as the most flexible and accurate method. The implementations of this approach by Sun et al [138] and EPRI [44] which are based upon typical load duration curves have been discussed.

A new method based upon discrete time simulation has been presented which derives energy losses by integrating demand losses calculated throughout the system at each time step over the study period. It has been noted that this provides an accurate basis for the time related allocation of the costs of losses to consumers. It has been shown that the method inherits the advantages and disadvantages of discrete time simulation, namely accurate time based modelling, but at the expense of large data and computational requirements. Tests on real systems have compared the results of the proposed method with the Loss Load Factor method and the duration curve approach. The results have demonstrated that the duration curve approach is capable of accurate results for the system as a whole when levels of load diversity are low, but that errors in results for individual network components can be substantial and are increased in cases of high diversity. Similarly the Loss Load Factor method is badly affected by load diversity. These limitations are of particular relevance in the costing of losses to major industrial consumers whose demand profiles are frequently diverse in nature. The proposed loss calculation method represents an important step forward in accounting for such cases.

10.2.7 Calculation of Losses - Reduction in Computational Requirements by Interpolation

In Chapter 8 two new loss calculation algorithms based upon discrete time simulation are presented in which the execution times are reduced through interpolation of the system loading data.

The first of the proposed methods, which uses archetypal daily loss curves to interpolate between reference loss points at 24 hour intervals, has been described and shown to provide reasonable accuracy at a small fraction of the execution time of the full discrete time simulation method. Test results show that the accuracy of the method compares favourably with that of the duration curve approaches described in Chapter 2. The assumptions underlying the method have been explored, and it has been shown that errors introduced in the linear scaling of archetypal loss profiles are small in comparison with errors in the results generally. Departures in individual demands from the archetypal equivalents used in the algorithm are the primary source of error. It has been shown that these errors can be significantly reduced by scaling the archetypal curves about certain reference times.

The second of the proposed methods, which uses loss coefficients to relate losses in individual lines to the system demand, has been described and shown to yield approximate results with very low execution times. The use of linear and quadratic loss coefficients has been explored, and it has been shown that linear coefficients offer greater accuracy in systems with mostly conforming loads, while quadratic coefficients offer greater accuracy in systems with significant numbers of diverse loads. The method has been proposed as suitable for the early stages of planning studies in which many cases need to be run and compared quickly. The assumptions underlying the method have been explored, and it has been shown that, as with other approximate algorithms, high levels of load diversity are the most significant source of error in this algorithm.

10.2.8 Allocation of Losses

In Chapter 9 the problem of allocating losses and their associated costs to consumers has been described. The objectives of energy pricing policy have been reviewed, and the issues associated with average cost and marginal cost based charging schemes have been discussed.

A new loss allocation algorithm based upon graph theory is presented, which permits charging for losses on an average cost basis as a function of time. The algorithm uses time based loss results from discrete time simulation and accounts for the diversity of individual consumers. The algorithm has been shown to satisfy pricing objectives concerning efficient resource allocation and equity in the allocation of costs. Variations of the basic algorithm which allow different treatment of fixed and variable losses have been explored, and a technique based upon superposition has been proposed. It has been shown that the additional flexibility afforded by this technique is available at some cost in terms of substantially increased complexity and execution times.

A number of loss allocation formulae have been presented which share losses at a given location between two or more consumers. A formula which allocates losses on the basis of consumer demand has been proposed as the most suitable for the allocation of both demand and energy losses.

The procedure for allocating losses on a marginal basis using discrete time simulation has also been described.

Worked examples have been presented which illustrate the features of average and marginal based loss allocation. It has been noted that a combination of the two methods provides the most effective means of catering for both existing and new consumers.

10.3 Proposals for Further Work

10.3.1 Improvement to the Proposed Load-flow Algorithm

Test results have shown that the improvement in speed of the proposed load-flow when compared with the existing Newton-Raphson algorithm is small if significant numbers of generators reach their reactive limits during the iterative procedure. This effect limits the scope for the use of a constant Jacobian.

A simple modification to the load-flow algorithm would alleviate this problem in most cases. Generators which have reached reactive limits and have been switched to PQ operation should be flagged, and should not be reset to PV operation prior to the next time step. Instead, when convergence has almost been reached at each subsequent time step, flagged generators should be checked and switched back to PV only if required. In the majority of cases generators which reach their limits for one time step will remain at the limit for many subsequent steps.

10.3.2 Allocation of Capital Costs to Consumers

In addition to the allocation of losses, the directed graph algorithm described in Chapter 9 could be applied to the allocation of network capacity. Such an algorithm could form the basis of a novel tariff structure in which consumers are charged a capacity element which depends upon their usage of individual lines and transformers during periods of peak demand.

The allocation algorithm is able to determine which lines and transformers are utilised to supply a given consumer, and how much of the capacity of each line and transformer is occupied. By assigning an annual charge to each line and transformer using standard techniques based upon rate of return on capital, the capital costs of each line could be assigned to consumers in proportion to their usage.

An extension to this scheme could employ a variable charge for each line, calculated to increase with the utilisation of the line, such that as the utilisation approaches 100% the revenue recovered would be equivalent to that required to build a new line.

10.3.3 New Time Based Applications

A wide range of possibilities exist for new time based applications. The following sections outline briefly some of the more important of these.

10.3.3.1 Simulation Event Handling

The discrete time simulator currently assumes that network topology is fixed during a simulation. The work required to extend the simulator to accommodate events such as switching is not excessive.

An event handling application would be necessary to permit the user to specify in advance which events should occur and at what times. Extensions to this application could allow for random events based upon equipment reliabilities, or the triggering of events under certain circumstances, such as the operation of protection equipment under overload conditions.

10.3.3.2 Time Based Loss Minimisation

Loss minimisation algorithms are in widespread use, but the majority minimise losses on the basis of a single loading condition. The proposed discrete time simulator could be combined with an efficient loss minimisation algorithm to permit minimisation of losses over a predefined period.

10.3.3.3 Time Based Security Assessment

Conventional security assessment algorithms determine constraint violations due to specified contingencies for a single loading condition. The incorporation of time based analysis could identify the risks to system security of given outages as a function of time, and help to identify which contingencies only pose a threat for very short periods of time, and which represent a more significant threat to the system.

10.4 Summary

The research presented here has shown that discrete time simulation at the distribution level is feasible using current workstation hardware, and that it offers many advantages over existing load-flow analysis methods.

The accurate modelling of the individual variations in load and generation profiles with time provides the engineer with a better understanding of the state of the system on which to base decisions or perform further analysis. Safe operation of the system closer to its design limits is possible, and capital costs can be reduced.

The research has also shown that discrete time simulation, when combined with other time based analysis algorithms, can offer advantages in the accurate costing and allocation of losses. The results from such studies can be used to identify opportunities for loss reduction, to assess the accuracy of existing tariffs, and to design improved tariff structures.

The work has highlighted the fact that the success of time based analysis at this level relies on both the efficiency of the time based algorithms, and the design of the software environment in which these algorithms run. The use of interactive graphics to provide efficient management of large volumes of data and reduce the workload of the user is very important in this respect.

Appendix A. Definitions

This appendix contains definitions of terms used in the body of the thesis.

A.1 Load Diversity

A.1.1 Diversity Factor

Diversity Factor, F_{Div}, is defined as the *ratio* of the sum of individual maximum demands of the various subdivisions of the system to the maximum demand of the whole system:

$$F_{Div} = \frac{\left(\sum_{i=1}^{n} P_{Dmax,i}\right)}{P_{Dmax,g}} \tag{A-1}$$

A.1.2 Load Diversity

Load Diversity, *LD*, is defined as the difference between the sum of the peaks of two or more loads and the peak of the combined load (Gönen, [55]).

$$LD = \left(\sum_{i=1}^{n} P_{Dmax,\,i}\right) - P_{Dmax,\,g} \tag{A-2}$$

where $P_{Dmax,\,i}$ is the maximum demand of load *i*, irrespective of time of occurrence, and $P_{Dmax,\,g}$ is the coincident maximum demand of the group of *n* loads.

A.2 Losses

A.2.1 Demand Loss

Demand loss is defined as the difference between power (in MW) input to the system and the power which exits the system (EPRI [44]).

$$P_L(t) = P_{in}(t) - P_{out}(t) \tag{A-3}$$

A.2.2 Energy Loss

Energy loss is defined as the difference between energy (in MWh) input to the system and the energy which exits the system [44].

$$W_L = W_{in} - W_{out} \tag{A-4}$$

A.3 Load and Loss Factor

A.3.1 Load Factor

Load Factor, F_D, is defined as "the ratio of the average load over a designated period of time to the peak load occurring during that period" [55].

$$F_D = \frac{\text{average load}}{\text{peak load}} = \frac{P_{Dav}}{P_{Dmax}} \tag{A-5}$$

A.3.2 Loss Factor

Loss Factor, F_L, is defined as the "the ratio of the average power loss to the peak power loss during a specified period of time".

$$F_L = \frac{\text{average loss}}{\text{peak loss}} = \frac{P_{Lav}}{P_{Lmax}} \tag{A-6}$$

A.3.3 Allocation Loss Factor

Active and reactive Allocation Loss Factors, F_{Lr} and F_{Lx}, relate to loads, and are defined as the mean active and reactive losses respectively incurred on the system between the system Grid Supply Points and a given load during a specified period of time, expressed as a ratio of the mean load active or reactive demand.

$$F_{Lr} = \frac{[P_{Lav}]_{\text{GSP to Load}}}{P_{Dav}} \tag{A-7}$$

$$F_{Lx} = \frac{[Q_{Lav}]_{\text{GSP to Load}}}{Q_{Dav}} \tag{A-8}$$

Appendix B. Load-flow Analysis Approach Test Results

B.1 Introduction

This appendix contains full results for the tests in Section 2.5.3 of Chapter 2. The results compare the accuracy of three load-flow analysis approaches: multiple-case chronological simulation, multiple-case duration curve simulation and discrete time simulation.

The tables list results for load demand, line loading and line loss for each load or line in each of the test systems. The results for the discrete time simulation approach are used as a reference. The maximum, minimum and mean results for the study period are compared, and the errors and deviations on the mean are listed.

B.2 Test Results

B.2.1 7 Node Test System

Table B.1 Demand Profile Results for the 7 Node Test System

Load No.	Simulation Type	Comparison with Discrete Time Simulation				
		Demand (MW)			Errors on the Mean (MW)	
		Max	Min	Mean	Mean Error	Mean Devia. on the Error
1	DTS	54.18	5.61	27.95		
	MC Chron	44.83	12.80	27.68	-0.27	3.46
	MC Dur	44.83	12.80	27.67	-0.29	3.04
2	DTS	11.95	0.26	9.11		
	MC Chron	11.70	3.04	9.37	0.25	1.60
	MC Dur	11.70	3.04	9.37	0.26	1.35
3	DTS	4.00	0.00	2.39		
	MC Chron	4.00	0.00	2.50	0.11	0.22
	MC Dur	4.00	0.00	2.48	0.09	0.23
4	DTS	3.51	0.36	1.81		
	MC Chron	2.91	0.83	1.79	-0.02	0.22
	MC Dur	2.90	0.83	1.79	-0.02	0.20

Table B.2 Line Loading Results for the 7 Node Test System

Line No.	Simulation Type	Comparison with Discrete Time Simulation				
		Line Loading (MVA)			Errors on the Mean (MVA)	
		Max	Min	Mean	Mean Error	Mean Devia on the Error
1	DTS	38.30	9.64	22.80		
	MC Chron	32.86	13.09	22.85	0.05	2.08
	MC Dur	35.39	11.34	22.85	0.05	2.07
2	DTS	38.34	9.65	22.83		
	MC Chron	32.90	13.10	22.87	0.05	2.08
	MC Dur	35.43	11.35	22.87	0.05	2.07
3	DTS	10.45	1.31	7.42		
	MC Chron	9.23	2.77	7.61	0.19	0.97
	MC Dur	10.26	2.44	7.61	0.19	0.88
4	DTS	10.17	1.28	7.23		
	MC Chron	8.99	2.70	7.41	0.19	0.95
	MC Dur	9.99	2.38	7.41	0.18	0.86

Table B.3 Line Loss Results for the 7 Node Test System

Line No.	Simulation Type	Comparison with Discrete Time Simulation				
		Line Loss (kW)			Errors on the Mean (kW)	
		Max	Min	Mean	Mean Error	Mean Devia on the Error
1	DTS	179.2	11.4	66.3		
	MC Chron	132.0	20.9	65.9	-0.4	11.6
	MC Dur	153.1	15.7	67.1	0.8	11.7
2	DTS	179.6	11.4	66.5		
	MC Chron	132.2	21.0	66.1	-0.4	11.6
	MC Dur	153.4	15.7	67.3	0.8	11.7
3	DTS	172.8	2.6	88.6		
	MC Chron	133.5	11.7	91.7	3.0	21.6
	MC Dur	167.6	9.0	93.6	4.9	20.5
4	DTS	157.9	2.4	81.1		
	MC Chron	122.1	10.8	83.9	2.8	19.7
	MC Dur	153.1	8.3	85.6	4.5	18.8

B.2.2 10 Node Test System

Table B.4 Demand Profile results for the 10 Node Test System

Load No.	Simulation Type	Comparison with Discrete Time Simulation				
		Demand (MW)			Errors on the Mean (MVA)	
		Max	Min	Mean	Mean Error	Mean Devia on the Error
1	DTS	6.91	0.93	3.44		
	MC Chron	6.56	1.02	3.42	-0.02	0.77
	MC Dur	6.56	1.02	3.45	0.01	0.50
2	DTS	16.90	0.00	9.21		
	MC Chron	15.20	0.00	9.31	0.10	1 23
	MC Dur	15.20	0.00	9.31	0.10	1.09
3	DTS	22.62	0.00	15.14		
	MC Chron	20.75	5.32	15.44	0.30	3 64
	MC Dur	20.75	5.32	15.44	0.30	3 34

Table B.5 Line Loading Results for the 10 Node Test System

Line No.	Simulation Type	Comparison with Discrete Time Simulation				
		Line Loading (MVA)			Errors on the Mean (MVA)	
		Max	Min	Mean	Mean Error	Mean Devia on the Error
1	DTS	23.73	1.84	15.20		
	MC Chron	21.00	6.32	15.27	0.068	2.57
	MC Dur	22.25	3.88	15.26	0.063	2.29
2	DTS	19.07	0.81	8.34		
	MC Chron	11.80	2.68	8.33	-0.003	2.11
	MC Dur	11.81	2.68	8.30	-0.039	1.89
3	DTS	11.21	0.63	6.88		
	MC Chron	9.78	3.02	6.94	0.063	0.88
	MC Dur	10.45	1.07	6.99	0.107	0.75
4	DTS	23.75	1.85	15.22		
	MC Chron	21.02	6.33	15.29	0.068	2.58
	MC Dur	22.27	3.89	15.28	0.062	2.29
5	DTS	19.06	0.81	8.33		
	MC Chron	11.80	2.68	8.33	-0.003	2.11
	MC Dur	11.80	2.68	8.30	-0.038	1.89
6	DTS	11.24	0.64	6.89		
	MC Chron	9.80	3.04	6.95	0.063	0.89
	MC Dur	10.46	1.08	7.00	0.107	0.75

Table B.6 Line Loss Results for 10 Node Test System

Line No.	Simulation Type	Comparison with Discrete Time Simulation				
		Line Loss (kW)			Errors on the Mean (kW)	
		Max	Min	Mean	Mean Error	Mean Devia on the Error
1	DTS	371.7	2.4	165.5		
	MC Chron	291.4	26.3	160.9	-4.6	47.6
	MC Dur	326.3	9.8	162.3	-3.1	41.3
2	DTS	85.2	0.0	18.1		
	MC Chron	31.5	1.6	16.7	-1.3	7.1
	MC Dur	31.6	1.6	16.5	-1.5	6.1
3	DTS	0.9	0.0	0.4		
	MC Chron	0.7	0.1	0.4	0.0	0.1
	MC Dur	0.8	0.4		0.0	0.1
4	DTS	371.7	2.4	165.5		
	MC Chron	291.4	26.3	160.9	-4.5	47.6
	MC Dur	326.3	9.8	162.4	-3.1	41.3
5	DTS	85.5	0.0	18.1		
	MC Chron	31.6	1.6	16.8	-1.3	7.2
	MC Dur	31.8	1.6	16.6	-1.5	6.1
6	DTS	1.0	0.0	0.4		
	MC Chron	0.7	0.1	0.4	0.0	0.1
	MC Dur	0.8	0.0	0.4	0.0	0.1

B.2.3 15 Node Test System

Table B.7 Demand Profile Results for the 15 Node Test System

Load No.	Simulation Type	Comparison with Discrete Time Simulation				
		Demand (MW)			Errors on the Mean (MW)	
		Max	Min	Mean	Mean Error	Mean Devia on the Error
1	DTS	44.20	10.70	27.29		
	MC Chron	37.10	16.10	27.18	-0.11	2.27
	MC Dur	37.10	16.10	27.12	-0.17	2.03
2	DTS	37.30	8.90	20.30		
	MC Chron	33.30	9.50	20.11	-0.19	1.74
	MC Dur	33.30	9.50	20.05	-0.26	1.62
3	DTS	34.60	8.60	19.27		
	MC Chron	31.30	8.90	19.24	-0.02	1.61
	MC Dur	31.30	8.90	19.27	0.00	1.45
4	DTS	16.70	5.20	10.75		
	MC Chron	15.10	5.40	10.70	-0.05	0.78
	MC Dur	15.10	5.40	10.70	-0.05	0.65
5	DTS	65.40	19.40	42.05		
	MC Chron	55.00	24.10	42.09	0.04	4.01
	MC Dur	55.00	24.10	42.09	0.05	3.50
6	DTS	54.90	12.20	30.67		
	MC Chron	50.50	13.70	30.48	-0.19	2.48
	MC Dur	50.50	13.70	30.52	-0.15	2.27

Table B.8 Line Loading Results for the 15 Node Test System

Line No.	Simulation Type	Comparison with Discrete Time Simulation				
		Line Loading (MVA)			Errors on the Mean (MVA)	
		Max	Min	Mean	Mean Error	Mean Devia on the Error
1	DTS	19.18	1.83	8.27		
	MC Chron	16.79	2.66	8.21	-0.062	1.04
	MC Dur	16.66	2.69	8.21	-0.062	0.95
2	DTS	15.43	4.61	8.91		
	MC Chron	13.18	5.43	8.88	-0.033	0.73
	MC Dur	13.49	5.47	8.87	-0.050	0.67
3	DTS	54.15	14.32	31.36		
	MC Chron	47.88	15.05	31.20	-0.158	2.38
	MC Dur	48.02	15.91	31.16	-0.200	2.19
4	DTS	48.32	12.67	28.34		
	MC Chron	41.99	15.09	28.20	-0.141	2.14
	MC Dur	42.00	14.98	28.15	-0.188	1.96
5	DTS	76.55	26.05	49.34		
	MC Chron	64.92	28.98	49.25	-0.092	3.57
	MC Dur	67.47	28.91	49.21	-0.131	3.20
6	DTS	126.17	38.31	78.06		
	MC Chron	111.64	41.43	77.80	-0.267	5.75
	MC Dur	115.36	41.09	77.79	-0.274	5.28
7	DTS	31.80	8.51	20.08		
	MC Chron	26.60	10.90	20.09	0.009	2.09
	MC Dur	26.41	10.90	20.06	-0.016	1.82
8	DTS	30.52	9.11	18.73		
	MC Chron	26.89	9.99	18.65	-0.083	1.28
	MC Dur	27.19	9.88	18.63	-0.099	1.17
9	DTS	44.47	14.43	28.51		
	MC Chron	38.22	16.34	28.46	-0.052	2.11
	MC Dur	39.85	16.22	28.45	-0.059	1.91
10	DTS	178.72	54.03	109.38		
	MC Chron	158.65	57.85	108.95	-0.426	7.93
	MC Dur	163.12	57.30	108.91	-0.470	7.30
11	DTS	30.51	8.86	18.53		
	MC Chron	26.80	9.75	18.45	-0.085	1.30
	MC Dur	27.10	9.64	18.44	-0.101	1.19

Table B.9 Line Loss Results for the 15 Node Test System

Line No.	Simulation Type	Comparison with Discrete Time Simulation				
		Line Loss (kW)			Errors on the Mean (kW)	
		Max	Min	Mean	Mean Error	Mean Devia on the Error
1	DTS	30.6	0.3	6.5		
	MC Chron	23.4	0.6	6.3	-0.2	1.5
	MC Dur	23.1	0.7	6.3	-0.3	1.4
2	DTS	53.1	3.8	17.6		
	MC Chron	38.2	5.6	17.3	-0.3	3.0
	MC Dur	40.1	5.7	17.2	-0.4	2.8
3	DTS	436.5	30.1	151.8		
	MC Chron	339.2	37.6	149.1	-2.7	22.8
	MC Dur	341.4	37.0	148.9	-2.9	20.8
4	DTS	375.9	26.0	134.1		
	MC Chron	282.4	36.5	131.8	-2.3	20.0
	MC Dur	282.8	35.9	131.5	-2.6	18.1
5	DTS	22.6	2.5	9.6		
	MC Chron	16.1	3.2	9.4	-0.1	1.4
	MC Dur	17.5	3.1	9.5	-0.1	1.2
6	DTS	71.9	6.5	28.3		
	MC Chron	56.0	7.6	27.9	-0.5	4.1
	MC Dur	59.9	7.4	27.9	-0.4	3.7
7	DTS	40.6	3.7	17.3		
	MC Chron	28.6	5.8	17.1	-0.2	3.2
	MC Dur	28.7	5.8	17.1	-0.2	2.8
8	DTS	261.3	22.0	100.4		
	MC Chron	201.4	26.6	98.8	-1.7	13.8
	MC Dur	206.0	26.0	98.8	-1.6	12.4
9	DTS	227.8	21.5	93.6		
	MC Chron	165.4	28.3	92.3	-1.2	14.1
	MC Dur	180.7	27.9	92.5	-1.1	12.7
10	DTS	3140.0	286.3	1219.1		
	MC Chron	2466.0	327.6	1198.8	-20.3	173.0
	MC Dur	2609.0	321.4	1200.3	-18.9	158.2
11	DTS	15.5	25.8	66.8		
	MC Chron	121.6	28.3	65.9	-0.9	7.4
	MC Dur	123.8	28.0	65.9	-0.9	6.7

B.2.4 348 Node Test System

Table B.10 Demand Results for the 348 Node Test System

Load No.	Simu-lation Type	Comparison with Discrete Time Sim.					Load No.	Simu-lation Type	Comparison with Discrete Time Sim.				
		Demand (MW)			Errors (MW)				Demand (MW)			Errors (MW)	
		Max	Min	Mean	Mean	Devia			Max	Min	Mean	Mean	Devia
1	DTS	89.70	41.40	62.09			21	DTS	79.80	34.80	54.86		
	Chron	80.90	42.50	60.01	-2.08	2.58		Chron	70.40	36.50	52.27	-2.59	2.32
	Dur	80.90	42.50	60.01	-2.08	2.33		Dur	70.40	36.50	52.27	-2.59	2.12
2	DTS	0.00	0.00	0.00			22	DTS	71.00	27.10	43.03		
	Chron	0.00	0.00	0.00	0.00	0.00		Chron	62.50	27.20	41.22	-1.81	2.06
	Dur	0.00	0.00	0.00	0.00	0.00		Dur	62.50	27.20	41.22	-1.81	1.87
3	DTS	114.00	45.80	74.27			23	DTS	85.60	38.10	58.81		
	Chron	102.70	47.90	71.08	-3.19	3.19		Chron	77.60	40.40	56.71	-2.10	2.31
	Dur	102.70	47.90	71.08	-3.19	2.89		Dur	77.60	40.40	56.71	-2.10	2.09
4	DTS	45.20	28.60	36.15			24	DTS	11.35	4.05	6.81		
	Chron	42.30	28.60	35.18	-0.98	1.04		Chron	9.85	4.25	6.57	-0.24	0.25
	Dur	42.30	28.60	35.18	-0.98	0.95		Dur	9.85	4.25	6.57	-0.24	0.23
5	DTS	68.80	28.80	46.45			25	DTS	11.35	4.05	6.81		
	Chron	59.30	30.00	44.41	-2.04	2.31		Chron	9.85	4.35	6.63	-0.17	0.27
	Dur	59.30	30.00	44.41	-2.04	2.10		Dur	9.85	4.35	6.63	-0.17	0.25
6	DTS	65.57	41.35	53.41			26	DTS	88.10	36.70	60.05		
	Chron	61.69	43.39	52.28	-1.12	1.20		Chron	81.30	37.80	58.41	-1.64	2.52
	Dur	61.69	43.39	52.28	-1.12	1.06		Dur	81.30	37.80	58.41	-1.64	2.31
7	DTS	65.57	41.35	53.41			27	DTS	30.10	12.40	19.65		
	Chron	61.69	43.39	52.28	-1.12	1.20		Chron	26.40	12.60	18.87	-0.77	0.94
	Dur	61.69	43.39	52.28	-1.12	1.06		Dur	26.40	12.60	18.87	-0.77	0.86
8	DTS	21.20	8.80	13.99			28	DTS	60.50	29.80	44.29		
	Chron	17.70	9.70	13.44	-0.55	0.90		Chron	52.90	30.50	42.59	-1.70	1.96
	Dur	17.70	9.70	13.44	-0.55	0.78		Dur	52.90	30.50	42.59	-1.70	1.67
9	DTS	61.80	26.00	42.28			29	DTS	53.90	20.60	34.38		
	Chron	56.50	27.80	41.19	-1.09	1.71		Chron	44.90	24.00	32.81	-1.57	4.22
	Dur	56.50	27.80	41.19	-1.09	1.49		Dur	44.90	24.00	32.81	-1.57	4.09
10	DTS	28.90	12.60	19.90			30	DTS	33.95	17.48	25.39		
	Chron	25.40	13.35	19.12	-0.79	0.93		Chron	30.25	18.10	24.68	-0.71	0.96
	Dur	25.40	13.35	19.12	-0.79	0.82		Dur	30.25	18.10	24.68	-0.71	0.86
11	DTS	28.90	12.60	19.90			31	DTS	101.85	52.43	76.16		
	Chron	25.40	13.35	19.12	-0.79	0.93		Chron	90.75	54.30	74.03	-2.13	2.89
	Dur	25.40	13.35	19.12	-0.79	0.82		Dur	90.75	54.30	74.03	-2.13	2.56
12	DTS	30.95	12.70	21.15			32	DTS	36.00	16.80	25.95		
	Chron	28.30	13.70	20.26	-0.88	0.95		Chron	31.30	17.30	25.15	-0.80	1.19
	Dur	28.30	13.70	20.26	-0.88	0.87		Dur	31.30	17.30	25.15	-0.80	1.00
13	DTS	30.95	12.70	21.15			33	DTS	18.40	9.20	13.61		
	Chron	28.30	13.70	20.26	-0.88	0.95		Chron	17.10	9.20	13.20	-0.41	0.56
	Dur	28.30	13.70	20.26	-0.88	0.87		Dur	17.10	9.20	13.20	-0.41	0.47
14	DTS	59.60	27.15	43.29			34	DTS	73.50	33.30	53.02		
	Chron	55.75	27.75	41.86	-1.43	1.57		Chron	65.70	34.00	52.03	-0.99	2.06
	Dur	55.75	27.75	41.86	-1.43	1.41		Dur	65.70	34.00	52.03	-0.99	1.85
15	DTS	0.00	0.00	0.00			35	DTS	32.30	14.60	23.34		
	Chron	0.00	0.00	0.00	0.00	0.00		Chron	30.00	14.80	22.66	-0.68	1.02
	Dur	0.00	0.00	0.00	0.00	0.00		Dur	30.00	14.80	22.66	-0.68	0.89
16	DTS	47.46	19.35	32.02			36	DTS	49.05	22.55	33.26		
	Chron	41.77	20.57	31.11	-0.91	1.39		Chron	44.55	22.55	32.45	-0.81	1.07
	Dur	41.77	20.57	31.11	-0.91	1.27		Dur	44.55	22.55	32.45	-0.81	0.98
17	DTS	62.72	39.56	51.09			37	DTS	49.05	22.55	33.26		
	Chron	59.01	41.50	50.01	-1.08	1.15		Chron	44.55	22.55	32.45	-0.81	1.07
	Dur	59.01	41.50	50.01	-1.08	1.01		Dur	44.55	22.55	32.45	-0.81	0.98
18	DTS	49.05	23.60	35.64			38	DTS	26.50	12.10	18.47		
	Chron	44.20	23.90	34.71	-0.93	1.41		Chron	24.10	12.50	17.95	-0.52	0.81
	Dur	44.20	23.90	34.71	-0.93	1.20		Dur	24.10	12.50	17.95	-0.52	0.74
19	DTS	49.05	23.60	35.64			39	DTS	65.40	29.20	43.42		
	Chron	44.20	23.90	34.71	-0.93	1.41		Chron	55.40	31.00	41.62	-1.80	2.35
	Dur	44.20	23.90	34.71	-0.93	1.20		Dur	55.40	31.00	41.62	-1.80	2.03
20	DTS	62.70	29.10	44.53			40	DTS	37.10	15.50	25.73		
	Chron	57.00	30.00	42.96	-1.57	1.66		Chron	31.50	17.00	24.77	-0.96	1.15
	Dur	57.00	30.00	42.96	-1.57	1.51		Dur	31.50	17.00	24.77	-0.96	1.00

Table B.11 Demand Results for the 348 Node Test System (Cont.)

Load No.	Simulation Type	Comparison with Discrete Time Sim. Demand (MW) Max	Min	Mean	Errors (MW) Mean	Devia	Load No.	Simulation Type	Comparison with Discrete Time Sim. Demand (MW) Max	Min	Mean	Errors (MW) Mean	Devia
41	DTS	29.10	13.70	20.04			61	DTS	101.80	42.80	67.51		
	Chron	29.10	14.50	19.73	-0.31	0.94		Chron	86.10	49.20	65.39	-2.12	4.29
	Dur	29.10	14.50	19.73	-0.31	0.82		Dur	86.10	49.20	65.39	-2.12	4.12
42	DTS	35.20	16.00	25.02			62	DTS	30.20	2.00	10.99		
	Chron	32.20	16.60	24.53	-0.50	1.18		Chron	19.30	3.40	9.39	-1.60	5.16
	Dur	32.20	16.60	24.53	-0.50	0.97		Dur	19.30	3.40	9.39	-1.60	4.88
43	DTS	77.40	34.90	53.84			63	DTS	0.00	0.00	0.00		
	Chron	65.70	35.50	51.88	-1.95	2.75		Chron	0.00	0.00	0.00	0.00	0.00
	Dur	65.70	35.50	51.88	-1.95	2.48		Dur	0.00	0.00	0.00	0.00	0.00
44	DTS	72.10	32.50	49.91			64	DTS	21.20	8.25	14.49		
	Chron	64.80	34.00	47.71	-2.20	3.30		Chron	18.85	9.45	13.81	-0.69	0.73
	Dur	64.80	34.00	47.71	-2.20	2.80		Dur	18.85	9.45	13.81	-0.69	0.67
45	DTS	37.90	5.40	24.46			65	DTS	21.20	8.25	14.49		
	Chron	32.10	16.50	23.43	-1.04	1.22		Chron	18.85	9.45	13.81	-0.69	0.73
	Dur	32.10	16.50	23.43	-1.04	1.08		Dur	18.85	9.45	13.81	-0.69	0.67
46	DTS	76.60	32.90	52.97			66	DTS	29.50	18.61	24.03		
	Chron	67.10	35.90	51.30	-1.67	2.10		Chron	27.76	19.52	23.52	-0.51	0.54
	Dur	67.10	35.90	51.30	-1.67	1.91		Dur	27.76	19.52	23.52	-0.51	0.48
47	DTS	30.10	13.60	20.62			67	DTS	35.20	6.60	22.82		
	Chron	25.80	13.90	19.80	-0.81	1.31		Chron	31.27	15.07	22.19	-0.63	0.92
	Dur	25.80	13.90	19.80	-0.81	1.07		Dur	31.27	15.07	22.19	-0.63	0.84
48	DTS	40.75	17.80	27.83			68	DTS	0.00	0.00	0.00		
	Chron	35.20	18.70	27.20	-0.63	1.33		Chron	0.00	0.00	0.00	0.00	0.00
	Dur	35.20	18.70	27.20	-0.63	1.16		Dur	0.00	0.00	0.00	0.00	0.00
49	DTS	40.75	17.80	27.83			69	DTS	8.83	5.57	7.19		
	Chron	35.20	19.15	27.22	-0.61	1.31		Chron	8.31	5.84	7.04	-0.15	0.16
	Dur	35.20	19.15	27.22	-0.61	1.17		Dur	8.31	5.84	7.04	-0.15	0.14
50	DTS	49.45	22.20	33.54			70	DTS	8.83	5.57	7.19		
	Chron	43.25	22.90	32.21	-1.33	1.38		Chron	8.31	5.84	7.04	-0.15	0.16
	Dur	43.25	22.90	32.21	-1.33	1.14		Dur	8.31	5.84	7.04	-0.15	0.14
51	DTS	49.45	22.20	33.54			71	DTS	23.80	10.35	16.96		
	Chron	43.25	22.90	32.21	-1.33	1.38		Chron	21.90	11.30	16.56	-0.40	0.89
	Dur	43.25	22.90	32.21	-1.33	1.14		Dur	21.90	11.30	16.56	-0.40	0.80
52	DTS	76.90	38.80	56.96			72	DTS	23.80	10.35	16.96		
	Chron	68.10	40.60	55.27	-1.69	2.12		Chron	21.90	11.30	16.54	-0.42	0.89
	Dur	68.10	40.60	55.27	-1.69	1.90		Dur	21.90	11.30	16.54	-0.42	0.80
53	DTS	79.80	40.00	58.15			73	DTS	35.60	15.10	24.39		
	Chron	70.90	41.10	56.62	-1.53	2.36		Chron	31.70	14.60	23.58	-0.82	1.24
	Dur	70.90	41.10	56.62	-1.53	1.88		Dur	31.70	14.60	23.58	-0.82	1.10
54	DTS	26.80	0.00	18.27			74	DTS	19.80	8.10	13.24		
	Chron	21.00	12.60	17.89	-0.37	2.07		Chron	17.40	8.20	12.83	-0.41	0.60
	Dur	21.00	12.60	17.89	-0.37	1.72		Dur	17.40	8.20	12.83	-0.41	0.56
55	DTS	50.60	19.65	36.45			75	DTS	46.40	21.20	32.44		
	Chron	47.15	23.95	34.42	-2.03	3.85		Chron	42.20	22.20	31.61	-0.84	1.18
	Dur	47.15	23.95	34.42	-2.03	3.80		Dur	42.20	22.20	31.61	-0.84	1.05
56	DTS	50.60	19.65	36.45			76	DTS	5.92	3.73	4.82		
	Chron	47.15	23.95	34.42	-2.03	3.85		Chron	5.57	3.92	4.72	-0.10	0.11
	Dur	47.15	23.95	34.42	-2.03	3.80		Dur	5.57	3.92	4.72	-0.10	0.10
57	DTS	50.30	7.00	30.32			77	DTS	16.70	5.90	11.21		
	Chron	42.70	21.10	30.31	-0.02	6.28		Chron	14.60	7.10	10.89	-0.32	0.49
	Dur	42.70	21.10	30.31	-0.02	5.59		Dur	14.60	7.10	10.89	-0.32	0.43
58	DTS	73.40	29.60	49.55			78	DTS	24.50	11.40	16.77		
	Chron	64.00	31.60	47.74	-1.81	2.07		Chron	21.70	12.10	16.01	-0.76	0.73
	Dur	64.00	31.60	47.74	-1.81	1.91		Dur	21.70	12.10	16.01	-0.76	0.63
59	DTS	42.45	16.95	31.11			79	DTS	17.60	7.70	11.94		
	Chron	40.20	22.30	30.45	-0.65	1.21		Chron	16.20	8.10	11.61	-0.33	0.48
	Dur	40.20	22.30	30.45	-0.65	1.11		Dur	16.20	8.10	11.61	-0.33	0.41
60	DTS	42.45	16.95	31.11			80	DTS	26.70	11.80	18.80		
	Chron	40.20	22.30	30.45	-0.65	1.21		Chron	24.40	12.10	18.21	-0.59	0.78
	Dur	40.20	22.30	30.45	-0.65	1.11		Dur	24.40	12.10	18.21	-0.59	0.70

Table B.12 Demand results for the 348 Node Test System (Cont.)

Load No.	Simulation Type	Comparison with Discrete Time Sim. Demand (MW)			Errors (MW)	
		Max	Min	Mean	Mean	Devia
81	DTS	0.00	0.00	0.00		
	Chron	0.00	0.00	0.00	0.00	0.00
	Dur	0.00	0.00	0.00	0.00	0.00
82	DTS	0.00	0.00	0.00		
	Chron	0.00	0.00	0.00	0.00	0.00
	Dur	0.00	0.00	0.00	0.00	0.00
83	DTS	0.00	0.00	0.00		
	Chron	0.00	0.00	0.00	0.00	0.00
	Dur	0.00	0.00	0.00	0.00	0.00
84	DTS	188.37	118.80	153.43		
	Chron	177.22	124.64	150.20	-3.23	3.45
	Dur	177.22	124.64	150.20	-3.23	3.04
85	DTS	0.00	0.00	0.00		
	Chron	0.00	0.00	0.00	0.00	0.00
	Dur	0.00	0.00	0.00	0.00	0.00
86	DTS	0.00	0.00	0.00		
	Chron	0.00	0.00	0.00	0.00	0.00
	Dur	0.00	0.00	0.00	0.00	0.00
87	DTS	0.00	0.00	0.00		
	Chron	0.00	0.00	0.00	0.00	0.00
	Dur	0.00	0.00	0.00	0.00	0.00
88	DTS	12.75	8.04	10.39		
	Chron	12.00	8.44	10.17	-0.22	0.23
	Dur	12.00	8.44	10.17	-0.22	0.21
89	DTS	39.67	25.02	32.31		
	Chron	37.32	26.25	31.63	-0.68	0.73
	Dur	37.32	26.25	31.63	-0.68	0.64
90	DTS	51.59	32.54	42.02		
	Chron	48.54	34.14	41.14	-0.88	0.94
	Dur	48.54	34.14	41.14	-0.88	0.83
91	DTS	41.33	19.45	30.24		
	Chron	37.67	21.15	29.20	-1.04	1.08
	Dur	37.67	21.15	29.20	-1.04	0.96
92	DTS	24.15	15.23	19.67		
	Chron	22.72	15.98	19.25	-0.41	0.44
	Dur	22.72	15.98	19.25	-0.41	0.39
93	DTS	28.67	18.08	23.35		
	Chron	26.97	18.97	22.86	-0.49	0.52
	Dur	26.97	18.97	22.86	-0.49	0.46
94	DTS	22.64	14.28	18.44		
	Chron	21.30	14.98	18.05	-0.39	0.41
	Dur	21.30	14.98	18.05	-0.39	0.37
95	DTS	42.15	26.58	34.33		
	Chron	39.65	27.89	33.61	-0.72	0.77
	Dur	39.65	27.89	33.61	-0.72	0.68
96	DTS	49.47	31.20	40.30		
	Chron	46.55	32.74	39.45	-0.85	0.91
	Dur	46.55	32.74	39.45	-0.85	0.80
97	DTS	18.85	11.89	15.35		
	Chron	17.74	12.47	15.03	-0.32	0.34
	Dur	17.74	12.47	15.03	-0.32	0.30
98	DTS	20.42	12.88	16.63		
	Chron	19.21	13.51	16.28	-0.35	0.37
	Dur	19.21	13.51	16.28	-0.35	0.33
99	DTS	291.31	183.72	237.27		
	Chron	274.07	192.76	232.28	-5.00	5.33
	Dur	274.07	192.76	232.28	-5.00	4.70
100	DTS	291.31	183.72	237.27		
	Chron	274.07	192.76	232.28	-5.00	5.33
	Dur	274.07	192.76	232.28	-5.00	4.70

Load No.	Simulation Type	Comparison with Discrete Time Sim. Demand (MW)			Errors (MW)	
		Max	Min	Mean	Mean	Devia
101	DTS	241.78	152.49	196.94		
	Chron	227.48	159.99	192.79	-4.15	4.42
	Dur	227.48	159.99	192.79	-4.15	3.90
102	DTS	291.31	183.72	237.27		
	Chron	274.07	192.76	232.28	-5.00	5.33
	Dur	274.07	192.76	232.28	-5.00	4.70
103	DTS	163.13	102.88	132.87		
	Chron	153.48	107.95	130.07	-2.80	2.98
	Dur	153.48	107.95	130.07	-2.80	2.63
104	DTS	163.13	102.88	132.87		
	Chron	153.48	107.95	130.07	-2.80	2.98
	Dur	153.48	107.95	130.07	-2.80	2.63
105	DTS	163.13	102.88	132.87		
	Chron	153.48	107.95	130.07	-2.80	2.98
	Dur	153.48	107.95	130.07	-2.80	2.63
106	DTS	163.13	102.88	132.87		
	Chron	153.48	107.95	130.07	-2.80	2.98
	Dur	153.48	107.95	130.07	-2.80	2.63
107	DTS	142.74	90.02	116.26		
	Chron	134.29	94.45	113.81	-2.45	2.61
	Dur	134.29	94.45	113.81	-2.45	2.30
108	DTS	142.74	90.02	116.26		
	Chron	134.29	94.45	113.81	-2.45	2.61
	Dur	134.29	94.45	113.81	-2.45	2.30
109	DTS	563.19	355.20	458.72		
	Chron	529.87	372.67	449.07	-9.66	10.30
	Dur	529.87	372.67	449.07	-9.66	9.08
110	DTS	160.65	101.32	130.85		
	Chron	151.14	106.30	128.10	-2.75	2.94
	Dur	151.14	106.30	128.10	-2.75	2.59
111	DTS	0.00	0.00	0.00		
	Chron	0.00	0.00	0.00	0.00	0.00
	Dur	0.00	0.00	0.00	0.00	0.00
112	DTS	0.00	0.00	0.00		
	Chron	0.00	0.00	0.00	0.00	0.00
	Dur	0.00	0.00	0.00	0.00	0.00
113	DTS	145.65	91.86	118.64		
	Chron	137.03	96.38	116.14	-2.50	2.66
	Dur	137.03	96.38	116.14	-2.50	2.35
114	DTS	2.24	1.41	1.82		
	Chron	2.10	1.48	1.78	-0.04	0.04
	Dur	2.10	1.48	1.78	-0.04	0.04

Table B.13 Line Loading Results for the 348 Node Test System

Load No.	Simulation Type	Comparison with Discrete Time Sim.					Load No.	Simulation Type	Comparison with Discrete Time Sim.				
		Line Loading (MVA)			Errors (MVA)				Line Loading (MVA)			Errors (MVA)	
		Max	Min	Mean	Mean	Devia			Max	Min	Mean	Mean	Devia
1	DTS	285.42	-576.69	-166.43			21	DTS	-20.43	-36.22	-27.31		
	Chron	136.54	-522.80	-204.87	-38.44	39.90		Chron	-20.50	-31.73	-26.63	0.67	1.01
	Dur	150.64	-525.02	-204.14	-37.70	36.14		Dur	-20.55	-32.23	-26.66	0.64	3.13
2	DTS	286.00	-577.78	-166.74			22	DTS	25.22	8.10	15.64		
	Chron	136.83	-523.79	-205.25	-38.51	39.98		Chron	21.26	9.44	15.11	-0.53	0.92
	Dur	150.96	-526.01	-204.51	-37.77	36.21		Dur	20.68	9.71	15.19	-0.45	1.18
3	DTS	51.61	-608.49	-267.06			23	DTS	-57.43	-78.53	-66.87		
	Chron	19.53	-490.54	-235.68	31.38	31.87		Chron	-58.12	-74.58	-65.57	1.30	2.08
	Dur	22.09	-497.65	-235.26	31.80	165.86		Dur	-57.28	-74.57	-65.62	1.25	5.06
4	DTS	51.53	-605.88	-265.92			24	DTS	49.83	33.84	42.75		
	Chron	19.59	-488.41	-234.63	31.29	31.74		Chron	49.76	37.34	43.33	0.58	1.40
	Dur	22.12	-495.48	-234.20	31.72	165.17		Dur	49.03	37.92	43.06	0.31	3.18
5	DTS	-650.65	1299.60	-964.91			25	DTS	37.87	7.25	24.49		
	Chron	-682.33	1184.30	-934.05	30.86	31.35		Chron	36.51	14.25	25.67	1.18	1.66
	Dur	-679.86	1191.30	-933.62	31.29	163.19		Dur	36.46	13.91	25.83	1.34	6.67
6	DTS	-654.32	1307.00	-970.39			26	DTS	41.40	17.96	28.17		
	Chron	-686.18	1191.10	-939.36	31.04	31.53		Chron	35.70	19.33	27.53	-0.63	1.35
	Dur	-683.70	1198.10	-938.92	31.47	164.13		Dur	35.70	19.10	27.53	-0.63	1.19
7	DTS	-563.14	1092.10	-823.01			27	DTS	41.04	17.80	27.92		
	Chron	-594.57	1004.20	-797.70	25.32	24.93		Chron	35.39	19.16	27.30	-0.63	1.34
	Dur	-593.36	1007.30	-797.57	25.45	135.08		Dur	35.39	18.93	27.29	-0.63	1.18
8	DTS	-563.14	1092.10	-823.01			28	DTS	21.02	-29.17	-0.11		
	Chron	-594.57	1004.20	-797.70	25.32	24.93		Chron	19.56	-17.46	2.05	2.16	2.49
	Dur	-593.36	1007.30	-797.57	25.45	135.08		Dur	19.52	-17.79	2.20	2.31	11.44
9	DTS	5.74	-5.07	-0.43			29	DTS	20.86	-29.37	-0.63		
	Chron	3.73	-3.84	-1.19	-0.77	2.09		Chron	19.92	-18.47	1.63	2.26	2.74
	Dur	3.88	-3.72	-1.27	-0.85	2.04		Dur	19.21	-17.91	1.38	2.01	11.00
10	DTS	-25.13	-48.93	-34.93			30	DTS	109.53	-623.91	-272.46		
	Chron	-27.38	-41.51	-34.11	0.81	2.27		Chron	-15.01	-575.68	-304.95	-32.50	33.90
	Dur	-26.98	-41.19	-34.19	0.74	5.12		Dur	-3.51	-577.62	-304.17	-31.71	30.52
11	DTS	-37.59	-73.46	-52.76			31	DTS	270.27	-561.51	-164.67		
	Chron	-40.01	-62.79	-51.44	1.32	2.65		Chron	128.12	-507.82	-201.44	-36.77	38.36
	Dur	-39.13	-62.26	-51.51	1.25	7.50		Dur	140.95	-510.12	-200.57	-35.90	34.50
12	DTS	-37.79	-49.86	-43.99			32	DTS	77.00	38.59	56.46		
	Chron	-39.33	-48.79	-44.23	-0.23	0.96		Chron	70.01	39.88	54.53	-1.93	2.12
	Dur	-39.98	-46.65	-44.30	-0.31	1.20		Dur	71.02	39.81	54.29	-2.16	1.96
13	DTS	63.99	12.15	37.35			33	DTS	27.68	7.60	18.55		
	Chron	55.69	14.68	34.90	-2.45	2.60		Chron	24.58	11.17	17.80	-0.75	1.67
	Dur	55.61	14.51	34.82	-2.53	2.41		Dur	25.50	11.10	17.71	-0.84	1.44
14	DTS	34.13	-36.59	-2.96			34	DTS	85.83	40.93	59.14		
	Chron	22.60	-33.27	-6.20	-3.24	3.52		Chron	71.76	44.74	57.51	-1.62	2.52
	Dur	22.88	-33.45	-6.34	-3.38	3.29		Dur	71.44	43.87	57.08	-2.06	1.97
15	DTS	-41.83	-84.68	-61.17			35	DTS	32.50	-0.23	7.18		
	Chron	-42.87	-75.38	-59.17	1.99	2.23		Chron	14.42	2.72	7.05	-0.13	1.10
	Dur	-42.94	-76.43	-59.08	2.08	10.72		Dur	11.05	3.86	6.78	-0.40	3.38
16	DTS	24.98	6.67	13.94			36	DTS	20.55	-5.25	6.91		
	Chron	19.96	7.07	13.35	-0.59	1.04		Chron	16.80	-4.60	5.64	-1.26	1.58
	Dur	19.06	7.39	13.44	-0.50	1.17		Dur	17.83	-3.28	5.32	-1.59	2.31
17	DTS	33.21	6.22	19.67			37	DTS	24.35	10.56	17.33		
	Chron	27.45	6.52	18.07	-1.60	1.95		Chron	22.39	11.53	16.91	-0.42	0.91
	Dur	31.60	6.14	17.73	-1.94	2.08		Dur	22.39	11.53	16.91	-0.42	0.82
18	DTS	-17.94	-37.01	-24.00			38	DTS	23.44	10.17	16.69		
	Chron	-18.54	-32.35	-23.78	0.22	1.26		Chron	21.56	11.11	16.28	-0.41	0.88
	Dur	-22.26	-25.82	-24.11	-0.11	3.39		Dur	21.56	11.11	16.28	-0.41	0.79
19	DTS	-29.76	-48.79	-40.31			39	DTS	-25.00	-73.33	-48.00		
	Chron	-33.10	-47.99	-41.10	-0.79	1.01		Chron	-25.77	-64.04	-45.51	2.49	2.74
	Dur	-32.76	-48.00	-41.16	-0.85	0.96		Dur	-25.29	-67.16	-45.26	2.75	12.97
20	DTS	24.88	6.12	16.81			40	DTS	-17.39	-68.04	-40.92		
	Chron	24.48	9.43	17.72	0.91	1.29		Chron	-19.30	-57.13	-38.83	2.09	2.97
	Dur	24.46	9.31	17.77	0.96	5.00		Dur	-19.36	-58.15	-38.51	2.42	12.41

Table B.14 Line Loading Results for the 348 Node Test System (Cont.)

Load No.	Simulation Type	Comparison with Discrete Time Sim.					Load No.	Simulation Type	Comparison with Discrete Time Sim.				
		Line Loading (MVA)			Errors (MVA)				Line Loading (MVA)			Errors (MVA)	
		Max	Min	Mean	Mean	Devia			Max	Min	Mean	Mean	Devia
41	DTS	53.06	25.30	38.71			61	DTS	-69.18	-142.73	-104.57		
	Chron	48.30	26.18	37.75	-0.96	1.58		Chron	-69.79	-129.10	-101.92	2.65	3.89
	Dur	48.53	26.10	37.72	-0.99	1.66		Dur	-70.30	-129.27	-102.10	2.47	17.78
42	DTS	133.21	64.74	98.29			62	DTS	0.00	0.00	0.00		
	Chron	119.48	66.26	95.15	-3.13	4.12		Chron	0.00	0.00	0.00	0.00	0.00
	Dur	120.20	66.06	95.16	-3.13	3.72		Dur	0.00	0.00	0.00	0.00	0.00
43	DTS	31.82	15.58	23.55			63	DTS	43.71	19.56	29.83		
	Chron	29.16	16.13	22.95	-0.61	0.97		Chron	38.53	19.55	28.63	-1.21	1.33
	Dur	29.77	16.06	22.93	-0.62	1.16		Dur	38.87	20.38	28.65	-1.19	1.20
44	DTS	117.48	57.82	87.38			64	DTS	48.35	21.58	32.96		
	Chron	105.80	59.28	84.45	-2.92	3.68		Chron	43.15	21.67	31.71	-1.25	1.39
	Dur	106.54	59.07	84.46	-2.92	3.36		Dur	43.55	21.92	31.57	-1.39	1.30
45	DTS	-46.98	-94.72	-70.68			65	DTS	62.50	27.64	42.09		
	Chron	-47.98	-84.84	-68.15	2.53	3.02		Chron	55.01	27.96	40.71	-1.38	1.74
	Dur	-47.98	-84.82	-68.14	2.53	12.95		Dur	54.80	27.94	40.70	-1.39	1.62
46	DTS	-42.61	-75.79	-57.83			66	DTS	113.20	52.26	78.43		
	Chron	-44.59	-68.75	-56.84	0.99	2.16		Chron	100.73	53.26	75.90	-2.54	3.24
	Dur	-42.80	-67.24	-57.15	0.69	7.17		Dur	101.28	52.75	75.93	-2.51	3.03
47	DTS	10.36	-8.18	1.57			67	DTS	-11.39	-24.85	-17.40		
	Chron	10.27	-5.70	2.35	0.78	1.23		Chron	-11.87	-22.59	-16.95	0.45	0.63
	Dur	8.15	-6.54	2.65	1.08	6.41		Dur	-11.87	-22.56	-16.95	0.45	3.56
48	DTS	20.92	10.08	15.46			68	DTS	-9.90	-21.90	-15.24		
	Chron	19.64	10.62	15.15	-0.31	0.67		Chron	-10.39	-19.94	-14.84	0.40	0.57
	Dur	19.92	10.59	15.17	-0.29	0.88		Dur	-10.39	-19.98	-14.84	0.40	3.24
49	DTS	0.00	0.00	0.00			69	DTS	40.55	16.17	26.83		
	Chron	0.00	0.00	0.00	0.00	0.00		Chron	35.03	16.48	25.85	-0.98	1.29
	Dur	0.00	0.00	0.00	0.00	0.00		Dur	35.25	17.50	25.84	-0.99	1.26
50	DTS	0.51	-0.31	0.12			70	DTS	88.27	40.37	61.00		
	Chron	0.54	-0.23	0.13	0.01	0.16		Chron	78.08	41.35	58.91	-2.09	2.66
	Dur	0.39	-0.18	0.16	0.03	0.13		Dur	78.66	40.83	58.94	-2.05	2.51
51	DTS	0.46	-0.28	0.11			71	DTS	12.96	8.20	10.32		
	Chron	0.48	-0.20	0.12	0.01	0.14		Chron	11.78	8.66	10.02	-0.30	0.52
	Dur	0.35	-0.16	0.14	0.03	0.12		Dur	12.05	7.77	10.07	-0.25	0.54
52	DTS	0.51	-0.31	0.12			72	DTS	12.97	8.21	10.33		
	Chron	0.54	-0.23	0.13	0.01	0.16		Chron	11.79	8.67	10.02	-0.30	0.52
	Dur	0.39	-0.18	0.16	0.03	0.13		Dur	12.06	7.77	10.08	-0.25	0.54
53	DTS	40.54	17.14	28.30			73	DTS	34.76	14.46	23.38		
	Chron	36.26	17.17	27.70	-0.59	1.18		Chron	29.92	15.06	22.35	-1.03	1.17
	Dur	36.36	17.20	27.50	-0.80	1.18		Dur	29.92	15.06	22.35	-1.03	1.06
54	DTS	21.51	9.02	15.25			74	DTS	34.76	14.45	23.38		
	Chron	19.39	9.12	14.95	-0.30	0.63		Chron	29.92	15.06	22.35	-1.03	1.17
	Dur	19.31	9.27	14.97	-0.28	0.65		Dur	29.92	15.06	22.35	-1.03	1.06
55	DTS	29.31	11.17	19.81			75	DTS	-71.62	-143.48	-100.20		
	Chron	26.46	11.49	19.38	-0.43	0.89		Chron	-75.72	-118.56	-97.68	2.51	4.25
	Dur	26.72	11.52	19.15	-0.66	1.00		Dur	-73.11	-118.95	-97.38	2.82	16.09
56	DTS	33.11	14.90	23.92			76	DTS	0.00	-0.00	0.00		
	Chron	29.77	15.01	23.44	-0.48	1.01		Chron	0.00	-0.00	0.00	0.00	0.00
	Dur	29.43	15.01	23.48	-0.43	0.91		Dur	0.00	-0.00	0.00	0.00	0.00
57	DTS	113.89	55.42	83.51			77	DTS	0.00	-0.00	0.00		
	Chron	102.60	56.76	81.30	-2.22	3.16		Chron	0.00	-0.00	0.00	0.00	0.00
	Dur	102.90	56.80	81.07	-2.44	2.93		Dur	0.00	-0.00	0.00	0.00	0.00
58	DTS	84.57	41.55	62.45			78	DTS	-102.46	-720.43	-429.56		
	Chron	75.66	42.45	60.88	-1.57	2.39		Chron	-212.54	-685.67	-457.65	-28.09	28.22
	Dur	75.14	42.45	60.91	-1.54	2.15		Dur	-203.58	-687.13	-456.78	-27.22	24.99
59	DTS	-60.20	-123.17	-90.38			79	DTS	-725.74	-986.97	-861.69		
	Chron	-61.41	-111.29	-87.96	2.42	3.38		Chron	-774.51	-972.29	-874.21	-12.52	12.06
	Dur	-61.39	-111.63	-87.76	2.62	15.25		Dur	-770.47	-972.11	-873.61	-11.92	10.53
60	DTS	-46.37	-93.42	-69.21			80	DTS	912.58	380.19	624.99		
	Chron	-47.11	-84.03	-67.44	1.78	2.61		Chron	816.65	408.64	602.04	-22.95	24.50
	Dur	-47.06	-83.53	-67.45	1.77	11.19		Dur	823.96	407.54	602.47	-22.53	21.97

Table B.15 Line Loading Results for the 348 Node Test System (Cont.)

Load No.	Simulation Type	Comparison with Discrete Time Sim.				
		Line Loading (MVA)			Errors (MVA)	
		Max	Min	Mean	Mean	Devia
81	DTS	114.00	45.79	77.07		
	Chron	101.72	49.37	74.19	-2.88	3.15
	Dur	102.68	49.29	74.24	-2.83	2.83
82	DTS	-27.60	-47.40	-37.55		
	Chron	-28.31	-43.71	-36.57	0.98	1.18
	Dur	-27.43	-45.39	-36.90	0.65	5.06
83	DTS	-13.69	-52.96	-34.43		
	Chron	-22.21	-43.36	-34.45	-0.02	5.88
	Dur	-27.49	-41.77	-35.58	-1.15	6.49
84	DTS	-16.99	-42.65	-31.22		
	Chron	-22.37	-40.38	-30.56	0.66	1.22
	Dur	-22.37	-40.38	-30.56	0.66	5.94
85	DTS	-16.95	-42.54	-31.15		
	Chron	-22.31	-40.28	-30.49	0.66	1.21
	Dur	-22.31	-40.28	-30.49	0.66	5.92
86	DTS	-22.33	-57.65	-41.10		
	Chron	-26.76	-53.81	-38.91	2.19	3.88
	Dur	-26.76	-53.81	-38.91	2.19	8.65
87	DTS	-17.03	-44.35	-32.01		
	Chron	-21.22	-40.84	-30.11	1.90	3.87
	Dur	-21.23	-40.84	-30.11	1.90	6.19
88	DTS	57.72	23.53	39.96		
	Chron	51.61	25.71	38.34	-1.63	1.62
	Dur	51.61	25.71	38.33	-1.63	1.51
89	DTS	78.11	30.65	55.61		
	Chron	68.91	36.17	52.73	-2.89	4.06
	Dur	68.91	36.17	52.72	-2.89	3.97
90	DTS	79.56	31.61	56.49		
	Chron	70.93	36.77	53.69	-2.80	3.74
	Dur	70.93	36.77	53.69	-2.80	3.64
91	DTS	-8.32	-21.30	-14.62		
	Chron	-9.54	-18.96	-13.93	0.69	0.74
	Dur	-9.54	-18.96	-13.93	0.69	2.81
92	DTS	-8.17	-21.15	-14.40		
	Chron	-9.34	-18.83	-13.72	0.68	0.73
	Dur	-9.34	-18.80	-13.72	0.68	2.80
93	DTS	0.00	0.00	0.00		
	Chron	0.00	0.00	0.00	0.00	0.00
	Dur	0.00	0.00	0.00	0.00	0.00
94	DTS	558.15	-52.06	239.78		
	Chron	447.56	-16.54	210.41	-29.36	27.13
	Dur	457.53	-27.59	211.56	-28.21	23.93
95	DTS	635.15	365.15	490.03		
	Chron	586.73	379.11	477.96	-12.07	12.72
	Dur	589.77	371.70	478.29	-11.74	11.14
96	DTS	656.57	486.67	562.09		
	Chron	625.50	494.50	555.60	-6.49	8.89
	Dur	626.13	494.96	555.61	-6.47	7.80
97	DTS	0.00	0.00	0.00		
	Chron	0.00	0.00	0.00	0.00	0.00
	Dur	0.00	0.00	0.00	0.00	0.00
98	DTS	1633.80	1305.90	1457.34		
	Chron	1573.70	1320.60	1441.92	-15.42	15.36
	Dur	1581.80	1310.00	1443.05	-14.29	14.03
99	DTS	320.56	18.29	179.08		
	Chron	300.18	70.99	191.75	12.67	13.57
	Dur	301.00	67.56	191.45	12.37	77.76
100	DTS	429.71	374.87	399.82		
	Chron	419.13	377.09	397.27	-2.54	2.68
	Dur	420.31	374.97	397.31	-2.50	2.46

Load No.	Simulation Type	Comparison with Discrete Time Sim.				
		Line Loading (MVA)			Errors (MVA)	
		Max	Min	Mean	Mean	Devia
101	DTS	-695.60	-919.98	-797.40		
	Chron	-704.45	-878.36	-787.41	9.99	10.65
	Dur	-701.11	-882.15	-787.52	9.88	61.78
102	DTS	-419.81	-541.08	-474.77		
	Chron	-424.65	-518.41	-469.38	5.38	5.77
	Dur	-422.54	-520.53	-469.47	5.30	33.43
103	DTS	0.00	0.00	0.00		
	Chron	0.00	0.00	0.00	0.00	0.00
	Dur	0.00	0.00	0.00	0.00	0.00
104	DTS	0.00	0.00	0.00		
	Chron	0.00	0.00	0.00	0.00	0.00
	Dur	0.00	0.00	0.00	0.00	0.00
105	DTS	51.54	21.46	33.99		
	Chron	43.42	24.69	32.89	-1.09	2.19
	Dur	43.41	24.69	32.89	-1.10	2.10
106	DTS	51.84	21.58	34.18		
	Chron	43.66	24.83	33.08	-1.10	2.20
	Dur	43.65	24.83	33.07	-1.11	2.11
107	DTS	30.44	2.00	11.03		
	Chron	19.38	3.40	9.40	-1.63	5.19
	Dur	19.38	3.40	9.40	-1.63	4.91
108	DTS	0.00	0.00	0.00		
	Chron	0.00	0.00	0.00	0.00	0.00
	Dur	0.00	0.00	0.00	0.00	0.00
109	DTS	473.12	359.53	411.04		
	Chron	452.08	364.02	405.98	-5.06	5.41
	Dur	454.02	362.29	405.99	-5.05	4.87
110	DTS	445.97	335.57	385.70		
	Chron	425.48	339.92	380.79	-4.91	5.23
	Dur	427.32	338.31	380.88	-4.81	4.72
111	DTS	101.07	20.37	55.60		
	Chron	84.27	23.92	51.92	-3.67	3.89
	Dur	84.12	20.93	51.93	-3.67	3.56
112	DTS	217.16	118.34	161.68		
	Chron	196.84	122.85	157.19	-4.49	4.75
	Dur	197.16	119.27	157.27	-4.41	4.29
113	DTS	11.28	4.16	7.87		
	Chron	11.57	3.61	7.87	0.01	0.79
	Dur	10.21	3.52	6.08	-1.78	2.55
114	DTS	-4.84	-11.33	-8.04		
	Chron	-5.52	-10.12	-7.82	0.21	0.29
	Dur	-5.53	-10.12	-7.82	0.21	1.73
115	DTS	-4.81	-11.29	-8.01		
	Chron	-5.50	-10.08	-7.80	0.21	0.29
	Dur	-5.49	-10.08	-7.80	0.21	1.73
116	DTS	-13.09	-34.39	-20.81		
	Chron	-13.14	-30.26	-19.93	0.88	1.00
	Dur	-13.14	-30.26	-19.93	0.88	7.18
117	DTS	-14.05	-36.88	-22.32		
	Chron	-14.10	-32.45	-21.38	0.94	1.07
	Dur	-14.10	-32.45	-21.38	0.94	7.69
118	DTS	54.57	23.74	37.67		
	Chron	48.60	25.06	36.21	-1.46	1.63
	Dur	49.33	25.23	36.25	-1.42	1.49
119	DTS	8.89	3.88	6.03		
	Chron	8.18	4.08	5.86	-0.17	0.24
	Dur	8.18	4.08	5.86	-0.17	0.21
120	DTS	-5.22	-15.14	-8.20		
	Chron	-5.27	-10.22	-7.91	0.29	0.52
	Dur	-5.56	-10.19	-7.87	0.33	1.89

Table B.16 Line Loading Results for the 348 Node Test System (Cont.)

Load No.	Simulation Type	Comparison with Discrete Time Sim.				
		Line Loading (MVA)			Errors (MVA)	
		Max	Min	Mean	Mean	Devia
121	DTS	46.15	20.87	31.50		
	Chron	41.16	21.36	30.36	-1.14	1.37
	Dur	41.16	21.36	30.36	-1.15	1.23
122	DTS	46.17	20.88	31.52		
	Chron	41.18	21.37	30.38	-1.14	1.37
	Dur	41.19	21.37	30.38	-1.15	1.23
123	DTS	0.00	0.00	0.00		
	Chron	0.00	0.00	0.00	0.00	0.00
	Dur	0.00	0.00	0.00	0.00	0.00
124	DTS	0.00	-0.00	0.00		
	Chron	0.00	-0.00	0.00	0.00	0.00
	Dur	0.00	-0.00	0.00	0.00	0.00
125	DTS	-26.97	-64.23	-44.96		
	Chron	-28.49	-57.55	-43.69	1.28	2.35
	Dur	-28.26	-51.26	-43.78	1.18	5.82
126	DTS	-34.00	-78.33	-53.46		
	Chron	-35.73	-69.08	-51.27	2.19	2.22
	Dur	-35.58	-69.69	-51.27	2.19	12.77
127	DTS	0.00	0.00	0.00		
	Chron	0.00	0.00	0.00	0.00	0.00
	Dur	0.00	0.00	0.00	0.00	0.00
128	DTS	1433.60	1188.40	1298.15		
	Chron	1389.40	1200.00	1287.75	-10.40	11.94
	Dur	1389.80	1193.10	1287.38	-10.77	10.72
129	DTS	0.00	-0.00	0.00		
	Chron	0.00	-0.00	0.00	0.00	0.00
	Dur	0.00	-0.00	0.00	0.00	0.00
130	DTS	-524.42	-642.94	-577.08		
	Chron	-528.99	-619.06	-571.89	5.19	5.56
	Dur	-526.96	-621.03	-572.01	5.08	31.90
131	DTS	-70.96	-86.97	-78.30		
	Chron	-71.75	-83.97	-77.62	0.67	0.87
	Dur	-70.98	-84.13	-77.70	0.60	3.69
132	DTS	-72.09	-88.34	-79.53		
	Chron	-72.89	-85.29	-78.85	0.69	0.88
	Dur	-72.10	-85.45	-78.93	0.61	3.75
133	DTS	-400.70	-432.73	-419.61		
	Chron	-406.59	-432.51	-420.90	-1.29	1.53
	Dur	-406.40	-432.12	-420.94	-1.33	1.61
134	DTS	-172.13	-240.18	-212.02		
	Chron	-186.23	-238.90	-215.01	-3.00	3.14
	Dur	-184.56	-240.46	-214.91	-2.89	3.10
135	DTS	0.00	0.00	0.00		
	Chron	0.00	0.00	0.00	0.00	0.00
	Dur	0.00	0.00	0.00	0.00	0.00
136	DTS	0.00	-0.00	0.00		
	Chron	0.00	-0.00	0.00	0.00	0.00
	Dur	0.00	-0.00	0.00	0.00	0.00
137	DTS	60.83	42.04	53.53		
	Chron	60.39	47.23	53.69	0.16	1.10
	Dur	61.44	47.59	53.77	0.24	2.96
138	DTS	-78.51	-177.50	-121.15		
	Chron	-80.93	-160.07	-116.33	4.82	4.78
	Dur	-80.52	-162.26	-116.31	4.84	31.19
139	DTS	-184.77	-220.45	-203.00		
	Chron	-187.01	-214.98	-201.29	1.72	1.65
	Dur	-186.89	-215.47	-201.37	1.63	10.49
140	DTS	55.66	19.32	40.45		
	Chron	53.88	26.88	41.84	1.39	1.81
	Dur	56.27	27.25	41.92	1.47	8.63
141	DTS	55.66	19.32	40.45		
	Chron	53.88	26.88	41.84	1.39	1.81
	Dur	56.27	27.25	41.92	1.47	8.63
142	DTS	8.55	5.00	6.62		
	Chron	8.01	5.11	6.45	-0.17	0.18
	Dur	8.23	5.11	6.55	-0.07	0.17
143	DTS	8.60	5.03	6.65		
	Chron	8.04	5.14	6.48	-0.17	0.18
	Dur	8.27	5.14	6.58	-0.07	0.17
144	DTS	8.58	5.02	6.64		
	Chron	8.03	5.13	6.47	-0.17	0.18
	Dur	8.26	5.13	6.57	-0.07	0.17
145	DTS	81.18	42.88	60.52		
	Chron	74.09	43.95	58.73	-1.79	1.98
	Dur	75.15	43.95	58.91	-1.62	1.79
146	DTS	75.69	38.37	56.70		
	Chron	70.41	41.08	55.18	-1.52	1.91
	Dur	71.38	41.07	55.16	-1.54	1.72
147	DTS	35.99	16.69	25.20		
	Chron	31.85	17.00	24.35	-0.85	1.09
	Dur	32.90	17.00	24.54	-0.66	0.98
148	DTS	28.02	10.57	19.34		
	Chron	25.84	12.48	18.82	-0.52	0.96
	Dur	26.82	12.48	18.79	-0.55	0.94
149	DTS	4.46	-5.33	-0.21		
	Chron	3.98	-4.12	-0.07	0.14	0.67
	Dur	3.44	-4.55	0.00	0.21	3.51
150	DTS	20.74	14.39	17.43		
	Chron	20.77	14.26	17.35	-0.08	0.73
	Dur	19.46	15.15	17.12	-0.31	1.40
151	DTS	-5.16	-12.17	-8.64		
	Chron	-6.12	-12.06	-8.67	-0.03	0.57
	Dur	-5.80	-11.49	-8.59	0.05	0.60
152	DTS	-5.14	-12.09	-8.58		
	Chron	-6.09	-11.98	-8.61	-0.03	0.57
	Dur	-5.78	-11.42	-8.54	0.05	0.60
153	DTS	-50.40	-72.22	-62.21		
	Chron	-53.77	-68.77	-61.10	1.10	1.22
	Dur	-53.51	-68.01	-61.02	1.18	3.91
154	DTS	-50.36	-72.20	-62.17		
	Chron	-53.73	-68.75	-61.07	1.10	1.22
	Dur	-53.47	-67.99	-60.99	1.18	3.93
155	DTS	-389.30	-731.65	-566.99		
	Chron	-420.65	-682.15	-549.36	17.64	16.54
	Dur	-421.42	-683.28	-549.28	17.71	87.44
156	DTS	-389.36	-731.75	-567.07		
	Chron	-420.70	-682.26	-549.44	17.63	16.54
	Dur	-421.47	-683.38	-549.37	17.70	87.47
157	DTS	372.07	262.42	317.37		
	Chron	354.80	271.89	312.13	-5.24	5.40
	Dur	354.86	271.95	312.13	-5.25	4.80
158	DTS	368.26	259.68	314.07		
	Chron	351.14	269.06	308.88	-5.19	5.34
	Dur	351.20	269.12	308.87	-5.20	4.75
159	DTS	297.28	198.02	247.54		
	Chron	281.47	206.46	242.88	-4.67	4.90
	Dur	281.49	206.48	242.87	-4.67	4.34
160	DTS	391.04	306.35	349.40		
	Chron	378.18	314.00	345.17	-4.23	4.13
	Dur	378.32	314.13	345.16	-4.24	3.74

Table B.17 Line Loading Results for the 348 Node Test System (Cont.)

Load No.	Simulation Type	Comparison with Discrete Time Sim.					Load No.	Simulation Type	Comparison with Discrete Time Sim.				
		Line Loading (MVA)			Errors (MVA)				Line Loading (MVA)			Errors (MVA)	
		Max	Min	Mean	Mean	Devia			Max	Min	Mean	Mean	Devia
161	DTS	-265.32	-308.81	-285.06			181	DTS	-0.06	-0.13	-0.09		
	Chron	-273.71	-307.70	-288.00	-2.94	2.13		Chron	-0.06	-0.12	-0.09	0.00	0.00
	Dur	-273.78	-303.42	-288.05	-3.00	3.10		Dur	-0.05	-0.12	-0.09	0.00	0.03
162	DTS	-265.32	-308.81	-285.06			182	DTS	4.83	1.93	3.21		
	Chron	-273.71	-307.70	-288.00	-2.94	2.13		Chron	4.26	1.98	3.11	-0.10	0.15
	Dur	-273.78	-303.42	-288.05	-3.00	3.10		Dur	4.28	1.96	3.11	-0.10	0.14
163	DTS	142.01	78.37	109.79			183	DTS	4.83	1.93	3.21		
	Chron	131.63	83.53	106.90	-2.89	3.17		Chron	4.26	1.98	3.11	-0.10	0.15
	Dur	131.61	83.11	106.90	-2.89	2.78		Dur	4.28	1.96	3.11	-0.10	0.14
164	DTS	354.87	290.58	323.66			184	DTS	0.00	0.00	0.00		
	Chron	345.40	296.67	320.31	-3.35	3.12		Chron	0.00	0.00	0.00	0.00	0.00
	Dur	345.54	296.82	320.30	-3.36	2.85		Dur	0.00	0.00	0.00	0.00	0.00
165	DTS	0.00	-0.00	0.00			185	DTS	0.00	0.00	0.00		
	Chron	0.00	-0.00	0.00	0.00	0.00		Chron	0.00	0.00	0.00	0.00	0.00
	Dur	0.00	-0.00	0.00	0.00	0.00		Dur	0.00	0.00	0.00	0.00	0.00
166	DTS	-40.83	-78.27	-63.71			186	DTS	0.00	0.00	0.00		
	Chron	-39.49	-79.46	-62.76	0.95	2.33		Chron	0.00	0.00	0.00	0.00	0.00
	Dur	-50.13	-75.68	-62.75	0.96	12.14		Dur	0.00	0.00	0.00	0.00	0.00
167	DTS	603.97	514.30	552.67			187	DTS	14.26	9.62	12.06		
	Chron	585.01	519.14	549.99	-2.68	5.06		Chron	13.34	10.15	11.84	-0.22	0.24
	Dur	583.98	506.29	550.05	-2.62	5.11		Dur	13.04	10.06	11.69	-0.37	0.23
168	DTS	603.97	514.30	552.67			188	DTS	12.70	8.44	10.86		
	Chron	585.01	519.14	549.99	-2.68	5.06		Chron	12.07	9.18	10.68	-0.18	0.22
	Dur	583.98	506.29	550.05	-2.62	5.11		Dur	11.76	9.10	10.51	-0.35	0.20
169	DTS	0.00	0.00	0.00			189	DTS	-3.45	-6.53	-4.76		
	Chron	0.00	0.00	0.00	0.00	0.00		Chron	-3.47	-6.04	-4.62	0.14	0.16
	Dur	0.00	0.00	0.00	0.00	0.00		Dur	-3.47	-6.38	-4.76	-0.00	0.95
170	DTS	-2.61	-7.57	-4.10			190	DTS	-3.45	-6.53	-4.76		
	Chron	-2.64	-5.11	-3.96	0.14	0.26		Chron	-3.47	-6.04	-4.62	0.14	0.16
	Dur	-2.78	-5.10	-3.94	0.16	0.94		Dur	-3.47	-6.38	-4.76	-0.00	0.95
171	DTS	-2.61	-7.57	-4.10			191	DTS	6.53	3.45	4.76		
	Chron	-2.64	-5.11	-3.96	0.14	0.26		Chron	6.04	3.47	4.62	-0.14	0.16
	Dur	-2.78	-5.10	-3.94	0.16	0.94		Dur	6.38	3.47	4.76	0.00	0.17
172	DTS	7.57	2.61	4.10			192	DTS	6.53	3.45	4.76		
	Chron	5.11	2.64	3.96	-0.14	0.26		Chron	6.04	3.47	4.62	-0.14	0.16
	Dur	5.10	2.78	3.94	-0.16	0.23		Dur	6.38	3.47	4.76	0.00	0.17
173	DTS	7.57	2.61	4.10			193	DTS	-8.11	-12.91	-10.48		
	Chron	5.11	2.64	3.96	-0.14	0.26		Chron	-8.51	-12.15	-10.26	0.22	0.24
	Dur	5.10	2.78	3.94	-0.16	0.23		Dur	-8.51	-12.07	-10.25	0.23	1.13
174	DTS	29.78	13.55	21.62			194	DTS	-8.11	-12.91	-10.48		
	Chron	27.86	13.84	20.90	-0.72	0.79		Chron	-8.51	-12.15	-10.26	0.22	0.24
	Dur	27.86	13.84	20.90	-0.72	0.70		Dur	-8.51	-12.07	-10.25	0.23	1.13
175	DTS	0.00	0.00	0.00			195	DTS	-7.29	-11.58	-9.52		
	Chron	0.00	0.00	0.00	0.00	0.00		Chron	-7.75	-10.89	-9.33	0.19	0.21
	Dur	0.00	0.00	0.00	0.00	0.00		Dur	-7.75	-11.10	-9.36	0.16	1.02
176	DTS	29.92	13.62	21.73			196	DTS	-7.32	-11.62	-9.52		
	Chron	27.99	13.93	21.01	-0.72	0.79		Chron	-7.74	-10.93	-9.33	0.19	0.21
	Dur	27.99	13.93	21.01	-0.72	0.71		Dur	-7.74	-11.06	-9.34	0.17	1.02
177	DTS	0.00	0.00	0.00			197	DTS	-7.83	-12.53	-10.15		
	Chron	0.00	0.00	0.00	0.00	0.00		Chron	-8.24	-11.79	-9.93	0.23	0.24
	Dur	0.00	0.00	0.00	0.00	0.00		Dur	-8.24	-11.66	-9.91	0.24	1.10
178	DTS	0.00	0.00	0.00			198	DTS	-8.76	-13.90	-11.31		
	Chron	0.00	0.00	0.00	0.00	0.00		Chron	-9.18	-13.08	-11.05	0.25	0.27
	Dur	0.00	0.00	0.00	0.00	0.00		Dur	-9.18	-13.03	-11.05	0.26	1.23
179	DTS	0.13	0.06	0.09			199	DTS	0.00	0.00	0.00		
	Chron	0.12	0.06	0.09	-0.00	0.00		Chron	0.00	0.00	0.00	0.00	0.00
	Dur	0.12	0.05	0.09	-0.00	0.00		Dur	0.00	0.00	0.00	0.00	0.00
180	DTS	0.00	0.00	0.00			200	DTS	0.00	0.00	0.00		
	Chron	0.00	0.00	0.00	0.00	0.00		Chron	0.00	0.00	0.00	0.00	0.00
	Dur	0.00	0.00	0.00	0.00	0.00		Dur	0.00	0.00	0.00	0.00	0.00

Table B.18 Line Loading Results for the 348 Node Test System (Cont.)

Load No.	Simulation Type	Comparison with Discrete Time Sim.					Load No.	Simulation Type	Comparison with Discrete Time Sim.				
		Line Loading (MVA)			Errors (MVA)				Line Loading (MVA)			Errors (MVA)	
		Max	Min	Mean	Mean	Devia			Max	Min	Mean	Mean	Devia
201	DTS	0.00	0.00	0.00			221	DTS	-23.97	-32.00	-27.43		
	Chron	0.00	0.00	0.00	0.00	0.00		Chron	-24.29	-30.50	-27.08	0.35	0.39
	Dur	0.00	0.00	0.00	0.00	0.00		Dur	-24.09	-30.59	-27.08	0.34	2.12
202	DTS	0.00	0.00	0.00			222	DTS	-24.15	-32.25	-27.64		
	Chron	0.00	0.00	0.00	0.00	0.00		Chron	-24.48	-30.73	-27.29	0.35	0.39
	Dur	0.00	0.00	0.00	0.00	0.00		Dur	-24.27	-30.82	-27.29	0.35	2.13
203	DTS	-40.93	-85.83	-59.14			223	DTS	4.30	-3.86	-0.68		
	Chron	-44.74	-71.76	-57.51	1.62	2.52		Chron	2.11	-3.46	-0.78	-0.09	0.48
	Dur	-43.87	-71.44	-57.08	2.06	9.36		Dur	1.92	-4.11	-0.79	-0.10	0.92
204	DTS	32.62	-0.14	7.25			224	DTS	0.08	0.07	0.08		
	Chron	14.47	2.82	7.12	-0.13	1.10		Chron	0.08	0.07	0.08	-0.00	0.00
	Dur	11.11	3.96	6.86	-0.39	3.36		Dur	0.08	0.07	0.08	-0.00	0.00
205	DTS	0.00	0.00	0.00			225	DTS	5.53	4.28	4.76		
	Chron	0.00	0.00	0.00	0.00	0.00		Chron	5.22	4.35	4.73	-0.03	0.07
	Dur	0.00	0.00	0.00	0.00	0.00		Dur	5.21	4.20	4.73	-0.03	0.08
206	DTS	26.22	4.22	16.10			226	DTS	-29.98	-43.56	-36.17		
	Chron	22.45	11.42	16.07	-0.03	3.16		Chron	-30.62	-41.05	-35.57	0.59	0.64
	Dur	22.45	11.30	16.07	-0.03	2.82		Dur	-30.25	-41.19	-35.59	0.58	3.55
207	DTS	26.22	4.22	16.10			227	DTS	-31.20	-44.43	-37.17		
	Chron	22.45	11.42	16.07	-0.03	3.16		Chron	-31.78	-41.97	-36.62	0.56	0.63
	Dur	22.45	11.30	16.07	-0.03	2.82		Dur	-31.38	-42.09	-36.63	0.55	3.47
208	DTS	256.82	223.16	238.69			228	DTS	-5.09	-10.14	-7.34		
	Chron	250.45	225.17	237.59	-1.10	1.81		Chron	-5.32	-9.20	-7.13	0.21	0.24
	Dur	250.21	222.19	237.60	-1.09	1.65		Dur	-5.19	-9.23	-7.13	0.21	1.31
209	DTS	-0.56	-0.74	-0.67			229	DTS	0.04	0.02	0.03		
	Chron	-0.57	-0.74	-0.66	0.00	0.01		Chron	0.04	0.03	0.03	0.00	0.00
	Dur	-0.62	-0.73	-0.66	0.00	0.05		Dur	0.04	0.03	0.03	0.00	0.00
210	DTS	0.15	0.12	0.13			230	DTS	-8.33	-11.40	-9.72		
	Chron	0.14	0.12	0.13	-0.00	0.00		Chron	-8.47	-10.83	-9.59	0.13	0.15
	Dur	0.14	0.12	0.13	-0.00	0.00		Dur	-8.40	-10.86	-9.59	0.13	0.79
211	DTS	-19.39	-37.73	-28.82			231	DTS	-8.39	-11.49	-9.79		
	Chron	-20.90	-34.68	-28.10	0.72	1.35		Chron	-8.53	-10.91	-9.66	0.13	0.15
	Dur	-20.52	-32.84	-28.25	0.57	2.93		Dur	-8.47	-10.94	-9.66	0.13	0.79
212	DTS	205.55	87.03	139.70			232	DTS	330.95	224.72	274.06		
	Chron	181.67	91.61	134.50	-5.19	5.56		Chron	311.94	230.08	269.50	-4.56	5.27
	Dur	183.64	89.58	134.62	-5.08	5.01		Dur	312.47	224.91	269.57	-4.49	4.54
213	DTS	22.96	2.88	11.65			233	DTS	6.02	4.31	5.07		
	Chron	18.53	3.32	11.25	-0.39	1.37		Chron	5.71	4.39	4.99	-0.07	0.08
	Dur	17.75	1.94	11.28	-0.36	2.52		Dur	5.73	4.34	4.99	-0.07	0.07
214	DTS	0.61	0.50	0.56			234	DTS	33.46	24.74	28.88		
	Chron	0.59	0.51	0.56	-0.00	0.01		Chron	31.93	25.19	28.52	-0.36	0.44
	Dur	0.59	0.51	0.56	-0.00	0.00		Dur	31.95	24.71	28.52	-0.36	0.38
215	DTS	14.51	8.42	12.17			235	DTS	-7.76	-55.10	-32.19		
	Chron	13.62	9.31	11.95	-0.22	0.33		Chron	-16.95	-52.34	-34.62	-2.43	2.03
	Dur	13.63	9.29	11.99	-0.18	0.28		Dur	-15.95	-52.12	-34.49	-2.30	1.83
216	DTS	14.52	11.47	12.82			236	DTS	84.01	66.83	74.54		
	Chron	13.88	11.72	12.74	-0.08	0.18		Chron	80.99	67.62	73.81	-0.74	0.82
	Dur	13.83	11.36	12.74	-0.08	0.21		Dur	81.34	67.09	73.85	-0.69	0.74
217	DTS	-115.11	-164.48	-136.83			237	DTS	4.06	3.03	3.49		
	Chron	-117.11	-155.43	-134.66	2.18	2.38		Chron	3.87	3.07	3.45	-0.04	0.05
	Dur	-115.63	-156.03	-134.69	2.14	13.16		Dur	3.88	3.04	3.45	-0.04	0.04
218	DTS	-119.85	-167.44	-140.57			238	DTS	26.52	14.81	20.08		
	Chron	-121.64	-158.65	-138.53	2.05	2.33		Chron	24.37	15.37	19.60	-0.49	0.55
	Dur	-120.05	-159.19	-138.55	2.02	12.72		Dur	24.53	14.98	19.61	-0.47	0.49
219	DTS	-14.41	-28.04	-20.17			239	DTS	26.71	14.92	20.23		
	Chron	-14.91	-25.51	-19.58	0.59	0.67		Chron	24.55	15.49	19.74	-0.49	0.55
	Dur	-14.51	-25.60	-19.57	0.60	3.61		Dur	24.71	15.09	19.75	-0.48	0.50
220	DTS	0.33	0.27	0.31			240	DTS	338.16	234.31	282.12		
	Chron	0.33	0.28	0.31	0.00	0.00		Chron	319.46	239.19	277.83	-4.29	5.22
	Dur	0.32	0.29	0.31	0.00	0.01		Dur	319.84	233.76	277.88	-4.25	4.52

Table B.19 Line Loading Results for the 348 Node Test System (Cont.)

Load No.	Simulation Type	Comparison with Discrete Time Sim.					Load No.	Simulation Type	Comparison with Discrete Time Sim.				
		Line Loading (MVA)			Errors (MVA)				Line Loading (MVA)			Errors (MVA)	
		Max	Min	Mean	Mean	Devia			Max	Min	Mean	Mean	Devia
241	DTS	6.13	4.49	5.20			261	DTS	4.82	3.70	4.19		
	Chron	5.83	4.56	5.13	-0.07	0.08		Chron	4.61	3.74	4.14	-0.05	0.06
	Dur	5.85	4.51	5.13	-0.07	0.07		Dur	4.63	3.72	4.14	-0.05	0.05
242	DTS	34.17	25.58	29.63			262	DTS	10.15	7.84	8.91		
	Chron	32.65	26.00	29.28	-0.34	0.44		Chron	9.72	7.95	8.82	-0.09	0.12
	Dur	32.66	25.49	29.29	-0.34	0.38		Dur	9.72	7.81	8.82	-0.09	0.10
243	DTS	85.90	70.73	77.43			263	DTS	3.20	2.57	2.85		
	Chron	83.22	71.37	76.79	-0.64	0.74		Chron	3.08	2.60	2.82	-0.03	0.03
	Dur	83.53	70.78	76.83	-0.60	0.67		Dur	3.09	2.59	2.82	-0.03	0.03
244	DTS	4.14	3.14	3.59									
	Chron	3.95	3.19	3.54	-0.04	0.05							
	Dur	3.96	3.16	3.55	-0.04	0.04							
245	DTS	27.25	16.74	21.41									
	Chron	25.30	17.23	20.99	-0.42	0.50							
	Dur	25.44	16.79	21.00	-0.41	0.45							
246	DTS	27.44	16.87	21.57									
	Chron	25.49	17.36	21.14	-0.42	0.51							
	Dur	25.62	16.91	21.15	-0.42	0.46							
247	DTS	74.24	35.54	53.25									
	Chron	67.37	37.51	51.66	-1.59	2.01							
	Dur	67.24	35.16	51.64	-1.61	1.73							
248	DTS	308.72	179.93	237.35									
	Chron	285.44	186.09	231.80	-5.56	6.23							
	Dur	286.22	183.13	231.78	-5.58	5.56							
249	DTS	10.97	7.51	9.14									
	Chron	10.37	7.69	9.00	-0.13	0.18							
	Dur	10.35	7.46	9.00	-0.14	0.16							
250	DTS	196.01	117.27	152.51									
	Chron	181.93	120.40	149.11	-3.41	3.73							
	Dur	182.91	119.12	149.04	-3.47	3.41							
251	DTS	-118.62	-121.44	-120.11									
	Chron	-118.89	-121.18	-120.18	-0.07	0.23							
	Dur	-119.38	-121.34	-120.26	-0.14	0.27							
252	DTS	-119.55	-122.38	-121.04									
	Chron	-119.81	-122.12	-121.11	-0.07	0.24							
	Dur	-120.31	-122.28	-121.19	-0.15	0.28							
253	DTS	-0.20	-0.42	-0.31									
	Chron	-0.21	-0.41	-0.31	-0.00	0.01							
	Dur	-0.27	-0.41	-0.31	-0.00	0.04							
254	DTS	0.12	0.09	0.11									
	Chron	0.12	0.09	0.11	-0.00	0.00							
	Dur	0.11	0.09	0.11	-0.00	0.00							
255	DTS	88.59	63.32	74.85									
	Chron	83.89	64.58	73.85	-1.00	1.28							
	Dur	83.92	63.19	73.86	-0.99	1.10							
256	DTS	4.79	3.67	4.15									
	Chron	4.58	3.72	4.11	-0.05	0.05							
	Dur	4.59	3.69	4.11	-0.05	0.05							
257	DTS	10.07	7.78	8.84									
	Chron	9.65	7.89	8.75	-0.09	0.12							
	Dur	9.64	7.75	8.76	-0.09	0.10							
258	DTS	3.17	2.55	2.83									
	Chron	3.05	2.58	2.80	-0.03	0.03							
	Dur	3.06	2.57	2.80	-0.03	0.03							
259	DTS	0.00	0.00	0.00									
	Chron	0.00	0.00	0.00	0.00	0.00							
	Dur	0.00	0.00	0.00	0.00	0.00							
260	DTS	89.28	63.79	75.42									
	Chron	84.54	65.07	74.41	-1.01	1.29							
	Dur	84.57	63.66	74.42	-1.00	1.11							

Table B.20 Line Loss Results for the 348 Node Test System

Line No.	Simulation Type	Comparison with Discrete Time Sim. Line Loss (kW)			Errors (kW)		Line No.	Simulation Type	Comparison with Discrete Time Sim. Line Loss (kW)			Errors (kW)	
		Max	Min	Mean	Mean	Devia			Max	Min	Mean	Mean	Devia
1	DTS	1737.0	32.5	315.1			21	DTS	295.3	103.7	172.5		
	Chron	1442.4	59.1	365.8	50.7	74.3		Chron	224.4	108.1	163.7	-8.8	11.9
	Dur	1445.6	56.8	376.2	61.1	390.0		Dur	232.6	101.0	163.4	-9.1	10.9
2	DTS	1743.8	32.6	316.3			22	DTS	223.4	16.1	79.0		
	Chron	1448.1	59.3	367.2	50.9	74.6		Chron	206.9	17.8	73.2	-5.8	21.4
	Dur	1451.2	57.0	377.6	61.3	391.5		Dur	207.5	18.8	74.0	-5.0	25.1
3	DTS	2638.3	0.7	589.3			23	DTS	359.7	167.6	244.0		
	Chron	1889.0	87.8	645.0	55.7	117.4		Chron	312.1	174.0	232.8	-11.2	17.0
	Dur	2052.7	128.8	705.5	116.2	123.1		Dur	315.1	172.4	232.7	-11.3	14.3
4	DTS	2617.1	0.7	584.6			24	DTS	521.0	242.7	382.9		
	Chron	1873.8	87.1	639.8	55.2	116.4		Chron	530.4	289.0	392.9	10.0	26.0
	Dur	2036.2	127.8	699.9	115.3	122.1		Dur	499.0	299.5	384.2	1.2	58.4
5	DTS	10004.0	2139.6	5049.4			25	DTS	313.3	15.9	140.8		
	Chron	7986.0	2352.3	4701.7	-347.7	368.7		Chron	294.4	47.0	151.0	10.2	17.5
	Dur	8098.9	2343.3	4708.3	-341.1	324.4		Dur	291.5	40.6	154.3	13.5	70.7
6	DTS	10116.0	2163.7	5106.2			26	DTS	334.6	56.5	149.2		
	Chron	8075.8	2378.7	4754.6	-351.6	372.8		Chron	245.9	64.8	141.8	-7.4	14.5
	Dur	8189.9	2369.7	4761.2	-345.0	328.0		Dur	245.2	62.9	141.1	-8.1	13.0
7	DTS	8091.1	1883.5	4224.4			27	DTS	328.9	55.5	146.7		
	Chron	6578.6	2085.6	3951.8	-272.6	291.1		Chron	241.8	63.6	139.4	-7.3	14.2
	Dur	6640.3	2086.9	3958.8	-265.6	258.5		Dur	241.1	61.8	138.7	-8.0	12.8
8	DTS	8091.1	1883.5	4224.4			28	DTS	0.4	0.0	0.0		
	Chron	6578.6	2085.6	3951.8	-272.6	291.1		Chron	0.2	0.0	0.0	0.0	0.0
	Dur	6640.3	2086.9	3958.8	-265.6	258.5		Dur	0.2	0.0	0.0	0.0	0.0
9	DTS	63.2	0.8	12.9			29	DTS	1.0	0.0	0.1		
	Chron	30.3	2.7	8.7	-4.1	5.6		Chron	0.5	0.0	0.1	0.0	0.1
	Dur	26.9	3.0	7.9	-5.0	6.2		Dur	0.4	0.0	0.1	0.0	0.1
10	DTS	692.3	166.2	343.8			30	DTS	2219.3	77.7	597.8		
	Chron	488.6	196.7	324.1	-19.8	46.9		Chron	1921.9	105.6	689.7	91.9	94.0
	Dur	480.8	190.5	320.5	-23.3	45.7		Dur	1914.6	107.5	696.3	98.5	568.9
11	DTS	1879.7	450.9	948.3			31	DTS	1784.2	69.6	350.8		
	Chron	1343.6	508.3	891.1	-57.2	101.6		Chron	1488.3	82.9	404.8	54.0	73.7
	Dur	1315.4	486.3	881.6	-66.7	97.0		Dur	1485.9	82.8	414.9	64.0	403.4
12	DTS	113.0	65.7	88.7			32	DTS	2973.7	784.9	1681.8		
	Chron	108.1	70.7	89.5	0.8	3.8		Chron	2410.1	865.7	1558.1	-123.6	117.9
	Dur	99.7	73.5	89.2	0.6	12.2		Dur	2574.2	874.8	1585.2	-96.6	110.5
13	DTS	216.1	14.2	77.9			33	DTS	373.7	25.3	188.8		
	Chron	163.6	12.2	68.0	-9.9	10.7		Chron	300.6	66.8	177.1	-11.7	28.0
	Dur	156.3	12.1	67.4	-10.4	10.1		Dur	314.1	66.9	180.8	-7.9	25.2
14	DTS	65.3	0.3	9.1			34	DTS	1346.4	375.8	687.5		
	Chron	47.3	0.1	8.7	-0.4	3.8		Chron	947.3	400.4	635.5	-51.9	53.6
	Dur	47.8	0.1	9.1	0.1	9.3		Dur	995.3	405.0	659.3	-28.1	47.4
15	DTS	988.9	212.5	488.0			35	DTS	222.9	54.2	118.3		
	Chron	732.5	217.5	454.0	-34.0	42.1		Chron	174.5	50.0	118.0	-0.3	18.8
	Dur	750.3	219.2	450.5	-37.5	40.0		Dur	211.5	82.2	138.7	20.4	19.1
16	DTS	527.1	37.1	185.9			36	DTS	506.0	21.5	160.6		
	Chron	479.3	43.4	176.2	-9.7	53.6		Chron	363.5	30.9	150.2	-10.4	46.8
	Dur	517.6	49.8	182.2	-3.7	62.8		Dur	340.1	28.4	121.4	-39.2	48.2
17	DTS	310.7	18.9	126.3			37	DTS	8.5	1.5	4.2		
	Chron	230.6	19.6	111.2	-15.1	26.5		Chron	6.8	1.7	3.9	-0.2	0.5
	Dur	288.6	18.2	105.1	-21.2	21.4		Dur	6.8	1.7	3.9	-0.3	0.4
18	DTS	670.8	159.8	301.9			38	DTS	7.9	1.4	3.9		
	Chron	515.2	158.2	286.6	-15.3	35.9		Chron	6.3	1.6	3.6	-0.2	0.4
	Dur	432.4	228.9	298.8	-3.1	79.5		Dur	6.3	1.6	3.6	-0.3	0.4
19	DTS	332.2	125.1	232.7			39	DTS	497.5	81.9	228.0		
	Chron	329.2	154.1	241.4	8.7	12.2		Chron	381.9	72.1	211.0	-17.1	28.4
	Dur	329.5	150.6	242.1	9.5	58.2		Dur	396.4	68.2	203.8	-24.2	26.1
20	DTS	81.2	5.7	38.4			40	DTS	427.8	29.1	152.2		
	Chron	78.7	11.8	42.2	3.8	5.7		Chron	277.8	32.5	136.8	-15.4	26.0
	Dur	78.6	11.7	42.4	4.0	22.0		Dur	279.2	33.4	130.0	-22.2	26.2

Table B.21 Line Loss Results for the 348 Node Test System (Cont.)

Line No.	Simulation Type	Comparison with Discrete Time Sim.					Line No.	Simulation Type	Comparison with Discrete Time Sim.				
		Line Loss (kW)			Errors (kW)				Line Loss (kW)			Errors (kW)	
		Max	Min	Mean	Mean	Devia			Max	Min	Mean	Mean	Devia
41	DTS	390.7	49.8	136.9			61	DTS	1934.7	388.6	983.0		
	Chron	217.5	52.4	126.7	-10.2	19.4		Chron	1553.9	393.1	929.0	-54.0	80.0
	Dur	219.4	52.2	125.9	-11.0	18.3		Dur	1545.8	404.2	926.0	-57.0	72.9
42	DTS	1755.2	335.8	842.3			62	DTS	0.0	0.0	0.0		
	Chron	1288.1	337.9	787.0	-55.3	78.2		Chron	0.0	0.0	0.0	0.0	0.0
	Dur	1273.1	335.9	781.2	-61.1	71.7		Dur	0.0	0.0	0.0	0.0	0.0
43	DTS	103.1	9.4	27.6			63	DTS	383.4	67.7	178.2		
	Chron	43.0	10.1	24.5	-3.1	6.0		Chron	300.6	67.0	166.8	-11.4	17.5
	Dur	44.2	10.1	24.4	-3.2	5.8		Dur	315.3	72.9	169.4	-8.8	15.9
44	DTS	75.4	14.2	35.6			64	DTS	464.1	80.0	211.0		
	Chron	54.3	14.3	33.2	-2.5	3.5		Chron	375.7	80.4	196.2	-14.7	19.9
	Dur	53.7	14.2	32.9	-2.7	3.2		Dur	383.1	82.2	187.7	-23.3	18.9
45	DTS	2298.9	467.1	1202.9			65	DTS	15.9	2.9	7.3		
	Chron	1785.4	485.0	1120.5	-82.4	110.2		Chron	12.5	2.9	6.8	-0.5	0.6
	Dur	1740.2	485.0	1110.3	-92.6	100.1		Dur	12.8	3.0	6.7	-0.5	0.6
46	DTS	2942.5	856.1	1657.8			66	DTS	50.6	11.3	25.0		
	Chron	2405.4	931.4	1593.6	-64.2	130.7		Chron	39.8	11.5	23.4	-1.6	2.0
	Dur	2271.1	850.8	1587.1	-70.8	122.0		Dur	39.9	11.2	23.2	-1.8	1.9
47	DTS	29.3	3.2	10.8			67	DTS	31.8	6.7	16.0		
	Chron	22.8	3.5	10.9	0.1	3.3		Chron	26.7	7.1	15.2	-0.8	1.2
	Dur	19.9	3.6	8.8	-2.0	3.5		Dur	26.7	7.1	15.0	-1.0	1.1
48	DTS	53.4	3.5	11.3			68	DTS	24.9	5.0	12.3		
	Chron	16.4	3.9	9.3	-1.9	3.4		Chron	20.9	5.4	11.7	-0.6	1.0
	Dur	17.4	3.9	9.4	-1.9	3.3		Dur	21.0	5.4	11.6	-0.7	0.9
49	DTS	0.0	0.0	0.0			69	DTS	426.5	58.3	184.7		
	Chron	0.0	0.0	0.0	0.0	0.0		Chron	305.7	62.3	173.8	-10.9	22.7
	Dur	0.0	0.0	0.0	0.0	0.0		Dur	328.0	67.5	173.1	-11.6	19.9
50	DTS	3.5	0.0	0.4			70	DTS	1488.5	305.7	718.6		
	Chron	2.1	0.0	0.3	-0.1	0.4		Chron	1156.1	316.5	667.5	-51.2	63.7
	Dur	2.0	0.0	0.2	-0.2	0.4		Dur	1170.6	312.4	661.5	-57.1	60.0
51	DTS	3.1	0.0	0.3			71	DTS	17.1	5.6	9.4		
	Chron	1.9	0.0	0.2	-0.1	0.4		Chron	12.1	6.1	8.8	-0.5	1.0
	Dur	1.7	0.0	0.2	-0.2	0.3		Dur	13.4	4.9	8.9	-0.5	1.0
52	DTS	3.5	0.0	0.4			72	DTS	17.0	5.6	9.3		
	Chron	2.1	0.0	0.3	-0.1	0.4		Chron	12.1	6.1	8.8	-0.5	1.0
	Dur	2.0	0.0	0.2	-0.2	0.4		Dur	13.3	4.9	8.9	-0.5	1.0
53	DTS	6.5	1.1	3.1			73	DTS	115.7	16.0	49.0		
	Chron	5.1	1.1	3.0	-0.2	0.3		Chron	85.1	18.7	46.0	-2.9	5.4
	Dur	5.3	1.1	2.9	-0.2	0.3		Dur	85.0	18.9	45.5	-3.4	5.0
54	DTS	2.4	0.4	1.2			74	DTS	124.8	17.2	52.8		
	Chron	1.9	0.4	1.1	-0.1	0.1		Chron	91.7	20.2	49.6	-3.2	5.8
	Dur	2.0	0.4	1.1	-0.1	0.1		Dur	91.7	20.3	49.1	-3.7	5.4
55	DTS	160.4	20.7	71.1			75	DTS	426.1	110.0	213.2		
	Chron	127.8	22.0	67.6	-3.5	7.6		Chron	291.0	121.3	200.7	-12.5	17.7
	Dur	131.6	22.1	64.3	-6.8	8.1		Dur	296.2	114.0	198.5	-14.8	14.9
56	DTS	230.4	39.9	112.8			76	DTS	0.0	0.0	0.0		
	Chron	177.1	41.5	107.7	-5.1	11.6		Chron	0.0	0.0	0.0	0.0	0.0
	Dur	184.7	41.4	106.9	-5.9	10.0		Dur	0.0	0.0	0.0	0.0	0.0
57	DTS	487.9	102.3	252.6			77	DTS	0.0	0.0	0.0		
	Chron	389.8	108.3	238.1	-14.5	20.4		Chron	0.0	0.0	0.0	0.0	0.0
	Dur	395.0	108.4	233.5	-19.1	18.8		Dur	0.0	0.0	0.0	0.0	0.0
58	DTS	282.9	58.2	144.6			78	DTS	538.2	28.8	213.3		
	Chron	219.3	61.4	136.7	-7.9	12.1		Chron	489.1	64.4	237.0	23.7	22.1
	Dur	216.5	61.3	135.4	-9.2	10.9		Dur	486.9	61.0	237.7	24.4	137.3
59	DTS	1001.9	221.6	524.6			79	DTS	910.9	479.7	676.8		
	Chron	802.1	231.4	494.3	-30.3	41.2		Chron	882.4	546.0	700.9	24.1	18.3
	Dur	812.9	231.3	486.9	-37.7	38.0		Dur	875.0	541.2	700.5	23.7	106.7
60	DTS	582.7	132.2	306.0			80	DTS	5624.1	1001.1	2691.6		
	Chron	458.5	135.7	288.7	-17.3	24.5		Chron	4499.3	1137.6	2493.7	-197.9	216.6
	Dur	448.8	136.2	285.6	-20.4	22.2		Dur	4582.6	1133.6	2501.3	-190.4	193.3

Table B.22 Line Loss Results for the 348 Node Test System (Cont.)

Line No.	Simulation Type	Comparison with Discrete Time Sim.					Line No.	Simulation Type	Comparison with Discrete Time Sim.				
		Line Loss (kW)			Errors (kW)				Line Loss (kW)			Errors (kW)	
		Max	Min	Mean	Mean	Devia			Max	Min	Mean	Mean	Devia
81	DTS	88.0	14.7	41.0			101	DTS	5262.0	2992.2	3920.4		
	Chron	69.9	16.7	37.9	-3.1	3.4		Chron	4775.4	3070.4	3821.6	-98.8	108.2
	Dur	71.2	16.6	38.0	-3.0	3.1		Dur	4818.6	3040.5	3823.4	-97.1	97.4
82	DTS	52.1	10.9	26.3			102	DTS	2143.8	1385.9	1690.0		
	Chron	38.2	11.7	25.7	-0.6	3.3		Chron	1974.9	1410.2	1656.8	-33.2	37.0
	Dur	43.0	12.3	27.7	1.4	3.3		Dur	1991.3	1399.3	1657.7	-32.3	33.2
83	DTS	80.8	5.6	35.9			103	DTS	0.0	0.0	0.0		
	Chron	61.2	9.9	29.5	-6.4	8.6		Chron	0.0	0.0	0.0	0.0	0.0
	Dur	61.4	18.6	37.3	1.4	8.9		Dur	0.0	0.0	0.0	0.0	0.0
84	DTS	125.6	19.3	65.8			104	DTS	0.0	0.0	0.0		
	Chron	111.3	34.1	62.9	-3.0	5.1		Chron	0.0	0.0	0.0	0.0	0.0
	Dur	111.4	34.0	62.9	-3.0	4.6		Dur	0.0	0.0	0.0	0.0	0.0
85	DTS	125.5	19.3	65.8			105	DTS	535.1	79.0	219.0		
	Chron	111.3	34.1	62.8	-3.0	5.1		Chron	357.7	105.4	193.9	-25.1	32.8
	Dur	111.3	34.0	62.8	-3.0	4.6		Dur	356.4	105.4	191.1	-28.0	31.7
86	DTS	86.0	11.8	42.8			106	DTS	539.3	79.7	220.8		
	Chron	74.8	16.8	37.7	-5.1	8.5		Chron	360.6	106.3	195.3	-25.5	33.1
	Dur	74.9	16.8	37.3	-5.5	8.5		Dur	359.3	106.3	192.4	-28.4	32.1
87	DTS	52.0	6.7	26.4			107	DTS	21.9	0.1	3.0		
	Chron	43.8	10.5	22.7	-3.7	6.7		Chron	5.3	0.1	1.1	-1.9	2.6
	Dur	43.8	10.5	22.4	-3.9	6.7		Dur	5.3	0.1	1.1	-1.9	2.6
88	DTS	75.4	11.5	36.0			108	DTS	0.0	0.0	0.0		
	Chron	59.6	13.6	32.8	-3.2	3.2		Chron	0.0	0.0	0.0	0.0	0.0
	Dur	59.8	13.6	32.5	-3.5	3.2		Dur	0.0	0.0	0.0	0.0	0.0
89	DTS	131.9	24.3	67.7			109	DTS	406.2	221.9	298.3		
	Chron	102.4	30.7	60.7	-6.9	9.5		Chron	367.6	228.1	290.3	-8.1	8.7
	Dur	102.5	30.7	60.2	-7.5	9.4		Dur	371.1	225.9	290.4	-7.9	7.8
90	DTS	150.4	27.5	76.3			110	DTS	361.5	193.8	263.4		
	Chron	119.2	34.2	68.7	-7.6	9.9		Chron	326.4	199.4	256.1	-7.3	7.9
	Dur	119.3	34.2	68.1	-8.2	9.8		Dur	329.4	197.5	256.3	-7.1	7.1
91	DTS	0.2	0.0	0.1			111	DTS	318.7	122.4	182.9		
	Chron	0.2	0.0	0.1	0.0	0.0		Chron	231.1	121.9	172.6	-10.3	12.9
	Dur	0.2	0.0	0.1	0.0	0.0		Dur	230.7	119.6	170.6	-12.4	12.6
92	DTS	0.2	0.0	0.1			112	DTS	578.5	163.1	314.2		
	Chron	0.2	0.0	0.1	0.0	0.0		Chron	444.5	174.3	294.9	-19.3	18.9
	Dur	0.2	0.0	0.1	0.0	0.0		Dur	445.5	165.9	296.6	-17.6	18.0
93	DTS	0.0	0.0	0.0			113	DTS	0.2	0.0	0.0		
	Chron	0.0	0.0	0.0	0.0	0.0		Chron	0.1	0.0	0.0	0.0	0.0
	Dur	0.0	0.0	0.0	0.0	0.0		Dur	0.4	0.0	0.3	0.2	0.1
94	DTS	416.9	1.3	98.5			114	DTS	0.1	0.0	0.1		
	Chron	270.5	16.3	82.3	-16.2	22.4		Chron	0.1	0.0	0.1	0.0	0.0
	Dur	283.4	16.6	84.8	-13.7	19.9		Dur	0.1	0.0	0.1	0.0	0.0
95	DTS	1368.5	468.9	830.3			115	DTS	0.2	0.0	0.1		
	Chron	1160.8	502.4	786.9	-43.3	40.7		Chron	0.1	0.0	0.1	0.0	0.0
	Dur	1173.6	491.5	789.1	-41.1	35.6		Dur	0.1	0.0	0.1	0.0	0.0
96	DTS	875.6	474.0	684.2			116	DTS	108.3	15.1	39.7		
	Chron	774.9	477.9	633.8	-50.4	17.3		Chron	82.2	15.2	36.4	-3.3	3.8
	Dur	776.5	514.7	634.6	-49.5	17.0		Dur	82.8	15.1	36.3	-3.4	3.6
97	DTS	0.0	0.0	0.0			117	DTS	121.5	16.5	44.3		
	Chron	0.0	0.0	0.0	0.0	0.0		Chron	92.3	16.6	40.7	-3.7	4.3
	Dur	0.0	0.0	0.0	0.0	0.0		Dur	93.0	16.6	40.5	-3.8	4.0
98	DTS	9654.2	6077.0	7636.1			118	DTS	53.7	10.2	25.3		
	Chron	8887.7	6231.6	7456.0	-180.1	166.2		Chron	42.6	11.6	23.5	-1.8	2.3
	Dur	8996.1	6123.8	7479.1	-157.0	152.0		Dur	45.3	12.9	23.5	-1.8	2.1
99	DTS	187.9	4.1	64.3			119	DTS	1.4	0.2	0.6		
	Chron	166.7	10.6	71.4	7.1	8.5		Chron	1.2	0.3	0.6	0.0	0.1
	Dur	166.3	10.0	71.6	7.3	51.6		Dur	1.2	0.3	0.6	0.0	0.0
100	DTS	404.1	376.0	386.3			120	DTS	0.0	0.0	0.0		
	Chron	395.9	377.1	384.5	-1.8	2.2		Chron	0.0	0.0	0.0	0.0	0.0
	Dur	396.1	376.5	384.6	-1.7	2.0		Dur	0.0	0.0	0.0	0.0	0.0

Table B.23 Line Loss Results for the 348 Node Test System (Cont.)

Line No.	Simulation Type	Comparison with Discrete Time Sim.				
		Line Loss (kW)			Errors (kW)	
		Max	Min	Mean	Mean	Devia
121	DTS	1149.1	64.4	260.5		
	Chron	472.3	64.8	202.1	-58.4	68.1
	Dur	475.0	64.8	199.8	-60.7	65.6
122	DTS	1149.3	64.4	260.5		
	Chron	472.4	64.8	202.1	-58.4	68.1
	Dur	475.1	64.8	199.8	-60.7	65.6
123	DTS	0.0	0.0	0.0		
	Chron	0.0	0.0	0.0	0.0	0.0
	Dur	0.0	0.0	0.0	0.0	0.0
124	DTS	0.0	0.0	0.0		
	Chron	0.0	0.0	0.0	0.0	0.0
	Dur	0.0	0.0	0.0	0.0	0.0
125	DTS	279.9	131.1	212.1		
	Chron	272.0	145.3	212.5	0.4	11.9
	Dur	264.9	140.2	212.2	0.0	53.4
126	DTS	72.8	10.1	28.0		
	Chron	47.8	10.2	24.6	-3.4	3.4
	Dur	48.3	10.1	24.6	-3.4	3.2
127	DTS	0.6	0.5	0.5		
	Chron	0.6	0.5	0.6	0.0	0.0
	Dur	0.6	0.5	0.5	0.0	0.0
128	DTS	12518.0	8478.6	10205.9		
	Chron	11704.0	8660.9	10041.4	-164.4	192.7
	Dur	11729.0	8564.2	10038.7	-167.2	173.1
129	DTS	0.7	0.7	0.7		
	Chron	0.7	0.7	0.7	0.0	0.0
	Dur	0.7	0.7	0.7	0.0	0.0
130	DTS	1229.6	803.7	979.1		
	Chron	1135.9	818.4	960.8	-18.3	20.0
	Dur	1143.8	812.0	961.3	-17.8	18.0
131	DTS	14.8	10.8	11.9		
	Chron	13.5	10.8	11.7	-0.2	0.2
	Dur	13.6	10.9	11.8	-0.2	0.2
132	DTS	14.6	10.4	11.6		
	Chron	13.3	10.5	11.4	-0.2	0.2
	Dur	13.4	10.6	11.5	-0.2	0.2
133	DTS	838.5	776.5	800.5		
	Chron	816.3	782.5	800.5	0.0	4.1
	Dur	813.5	781.9	801.9	1.4	10.0
134	DTS	238.2	178.6	208.7		
	Chron	235.0	186.5	211.1	2.4	3.8
	Dur	237.2	187.3	213.8	5.1	19.7
135	DTS	0.0	0.0	0.0		
	Chron	0.0	0.0	0.0	0.0	0.0
	Dur	0.0	0.0	0.0	0.0	0.0
136	DTS	4.9	4.5	4.7		
	Chron	4.9	4.6	4.7	0.0	0.0
	Dur	4.9	4.6	4.8	0.1	0.1
137	DTS	123.4	17.9	35.7		
	Chron	79.1	19.1	33.2	-2.5	4.0
	Dur	81.8	18.9	33.4	-2.3	3.7
138	DTS	417.0	276.5	325.0		
	Chron	393.2	301.2	327.0	2.0	16.1
	Dur	391.0	295.5	327.2	2.1	14.9
139	DTS	515.1	399.7	426.3		
	Chron	498.3	400.4	427.4	1.1	8.3
	Dur	497.8	404.2	425.8	-0.4	17.0
140	DTS	39.6	13.7	18.7		
	Chron	27.1	14.0	17.3	-1.4	1.8
	Dur	27.9	14.2	17.2	-1.5	2.6

Line No.	Simulation Type	Comparison with Discrete Time Sim.				
		Line Loss (kW)			Errors (kW)	
		Max	Min	Mean	Mean	Devia
141	DTS	39.6	13.7	18.7		
	Chron	27.1	14.0	17.3	-1.4	1.8
	Dur	27.9	14.2	17.2	-1.5	2.6
142	DTS	1.8	0.6	1.1		
	Chron	1.6	0.6	1.1	-0.1	0.1
	Dur	1.8	0.6	1.1	0.0	0.1
143	DTS	1.9	0.6	1.1		
	Chron	1.6	0.6	1.1	-0.1	0.1
	Dur	1.8	0.6	1.1	0.0	0.1
144	DTS	1.8	0.6	1.1		
	Chron	1.6	0.6	1.1	-0.1	0.1
	Dur	1.8	0.6	1.1	0.0	0.1
145	DTS	164.5	58.7	104.6		
	Chron	143.5	69.7	100.9	-3.7	6.2
	Dur	145.4	69.0	99.3	-5.2	6.0
146	DTS	158.9	67.6	101.5		
	Chron	132.9	67.6	96.4	-5.1	5.5
	Dur	132.9	65.5	96.8	-4.7	5.5
147	DTS	28.2	10.3	20.1		
	Chron	25.8	10.8	20.2	0.2	2.2
	Dur	25.9	12.7	19.5	-0.5	2.4
148	DTS	60.8	28.4	40.1		
	Chron	51.5	28.7	38.1	-2.0	4.4
	Dur	57.7	26.2	38.7	-1.4	8.1
149	DTS	15.1	0.8	5.8		
	Chron	13.9	0.7	5.3	-0.5	2.3
	Dur	16.1	0.6	5.9	0.1	4.6
150	DTS	32.7	6.7	15.9		
	Chron	27.9	6.9	16.1	0.2	3.7
	Dur	22.6	8.6	14.1	-1.7	4.6
151	DTS	81.3	26.6	54.0		
	Chron	77.3	36.1	54.8	0.7	7.6
	Dur	82.4	37.4	55.8	1.8	12.2
152	DTS	81.0	26.6	53.8		
	Chron	77.0	35.9	54.6	0.7	7.6
	Dur	82.1	37.2	55.6	1.8	12.1
153	DTS	265.6	178.8	220.0		
	Chron	243.6	187.7	215.9	-4.1	8.0
	Dur	246.8	186.9	216.1	-3.9	9.5
154	DTS	264.7	178.0	219.1		
	Chron	242.9	186.9	215.0	-4.1	7.9
	Dur	245.8	186.1	215.1	-3.9	9.4
155	DTS	4635.4	1152.5	2579.8		
	Chron	3898.4	1344.8	2415.6	-164.1	168.6
	Dur	3925.7	1350.9	2417.9	-161.9	155.6
156	DTS	4576.6	1137.9	2547.0		
	Chron	3848.9	1327.7	2385.0	-162.1	166.5
	Dur	3875.9	1333.7	2387.2	-159.8	153.7
157	DTS	470.1	199.8	307.8		
	Chron	408.3	215.2	296.0	-11.7	12.7
	Dur	409.4	216.7	296.2	-11.6	11.4
158	DTS	475.7	202.2	311.4		
	Chron	413.0	217.8	299.5	-11.9	12.9
	Dur	414.2	219.2	299.7	-11.7	11.6
159	DTS	517.8	188.0	315.8		
	Chron	439.4	205.8	301.3	-14.5	15.6
	Dur	440.7	206.8	301.5	-14.4	14.1
160	DTS	1661.9	873.1	1222.3		
	Chron	1509.4	916.6	1194.4	-27.9	37.8
	Dur	1515.1	922.8	1195.4	-26.9	34.3

Table B.24 Line Loss Results for the 348 Node Test System (Cont.)

Line No.	Simu-lation Type	Comparison with Discrete Time Sim.					Line No.	Simu-lation Type	Comparison with Discrete Time Sim.				
		Line Loss (kW)			Errors (kW)				Line Loss (kW)			Errors (kW)	
		Max	Min	Mean	Mean	Devia			Max	Min	Mean	Mean	Devia
161	DTS	990.1	608.4	707.3			181	DTS	0.0	0.0	0.0		
	Chron	869.5	619.4	715.1	7.8	18.9		Chron	0.0	0.0	0.0	0.0	0.0
	Dur	878.0	650.2	718.0	10.7	33.3		Dur	0.0	0.0	0.0	0.0	0.0
162	DTS	990.1	608.4	707.3			182	DTS	3.7	0.6	1.7		
	Chron	869.5	619.4	715.1	7.8	18.9		Chron	2.9	0.6	1.6	-0.1	0.2
	Dur	878.0	650.2	718.0	10.7	33.3		Dur	3.0	0.6	1.6	-0.1	0.2
163	DTS	92.4	22.0	49.4			183	DTS	3.7	0.6	1.7		
	Chron	75.8	24.8	46.8	-2.7	3.5		Chron	2.9	0.6	1.6	-0.1	0.2
	Dur	76.1	24.7	46.8	-2.7	3.1		Dur	3.0	0.6	1.6	-0.1	0.2
164	DTS	1144.2	621.2	862.0			184	DTS	0.0	0.0	0.0		
	Chron	1051.4	646.8	846.4	-15.5	25.7		Chron	0.0	0.0	0.0	0.0	0.0
	Dur	1056.0	651.4	847.2	-14.7	23.4		Dur	0.0	0.0	0.0	0.0	0.0
165	DTS	2.7	2.5	2.6			185	DTS	0.0	0.0	0.0		
	Chron	2.7	2.5	2.6	0.0	0.0		Chron	0.0	0.0	0.0	0.0	0.0
	Dur	2.7	2.5	2.6	0.0	0.0		Dur	0.0	0.0	0.0	0.0	0.0
166	DTS	472.4	72.8	137.6			186	DTS	0.0	0.0	0.0		
	Chron	299.0	94.0	134.4	-3.2	16.3		Chron	0.0	0.0	0.0	0.0	0.0
	Dur	315.6	98.1	134.8	-2.8	15.5		Dur	0.0	0.0	0.0	0.0	0.0
167	DTS	1104.7	554.0	727.5			187	DTS	5.6	2.5	3.6		
	Chron	958.5	577.4	714.8	-12.7	26.6		Chron	4.6	2.6	3.5	-0.1	0.2
	Dur	963.4	553.7	716.6	-10.9	24.2		Dur	4.3	2.6	3.5	-0.2	0.3
168	DTS	1104.7	554.0	727.5			188	DTS	4.8	1.9	3.0		
	Chron	958.5	577.4	714.8	-12.7	26.6		Chron	3.7	2.1	2.8	-0.1	0.1
	Dur	963.4	553.7	716.6	-10.9	24.2		Dur	3.5	2.1	2.8	-0.2	0.2
169	DTS	0.0	0.0	0.0			189	DTS	0.6	0.1	0.3		
	Chron	0.0	0.0	0.0	0.0	0.0		Chron	0.4	0.1	0.3	0.0	0.0
	Dur	0.0	0.0	0.0	0.0	0.0		Dur	0.4	0.1	0.2	-0.1	0.0
170	DTS	0.1	0.0	0.0			190	DTS	0.6	0.1	0.3		
	Chron	0.1	0.0	0.0	0.0	0.0		Chron	0.4	0.1	0.3	0.0	0.0
	Dur	0.1	0.0	0.0	0.0	0.0		Dur	0.4	0.1	0.2	-0.1	0.0
171	DTS	0.1	0.0	0.0			191	DTS	0.6	0.1	0.3		
	Chron	0.1	0.0	0.0	0.0	0.0		Chron	0.5	0.1	0.3	0.0	0.0
	Dur	0.1	0.0	0.0	0.0	0.0		Dur	0.4	0.1	0.2	-0.1	0.0
172	DTS	0.1	0.0	0.0			192	DTS	0.6	0.1	0.3		
	Chron	0.1	0.0	0.0	0.0	0.0		Chron	0.5	0.1	0.3	0.0	0.0
	Dur	0.1	0.0	0.0	0.0	0.0		Dur	0.4	0.1	0.2	-0.1	0.0
173	DTS	0.1	0.0	0.0			193	DTS	0.3	0.1	0.2		
	Chron	0.1	0.0	0.0	0.0	0.0		Chron	0.3	0.1	0.2	0.0	0.0
	Dur	0.1	0.0	0.0	0.0	0.0		Dur	0.3	0.1	0.2	0.0	0.0
174	DTS	72.8	13.3	37.4			194	DTS	0.3	0.1	0.2		
	Chron	62.4	13.4	34.8	-2.6	2.9		Chron	0.3	0.1	0.2	0.0	0.0
	Dur	62.4	13.4	34.8	-2.6	2.6		Dur	0.3	0.1	0.2	0.0	0.0
175	DTS	0.0	0.0	0.0			195	DTS	0.2	0.1	0.2		
	Chron	0.0	0.0	0.0	0.0	0.0		Chron	0.2	0.1	0.2	0.0	0.0
	Dur	0.0	0.0	0.0	0.0	0.0		Dur	0.3	0.1	0.2	0.0	0.0
176	DTS	36.8	6.8	19.0			196	DTS	0.2	0.1	0.2		
	Chron	31.7	6.8	17.7	-1.3	1.5		Chron	0.2	0.1	0.2	0.0	0.0
	Dur	31.8	6.8	17.7	-1.3	1.3		Dur	0.2	0.1	0.2	0.0	0.0
177	DTS	0.0	0.0	0.0			197	DTS	0.3	0.1	0.2		
	Chron	0.0	0.0	0.0	0.0	0.0		Chron	0.3	0.1	0.2	0.0	0.0
	Dur	0.0	0.0	0.0	0.0	0.0		Dur	0.2	0.1	0.2	0.0	0.0
178	DTS	0.0	0.0	0.0			198	DTS	0.3	0.1	0.2		
	Chron	0.0	0.0	0.0	0.0	0.0		Chron	0.3	0.1	0.2	0.0	0.0
	Dur	0.0	0.0	0.0	0.0	0.0		Dur	0.3	0.1	0.2	0.0	0.0
179	DTS	0.0	0.0	0.0			199	DTS	0.0	0.0	0.0		
	Chron	0.0	0.0	0.0	0.0	0.0		Chron	0.0	0.0	0.0	0.0	0.0
	Dur	0.0	0.0	0.0	0.0	0.0		Dur	0.0	0.0	0.0	0.0	0.0
180	DTS	0.0	0.0	0.0			200	DTS	0.0	0.0	0.0		
	Chron	0.0	0.0	0.0	0.0	0.0		Chron	0.0	0.0	0.0	0.0	0.0
	Dur	0.0	0.0	0.0	0.0	0.0		Dur	0.0	0.0	0.0	0.0	0.0

Table B.25 Line Loss Results for the 348 Node Test System (Cont.)

Line No.	Simu-lation Type	Comparison with Discrete Time Sim.					Line No.	Simu-lation Type	Comparison with Discrete Time Sim.				
		Line Loss (kW)			Errors (kW)				Line Loss (kW)			Errors (kW)	
		Max	Min	Mean	Mean	Devia			Max	Min	Mean	Mean	Devia
201	DTS	0.0	0.0	0.0			221	DTS	213.6	115.2	155.2		
	Chron	0.0	0.0	0.0	0.0	0.0		Chron	192.1	118.6	151.1	-4.1	4.6
	Dur	0.0	0.0	0.0	0.0	0.0		Dur	193.3	116.6	151.1	-4.0	4.2
202	DTS	0.0	0.0	0.0			222	DTS	219.7	118.5	159.6		
	Chron	0.0	0.0	0.0	0.0	0.0		Chron	197.6	122.0	155.4	-4.2	4.8
	Dur	0.0	0.0	0.0	0.0	0.0		Dur	198.8	120.0	155.5	-4.2	4.3
203	DTS	2096.5	595.0	1076.4			223	DTS	277.3	1.7	38.7		
	Chron	1477.7	629.6	994.9	-81.5	83.7		Chron	144.8	3.0	33.3	-5.4	9.7
	Dur	1555.2	639.0	1034.1	-42.3	74.4		Dur	151.9	3.2	33.9	-4.8	9.0
204	DTS	119.7	29.9	64.7			224	DTS	0.1	0.1	0.1		
	Chron	95.0	27.5	64.5	-0.2	10.2		Chron	0.1	0.1	0.1	0.0	0.0
	Dur	114.9	45.2	75.7	11.0	10.3		Dur	0.1	0.1	0.1	0.0	0.0
205	DTS	0.0	0.0	0.0			225	DTS	56.2	21.6	29.6		
	Chron	0.0	0.0	0.0	0.0	0.0		Chron	43.2	22.7	28.8	-0.8	1.4
	Dur	0.0	0.0	0.0	0.0	0.0		Dur	43.5	21.3	28.8	-0.7	1.4
206	DTS	68.5	1.0	20.5			226	DTS	1366.1	633.3	928.4		
	Chron	43.3	8.1	20.4	-0.1	9.3		Chron	1206.9	657.9	897.7	-30.7	34.9
	Dur	43.2	7.8	20.3	-0.2	8.3		Dur	1216.4	641.2	898.7	-29.7	31.1
207	DTS	68.5	1.0	20.5			227	DTS	1431.0	696.7	993.4		
	Chron	43.3	8.1	20.4	-0.1	9.3		Chron	1272.4	723.5	962.9	-30.5	35.1
	Dur	43.2	7.8	20.3	-0.2	8.3		Dur	1281.5	704.6	963.8	-29.6	31.3
208	DTS	1176.3	758.8	904.6			228	DTS	16.4	5.1	9.2		
	Chron	1064.8	780.8	892.3	-12.2	19.2		Chron	13.5	5.3	8.7	-0.5	0.5
	Dur	1066.6	761.6	893.1	-11.5	17.4		Dur	13.6	5.1	8.7	-0.5	0.5
209	DTS	5.3	0.9	1.6			229	DTS	0.1	0.0	0.1		
	Chron	3.4	1.0	1.5	-0.1	0.2		Chron	0.1	0.0	0.1	0.0	0.0
	Dur	3.5	1.0	1.5	-0.1	0.1		Dur	0.1	0.0	0.1	0.0	0.0
210	DTS	2.7	0.8	1.2			230	DTS	209.8	112.4	152.3		
	Chron	2.0	0.9	1.2	0.0	0.1		Chron	188.9	115.6	148.2	-4.2	4.7
	Dur	2.0	0.8	1.2	0.0	0.1		Dur	189.9	113.7	148.3	-4.0	4.2
211	DTS	26.0	4.2	10.8			231	DTS	213.1	114.2	154.7		
	Chron	20.4	4.8	11.0	0.2	1.3		Chron	191.8	117.4	150.5	-4.2	4.7
	Dur	21.1	4.7	11.4	0.5	7.7		Dur	192.8	115.5	150.6	-4.1	4.2
212	DTS	182.2	25.4	70.3			232	DTS	11448.0	5273.1	7758.6		
	Chron	116.0	28.3	64.7	-5.5	5.8		Chron	10065.0	5496.1	7499.5	-259.1	304.9
	Dur	118.4	27.4	64.9	-5.4	5.3		Dur	10108.0	5248.8	7504.9	-253.7	263.9
213	DTS	131.3	3.0	13.3			233	DTS	151.4	75.4	106.1		
	Chron	52.3	2.1	10.9	-2.5	4.0		Chron	135.3	78.1	102.8	-3.2	3.7
	Dur	56.5	4.1	10.7	-2.6	4.1		Dur	136.4	76.4	102.9	-3.1	3.2
214	DTS	5.2	2.8	4.0			234	DTS	1119.6	572.0	791.8		
	Chron	4.5	2.9	3.9	-0.1	0.1		Chron	993.2	592.1	770.5	-21.3	26.4
	Dur	4.5	2.9	3.9	-0.1	0.1		Dur	996.4	569.4	770.9	-20.8	22.9
215	DTS	14.6	2.5	8.3			235	DTS	35.9	2.2	12.4		
	Chron	10.5	2.6	7.9	-0.3	0.7		Chron	36.6	3.8	12.8	0.4	1.8
	Dur	10.5	2.5	8.0	-0.3	0.6		Dur	35.6	3.6	13.0	0.6	9.8
216	DTS	67.7	32.9	42.8			236	DTS	508.1	320.7	401.3		
	Chron	56.0	34.4	42.0	-0.9	1.6		Chron	470.1	328.2	393.3	-8.1	8.7
	Dur	56.1	32.3	42.0	-0.8	1.7		Dur	474.0	323.2	393.8	-7.5	7.8
217	DTS	1901.2	899.9	1300.0			237	DTS	79.8	42.6	57.7		
	Chron	1685.6	934.0	1257.2	-42.9	47.7		Chron	71.8	44.0	56.1	-1.6	1.8
	Dur	1699.6	909.9	1258.2	-41.8	42.7		Dur	72.4	43.3	56.2	-1.5	1.6
218	DTS	2106.7	1046.3	1469.9			238	DTS	101.8	30.4	58.0		
	Chron	1879.1	1085.2	1425.4	-44.6	50.9		Chron	85.8	33.4	55.4	-2.6	3.3
	Dur	1893.1	1056.3	1426.3	-43.6	45.6		Dur	87.2	31.7	55.5	-2.5	3.0
219	DTS	136.0	38.6	71.4			239	DTS	104.3	31.2	59.5		
	Chron	111.7	41.4	67.2	-4.2	4.8		Chron	88.0	34.2	56.8	-2.7	3.4
	Dur	112.5	39.6	67.2	-4.3	4.3		Dur	89.4	32.5	56.9	-2.6	3.0
220	DTS	3.0	1.4	2.5			240	DTS	11978.0	5801.0	8268.1		
	Chron	2.9	1.5	2.6	0.1	0.1		Chron	10584.0	6021.5	8012.2	-255.8	307.8
	Dur	2.9	1.5	2.6	0.1	0.5		Dur	10620.0	5749.3	8016.7	-251.4	266.7

Table B.26 Line Loss Results for the 348 Node Test System (Cont.)

Line No.	Simulation Type	Comparison with Discrete Time Sim.					Line No.	Simulation Type	Comparison with Discrete Time Sim.				
		Line Loss (kW)			Errors (kW)				Line Loss (kW)			Errors (kW)	
		Max	Min	Mean	Mean	Devia			Max	Min	Mean	Mean	Devia
241	DTS	148.2	77.1	105.9			261	DTS	73.9	42.7	55.4		
	Chron	133.2	79.9	102.9	-3.0	3.4		Chron	67.3	43.8	54.0	-1.4	1.5
	Dur	134.1	78.1	102.9	-2.9	3.0		Dur	67.7	43.3	54.1	-1.3	1.3
242	DTS	1180.3	621.0	844.3			262	DTS	234.5	126.0	166.7		
	Chron	1050.4	641.7	823.1	-21.3	27.1		Chron	206.8	130.1	162.9	-3.8	5.1
	Dur	1053.1	616.9	823.5	-20.8	23.5		Dur	207.3	125.5	163.0	-3.7	4.4
243	DTS	489.1	327.4	397.1			263	DTS	36.4	23.2	28.4		
	Chron	456.6	334.4	390.6	-6.5	7.6		Chron	33.4	23.5	27.8	-0.6	0.6
	Dur	459.8	328.8	391.1	-6.1	6.8		Dur	33.7	23.3	27.8	-0.6	0.6
244	DTS	77.4	43.2	57.1									
	Chron	70.0	44.7	55.7	-1.4	1.6							
	Dur	70.6	43.9	55.7	-1.4	1.5							
245	DTS	109.4	40.2	67.9									
	Chron	94.5	44.2	65.3	-2.6	3.2							
	Dur	95.8	42.0	65.4	-2.5	2.9							
246	DTS	112.1	41.2	69.6									
	Chron	96.8	45.3	66.9	-2.6	3.3							
	Dur	98.1	43.0	67.0	-2.5	2.9							
247	DTS	257.6	74.4	130.5									
	Chron	201.4	76.0	122.8	-7.7	9.1							
	Dur	201.2	69.4	122.7	-7.9	7.9							
248	DTS	110.7	45.9	69.4									
	Chron	95.2	48.0	66.6	-2.8	3.2							
	Dur	95.6	46.7	66.6	-2.8	2.8							
249	DTS	23.6	9.6	14.6									
	Chron	19.9	10.1	14.1	-0.5	0.7							
	Dur	19.9	9.5	14.1	-0.5	0.6							
250	DTS	313.4	177.4	225.0									
	Chron	274.0	186.4	219.5	-5.6	6.4							
	Dur	276.1	183.3	219.5	-5.5	5.8							
251	DTS	93.2	88.1	91.5									
	Chron	93.1	90.0	91.7	0.1	0.4							
	Dur	92.8	90.6	91.8	0.2	0.8							
252	DTS	102.6	97.0	100.8									
	Chron	102.5	99.1	101.0	0.2	0.4							
	Dur	102.2	99.8	101.1	0.3	0.8							
253	DTS	1.6	0.5	0.8									
	Chron	1.0	0.6	0.8	0.0	0.1							
	Dur	1.1	0.6	0.8	0.0	0.1							
254	DTS	1.6	0.6	0.9									
	Chron	1.2	0.7	0.9	0.0	0.0							
	Dur	1.2	0.7	0.9	0.0	0.1							
255	DTS	1956.6	959.0	1330.5									
	Chron	1701.5	990.4	1292.1	-38.3	48.0							
	Dur	1706.1	947.9	1292.9	-37.6	41.7							
256	DTS	74.1	42.8	55.6									
	Chron	67.5	43.9	54.2	-1.4	1.5							
	Dur	67.9	43.4	54.2	-1.3	1.3							
257	DTS	230.3	123.8	163.7									
	Chron	203.1	127.8	160.0	-3.7	5.0							
	Dur	203.5	123.2	160.1	-3.6	4.4							
258	DTS	36.6	23.3	28.5									
	Chron	33.6	23.6	27.9	-0.6	0.6							
	Dur	33.9	23.5	27.9	-0.6	0.6							
259	DTS	0.0	0.0	0.0									
	Chron	0.0	0.0	0.0	0.0	0.0							
	Dur	0.0	0.0	0.0	0.0	0.0							
260	DTS	1984.6	972.8	1349.6									
	Chron	1725.9	1004.6	1310.7	-38.9	48.7							
	Dur	1730.6	961.5	1311.5	-38.1	42.3							

Appendix C. Calculation of Losses Test Results

C.1 Introduction

This appendix contains full results for the tests in Section 8.4 of Chapter 8. The results compare the accuracy of four methods for calculating losses: archetypal days, linear loss coefficients, quadratic loss coefficients and discrete time simulation.

The tables list results for maximum and minimum demand loss and energy loss for each line in each of the test systems. The results for the discrete time simulation approach are used as a reference, and the errors and deviations from this reference are listed for each of the approximate loss calculation methods.

C.2 Test Results

C.2.1 7 Node Test System

Table C.1 Comparison of Loss Results for the 7 Node Test System

Line No.	Simulation Type	Comparison with Discrete Time Simulation				
		Loss (kW)			Errors on the Mean (kW)	
		Max	Min	Mean	Mean Error	Mean Devia on the Error
1	DTS	179.2	11.4	66.3		
	Arch Days	193.2	10.5	67.5	1.1	9.8
	Linear LC	179.2	11.4	66.3	0.0	0.0
	Quad LC	170.4	11.4	62.7	-3.7	16.9
2	DTS	179.6	11.4	66.5		
	Arch Days	193.7	10.5	67.6	1.2	9.8
	Linear LC	179.6	11.4	66.5	0.0	0.0
	Quad LC	170.8	11.4	62.8	-3.7	16.9
3	DTS	172.8	2.6	88.6		
	Arch Days	236.8	1.3	90.8	2.2	22.2
	Linear LC	361.7	22.9	133.9	45.2	42.9
	Quad LC	145.2	-7.2	100.2	11.6	42.8
4	DTS	157.9	2.4	81.1		
	Arch Days	216.3	1.2	83.1	2.0	20.3
	Linear LC	331.1	21.0	122.6	41.4	39.3
	Quad LC	132.9	-6.7	91.7	10.6	39.2

C.2.2 10 Node Test System

Table C.2 Comparison of Loss Results for the 10 Node Test System

Line No.	Simulation Type	Comparison with Discrete Time Simulation				
		Loss (kW)			Errors on the Mean (kW)	
		Max	Min	Mean	Mean Error	Mean Devia on the Error
1	DTS	369.0	2.4	164.7		
	Arch Days	412.2	2.2	154.9	-9.9	39.2
	Linear LC	369.8	2.3	164.7	0.0	0.3
	Quad LC	329.1	2.5	164.8	0.1	35.6
2	DTS	82.8	0.0	17.9		
	Arch Days	54.9	0.0	17.1	-0.8	5.9
	Linear LC	42.6	0.3	19.0	1.0	3.3
	Quad LC	35.5	0.4	18.0	0.0	5.5
3	DTS	0.9	0.0	0.4		
	Arch Days	1.0	0.0	0.3	0.0	0.1
	Linear LC	0.7	0.0	0.3	-0.1	0.1
	Quad LC	0.8	0.0	0.4	0.0	0.1
4	DTS	369.0	2.4	164.7		
	Arch Days	412.3	2.3	154.9	-9.9	39.2
	Linear LC	369.9	2.3	164.7	0.0	0.4
	Quad LC	329.2	2.5	164.8	0.1	35.7
5	DTS	83.2	0.0	18.0		
	Arch Days	55.2	0.0	17.2	-0.8	5.9
	Linear LC	42.8	0.3	19.0	1.0	3.3
	Quad LC	35.7	0.4	18.0	0.0	5.5
6	DTS	0.9	0.0	0.4		
	Arch Days	1.0	0.0	0.4	0.0	0.1
	Linear LC	0.7	0.0	0.3	-0.1	0.1
	Quad LC	0.8	0.0	0.4	0.0	0.1

C.2.3 15 Node Test System

Table C.3 Comparison of Loss Results for the 15 Node Test System

Line No.	Simulation Type	Comparison with Discrete Time Simulation				
		Loss (kW)			Errors on the Mean (kW)	
		Max	Min	Mean	Mean Error	Mean Devia on the Error
1	DTS	30.6	0.3	6.5		
	Arch Days	32.7	0.4	6.4	-0.1	1.1
	Linear LC	13.1	1.5	5.3	-1.2	2.5
	Quad LC	29.6	1.2	6.6	0.0	2.3
2	DTS	53.1	3.8	17.6		
	Arch Days	51.8	3.8	17.1	-0.5	2.0
	Linear LC	44.0	5.1	17.9	0.3	2.9
	Quad LC	47.6	4.3	17.4	-0.2	4.8
3	DTS	436.5	14.8	151.8		
	Arch Days	447.6	12.9	149.1	-2.7	14.6
	Linear LC	363.7	41.9	148.2	-3.6	27.2
	Quad LC	423.2	32.4	145.9	-5.9	41.0
4	DTS	375.9	26.0	134.1		
	Arch Days	377.0	29.4	131.8	-2.3	13.2
	Linear LC	325.7	37.5	132.7	-1.4	27.2
	Quad LC	348.9	29.6	128.0	-6.1	37.5
5	DTS	167.6	2.5	9.6		
	Arch Days	156.4	2.4	9.5	-0.1	0.9
	Linear LC	24.6	2.8	10.0	0.4	2.0
	Quad LC	20.4	2.7	9.1	-0.5	2.6
6	DTS	71.9	6.4	28.3		
	Arch Days	74.0	5.7	27.9	-0.4	2.7
	Linear LC	69.1	8.0	28.2	-0.2	6.6
	Quad LC	68.9	6.6	26.8	-1.6	8.6
7	DTS	40.6	3.7	17.4		
	Arch Days	41.4	3.2	17.3	-0.1	2.3
	Linear LC	46.1	5.3	18.8	1.4	4.6
	Quad LC	32.3	5.2	16.4	-0.9	5.2
8	DTS	261.3	9.0	100.4		
	Arch Days	266.5	7.9	99.1	-1.3	9.3
	Linear LC	243.0	28.0	99.0	-1.4	26.9
	Quad LC	246.2	23.0	94.4	-6.0	31.7
9	DTS	227.8	21.5	93.6		
	Arch Days	224.0	20.3	92.3	-1.2	9.7
	Linear LC	237.0	27.3	96.6	3.0	25.4
	Quad LC	207.8	24.8	88.9	-4.6	28.5

Table C.4 Comparison of Loss Results for the 15 Node Test System (Cont.)

Line No.	Simulation Type	Comparison with Discrete Time Simulation				
		Loss (kW)			Errors on the Mean (kW)	
		Max	Min	Mean	Mean Error	Mean Dev on Error
10	DTS	3140.2	63.7	1218.4		
	Arch Days	3205.9	56.2	1199.5	-18.9	111.7
	Linear LC	2963.7	341.3	1207.7	-10.7	359.7
	Quad LC	3058.7	285.8	1157.7	-60.7	410.5
11	DTS	2142.1	25.8	67.7		
	Arch Days	1964.9	23.7	66.9	-0.8	5.1
	Linear LC	162.7	18.7	66.3	-1.4	19.6
	Quad LC	148.9	26.5	64.0	-3.7	18.8

C.2.4 348 Node Test System

Table C.5 Comparison of Loss Results for the 348 Node Test System

Line No.	Simulation Type	Comparison with Discrete Time Sim.					Line No.	Simulation Type	Comparison with Discrete Time Sim.				
		Line Loss (kW)			Errors (kW)				Line Loss (kW)			Errors (kW)	
		Max	Min	Mean	Mean	Devia			Max	Min	Mean	Mean	Devia
1	DTS	1737.0	32.5	314.9			16	DTS	527.1	37.1	185.8		
	Arch D	2547.2	21.9	284.8	-30.1	90.0		Arch D	720.4	19.4	172.3	-13.5	49.2
	Lin LC	363.4	112.0	218.5	-96.3	241.7		Lin LC	288.6	89.0	173.6	-12.3	67.6
	Q LC	1627.4	-29.0	509.8	195.0	419.8		Q LC	484.6	30.1	184.5	-1.4	72.7
2	DTS	1743.8	32.6	316.1			17	DTS	310.7	18.9	126.4		
	Arch D	2557.2	22.0	285.9	-30.2	90.3		Arch D	332.3	23.4	121.4	-5.	24.7
	Lin LC	364.9	112.5	219.4	-96.6	242.7		Lin LC	280.8	86.6	168.9	42.5	32.1
	Q LC	1633.7	-29.1	511.7	195.7	421.5		Q LC	299.4	37.5	134.5	8.1	32.8
3	DTS	2638.3	0.7	589.9			18	DTS	670.8	159.8	302.1		
	Arch D	3024.9	133.0	848.4	258.5	191.1		Arch D	640.3	116.4	283.2	-18.8	39.9
	Lin LC	1998.8	616.0	1201.9	612.3	198.4		Lin LC	441.4	136.1	265.4	-36.5	109.6
	Q LC	2742.9	645.8	1299.5	709.9	168.8		Q LC	334.1	218.8	297.8	-4.1	77.7
4	DTS	2617.1	0.7	585.1			19	DTS	332.2	125.1	232.7		
	Arch D	3000.6	132.0	841.6	256.5	189.6		Arch D	338.5	114.6	229.7	-3.	10.1
	Lin LC	1982.9	611.1	1192.4	607.5	196.8		Lin LC	387.1	119.3	232.7	0.1	68.6
	Q LC	2721.0	640.6	1289.1	704.2	167.4		Q LC	317.4	139.3	230.3	-2.3	19.8
5	DTS	10004.0	2139.6	5050.1			20	DTS	81.2	5.7	38.4		
	Arch D	11703.0	2008.3	5111.7	61.7	314.4		Arch D	113.6	5.9	41.0	2.6	6.7
	Lin LC	8406.7	2590.9	5055.2	4.6	234.6		Lin LC	63.1	19.4	37.9	-0.5	17.7
	Q LC	9895.2	2121.1	5253.8	203.3	618.3		Q LC	75.3	11.7	39.3	0.9	9.
6	DTS	10116.0	2163.7	5106.8			21	DTS	295.3	103.7	172.5		
	Arch D	11835.0	2030.9	5169.1	62.3	317.9		Arch D	313.6	101.0	169.1	-3.4	11.9
	Lin LC	8501.0	2620.0	5111.9	4.5	237.3		Lin LC	295.7	91.1	177.8	5.3	18.7
	Q LC	10006.0	2144.9	5312.9	205.6	625.2		Q LC	287.0	111.6	182.1	9.6	20.9
7	DTS	8091.1	1883.5	4224.9			22	DTS	223.4	16.1	79.0		
	Arch D	9441.1	1775.1	4301.1	76.3	251.7		Arch D	296.4	9.2	73.7	-5.3	19.
	Lin LC	6999.6	2157.3	4209.0	-16.3	181.1		Lin LC	118.8	36.6	71.4	-7.6	31.2
	Q LC	8041.0	1911.6	4377.7	152.3	507.1		Q LC	197.3	13.2	77.3	-1.7	31.4
8	DTS	8091.1	1883.5	4224.9			23	DTS	359.7	167.6	244.0		
	Arch D	9441.1	1775.1	4301.1	76.3	251.7		Arch D	369.9	139.5	234.0	-10.	17.
	Lin LC	6999.6	2157.3	4209.0	-16.3	181.1		Lin LC	402.8	124.1	242.2	-1.8	20.7
	Q LC	8041.0	1911.6	4377.7	152.4	507.1		Q LC	323.3	173.1	242.3	-1.7	20.
9	DTS	63.2	0.8	12.9			24	DTS	521.0	242.7	382.9		
	Arch D	34.6	0.9	13.1	0.2	5.9		Arch D	614.0	231.4	382.2	-0.7	25.9
	Lin LC	29.4	9.1	17.7	4.8	4.8		Lin LC	604.3	186.3	363.4	-19.5	95.4
	Q LC	15.7	-12.2	14.1	1.3	5.7		Q LC	554.9	301.4	394.9	12.	38.7
10	DTS	692.3	166.2	343.9			25	DTS	313.3	15.9	140.8		
	Arch D	754.1	168.7	351.4	7.6	22.8		Arch D	392.3	17.1	151.4	10.6	22.8
	Lin LC	593.9	183.0	357.1	13.2	42.0		Lin LC	235.6	72.6	141.7	0.9	64.
	Q LC	604.7	180.2	362.1	18.2	50.6		Q LC	318.6	42.1	144.6	3.8	36.5
11	DTS	1879.7	450.9	948.5			26	DTS	334.6	56.5	149.3		
	Arch D	2010.8	452.2	953.1	4.6	58.2		Arch D	393.7	58.8	150.8	1.5	13.5
	Lin LC	1660.1	511.7	998.3	49.7	86.0		Lin LC	256.1	78.9	154.0	4.8	11.6
	Q LC	1636.7	457.6	1001.8	53.3	127.4		Q LC	318.6	55.6	161.9	12.7	20.7
12	DTS	113.0	65.7	88.7			27	DTS	328.9	55.5	146.7		
	Arch D	118.0	63.6	87.2	-1.4	4.0		Arch D	387.1	57.8	148.2	1.5	13.2
	Lin LC	151.1	46.6	90.9	2.2	19.5		Lin LC	251.8	77.6	151.4	4.7	11.4
	Q LC	93.2	74.7	88.8	0.2	8.7		Q LC	313.2	54.6	159.2	12.5	20.4
13	DTS	216.1	14.2	77.9			28	DTS	0.4	0.0	0.0		
	Arch D	274.9	13.5	75.9	-2.0	8.8		Arch D	31.8	0.0	0.9	0.9	1.2
	Lin LC	133.4	41.1	80.2	2.3	14.5		Lin LC	0.0	0.0	0.0	0.	0.
	Q LC	196.7	14.6	85.8	7.9	14.5		Q LC	0.7	-1.1	0.1	0.1	0.1
14	DTS	65.3	0.3	9.0			29	DTS	1.0	0.0	0.1		
	Arch D	172.5	0.1	11.6	2.6	7.7		Arch D	9.5	0.0	0.3	0.2	0.4
	Lin LC	3.8	1.2	2.3	-6.8	6.9		Lin LC	0.1	0.0	0.1	0.	0.1
	Q LC	103.7	-9.3	18.7	9.6	17.7		Q LC	1.1	-0.1	0.2	0.1	0.1
15	DTS	988.9	212.5	488.1			30	DTS	2219.3	77.7	597.6		
	Arch D	1025.7	176.6	473.6	-14.5	43.5		Arch D	2791.5	27.5	563.2	-34.3	111.7
	Lin LC	830.4	255.9	499.4	11.2	49.0		Lin LC	897.4	276.6	539.6	-57.8	406.6
	Q LC	892.2	206.5	514.9	26.8	76.7		Q LC	2125.3	340.8	765.8	168.4	395.1

Table C.6 Comparison of Loss Results for the 348 Node Test System (Cont.)

Line No.	Simulation Type	Comparison with Discrete Time Sim.					Line No.	Simulation Type	Comparison with Discrete Time Sim.				
		Line Loss (kW)			Errors (kW)				Line Loss (kW)			Errors (kW)	
		Max	Min	Mean	Mean	Devia			Max	Min	Mean	Mean	Devia
31	DTS	1784.2	69.6	350.6			46	DTS	2942.5	856.1	1658.2		
	Arch D	2508.8	36.1	323.9	-26.7	86.1		Arch D	3424.0	820.9	1696.2	38.1	107.8
	Lin LC	423.0	130.4	254.4	-96.2	257.5		Lin LC	2991.6	922.0	1798.9	140.7	190.3
	Q LC	1675.8	15.9	544.6	194.0	419.5		Q LC	2548.5	830.9	1749.5	91.3	214.9
32	DTS	2973.7	784.9	1681.9			47	DTS	29.3	3.2	10.8		
	Arch D	3296.9	691.7	1695.4	13.5	106.1		Arch D	40.1	2.6	11.1	0.3	3.7
	Lin LC	2764.6	852.0	1662.4	-19.7	56.1		Lin LC	19.6	6.0	11.8	1.	3.1
	Q LC	2906.6	781.1	1711.9	29.8	185.0		Q LC	24.8	8.6	11.4	0.5	3.4
33	DTS	373.7	25.3	188.7			48	DTS	53.4	3.5	11.3		
	Arch D	466.7	28.2	206.7	18.0	27.5		Arch D	46.9	3.2	11.4	0.1	1.6
	Lin LC	289.9	89.3	174.3	-14.5	27.6		Lin LC	16.9	5.2	10.2	-1.1	3.7
	Q LC	281.3	67.8	171.4	-17.4	37.9		Q LC	14.7	3.0	9.7	-1.5	3.7
34	DTS	1346.4	375.8	687.6			49	DTS	0.0	0.0	0.0		
	Arch D	1352.9	396.5	677.7	-9.9	49.4		Arch D	0.0	0.0	0.0	0.	0.
	Lin LC	1093.0	336.8	657.2	-30.3	55.3		Lin LC	0.0	0.0	0.0	0.	0.
	Q LC	1304.9	379.7	718.2	30.7	81.9		Q LC	0.2	0.0	0.0	0.	0.
35	DTS	222.9	54.2	118.3			50	DTS	3.5	0.0	0.4		
	Arch D	261.1	22.8	108.6	-9.7	30.0		Arch D	11.6	0.0	1.3	0.9	1.2
	Lin LC	117.8	36.3	70.9	-47.4	16.3		Lin LC	1.5	0.5	0.9	0.6	0.4
	Q LC	256.4	28.9	116.7	-1.6	28.6		Q LC	0.6	-0.1	0.1	-0.2	0.4
36	DTS	506.0	21.5	160.7			51	DTS	3.1	0.0	0.3		
	Arch D	594.5	25.6	173.3	12.6	52.5		Arch D	10.3	0.0	1.1	0.8	1.1
	Lin LC	268.8	82.8	161.6	0.9	57.0		Lin LC	1.4	0.4	0.8	0.5	0.3
	Q LC	512.1	79.9	172.2	11.5	56.6		Q LC	0.5	-0.1	0.1	-0.2	0.3
37	DTS	8.5	1.5	4.2			52	DTS	3.5	0.0	0.4		
	Arch D	9.7	1.5	4.1	0.0	0.4		Arch D	11.6	0.0	1.3	0.9	1.2
	Lin LC	7.3	2.3	4.4	0.2	0.6		Lin LC	1.5	0.5	0.9	0.6	0.4
	Q LC	7.2	-3.9	4.3	0.2	0.7		Q LC	0.6	-0.1	0.1	-0.2	0.4
38	DTS	7.9	1.4	3.9			53	DTS	6.5	1.1	3.1		
	Arch D	9.0	1.4	3.8	0.0	0.3		Arch D	7.2	0.7	2.9	-0.2	0.3
	Lin LC	6.8	2.1	4.1	0.2	0.6		Lin LC	5.2	1.6	3.1	0.	0.4
	Q LC	6.7	1.3	4.0	0.2	0.6		Q LC	6.7	1.1	3.3	0.1	0.5
39	DTS	497.5	81.9	228.1			54	DTS	2.4	0.4	1.2		
	Arch D	507.9	69.3	215.4	-12.7	30.1		Arch D	2.7	0.3	1.1	-0.1	0.1
	Lin LC	436.9	134.7	262.7	34.6	26.3		Lin LC	1.9	0.6	1.2	0.	0.1
	Q LC	484.7	65.4	237.7	9.6	40.9		Q LC	2.5	0.4	1.2	0.1	0.2
40	DTS	427.8	29.1	152.2			55	DTS	160.4	20.7	71.1		
	Arch D	464.9	30.7	150.2	-2.0	20.0		Arch D	179.7	14.3	67.9	-3.2	8.2
	Lin LC	260.0	80.1	156.3	4.1	28.8		Lin LC	117.2	36.1	70.5	-0.7	11.1
	Q LC	394.6	34.9	165.0	12.8	32.5		Q LC	166.4	22.9	75.7	4.6	13.8
41	DTS	390.7	49.8	136.9			56	DTS	230.4	39.9	112.8		
	Arch D	386.4	45.3	134.5	-2.4	13.3		Arch D	256.5	25.8	104.0	-8.8	11.4
	Lin LC	239.7	73.9	144.1	7.2	26.8		Lin LC	183.3	56.5	110.2	-2.6	12.1
	Q LC	222.3	41.3	139.2	2.3	28.3		Q LC	222.2	41.2	114.9	2.	17.5
42	DTS	1755.2	335.8	842.5			57	DTS	487.9	102.3	252.6		
	Arch D	1775.2	299.0	821.1	-21.4	73.0		Arch D	516.5	85.2	237.8	-14.9	20.4
	Lin LC	1498.2	461.7	900.9	58.4	125.4		Lin LC	427.7	131.8	257.2	4.5	23.8
	Q LC	1392.8	273.1	874.1	31.6	148.3		Q LC	471.2	94.9	262.6	10.	37.5
43	DTS	103.1	9.4	27.6			58	DTS	282.9	58.2	144.7		
	Arch D	96.1	8.4	27.3	-0.3	3.0		Arch D	298.2	46.1	134.7	-10.	11.7
	Lin LC	46.2	14.2	27.8	0.1	7.3		Lin LC	242.4	74.7	145.7	1.1	13.9
	Q LC	40.7	7.9	26.5	-1.1	7.4		Q LC	264.0	54.4	148.6	3.9	21.2
44	DTS	75.4	14.2	35.6			59	DTS	1001.9	221.6	524.7		
	Arch D	75.9	12.5	34.7	-1.0	3.2		Arch D	1076.8	187.7	498.2	-26.5	40.5
	Lin LC	63.3	19.5	38.1	2.4	5.4		Lin LC	884.1	272.5	531.6	6.9	48.9
	Q LC	58.1	11.6	36.9	1.2	6.4		Q LC	968.8	209.1	543.6	18.9	76.4
45	DTS	2298.9	467.1	1203.2			60	DTS	582.7	132.2	306.1		
	Arch D	2614.3	418.2	1166.0	-37.2	112.4		Arch D	621.6	107.8	288.6	-17.5	23.5
	Lin LC	2146.7	661.6	1290.8	87.6	175.2		Lin LC	512.8	158.1	308.4	2.3	29.7
	Q LC	1990.5	401.5	1252.2	49.0	212.8		Q LC	548.6	124.5	314.3	8.2	44.1

Table C.7 Comparison of Loss Results for the 348 Node Test System (Cont.)

Line No.	Simulation Type	Comparison with Discrete Time Sim.				
		Line Loss (kW)			Errors (kW)	
		Max	Min	Mean	Mean	Devia
61	DTS	1934.7	388.6	983.2		
	Arch D	2099.8	328.1	940.5	-42.7	74.2
	Lin LC	1633.2	503.4	982.1	-1.2	83.3
	Q LC	1840.8	363.7	1007.4	24.1	137.9
62	DTS	0.0	0.0	0.0		
	Arch D	0.0	0.0	0.0	0.0	0.0
	Lin LC	0.0	0.0	0.0	0.0	0.0
	Q LC	0.0	-2.8	0.0	0.0	0.0
63	DTS	383.4	67.7	178.2		
	Arch D	394.2	57.6	178.8	0.5	17.1
	Lin LC	280.1	86.3	168.4	-9.9	30.4
	Q LC	371.5	76.2	179.9	1.6	35.5
64	DTS	464.1	80.0	211.0		
	Arch D	471.4	66.7	205.9	-5.1	17.6
	Lin LC	343.3	105.8	206.5	-4.6	35.4
	Q LC	486.4	86.3	223.3	12.2	42.7
65	DTS	15.9	2.9	7.3		
	Arch D	16.4	2.6	7.0	-0.3	0.5
	Lin LC	11.5	3.5	6.9	-0.4	1.4
	Q LC	16.0	2.9	7.4	0.2	1.5
66	DTS	50.6	11.3	25.0		
	Arch D	55.4	10.0	24.4	-0.7	1.6
	Lin LC	41.8	12.9	25.1	0.1	1.9
	Q LC	50.5	10.8	26.3	1.3	3.5
67	DTS	31.8	6.7	16.0		
	Arch D	35.4	5.9	15.5	-0.5	1.1
	Lin LC	26.3	8.1	15.8	-0.2	1.3
	Q LC	31.3	6.5	16.5	0.5	2.3
68	DTS	24.9	5.0	12.3		
	Arch D	27.9	4.6	12.0	-0.3	0.8
	Lin LC	20.3	6.3	12.2	-0.1	1.2
	Q LC	24.6	5.1	12.8	0.4	1.8
69	DTS	426.5	58.3	184.7		
	Arch D	417.1	59.5	174.0	-10.7	19.1
	Lin LC	282.6	87.1	169.9	-14.9	41.1
	Q LC	397.5	72.8	183.2	-1.5	43.8
70	DTS	1488.5	305.7	718.7		
	Arch D	1638.6	278.1	702.5	-16.2	49.4
	Lin LC	1210.5	373.1	727.9	9.1	63.5
	Q LC	1501.1	310.4	765.8	47.0	106.9
71	DTS	17.1	5.6	9.4		
	Arch D	17.0	4.6	9.3	0.0	1.3
	Lin LC	14.9	4.6	9.0	-0.4	1.2
	Q LC	15.0	1.6	9.4	0.1	1.2
72	DTS	17.0	5.6	9.3		
	Arch D	17.0	4.6	9.3	0.0	1.3
	Lin LC	14.9	4.6	9.0	-0.4	1.2
	Q LC	15.0	7.0	9.4	0.1	1.2
73	DTS	115.7	16.0	49.0		
	Arch D	123.8	15.4	47.9	-1.1	4.0
	Lin LC	79.7	24.6	48.0	-1.0	7.8
	Q LC	115.9	16.8	51.9	3.0	9.0
74	DTS	124.8	17.2	52.8		
	Arch D	133.6	16.6	51.6	-1.2	4.3
	Lin LC	86.0	26.5	51.7	-1.1	8.4
	Q LC	125.0	18.1	56.0	3.2	9.7
75	DTS	426.1	110.0	213.3		
	Arch D	406.3	107.7	206.2	-7.1	15.9
	Lin LC	349.0	107.6	209.9	-3.4	14.2
	Q LC	409.0	124.9	224.3	11.1	25.8

Line No.	Simulation Type	Comparison with Discrete Time Sim.				
		Line Loss (kW)			Errors (kW)	
		Max	Min	Mean	Mean	Devia
76	DTS	0.0	0.0	0.0		
	Arch D	0.0	0.0	0.0	0.	0.
	Lin LC	0.0	0.0	0.0	0.	0.
	Q LC	0.0	-2.4	0.0	0.	0.
77	DTS	0.0	0.0	0.0		
	Arch D	0.0	0.0	0.0	0.	0.
	Lin LC	0.0	0.0	0.0	0.	0.
	Q LC	0.0	0.0	0.0	0.	0.
78	DTS	538.2	28.8	213.2		
	Arch D	614.4	26.4	205.9	-7.3	25.1
	Lin LC	349.4	107.7	210.1	-3.1	114.
	Q LC	528.9	78.8	239.3	26.1	68.9
79	DTS	910.9	479.7	676.8		
	Arch D	939.9	457.6	676.5	-0.3	18.3
	Lin LC	1165.1	359.1	700.6	23.9	183.7
	Q LC	916.6	501.9	702.9	26.1	44.6
80	DTS	5624.1	1001.1	2692.0		
	Arch D	6850.8	952.7	2774.8	82.8	184.9
	Lin LC	4499.8	1386.8	2705.8	13.6	236.7
	Q LC	5649.7	1039.3	2846.6	154.3	386.2
81	DTS	88.0	14.7	41.0		
	Arch D	108.0	13.9	42.4	1.4	2.9
	Lin LC	68.8	21.2	41.4	0.4	4.
	Q LC	88.6	15.3	43.7	2.7	6.1
82	DTS	52.1	10.9	26.3		
	Arch D	69.7	8.8	36.4	10.	4.
	Lin LC	36.3	11.2	21.8	-4.5	2.4
	Q LC	61.2	10.2	26.8	0.5	4.8
83	DTS	80.8	5.6	35.9		
	Arch D	85.5	1.8	23.0	-12.9	9.6
	Lin LC	48.5	15.0	29.2	-6.7	8.7
	Q LC	54.7	3.9	38.4	2.5	11.5
84	DTS	125.6	19.3	65.8		
	Arch D	160.1	21.2	68.2	2.4	5.
	Lin LC	105.1	32.4	63.2	-2.6	6.1
	Q LC	122.8	30.2	66.1	0.2	9.6
85	DTS	125.5	19.3	65.8		
	Arch D	160.0	21.2	68.2	2.4	5.
	Lin LC	105.0	32.4	63.2	-2.6	6.1
	Q LC	122.7	30.2	66.1	0.2	9.6
86	DTS	86.0	11.8	42.8		
	Arch D	76.9	10.6	41.1	-1.8	3.9
	Lin LC	60.8	18.7	36.6	-6.3	9.5
	Q LC	61.4	19.4	38.3	-4.5	10.3
87	DTS	52.0	6.7	26.4		
	Arch D	51.1	6.0	25.4	-1.	2.8
	Lin LC	36.3	11.2	21.8	-4.6	7.1
	Q LC	33.0	12.5	22.5	-3.9	7.4
88	DTS	75.4	11.5	36.0		
	Arch D	75.7	10.8	34.9	-1.1	2.4
	Lin LC	57.4	17.7	34.5	-1.5	5.5
	Q LC	72.9	11.5	37.1	1.1	6.9
89	DTS	131.9	24.3	67.7		
	Arch D	121.7	21.3	65.9	-1.8	5.1
	Lin LC	100.4	30.9	60.4	-7.3	10.5
	Q LC	104.4	33.0	63.5	-4.2	12.4
90	DTS	150.4	27.5	76.3		
	Arch D	136.9	24.2	74.1	-2.2	5.6
	Lin LC	113.6	35.0	68.3	-8.	11.4
	Q LC	122.2	36.8	72.2	-4.1	13.7

Table C.8 Comparison of Loss Results for the 348 Node Test System (Cont.)

Line No.	Simulation Type	Comparison with Discrete Time Sim.					Line No.	Simulation Type	Comparison with Discrete Time Sim.				
		Line Loss (kW)			Errors (kW)				Line Loss (kW)			Errors (kW)	
		Max	Min	Mean	Mean	Devia			Max	Min	Mean	Mean	Devia
91	DTS	0.2	0.0	0.1			106	DTS	539.3	79.7	220.8		
	Arch D	0.2	0.0	0.1	0.0	0.0		Arch D	516.9	76.7	214.7	-6.1	17.7
	Lin LC	0.2	0.1	0.1	0.0	0.0		Lin LC	344.9	106.3	207.4	-13.4	35.7
	Q LC	0.2	-0.2	0.1	0.0	0.0		Q LC	517.8	102.9	228.1	7.3	40.1
92	DTS	0.2	0.0	0.1			107	DTS	21.9	0.1	3.0		
	Arch D	0.2	0.0	0.1	0.0	0.0		Arch D	18.8	0.0	2.4	-0.5	1.6
	Lin LC	0.2	0.0	0.1	0.0	0.0		Lin LC	1.1	0.4	0.7	-2.3	2.8
	Q LC	0.2	0.0	0.1	0.0	0.0		Q LC	1.3	-4.5	0.8	-2.2	2.7
93	DTS	0.0	0.0	0.0			108	DTS	0.0	0.0	0.0		
	Arch D	0.0	0.0	0.0	0.0	0.0		Arch D	0.0	0.0	0.0	0.	0.
	Lin LC	0.0	0.0	0.0	0.0	0.0		Lin LC	0.0	0.0	0.0	0.	0.
	Q LC	0.0	0.0	0.0	0.0	0.0		Q LC	0.0	0.0	0.0	0.	0.
94	DTS	416.9	1.3	98.6			109	DTS	406.2	221.9	298.3		
	Arch D	590.9	20.7	111.5	12.9	22.4		Arch D	433.3	216.5	301.0	2.6	7.5
	Lin LC	202.0	62.3	121.5	22.9	40.0		Lin LC	499.6	154.0	300.4	2.	23.4
	Q LC	539.7	84.0	167.2	68.7	31.8		Q LC	397.2	223.7	302.1	3.8	17.2
95	DTS	1368.5	468.9	830.3			110	DTS	361.5	193.8	263.4		
	Arch D	1541.5	447.5	838.4	8.0	36.8		Arch D	386.6	189.1	265.9	2.5	6.8
	Lin LC	1380.6	425.5	830.2	-0.2	15.9		Lin LC	441.0	135.9	265.2	1.8	20.
	Q LC	1364.2	471.5	849.5	19.1	76.0		Q LC	353.1	195.4	266.8	3.4	15.5
96	DTS	875.6	474.0	684.1			111	DTS	318.7	122.4	182.9		
	Arch D	943.8	454.0	645.7	-38.5	31.2		Arch D	281.0	120.8	181.7	-1.3	7.2
	Lin LC	1021.5	314.8	614.3	-69.9	73.4		Lin LC	307.0	94.6	184.6	1.6	13.1
	Q LC	841.7	446.4	618.9	-65.3	40.9		Q LC	325.5	141.0	194.4	11.4	18.6
97	DTS	0.0	0.0	0.0			112	DTS	578.5	163.1	314.2		
	Arch D	0.0	0.0	0.0	0.0	0.0		Arch D	588.5	169.6	315.9	1.7	14.7
	Lin LC	0.0	0.0	0.0	0.0	0.0		Lin LC	529.6	163.2	318.5	4.2	11.1
	Q LC	0.0	-0.7	0.0	0.0	0.0		Q LC	570.2	182.8	330.3	16.1	36.1
98	DTS	9654.2	6077.0	7636.4			113	DTS	0.2	0.0	0.0		
	Arch D	10092.0	5920.0	7649.8	13.4	144.3		Arch D	0.1	0.0	0.0	0.	0.
	Lin LC	12710.0	3917.3	7643.0	6.4	807.2		Lin LC	0.1	0.0	0.0	0.	0.
	Q LC	9446.4	6067.1	7670.2	33.6	312.0		Q LC	0.0	-2.4	0.0	0.	0.
99	DTS	187.9	4.1	64.3			114	DTS	0.1	0.0	0.1		
	Arch D	221.4	2.9	59.5	-4.8	10.0		Arch D	0.1	0.0	0.1	0.	0.
	Lin LC	93.0	28.7	55.9	-8.4	38.8		Lin LC	0.1	0.0	0.1	0.	0.
	Q LC	175.4	24.5	69.3	5.0	29.8		Q LC	0.1	0.0	0.1	0.	0.
100	DTS	404.1	376.0	386.3			115	DTS	0.2	0.0	0.1		
	Arch D	409.0	372.2	386.7	0.3	1.8		Arch D	0.2	0.0	0.1	0.	0.
	Lin LC	642.8	198.1	386.5	0.2	63.0		Lin LC	0.1	0.0	0.1	0.	0.
	Q LC	407.4	376.0	386.4	0.1	3.0		Q LC	0.2	0.0	0.1	0.	0.
101	DTS	5262.0	2992.2	3920.7			116	DTS	108.3	15.1	39.7		
	Arch D	5593.5	2920.2	3956.6	35.9	93.7		Arch D	134.6	12.4	40.3	0.6	3.6
	Lin LC	6573.3	2025.9	3952.7	31.9	333.3		Lin LC	61.1	18.8	36.7	-3.	11.6
	Q LC	5154.7	3012.0	3974.2	53.4	208.6		Q LC	109.8	18.2	42.7	3.	10.7
102	DTS	2143.8	1385.9	1690.1			117	DTS	121.5	16.5	44.4		
	Arch D	2247.0	1357.3	1703.4	13.3	32.4		Arch D	151.3	13.6	45.0	0.7	4.1
	Lin LC	2833.8	873.4	1704.1	13.9	177.9		Lin LC	68.2	21.0	41.0	-3.3	13.1
	Q LC	2109.5	1389.5	1710.2	20.1	69.0		Q LC	123.0	19.9	47.7	3.3	12.
103	DTS	0.0	0.0	0.0			118	DTS	53.7	10.2	25.3		
	Arch D	0.0	0.0	0.0	0.0	0.0		Arch D	59.7	9.9	24.2	-1.1	1.7
	Lin LC	0.0	0.0	0.0	0.0	0.0		Lin LC	42.4	13.1	25.5	0.2	2.9
	Q LC	0.0	-0.8	0.0	0.0	0.0		Q LC	53.2	10.1	26.0	0.7	4.2
104	DTS	0.0	0.0	0.0			119	DTS	1.4	0.2	0.6		
	Arch D	0.0	0.0	0.0	0.0	0.0		Arch D	1.7	0.2	0.6	0.	0.1
	Lin LC	0.0	0.0	0.0	0.0	0.0		Lin LC	1.0	0.3	0.6	0.	0.1
	Q LC	0.0	0.0	0.0	0.0	0.0		Q LC	1.5	0.3	0.7	0.	0.1
105	DTS	535.1	79.0	219.1			120	DTS	0.0	0.0	0.0		
	Arch D	512.5	76.2	213.0	-6.1	17.5		Arch D	0.0	0.0	0.0	0.	0.
	Lin LC	342.2	105.5	205.8	-13.3	35.4		Lin LC	0.0	0.0	0.0	0.	0.
	Q LC	513.6	102.2	226.3	7.2	39.8		Q LC	0.0	0.0	0.0	0.	0.

Table C.9 Comparison of Loss Results for the 348 Node Test System (Cont.)

Line No.	Simulation Type	Comparison with Discrete Time Sim.				
		Line Loss (kW)			Errors (kW)	
		Max	Min	Mean	Mean	Devia
121	DTS	1149.1	64.4	260.5		
	Arch D	826.5	53.6	247.7	-12.8	31.4
	Lin LC	395.5	121.9	237.8	-22.7	66.7
	Q LC	878.8	87.8	291.6	31.0	76.0
122	DTS	1149.3	64.4	260.6		
	Arch D	826.6	53.6	247.7	-12.8	31.4
	Lin LC	395.6	121.9	237.9	-22.7	66.7
	Q LC	878.9	87.8	291.6	31.0	76.0
123	DTS	0.0	0.0	0.0		
	Arch D	0.0	0.0	0.0	0.0	0.0
	Lin LC	0.0	0.0	0.0	0.0	0.0
	Q LC	0.0	-12.5	0.0	0.0	0.0
124	DTS	0.0	0.0	0.0		
	Arch D	0.0	0.0	0.0	0.0	0.0
	Lin LC	0.0	0.0	0.0	0.0	0.0
	Q LC	0.0	0.0	0.0	0.0	0.0
125	DTS	279.9	131.1	212.1		
	Arch D	281.8	131.7	210.6	-1.6	8.8
	Lin LC	374.2	115.3	225.0	12.9	66.4
	Q LC	254.9	185.3	222.0	9.9	24.2
126	DTS	72.8	10.1	28.0		
	Arch D	77.1	9.6	27.3	-0.6	2.1
	Lin LC	44.6	13.8	26.8	-1.1	4.4
	Q LC	74.9	10.7	30.3	2.3	5.2
127	DTS	0.6	0.5	0.5		
	Arch D	0.6	0.5	0.5	0.0	0.0
	Lin LC	0.9	0.3	0.6	0.0	0.1
	Q LC	0.6	-0.2	0.5	0.0	0.0
128	DTS	12518.0	8478.6	10206.3		
	Arch D	13057.0	8421.6	10294.7	88.5	172.5
	Lin LC	17115.0	5274.8	10291.8	85.3	1167.0
	Q LC	12257.0	8562.3	10286.4	79.9	367.7
129	DTS	0.7	0.7	0.7		
	Arch D	0.7	0.7	0.7	0.0	0.0
	Lin LC	1.1	0.4	0.7	0.0	0.1
	Q LC	3.7	0.7	0.7	0.0	0.0
130	DTS	1229.6	803.7	979.1		
	Arch D	1277.8	790.1	985.7	6.5	17.4
	Lin LC	1640.6	505.6	986.5	7.4	105.4
	Q LC	1204.0	808.0	988.8	9.6	39.1
131	DTS	14.8	10.8	11.9		
	Arch D	15.2	10.7	12.0	0.1	0.2
	Lin LC	19.8	6.1	11.9	0.0	1.7
	Q LC	15.1	10.7	12.1	0.2	0.4
132	DTS	14.6	10.4	11.6		
	Arch D	15.0	10.4	11.7	0.1	0.2
	Lin LC	19.4	6.0	11.7	0.0	1.6
	Q LC	14.8	10.3	11.9	0.2	0.4
133	DTS	838.5	776.5	800.5		
	Arch D	828.2	778.7	802.0	1.5	4.4
	Lin LC	1336.9	412.0	803.9	3.5	138.8
	Q LC	827.5	798.9	804.2	3.7	8.6
134	DTS	238.2	178.6	208.7		
	Arch D	244.3	181.2	210.3	1.6	3.3
	Lin LC	344.6	106.2	207.2	-1.5	45.2
	Q LC	236.0	199.9	210.0	1.3	10.6
135	DTS	0.0	0.0	0.0		
	Arch D	0.0	0.0	0.0	0.0	0.0
	Lin LC	0.0	0.0	0.0	0.0	0.0
	Q LC	0.0	-1.1	0.0	0.0	0.0

Line No.	Simulation Type	Comparison with Discrete Time Sim.				
		Line Loss (kW)			Errors (kW)	
		Max	Min	Mean	Mean	Devia
136	DTS	4.9	4.5	4.7		
	Arch D	4.9	4.5	4.7	0.	0.
	Lin LC	8.0	2.5	4.8	0.1	0.9
	Q LC	4.9	4.7	4.8	0.1	0.1
137	DTS	123.4	17.9	35.7		
	Arch D	160.6	17.3	38.4	2.7	4.5
	Lin LC	53.6	16.5	32.3	-3.5	5.9
	Q LC	151.8	21.5	44.5	8.8	13.
138	DTS	417.0	276.5	325.0		
	Arch D	392.6	270.9	322.7	-2.4	12.2
	Lin LC	562.3	173.3	338.1	13.1	56.4
	Q LC	415.2	318.2	343.2	18.2	19.6
139	DTS	515.1	399.7	426.2		
	Arch D	512.4	402.9	430.4	4.1	7.8
	Lin LC	689.4	212.5	414.6	-11.7	71.8
	Q LC	498.4	400.1	429.5	3.2	15.4
140	DTS	39.6	13.7	18.7		
	Arch D	47.5	14.1	20.1	1.4	1.9
	Lin LC	26.6	8.2	16.0	-2.7	2.9
	Q LC	58.0	9.6	21.6	2.9	6.2
141	DTS	39.6	13.7	18.7		
	Arch D	47.5	14.1	20.1	1.4	1.9
	Lin LC	26.6	8.2	16.0	-2.7	2.9
	Q LC	58.0	11.8	21.6	2.9	6.2
142	DTS	1.8	0.6	1.1		
	Arch D	2.1	0.6	1.1	0.	0.
	Lin LC	1.8	0.6	1.1	0.	0.
	Q LC	1.9	-0.4	1.1	0.	0.1
143	DTS	1.9	0.6	1.1		
	Arch D	2.1	0.6	1.1	0.	0.
	Lin LC	1.9	0.6	1.1	0.	0.
	Q LC	1.9	0.6	1.1	0.	0.1
144	DTS	1.8	0.6	1.1		
	Arch D	2.1	0.6	1.1	0.	0.
	Lin LC	1.8	0.6	1.1	0.	0.
	Q LC	1.8	0.6	1.1	0.	0.1
145	DTS	164.5	58.7	104.6		
	Arch D	186.5	70.7	110.3	5.8	6.6
	Lin LC	168.1	51.8	101.1	-3.5	5.9
	Q LC	170.8	70.0	105.8	1.2	8.2
146	DTS	158.9	67.6	101.5		
	Arch D	182.2	66.3	105.4	3.8	6.5
	Lin LC	155.8	48.0	93.7	-7.8	7.6
	Q LC	157.0	67.8	98.0	-3.5	6.9
147	DTS	28.2	10.3	20.1		
	Arch D	35.6	16.4	23.0	2.9	3.3
	Lin LC	29.8	9.2	17.9	-2.2	3.2
	Q LC	27.2	16.1	19.1	-1.	2.5
148	DTS	60.8	28.4	40.1		
	Arch D	73.6	28.6	44.7	4.6	7.9
	Lin LC	49.9	15.4	30.0	-10.1	8.1
	Q LC	39.8	29.6	31.6	-8.5	6.2
149	DTS	15.1	0.8	5.8		
	Arch D	81.4	1.1	12.3	6.5	8.5
	Lin LC	2.5	0.8	1.5	-4.3	3.4
	Q LC	2.7	1.9	2.3	-3.6	3.3
150	DTS	32.7	6.7	15.9		
	Arch D	46.8	7.5	20.7	4.8	6.2
	Lin LC	20.6	6.3	12.4	-3.5	4.4
	Q LC	13.9	8.7	12.0	-3.9	4.1

Table C.10 Comparison of Loss Results for the 348 Node Test System (Cont.)

Line No.	Simu-lation Type	Comparison with Discrete Time Sim.					Line No.	Simu-lation Type	Comparison with Discrete Time Sim.				
		Line Loss (kW)			Errors (kW)				Line Loss (kW)			Errors (kW)	
		Max	Min	Mean	Mean	Devia			Max	Min	Mean	Mean	Devia
151	DTS	81.3	26.6	54.0			166	DTS	472.4	72.8	137.6		
	Arch D	73.0	18.6	45.5	-8.5	10.0		Arch D	695.2	83.0	153.9	16.3	24.4
	Lin LC	117.8	36.3	70.9	16.8	12.8		Lin LC	192.1	59.2	115.5	-22.	24.9
	Q LC	82.8	64.7	69.1	15.0	10.1		Q LC	636.8	71.8	174.8	37.2	74.7
152	DTS	81.0	26.6	53.8			167	DTS	1104.7	554.0	727.5		
	Arch D	72.7	18.6	45.3	-8.5	10.0		Arch D	1174.6	572.0	751.6	24.1	28.1
	Lin LC	117.4	36.2	70.6	16.8	12.8		Lin LC	1256.6	387.3	755.6	28.1	62.
	Q LC	82.5	64.5	68.8	15.0	10.0		Q LC	1120.2	580.4	773.1	45.5	42.
153	DTS	265.6	178.8	220.0			168	DTS	1104.7	554.0	727.5		
	Arch D	267.0	161.7	216.3	-3.7	8.1		Arch D	1174.6	572.0	751.6	24.1	28.1
	Lin LC	384.2	118.4	231.0	11.0	27.0		Lin LC	1256.6	387.3	755.6	28.1	62.
	Q LC	267.3	192.9	228.9	8.8	11.5		Q LC	1120.2	580.4	773.1	45.5	42.
154	DTS	264.7	178.0	219.1			169	DTS	0.0	0.0	0.0		
	Arch D	266.6	161.2	215.5	-3.6	8.1		Arch D	0.0	0.0	0.0	0.	0.
	Lin LC	382.4	117.9	230.0	10.9	26.7		Lin LC	0.0	0.0	0.0	0.	0.
	Q LC	266.4	191.7	227.8	8.7	11.4		Q LC	0.0	-4.3	0.0	0.	0.
155	DTS	4635.4	1152.5	2580.0			170	DTS	0.1	0.0	0.0		
	Arch D	5513.5	1149.3	2669.3	89.3	157.4		Arch D	0.1	0.0	0.0	0.	0.
	Lin LC	4272.8	1316.9	2569.3	-10.9	102.3		Lin LC	0.1	0.0	0.0	0.	0.
	Q LC	4568.9	1217.0	2641.0	60.8	306.3		Q LC	0.1	0.0	0.0	0.	0.
156	DTS	4576.6	1137.9	2547.2			171	DTS	0.1	0.0	0.0		
	Arch D	5443.6	1134.7	2635.4	88.2	155.4		Arch D	0.1	0.0	0.0	0.	0.
	Lin LC	4218.7	1300.2	2536.8	-10.7	101.0		Lin LC	0.1	0.0	0.0	0.	0.
	Q LC	4510.9	1201.6	2607.5	60.0	302.4		Q LC	0.1	0.0	0.0	0.	0.
157	DTS	470.1	199.8	307.8			172	DTS	0.1	0.0	0.0		
	Arch D	521.8	199.7	315.3	7.5	12.4		Arch D	0.1	0.0	0.0	0.	0.
	Lin LC	512.0	157.8	307.9	0.1	15.7		Lin LC	0.1	0.0	0.0	0.	0.
	Q LC	467.2	208.6	314.0	6.2	21.2		Q LC	0.1	0.0	0.0	0.	0.
158	DTS	475.7	202.2	311.4			173	DTS	0.1	0.0	0.0		
	Arch D	527.9	202.1	319.0	7.6	12.6		Arch D	0.1	0.0	0.0	0.	0.
	Lin LC	518.0	159.6	311.5	0.1	15.9		Lin LC	0.1	0.0	0.0	0.	0.
	Q LC	472.6	211.0	317.7	6.3	21.4		Q LC	0.1	0.0	0.0	0.	0.
159	DTS	517.8	188.0	315.9			174	DTS	72.8	13.3	37.4		
	Arch D	588.0	188.3	325.1	9.3	15.3		Arch D	87.2	13.3	39.6	2.2	3.1
	Lin LC	524.2	161.6	315.2	-0.7	9.2		Lin LC	63.1	19.5	38.0	0.5	5.8
	Q LC	518.0	197.5	324.1	8.2	25.5		Q LC	69.3	12.5	38.6	1.2	8.1
160	DTS	1661.9	873.1	1222.4			175	DTS	0.0	0.0	0.0		
	Arch D	1774.2	851.0	1244.6	22.2	36.9		Arch D	0.0	0.0	0.0	0.	0.
	Lin LC	2073.7	639.1	1247.0	24.5	98.7		Lin LC	0.0	0.0	0.0	0.	0.
	Q LC	1604.3	884.9	1241.4	18.9	71.2		Q LC	0.0	0.0	0.0	0.	0.
161	DTS	990.1	608.4	707.3			176	DTS	36.8	6.8	19.0		
	Arch D	975.6	582.8	730.6	23.3	25.2		Arch D	44.4	6.8	20.1	1.1	1.5
	Lin LC	1248.9	384.9	751.0	43.7	109.9		Lin LC	32.1	9.9	19.3	0.3	2.9
	Q LC	1074.7	718.2	779.3	71.9	45.6		Q LC	35.3	6.3	19.7	0.6	4.1
162	DTS	990.1	608.4	707.3			177	DTS	0.0	0.0	0.0		
	Arch D	975.6	582.8	730.6	23.3	25.2		Arch D	0.0	0.0	0.0	0.	0.
	Lin LC	1248.9	384.9	751.0	43.7	109.9		Lin LC	0.0	0.0	0.0	0.	0.
	Q LC	1074.7	718.2	779.3	71.9	45.6		Q LC	0.0	0.0	0.0	0.	0.
163	DTS	92.4	22.0	49.5			178	DTS	0.0	0.0	0.0		
	Arch D	108.0	21.2	51.5	2.1	3.3		Arch D	0.0	0.0	0.0	0.	0.
	Lin LC	84.5	26.0	50.8	1.3	1.6		Lin LC	0.0	0.0	0.0	0.	0.
	Q LC	88.4	21.8	51.7	2.2	5.7		Q LC	0.0	0.0	0.0	0.	0.
164	DTS	1144.2	621.2	862.0			179	DTS	0.0	0.0	0.0		
	Arch D	1208.9	595.9	877.3	15.3	25.9		Arch D	0.1	0.0	0.0	0.	0.
	Lin LC	1478.6	455.7	889.1	27.0	73.2		Lin LC	0.0	0.0	0.0	0.	0.
	Q LC	1097.2	619.6	876.4	14.3	54.2		Q LC	0.0	0.0	0.0	0.	0.
165	DTS	2.7	2.5	2.6			180	DTS	0.0	0.0	0.0		
	Arch D	2.7	2.4	2.6	0.0	0.0		Arch D	0.0	0.0	0.0	0.	0.
	Lin LC	4.4	1.3	2.6	0.0	0.5		Lin LC	0.0	0.0	0.0	0.	0.
	Q LC	7.0	2.4	2.6	0.0	0.0		Q LC	0.0	0.0	0.0	0.	0.

Table C.11 Comparison of Loss Results for the 348 Node Test System (Cont.)

Line No.	Simulation Type	Comparison with Discrete Time Sim.					Line No.	Simulation Type	Comparison with Discrete Time Sim.				
		Line Loss (kW)			Errors (kW)				Line Loss (kW)			Errors (kW)	
		Max	Min	Mean	Mean	Devia			Max	Min	Mean	Mean	Devia
181	DTS	0.0	0.0	0.0			196	DTS	0.2	0.1	0.2		
	Arch D	0.1	0.0	0.0	0.0	0.0		Arch D	0.2	0.1	0.2	0.	0.
	Lin LC	0.0	0.0	0.0	0.0	0.0		Lin LC	0.3	0.1	0.2	0.	0.
	Q LC	0.0	0.0	0.0	0.0	0.0		Q LC	0.3	0.1	0.2	0.	0.
182	DTS	3.7	0.6	1.7			197	DTS	0.3	0.1	0.2		
	Arch D	4.3	0.5	1.7	-0.1	0.1		Arch D	0.4	0.1	0.2	0.	0.
	Lin LC	3.3	1.0	2.0	0.3	0.2		Lin LC	0.3	0.1	0.2	0.	0.
	Q LC	3.4	0.7	1.8	0.1	0.3		Q LC	0.3	0.1	0.2	0.	0.
183	DTS	3.7	0.6	1.7			198	DTS	0.3	0.1	0.2		
	Arch D	4.3	0.5	1.7	-0.1	0.1		Arch D	0.4	0.1	0.2	0.	0.
	Lin LC	3.3	1.0	2.0	0.3	0.2		Lin LC	0.4	0.1	0.2	0.	0.
	Q LC	3.4	0.7	1.8	0.1	0.3		Q LC	0.3	0.1	0.2	0.	0.
184	DTS	0.0	0.0	0.0			199	DTS	0.0	0.0	0.0		
	Arch D	0.0	0.0	0.0	0.0	0.0		Arch D	0.0	0.0	0.0	0.	0.
	Lin LC	0.0	0.0	0.0	0.0	0.0		Lin LC	0.0	0.0	0.0	0.	0.
	Q LC	0.0	0.0	0.0	0.0	0.0		Q LC	0.0	0.0	0.0	0.	0.
185	DTS	0.0	0.0	0.0			200	DTS	0.0	0.0	0.0		
	Arch D	0.0	0.0	0.0	0.0	0.0		Arch D	0.0	0.0	0.0	0.	0.
	Lin LC	0.0	0.0	0.0	0.0	0.0		Lin LC	0.0	0.0	0.0	0.	0.
	Q LC	0.0	0.0	0.0	0.0	0.0		Q LC	0.0	0.0	0.0	0.	0.
186	DTS	0.0	0.0	0.0			201	DTS	0.0	0.0	0.0		
	Arch D	0.0	0.0	0.0	0.0	0.0		Arch D	0.0	0.0	0.0	0.	0.
	Lin LC	0.0	0.0	0.0	0.0	0.0		Lin LC	0.0	0.0	0.0	0.	0.
	Q LC	0.0	0.0	0.0	0.0	0.0		Q LC	0.0	0.0	0.0	0.	0.
187	DTS	5.6	2.5	3.6			202	DTS	0.0	0.0	0.0		
	Arch D	5.8	2.4	3.7	0.1	0.2		Arch D	0.0	0.0	0.0	0.	0.
	Lin LC	5.9	1.8	3.5	-0.1	0.2		Lin LC	0.0	0.0	0.0	0.	0.
	Q LC	4.7	2.7	3.6	-0.1	0.3		Q LC	0.0	0.0	0.0	0.	0.
188	DTS	4.8	1.9	3.0			203	DTS	2096.5	595.0	1076.6		
	Arch D	4.8	2.0	3.1	0.1	0.2		Arch D	2102.1	622.7	1059.9	-16.7	77.8
	Lin LC	4.9	1.5	2.9	0.0	0.2		Lin LC	1709.3	526.8	1027.9	-48.7	86.7
	Q LC	4.0	2.4	2.9	0.0	0.2		Q LC	2032.2	596.3	1123.8	47.3	127.5
189	DTS	0.6	0.1	0.3			204	DTS	119.7	29.9	64.7		
	Arch D	0.5	0.1	0.3	0.0	0.0		Arch D	141.5	12.7	59.4	-5.3	16.2
	Lin LC	0.3	0.1	0.2	-0.1	0.0		Lin LC	64.9	20.0	39.0	-25.7	8.8
	Q LC	0.3	0.1	0.2	-0.1	0.1		Q LC	138.7	16.1	63.7	-0.9	15.4
190	DTS	0.6	0.1	0.3			205	DTS	0.0	0.0	0.0		
	Arch D	0.5	0.1	0.3	0.0	0.0		Arch D	0.0	0.0	0.0	0.	0.
	Lin LC	0.3	0.1	0.2	-0.1	0.0		Lin LC	0.0	0.0	0.0	0.	0.
	Q LC	0.3	0.1	0.2	-0.1	0.1		Q LC	0.0	-0.7	0.0	0.	0.
191	DTS	0.6	0.1	0.3			206	DTS	68.5	1.0	20.5		
	Arch D	0.5	0.1	0.3	0.0	0.0		Arch D	86.9	1.5	21.2	0.7	6.9
	Lin LC	0.4	0.1	0.2	-0.1	0.0		Lin LC	34.7	10.7	20.8	0.3	9.7
	Q LC	0.4	0.1	0.3	-0.1	0.1		Q LC	24.0	1.7	16.7	-3.8	10.9
192	DTS	0.6	0.1	0.3			207	DTS	68.5	1.0	20.5		
	Arch D	0.5	0.1	0.3	0.0	0.0		Arch D	86.9	1.5	21.2	0.7	6.9
	Lin LC	0.4	0.1	0.2	-0.1	0.0		Lin LC	34.7	10.7	20.8	0.3	9.7
	Q LC	0.4	0.1	0.3	-0.1	0.1		Q LC	24.0	1.7	16.7	-3.8	10.9
193	DTS	0.3	0.1	0.2			208	DTS	1176.3	758.8	904.6		
	Arch D	0.4	0.1	0.2	0.0	0.0		Arch D	1221.5	771.3	919.1	14.5	20.7
	Lin LC	0.3	0.1	0.2	0.0	0.0		Lin LC	1522.3	469.2	915.4	10.7	110.4
	Q LC	0.3	0.1	0.2	0.0	0.0		Q LC	1188.2	785.8	928.1	23.4	29.6
194	DTS	0.3	0.1	0.2			209	DTS	5.3	0.9	1.6		
	Arch D	0.4	0.1	0.2	0.0	0.0		Arch D	7.2	1.0	1.7	0.1	0.2
	Lin LC	0.3	0.1	0.2	0.0	0.0		Lin LC	2.3	0.7	1.4	-0.2	0.2
	Q LC	0.3	0.1	0.2	0.0	0.0		Q LC	6.8	-2.1	2.0	0.4	0.7
195	DTS	0.2	0.1	0.2			210	DTS	2.7	0.8	1.2		
	Arch D	0.3	0.1	0.2	0.0	0.0		Arch D	3.1	0.9	1.3	0.1	0.1
	Lin LC	0.3	0.1	0.2	0.0	0.0		Lin LC	2.0	0.6	1.2	0.	0.1
	Q LC	0.3	0.1	0.2	0.0	0.0		Q LC	3.1	1.0	1.4	0.2	0.2

Table C.12 Comparison of Loss Results for the 348 Node Test System (Cont.)

Line No.	Simulation Type	Comparison with Discrete Time Sim.					Line No.	Simulation Type	Comparison with Discrete Time Sim.				
		Line Loss (kW)			Errors (kW)				Line Loss (kW)			Errors (kW)	
		Max	Min	Mean	Mean	Devia			Max	Min	Mean	Mean	Devia
211	DTS	26.0	4.2	10.8			226	DTS	1366.1	633.3	928.5		
	Arch D	26.7	3.6	11.1	0.3	1.5		Arch D	1488.6	609.5	942.3	13.8	31.1
	Lin LC	14.1	4.3	8.5	-2.4	5.4		Lin LC	1565.1	482.4	941.1	12.6	52.3
	Q LC	29.4	5.1	12.2	1.3	7.2		Q LC	1323.1	635.5	948.4	19.8	64.6
212	DTS	182.2	25.4	70.3			227	DTS	1431.0	696.7	993.5		
	Arch D	172.7	24.8	71.3	1.1	4.5		Arch D	1551.7	673.7	1007.5	14.	31.4
	Lin LC	115.2	35.5	69.3	-1.0	7.0		Lin LC	1675.8	516.5	1007.7	14.2	63.8
	Q LC	176.1	27.5	76.5	6.2	11.7		Q LC	1385.6	700.1	1014.0	20.4	64.8
213	DTS	131.3	3.0	13.3			228	DTS	16.4	5.1	9.2		
	Arch D	160.5	2.6	12.7	-0.6	4.6		Arch D	18.4	4.8	9.4	0.2	0.5
	Lin LC	21.3	6.6	12.8	-0.5	6.1		Lin LC	15.3	4.7	9.2	0.	0.2
	Q LC	172.9	0.6	29.8	16.5	25.4		Q LC	16.2	5.0	9.5	0.3	0.9
214	DTS	5.2	2.8	4.0			229	DTS	0.1	0.0	0.1		
	Arch D	5.1	2.7	4.0	0.1	0.1		Arch D	0.2	0.0	0.0	0.	0.
	Lin LC	7.1	2.2	4.2	0.3	0.4		Lin LC	0.1	0.0	0.0	0.	0.
	Q LC	4.5	0.1	4.1	0.1	0.4		Q LC	0.1	0.0	0.1	0.	0.
215	DTS	14.6	2.5	8.3			230	DTS	209.8	112.4	152.3		
	Arch D	14.1	2.0	8.3	0.0	0.6		Arch D	224.6	108.9	154.1	1.8	4.2
	Lin LC	16.5	5.1	9.9	1.6	1.0		Lin LC	255.9	78.9	153.9	1.6	11.9
	Q LC	11.0	1.8	8.8	0.5	2.4		Q LC	203.7	112.4	154.5	2.2	8.7
216	DTS	67.7	32.9	42.8			231	DTS	213.1	114.2	154.7		
	Arch D	71.2	33.5	44.1	1.3	1.8		Arch D	228.1	110.6	156.6	1.9	4.3
	Lin LC	72.2	22.3	43.4	0.6	4.7		Lin LC	259.9	80.1	156.3	1.6	12.
	Q LC	70.8	34.3	45.2	2.4	3.0		Q LC	206.8	114.2	156.9	2.2	8.8
217	DTS	1901.2	899.9	1300.1			232	DTS	11448.0	5273.1	7759.2		
	Arch D	2076.8	873.5	1317.0	16.9	41.9		Arch D	12426.0	5104.1	7884.8	125.6	273.2
	Lin LC	2179.7	671.8	1310.7	10.5	74.6		Lin LC	13139.0	4049.4	7900.8	141.2	452.2
	Q LC	1865.4	906.0	1325.2	25.0	87.9		Q LC	11011.0	5223.4	7928.7	169.1	543.6
218	DTS	2106.7	1046.3	1470.0			233	DTS	151.4	75.4	106.1		
	Arch D	2289.6	1021.0	1488.9	18.9	44.8		Arch D	164.5	73.0	107.6	1.5	3.3
	Lin LC	2466.3	760.1	1483.0	12.9	95.5		Lin LC	178.4	55.0	107.3	1.2	6.9
	Q LC	2065.7	1055.2	1497.4	27.3	92.9		Q LC	147.8	75.7	108.1	2.1	6.8
219	DTS	136.0	38.6	71.4			234	DTS	1119.6	572.0	791.8		
	Arch D	162.8	37.4	73.3	1.9	4.2		Arch D	1197.4	559.4	804.0	12.2	24.6
	Lin LC	117.2	36.1	70.5	-1.0	3.1		Lin LC	1336.5	411.9	803.6	11.8	62.8
	Q LC	141.0	38.7	74.4	3.0	7.9		Q LC	1081.2	572.6	807.0	15.1	44.9
220	DTS	3.0	1.4	2.5			235	DTS	35.9	2.2	12.4		
	Arch D	3.1	1.1	2.5	0.0	0.1		Arch D	38.4	2.0	10.6	-1.8	2.3
	Lin LC	4.5	1.4	2.7	0.2	0.8		Lin LC	17.0	5.2	10.2	-2.2	7.3
	Q LC	3.0	0.9	2.5	0.0	0.1		Q LC	30.6	4.7	12.5	0.2	5.6
221	DTS	213.6	115.2	155.2			236	DTS	508.1	320.7	401.3		
	Arch D	227.0	113.1	156.7	1.5	4.0		Arch D	532.2	314.5	404.2	2.9	7.7
	Lin LC	260.9	80.4	156.9	1.7	12.2		Lin LC	673.6	207.6	405.0	3.7	41.8
	Q LC	207.6	116.3	157.7	2.5	8.8		Q LC	498.1	323.4	405.8	4.5	16.8
222	DTS	219.7	118.5	159.6			237	DTS	79.8	42.6	57.7		
	Arch D	233.5	116.3	161.1	1.5	4.2		Arch D	85.4	41.6	58.4	0.7	1.5
	Lin LC	268.4	82.7	161.4	1.7	12.6		Lin LC	97.0	29.9	58.3	0.6	4.4
	Q LC	213.6	119.6	162.2	2.6	9.1		Q LC	78.0	43.3	58.7	1.	3.4
223	DTS	277.3	1.7	38.7			238	DTS	101.8	30.4	58.0		
	Arch D	565.4	2.9	47.9	9.2	14.0		Arch D	115.9	30.1	59.5	1.4	2.9
	Lin LC	51.8	16.0	31.2	-7.5	18.7		Lin LC	100.5	31.0	60.4	2.4	1.1
	Q LC	344.0	5.7	63.6	24.9	38.6		Q LC	97.9	32.9	61.5	3.5	5.9
224	DTS	0.1	0.1	0.1			239	DTS	104.3	31.2	59.5		
	Arch D	0.1	0.1	0.1	0.0	0.0		Arch D	118.8	30.9	61.0	1.5	3.
	Lin LC	0.2	0.1	0.1	0.0	0.0		Lin LC	103.0	31.7	61.9	2.4	1.2
	Q LC	0.1	-7.9	0.1	0.0	0.0		Q LC	100.4	33.7	63.1	3.6	6.1
225	DTS	56.2	21.6	29.6			240	DTS	11978.0	5801.0	8268.7		
	Arch D	60.0	22.5	30.8	1.2	1.7		Arch D	12930.0	5622.5	8399.8	131.1	276.4
	Lin LC	49.7	15.3	29.9	0.3	2.5		Lin LC	14007.0	4316.8	8422.6	153.5	543.7
	Q LC	61.0	23.6	32.4	2.9	3.1		Q LC	11508.0	5736.4	8443.2	174.1	543.3

Table C.13 Comparison of Loss Results for the 348 Node Test System (Cont.)

Line No.	Simulation Type	Comparison with Discrete Time Sim.				
		Line Loss (kW)			Errors (kW)	
		Max	Min	Mean	Mean	Devia
241	DTS	148.2	77.1	105.9		
	Arch D	160.2	75.0	107.3	1.4	3.1
	Lin LC	178.2	54.9	107.1	1.3	7.7
	Q LC	144.6	77.6	107.9	2.0	6.3
242	DTS	1180.3	621.0	844.4		
	Arch D	1257.8	609.0	857.5	13.1	25.3
	Lin LC	1425.5	439.3	857.2	12.8	70.8
	Q LC	1138.4	621.8	860.1	15.7	45.5
243	DTS	489.1	327.4	397.2		
	Arch D	509.2	323.7	400.2	3.0	6.7
	Lin LC	667.3	205.7	401.3	4.1	45.1
	Q LC	479.6	331.1	401.5	4.4	14.5
244	DTS	77.4	43.2	57.1		
	Arch D	82.4	42.4	57.7	0.6	1.4
	Lin LC	96.1	29.6	57.8	0.6	4.8
	Q LC	75.7	43.9	58.1	1.0	3.1
245	DTS	109.4	40.2	67.9		
	Arch D	122.0	40.2	69.1	1.2	2.8
	Lin LC	117.7	36.3	70.8	2.9	2.6
	Q LC	105.2	43.4	71.6	3.7	5.8
246	DTS	112.1	41.2	69.6		
	Arch D	125.0	41.2	70.8	1.2	2.9
	Lin LC	120.7	37.2	72.5	3.0	2.7
	Q LC	107.9	44.5	73.4	3.8	5.9
247	DTS	257.6	74.4	130.5		
	Arch D	290.6	68.2	134.4	3.9	8.0
	Lin LC	220.6	68.0	132.7	2.1	4.2
	Q LC	253.0	66.8	138.0	7.4	15.0
248	DTS	110.7	45.9	69.4		
	Arch D	123.0	44.4	71.0	1.6	2.8
	Lin LC	115.4	35.6	69.4	-0.1	2.3
	Q LC	112.1	45.9	71.3	1.9	5.6
249	DTS	23.6	9.6	14.6		
	Arch D	25.8	9.4	15.0	0.4	0.6
	Lin LC	24.7	7.6	14.8	0.2	0.8
	Q LC	23.0	9.6	15.1	0.5	1.0
250	DTS	313.4	177.4	225.0		
	Arch D	326.4	182.9	228.4	3.3	5.4
	Lin LC	370.8	114.3	223.0	-2.1	20.6
	Q LC	325.6	187.9	229.2	4.1	10.4
251	DTS	93.2	88.1	91.5		
	Arch D	93.1	87.9	91.4	-0.2	0.4
	Lin LC	153.4	47.3	92.2	0.7	16.3
	Q LC	93.2	90.4	92.3	0.8	0.7
252	DTS	102.6	97.0	100.8		
	Arch D	102.5	96.8	100.6	-0.2	0.5
	Lin LC	168.9	52.1	101.6	0.8	18.0
	Q LC	102.6	101.3	101.7	0.9	0.8
253	DTS	1.6	0.5	0.8		
	Arch D	1.7	0.5	0.8	0.1	0.1
	Lin LC	1.1	0.4	0.7	-0.1	0.2
	Q LC	2.2	0.5	0.9	0.1	0.3
254	DTS	1.6	0.6	0.9		
	Arch D	1.7	0.7	0.9	0.0	0.1
	Lin LC	1.5	0.5	0.9	0.0	0.1
	Q LC	1.8	0.8	1.0	0.1	0.1
255	DTS	1956.6	959.0	1330.6		
	Arch D	2083.3	933.2	1352.9	22.3	45.3
	Lin LC	2251.6	693.9	1354.0	23.4	99.6
	Q LC	1895.6	951.2	1365.9	35.3	80.6

Line No.	Simulation Type	Comparison with Discrete Time Sim.				
		Line Loss (kW)			Errors (kW)	
		Max	Min	Mean	Mean	Devia
256	DTS	74.1	42.8	55.6		
	Arch D	79.1	41.7	56.2	0.6	1.4
	Lin LC	93.1	28.7	56.0	0.4	4.8
	Q LC	72.5	42.8	56.3	0.7	2.8
257	DTS	230.3	123.8	163.7		
	Arch D	242.8	122.8	166.4	2.7	4.9
	Lin LC	276.5	85.2	166.3	2.6	15.2
	Q LC	225.4	125.5	167.9	4.1	8.
258	DTS	36.6	23.3	28.5		
	Arch D	38.4	22.7	28.7	0.2	0.5
	Lin LC	47.6	14.7	28.6	0.1	2.9
	Q LC	36.2	23.3	28.8	0.3	1.2
259	DTS	0.0	0.0	0.0		
	Arch D	0.0	0.0	0.0	0.	0.
	Lin LC	0.0	0.0	0.0	0.	0.
	Q LC	0.0	0.0	0.0	0.	0.
260	DTS	1984.6	972.8	1349.7		
	Arch D	2113.2	946.6	1372.3	22.7	45.9
	Lin LC	2283.9	703.9	1373.3	23.6	101.
	Q LC	1922.9	964.9	1385.5	35.8	81.8
261	DTS	73.9	42.7	55.4		
	Arch D	78.8	41.5	56.0	0.6	1.4
	Lin LC	92.9	28.6	55.8	0.4	4.8
	Q LC	72.3	42.6	56.1	0.7	2.8
262	DTS	234.5	126.0	166.7		
	Arch D	247.3	125.0	169.5	2.8	5.
	Lin LC	281.6	86.8	169.3	2.6	15.5
	Q LC	229.6	127.8	170.9	4.2	8.2
263	DTS	36.4	23.2	28.4		
	Arch D	38.2	22.6	28.6	0.2	0.5
	Lin LC	47.3	14.6	28.5	0.1	2.8
	Q LC	36.0	23.1	28.6	0.3	1.2

Appendix D. Database Entities and Attributes Required for Time Based Load-flow Analysis

D.1 Plant Data

The following sections describe the static plant data attributes which must be specified for each database entity to perform a time-based load-flow study. Omitted from this data are the attributes which define the connectivity of the network. These attributes are maintained automatically by the SQL server whenever plant is added, deleted, connected or disconnected within the system.

In addition to the attributes described in the following section, every entity has the attribute In Study, which defines whether the entity is a member of the current 'study'. The proposed Insight application uses the In Study attribute to determine whether an item of plant is part of the network to be analysed.

Further information is provided in references [17] and [19].

D.1.1 Generator Entity

Table D.1 lists the plant data attributes required for the generator entity.

Table D.1 Plant Data Attributes for the Generator Entity

Attribute Name	Data Type	Description
Number	Integer	Unique database identifier. Assigned automatically when entity is created
Name	String	A unique name must be entered for each generator
Profile Library Type	Integer	If the generator uses library profiles, an integer corresponding to the consumer type code in the load library must be entered. Otherwise a zero is entered
Meter File Type	Integer	If the generator has metered data a non-zero integer is entered specifying the source format of the metered data. If the generator does not have metered data, a zero is entered.
Active Power Minimum	Real MW	Minimum active power output of the generator
Active Power Maximum	Real MW	Maximum active power output of the generator
Reactive Power Minimum	Real MVAr	Minimum reactive power output of the generator
Reactive Power Maximum	Real MVAr	Maximum reactive power output of the generator
Voltage Magnitude	Real kV	Target voltage V of generator
Annual Active Power Maximum	Real MW	The annual active max demand for the generator. May be used in the Generator Constrained mode of simulation
Annual Reactive Power Maximum	Real MVAr	The annual reactive max demand for the generator
Loss Factor	Real %	An estimate of the average percentage MW loss occurring between the generator and the nearest Grid Supply Point. Zero can be entered in the absence of data

D.1.2 Infeed Entity

Infeeds are used to model Grid Supply Points and other forms of interconnection with external systems. Table D.2 lists the plant data attributes for the infeed entity.

Table D.2 Plant Data Attributes for the Infeed Entity

Attribute Name	Data Type	Description
Number	Integer	Unique database identifier. Assigned automatically when entity is created
Name	String	The name is optional for infeeds, but if used it must be unique.
Fault Level Current Magnitude	Real MVA	Fault level of the infeed in MVA. Used to calculate the equivalent impedance of the infeed.
Fault Level Power Factor	Real	Fault level power factor. Used to calculate the equivalent impedance of the infeed.

D.1.3 Junction Entity

Junctions are used for the connection of plant. The busbar is a type of junction. Table D.3 lists the plant data attributes of the junction entity.

Table D.3 Plant Data Attributes for the Junction Entity

Attribute Name	Data Type	Description
Number	Integer	Unique database identifier. Assigned automatically when entity is created
Name	String	The name is optional for junctions, but if used it must be unique
Voltage Magnitude Level	Real kV	The nominal or base voltage *V* for the junction
Voltage Magnitude Minimum	Real kV	The minimum permitted voltage V_{min} for the junction. Used by the constrained mode of simulation
Voltage Magnitude Maximum	Real kV	The maximum permitted voltage *Vmax for* the junction. Used by the constrained mode of simulation

D.1.4 Line Entity

Table D.4 lists the plant data attributes of the line entity. The load-flow program uses a pi model for transmission lines, as illustrated in Figure D.1.

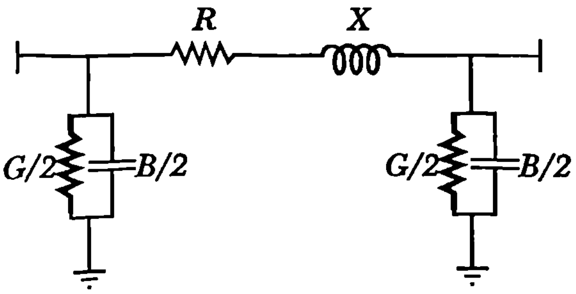

Figure D.1 Transmission Line Model Used in the Load-flow Program

Table D.4 Plant Data Attributes for the Line Entity

Attribute Name	Data Type	Description
Number	Integer	Unique database identifier. Assigned automatically when entity is created
Name	String	The name is optional for lines. If used, the name must be unique
Temperature Type	Logical	Specifies whether the resistance of the line is modified according to temperature in the load flow computations. Enter T or F
Resistance Positive Sequence	Real	The resistance R of the line in per unit.
Reactance Positive Sequence	Real	The reactance X of the line in per unit.
Susceptance Positive Sequence	Real	The susceptance B of the line in per unit.
Conductance Positive Sequence	Real	The conductance G of the line in per unit.

D.1.5 Load Entity

Table D.5 lists the plant data attributes for the load entity. The variation of load power with voltage is accounted for using the polynomials:

$$\begin{aligned} P_{Di} &= P_{Dnom,i}(\alpha_1 V_i^{\mu_1} + \alpha_2 V_i^{\mu_2} + \alpha_3 V_i^{\mu_3}) \\ Q_{Di} &= Q_{Dnom,i}(\beta_1 V_i^{\nu_1} + \beta_2 V_i^{\nu_2} + \beta_3 V_i^{\nu_3}) \end{aligned}$$

where α and β are active and reactive coefficients, and μ and ν are active and reactive exponents respectively.

Table D.5 Plant Data Attributes for the Load Entity

Attribute Name	Data Type	Description
Number	Integer	Unique database identifier. Assigned automatically when entity is created
Name	String	A unique name must be entered for each Load
Profile Library Type	Integer	If the load is a library consumer, an integer corresponding to the consumer type code in the load library must be entered. Otherwise a zero is entered
Meter File Type	Integer	If the load is a metered consumer a non-zero integer is entered specifying the source format of the metered data. If the load is not a metered consumer, a zero is entered.
Active Power Coefficients and Exponents	Real	Coefficients α_1, α_2, α_3. Exponents μ_1, μ_2, μ_3. For a load whose active power is independent of voltage (the default) Coefficient 1 are set to 1.0 and all the other coefficients and exponents are set to zero.
Reactive Power Coefficients and Exponents	Real	Coefficients β_1, β_2, β_3. Exponents v_1, v_2, v_3. For a load whose reactive power is independent of voltage (the default) Coefficient 1 are set to 1.0 and all the other coefficients and exponents are set to zero
Annual Active Power Maximum	Real MW	The annual active maximum demand for the load. May be used in the Load Constrained mode of simulation
Annual Reactive Power Maximum	Real MVAr	The annual reactive maximum demand for the load
Loss Factor	Real %	An estimate of the average percentage MW loss occurring between the nearest Grid Supply Point and the specified load. Zero can be entered in the absence of data
Tariff Group	Integer	Integer code corresponding to a tariff group defined in an INSIGHT Tariff Library file. If not used, a zero may be entered

D.1.6 Shunt Entity

The shunt entity is used to model shunt admittances such as capacitor banks. Table D.6 lists the plant data attributes for the shunt entity.

Table D.6 Plant Data Attributes for the Shunt Entity

Attribute Name	Data Type	Description
Number	Integer	Unique database identifier. Assigned automatically when entity is created
Name	String	The name is optional for shunts. If used, the name must be unique
Susceptance Positive Sequence	Real	The susceptance B in per unit of the shunt
Conductance Positive Sequence	Real	The conductance G in per unit of the shunt

D.1.7 Switch Entity

The switch entity is used to model switching devices such as circuit breakers and isolators. It is also used to model very low impedance links between busbars in substations. Table D.7 lists the plant data attributes of the switch entity.

Table D.7 Plant Data Attributes for the Switch Entity

Attribute Name	Data Type	Description
Number	Integer	Unique database identifier. Assigned automatically when entity is created
Name	String	The name is optional for switches. If used, the name must be unique
State	Integer	Specifies the state of the switch: 0 Open 1 Closed

D.1.8 Terminal Entity

Terminals are the entities by which connections are made. Terminals connect to junctions via a many-to-one relation. Table D.8 lists the plant data attributes required for the terminal entity.

Table D.8 Plant Data Attributes for the Terminal Entity

Attribute Name	Data Type	Description
Number	Integer	Unique database identifier. Assigned automatically when entity is created

D.1.9 Transformer Entity

The database model developed at Brunel University contains a flexible transformer model which caters for tap changers on the primary and/or secondary side, and which models the core losses. Figure D.2 illustrates the transformer model. A transformer has two windings, plus an optional tertiary winding. Each winding can have a tap stepper which in turn can have a servo for on-load tap changing. The windings can also have an earthing connection. The entities which comprise a transformer are listed in the following sections. Table D.9 lists the plant data required for the transformer entity.

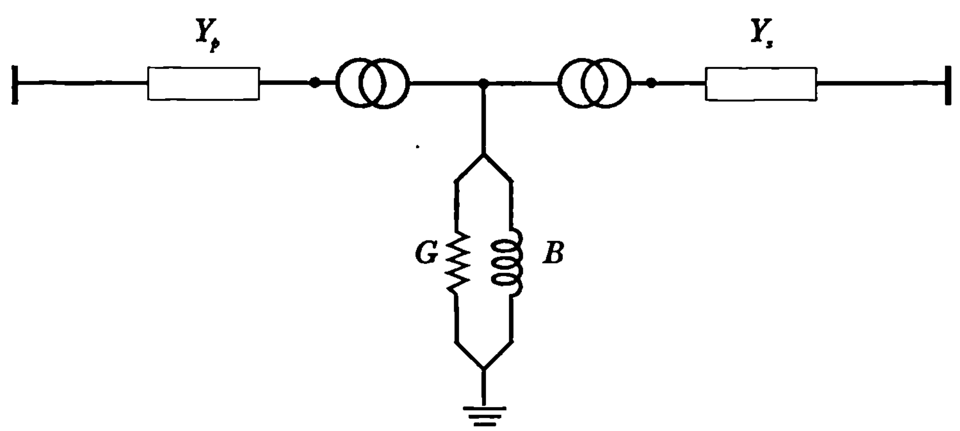

Figure D.2 Transformer Model Used in the Load-flow Program

Table D.9 Plant Data Attributes for the Transformer Entity

Attribute Name	Data Type	Description
Number	Integer	Unique database identifier. Assigned automatically when entity is created
Name	String	The name is optional for transformers. If used, the name must be unique
Group Leader Transformer Number	Integer	Transformers can be operated in parallel in master-slave configuration. This field allows specifies which of the parallel transformers is the group leader or master. For non-parallel operation, zero is entered.
Susceptance of Iron	Real	Susceptance B of the magnetising branch of the transformer in per unit.
Conductance of Iron	Real	Conductance G of the magnetising branch of the transformer in per unit.

D.1.10 Winding Entity

Table D.10 lists the plant data required for the winding entity.

Table D.10 Plant Data Attributes for the Winding Entity

Attribute Name	Data Type	Description
Number	Integer	Unique database identifier. Assigned automatically when entity is created
Resistance Positive Sequence	Real	The resistance R of the winding in per unit.
Reactance Positive Sequence	Real	The reactance X of the winding in per unit.

D.1.11 Stepper Entity

Table D.11 lists the plant data required for the stepper entity.

Table D.11 Plant Data Attributes for the Stepper Entity

Attribute Name	Data Type	Description
Number	Integer	Unique database identifier. Assigned automatically when entity is created
Position Minimum	Real	The minimum tap ratio in per unit
Position Maximum	Real	The maximum tap ratio in per unit
Position Steps	Integer	The number of tap steps
Position Nominal	Integer	The nominal tap position

D.1.12 Servo Entity

The servo entity is used to drive tap and phase steppers for on-load tap changing transformers. Table D.12 lists the plant data required for the servo entity.

Table D.12 Plant Data Attributes for the Servo Entity

Attribute Name	Data Type	Description
Number	Integer	Unique database identifier. Assigned automatically when entity is created
Load Drop Compensation Resistance	Real	LDC resistance setting in per unit. Zero if not used
Load Drop Compensation Reactance	Real	LDC reactance setting in per unit. Zero if not used
Set Point	Real kV I MW	The target voltage (or MW for phase stepper servos) of the servo. The tap position will be adjusted within its limits to maintain this target.
State	Integer	The operating state of the servo: 0 Inactive/Disabled 1 Active/Enabled

D.1.13 Earthing Entity

Table D.13 lists the plant data required for the earthing entity.

Table D.13 Plant Data Attributes for the Earthing Entity

Attribute Name	Data Type	Description
Number	Integer	Unique database identifier. Assigned automatically when entity is created
Resistance	Real	Earthing resistance R in per unit
Reactance	Real	Earthing reactance X in per unit
State	Integer	Earthing state: 0 Off/Disconnected 1 On/Connected

D.2 Profiles Data

The time based profiles data forms part of the input data to the discrete time simulator. Values are specified for each time step t of the simulation. The attributes are described in the following sections.

D.2.1 Generator Entity

Table D.14 lists the profiles data attributes required for the generator entity. The values specified dictate the mode of the generator according to the following conventions given in Table D.15.

Table D.14 Profiles Data Attributes for the Generator Entity

Attribute Name	Data Type	Description
Active power	Real MW	Active power generation $P_G(t)$ of the generator
Reactive power	Real MVAr	Reactive power generation $Q_G(t)$ of the generator

Table D.15 Conventions for Generation Mode Selection

Generation Mode	Active Power P(t)	Reactive Profile Q(t)	Remarks
PV	> 0	= 0	Generator operates at specified MW output, while MVAr output varies within limits to maintain a constant target voltage
PQ	> 0	> 0	Generator operates at specified MW and MVAr voltage, while voltage is allowed to vary
Vθ	= 0	= 0	Implies a slack generator. Generator operates at specified voltage magnitude and angle, while MW and MVAr output vary to supply any mismatch in supply and demand in the system

D.2.2 Load Entity

Table D.16 lists the profiles data required for the load entity.

Table D.16 Profiles Data Attributes for the Load Entity

Attribute Name	Data Type	Description
Active power	Real MW	Active power demand $P_D(t)$ of the load
Reactive power	Real MVAr	Reactive power demand $Q_D(t)$ of the load

D.3 Results Data

This section describes the time based results data generated by the discrete time simulator. The results data is held in just three entities: junction, terminal and stepper. From this data, time based load-flow results for all the other entities can be derived, based upon knowledge of the connectivity of the network and the static plant data described in Section D.1. For example, the loss in a line can be determined by studying the power flow through the terminals at each end of the line, and taking the difference between the two.

D.3.1 Junction Entity

Table D.17 lists the time based results data for the junction entity.

Table D.17 Results Data Attributes for the Junction Entity

Attribute Name	Data Type	Description
Voltage Magnitude	Real kV	Voltage *V(t)* of the junction
Voltage Angle	Real Deg	Angle $\theta(t)$ of the junction

D.3.2 Terminal Entity

Table D.18 lists the time based results data for the terminal entity.

Table D.18 Results Data Attributes for the Terminal Entity

Attribute Name	Data Type	Description
Current Magnitude	Real A	Magnitude of current flowing through the terminal
Current Angle	Real Deg	Angle of current flowing through the terminal
Active Power	Real MW	Active power *P(t)* flowing through the terminal
Reactive Power	Real MVAr	Reactive power *Q(t)* flowing through the terminal

D.3.3 Stepper Entity

Table D.19 lists the time based results data for the stepper entity.

Table D.19 Results Data Attributes for the Stepper Entity

Attribute Name	Data Type	Description
Tap Position	Integer	Tap position of the stepper

Appendix E. Distribution Test Networks

E.1 Introduction

The following sections describe the distribution networks used in the tests reported in the thesis. In certain cases network details have been omitted to comply with restrictions related to the commercially sensitive nature of the data.

E.2 7 Node Test System

E.2.1 System Configuration

The 7 Node system is a primary feeder from a distribution system in the United Kingdom, and supplies a mixture of industrial and domestic loads as shown in Figure E.1.

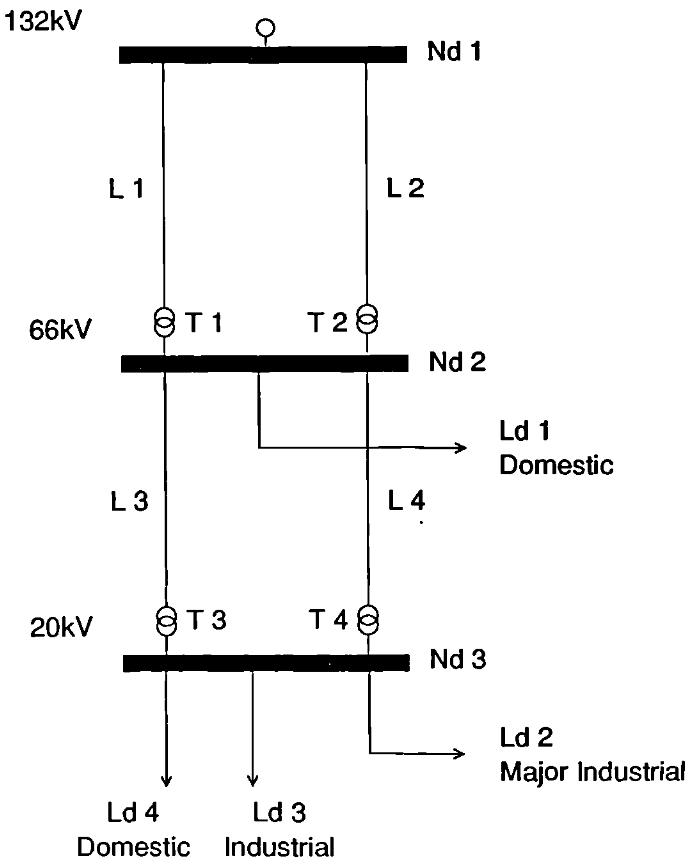

Figure E.1 7 Node Test System Configuration

E.2.2 Plant Data

The plant data is given in Tables E.1 to E.3.

Table E.1 7 Node Test System Impedance Data

Line No.	From	To	R p.u.	X p.u.	S p.u.	Line No.	From	To	R p.u.	X p.u.	S p.u.
1	1	2	0.0122	0.0271	0.0000	3	2	3	0.1476	0.2679	0.0000
2	1	2	0.0122	0.0271	0.0000	4	2	3	0.1424	0.3087	0.0000

Table E.2 7 Node Test System Transformer Data

Transformer			Taps			Impedance			Controls			
No.	From	To	Max	Min	Steps	R	X	G	LTC	Set P	LDC R	LDC X
1	1	2	1.100	0.800	18	0.0062	0.1910	0.00045	✓	0.977	0.0000	0.0000
2	1	2	1.100	0.800	18	0.0062	0.1905	0.00040	✓	0.977	0.0000	0.0000
3	2	3	1.105	0.895	14	0.0023	0.6476	0.00021	✓	1.025	0.0000	0.0000
4	2	3	1.105	0.895	14	0.0023	0.6300	0.00021	✓	1.025	0.0000	0.0000

Table E.3 7 Node Test System PV Node Data

Node	Voltage p.u.	Minimum MVAr	Maximum MVAr
2	1.000	$-\infty$	∞

E.2.3 Profiles Data

Metered data for the period 1 January to 31 December 1987, recorded at half hour intervals, is stored for this system. Table E.4 summarises the demand profile characteristics of the individual loads, and indicates the high levels of load diversity on the system.

Table E.4 7 Node Test System Profiles Data

Load	Voltage	Load Type	Profile Characteristics
Ld 1	66kV	Domestic feeder	Predictable, repetitive domestic pattern showing normal week and weekend trends.
Ld 2	20kV	Major industrial. Chemical manufacturing process	Predictable, industrial pattern with heavy overnight usage
Ld 3	20kV	Industrial. Steel component manufacture.	Repetitive pattern showing double day shift working. No Sunday load.
Ld 4	20kV	Domestic feeder with some commercial.	Moderately predictable, overall domestic pattern.

E.3 9 Node Test System

E.3.1 System Configuration

The 9 Node system is a radial 11kV feeder supplying a rural system, as shown in Figure E.2. A 200kVA embedded generator is connected via a 415V/11kV transformer at the far end of the feeder.

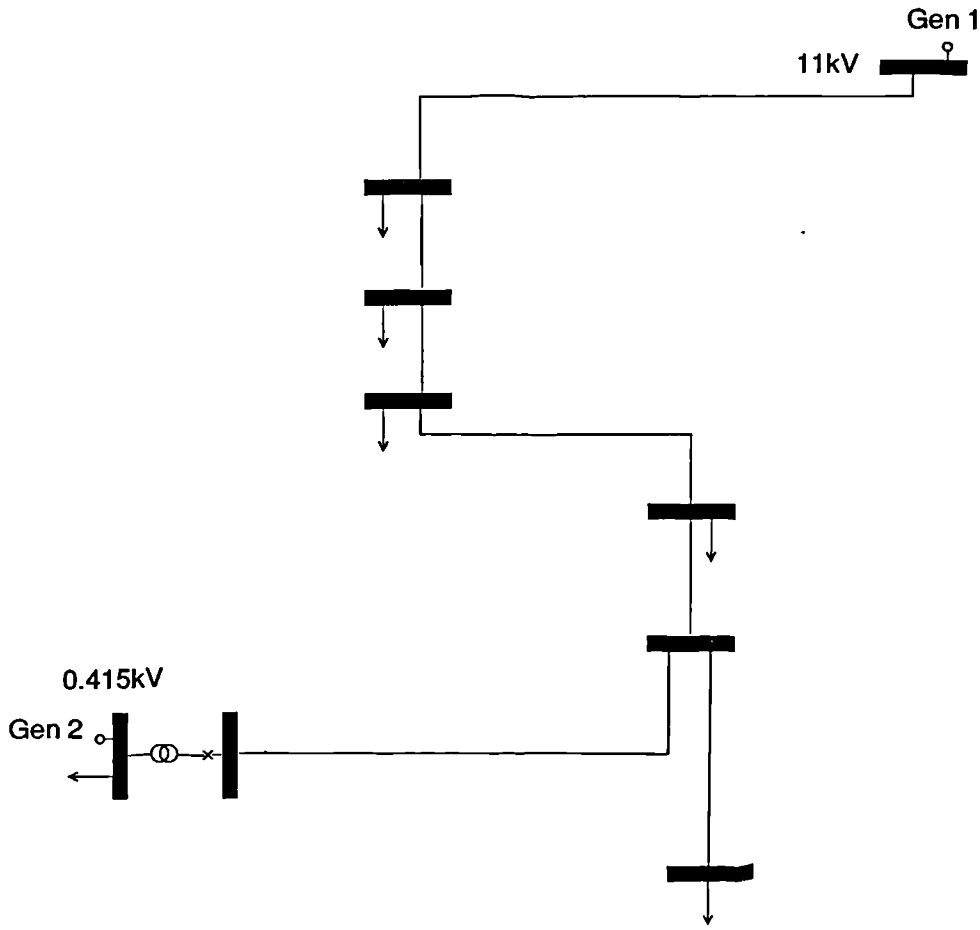

Figure E.2 9 Node Test System Configuration

E.3.2 Profiles Data

Time based load and generation data was not available for this system, and therefore had to be created. Demand profiles were created for the period 7 to 10 January 1990 at half hour intervals using the Load Allocation application. Domestic Winter Weekday and Weekend library profiles were used to model the six loads on the system.

E.4 10 Node Test System

E.4.1 System Configuration

The 10 Node system is a primary feeder from a distribution system in the United Kingdom, and supplies a mixture of heavy industrial and rural loads as shown in Figure E.3.

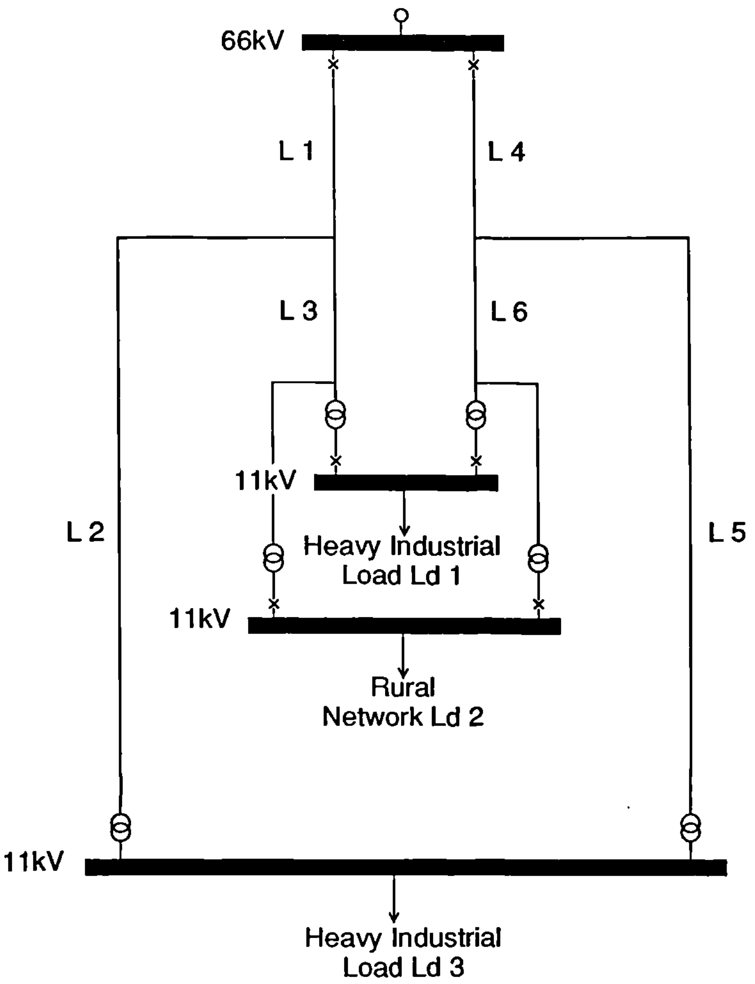

Figure E.3 10 Node Test System Configuration

E.4.2 Profiles Data

Metered data for the period 1 January to 31 June 1993, recorded at half hour intervals, is stored for this system. Table E.5 summarises the demand profile characteristics of the individual loads, and indicates the high levels of diversity on the system.

Table E.5 10 Node Test System Profiles Data

Load	Voltage	Load Type	Profile Characteristics
Ld 1	11kV	Heavy industrial with large scale electrical machinery	General weekly trend, but large random variations from one hour to the next.
Ld 2	11kV	Rural network. Domestic and agricultural loads	Predictable pattern, with large early morning demand.
Ld 3	20kV	Industrial. Mineral processing plant	General weekly trend, but very large random variations during the day

E.5 15 Node Test System

E.5.1 System Configuration

The 15 Node test system is shown in Figure E.3

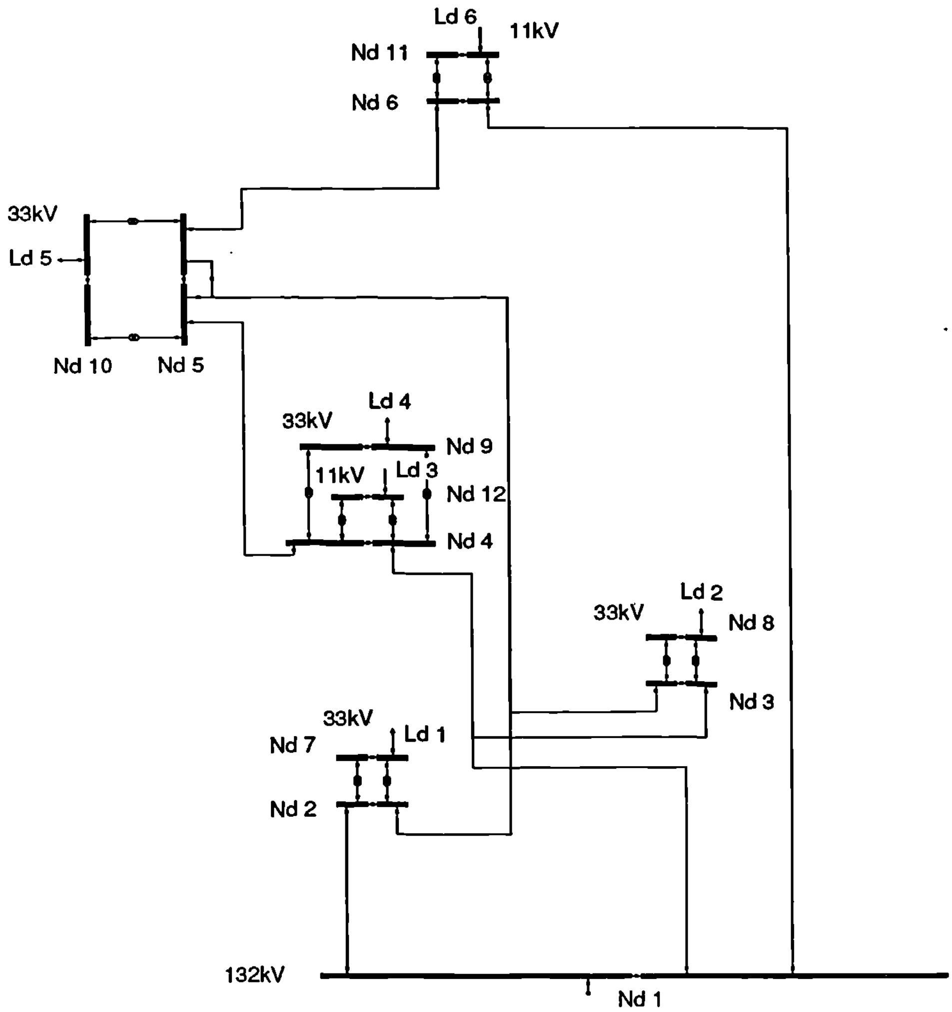

Figure E.4 15 Node Test System Configuration

E.5.2 Profiles Data

Metered data for the period 1 January to 31 December 1992, recorded at half hour intervals, is stored for this system. Table E.6 summarises the demand profile characteristics of the individual loads.

Table E.6 15 Node Test System Profiles Data

Load	Voltage	Load Type	Profile Characteristics
Ld 1	33kV	Domestic/Rural	Fairly predictable, domestic pattern
Ld 2	33kV	Domestic/Rural	Predictable domestic pattern
Ld 3	11kV	Domestic	Predictable domestic pattern
Ld 4	33kV	Domestic/Commercial	Predictable pattern
Ld 5	33kV	Domestic/Rural	General weekly trend, but large variations from day to day
Ld 6	11kV	Rural	General weekly trend, but large variations from day to day. Large early morning load

E.6 IEEE 30 Node Test System

E.6.1 System Configuration

The configuration of the IEEE 30 Node test system is shown in Figure E.5. The system is interconnected and operates at a nominal voltage of 33kV.

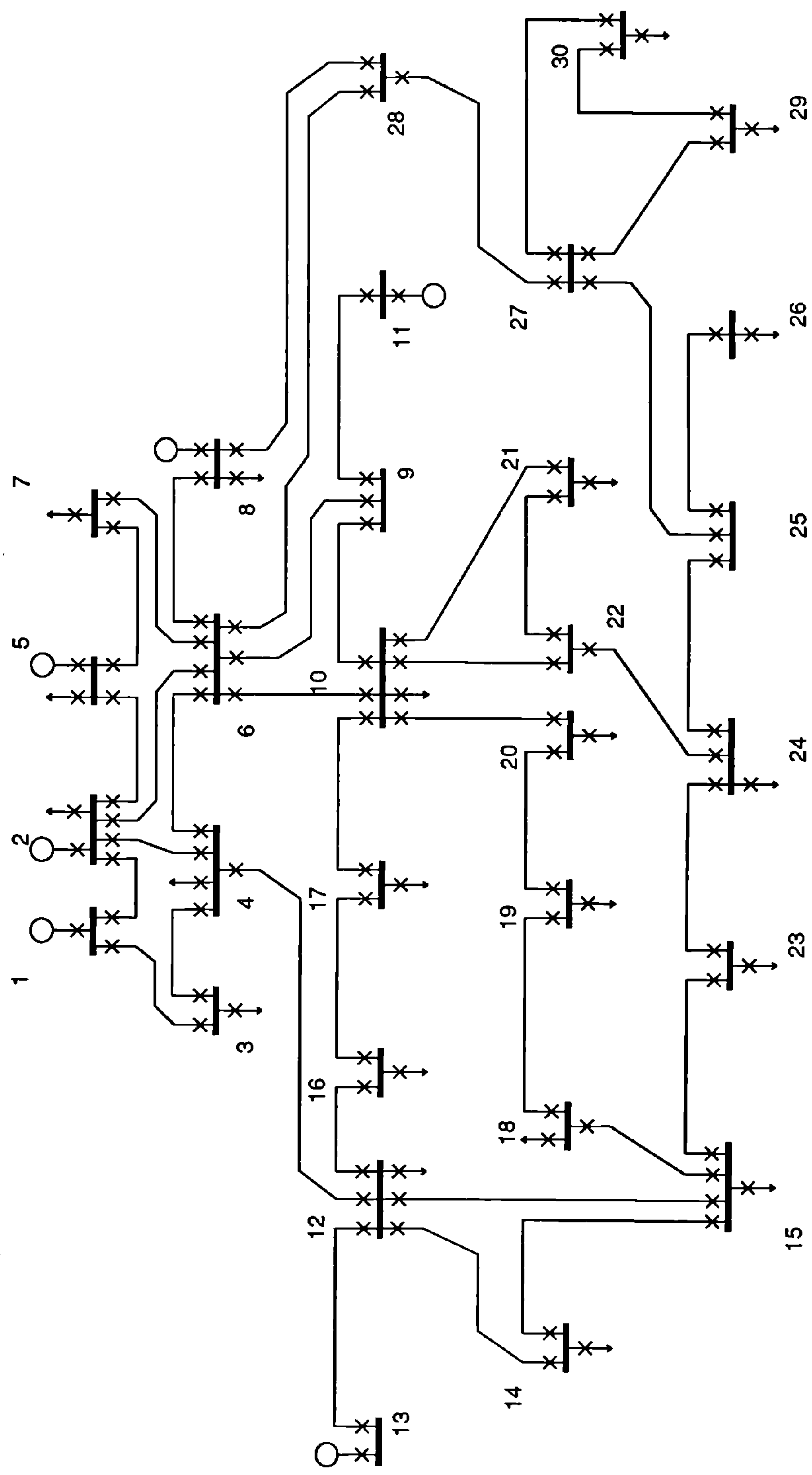

Figure E.5 IEEE 30 Node Test System Configuration

E.6.2 Plant Data

Plant data is given in Tables E.7 and E.8, and is taken from Freris [49].

Table E.7 IEEE 30 Node Test System Impedance Data

Line From	To	R p.u.	X p.u.	S p.u.		Line From	To	R p.u.	X p.u.	S p.u.
1	2	0.0192	0.0575	0.0264		15	18	0.1070	0.2185	0.0000
1	3	0.0452	0.1852	0.0204		18	19	0.0639	0.1292	0.0000
2	4	0.0570	0.1737	0.0184		19	20	0.0340	0.0680	0.0000
3	4	0.0132	0.0379	0.0042		10	20	0.0936	0.2090	0.0000
2	5	0.0472	0.1983	0.0209		10	17	0.0324	0.0845	0.0000
2	6	0.0581	0.1763	0.0187		10	21	0.0348	0.0749	0.0000
4	6	0.0119	0.0414	0.0045		10	22	0.0727	0.1499	0.0000
5	7	0.0460	0.1160	0.0102		21	22	0.0116	0.0236	0.0000
6	7	0.0267	0.0820	0.0085		15	23	0.1000	0.2020	0.0000
6	8	0.0120	0.0420	0.0045		22	24	0.1150	0.1790	0.0000
6	9	0.0000	0.2080	0.0000		23	23	0.1320	0.2700	0.0000
6	10	0.0000	0.5560	0.0000		24	25	0.1885	0.3292	0.0000
9	11	0.0000	0.2080	0.0000		25	26	0.2544	0.3800	0.0000
9	10	0.0000	0.1100	0.0000		25	27	0.1093	0.2087	0.0000
4	12	0.0000	0.2560	0.0000		27	28	0.0000	0.3960	0.0000
12	13	0.0000	0.1400	0.0000		27	29	0.2198	0.4153	0.0000
12	14	0.1231	0.2559	0.0000		27	30	0.3202	0.6027	0.0000
12	15	0.0662	0.1304	0.0000		29	30	0.2399	0.4533	0.0000
12	16	0.0945	0.1987	0.0000		8	28	0.0636	0.2000	0.0214
14	15	0.2210	0.1997	0.0000		6	28	0.0169	0.0599	0.0065
16	17	0.0824	0.1923	0.0000						

Table E.8 IEEE 30 Node Test System PV Node Data

Node	Voltage p.u.	Minimum MVAr	Maximum MVAr
2	1.045	-40.0	50.0
5	1.010	-40.0	40.0
7	1.010	-10.0	40.0
11	1.082	-6.0	24.0
13	1.071	-6.0	24.0

E.6.3 Profiles Data

Time based load and generation data was not available for this system, and therefore had to be created. Demand profiles were imported for the period 7 to 10 January 1990 at half hour intervals from substations of another distribution system operating at similar voltage. The power injection values given in reference [49] were used as maximum demands for the scaling of imported profiles. The load categories are summarised in Table E.9.

Table E.9 30 Node Test System Load Categories

Load Type	Number of Loads
Domestic	15
Commercial	1
Light Industrial	1
Heavy Industrial	2

E.7 52 Node Test Network

E.7.1 System Configuration

The 52 Node test system comprises a collection of 33kV and 11kV feeders supplied from a grid supply point at 400kV. Part of the 33kV system is operated in a meshed configuration. The configuration is shown in Figure E.6.

E.7.2 Profiles Data

Time based load and generation data was not available for this system, and therefore had to be created. Demand profiles were imported for the period 7 to 10 January 1990 at half hour intervals from substations of other distribution systems operating at similar voltage. Maximum demand readings were available and were used for the scaling of imported profiles. The load categories are summarised in Table E.10.

Table E.10 52 Node Test System Load Categories

Load Type	Number of Loads
Domestic	9
Commercial	1
Light Industrial	1
Heavy Industrial	4

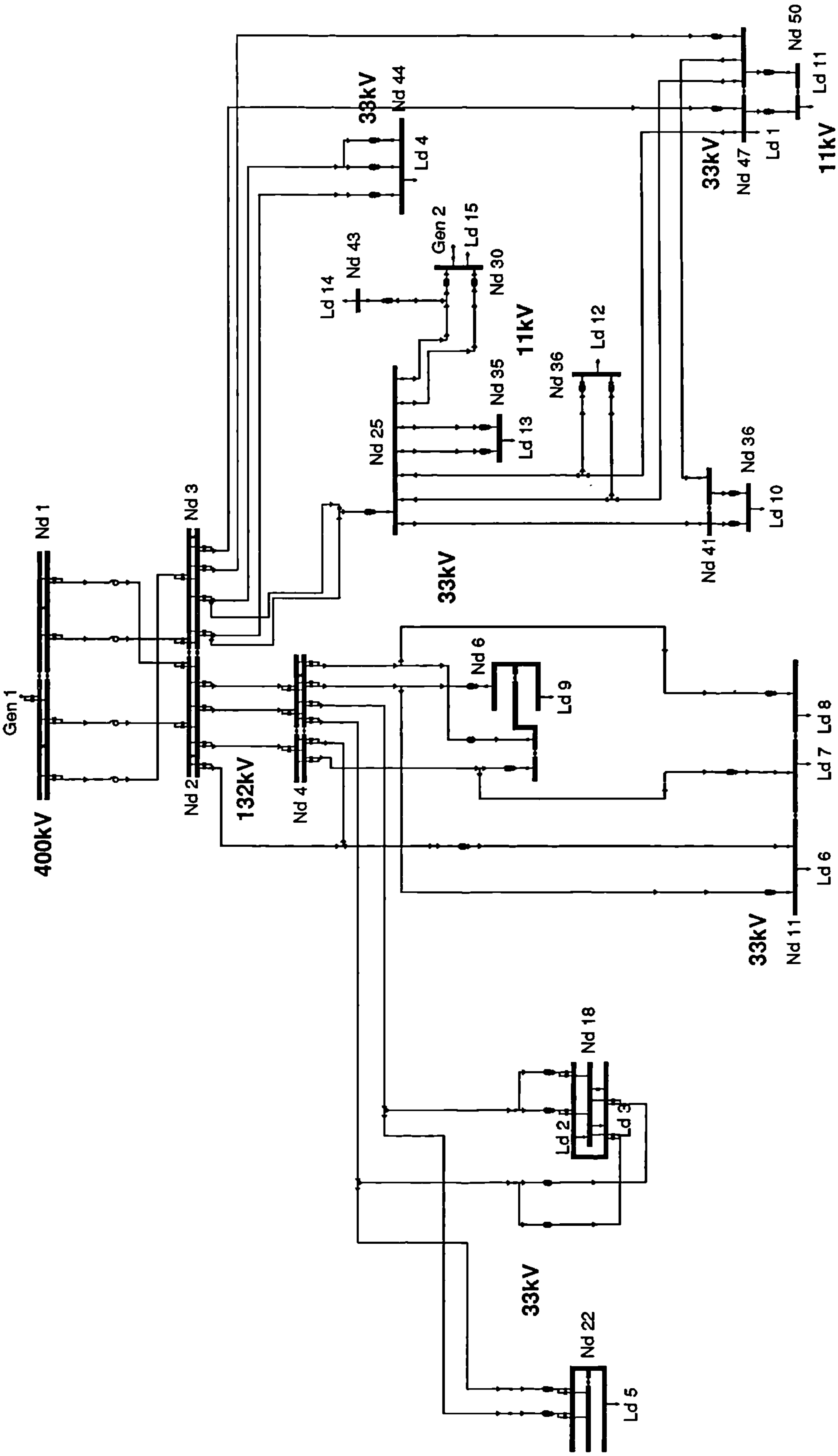

Figure E.6 52 Node Test System Configuration

E.8 122 Node Test Network

E.8.1 System Configuration

The 122 node test system is a radial 11kV circuit feeding five 11kV/433V transformers which serve individual streets in a residential urban area.

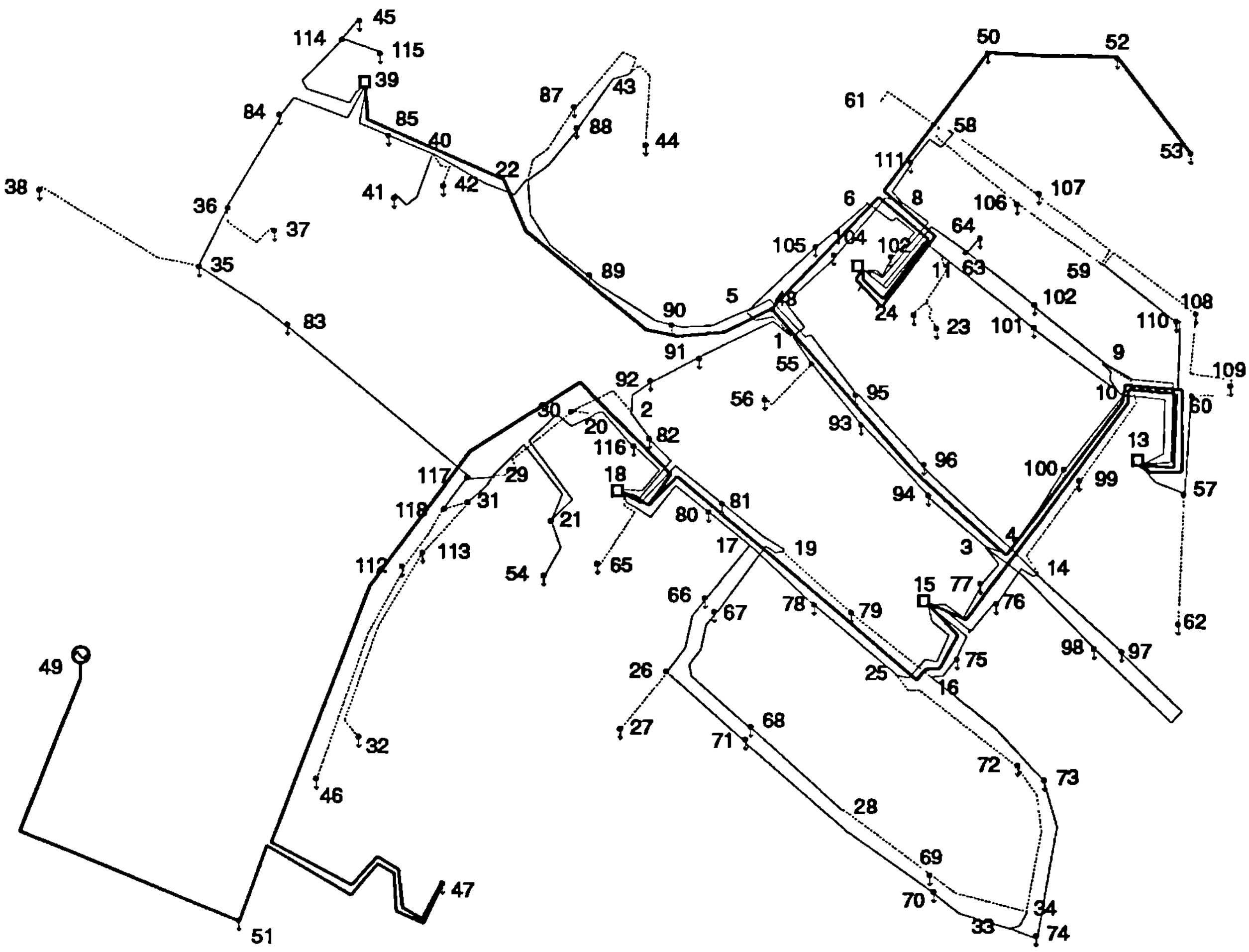

Figure E.7 122 Node Test System Configuration

E.8.2 Plant Data

Plant data is given in Tables E.11 to E.13.

Table E.11 122 Node Test System Impedance Data

Line From	To	R p.u.	X p.u.	S p.u.		Line From	To	R p.u.	X p.u.	S p.u.
1	91	10.9810	3.7904	0.0000		81	19	8.5789	2.9612	0.0000
1	55	3.5459	1.2240	0.0000		19	67	10.6378	3.6719	0.0000
5	1	6.2912	2.1716	0.0000		116	20	5.2617	1.8167	0.0000
104	1	11.8961	4.1063	0.0000		20	21	18.7592	6.4752	0.0000
92	2	4.2323	1.4609	0.0000		20	30	4.8773	1.1673	0.0000
82	2	3.3172	1.1450	0.0000		21	29	13.4975	4.6590	0.0000
30	2	12.1934	2.9183	0.0000		21	54	6.9775	2.4085	0.0000
94	3	7.8926	2.7243	0.0000		89	22	13.6798	4.9679	0.0000
3	4	3.4316	1.1845	0.0000		86	22	5.4905	1.8952	0.0000
98	3	15.6708	5.4092	0.0000		22	87	25.5944	3.3096	0.0000
3	77	5.2617	1.8162	0.0000		88	22	7.6638	2.6454	0.0000
4	96	12.1248	4.1852	0.0000		78	25	11.0954	3.8299	0.0000
14	4	3.7747	1.3029	0.0000		25	72	25.4319	6.0867	0.0000
100	4	9.9515	3.4350	0.0000		66	26	9.1508	3.1587	0.0000
95	5	16.8146	5.8040	0.0000		26	27	13.0295	2.7975	0.0000
5	105	10.1803	3.5140	0.0000		26	71	10.4091	3.5930	0.0000
5	90	6.6192	2.4038	0.0000		28	68	12.9255	4.4616	0.0000
105	6	6.8631	2.3690	0.0000		71	28	13.6119	4.6985	0.0000
6	103	10.0659	3.4745	0.0000		28	70	13.0399	4.5011	0.0000
103	119	4.3466	1.5004	0.0000		28	69	33.3401	4.3112	0.0000
119	8	13.2687	4.5801	0.0000		29	30	18.1158	4.3357	0.0000
119	63	15.7852	5.4487	0.0000		29	31	7.3160	1.7510	0.0000
11	119	12.5824	4.3432	0.0000		29	117	2.4021	0.8291	0.0000
48	7	0.0364	0.0250	0.0000		31	118	1.9161	0.4586	0.0000
7	50	0.0407	0.0229	0.0000		31	113	21.2164	2.7435	0.0000
8	104	10.0659	3.4745	0.0000		113	32	64.9964	8.4047	0.0000
8	111	5.2617	1.8162	0.0000		74	33	3.2028	1.1055	0.0000
9	102	9.0364	3.1192	0.0000		70	33	9.9515	3.4350	0.0000
9	10	4.3466	1.5004	0.0000		34	33	2.6477	0.9615	0.0000
120	9	18.3016	6.3173	0.0000		72	34	23.5158	5.6281	0.0000
9	99	24.3867	5.8365	0.0000		69	34	32.3298	4.1806	0.0000
10	100	9.7228	3.3561	0.0000		83	35	11.0954	3.8299	0.0000
10	101	11.0954	3.8299	0.0000		35	36	6.4056	2.2111	0.0000
10	120	12.9255	4.4616	0.0000		35	38	28.0447	6.7120	0.0000
101	11	12.3536	4.2642	0.0000		36	37	14.5589	2.7069	0.0000
11	12	8.7090	2.0845	0.0000		36	84	11.2098	3.8694	0.0000
12	23	14.8178	1.3302	0.0000		84	122	12.3536	4.2642	0.0000
12	24	2.4387	0.5837	0.0000		122	85	7.8328	2.8445	0.0000
15	13	0.0635	0.0298	0.0000		122	114	13.9550	4.8170	0.0000
13	48	0.0783	0.0441	0.0000		48	39	0.1288	0.0353	0.0000
120	57	5.0330	1.7373	0.0000		40	86	6.5200	2.2505	0.0000
110	120	18.3016	6.3173	0.0000		85	40	4.6335	1.6827	0.0000
14	97	11.7817	4.0668	0.0000		40	41	8.3501	2.8823	0.0000
99	14	18.4642	4.4191	0.0000		40	42	17.8836	1.6055	0.0000
76	14	6.7487	2.3295	0.0000		87	43	33.6769	4.3548	0.0000
77	121	7.8926	2.7243	0.0000		43	88	8.2357	2.8428	0.0000
121	76	9.4940	3.2771	0.0000		43	44	36.7078	4.7467	0.0000
121	75	7.7782	2.6849	0.0000		114	45	2.7452	0.9476	0.0000
25	121	12.5824	4.3432	0.0000		112	46	35.7091	8.5464	0.0000
47	15	0.1208	0.0864	0.0000		51	47	0.0469	0.0264	0.0000
75	16	3.5459	1.2240	0.0000		51	49	0.1408	0.0793	0.0000
79	16	15.3288	3.6687	0.0000		50	52	0.0136	0.0077	0.0000
16	73	16.2427	5.6066	0.0000		52	53	0.0130	0.0073	0.0000
17	80	5.2617	1.8162	0.0000		55	93	8.0070	2.7638	0.0000
17	78	9.1508	3.1587	0.0000		55	56	11.4966	2.7515	0.0000
17	66	7.2063	2.4874	0.0000		60	57	10.6378	3.6719	0.0000
18	80	10.6378	3.6719	0.0000		57	62	30.2337	5.1619	0.0000
82	18	13.1543	4.5406	0.0000		111	58	7.7782	2.6849	0.0000
18	81	14.1838	4.8959	0.0000		58	107	17.0707	4.0856	0.0000
18	116	10.0659	3.4745	0.0000		107	59	17.2449	4.1273	0.0000
18	65	16.5830	3.5605	0.0000		59	108	18.8126	4.5025	0.0000
19	79	14.9804	3.5853	0.0000		59	106	16.5481	3.9605	0.0000

Table E.12 122 Node Test System Impedances (Cont.)

Line From	To	R p.u.	X p.u.	S p.u.		Line From	To	R p.u.	X p.u.	S p.u.
59	110	9.1508	3.1587	0.0000		93	94	10.0659	3.4745	0.0000
109	60	8.0128	1.9177	0.0000		96	95	10.5234	3.6325	0.0000
106	61	30.3092	7.2540	0.0000		97	98	21.0469	7.2649	0.0000
63	102	8.9221	3.0797	0.0000		108	109	17.7675	4.2523	0.0000
63	64	2.0589	0.7107	0.0000		118	112	12.5417	3.0017	0.0000
67	68	15.5564	5.3697	0.0000		114	115	4.3466	1.5004	0.0000
73	74	16.4715	5.6856	0.0000		7	119	1.8120	9.3250	0.0000
117	83	25.3935	8.7653	0.0000		13	120	1.8120	9.3250	0.0000
90	89	9.8186	3.5657	0.0000		15	121	1.8120	9.3250	0.0000
91	92	5.6049	1.9347	0.0000		39	122	1.8120	9.3250	0.0000

Table E.13 122 Node Test System PV Node Data

Node	Voltage p.u.	Minimum MVAr	Maximum MVAr
49	1.037	$-\infty$	∞

E.8.3 Profiles Data

Time based load and generation data was not available for this system. The demand profile from an alternative 11kV feeder as used to model the source breaker flow. The Load Allocation procedure was used in to assign demand profiles to each load using distribution factors derived from annual maximum demand readings.

E.9 348 Node Test Network

E.9.1 System Configuration

The 348 Node test network is a complete distribution system from Grid Supply Points at 400kV and 275kV down to and including the 33kV system, with selected feeders at 22kV, 11kV and 6.6kV. The systems at 132kV and 33kV are operated in an interconnected configuration. Most of the area served by the system is classed as residential or rural/agricultural.

E.9.2 Profiles Data

Metered data for the period 1 January to 31 January 1993, recorded at half hour intervals, is stored for this system. The loads served by the system are summarised in Table E.14 in terms of the predominant load type category.

Table E.14 348 Node Test System Load Categories

Load Type	Number of Loads
Domestic	49
Domestic/Commercial	22
Domestic/Agricultural	11
Industrial	4

Appendix F. Insight Application Program Implementation

F.1 Introduction

The following sections describe briefly the implementation details of the programs which comprise the Insight application. The menu options and major dialog boxes are listed, and their purpose described.

F.2 Insight Load Allocation Component

F.2.1 Program Functions

F.2.1.1 Main Window

Figure F.1 shows the main window of the Load Allocation component during a study. All the functions of the program are accessed from the menu at the top of the window. The area in the centre of the window displays the names of the current plant and profiles databases. At the bottom of the main window is the command window, which contains the command line and a scrolling display of the previous four commands. Commands are generated automatically when the user interacts with the program menus and dialog boxes using the mouse. Alternatively commands can be entered into the command line directly from the keyboard.

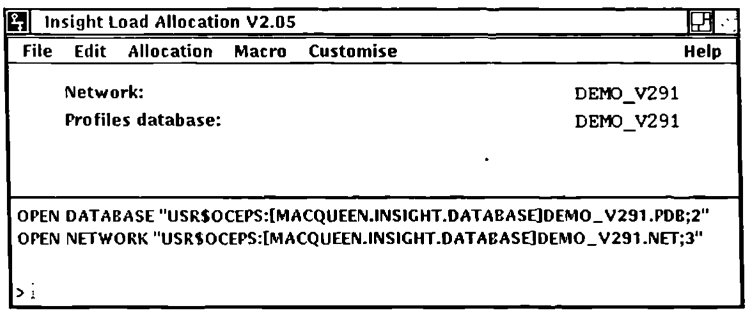

Figure F.1 Main Window of the Insight Load Allocation Component

The following sections describe briefly the functions of the program as they appear in the main menu. For a detailed description of the functions of the program, the reader is referred to reference [16].

F.2.1.2 File Related Functions

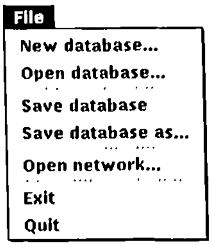

The functions in the file menu enable the user to create new profiles databases, edit existing profiles databases and save any changes made during a study.

Because the power profiles stored in a given profiles database are related to items of plant in a plant database, the Load Allocation application insists that a plant database is specified prior to commencing a study. The Open network option allows the user to specify a plant database.

The final options on the menu allow the user to leave the program.

F.2.1.3 Editing Functions

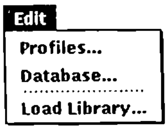

Edit profiles

The load allocation procedure performs a global update of power profiles for all selected loads and generators. However, changes to specific individual profiles can be made using the Edit profiles facility. This facility contains the following functions:

1. Editing of the attributes which dictate the treatment of an individual load or generator during the load allocation procedure.
2. Importing of time based profile data from another application for individual loads and generators.
3. Scaling of individual profiles using fixed scaling factors or annual growth factors
4. Plotting of profiles on a graph using the Graph utility described in Section 4.8.

Edit database

The profiles database itself can be edited using the Edit database facility. The contents of the database can be viewed, and individual profiles can be deleted. A consistency check can be performed to ensure that all the profiles in the profiles database correspond to valid items of plant in the plant database.

Edit load library

The profile data held in the load library can be edited using the dedicated Load Library application described in Section 4.7.

F.2.1.4 Performing a Load Allocation

Allocation

Start allocation

Once the user has specified the desired program options using the Customise menu, the load allocation is initiated using the Start allocation option.

F.2.1.5 Macro Related Functions

Macro

Record macro...
Edit macro...
Run macro...

The options in the Macro menu allow the user to record sequences of commands as a macro, to edit the resulting macro files and to run previously recorded macros.

F.2.1.6 Customising the Program Options

Customise

Hide command line
Allocation options...
Macro options...
Save current settings
Save current settings as...
Load current settings from...

The options in the Customise menu permit the user to specify settings which dictate the behaviour of the load allocation algorithm. The most important of these are accessed via the Allocation options menu item, which displays the allocation options dialog box as shown in Figure F.2.

The options at the top of the dialog allow the user to specify which classes of consumer are to be considered in the allocation study, and the time period under consideration. The remaining options specify the format of metered data to be imported, the filename of a load library file to be used in the study, and the details of the 'system load' profile which is used in the allocation procedure.

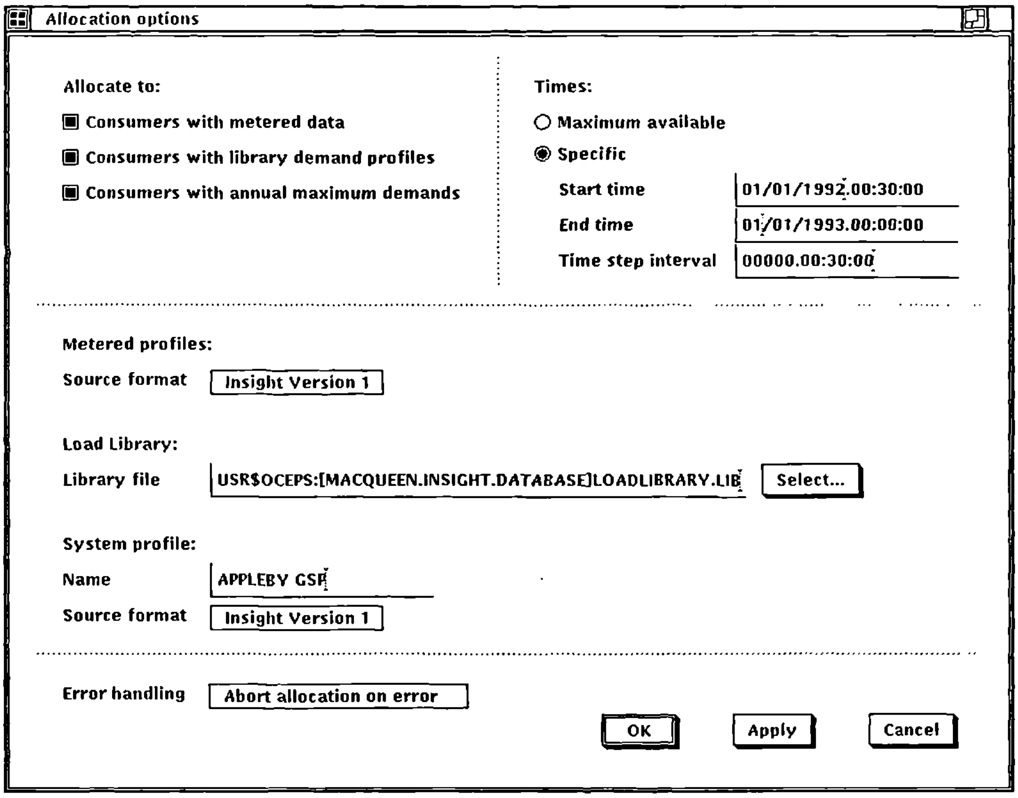

Figure F.2 Load Allocation Options Dialog Box

The final options in the customise menu permit the user to save program settings for future use, and to retrieve previously stored settings.

F.3 Insight Simulation Component

F.3.1 Program Functions

F.3.1.1 Main Window

The main window of the Insight Simulation component is shown in Figure F.3. As with the Load Allocation program, all the facilities of the program can be accessed via the main menu at the top of the main window, or alternatively by entering commands into the command line. The status of the simulation is displayed in the middle section of the window.

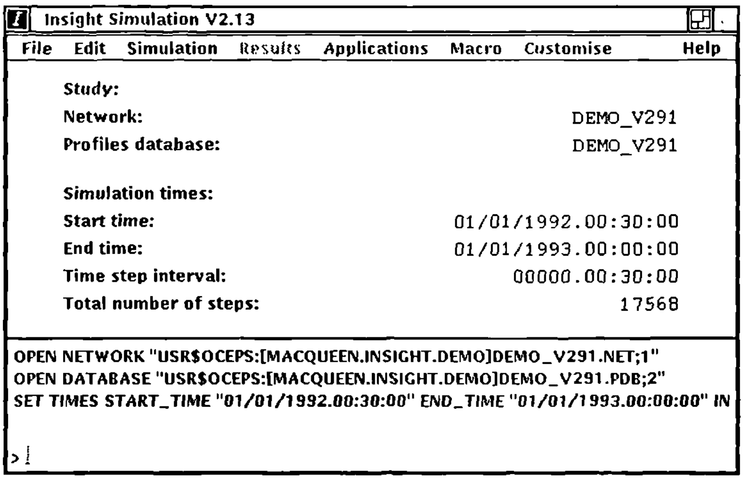

Figure F.3 Main Window of the Insight Simulation Component

The following sections describe briefly the main functions of the program as they appear in the main menu, and highlight novel features of the design. For a detailed description of these functions, the user is referred to reference [18].

F.3.1.2 File Related Functions

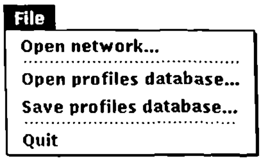

The options in the file menu allow the user to specify a plant database (network) for use in the study, and an associated profiles database. The Open network option is disabled if the program is initiated from the PACS graphics system. In this case the program establishes an API communication link with the PACS system and determines the name of the current database directly through an API query. This procedure avoids potential inconsistencies by ensuring that the two systems share the same database during the Insight study.

F.3.1.3 Editing Functions

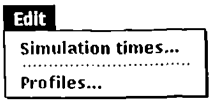

The options in the edit menu permit the user to set the times of the load-flow simulation, and to edit individual load and generation profiles.

When the Edit profiles option is selected the program uses the graphical selection techniques described in Section 4.4.5 to present just the selected loads and generators to the user.

F.3.1.4 Performing a Discrete Time Simulation

The Simulation control option presents a control dialog with buttons which allow the user to start a discrete time simulation, and additionally to pause, restart or abort the simulation once in progress. The control dialog also displays the progress of the simulation at regular intervals.

F.3.1.5 Results Analysis

The results menu contains options for the selective display of results data. The Statistics option provides a summary of the performance of the discrete time simulator. The Results option displays the main results selection dialog, as shown in Figure F.4.

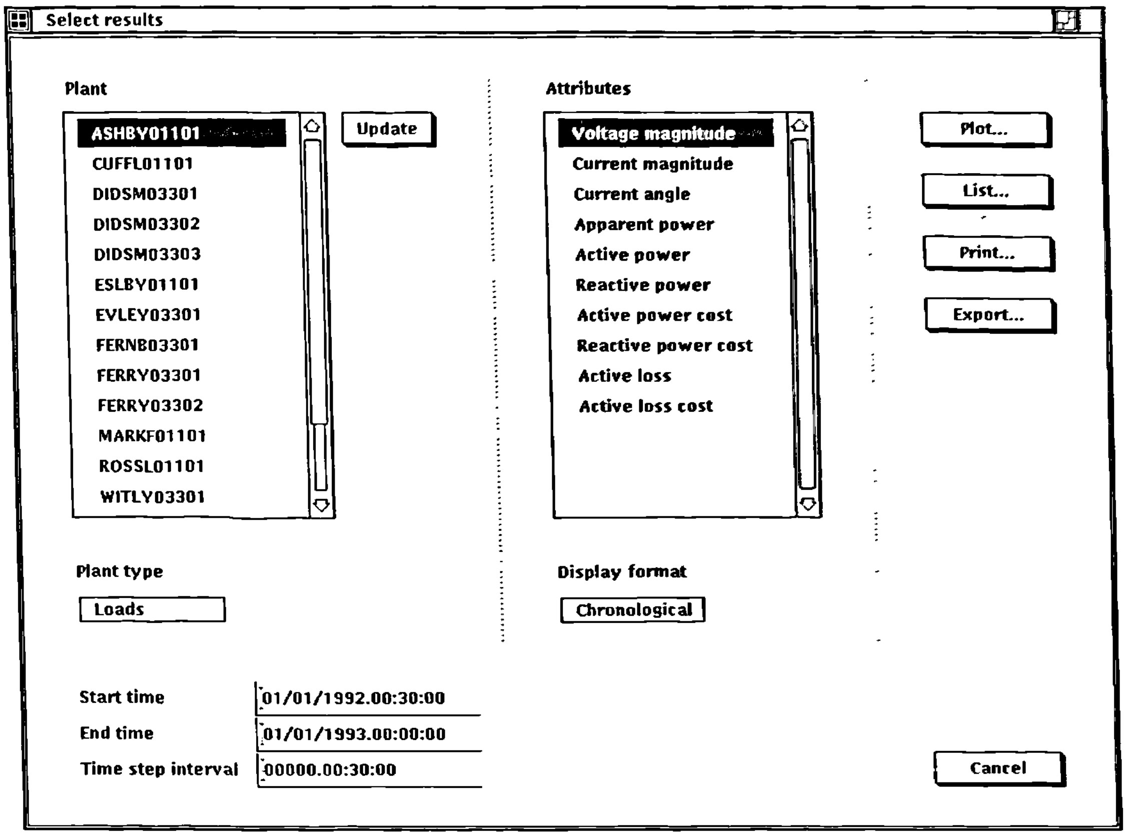

Figure F.4 Insight Simulation Results Dialog Box

The program uses the graphical selection technique described in Section 4.4.5 is in the display of plant in the plant list box on the left hand side of the dialog. Facilities are provided for plotting selected results on a graph, listing them in tabular form, sending them to a printer, or saving them to disk. Results can be presented in chronological form, in which the time sequence of changes in the system state is preserved, or in duration form which rearranges the data in descending order of magnitude.

The **Playback** menu option allows for the copying of results for a given time step to the relational plant database for subsequent display on the PACS diagram, or for use by other applications such as security assessment. The playback dialog is shown in Figure F.5, and operates like a video recorder.

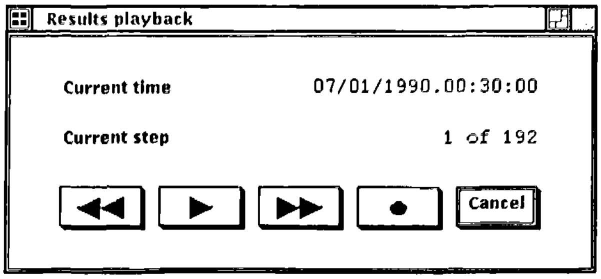

Figure F.5 Insight Simulation Results Playback Facility

When the play button is pressed, the program starts copying the results to the plant database step by step, instructing the PACS system to update its display at each step. The user can proceed directly to particular times through the use of the rewind or fast forward buttons.

F.3.1.6 Calling Other Applications

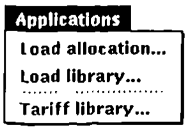

The applications menu provides a means for initiating other components within the Insight application, including Load Allocation and the Load and Tariff Library maintenance programs.

F.3.1.7 Macro Related Functions

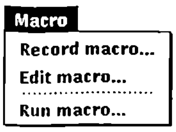

The macro related functions permit the recording, editing and subsequent execution of macros: sequences of Insight commands. The recording procedure operates like a tape recorder; once recording has started the user proceeds as normal, and any commands generated during the study are stored in a macro file until recording is terminated.

F.3.1.8 Customising the Program Options

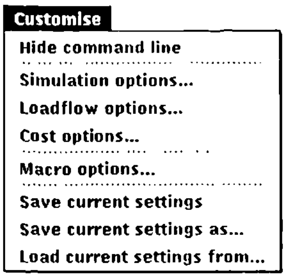

The options in the customise menu permit the user to specify the program settings which govern the behaviour of routines such as the discrete time simulator. The simulation options are illustrated in Figure F.6.

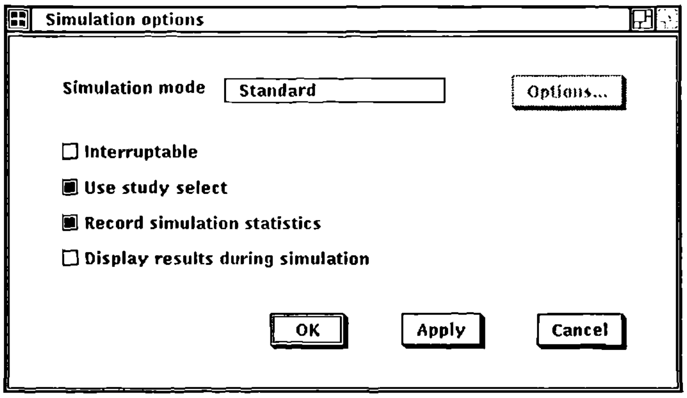

Figure F.6 Insight Simulation Options Dialog Box

The simulation mode shown in the figure permits the user to select the standard discrete time simulation, or the constrained mode of simulation. The additional settings which are required for the constrained mode are specified via the Options button.

F.4 Insight Load and Tariff Library Components

F.4.1 Program Functions

F.4.1.1 Main Window

The main window of the Load Library program is illustrated in Figure F.7. The list on the left hand side of the window contains the names of the cons'umer types defined in the current library file. On the right hand side is a preview window which displays the Profiles for the currently selected consumer type. The push buttons at the bottom of the window permit the user to add and delete consumer types, and to edit existing consumer type records.

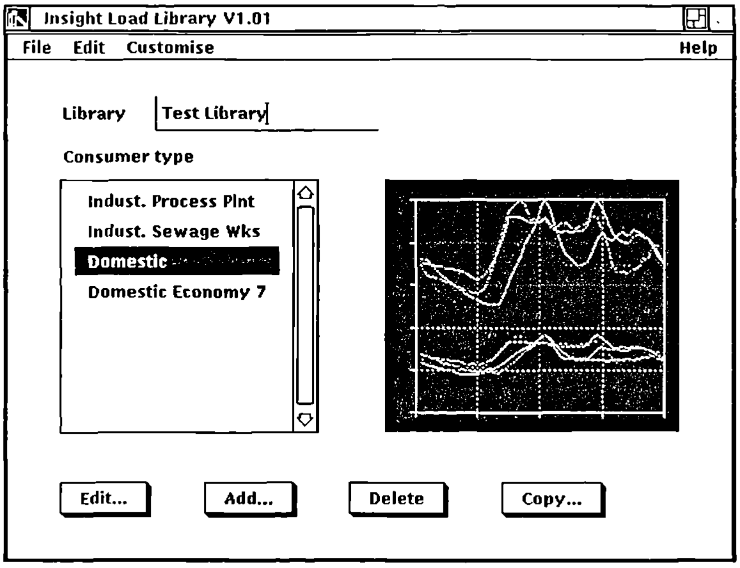

Figure F.7 Main Window of the Insight Load Library Component

F.4.1.2 Consumer Type Editing Dialog

The consumer type editing dialog provides facilities for adding and deleting profiles for the current consumer type, and for editing specific profile data. The dialog is shown in Figure F.8.

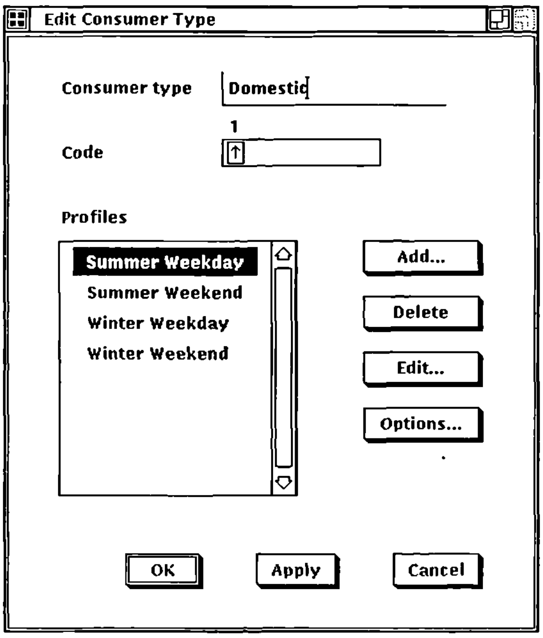

Figure F.8 Load Library Consumer Editing Dialog

F.4.1.3 Profile Editing Dialog

Individual profiles can be edited via the Edit button which displays the profile editing dialog as shown in Figure F.9.

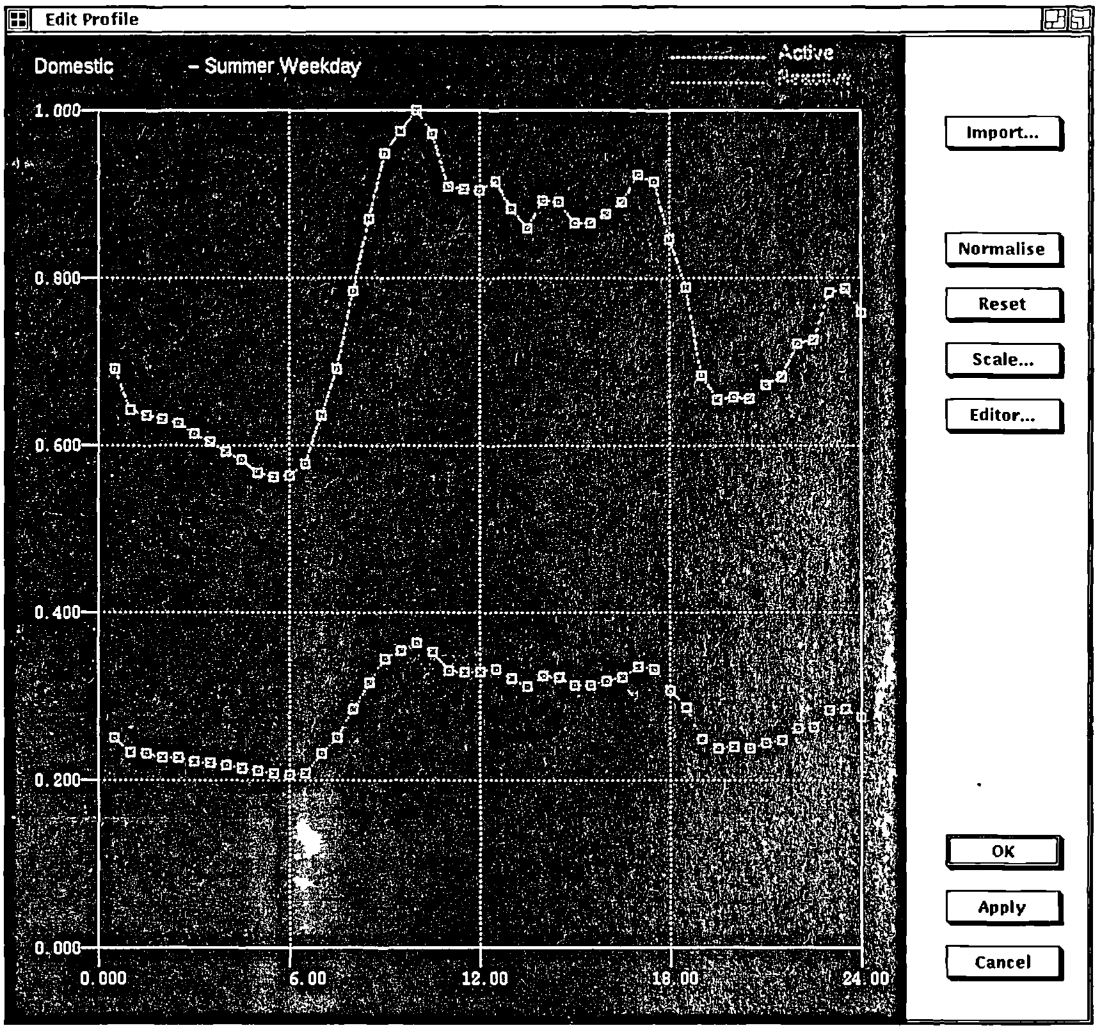

Figure F.9 Load Library Profile Editing Dialog

A novel feature of the design is the graphical editing capability. Points on the curve can be selected using the mouse and dragged vertically to reshape the curve dynamically. Additional program facilities allow coupling of the active and reactive curves to maintain the power factor during the editing process, and coupling of adjacent data points to allow smooth shaping of curves. Figure F.10 illustrates the effect of linear and non linear coupling on adjacent points when one point is dragged to a new position.

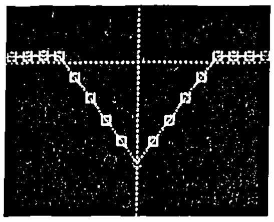

Linear Coupling

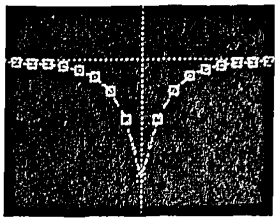

Nonlinear Coupling

Figure F.10 Graphical Shaping of Profiles with Linear and Nonlinear Coupling of Adjacent Data Points

An alternative to the manual creation of profile curves is the import facility which permits data from other applications to be captured for use in the library.

F.4.1.4 Profile Options Dialog

The options dialog, accessed via the Options button allows the user to specify which days of the week and seasons of the year a given profile relates to. The dialog is shown in Figure F.11.

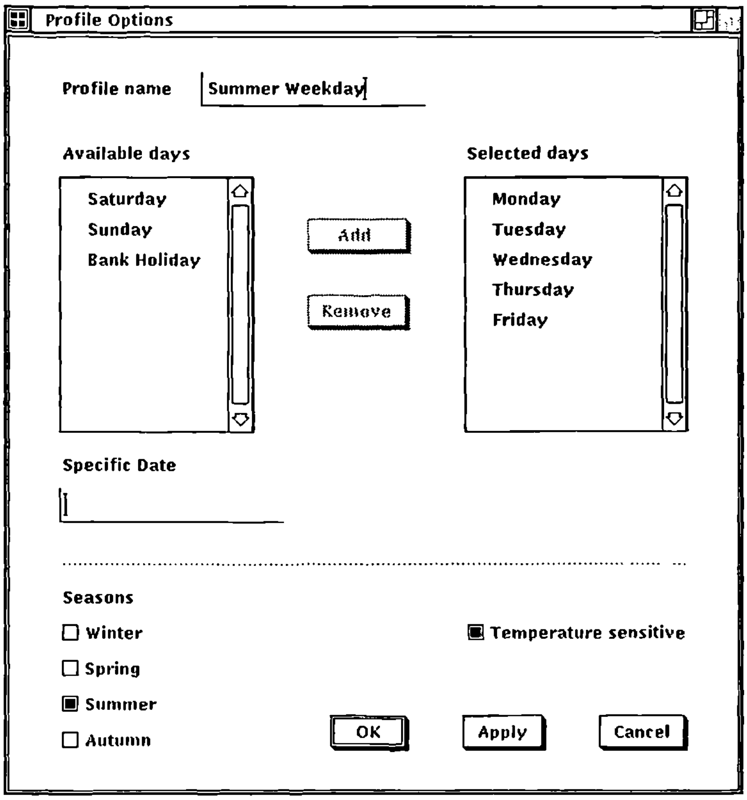

Figure F.11 Load Library Profile Options Dialog

References

[1] Allan, R.N. and Al-Shakarchi, M.R.G., 'Probabilistic a.c. load flow', Proc. IEE, Vol. 123, No. 6, June 1976, pp. 531-536.

[2] Allan, R.N., Leite da Silva, A.M. and Burchett, R.C., 'Evaluation methods and accuracy in probabilistic load flow solutions', IEEE Trans. Power Apparatus and Systems, Vol. PAS-100, No. 5, May 1981, pp. 2539-2546.

[3] Allera, S.V., Alcock, N.D. and Cook, A. A., 'Load research in a privatised electricity supply industry', Proc. 6th IEE Metering Apparatus and Tariffs for Electricity Supply Conference, Manchester, UK, 1990.

[4] Amerongen, R.A.M., 'A general-purpose version of the fast decoupled loadflow', IEEE Trans. Power Systems, Vol. 4, No. 2, May 1989, pp. 760-770.

[5] Anders, G.J., 'Probability concepts in electric power systems', Wiley, New York, 1990.

[6] Andersson, A., Jansson, A. and Klevas, J., 'Model for load simulations by means of load pattern curves', Proc. CIRED, 1989, pp. 545-549.

[7] Arrillaga, J. and Arnold, C.P., 'Computer analysis of power systems', Wiley, Chichester, 1990.

[8] Arrow, R.J. and Solow, R.M., 'Studies in linear and nonlinear programming', Edited by Arrow, R.J., Hurwics, L. and Uzawa, H., Stanford University Press, Stanford, 1958, pp. 166-169.

[9] Babic, B.S., 'Decoupled load flow with variables in rectangular form', IEE Proc. Vol. 130, Pt. C, No. 3, May 1983, pp. 98-102.

[10] Bacher, R., and Tinney, W.F., 'Faster local power flow solutions: the zero mismatch approach', IEEE Trans. Power Systems, Vol. 4, No. 4, October 1989, pp. 1345-1354.

[11] Baran, M.E. and Wu, F.F., 'Network reconfiguration in distribution systems for loss reduction and load balancing', IEEE Trans. Power Delivery, Vol. PWRD-4, 1989, pp. 1401-1407.

[12] Bengiamin, N.N. and Holcomb, F.H., 'PC-based power systems software: comparing functions and features', IEEE Computer Applications in Power, January 1991, pp. 35-40.

[13] Benham-Guilani, K., 'Fast decoupled load flow: the hybrid model', IEEE Trans. Power Systems, Vol. 3, No. 2, May 1988, pp. 734-742.

[14] Berrie, T.W., 'Electricity economics and planning', Peter Peregrinus, London, 1992.

[15] Berrie, T.W., 'Power system economics', Peter Peregrinus, London, 1983.

[16] BIPS, 'Insight Load Allocation reference manual', Brunel Institute of Power Systems, Brunel University, Uxbridge, UK, 1993.

[17] BIPS, 'Insight Load Allocation technical reference manual', Brunel Institute of Power Systems, Brunel University, Uxbridge, UK, 1993.

[18] BIPS, 'Insight Simulation reference manual', Brunel Institute of Power Systems, Brunel University, Uxbridge, UK, 1993.

[19] BIPS, 'Insight Simulation technical reference manual', Brunel Institute of Power Systems, Brunel University, Uxbridge, UK, 1993.

[20] Boice, D.G. and Gursky, R.J., Discussion of Reference [61], IEEE Trans. Power Apparatus and Systems, Vol. PAS-102, No. 9, September 1983, p. 3194.

[21] Bowers, B., 'A history of light electric light and power', Peter Peregrinus, Stevenage, UK, 1982.

[22] Brameller, A. and Denmead, J.K., 'Some improved methods of digital network analysis', IEE Proc., Vol 109A, February 1962, pp.109-116.

[23] Breipohl, A., Lee, F.N., Huang, J. and Feng, Q., 'Sample size reduction in stochastic production simulation', IEEE Trans. Power Systems, Vol. 5, No. 3, August 1990, pp. 984-992.

[24] British Electricity International, 'Modern Power Station Practice', Vol. L (System Operation), Pergamon Press, Oxford, 1991.

[25] Broadwater, R.P., Khan, A.H., Shaalan, H.E. and Lee, R.E., 'Time varying load analysis to reduce distribution losses through reconfiguration', IEEE Trans. Power Delivery, Vol. 8, No. 1, January 1993, pp. 294-300.

[26] Brown, H.E., Carter, G.K., Happ, H.H. and Person, C.E., 'Power flow solution by impedance matrix iterative method', IEEE Trans. Power Apparatus and Systems, Vol. PAS-82, April 1963, pp. 1-10.

[27] Brown, H.E., Carter, G.K., Happ, H.H. and Person, C.E., 'Z-matrix algorithms in load-flow programs', IEEE Trans. Power Apparatus and Systems, Vol. PAS-82, April 1963, pp. 1-10.

[28] Brown, R.J. and Tinney, W.F., 'Digital solutions for large power networks', AIEE Trans. Power Apparatus and Systems, Vol. 76, June 1957, pp. 347-355.

[29] Buller, F.H. and Woodrow, C.A., 'Load factor - equivalent hour values compared', Electrical World, Vol. 92, No. 2, July 1928, pp. 59-60.

[30] Cheung, C.H., '"FAULT": Computation of electrical power system fault conditions', OCEPS Research Report, University of Durham, Durham, UK, April 1989.

[31] Clark, S.L., Steventon, J. and Masiello, R.D., 'Full-graphics man-machine interface for power system control centers', IEEE Computer Applications in Power, July 1988, pp. 27-32.

[32] Cory, B.J., Ekwue, A.O. and Johnson, R.B.I., 'Comparative analysis of the convergence characteristics of second-order loadflow methods', Electrical Power & Energy Systems, Vol. 12, No. 4, October 1990, pp. 251-256.

[33] Date, C.J., 'An introduction to database systems', Addison-Wesley, Reading, Massachusetts, 1990.

[34] Del Toro, V., 'Electric power systems', Prentice Hall, Englewood Cliffs, 1992.

[35] Distribution code of the Public Electricity Suppliers of England and Wales, HMSO, March 1990.

[36] Dodson, D.S., 'A study of sparse matrix algorithms applicable to electric power flow problems', Proc. 1982 'Array' Conference, Floating Point Systems User Society, USA.

[37] Duran, H., Discussion of Reference [74]. IEEE Trans. Power Apparatus and Systems, Vol. PAS-97, No. 5, September/October 1978, p. 1594.

[38] Dy Liacco, T.E., Discussion of Reference [65]. IEEE Trans. Power Apparatus and Systems, Vol. PAS-96, No. 3, May/June 1977, pp. 841-854.

[39] Ekwue, A.O. and Adams, R.N., 'Algorithmic development of the second order loadflow for real time applications', Proc. 8th Power Systems Computation Conference, Helsinki, Finland, August 1984, pp. 724-731.

[40] El-Abiad, A.H., 'Power systems analysis and planning', Hemisphere Publishing, Washington, 1983.

[41] Electrical World, 'Power delivery software: what's out there?', Electrical World, Vol. 200, No. 7, July 1986, pp. 61-65.

[42] Electricity Council, 'The cost of losses for transformers used on distribution systems', Engineering Recommendation T8/6, December 1987.

[43] El-Hawary, M.E. and Wellon, O.K., 'The alpha-modified quasi-second order Newton-Raphson method for load flow solutions in rectangular form', IEEE Trans. Power Apparatus and Systems, Vol. PAS-101, No. 4, April 1982, pp. 854-866.

[44] EPRI, 'Bulk Transmission System Loss Analysis', Report EL-6814, Vol. 1, Electric Power Research Institute, May 1990.

[45] EPRI, 'Improved methods for distribution loss evaluation', Report EL3261, Vol. 1, Electric Power Research Institue, November 1983.

[46] EPRI, 'Technical Assessment Guide', Report P-2410-SR, Electric Power Research Institute, May 1982.

[47] Flaten, D.L., 'Distribution system losses calculated by percent loading', IEEE Trans. Power Systems, Vol. 3, No. 3, August 1988, pp. 1263-1269.

[48] Foley, M., Bose, A., Mitchell, W. and Faustini, A., 'An object oriented graphical user interface for power systems', IEEE Trans. Power Systems, Vol. 8, no. 1, February 1993, pp. 97-104.

[49] Freris, L.L. and Sasson, A.M., 'Investigation of the load-flow problem', Proc. IEE, Vol. 115, No. 10, October 1968, pp. 1459-1470.

[50] Gann, J.O., 'Integrated graphical simulation and analysis environment for distribution power systems: database evaluation', Progress Report 89/3, Distribution Research Centre, Power Systems Research Group, University of Durham, UK, April 1989.

[51] Gann, J.O., 'Integrated graphical simulation and analysis environment for distribution power systems: database evaluation continued', Progress Report 89/5, Distribution Research Centre, Power Systems Research Group, University of Durham, UK, October 1989.

[52] Geisler, K.I., Neumann, S.A., Nielsen, T.D., Bower, P.K. and Hughes, B.A., 'A generalized information management system applied to electrical distribution', IEEE Computer Applications in Power, July 1990, pp. 9-13.

[53] Glimn, A.F. and Stagg, G.W., 'Automatic calculation of load flows', AIEE Trans. Power Apparatus and Systems, Vol. 76, October 1957, pp. 817-828.

[54] Gnadt, P.A., Lawler, J.S. and Whitfield, E.W., 'Automating electric utility distribution systems : the Athens automation and control experiment', Prentice Hall, Englewood Cliffs, 1990.

[55] Gönen, T., 'Electric Power Distribution System Engineering', McGraw-Hill, New York, 1986.

[56] Goswami, S.K. and Basu, S.K., 'Direct solution of distribution systems', IEE Proc., Vol. 138, Pt. C, No. 1, January 1991, pp. 78 - 88.

[57] Grainger, J.J., 'Capacitive compensation of primary feeders for loss reduction', Transmission and Distribution, July 1982, pp. 38-39.

[58] Grainger, J.J. and Kendrew, T.J., 'Evaluation of technical losses on electric distribution systems', Proc. CIRED, 1989, pp. 488-493.

[59] Gross, C.A., 'Power system analysis', Wiley, New York, 1986.

[60] Gupta, P.P. and Humphrey Davies, M.W., 'Digital computers in power system analysis', IEE Proc., Vol. 108A, January 1961, pp. 383-404.

[61] Gustafson, M.W., 'Demand, energy, and marginal electric system losses', IEEE Trans. Power Apparatus and Systems, Vol. PAS-102, No. 9, September 1983.

[62] Gustafson, M.W. and Baylor, J.S., 'Transmission loss evaluation for electric systems', IEEE Trans. Power Systems, Vol. 3, No. 3, August 1988, pp. 1026-1032.

[63] Gustafson, M.W. and Baylor, J.S., 'Approximating the system losses equation', IEEE Trans. Power Apparatus and Systems, Vol. 4, No. 3, August 1989, pp. 850-855.

[64] Haley, P.H. and Ayres, M., 'Super decoupled loadflow with distributed slack bus', IEEE Trans. Power Apparatus and Systems, Vol. PAS-104, No. 1, January 1985, pp. 104-113.

[65] Happ, H.H., 'Optimal power dispatch - a comprehensive survey', IEEE Trans. Power Apparatus and Systems, Vol. PAS-96, No. 3, May/June 1977, pp. 841-854.

[66] Hartley, P.J. and Wynn-Evans, A., 'A structured introduction to numerical mathematics', Stanley Thornes, Cheltenham, 1979.

[67] Hickok, H.N., 'Electrical energy losses in power systems', IEEE Trans. Industry Applications, Vol. IA-14, No. 5, September/October 1978, pp. 373-387.

[68] Hill, E.F. and Stevenson, W.D., 'A new method of determining loss coefficients', IEEE Trans. Power Apparatus and Systems, Vol. PAS-87, No. 7, July 1968, pp. 1548-1553.

[69] H.M.Government, 'Privatising electricity: the Government's proposals for the privatisation of the electricity supply industry in England and Wales', HMSO, London, February 1988.

[70] Hubbi, W., 'The mismatch theorem and second-order load flow algorithms' IEE Proc. Vol. 132, Pt. C, No. 4, July 1985, pp. 189-194.

[71] ICL Electricity, 'Dinis (E) Technical information for engineers', Ref. 19285/004, International Computers Limited, Leeds, UK, March 1992.

[72] Imhof, K. and Arias, C., 'Show it with colors: connectivity, status, and value information in energy management systems', IEEE Computer Applications in Power, October 1990, pp. 11-16.

[73] Irving, M.R. and Sterling, M.J.H.S., 'Efficient Newton-Raphson algorithm for load-flow calculation in transmission and distribution networks', IEE Proc., Vol. 134, Pt. C, No. 5, September 1987, pp. 325-328.

[74] Iwamoto, S. and Tamura, Y., 'A fast load flow method retaining nonlinearity', IEEE Trans. Power Apparatus and Systems, Vol. PAS-97, No. 5, September/October 1978, pp. 1586-1599.

[75] Jalali-Kushki, H. and Wvong, M.D., Discussion of Reference [74]. IEEE Trans. Power Apparatus and Systems, Vol. PAS-97, No. 5, September/October 1978, p. 1594.

[76] Jasmon, G.B. and Lee, L.H.C.C., 'Stability of loadflow techniques for distribution system voltage stability analysis', IEE Proc. C, Vol. 138, No. 6, November 1991, pp. 479-484.

[77] Keyhani, A., 'Study of fast decoupled load flow algorithms with substantially reduced memory requirements', Electric Power Systems Research, Vol. 9, 1985, pp. 1-9.

[78] Kirchmayer, L.K. and Stagg, G.W., 'Analysis of total and incremental losses in transmission systems', AIEE Trans., Vol. 70, Part I, 1951, pp. 1197- 1205.

[79] Kron, G., 'Tensorial analysis of integrated transmission systems, Part I - the six basic reference frames', AIEE Trans., Vol. 70, Part I, 1951, pp. 1239-1248.

[80] Kron, G., 'Tensorial analysis of integrated transmission systems, Part II - off-nominal turn ratios', AIEE Trans., Vol. 71, Part III (Power Apparatus and Systems), January 1952, pp. 505-512.

[81] Lakervi, E. and Holmes, E.J., 'Electricity distribution network design', Peter Peregrinus, London, 1989.

[82] Leite da Silva, A.M., Allan, R.M., Soares, S.M. and Arienti, V.L., 'Probabilistic load-flow considering network outages', IEE Proc., Vol. 132, Pt. C, No. 3, May 1985, pp. 139-145.

[83] Leite da Silva, A.M., Arienti, V.L. and Allan, R.M., 'Probabilistic load flow considering dependence between input nodal powers', IEEE Trans. Power Apparatus and Systems, Vol. PAS-103, No. 6, June 1984, pp. 1524-1530.

[84] Leite da Silva, A.M., Arienti, V.L. and Barbosa, M.H., 'Probabilistic techniques in load flow analysis - a practical application', *in Krishnasamy, S.G., 'Probabilistic methods applied to electric power systems'*, Pergamon Press, Oxford, 1987, pp. 643-651.

[85] Macqueen, C.N., 'Economic analysis of distribution systems - algorithms for costing losses', Research Report CNM89/1, School of Engineering and Applied Science, University of Durham, UK, October 1989.

[86] Macqueen, C.N., 'Power purchase and contracts in the United States - a report on the regulation operation and costing of wheeling contracts in the American electricity supply industry', IEE North Eastern Power Section Premium Award Paper, October 1990.

[87] Macqueen, C.N. and Bumby, J.R., 'Algorithms for evaluating and costing energy losses in distribution systems', Proc. 25th Universities Power Engineering Conference, Aberdeen, UK, September 1990.

[88] Macqueen, C.N. and Bumby, J.R., 'A load allocation algorithm for distribution system analysis', Proc. 26th Universities Power Engineering Conference, Brighton, UK, September 1991.

[89] Macqueen, C.N. and Irving, M.R., 'Discrete-time simulation of network distribution systems for technical and economic reasons', IEE Colloquium on Simulation of Power Systems, Digest 1992/221, December 1992.

[90] Macqueen, C.N., Irving, M.R. and Sterling, M.J.H., 'An integrated environment for operational planning and control in power distribution systems', IFAC World Congress, Sydney, Australia, July 1993.

[91] Macqueen, C.N., Irving, M.R., Morrison, S.A. and Sterling, M.J.H. 'An integrated software environment for distribution system planning', Proc. 18th IEEE Power Industry Computer Applications Conference, Phoenix, USA, May 1993, pp. 162-168.

[92] Masiello, R.D. and Wollenberg, B.F., 'Comments on "Review of load-flow calculation methods"' (Reference [134]), Proc. IEEE, Vol. 63, April 1975, pp. 713-714.

[93] Meisel, J. and Barnard, R.D., 'Application of fixed-point techniques to load-flow studies', IEEE Trans. Power Apparatus and Systems', Vol. PAS-89, No. 1, January 1970, pp. 136-140.

[94] Meyer, W.S., 'Efficient computer solution for Kron and Kron-Early loss formulas', Proc. IEEE Power Industry Computer Application Conference, Minneapolis, USA, June 1973, pp. 428-432.

[95] Morrison, S.A., 'Application Programmers Interface', Internal report, Brunel Institute of Power Systems, Brunel University, Uxbridge, UK, 1993.

[96] Munasinghe, M., 'Electricity pricing: a comprehensive framework', IEEE Trans. Power Apparatus and Systems, Vol. PAS-100, No. 8, August 1981, pp. 3959-3968.

[97] Munasinghe, M., 'Engineering-Economic Analysis of Electric Power Systems', Proc. IEEE, Vol. 72, No. 4, 1984, pp. 424-461.

[98] Murtagh, B.A. and Saunders, M.A., 'A projected Lagrangian algorithm and its implementation for sparse nonlinear constraints', Technical Report SOL 80-1R, Systems Optimisation Laboratory, Stanford University, Stanford, USA, February 1981.

[99] Nanda, J., Bijwe, P.R., Kothari, D.P. and Shenoy, D.L., 'Second order decoupled Newton load flow', Electric Macines and Power Systems, Vol. 12, 1987, pp. 301-312.

[100] OCEPS Limited, 'Power~PACS reference manual', Brunel University, Uxbridge, UK, 1993.

[101] OCEPS Limited, 'PACS dblib reference manual', Brunel University, Uxbridge, UK, 1993.

[102] OCEPS Limited, 'Transient user manual', Brunel University, Uxbridge, UK, 1993.

[103] Office of Electricity Regulation, Publications List, OFFER Library, Birmingham, UK, June 1993.

[104] Osborn, D.L., 'Factors for planning a static VAR system', Electric Power Systems Research, Vol. 17, 1989, pp. 5-12.

[105] Özveren, C.S., Bumby, J.R. and Macqueen, C.N., 'An integrated problem solving environment for distribution system planning', Proc. 25th Universities Power Engineering Conference, Aberdeen, UK, September 1990.

[106] Pansini, A.J., 'Power transmission and distribution', Fairmont Press, Lilburn, USA, 1991.

[107] Parton, K.C., Kendall, T.J., and Walton, C.M., 'Special graphics requirements for interactive analysis of high density city centre and urban distribution networks', Proc. CIRED, 1989, pp. 558-562.

[108] Peddie, J., 'Graphical user intefaces and graphic standards', McGraw-Hill, New York, 1992.

[109] Podmore, R., 'A simplified and improved method for calculating transmission loss formulas', Proc. 8th IEEE Power Industry Computer Applications Conference, Minneapolis, USA, June 1973, pp. 433-440.

[110] Pole, W., 'The life of Sir William Siemens', Siemens Limited, Sunbury-on-Thames, Middlesex, 1986.

[111] Press, W.H., Teukolsky, S.A., Vetterling, W.T. and Flannery, B.P., 'Numerical recipes in FORTRAN : the art of scientific computing', 2nd Edition, Cambridge University Press, Cambridge, UK, 1992.

[112] Rao, N.D. and Roy, L., 'A cartesian coordinate algorithm for power system state estimation', IEEE Trans. Power Apparatus and Systems, Vol. PAS-102, No. 5, May 1983, pp. 1070-1082.

[113] Rao, P.S.N., Rao, K.S.P. and Nanda, J., 'A novel hybrid load flow method', IEEE Trans. Power Apparatus and Systems, Vol. PAS-100, No. 1, January 1981, pp. 303-308.

[114] Rao, P.S.N., Rao, K.S.P. and Nanda, J., 'An empirical criterion for the convergence of the fast decoupled load flow method', IEEE Trans. Power Apparatus and Systems, Vol. PAS-103, No. 5, May 1984, pp. 974-981.

[115] Rao, P.S.N., Rao, K.S.P. and Nanda, J., 'An exact fast load flow method including second order terms in rectangular coordinates', IEEE Trans. Power Apparatus and Systems, Vol. PAS-101, No. 9, September 1982, pp. 3261-3268.

[116] Ridders, C.J.F., 'A new algorithm for computing a single root of a real continuous function', IEEE Trans. Circuits and Systems, Vol. CAS-26, 1979, pp. 979-980.

[117] Rumbaugh, J., Blaha, M., Premerlani, W., Eddy, F. and Lorensen, W., 'Object-oriented modeling and design', Prentice-Hall, Englewood Cliffs, USA, 1991.

[118] Roy, L., 'Exact second order load flow', Proc. 6th Power Systems Computation Conference, Darmstadt, Germany, Vol. 2, August 1978, pp. 711-718.

[119] Roy, L. and Rao, N.D., 'A cartesian coordinate algorithm for power system state estimation', IEEE Trans. Power Apparatus and Systems, Vol. PAS-102, No. 5, 1983, pp. 1070-1082.

[120] Sachdev, M.S., and Medicherla, T.K.P., 'A second order load flow technique', IEEE Trans. Power Apparatus and Systems, Vol. PAS-96, No. 1, January/February 1977, pp. 189-197.

[121] Sachdev, M.S., Medicherla, T.K.P. and Billinton, R. Discussion of Reference [74], IEEE Trans. Power Apparatus and Systems, Vol. PAS-97, No. 5, September/October 1978, pp 1597-1598.

[122] Sarikas, R.H. and Thacker, H.B., 'Distribution system load characteristics and their use in planning and design', AIEE Trans., Vol. 31, Part III, August 1957, pp. 564-573.

[123] Sasaki, H., Discussion of Reference [43], IEEE Trans. Power Apparatus and Systems, VOL. PAS-101, No. 4, April 1982, pp. 863-864.

[124] Sasson, A.M., Snyder, W. and Flam, M., 'Comments on "Review of load-flow calculation methods"' (Reference [134]), Proc. IEEE, Vol. 63, April 1975, pp. 712-713.

[125] Sasson, A.M., Trevino, C. and Aboytes, F., 'Improved Newton's load flow through a minimization technique', IEEE Trans. Power Apparatus and Systems, Vol. 90, 1971, pp. 1974-1981.

[126] Sato, N. and Tinney, W.F., 'Techniques for exploiting the sparsity of the network admittance matrix', IEEE Trans. Power Apparatus and Systems, Vol. 82, December 1963, pp. 944-950.

[127] Shoults, R.R., Grady, W.M. and Helmick, S., 'An efficient method for computing loss formula coefficients based upon the method of least squares', IEEE Trans. Power Apparatus and Systems, Vol. PAS-98, No. 6, November/December 1979, pp. 2144-2152.

[128] Shultz, R.D., Hickey, G.L. and Brunhart, A.D., 'Determination of subsystem loss factors for loss allocation with limited data', IEEE Trans. Power Apparatus and Systems, Vol. PAS-101, No. 5, May 1982, pp. 1053-1058.

[129] Siddall, J.N., 'Probabilistic engineering design', Marcel Dekker, New York, 1983.

[130] Slominski, A.P., 'Analysis of system electrical losses', Proc. American Power Conference, Vol. 44, April 1982, pp. 620-625.

[131] Stagg, G.W. and El-Abiad, A.H., 'Computer methods in power system analysis', McGraw-Hill, New York, 1968.

[132] Stott, B., 'Effective starting process for Newton-Raphson load flows', IEE Proc., Vol. 118, No. 8, August 1971, pp. 983-987.

[133] Stott, B., 'Decoupled Newton load flow', IEEE Trans. Power Apparatus and Systems, Vol. PAS-91, September 1972, pp. 1955-1959.

[134] Stott, B., 'Review of load-flow calculation methods', Proc. IEEE, Vol. 62, No. 7, July 1974, pp. 916-929.

[135] Stott, B., Discussion of Reference [153], IEEE Trans. Power Apparatus and Systems, Vol. PAS-96, No. 1, January/February 1977, p. 274.

[136] Stott, B., and Alsac, O. 'Fast-decoupled load flow', IEEE Trans. Power Apparatus and Systems, Vol. PAS-93, May/June 1974, pp. 859-869.

[137] Stott, B. and Thome, L.M., Discussion of Reference [74]. IEEE Trans. Power Apparatus and Systems, Vol. PAS-97, No. 5, September/October 1978, p. 1596.

[138] Sun, D.I.H., Abe, S., Shoults, R.R., Chen, M.S., Eichenberger, P. and Farris, D., 'Calculation of energy losses in a distribution system', IEEE Trans. Power Apparatus and Systems, Vol. PAS-99, No. 4, July/August 1980, pp. 1347-1356.

[139] Thomas, C.P., Evans, D. and Parton, K.C., 'CADARN - Computer aided design and rationalisation of networks', Proc. CIRED, 1987, Paper a.06.

[140] Tinney, W.F., Discussion of Reference [125]. IEEE Trans. Power Apparatus and Systems, Vol. 90, 1971, pp. 1980.

[141] Tinney, W.F. and Hart, C.E., 'Power flow solution by Newton's method', IEEE Trans. Power Apparatus and Systems, Vol PAS-86, No. 11, November 1967, pp. 1449-1460.

[142] Tinney, W.F. and Walker, J.W., 'Direct solutions of sparse network equations by optimally ordered triangular factorization', Proc. IEEE, Vol. 55, No. 11, November 1967, pp. 1801-1809.

[143] Tobin, N.P. and Glynn, B., 'Evaluation and management of distribution system losses', Proc. CIRED, pp. 6.5.1-6.5.6.

[144] Tripathy, S.C. and Purge Prasad, G.S.S.S.K., 'Load flow solution for ill-conditioned power systems by quadratically convergent Newton-like method', IEE Proc. Vol. 127, Pt. C, No. 5, September 1980, pp. 273-280.

[145] Van Ness, J.E., 'Iteration methods for digital load flow studies', AIEE Trans. Power Apparatus and Systems, Vol. 78, August 1959, pp. 583-588.

[146] Van Ness, J.E. and Griffin, J.H., 'Elimination methods for load-flow studies', AIEE Trans. Power Apparatus and Systems, Vol. 80, June 1961, pp.299-304.

[147] Walker, T.R. and Hutchins, W.H., 'Accuracy of loss formula coefficients on the TVA power system', AIEE Trans., December 1963, pp. 858-866.

[148] Wang, L., Xiang, N., Wang, S., Zhang, B., and Huang, M., 'Novel decoupled power flow', IEE Proc. Vol. 137, Pt. C, No. 1, January 1990, pp. 1-7.

[149] Ward, J.B. and Hale, H.W., 'Digital computer solution of power-flow problems', AIEE Trans. Power Apparatus & Systems, Vol. 75, June 1956, pp. 398-404.

[150] Webb, M.G., 'Energy', *in Gowland, D.H., 'Modern Economic Analysis'*, Butterworths, London, 1979, pp. 197-208.

[151] Willis, H.L., Vismor, T.D. and Powell, R.W., 'Some aspects of sampling load curve data on distribution systems', IEEE Trans. Power Apparatus and Systems, Vol. PAS-104, No. 11, November 1985, pp. 3221-3228.

[152] Wood, A.J. and Wollenburg, B.F., 'Power generation and control', Wiley, New York, 1984.

[153] Wu, F.F., 'Theoretical study of the convergence of the fast decoupled load flow', IEEE Trans. Power Apparatus and Systems, Vol. PAS-96, No. 1, January/February 1977, pp. 268-275.

[154] Zhang, B., Xiang, N., Wang, S., Yu, E. and Sun, S., 'A fast loop-based algorithm for computing loss formula coefficients', IFAC Symposium on Power System & Power Plant Control, Beijing, China, 1986, pp. 518-523.

[155] Zhang, S. and Irving, M.R., 'An enhanced Newton-Raphson algorithm for normal, controlled and optimal powerflow solutions using column exchange techniques', Research Report, Brunel Institute of Power Systems, Brunel University, Uxbridge, UK, October 1993.

[156] Zollenkopf, K., 'Bifactorisation - basic computational algorithm and programming techniques', *in Reid, J.K., 'Large sparse sets of linear equations'*, Academic Press, UK, 1971, pp. 75-96.

[157] Borkowska, B., 'Probabilistic load flow', IEEE Trans. Power Apparatus and Systems, Vol. PAS-93, No. 3, May/June 1974, pp. 752-759.